Hostile takeover factors of *Pseudomonas*

Alice Christina Zammit Collins
BSc, MRes

Department of Respiratory Infections

National Heart and Lung Institute

Imperial College London

This thesis is submitted in partial fulfilment of the requirements for the degree of Doctor of Philosophy

Candidate's Declaration

I declare that the work presented in this thesis is my own and that the contributions of others are duly acknowledged and appropriately referenced.

Copyright Declaration

The copyright of this thesis rests with the author. Unless otherwise indicated, its contents are licensed under a Creative Commons Attribution-Non Commercial 4.0 International Licence (CC BY-NC). Under this licence, you may copy and redistribute the material in any medium or format. You may also create and distribute modified versions of the work. This is on the condition that: you credit the author and do not use it, or any derivative works, for a commercial purpose. When reusing or sharing this work, ensure you make the licence terms clear to others by naming the licence and linking to the licence text. Where a work has been adapted, you should indicate that the work has been changed and describe those changes. Please seek permission from the copyright holder for uses of this work that are not included in this licence or permitted under UK Copyright Law.

To my family, who inspired me to believe anything is possible when you put your mind to it.

Abstract

Pseudomonas aeruginosa is an opportunistic pathogen that causes chronic pulmonary infections in Cystic Fibrosis patients, dominating and damaging the lung environment. *P. aeruginosa* can deliver bacterial-derived toxins into competing neighbours to inhibit growth or kill via the contact-dependent inhibition (CDI) and Type VI Secretion Systems (T6SS). However, the role of CDI systems in *Pseudomonas* infection in Cystic Fibrosis clinical isolates remains unclear. Here we bioinformatically and experimentally investigate the CDI and T6SSs encoded in *P. aeruginosa* strain PA14. For CDI systems, bioinformatics was used to elucidate and evaluate genetic domains to determine putative toxin-immunity module functions. I show that PA14 encodes two CDI systems with putative tRNase activities and demonstrate that both CDI systems encode a functional toxin/immunity pair, further supporting their role in antibacterial activity. I identified regions conserved between and within genetically distinct system types to produce recombinant proteins for antibody production for use as a tool to determine CDI activation status in clinical isolates. We constructed whole operon deletion mutants and see no impact of these systems upon motility or biofilm formation. However, we show a role for both CDI systems in interbacterial competition with potential interplay between the CDI and T6SSs. Finally, we show an unprecedented level of control for the H2-T6SSs by enhancer binding protein Sfa2 in addition to a previously unseen role of RpoN in CDI system expression. This study further delineates the genomic organisation and role of CDI systems in *P. aeruginosa* interbacterial competition which may contribute to the niche dominance observed in *P. aeruginosa* infection. We propose the use of competitive systems as a mechanism of *P. aeruginosa* dominance in the CF lung.

Acknowledgements

Having started this position only a few months before the beginning of a global pandemic, I feel that this was one of the strangest and most difficult times in history to have been attempting a PhD. The irony of working at the National Heart and Lung Institute on a project in molecular respiratory microbiology during the COVID-19 pandemic is not lost on me and for that I have to thank Chaos for introducing this factor into the already full mix associated with taking on research at this level. Because of this, I feel that this thesis is the culmination of both my work but also my experience when the world was turned completely upside down.

Growing up with a sibling with Cystic Fibrosis, you build a different kind of awareness of the world around you. The inherent understanding of health and mortality at such a young age has been something that I think has been a driving force in me picking a career that can help understand this condition. Besides my inherent fascination in biology and wanting to be a scientist from the age of three, I feel that it is no surprise that I ended up in this field. Contributing to the research, to essentially play a part in the discovery of the future cure, is my way of hoping I can prevent others from having to endure the hardships of this condition. Being in the unique position of studying a condition that is so close to my heart, as well as having the opportunity to do so, has been a privilege that has made me feel lucky every single day of this process to have been afforded (ok maybe not during the late night labs or thesis writing stage but definitely the rest). For this I first must thank my grandmother, Barbara Zammit, who always believed I could do anything I put my mind to. Particularly for her saving the CF Trust magazines for me which incited my interest in the possibility of a career in the CF field, especially as many of these contained articles on Jane and her research team.

Next I'd like to thank Professor Eshwar Mahenthiralingam at Cardiff University, who gave me my first opportunity to work in the CF field during my MRes. For the amazing time I had there with the various members of his group, I'd like to thank him for ultimately solidifying and inciting within me the surety that I wanted to build a research career in this field.

It is a unique thing to be finishing a PhD not wanting to leave, and for this I must sincerely thank both Luke and Jane for making my PhD experience so wonderful. I will be forever grateful to them for giving me the opportunity to work with them, as well as all the incredible help and support they have given me through the ups and downs of this experience whether personally, professionally or coping with the fallout of the pandemic. To Luke, I would like to thank him for picking me to be his first PhD student and for having the faith in me to become a molecular biologist having had no previous experience in the field. I feel very privileged to have been his first PhD student and could not have succeeded or become the scientist I am today without his teaching, guidance, support, and encouragement. To Jane, it has been an honour to work with her and I would like to thank her for all her guidance, kindness and for being a truly epic role model as a woman in science. If I can be half the inspiration she has been to me for future generations of female scientists I will be incredibly proud. To both, this has been a truly life-changing experience that I will never be able to thank either of them enough for, and I sincerely hope our professional paths will cross again in the future.

Next I would like to thank all the amazing team members at EKB, both old and new. For all the long lab days, frustrations with experiments, hardships, and ultimate successes they saw

me through. Both professionally and personally they have been a source of constant support and kindness, they really are a special group. Particular thanks go to Matt Coates and Ronan Murphy who warmly welcomed me into the team when I started and were the only faces I saw during the various lockdowns, and for that I must acknowledge their help in preserving my sanity. Other special thanks go to Laura Gardner, Livia Spiga, Micaela Mossop, Alecks Cunanan, and Simone Hadjisymeou-Andreou who have always lent a sympathetic ear during hard days and celebrated with me during my successes. I couldn't have asked for a better group of inspirational female scientists to be around during this process. Special thanks go to Laura Nolan who has given me so much advice in next steps post-PhD and being a woman in science and I have valued our conversations immensely. Thanks also go to Luca Robinson who was my first long-term teammate in the Allsopp lab, a fantastic colleague and gifted scientist who was great for talking through various ideas and problems. Final thanks go to my MRes students Madeleine Humphrey and Nicholas Yuen for all their hard work on this project.

On a more personal note, I would like to thank the rest of my family. Firstly, my mother, Diane, who has been my rock and best friend for so many years. She has supported me through every success and failure with unending patience and love and I really wouldn't be where I am today were it not for her guidance. Without her unerring belief in me, and encouragement in applying for this position, I would not be here today. She has shaped every aspect of who I am as a person and no words can express the depth of my gratitude for having such an unwavering advocate in my corner. She is the strongest, bravest and all around most amazing woman I know. Next, I would like to thank my father, Brian, who showed me just how amazing the world around us is and for fostering my love for science. For all the experiments on weekends, to the science fair projects in school, and the ultimate and time-consuming essay editing during my university years (I promise I'm better now). I have so much gratitude for how much he has been there for me throughout this journey. His time, support and endless patience have meant so much throughout this process, as well as his belief in me that I can work to achieve anything I want to do in life. I am so thankful to both of them for everything they have done to support me, and no words can truly express the depth of my gratitude and love for them.

Lastly, I would like to thank my brother, Alexander, a CF sufferer. From a young age I have always had such admiration for his strength and resolve in the face of adversity with the many facets of his condition. This strength and my love for him have really shaped me as a person and he is the main inspiration in my pursual of a career in this field. During this PhD I had the privilege of seeing him receive Kaftrio, which was one of the best days of my life and I will be eternally grateful to the researchers that made this kind of treatment possible. As a scientist you get to marvel at the way the world works every day but to see that in action for a person you love is a life changing experience I will never forget. I feel that this process has enabled us to open up and talk about how CF has affected not only ourselves, but our family, which is something I did not anticipate but will treasure as a part of the experience. Whilst there have been incredible advancements in the CF field which have changed both my professional and personal life through the course of this PhD, the work is not done. We still have so much to learn. So as I leave this chapter of my life and PhD behind, I look to the future and the work it will entail to understand and cure this condition so that people with CF really can live a life unlimited.

Contents

ABBREVIATIONS **10**

LIST OF FIGURES **11**

LIST OF TABLES **15**

1. INTRODUCTION **17**

1.1 *PSEUDOMONAS*- FROM WAR WOUNDS TO THE ERA OF GENOMICS 17
1.1.1 Pseudomonas aeruginosa- an adaptable type species *19*
1.1.2 Bacterial cell envelopes and what we have learnt since Christian Gram *22*
1.1.2 P. AERUGINOSA PATHOGENESIS- THE PERFECT OPPORTUNISTIC PATHOGEN 27
1.2 CYSTIC FIBROSIS AND POLYMICROBIAL COMMUNITIES- A TALE AS OLD AS TIME 29
1.2.1 The original genetic condition, from salty sweat to CFTR *30*
1.2.2 CF lung physiology and pulmonary infections *34*
1.2.3 Polymicrobial communities and controlling pathogens *38*
1.3 BACTERIAL MECHANISMS OF MOVEMENT- FROM FLAGELLA BASED SWIMMING TO QUORUM SENSING MEDIATED SWARMING 42
1.3.1 The flagellar structure and bacterial movement *43*
1.3.2 The group mediated movement response and quorum sensing *46*
1.3.3 Other mechanisms of bacterial movement- from type IV pili mediated twitching to sliding *48*
1.4 PRODUCTION OF BIOFILM- THE SHIELD 50
1.4.1 The biofilm matrix- components matter *51*
1.4.2 Microscopic mushrooms- the biofilm maturation cycle *53*
1.4.3 Tough shields, bacterial persistence, and survival in hostile environments *56*
1.5 BACTERIAL SECRETION SYSTEMS- FROM CLASSICAL TO NON-CLASSICAL MECHANISMS OF PROTEIN EXPORT 58
1.5.1 The type I secretion system (T1SS)- an ABC autotransporter *60*
1.5.2 The type II secretion system (T2SS) and two-step secretion *62*
1.5.3 The type III secretion system (T3SS) injectosome *64*
1.5.4 The type IV secretion system (T4SS) sex pilus *66*
1.5.5 The non-classical secretion systems *67*
1.6 THE TYPE V SECRETION SYSTEM (T5SS) AND CONTACT DEPENDENT INHIBITION (CDI) SYSTEMS 68
1.6.1 The T5SS subtypes and classification *71*
1.6.2 The T5bSS CDI systems *74*
1.6.3. The mechanistic deployment of the CDI systems- a molecular spear for bacterial warfare *78*
1.7 THE TYPE VI SECRETION SYSTEM (T6SS) MOLECULAR HARPOON 82
1.7.1 The T6SS core operons and orphan islands *85*
1.7.2 A nano-harpoon apparatus- the mechanism of T6SS deployment in P. aeruginosa *89*
1.7.3 Transkingdom interactions and bacterial warfare *92*
1.8 REGULATION NETWORKS AND CONTROLLING BACTERIAL PHENOTYPES 96
1.8.1 The post-transcriptional Gac/Rsm regulation pathway *98*
1.8.2 Sigma factors and enhancer binding proteins in transcriptional regulation *101*
1.8.3 Post-translational regulation and other networks for virulence factor interplay *106*
1.9 PROJECT OVERVIEW AND AIMS 109

2. MATERIALS AND METHODS **112**

2.1 BACTERIA 112
2.2 MEDIA 116
2.3 PRIMERS 119
2.4 LOW TEMPERATURE STORAGE OF BACTERIAL CULTURES 122
2.5 BIOINFORMATIC ANALYSIS OF T5SS CDI OPERONS FOR IMMUNITY PROTEIN AND CONSERVED SEQUENCE IDENTIFICATION 122
2.5.1 Putative immunity identification through small ORF analysis *122*
2.5.2 Phylogenetic analysis of toxin genes from P. aeruginosa CDI systems *123*
2.5.3 Phylogenetic analysis of T5SS CDI toxin gene orthologues in P. aeruginosa and other Pseudomonas species *124*
2.6 PRIMER DESIGN FOR MUTATOR FRAGMENT CONSTRUCTION 125

2.7 Gene deletion mutator fragment construction through PCR amplification 125
2.7.1 PCR for cloning CDI genes and screening constructed transformant colonies *125*
2.7.2 Agarose gel electrophoresis of cloning/colony PCR products *127*
2.8 Ligation of mutator fragment into plasmid vectors in *Escherichia coli* 127
2.8.1 Restriction digest of PCR products and vector *128*
2.8.2 Ligation of restriction digest products *128*
2.9 Chemically competent cell production for transformations 129
2.10 Transformation into vectors and competent strains 129
2.11 Screening isolates through colony PCR 130
2.12 Three partner conjugation for transfer of gene deletion plasmids into *P. aeruginosa* strains 131
2.13 Inter and intrabacterial killing assays 134
2.14 Determining biofilm production of CDI mutants 136
2.15 Determining motility of CDI mutants 138
2.15.1 Determining swimming motility of CDI mutants *138*
2.15.2 Determining swarming motility of CDI mutants *139*
2.16 Determining growth rates of CDI mutants 140
2.17 Toxin-immunity module cloning, plus validation via growth rate and agar plate induction 141
2.18 SDS-PAGE and western blot analysis 142
2.18.1 SDS-PAGE and semi-dry transfer *142*
2.18.2 Tris-Acetate electrophoresis and wet transfer *143*
2.19 Protein purification for toxin-immunity validation and antibody production 144
2.20 Protein pull down for toxin-immunity validation 146
2.21 Site-directed mutagenesis for protein tag replacement 146
2.22 Determining regulation control of T6SS via b-galactosidase expression assay 147
2.23 Statistical analyses 148

3. BIOINFORMATIC ANALYSIS OF CDI OPERONS TO INVESTIGATE THE PUTATIVE FUNCTIONS OF CDI SYSTEMS IN *P. AERUGINOSA* PA14 AND PAO1 ..... **149**

3.1 Introduction 149
3.2 Aims of this study 152
3.3 Results 153
3.3.1 Identification and bioinformatic analysis of T5SS CDI operons in P. aeruginosa *153*
3.3.2 Comprehensive in silico identification orphan-immunity pairs and unannotated putative immunity genes through small ORF analysis *156*
3.3.3 Determining CDI operon genetic and protein structure homologies through in silico analysis *166*
3.3.4 Determining phylogenetic relatedness of CDI systems in Pseudomonas species *179*
3.3.5 Identification of conserved regions specific to P. aeruginosa PA14 CdiA proteins to enable cloning into inducible vectors for recombinant protein expression *183*
3.4 Discussion 187
3.4.1 Does the genome of P. aeruginosa PA14 contain multiple CDI systems? *188*
3.4.2 Do downstream small ORFs encode putative immunities and toxin/immunity modules? *189*
3.4.3 Do CDI operon structures and genes have homology? *194*
3.4.4 Are CDI systems in P. aeruginosa closely related to those found within other Pseudomonas species? *200*
3.4.5 Are there conserved regions in CDI systems that could enable identification of presence and activity of each system type? *202*
3.5 Conclusions 203

4. CDI SYSTEM ACTIVITY IN *P. AERUGINOSA* STRAIN PA14 ..... **206**

4.1 Introduction 206
4.2 Aims of this study 208
4.3 Results 209
4.3.1 Mutant strain background engineering *209*
4.3.2 CDI system deletion mutant engineering from in silico characterisation of CDI operons *213*
4.3.3 Cloning of CDI toxin and immunity pairs into inducible vectors *221*
4.3.4 CdiA^{PA14_00510} and CdiA^{PA14_32790} encode functional toxin-immunity pairs *228*
4.4 Discussion 240

4.4.1 Can rsmA be restored in PA14 rsmAH123 background? ... 240
4.4.2 Can whole system deletion mutants of each CDI system in P. aeruginosa strain PA14 be engineered? ... 241
4.4.3 Can the CDI toxins and immunities be cloned into expression vectors in E. coli? ... 242
4.4.4 Are the toxin-immunity modules from the CDI systems in P. aeruginosa strain PA14 functional and induce bacterial intoxication? ... 244
4.4.5 Are the toxin-immunity modules from the CDI systems in P. aeruginosa strain PA14 specific and interact via cognate binding? ... 247
4.5 Conclusions ... 250

5. GENERATION OF CDI SPECIFIC POLYCLONAL MOUSE ANTIBODIES VIA THE PRODUCTION OF RECOMBINANT PROTEINS FROM CONSERVED REGIONS OF THE CDIA EXTRACELLULAR TOXIN-PASSENGER DOMAIN ... 252

5.1 Introduction ... 252
5.2 Aims of this study ... 254
5.3 Results ... 255
5.3.1 Cloning conserved CdiA-NT regions enables generation of inducible recombinant protein vectors 255
5.3.2 Recombinant protein expression enables purification for antibody production ... 265
5.3.3 Polyclonal antibodies successfully detect their corresponding recombinant proteins ... 269
5.3.4 Polyclonal antibodies do not detect CdiA in P. aeruginosa laboratory strains or whole system deletion mutants ... 273
5.4 Discussion ... 280
5.4.1 Can conserved CdiA-NT regions be cloned to generate inducible recombinant protein vectors? ... 281
5.4.2 Can recombinant proteins be expressed and purified to enable antibody production? ... 282
5.4.3 Are polyclonal antibodies raised in rabbits effective at detecting both recombinant proteins and the presence of CDI systems in P. aeruginosa CDI deletion mutants? ... 283
5.5 Conclusions ... 286

6. DETERMINING THE ROLE OF CDI AND T6SS IN INTERBACTERIAL COMPETITION BETWEEN *P. AERUGINOSA* LABORATORY STRAINS ... 289

6.1 Introduction ... 289
6.2 Aims of this study ... 291
6.3 Results ... 291
6.3.1 CDI systems in P. aeruginosa strain PA14 do not play a role in motility ... 291
6.3.2 CDI systems in P. aeruginosa strain PA14 do not play a role in biofilm formation ... 298
6.3.3 Both CDI systems in P. aeruginosa strain PA14 play a role in interbacterial competition ... 302
6.4 Discussion ... 315
6.4.1 Do the CDI systems in P. aeruginosa strain PA14 play a role in bacterial motility? ... 316
6.4.2 Do the CDI systems in P. aeruginosa strain PA14 play a role in biofilm production? ... 319
6.4.3 Do the CDI systems in P. aeruginosa strain PA14 play a role in interbacterial competition? ... 321
6.5 Conclusions ... 327

7. REGULATION OF CONTACT DEPENDENT KILLING SYSTEMS IN *P. AERUGINOSA* STRAIN PA14 ... 330

7.1 Introduction ... 330
7.2 Aims of this study ... 333
7.3 Summary of findings ... 334
7.4 Results ... 335
7.4.1 Analysis of RNA-seq data identifies differential transcriptional regulators of the CDI, TPS and T6SSs ... 335
7.4.2 Transcriptional fusions enable investigation of the role of RpoN in the regulatory control of H2-T6SS in PA14 ... 345
7.4.3 In P. aeruginosa PA14, the regulator RpoN plays a clear role in motility, whilst enhancer binding protein Sfa2 may play a role, but Sfa3 does not ... 347
7.4.4 Regulators RpoN and Sfa2 do not play a role in biofilm production in P. aeruginosa strain PA14 ... 353
7.5 Discussion ... 355
7.5.1 Can transcriptomics analysis identify regulators of CDI and T6SS? ... 356
7.5.2 Is motility influenced by RpoN and SFA proteins? ... 360

7.5.3 Is biofilm production influenced by RsmA, RpoN and SFA proteins? *362*
7.6 CONCLUSIONS 364

8. FINAL DISCUSSION **367**

8.1 CDI SECRETION SYSTEMS IN *P. AERUGINOSA* 367
8.2 FUNCTION AND SPECIFICITY OF CDI ENCODED TOXIN-IMMUNITY MODULES FOR INTERBACTERIAL COMPETITION 372
8.3 REGULATION OF T6SS AND CDI IN *P. AERUGINOSA* 377
8.4 CONCLUSION 380

9. REFERENCES **381**

10. APPENDIX **434**

Abbreviations

ABC	ATP-Binding Cassette
AMR	Antimicrobial Resistance
BAM	β-barrel-assembly machinery
CDI	Contact Dependent Inhibition
CdiA	Toxin passenger domain
CdiB	Outer membrane β-barrel
c-di-GMP	Cyclic di-GMP
CDS	Contact Dependent Signalling
CF	Cystic Fibrosis
CFTR	Cystic Fibrosis Transmembrane Conductance Regulator
CdiI	Immunity
DUF	Domain of Unknown Function
EBP	Enhancer Binding Protein
eDNA	Extracellular DNA
ECM	Extracellular Milieu
EPS	Extracellular Polysaccharide
HGT	Horizontal Gene Transfer
HR	Homologous Recombination
HSL	Homoserine Lactone
IM	Inner Membrane
IPTG	isopropyl β-D-1-thiogalactopyranoside
OM	Outer Membrane
ORF	Open Reading Frame
PARA	*Pseudomonas aeruginosa* response to antagonism
PTPM	Pre-Toxin Peptide Motif
QS	Quorum Sensing
RBD	Receptor Binding Domain
RBS	Ribosomal Binding Site
RND	Resistance-Nodulation and Division
SFA	Sigma Factor Activator
sRNA	Small non-coding regulatory RNA

ST1	System Type 1 (homologous to CDI^{00510})
ST2	System Type 2 (homologous to CDI32790)
TCS	Two-Component System
TPS	Two-Partner Secretion
T5SS	Type V Secretion System
T6SS	Type VI Secretion System
WSDM	Whole System Deletion Mutant
WT	Wild Type
X-gal	5-bromo-4-chloro-indolyl-β-D-galactopyranoside

List of Figures

Figure 1.1: Bacterial cell envelopes.	23
Figure 1.2: Sec and BAM complex translocation machinery.	27
Figure 1.3: Ion dysregulation in epithelial cells with CFTR functional mutation.	31
Figure 1.4: Classes of CFTR mutations which result in cystic fibrosis manifestation.	32
Figure 1.5: Lower airway metagenome of cystic fibrosis patients.	36
Figure 1.6: Prevalence of infection by various pathogens in cystic fibrosis patients compared with age.	38
Figure 1.7: Metagenomic sequencing identification of other bacterial species associated with cystic fibrosis.	39
Figure 1.8: The flagellar motor complex.	45
Figure 1.9: Quorum sensing network of *P. aeruginosa*.	47
Figure 1.10: Twitching motility movement via the type IV pili.	49
Figure 1.11: The biofilm maturation cycle.	54
Figure 1.12: Gram-negative classical bacterial secretion systems.	59
Figure 1.13: The type I secretion system.	61
Figure 1.14: The type II secretion system.	63
Figure 1.15: The type III secretion system.	64
Figure 1.16: Classes of the Type V bacterial secretion systems.	71
Figure 1.17: The type Vb secretion system.	75
Figure 1.18: The CDI proteins and their domains.	77
Figure 1.19: Mechanistic deployment of the CDI system.	80
Figure 1.20: The type VI secretion system.	86
Figure 1.21: Core clusters and orphan islands of the type VI secretion system.	88
Figure 1.22: Mechanistic deployment of the T6SS system.	91
Figure 1.23: Mechanistic deployment of the T6SS system.	93
Figure 1.24: The Gac/Rsm global regulation pathway.	99
Figure 1.25: RpoN transcription initiation through the utilisation of enhancer binding proteins.	104
Figure 1.26: The threonine phosphorylation (TPP) post-translational regulation of the T6SS.	108
Figure 2.1: Primer positions and orientations.	125
Figure 2.2: Mutator fragment insertion into plasmid vector.	127
Figure 2.3: Mutator fragment insertion into pKNG.	130
Figure 2.4: Strain spotting on LB agar for conjugation incubation.	132
Figure 2.5: Culture processing for three partner conjugation.	133

Figure 2.6: Culture processing for competition assays.	135
Figure 2.7: Culture processing for biofilm biomass production assay.	137
Figure 2.8: Biofilm assay 96 well plate layout representation.	137
Figure 2.9: Swimming motility on low agar plates.	139
Figure 2.10: Swarming motility on low agar plates.	140
Figure 2.11: Site-direct mutagenesis for protein tag exchange.	147
Figure 3.1: CDI operons in PAO1 and PA14.	155
Figure 3.2: Small ORFs of toxin-Immunity regions downstream of CDI operons in PAO1 and PA14.	163
Figure 3.3: Phyre2 analysis of CdiI from CDI systems in PAO1 and PA14.	164
Figure 3.4: Phyre2 PA14 CdiB$_{00490}$ analysis.	167
Figure 3.5: Domains of CdiA proteins in *E. coli* type CDI systems in *Pseudomonas* spp.	168
Figure 3.6: Domains of CdiA proteins in CDI systems within *P. aeruginosa* strains PAO1 and PA14.	169
Figure 3.7: DUF domain situation in C-terminal CdiA from *P. aeruginosa* CDI systems.	172
Figure 3.8: Phyre2 analysis of CdiA-CT from homologous CDI system PAO1$_{0041}$ and PA14$_{00510}$.	174
Figure 3.9: InterPro ArgJ-like domain alignment to C-terminal DUF domain of CdiA in *P. aeruginosa* CDI systems.	176
Figure 3.10: Maximum-Likelihood phylogenetic tree of BLAST results homologous to PA2462 using amino acid sequence alignments.	178
Figure 3.11: Maximum-Likelihood phylogenetic trees of CDI toxins in PAO1 and PA14 using DNA and amino acid sequence alignments.	181
Figure 3.12: Maximum-Likelihood phylogenetic trees of CDI toxins in *P. aeruginosa* clonal lineages using DNA and amino acid sequence alignments.	181
Figure 3.13: Maximum-Likelihood phylogenetic trees of all CDI toxin homologues from *Pseudomonas* spp. using DNA and amino acid alignments.	182
Figure 3.14: CdiA toxin passenger domain alignment between homologous systems to identify conserved domain regions.	185
Figure 4.1: *P. aeruginosa* strain backgrounds for CDI mutant production.	211
Figure 4.2: PCR confirmation of successful *rsmA* repair on the chromosome of *P. aeruginosa* PA14.	212
Figure 4.3: Sequence alignment confirming successful chromosomal reinsertion of *rsmA* .	212
Figure 4.4: CDI mutant strains generated.	215
Figure 4.5: Primers for amplification of PA14 *cdiBAI*$_{00510}$ upstream and downstream fragments.	216
Figure 4.6: Splice overlap PCRs of PA14 *cdiBAI*$_{00510}$ and *cdiBAI*$_{32790}$ upstream and downstream fragments.	216
Figure 4.7: Successful generation of pKNG101*cdiBAI*$_{00510}$ mutator confirmed by PCR screening.	217
Figure 4.8: Sequencing alignment confirming successful construction of pKNG101cdi*BAI*$_{00510}$	217
Figure 4.9: PCR amplification confirming successful insertion of pKNG101*cdiBAI*$_{00510}$ mutator into PA14.	218
Figure 4.10: PCR amplification of successful PA14 Δ*cdiBAI*$_{00510}$ mutant construction in the PA14 background.	218
Figure 4.11: Sequencing alignment confirming successful construction of PA14 Δ*cdiBAI*$_{00510}$.	219
Figure 4.12: CDI mutations in all *P. aeruginosa* strain backgrounds have no significant impacts to growth rate.	220
Figure 4.13: Primers for amplification of PA14 CDI$_{00510}$ *cdiI* genes.	222

Figure 4.14: PCR amplification of successful insertion of cloned *cdiI*^{00510} or *cdiI*^{32790} into pCR Blunt II-TOPO.	223
Figure 4.15: Sequencing alignment confirming successful construction of pCR Blunt II-TOPO-*cdiI*^{00510}.	224
Figure 4.16: Amplification of successful insertion of cloned *cdiI*^{00510} and *cdiI*^{32790} into expression vector pBAD33.	224
Figure 4.17: Amplification of successful insertion of cloned *cdiA*^{00510} and *cdiA*^{32790} into expression vector pNDM220.	225
Figure 4.18: Sequencing alignment confirming successful construction of p*cdiI*^{00510}.	226
Figure 4.19: Sequencing alignment confirming successful construction of p*cdiA*^{00510}.	226
Figure 4.20: Model of *Escherichia coli* BL21 strains with cloned toxin-immunity pairs from CDI systems.	227
Figure 4.21: *cdiAI*^{00510} encodes a functional toxin-immunity pair which induces both bacterial intoxication and recovery when expressed in *E. coli* BL21.	230
Figure 4.22: *cdiAI*^{32790} encodes a functional toxin-immunity pair which induces both bacterial intoxication and recovery when expressed in *E. coli* BL21.	231
Figure 4.23: Liquid growth assays confirm CdiAI^{00510} and CdiAI^{32790} are functional toxin-immunity pairs.	232
Figure 4.24: Area under the curve parameters calculated from toxin-immunity expression assay growth rates show significant reduction in area during toxin induction when expressed.	233
Figure 4.25: Doubling time calculated from toxin-immunity expression assay growth rates show significant increase during toxin induction when expressed.	234
Figure 4.26: Western blot analysis confirms CDI toxin-immunity modules are expressed upon induction.	235
Figure 4.27: Model of BL21 strains with plasmids encoding the unmatched CdiA and CdiI pairs.	236
Figure 4.28: CdiI^{32790} does not recover from CdiA-CT^{00510} intoxication.	237
Figure 4.29: CdiI^{00510} does not recover from CdiA-CT^{32790} intoxication.	238
Figure 4.30: Protein pull-down confirms CDI toxin-immunity pairs interact via cognate binding.	239
Figure 5.1: Conserved extracellular CdiA-NT regions from *P. aeruginosa* CDI systems.	257
Figure 5.2: Model of *Escherichia coli* BL21 strains with cloned conserved *cdiA* regions from *P. aeruginosa* strain PA14 CDI systems.	258
Figure 5.3: Primers for amplification of PA14 CDI General and System Type 1 conserved regions.	259
Figure 5.4: PCR of CDI System Type 1 and System Type 2 amplified DNA fragments.	259
Figure 5.5: PCR confirms successful insertion System Type 1 and System Type 2 DNA fragments into high efficacy intermediary vector pCRBlunt II-TOPO.	260
Figure 5.6: Sequencing alignment confirming successful construction of pCR Blunt II-TOPO-System Type 1.	260
Figure 5.7: PCR confirms successful insertion System Type 1 and System Type 2 DNA fragments into expression vector pET29a.	261
Figure 5.8: Sequencing alignment confirming successful construction of pET29a-System Type 1.	261
Figure 5.9: GeneArt synthesised vectors with conserved *cdiA* regions from *P. aeruginosa* strain PA14 CDI systems	262
Figure 5.10: PCR confirms successful insertion of codon optimised General and System Type 2 DNA fragments into expression vector pET29a.	263
Figure 5.11: Sequencing alignment confirming successful construction of pET29a-System Type 2.	263
Figure 5.12: Western blot analysis confirms expression of all three CdiA^{Strep} proteins via StrepII tag detection and visualisation using Immobilon HRP substrate peroxidase.	264

Figure 5.13: SDS-PAGE Coomassie stained gel and western blot analysis confirms Strep-Tactin mediated purification of System Type 2 recombinant protein.	266
Figure 5.14: Direct mutagenesis of StrepII tag to His tag.	267
Figure 5.15: Sequencing alignment confirming successful mutagenesis and replacement of StrepII tag to His tag.	267
Figure 5.16: SDS-PAGE Coomassie stained gel and western blot analysis confirms TALON-resin purification of General and System Type 1 recombinant proteins.	268
Figure 5.17: Eurogentec speedy 28-day custom polyclonal antibody service protocol.	270
Figure 5.18: Western blot analysis shows cross-reaction between CdiA regions from final bleed sera.	272
Figure 5.19: Western blot analysis shows cross-reaction occurs between CdiA regions from pre-bleed sera using rabbit antibody detection and visualisation via Immobilon HRP substrate peroxidase.	275
Figure 5.20: Western blot analysis using final-bleed polyclonal antibodies shows no cross-reaction occurs with native CdiA from *P. aeruginosa* strain PA14 that should be absent in the corresponding deletion mutant strains.	277
Figure 5.21: Western blot analysis using adsorbed polyclonal antibodies shows no cross-reaction occurs with native CdiA from *P. aeruginosa* strain PA14 that should be absent in the corresponding deletion mutant strains.	278
Figure 5.22: Tris-Acetate NuPAGE, wet transfer and western blot analysis using adsorbed polyclonal antibodies shows no cross-reaction occurs with native CdiA from *P. aeruginosa* strain PA14 that should be absent in the corresponding deletion mutant strains.	279
Figure 6.1: Swimming motility of *cdiBAI*^{00510} and *cdiBAI*^{32790} whole system deletion mutants in the background strains.	294
Figure 6.2: Deletion of *cdiBAI*^{00510} and *cdiBAI*^{32790} has no effect on swimming motility.	295
Figure 6.3: Swarming motility of *cdiBAI*^{00510} and *cdiBAI*^{32790} whole system deletion mutants in their respective background strains.	296
Figure 6.4: Deletion of *cdiBAI*^{00510} and *cdiBAI*^{32790} has no effect on swarming motility.	297
Figure 6.5: Deletion of *cdiBAI*^{00510} and *cdiBAI*^{32790} has no effect on biofilm biomass production.	300
Figure 6.6: Randomised well format confirms deletion of *cdiBAI*^{00510} and *cdiBAI*^{32790} has no effect on biofilm biomass production.	301
Figure 6.7: Deletion of *cdiBAI*^{00510} in the PA14 backgrounds but not in the *rsmA* backgrounds render prey susceptible to killing by PA14::*lacZ* WT attacker.	304
Figure 6.8: X-gal based competition assays show a role for both CDI systems dependent on the strain background used.	306
Figure 6.9: Deletion of *cdiBAI*^{00510} in the PA14 background and deletion of *cdiBAI*^{000510} and *cdiBAI*^{32790} in the H123 background but not in the *rsmA* and *rsmA*H123 backgrounds render prey susceptible to killing by PA14 WT attacker.	309
Figure 6.10: Deletion of CDI^{00510} in the PA14 and *rsmA* backgrounds and deletion of CDI^{32790} in the H123, *rsmA* and *rsmA*H123 backgrounds enhances PA14 ΔCDI^{00510} ΔCDI^{32790} prey survival.	313
Figure 6.11: Deletion of CDI^{00510} in the PA14 and *rsmA* backgrounds and deletion of CDI^{32790} in the H123, *rsmA* and *rsmA*H123 backgrounds enhances H123 ΔCDI^{00510} ΔCDI^{32790} prey survival.	214
Figure 7.1: RpoN positively regulates the flagellar operon in *P. aeruginosa* strain PA14.	337
Figure 7.2: Deletion of *rpoN* significantly alters expression of T6SS associated genes.	338
Figure 7.3: Sfa2 is essential for expression of H2-T6SS associated genes.	339
Figure 7.4: Flagella gene expression is unaffected by Sfa2.	339
Figure 7.5: Flagella gene expression is unaffected by Sfa3.	340
Figure 7.6: Altered gene expression is observed in 10 genes upon deletion of *sfa3*.	340

Figure 7.7: Deletion of *rsmA* enhances expression of CDI$_{00510}$, CDI$_{32790}$ and TPS$_{61200}$.	343
Figure 7.8: Deletion of *rpoN* reduces expression of CDI$_{00510}$ and CDI$_{32790}$ but increases expression of TPS$_{61200}$.	344
Figure 7.9: Deletion of *rpoN* reduces expression of H2-T6SS but increases expression of H3-T6SS.	346
Figure 7.10: Swimming motility of *sfa2* and *sfa3* deletion mutants.	349
Figure 7.11: Deletion of *rpoN and rsmA* reduces swimming motility, but no effect is observed upon deletion of *sfa2* or *sfa3*.	350
Figure 7.12: Swarming motility of *sfa2* and *sfa3* deletion mutants.	351
Figure 7.13: Deletion of *rpoN and rsmA* reduces swarming motility, but no effect is observed upon deletion of *sfa2* or *sfa3*.	352
Figure 7.14: Deletion of *rpoN* and rsmA significantly alters biofilm formation, but no effect is observed upon deletion of *sfa2* or *sfa3*.	354

List of Tables

Table 2.1: *Pseudomonas* strains and strain background deletion mutant constructs	112
Table 2.2: Components for making 1L of LB broth	117
Table 2.3: Components for making 1L of LB agar	117
Table 2.4: Components for making 1L of VBM X10 stock	117
Table 2.5: Components for making 1L of Vogel-Bonner agar	118
Table 2.6: Components for making 1L of 20% Sucrose agar media	118
Table 2.7: Components for making 1L of 0.1% Crystal Violet solution	118
Table 2.8: Components for making 1L of *Burkholderia cepacia* Selective Agar	118
Table 2.9: Antibiotics used for media and bacterial growth maintenance of vectors	118
Table 2.10: Antibiotics used for media and bacterial growth maintenance of vectors	119
Table 2.11: Oligonucleotides	119
Table 2.12: Online bioinformatics tools used for small ORFs function identification	122
Table 2.13: MEGA settings for phylogenetic analysis from ClustalW toxin sequence alignment	123
Table 2.14: MEGA settings for phylogenetic analysis from ClustalW toxin sequence alignment	124
Table 2.15: PCR components for making 50 µl final volume sample for DNA amplification	126
Table 2.16: PCR components for making 50 µl final volume sample for overlap amplification	126
Table 2.17: PCR cycle step protocol for DNA fragment amplification	126
Table 2.18: Components for making a 50 µl final volume sample for double enzyme digest of mutator fragment or vector DNA	128
Table 2.19: Components for making 20 µl final volume sample for mutator fragment ligation into pKNG	128
Table 2.20: Components for making 6 µl final volume sample for mutator fragment ligation into pCR BluntII-TOPO	130
Table 2.21: PCR components for making 20 µl final volume sample for DNA amplification	131
Table 2.22: PCR cycle step protocol for DNA fragment amplification	131
Table 3.1: Kolaskar values for expression likelihood of immunity ORFs for PA14 and PAO1 CDI systems	164
Table 3.2: Percentage sequence identity of toxins based on bioinformatics software based database hits and UGENE sequence alignments	165

Table 3.3: Percentage sequence identity of region upstream second PTPM compared to Tse6 based on MUSCLE genome alignment	173
Table 3.4: Percentage sequence identity of toxins based on NCBI BLASTp hits and UGENE sequence alignments	175
Table 3.5: T5SS and TPS systems identified by Madeleine Humphrey during PAO1 and PA14 genome searches	185
Table 3.6: Maximum amino acid sequence identity stretches between TpsA found throughout the genome compared to *P. aeruginosa* CdiB	186
Table 5.1: Rabbit identification numbers with immunogen used for sera production	271
Table 5.2: Detection of CDI expected to be observed by final-bleed antibodies	276
Table 7.1: Diguanylate cyclase gene is downregulated upon deletion of RpoN	338
Table 7.2: TPS/CDI systems encoded in *P. aeruginosa* PA14	342
Supplementary 1 (S1): Bioinformatic analysis of annotated CDI system genes in PAO1 and PA14	434
Supplementary 2 (S2): Small ORF bioinformatics analysis	443

1. Introduction

1.1 *Pseudomonas*- from war wounds to the era of genomics

Since Antoni van Leeuwenhoeck first glimpsed the microbial world using his newly invented microscope in 1677 (van Leewenhoeck, 1677), bacteria have captured the fascination of scientists and doctors alike. Deemed 'animalcules' his first foray into the unseen world founded the field of microbiology. Since then many other scientists have been accredited with linking these organisms to human health, most notably Pasteur, Lister and Snow, almost 200 years after their discovery- founding the fields of vaccinology and epidemiology respectively (Lister, Wolter & Hanson, 2009; Tulchinsky, 2018). Koch's further enhancement of culturing techniques and isolation of individual bacteria from both environmental and human samples gave rise to the ability to study bacteria in depth and identify and classify different genera associated with human infection (Opal, 2009).

Pseudomonas spp. was first associated with human infection from the wounds of soldiers by Sédillot in 1850 (Lister, Wolter & Hanson, 2009), where the appearance of a blue/green colour emanated from their bandages, and was later isolated by Carle Gessard in 1882 (Moore & Flaws, 2011). Described by Walter Migula in 1894, *Pseudomonas* spp. was used to encompass bacteria that were gram-negative, aerobic and rod-shaped bacilli which had an observable tail-like appendage at its pole (Moore & Flaws, 2011). This broad definition meant many bacteria isolated from both human infection and the environment were classified as *Pseudomonadaceae* based on Migula's definition, which includes ~800 species in total. Previously considered one of the most complex genera due to its 144 members and 10

subspecies, most members were not well characterised until Stanier *et al.* in 1966 defined the biochemical and physiological properties of the genera, creating the basis for the taxonomic classification of these isolates (Stanier, Palleroni & Doudoroff, 1966; Parte, 2014). Then in 1984, the introduction of 16S rRNA sequencing enabled classification of many of these species into separate genera (Gomila *et al.*, 2015). Further classification using rRNA-DNA hybridisation categorised *Pseudomonas* into the *Gammaproteobacteria* Class, and further stratification has deemed only 31 species as 'true' of the genera (Mulet *et al.*, 2012; Gomila *et al.*, 2015). Whilst the original gram-negative bacilli classification of these species has remained true, many strains have now been categorised into new genera such as *Ralstonia*, *Burkholderia* and *Stentorophomonas* (Anzai *et al.*, 2000; Coenye *et al.*, 2001), and have can be associated with different oxic environments and possessing different motility-associated mechanisms (Alvarez-Ortega & Harwood, 2007; Schwab *et al.*, 2014; Dalsing *et al.*, 2015; Cowley *et al.*, 2015; Seveau *et al.*, 2019). Today, new strains are identified via analysis of four key housekeeping genes: 16S rRNA, *rpoB*, *rpoD*, and *gyrB*, which are utilised in multi-locus sequence analysis during sequencing studies (Tayeb *et al.*, 2015).

Based on these taxonomic, phenotypic and biochemical classifications, *Pseudomonas* spp. are identified as rod-shaped bacilli which are motile, inhabit generally aerobic environments, and are catalase and oxidase positive (Diggle & Whiteley, 2020; Alvarez-Ortega & Harwood, 2007). However, the species within the genera are diverse, inhabiting multiple niches including the environment as well as causing infections in both plants and human hosts (Ambreetha *et al.*, 2022). This is due to their large genomic and metabolic diversity which allows adaptation to a wide range of distinct niches (Stover *et al.*, 2000; Silby *et al.*, 2011; Loper *et al.*, 2012). This makes *Pseudomonas* spp. generally ubiquitous within the environment, and an opportunistic

pathogen in immunocompromised individuals (Thomas *et al.*, 2013; Moradali, Ghods & Rehm, 2017; Alwazzeh *et al.*, 2020; Singh, Montano & Bostick, 2021). Current metagenomics-based strain phylogeny has delineated two clear species: *P. aeruginosa* and *P. chlororaphis*, in addition to four closely linked species: *fluorescens*, *syringae*, *putida* and *stutzeri* (Nikolaidis *et al.*, 2020). *P. putida, P. syringae* and *P. fluorescens* are conduits for studying plant-associated *Pseudomonas* species (Sah, Krishnani & Singh, 2021), whilst *P. aeruginosa* is studied for its extensive links to virulent human pathogenic infections (Diggle & Whiteley, 2020).

1.1.1 Pseudomonas aeruginosa- an adaptable type species

As the genera's type species, *P. aeruginosa* is the most represented and characterised for its association with human infection (Diggle & Whiteley, 2020). First identified as the causative agent of soldier's discoloured bandages and associated as a transferable agent from surgical wounds, this lay the groundwork for Gessard's publication in 1882 (Lister, Wolter & Hanson, 2009). However its role in both acute and chronic infection wasn't outlined until Leonard Freeman determined its role in the wounds of WW1 frontline soldiers (Freeman, 1916). A ubiquitous bacterium, *P. aeruginosa* is highly adaptable to a multitude of niches attributed to its large and mosaic genome (Robinson *et al.*, 2023). A facultative aerobe (Diggle & Whiteley, 2020), it can perform both aerobic and anaerobic respiration. Anaerobic respiration can occur using nitrate as the electron transport chain terminal electron acceptor, enabling it to switch to nitrate-based respiration (Alvarez-Ortega & Harwood, 2007; Higashi, 1960). Anaerobic respiration is also possible due to its fermentative capabilities, utilising arginine as a carbon source- although this is associated with slow growth or bacterial senescence phenotypes (Diggle & Whiteley, 2020).

Whilst the bacterium is associated with the phenotypes outlined above, it is able to utilise >100 carbon sources and survive in minimal media on a single carbon source (Stover *et al.*, 2000). Additionally, it can survive a range of temperatures. Most commonly associated with growth at 37 °C, it can grow from 4 - 42 °C which helps colonisation of various environmental niches such as water and agriculture, as well as the human body (Stover *et al.*, 2000). It has also been linked with utilisation and production of polycyclic aromatic hydrocarbons- broken down for the production of volatile compounds for interbacterial interactions and control of its environment, as well as production of antimicrobial compounds (He *et al.*, 2018; Létoffé *et al.*, 2022; Nolan & Allsopp, 2022). *P. aeruginosa* can be further subcategorised due to its glucose and lactose non-fermenting nature (Qin *et al.*, 2003). Its survival in the environment and the human body means it remains a heavy burden to both human health and industry- particularly due to its inherent resistance to antibiotic treatment and pesticides (Jimenez, 2007; White *et al.*, 2011; Pang *et al.*, 2019; Paz De Oliveira *et al.*, 2021; Li *et al.*, 2022).

The *P. aeruginosa* large genome size of ~5-7 Mbp explains the bacterium's diverse nature (Stover *et al.*, 2000). However, even today the entire genome, its functions, association with bacterial behaviour and roles in infection are not fully elucidated. From research to date, its flexibility is attributed to its complex and specific regulatory networks at the transcriptional, post-transcriptional and post-translational levels which control traits in concert to enable the bacterium's individual and group-mediated response to various environmental stimuli (Moradali, Ghods & Rehm, 2017). This controls its ability to enter, colonise and establish itself within a new niche, frequently predominating said niches. The pangenome, comprising 665 core genes, is open and has an accessory genome highly enriched via horizontal gene transfer.

This reflects the strain's flexibility as a high level of variability is thus observable even on a sub-species level (Freschi *et al.*, 2019; Robinson *et al.*, 2023).

Research into *P. aeruginosa* largely utilises lab-based strains PAO1 and PA14. Other lab strains PAK and PA7 exist, but PA7 is less frequently used as it is more distantly related (Freschi *et al.*, 2018). PAO1 and PA14 are virulent and linked to common genetic backgrounds most frequently associated with human infection in immunocompromised individuals (Grace *et al.*, 2022). Originally isolated from a chronic wound infection in a hospital in Melbourne, Australia in the 1954, PAO1 was the first strain genomically sequenced and is one of the largest sequenced to date at 6.3 Mbp (Chandler *et al.*, 2019). PAO1 is considered moderately virulent with enhanced chloramphenicol resistance and is frequently used as the backbone for genome assembly and phylogenetic analysis of newly identified and sequenced strains (Holloway, 1955; Chandler *et al.*, 2019). PA14, also known as UCBPP-PA14, was isolated from a burn patient in Mercy Hospital, Pennsylvania and stored in the University of California Berkeley Plant Pathology laboratory in 1995. Exhibiting enhanced virulence, this was attributed to the acquisition of additional virulence factors (~800 genes) and its ability to induce a chronic infection phenotype with enhanced biofilm capabilities (Mathee, 2018; Grace *et al.*, 2022). Although these lab strains are the staple in phenotypic and mechanistic elucidation, studies have shown diversification between labs and outlines the reason for disparity between labs (Chandler *et al.*, 2019). Diversification in standard lab strains adds to the argument for the incorporation of clinical isolates in research for their relevance in mechanisms and phenotypes in human infection. Incorporating clinical strains is important for encompassing the high diversity observed at a substrain level. This diversity is owed to *P. aeruginosa* ability to adapt to a highly specific niche in similar environments or within patients

associated with the same medical condition, such as Cystic Fibrosis (CF), found in different countries throughout the world (De Soyza *et al.*, 2013). Sub-strain diversity can be attributed to the presence of genes acquired by horizontal gene transfer such as genomic islands, chromosomal phage insertions, plasmids and transposable elements and indicates its capacity to cause disease is dependent on an abundance of factors culminating in a colonisation event (Fischer *et al.*, 2021; Robinson *et al.*, 2023). Although PA14 has additional genes and is a hypervirulent strain, PAO1 and PA14 strain lineages maintain similar structural and physiological properties (Grace *et al.*, 2022).

1.1.2 Bacterial cell envelopes and what we have learnt since Christian Gram

One of the first classifications assigned to bacteria in 1883 by Christian Gram was based on the structure of the cellular envelope (Bartholomew & Mittwer, 1952), generally classified as either gram positive or negative by dye retention and the architecture of the cell envelope through the presence of certain layers (Figure 1.1) (Silhavy, Kahne & Walker, 2010). Gram-positive bacteria possess an inner membrane (IM), a classical lipid bilayer and a surrounding peptidoglycan layer which is a thick matrix consisting of linked lipoteichoic and teichoic acids that create a mesh-like structure (Erickson, 2021). In contrast, gram-negative bacteria have an additional classic lipid bilayer, the outer membrane (OM), and a thinner peptidoglycan layer between the IM and OM known as the periplasmic space (Leduc *et al.*, 1989). These two structural variants were originally classified via the Gram stain technique which utilises crystal violet, where fixation of the colour via the use of iodine and maintenance of the colour during the decolourisation step indicates a gram-positive bacteria. Whereas upon the decolourisation step, gram-negative bacteria do not retain the stain due to the disintegration

of the OM from the decolourisation solvent and instead counter strain red via safranin (O'Toole, 2016).

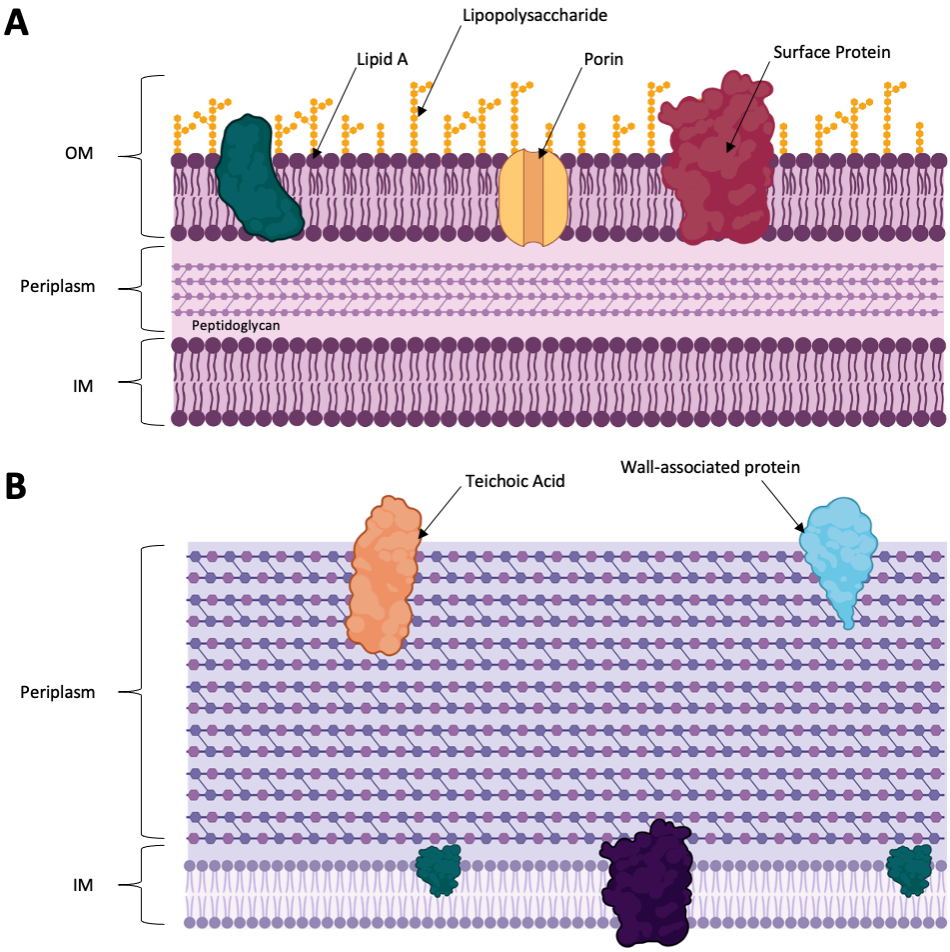


Figure 1.1: Bacterial cell envelopes. Diagram showing the bacterial cell envelopes of the two broad classifications of bacteria. (A) Gram-negative bacteria have three membranes, inner membrane (IM) classical lipid bilayer, peptidoglycan layer within the periplasmic space, finally the outer membrane (OM) lipid bilayer. The OM differs from the IM due to differences in the phospholipids in the outer leaflet of the membrane. Additional proteins and lipopolysaccharides are attached to the membrane here. (B) Gram-positive bacteria have two membranes, the IM classical lipid bilayer and a thick layer of peptidoglycan surrounding the IM.

As a gram-negative bacteria, *P. aeruginosa* possesses two membrane layers which play a role in its etiology as it determines the possession of various structures involved in bacterial phenotype and sensing the environment (Kimkes & Heinemann, 2019). The inner membrane fundamentally acts to compartmentalise the cytoplasm. It is important in the generation of the proton motive force, export of proteins from their internal site of assembly and production of membrane-associated lipids (Benarroch & Asally, 2020; Kaushik, He & Dalbey, 2022). This membrane is symmetrical and comprised of glycerophospholipids with

hydrophilic head groups and hydrophobic tail groups. IM enables diffusion as it is semi-permeable (Miller & Salama, 2018).

The peptidoglycan layer found within the periplasmic space is a major component of cellular structural integrity (Typas *et al.*, 2012). Consisting of a cross-linked mesh formed of strands of glycans and short peptides, it enables survival from turgor stresses (Figure 1.1). Cross links in gram-negative bacteria utilise the glycan pentapeptide chain, comprised of the L-alanine, D-glutamate, mDAP and D-alanine subunits, where D-glutamine and mDAP create isopeptide links crucial to the formation of the peptidoglycan structure (Schleifer & Kandler, 1972). Peptidoglycan is an essential component in the cell cycle enabling division via elongation and initiation of septa and is the defining structure for cell classification and shape (Kuru *et al.*, 2012). The presence of multiple enzymes enables expansion and contraction of the membrane for division and can be tethered to the OM via covalently linked Braun's proteins (Garde, Chodisetti & Reddy, 2021).

The OM is an asymmetric lipid bilayer that is the distinguishing feature of a gram negative cell envelope. It consists of multiple embedded lipids and differs between the inner and outer leaflets (Figure 1.1). The most notable difference between leaflets and a defining feature in the barrier protection function of the OM, is the presence of lipopolysaccharides (LPS) on the outer leaflet. LPS are long chains comprised of a glucosamine disaccharide, several acyl chains, a polysaccharide core and an extended chain 'tail' known as the O-antigen (King *et al.*, 2009). These LPS are tightly packed and create a charge across the cell surface from the presence of negatively charged phosphate groups and cations such as Mg^{2+}. This prevents diffusion of hydrophobic molecules into the cell and export of hydrophilic molecules >700 kDa

(Nikaido & Vaara, 1985). The large size of LPS creates a greatly antigenic molecule, and is frequently modified, most commonly at the O-antigen site, as a way to subvert the host immune system- a crucial tactic utilised by pathogenic bacteria during infection.

Both membranes in gram-negative bacteria require membrane-bound proteins to necessitate the export of various molecules and proteins. They somewhat connect via membrane spanning protein complexes, such as secretion systems and motility-associated structures such as the flagellar motor complex (Thomas, Morgan & DeRosier, 2001; Durand *et al.*, 2015). This enables the bacteria to sense and interact with its environment, often pertaining to a cascade first encountered at the OM, leading through to the cytosol where a gene-related response is initiated. Due to the complex nature of the cell envelope, multiple mechanisms are utilised in the export of proteins across or the situation of proteins within the membranes.

Proteins are most commonly targeted to the IM via Sec, Tat and lipoprotein signal peptides (Kaushik, He & Dalbey, 2022). Signal peptides are a string of amino acids recognised by various cytosolic chaperone proteins to target polypeptides to the IM where they are either inserted or translocated across. Periplasmic chaperone proteins bind to prevent premature folding whilst transporting polypeptides to their translocation machinery (e.g. SurA/Skp see Figure 1.2) (Hoffmann, Bukau & Kramer, 2010; Bruel & Genevaux, 2014). Sec is the most common pathway for protein export which utilises the Sec machinery for translocating unfolded proteins to the periplasm. SecB binds the signal sequence, handed over from the chaperone protein, maintaining the protein in an unfolded state. SecB interacts with ATPase SecA which guides the peptide through the SecYEG channel in an ATP-dependent manner (Randall & Hardy, 2002; Zimmer, Nam & Rapoport, 2008). Alternatively an additional protein SRP is

utilised for proteins bound for IM insertion which binds the nascent sequence at the ribosome, targeting the FtsY docking protein which delivers the complex to the SecYEG channel. The transmembrane portion of the nascent protein then inserts through a pore in the SecYEG channel (Bernstein, 2000).

OM transport commonly targets proteins to the β-barrel assembly or BAM complex, which employs a β-barrel to insert proteins laterally into the membrane (Figure 1.2) (Hagan, Silhavy & Kahne, 2011). Comprised of the BamA protein and BamBCDE accessory lipoproteins, its utilisation is essential for cell viability due to its role in the insertion of crucial membrane proteins such as the LPS export complex and porins. BamAD are crucial to cell survival whereas BamBCE are utilised for insertion of subsets of OM proteins (Buchanan, Botos & Noinaj, 2017). This inherent lethality encountered upon deletion of BamAD has hindered research and the exact insertion mechanism remains unknown. However, prevailing theories indicate either a BamA-assisted mechanism where the BAM complex recruits chaperone-OM protein complexes and insertion occurs through localised membrane destabilisation (Gessmann *et al.*, 2014). Alternatively insertion may occur via chaperone-OM proteins delivery to BAM, where a BamA-OM protein intermediate forms before budding into the membrane via lateral opening and conformational change of BamA occurs. This second theory has more evidence from *in vitro* data obtained indicating BamA undergoes conformational changes, switching from outward open to inward open states which enable the complex to open laterally in the membrane (Iadanza *et al.*, 2016). This is a crucial process in OM insertion and protein targeting and plays a role in the presentation of virulence related structures on the cell surface.

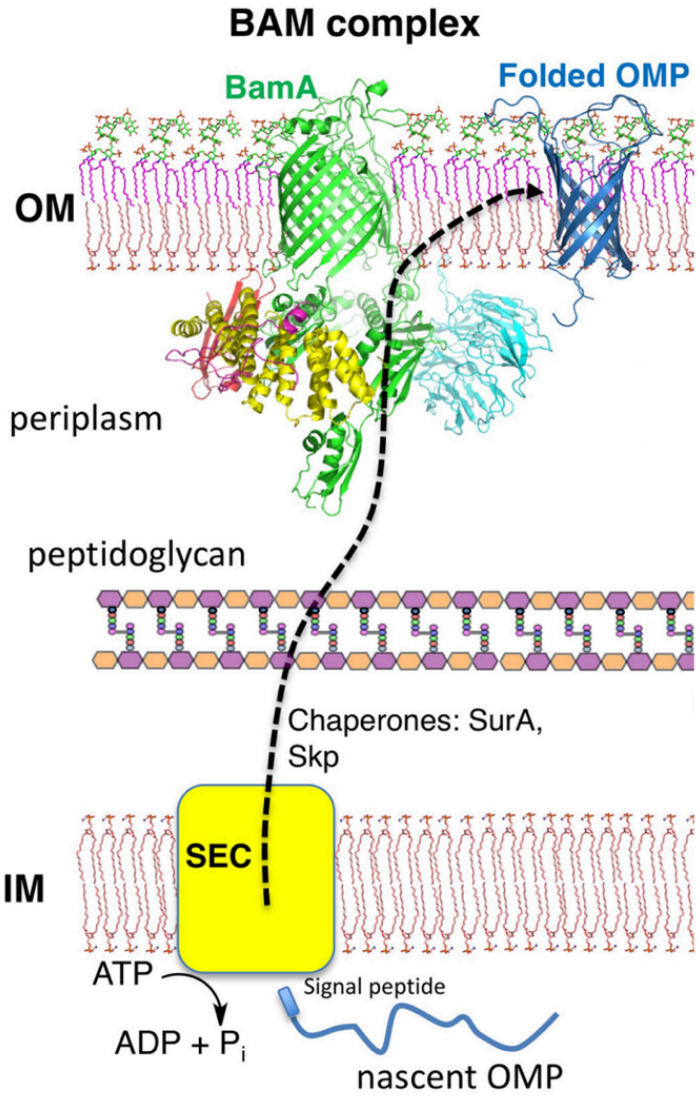


Figure 1.2: Sec and BAM complex translocation machinery. Insertion of a protein into the outer membrane occurs via movement of nascent protein through the IM SecYEG translocon before targeting to the BAM complex where it is inserted into the membrane in its mature form. Figure adapted from (Robinson, 2019).

1.1.2 P. aeruginosa pathogenesis- the perfect opportunistic pathogen

P. aeruginosa infections generally occur in patients who are somehow immunocompromised such as those with wounds, burns or genetic conditions resulting in impaired host defence such as Cystic Fibrosis (CF) (Moradali, Ghods & Rehm, 2017). It is a frequent nosocomial infection due to the bacterium's ubiquitous nature and association with the colonisation of medical devices such as urinary catheters and respirators (Cole *et al.*, 2014; Tsay *et al.*, 2016). As this infection does not establish in individuals with no underlying health conditions, *P. aeruginosa* is considered 'opportunistic' pertaining to its establishment in individuals after a host perturbation event. Whilst most infections are acute and later resolved, chronic infection can occur, most commonly in the lungs of patients with CF (Moradali, Ghods & Rehm, 2017). Due to its large genome and ability to survive in diverse

environmental niches, it exhibits both inherent and acquired antibiotic resistance. As such, heavy use of antibiotics in chronic infections has enhanced antimicrobial resistance (AMR) making them impossible to eradicate and creating an incredibly successful pathogen (Perikleous *et al.*, 2023). For this reason, in 2017 the World Health Organisation (WHO) listed *P. aeruginosa* on its 'critical pathogen' list due to its resistance to last line defence antibiotics-carbapenems (WHO, 2017). This highlights the threat to public health *P. aeruginosa* poses and as such requires the development of new treatments. However, much is still unknown about the exact mechanisms of *P. aeruginosa* infection which enables it to be so successful in comparison to other pathogens. So why is *P. aeruginosa* so persistent?

P. aeruginosa encodes multiple mechanisms and factors that make it successful in colonisation, dominance, and chronic survival within hosts. Virulence is multifactorial and therefore pathogenesis is attributed to a combination of mechanisms such as those utilised for the export of multiple bioactive molecules, proteins, and polysaccharides. Many of these exports play crucial roles at various infection stages and provide *P. aeruginosa* with selective advantages. These mechanisms encompass functions such as motility via flagella and pili, biofilm production, LPS and adhesins production, as well as competitive systems such as secretion systems which make it highly versatile in its responses to environmental stimuli. These mechanisms combined with its inherent antibiotic resistance play crucial roles from early to chronic infection stages through the mediation of host-pathogen and pathogen-pathogen interactions and subversions which drive infection pathology. I will further discuss these mechanisms in more depth in sections 1.3- 1.7 of this thesis.

As a new antibiotic has not been discovered for decades (Hutchings, Truman & Wilkinson, 2019), alternate treatments are required for bacterial eradication. Targeting virulence mechanisms such as quorum sensing (QS), biofilm formation and secretion systems through novel therapies could be used in combination with antibiotics to make more effective treatment regimens. This could result in elimination of infection via breakdown of its protective mechanisms. So far this has been successful for penicillin resistant pathogens through the dual use of clavulanic acid and amoxicillin. Clavulanic acid binds to penicillinases to allow amoxicillin to reach the peptidoglycan and shows scope for similar treatments to be developed in the future (Ribeiro Da Cunha, Fonseca & Calado, 2019). A further barrier to treatment to date is the presence of the biofilm which protects the bacteria from desiccation and attack via antimicrobial compounds and host defences through reduced penetration and lowering of cellular metabolic rates (Sharma, Misba & Khan, 2019). This is particularly prevalent in chronically established *P. aeruginosa* infection and is the reason eradication of infections in patients with CF is so difficult. CF airway physiology provides an environment conducive to chronic infection establishment. Therefore, understanding host and pathogen factors to discern host-pathogen interplay in CF patients through the utilisation of its various virulence mechanisms is required (Bhagirath *et al.*, 2016).

1.2 Cystic Fibrosis and polymicrobial communities- a tale as old as time

Cystic fibrosis is a condition that has afflicted humanity for thousands of years but has only started to be understood within the last century (Farrell *et al.*, 2018). Today ~1:2500 babies are born in the UK with CF annually and is frequently recognised within the Caucasian population (Scotet *et al.*, 2012). However, observed CF frequency in populations from the

Indian subcontinent and Afro-Caribbean lineages is increasing due to better disease surveillance (McCormick *et al.*, 2002). The name cystic fibrosis was first coined by Dr Dorothy Andersen who identified mucus plugging in the glandular ducts of the pancreas in children (Andersen, 1938). This initial classification as a severe celiac disease was observed at a later date to be associated with malabsorption and stunted growth, labelled a 'generalised exocrinopathy' (Farber, Shwachman & Maddock, 1943; di Sant'agnese, 1956). It was not initially linked to pulmonary infections due to the patient's lifespan which often did not stretch beyond the early childhood years. Pulmonary infection was therefore thought to be the end point from a vulnerability induced by insufficient nutritional uptake. It was not until other problems such as salt and water loss in children in New York during the 1948 heatwave was linked to the condition that the understanding of the systemic effect of CF was realised (di Sant'agnese *et al.*, 1953). From this point, with the development of the 'sweat test', CF was better diagnosed and treated which has been further enhanced in the decades since.

1.2.1 The original genetic condition, from salty sweat to CFTR

The underlying cause of CF is a mutation in the CFTR gene, which produces a membrane bound gated ion channel that enables the movement of chloride and bicarbonate ions across epithelial cells in an ATP-dependent manner (Veit *et al.*, 2016). The CFTR gene is located on chromosome seven (Newmark, 1985), where mutations cause protein misfolding leading to dysfunction of the CFTR protein that disrupts the movement of anions across epithelial cells (Figure 1.3). A member of the ATP-binding cassette (ABC) superfamily, the wild type protein is activated in an cAMP-dependent manner that enables ATP to bind, resulting in the opening of the channel in a stable state (Riordan *et al.*, 1989). Subsequent hydrolysis results in the

channel closing, which occurs in a cycle resulting in multiple opening and closing events allowing salt ions through (Carson, Travis & Welsh, 1995). As CFTR regulates the amiloride sensitive sodium channel in an inhibitory fashion, mutations in CFTR also result in a linked dysregulation of sodium ions and increased absorption into the airways (Ismailov *et al.*, 1996; Mall *et al.*, 1996), where thick dehydrated mucus forms on the apical epithelial cell surface.

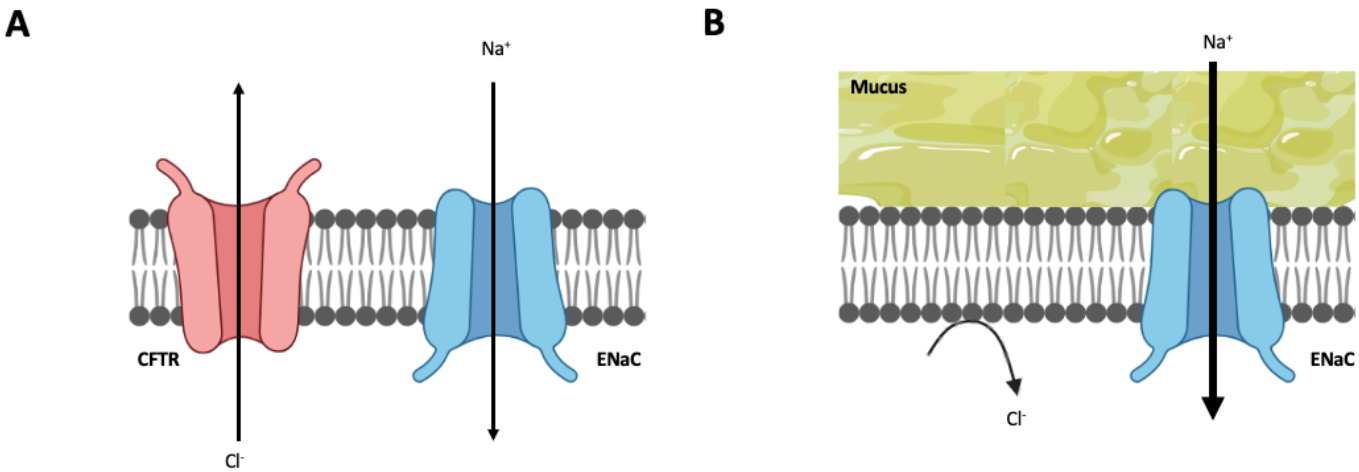
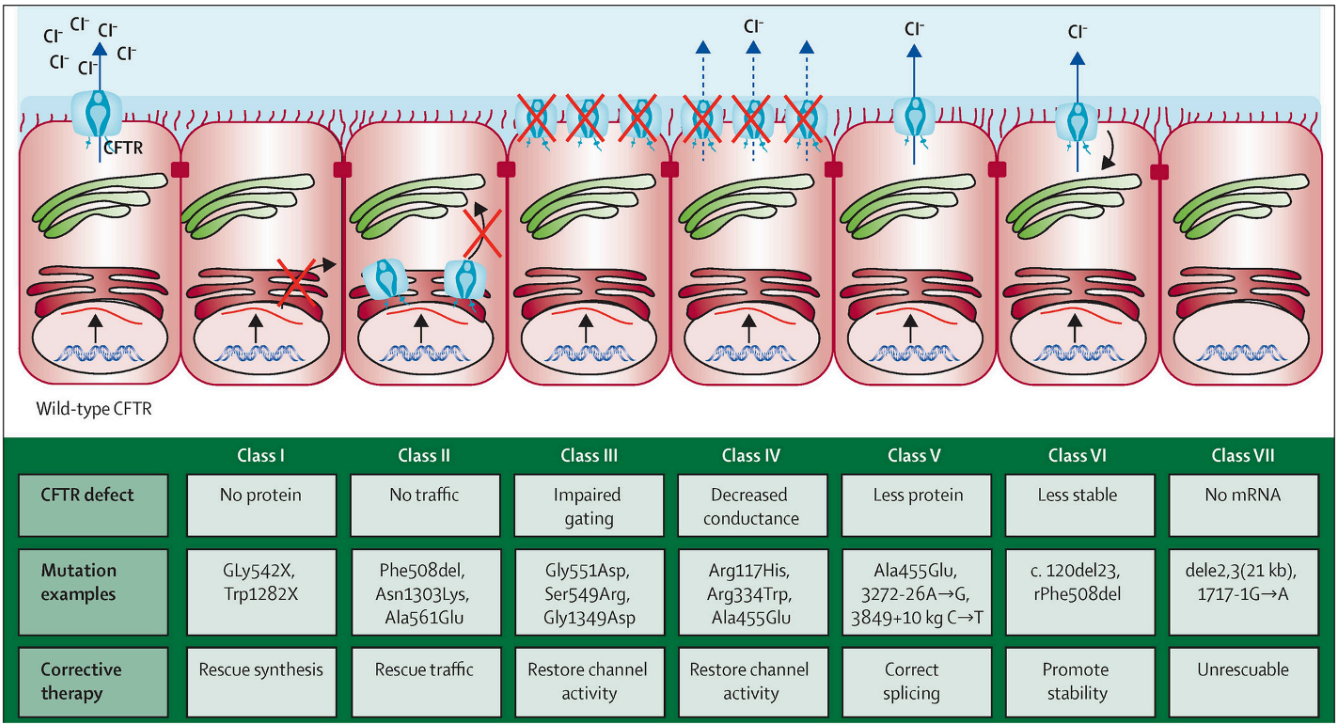


Figure 1.3: Ion dysregulation in epithelial cells with CFTR functional mutation. (A) Normal cell chloride and sodium ion movement across epithelial membrane, (B) CF cell chloride and ion movement across epithelial membrane in the absence of CFTR due to mutation. Dysregulation occurs when CFTR mutation disrupts flow of chloride ions through the epithelia. The lack of chloride ion secretion and excessive sodium absorption which, via osmotic forces, bring water paracellularly and dehydrate the airway surface.

CF was first linked to chloride and sodium ion dysregulation in epithelia in 1983 (Quinton, 1983), but it wasn't until 1989 Dr. Lap-Chee Tsui and his team were able to discover the gene (Tsui & Dorfman, 2013). It was the first condition linked to genetic material and was one of the first significant breakthroughs in human genomics. A recessive condition, requiring the acquisition of two mutated CFTR genes, the variation in genetic mutations varies greatly with ~2000 mutations identified to date resulting in a combination that leads to disease (Castellani *et al.*, 2008). Certain mutations are found in a large proportion of patients with the condition

such as F508del (Kerem *et al.*, 1989), whereas at the other end of the scale, some mutations are so rare they can be linked to a single family or individual (Castellani *et al.*, 2008). The many mutations identified result in multiple types of dysfunction within the protein and are categorised into seven classes based on their phenotype, which range from complete absence of the protein from the introduction of premature stop codons to decreased opening of ion channels (Figure 1.4). CF is proposed to be a mutation which arose from human evolution against the pathogen *Vibrio cholerae*, where cholera toxin activates the cystic fibrosis conductance regulator (CFTR). In addition, CF is particularly prevalent in populations associated with regions of endemic cholera outbreaks, and is considered one of the most commonly inherited genetic conditions (Azimi, 2015).



	Class I	Class II	Class III	Class IV	Class V	Class VI	Class VII
CFTR defect	No protein	No traffic	Impaired gating	Decreased conductance	Less protein	Less stable	No mRNA
Mutation examples	GLy542X, Trp1282X	Phe508del, Asn1303Lys, Ala561Glu	Gly551Asp, Ser549Arg, Gly1349Asp	Arg117His, Arg334Trp, Ala455Glu	Ala455Glu, 3272-26A→G, 3849+10 kg C→T	c. 120del23, rPhe508del	dele2,3(21 kb), 1717-1G→A
Corrective therapy	Rescue synthesis	Rescue traffic	Restore channel activity	Restore channel activity	Correct splicing	Promote stability	Unrescuable

Figure 1.4: Classes of CFTR mutations which result in cystic fibrosis manifestation. Seven classes of CF gene mutations exist which results in multiple ways for CF presentation in the clinic. Figure reproduced from (De Boeck, 2020).

CF is a multisystem condition, however initial diagnoses were made through an association with highly salty sweat due to this chloride and sodium ion dysregulation (di Sant'agnese *et al.*, 1953). This was found to be a hallmark of the condition and was utilised in the development of the first diagnostic test utilised by Gibson and Cooke called the Quantitative Pilocarpine Iontophoresis Test (Gibson & Cooke, 1959), more commonly known as the 'sweat test'. CF patients have abnormally high levels of sodium and chloride in their sweat where they fail to reabsorb ≥ 60 mmol/L compared to the norm which is < 30 mmol/L (Davis & Di Sant'Agnese, 1984; Farrell *et al.*, 2017). This level is often used as a biomarker of CFTR function and correlates to gene mutation severity. This test is highly specific to CF as few conditions exhibit elevated salt levels in sweat. Not all patients with CF have pancreatic insufficiency, therefore patient discrimination from high salt levels in sweat was and is even able to identify patients with milder clinical presentations of the condition. Although this test is still utilised in clinics today, most diagnoses are through the newborn screening programme which uses blood to test for commonly inherited conditions such as CF (Schlüter *et al.*, 2019).

Now it is understood CF also affects the intestines, liver and reproductive systems outlining the full systemic impact of the condition, and specialist CF centres have multidisciplinary clinical teams dedicated to understanding and treating each facet of the health of each individual patient. Patients have a range of symptoms that require management which can differ between individuals. Alongside the pancreatic dysregulation due to the organ's mucus-blocked ducts and fibrosis, patients can also frequently exhibit CF-associated diabetes, liver cirrhosis, bowel obstruction as well as infertility and pulmonary infection which all require specialist doctors for each facet of the condition (Davies, Alton & Bush, 2007).

1.2.2 CF lung physiology and pulmonary infections

The build-up of the viscous dehydrated mucus is particularly pronounced in the airways, which provides an environment for microbial colonisation. This is the most commonly associated physiological repercussion of the condition, where the presence of thick mucus due to CFTR dysregulation builds up in the lungs and becomes difficult to remove (Weiser *et al.*, 2022). Reduced cilial movement due to thick mucus prevents natural removal of infectious agents allowing bacteria to take hold of the lung environment (Chioccioli *et al.*, 2019). Additionally, dysregulation in CF macrophages indicates impaired immune clearance likely plays a role in the persistence of lung infections (Di *et al.*, 2006; del Porto *et al.*, 2011; Simonin-Le Jeune *et al.*, 2013; Assani *et al.*, 2017).

Microbial infection remains the largest burden to CF lung health and is directly linked to progressive decreases in lung function- the largest contributing factor to morbidity and mortality in patients (Durda-Masny *et al.*, 2021). The combination of impaired mucociliary clearance and microbial colonisation induces a pro-inflammatory environment (Cohen-Cymberknoh *et al.*, 2013). This is supported by evidence that shows an inability to effectively clear infections due to sequestered immune cells such as macrophages encoding deficient CFTR which further allow persistence of infection due to defects in phagocytosis and oxidative burst (Di *et al.*, 2006; del Porto *et al.*, 2011; Simonin-Le Jeune *et al.*, 2013; Assani *et al.*, 2017). This enhances lung damage in a cycle which leads to the development of bronchiectasis and eventual irreversible respiratory failure (Cantin *et al.*, 2015). Many patients reaching this stage require a double lung transplant which is at great risk to the individual where the survival rate 5 years post-operation is ~50% (Lynch *et al.*, 2015).

This build-up of mucus creates an environment conducive to bacterial growth due to the high humidity and warm conditions within the lungs (McFadden *et al.*, 1985; Khosravi *et al.*, 2021) which provides both aerobic and anaerobic niches based on mucus plugging commonly found in the bronchioles (Mall, Danahay & Boucher, 2018). Due to these favourable environments, a diverse range of bacteria, fungi and viruses can chronically infect a patient's lungs (Figure 1.5). From a bacterial perspective, both gram positive and negative organisms with both aerobic and anaerobic tolerances can establish themselves within the lungs. This creates a polymicrobial community specific to each individual based on microbes found within their immediate environment (Jean-Pierre *et al.*, 2021). This presents a great challenge for understanding these communities and providing treatments as microbe-microbe and microbe-host interactions are not fully elucidated in this condition. As a result of enhanced antibiotic regimens, today bacterial infections of common pathogens associated with the condition are managed more effectively. However this enables rare and less understood bacterial pathogens to increase in prevalence in these patients (Hatziagorou *et al.*, 2020).

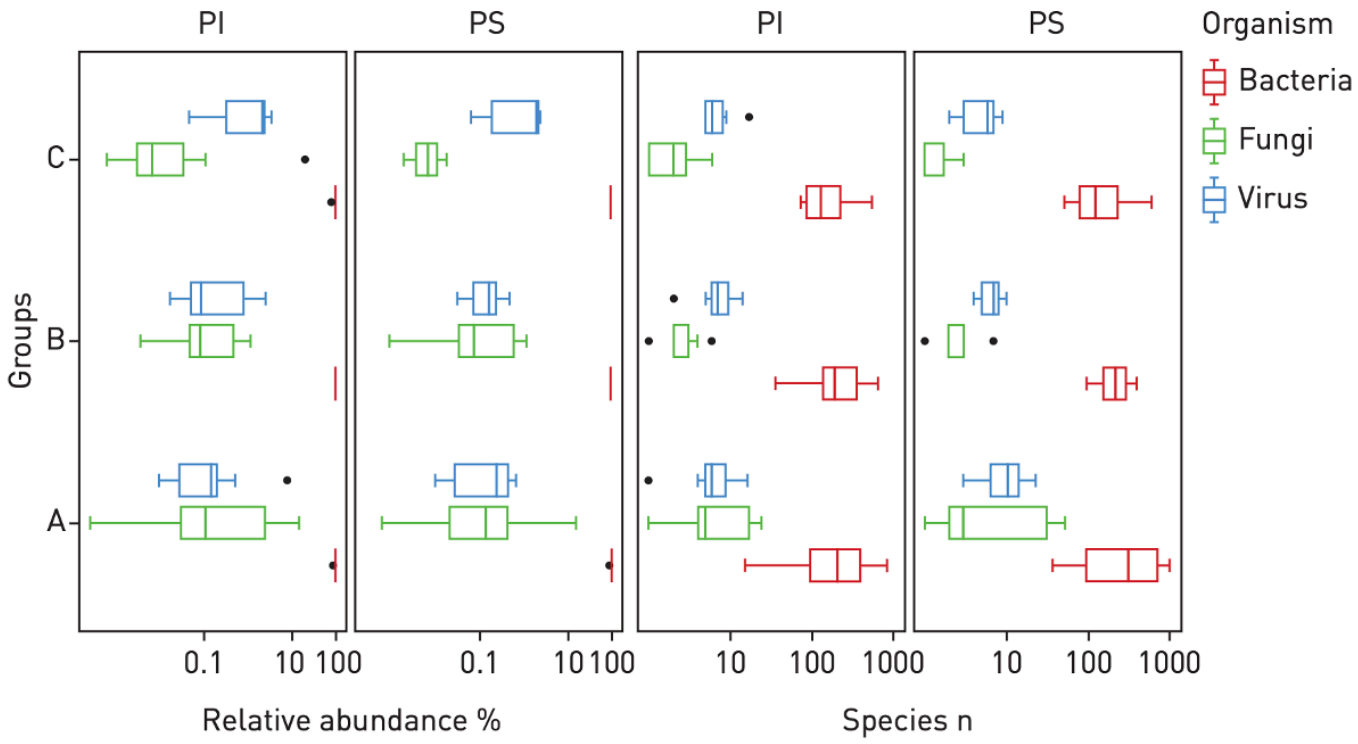


Figure 1.5: Lower airway metagenome of cystic fibrosis patients. (A) Children with CF, (B) Adolescents with CF, (C) Adults with CF. Metagenome sequencing of various CF patient age groups shows abundance and species number from lower airways. Patients were split into pancreatic insufficient (PI) and pancreatic sufficient groups (PS). Figure reproduced from (Losada *et al.*, 2016).

Generally, multiple acute infection events occur in childhood before an individual infection event leads to the induction of chronic colonisation. This is generally associated with *Staphylococcus aureus* which is most common in early childhood, whilst during the teenage and adult years *P. aeruginosa* is responsible for the largest proportion of infections in the CF population (Figure 1.6) (Schaffer, 2015). Chronic *P. aeruginosa* is associated with enhanced lung function decline. Its dominance of the lung and chronic infection progression has an observable reduction in the polymicrobial community diversity (Coburn *et al.*, 2015; Flight *et al.*, 2015; Cuthbertson *et al.*, 2020). However the exact mechanism of this dominance is currently unknown. Outbreak strains such as Liverpool Epidemic (LES) and adaptation to the

lung promotes strain succession during chronic infection where different *P. aeruginosa* strains can be isolated from an individual patient (Khanolkar *et al.*, 2020).

Multiple pathogens besides *P. aeruginosa* and *S. aureus* are frequently associated with CF pulmonary infection such as *Stenotrophomonas, Achromobacter* and *Haemophilus*. However, other pathogens such as *Burkholderia* and non-tuberculous *Mycobacteria* cause more aggressive infections (Parkins & Floto, 2015; Salsgiver *et al.*, 2016). They may in some cases replace *P. aeruginosa* (Sanguinetti *et al.*, 2001; Schwab *et al.*, 2014), and certain *Burkholderia* infections are extremely severe leading to pulmonary necrosis observed in 'cepacia syndrome' (Daccò *et al.*, 2023). Due to poorer prognosis observed with some of these pathogens, patients may no longer be eligible for lung transplantation as a result (Leard *et al.*, 2021). This provides a challenge for effective treatment and better health outcomes and presents a real burden on patient life expectancy and quality of life.

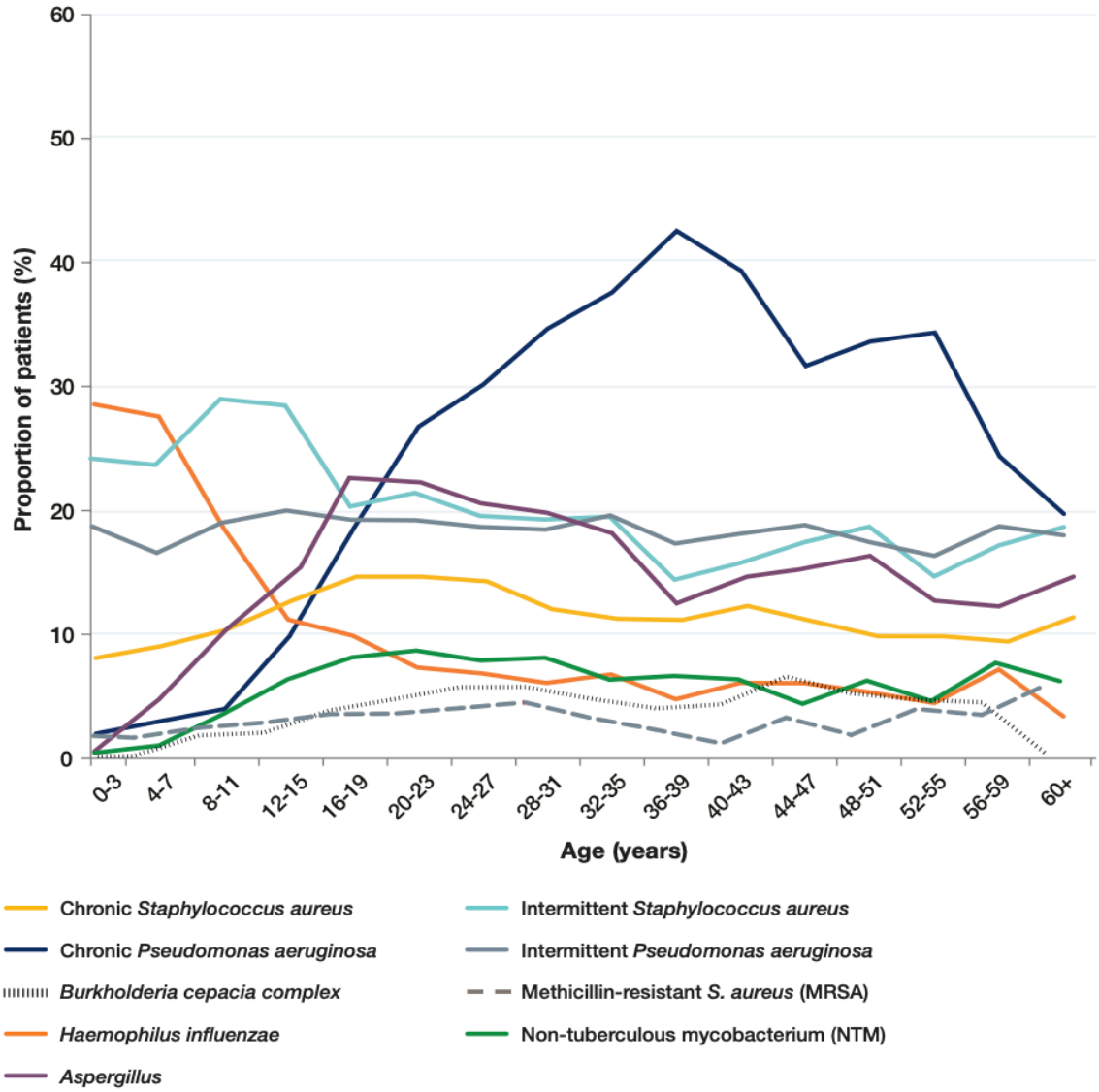


Figure 1.6: Prevalence of infection by various pathogens in cystic fibrosis patients compared with age. *P. aeruginosa* pertains highest prevalence and overtakes *S. aureus* throughout the teenage and adult years. Figure reproduced from the UK CF Registry annual data report 2020.

1.2.3 Polymicrobial communities and controlling pathogens

The era of genomics has allowed us to understand the complex diversity of polymicrobial communities and enabled the identification of previously unobserved genera associated with pulmonary infection, particularly those that are non-culturable. This is especially relevant to anaerobic bacteria such as *Prevotella, Porphyromonas and Veillonella* which confer a large

proportion of polymicrobial communities observed in patient microbiomes to date (Figure 1. 7) (Huang & LiPuma, 2016; Losada *et al.*, 2016). Increased diversity has been associated with better patient health outcomes, whilst reduced diversity and pathogen dominance is associated with worse outcomes and increased frequency of exacerbations.

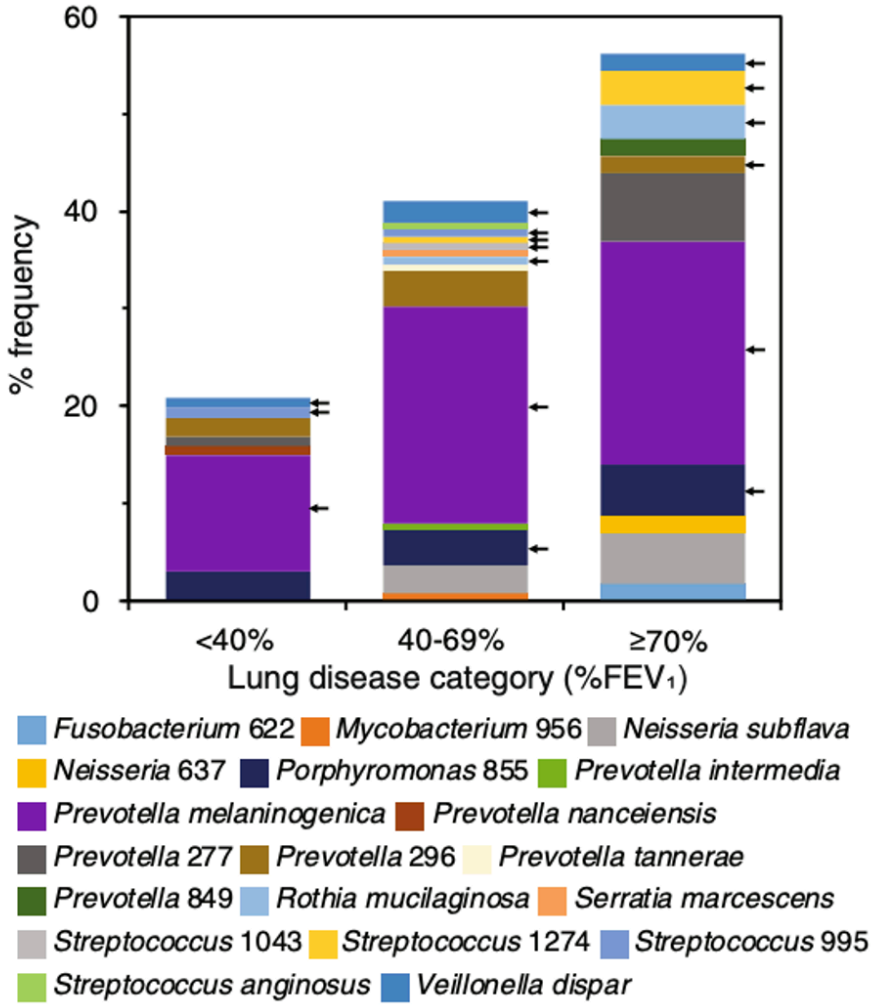


Figure 1.7: Metagenomic sequencing identification of other bacterial species associated with cystic fibrosis.

Bacteria associated with lung disease severity category. Figure adapted from (Cuthbertson *et al.*, 2020).

Exacerbations are defined as episodes of the patient feeling unwell, exhibiting worsened respiratory symptoms and decreased lung function (Gibson, Burns & Ramsey, 2003; Goss & Burns, 2007). An associated increase in airway inflammation which further damages the lungs occurs (Stanford, Dave & Simmonds, 2021). Patients are treated with high-dose oral or

intravenous antibiotics to limit any damage caused and manage symptoms, however 25% of patients do not recover their baseline lung function post-exacerbation (Sanders *et al.*, 2010). Although the link between worse patient outcomes and reduced community diversity has been found (Flight *et al.*, 2015; Cuthbertson *et al.*, 2020), the changes to community dynamics during exacerbation periods remains largely unknown. Furthermore, the exact mechanisms of exacerbation induction remain elusive; they may be due to influx of a new pathogen, particularly a virus, upsetting the community balance or dissemination of a previously established pathogen into a new niche within the lungs (Stanford, Dave & Simmonds, 2021).

The acquisition of new pathogens is particularly dangerous between patients where cross infection of more aggressive strains or pathogens can result in outcompeting the current dominant strain or organism and enhancing the rate of lung function decline. This is a major concern in clinical environments as the risk posed by cross-infection has led to changed clinical practice where patients are not allowed to mix (Conway, 2008).

Infection in people with CF is driven by an individual pathogen that ultimately predominates their pulmonary microbiota (Thornton *et al.*, 2022). To do this, bacteria must compete with the other residents of the microbiota for food, nutrients, and space, as well as evading hostile host responses such as the immune system to effectively colonise the niche. Frequently, these pathogens are associated with reduced community diversity, particularly observable in *P. aeruginosa* infection (Flight *et al.*, 2015; Cuthbertson *et al.*, 2020). This is in part due to the arsenal of virulence factors encoded which provide the pathogen with a selective advantage but also their ability to survive. Some of the mechanisms linked to enhanced pathogenesis to date include the production of biofilm, ability to move in a coordinated group mediated

response known as swarming (Liao *et al.*, 2022), utilisation of various secretion systems which mediate microbe-environment, microbe-microbe and host-microbe interactions (Green & Mecsas, 2016; Armbruster *et al.*, 2020), as well as the secretion of molecules such as homoserine lactone (HSL) and pyocyanin in QS and toxicity respectively (Jurado-Martín, Sainz-Mejías & McClean, 2021). These all influence pathogen fitness and ability to colonise which produces the effect observed in clinic. However, the mechanisms of pathogen dominance remain unknown and provides much scope for further research. This is important in understanding the establishment of these infections which will inform future treatments and may provide new targets for the development of novel therapies, particularly against highly conserved mechanisms such as secretion systems and biofilm formation.

Today, the future is looking much brighter for CF patients. Research has identified and implemented many new treatments which has vastly improved patient quality and length of life. From the realisation of enhance lung health in Australian surfers with CF which led to inhaled saline nebulisation (Elkins & Bye, 2011) to research-identified DNase therapy to help break up extracellular DNA to reduce sputum viscosity and bacterial biofilms to make antibiotic treatments more effective (Novotny *et al.*, 2013), CF patients are now frequently able to manage their conditions effectively when combining medication and physiotherapy. This has radically changed the CF landscape, particularly in recent years, and means that patients are living longer, healthier lives. With newborn screening (Southern *et al.*, 2007) and the introduction of modulator therapies such as Kaftrio to correct CFTR presentation at the cell surface (Condren & Bradshaw, 2013), children born with CF today will have a much better quality of life and may never acquire long term chronic infections. However, for those with established chronic pulmonary infections, modulator therapy treatment has not resolved

their burden on patient health and further research is required in order to eradicate them (Harvey *et al.*, 2022). Additionally, ~10% of CF population are ineligible for the current modulator therapies due to possessing mutation types which cannot be targeted by the current therapies, therefore there is much work yet to be done to enhance the life of all patients with CF.

1.3 Bacterial mechanisms of movement- from flagella based swimming to quorum sensing mediated swarming

When nutrients and space are limited within a niche, bacteria which can move to a new environment ensure their survival by exploiting resources and avoiding host-mediated removal via the immune system. An inherent requirement for most living organisms (Miyata *et al.*, 2020), bacteria have evolved a multitude of mechanisms which can be classified into either free swimming in aqueous solutions or movement over a solid surface and has been an observed trait since the initial discovery of bacteria by Antoni van Leeuwenhoeck (van Leewenhoeck, 1677; Henrichsen, 1972). These systems utilise appendages which move in particular ways to generate force to propel the cell either towards or away from various environmental stimuli. The advancements in microscopy capabilities since the days of Antoni van Leeuwenhoeck have meant that these appendages can be resolved and studied in greater detail, particularly portions of the machinery which sit within the bacterial cell. A recognised virulence factor due to its importance in infection, these systems are often coordinated in conjunction or opposition to other virulence mechanisms such as biofilm production and expression of defence systems such as the secretion systems (Pena *et al.*, 2019).

P. aeruginosa has three movement modalities: swimming, swarming and twitching (Kazmierczak, Schniederberend & Jain, 2015), which have been shown to play an important role, particularly in acute infection (Winstanley, O'Brien & Brockhurst, 2016). However, as these appendages can be large, they create highly immunogenic sites that can be identified by the host immune system. Research has shown these appendages can induce the inflammatory response and phagocytosis of cells in both mouse and human derived macrophages (Amiel *et al.*, 2010). Therefore downregulating these systems is associated with sessile bacterial behaviour which mediates chronic colonisation and is closely linked via the Gac/Rsm pathways to the upregulation of biofilm production known as the motile-sessile switch (Winstanley, O'Brien & Brockhurst, 2016; Li *et al.*, 2017). This motile-sessile switch is achieved by utilising motility appendages to adhere to surfaces and initiate changes in gene expression (O'Toole & Kolter, 1998; Klausen *et al.*, 2003a). This link to pathogenesis, chronic infection and regulation via a global regulator means that motility is often studied as a marker of enhanced or reduced virulence upon manipulation of the bacteria. The Gac/Rsm signal pathway will be discussed further in 1.8 of this chapter.

1.3.1 The flagellar structure and bacterial movement

The flagella is the classical motility appendage discovered in the 17th century by Antoni van Leeuwenhoeck who initially likened them to 'little feet' (van Leewenhoeck, 1677). Today we know it is a intricate multi-protein complex that has inspired the development of nanorobots for future medical applications due to the elegance of this evolved system (Ali *et al.*, 2017). A long whip-like appendage it is utilised for planktonic movement in aqueous environments. Comprised of five subunits and ~25 different proteins: the hook, L-ring, P-ring, MS-ring and

rod, this protein complex spans the entirety of the gram-negative cell envelope and produces a motor complex which is utilised to generate torque through the rod into the hook and through to the filament to generate movement of the cell (Figure 1.8) (Wadhwa & Berg, 2022). The motor is a multiprotein complex with homology to the T3SS and is believed to be the blueprint for the secretion system (Halte & Erhardt, 2021). The stator units embedded in the membrane constitute MotA and MotB which surround the rotor ring and are utilised in force generation. The C-ring is comprised of FliGMN proteins on the cytoplasmic side of the FliF MS-ring and are coupled to the stator units to control directional rotation. The rod is comprised of FliE and FlgBCFG which transfer the rotational force to the filament via the FlgE protein-based hook. The FlgI protein-based P-ring and FlgH protein-based L-ring anchor the rod within the cellular envelope to facilitate the rotation (Tan *et al.*, 2021). Rotation occurs as a single unit where the rotational speed in the C-ring generates that of the hook and filament (Hosu, Nathan & Berg, 2016).

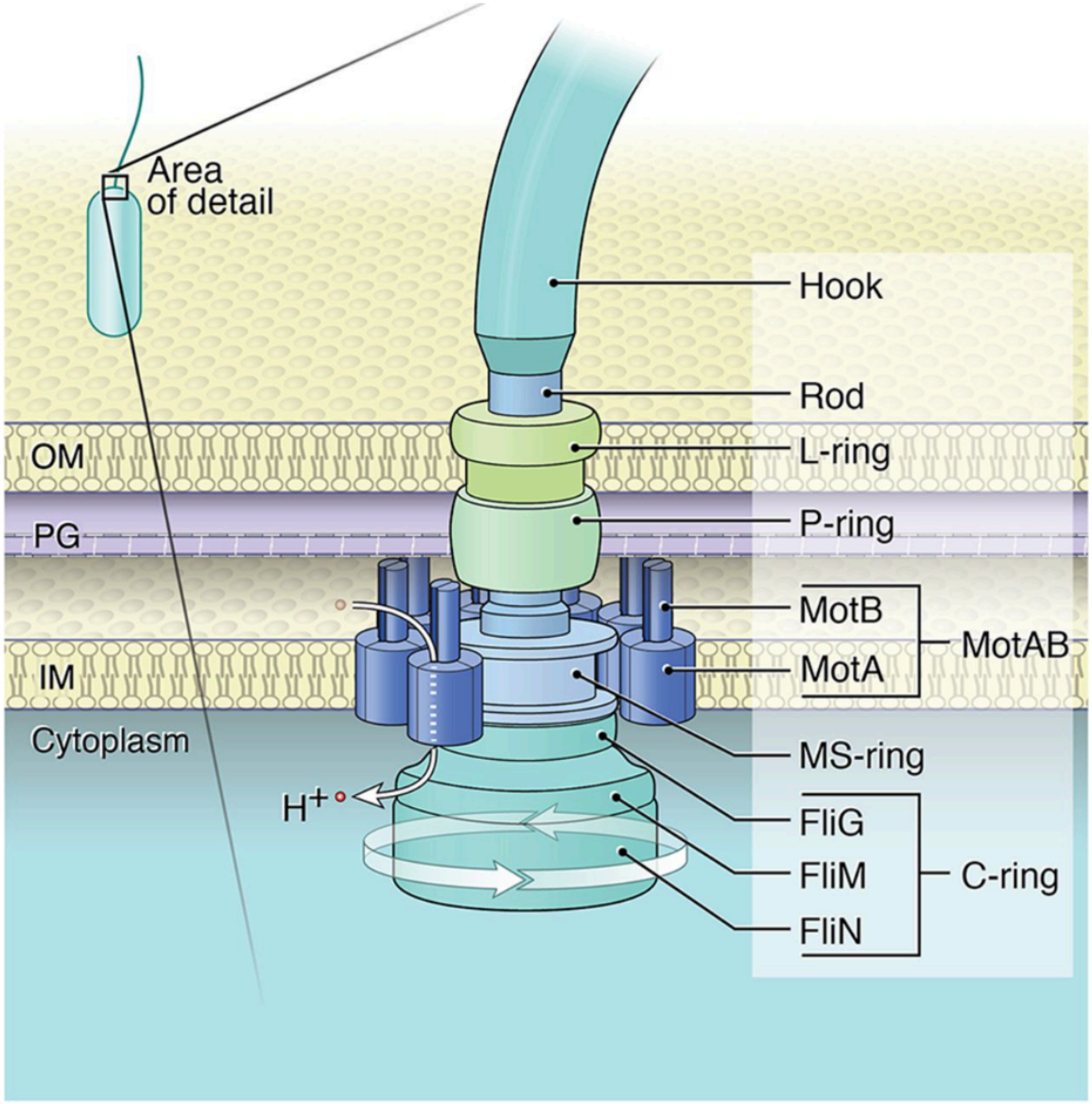


Figure 1.8: The flagellar motor complex. Schematic representation of gram-negative membrane associated flagellar motor complex consisting of the hook, rod, L-, P- and C-ring, and MotAB complex used for initiating flagellar based movement. Figure reproduced from (Baker & O'Toole, 2017).

P. aeruginosa has a single flagellum situated at one pole that is rotated in a helical manner to provide the torque for movement. This torque is generated by the stator proteins MotAB which utilise the proton motive force (pmf) for swimming phenotypes (Toutain, Zegans & O'Toole, 2005). This is driven by a reversible motor system which after the helical rotation of

the filament undergoes a rotary motor switch to dictate the direction cellular movement. During this time momentary reversal of the cell occurs before re-engagement of the motor propels the bacterium forward (Homma *et al.*, 1996). This is determined by CheY protein concentration which diffuses across the cytoplasm once phosphorylated to bind the flagellar motor to induce clockwise spinning, therefore increased concentration results in less 'tumble' events (Brown & Berg, 1974). The flagella is tightly regulated as it is highly energy expensive (Schavemaker & Lynch, 2022).

1.3.2 The group mediated movement response and quorum sensing

Swarming motility is an additional movement phenotype which utilises the flagella, defined as a group-mediated movement over semi-solid media (Henrichsen, 1972) and exhibits patterns generally specific to each bacterial genera. Controlled by the alternative stator units MotCD (Toutain, Zegans & O'Toole, 2005), this mechanism is negatively regulated by the cyclic di-GMP (c-di-GMP) secondary messenger through MotD binding to prevent motility within viscous environments (Kuchma *et al.*, 2015). C-di-GMP itself is regulated via AmrZ which in turn is a regulator of other virulence factors such as T6SS alongside the diguanylate cyclase SadC (Kuchma *et al.*, 2007; Allsopp *et al.*, 2017; Hou *et al.*, 2019). First described in *Proteus* in the 1970s (Williams & Schwarzhoff, 1978) swarming motility has now been reported in multiple genera such as *Escherichia, Vibrio* and *Pseudomonas* (Kohler *et al.*, 2000; Wah Liew *et al.*, 2021). This indicates a conserved mechanism by gram-negative bacteria important in surface exploration for colonisation of a niche and requires a thin layer of liquid to do so (Partridge & Harshey, 2013). The induction of swarming is through various sensed environmental factors but is readily linked to the utilisation of bacterial QS systems. QS utilise

the external expression of molecules such as homo-serine lactone (HSL). Upon reaching a threshold concentration based on the number of cells present, altered gene expression mediates a group response to bring about the swarming phenotype (Reimmann *et al.*, 2002; Zhang *et al.*, 2010). *P. aeruginosa* encodes three QS systems; Rhl, Las and PQS, which integrate to coordinate the expression of various virulence factors and behaviours at the transcriptional and post-transcriptional level such as motility via major alternative sigma factor RpoN and quorum signalling molecules such as 3-oxo-C12-HSL, C4-HSL and PQS (Figure 1.9) (Lee & Zhang, 2015; Liu *et al.*, 2021). In *P. aeruginosa* swarming motility is also dependent on rhamnolipids and an additional motility appendage the type IV pili (Kohler *et al.*, 2000). Due to its association with additional genes to those from the swimming motility phenotype, swarming motility is another mechanism frequently studied due to its link to virulence via the QS regulatory network.

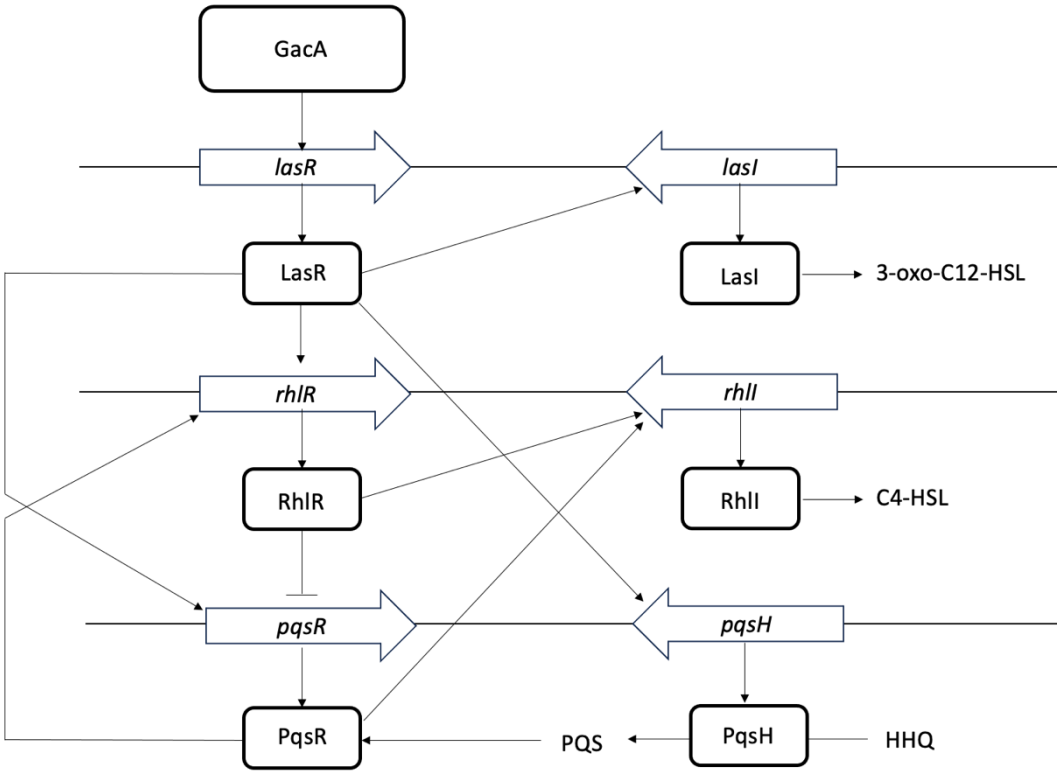


Figure 1.9: Quorum sensing network of *P. aeruginosa*. Schematic representation of Las, Rhl and PQS QS network integration.

1.3.3 Other mechanisms of bacterial movement- from type IV pili mediated twitching to sliding

Whilst swimming and swarming motility phenotypes are the most widely studied, other motility mechanisms are at play in bacterial movement. Twitching is a phenomenon which utilises the type IV pili that is frequently utilised in host cell adhesion, DNA uptake and other virulence mechanisms such as surface sensing, chemotaxis, and predation. The envelope-embedded basal body comprises 10 proteins, which form a PilQ/TsaP mediated OM pore, PilP and PilNO periplasmic rings, PilM cytoplasmic ring and PilC IM platform (Wadhwa & Berg, 2022). The pilus itself comprises a helical PilA-mediated polymer that is embedded in the IM and inserted via PilB and PilT ATPases which dock monomers to the cytoplasmic ring, driving polymerisation and depolymerisation respectively (Craig *et al.*, 2006; Koch *et al.*, 2021). Closely related to the T2SS (Korotkov, Sandkvist & Hol, 2012), type IV pili undergo a rapid succession of extension and retraction cycles (Merz, So & Sheetz, 2000; Skerker & Berg, 2001). These cycles are facilitated by binding the tip to a surface before retraction occurs in a grappling hook-like mechanism (Figure 1.10). This can occur at a rate of ~1 μm/s and forms the basis of the twitching phenotype (Merz, So & Sheetz, 2000; Skerker & Berg, 2001; Clausen, Koomey & Maier, 2009). The pili in *P. aeruginosa* are located at the cellular poles, where 'walking' phenotypes using pili at a single pole have been observed (Gibiansky *et al.*, 2010; Talà *et al.*, 2019).

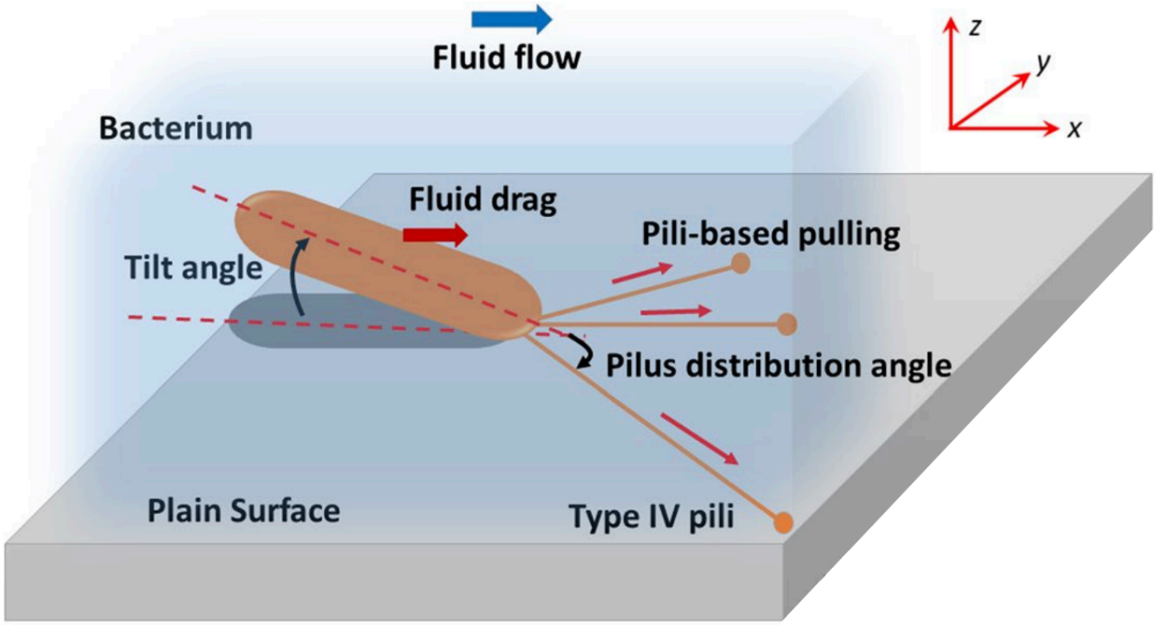


Figure 1.10: Twitching motility movement via the type IV pili. Schematic representation of directional movement via type IV pili for twitching motility. Figure adapted from (Jayathilake *et al.*, 2019)**.**

Another mechanism is known as sliding motility, which is utilised in the absence of flagella and pili on semisolid surfaces. First described in 1972 (Henrichsen, 1972), it was outlined as a *P. aeruginosa* mode of movement in 2008 (Murray & Kazmierczak, 2008). This study showed sliding occurs by secretion of rhamnolipids induced by the Gac/Rsm pathway and may enable cell spreading at the outside of a colony for passive spatiotemporal expansion. As *P. aeruginosa* downregulates expression of motile appendages during chronic infection, sliding may occur in CF airways in established infections as a pathoadaptive feature but this is unknown (Winstanley, O'Brien & Brockhurst, 2016). Additionally, the extent of the interplay of motility with other factors and mechanisms of virulence is yet to be determined.

1.4 Production of biofilm- the shield

Although bacteria exist as planktonic, free, individually floating cells, cells also exist in a group mediated structure called the biofilm matrix. This enables bacteria to associate with a surface, both biotic and abiotic, as well as interact with other microbes and protect themselves from environmental stressors by forming coated clusters. Biofilms are known for bacterial cell aggregation which promotes either competition, nutrient exchange or protection from lethal stressors such as desiccation or antibiotics (Flemming *et al.*, 2016). Biofilms are an evolved trait often seen in the environment but are frequently associated with virulent and nosocomially acquired infections (Devanga Ragupathi *et al.*, 2022). A change in gene regulation initiates the switch between a planktonic to group lifestyle and is initiated by the flagella, enabling attachment to a surface (Schniederberend *et al.*, 2019). This is followed by other mechanisms such as QS which instigates biofilm production through influencing gene regulation upon the presence of a threshold number of cells (Wang, Bian & Wang, 2022). Thus, biofilm is an inherently social trait which occurs through cooperation of multiple bacterial cells, where QS enables direct cell-cell communication for coordination on this scale. Although there is much debate in the field as to how many bacteria in an aggregate comprise a biofilm, generally it is considered to be an aggregate large enough to confer biofilm properties such as polysaccharide production or ranging in complexity with secondary/tertiary structures (Penesyan *et al.*, 2021).

P. aeruginosa uses biofilms and is generally considered one of the model organisms. *P. aeruginosa* chronic infections, particularly in CF, are mediated by biofilm production where it is a major factor in the bacteria's arsenal of advantageous mechanisms (Ciofu *et al.*, 2022).

The protective layer the biofilm decreases *P. aeruginosa* immunogenicity and protects the cells from various therapies and host defences, making them difficult to eradicate. Biofilms can be produced in hypoxic and anoxic environments, where *P. aeruginosa* is able to adapt to these environments through the biofilm matrix via strain diversification within an individual host (Sønderholm *et al.*, 2017; Schick & Kassen, 2018). An added layer of complexity of *P. aeruginosa* biofilms in CF is that they may be multispecies, making our understanding of microbial interactions during pulmonary infection more convoluted. Although most infections are not caused by an individual species, CF infection is associated with co-colonisation of many other infectious agents such as those discussed above in 1.2.2. These pathogens may be incorporated into the *P. aeruginosa* biofilm where, with the adaptation to the lung and the switch from the 'non-mucoid' to 'mucoid' phenotype, they form a matrix with a complex network called the polymicrobial community.

1.4.1 The biofilm matrix- components matter

Multiple components are required for biofilm assembly and can range from enzymes to polysaccharides and even DNA. The most associated components with the matrix are the polysaccharides such as alginate, which can be additionally mediated by either Pel or Psl. Various *P. aeruginosa* strains can produce either all three polysaccharides or a combination. Psl is an extracellular polysaccharide (EPS) associated with *P. aeruginosa* PAO1 biofilm. It is a neutral polymer which acts as both a scaffold and adhesin for organising other components of the matrix (Jackson *et al.*, 2004). Comprising of branched pentasaccharides D-glucose, L-rhamnose and D-mannose, it additionally provides trails for bacterial movement within the matrix in either a cell associated or ECM cell-free form (Liu *et al.*, 2022). Due to its importance

in the matrix structural foundation, its production is associated with a positive c-di-GMP loop to initiate further Psl production upon niche establishment (Lesic *et al.*, 2009). The Pel polysaccharide variant is also regulated by c-di-GMP but is utilised instead by *P. aeruginosa* strain PA14 (Friedman & Kolter, 2004b). It is rich in N-acetylglucosamine (N-glu) and N-acetylgalactosamine (N-gal) with a linear polymeric structure of partially de-*N*-acetylated α-1,4-*N*-acetylgalactosamine and N-glu-N-gal dimeric repeats (Le Mauff *et al.*, 2022). Crucially, it is cationic enabling crosslinking with other components such as DNA- initiating the formation of tertiary structures as well as enhancing resistance to antimicrobial compounds (Jennings *et al.*, 2015, 2021).

Alginate is a polysaccharide associated with 85% of chronic *P. aeruginosa* infections in CF. Overproduction of alginate in strains adapted to the variable oxygen environments in the lung are known as 'mucoid' strains- a major pathoadaptive feature associated with *P. aeruginosa* infection in CF (Doggett, 1969; Hentzer *et al.*, 2001). A polymer composed of β-1,4-D- linked L-guluronic and D-mannuronic acids, it is a high molecular weight structure comprised of 50-90% repetitive motifs of the mannuronic acid 'M' unit (Linker & Jones, 1964; Evans & Linker, 1973). Although it is not an essential biofilm component, it is maintained in the CF lung and is an example of adaptive host evolution through *mucA* mutations and subsequent constitutive *alg* operon activation (May *et al.*, 1991; Xie *et al.*, 1996). The induction of the mucoid phenotype makes treatment difficult due to the thick biofilm which protects the bacteria against antibiotics such as aminoglycosides via the M-rich region (Heriot *et al.*, 2019).

Unlike alginate, an additional component not solely associated with CF biofilms is the presence of extracellular DNA (eDNA). However, like alginate it is an anionic high molecular weight polymer due to the phosphate in its structural backbone and is in high abundance in

CF sputum (Picot, Das & Reid, 1978). This phosphate binds various cations which can prevent removal via cationic antibiotics such as aminoglycosides (Mulcahy, Charron-Mazenod & Lewenza, 2008; Ibáñez de Aldecoa, Zafra & González-Pastor, 2017). More recently it promotes cellular spatial organisation by concentrating in specific locations (Gloag *et al.*, 2013). Biofilms can utilise both bacterial and host eDNA (Lethem *et al.*, 1990), and is employed in early biofilm formation stages and microcolony stalks for stabilisation though colocalising with other components of the matrix such as Psl (Whitchurch *et al.*, 2002; Wang *et al.*, 2015). It is often additionally used as an alternative nutrient source through the secretion of DNase enzymes for its high proportion of phosphorus, carbon and nitrogen (Dell'Anno & Danovaro, 2005; Mulcahy, Charron-Mazenod & Lewenza, 2010).

1.4.2 Microscopic mushrooms- the biofilm maturation cycle

Laboratory based research has proposed that biofilm formation occurs in a five-step cycle closely linked to bacterial motility based on model systems (Figure 1.11). The shift between planktonic growing to sessile stages occur through complex, highly regulated mechanisms. This is controlled by a linked gene regulation pathway, Gac/Rsm, which downregulates motility genes upon surface attachment and subsequent upregulation of biofilm genes (Shang *et al.*, 2021). This is mediated through c-di-GMP which promotes motility upon low intracellular levels, and biofilm upon high intracellular levels (Simm *et al.*, 2004). There are multiple genetic regulatory pathways that act in concert, which is mediated by SuhB through RNA polymerase and ribosomal interactions and the diguanylate cyclase GcbA in *P. aeruginosa* (Wang *et al.*, 2007; Shi *et al.*, 2015; Hanson *et al.*, 2017). During this shift *P.*

aeruginosa demonstrates multiple distinct phenotypes with divergence in structural and metabolic characteristics which occur at distinct stages throughout biofilm development.

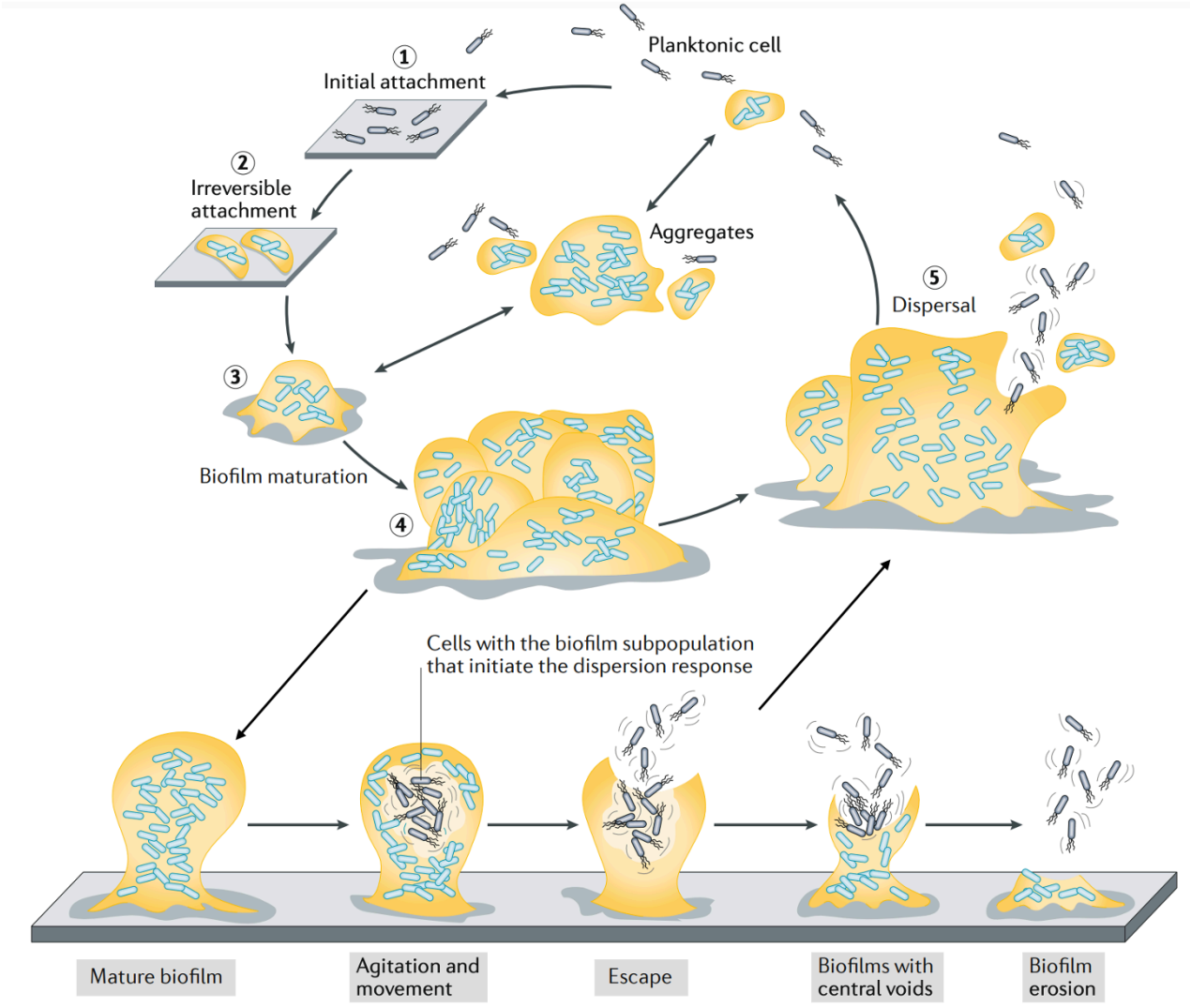


Figure 1.11: The biofilm maturation cycle. Schematic representation of biofilm production and maturation on a surface via the five-step cycle of reversible attachment, irreversible attachment, aggregation, biofilm maturation, and finally dispersal. Figure adapted from (Rumbaugh & Sauer, 2020).

Initially, *P. aeruginosa* attaches to a surface via their pole, usually involving the flagella or type IV pili (O'Toole & Kolter, 1998) which is mostly unstable, and this is known as reversible

attachment. Irreversible attachment is then initiated when the cell length associates with the surface and is mediated through SadB and LapA (Hinsa *et al.*, 2003; Caiazza & O'Toole, 2004). This transition is conveyed by a reduction in flagellar reversal rates, gene expression and the upregulation of biofilm genes such as the alginate operon to build the microcolony structure (Sauer *et al.*, 2022). At this early stage, bacteria begin to demonstrate enhanced resistance to antibiotic agents (Gupta *et al.*, 2013). Upon initiation of matrix component production, bacterial cells adhere more firmly to the surface and start to build complex structures. In *P. aeruginosa*, these are characterised by mushroom-like tertiary structures of mature biofilms (Klausen *et al.*, 2003a, 2003b). These structures are formed through a type IV pili dependent mechanism known as twitching motility (O'Toole & Kolter, 1998). During formation of the 3D structures, spatial heterogeneity is exhibited due to different levels of oxygen and nutrients in different locations within the matrix (Stewart & Franklin, 2008; Serra & Hengge, 2014; Sauer *et al.*, 2022). The final stage of biofilm development is known as dispersion, where bacteria switch from sessile back to motile phenotypes upon escape from the biofilm matrix which is utilised for active dissemination and colonisation of new niches (Purevdorj-Gage, Costerton & Stoodley, 2005; Rumbaugh & Sauer, 2020). C-di-GMP levels have a key role in the initiation of dispersal through reduced intracellular levels that results in enhanced expression of genes associated with motility (Roy, Petrova & Sauer, 2012; Cai *et al.*, 2020). Although this model is considered the standard, it is limited to a monoculture and bacterial attachment to a surface which does not occur in the CF lung but forms within sputum. Therefore more work is required to understand coculture and polymicrobial biofilms.

1.4.3 Tough shields, bacterial persistence, and survival in hostile environments

Various biofilm matrix components are crucial in infection establishment and preventing removal via antibiotic therapies. The flagellum is a major component of this- where it can bind epithelial cell surface molecules such as monosialylated glycolipid GM1 and N-glycans, inducing host signal transduction pathways to enable internalisation as a mechanism of immune evasion (Feldman *et al.*, 1998; Bucior, Pielage & Engel, 2012). However, due to the flagellum's immunogenic nature, to evade the immune system *P. aeruginosa* becomes non-motile to reduce their clearance particularly during chronic establishment, which coincides with epithelial internalisation and biofilm formation (Mahenthiralingam, Campbell & Speert, 1994). Other matrix components specifically promote adhesion to airway epithelia whilst preventing neutrophilic phagocytosis such as Psl and alginate (Boyd & Chakrabarty, 1995; Byrd *et al.*, 2010; Mishra *et al.*, 2012). Many of these components are recognised by the innate immune system's polymorphonuclear leukocytes (PMNs) which create a pro-inflammatory environment through the respiratory burst and degranulation of PMNs (Rybtke *et al.*, 2020; Moser *et al.*, 2021). This highly inflammatory environment enacts damage on the lungs and is associated with reduced lung function in patients with CF (Ghigo *et al.*, 2021). However, *P. aeruginosa* also utilises other factors of the CF pulmonary environment to aid in infection, creating cycles of infection and damage which makes colonisation of the lung the perfect storm for chronic infection establishment.

Components of the CF lung also contribute to *P. aeruginosa* biofilms and therefore infection persistence, which is chiefly associated with host-derived mucins. Mucins are a major component of sputum which can be transmembrane or secreted by epithelia. Mucins are high

molecular weight rod-shaped glycosylated proteins which range in diversity based on their carbohydrate-based backbones and encompass multiple O-linked glycans which account for ~85% of the protein's mass (Hansson, 2019). Negatively charged and assemble hydrophobic domains via covalent disulfide bonds, their complex structure contribute to both mucin's ability to form hydrogels and create the barrier effect and desiccation resistance of biofilms (Guillaume *et al.*, 2022). Their importance in the human body is in their ability to provide both hydration and lubrication to epithelia whilst acting as a receptor for endogenous cells and microbes (Petrou & Crouzier, 2018). This creates a 'track' to enable *P. aeruginosa* to initiate biofilm formation (Guillaume *et al.*, 2022). Therefore, production of mucus is associated with a positive feedback loop upon colonisation of the epithelia which is mediated by a combination of cytokines such as IL-9, TNF-α and IL-1β (Song *et al.*, 2003; Mitri *et al.*, 2020).

This barrier mechanism is the major contributor to bacterial persistence. There are many ways bacteria can persist after antibiotic therapy when located in an established biofilm, and this is due to the properties of the therapeutic agents as well as the inherent cellular heterogeneity exhibited in mature biofilms. Biofilms have the ability to interact with cationic antibiotics such as aminoglycosides (Heriot *et al.*, 2019), as well as prevent diffusion of antibiotics through the hydrogel (Drenkard, 2003; Pang *et al.*, 2019). This diffusion barrier combined with the cellular inherent heterogeneity gives rise to resistance from sublethal antibiotic levels in the matrix (Stewart & Franklin, 2008), making bacteria difficult to eradicate upon biofilm establishment. Extensive co-regulation occurs between biofilm formation and T6SS expression which contributes to biofilm formation and cell-cell interactions (Chen *et al.*, 2020), as well as protection against predation and competition from other bacterial cells (Toska, Ho & Mekalanos, 2018; Teschler *et al.*, 2022) however this is yet to be determined in

P. aeruginosa. Therefore, the interplay between *Pseudomonas*, biofilms and the CF lung environment remains to be fully elucidated and may have implications in clinical patient outcomes where they could provide novel targets for future therapies.

1.5 Bacterial secretion systems- from classical to non-classical mechanisms of protein export

One of the potential mechanisms bacteria employ to enable niche dominance is through secretion systems. Secretion systems are transmembrane protein complexes which allow the movement of protein effectors across the cell membrane allowing efflux into the extracellular milieu (ECM) or directly into target cells (Green & Mecsas, 2016). Previously they have been shown to play a role in virulence in a range of animal and plant models as well as host cell manipulation. Many are utilised for nutrient acquisition or are involved in mechanisms such as interbacterial competition through effector export (Costa *et al.*, 2015; Yang *et al.*, 2021). This export is mediated in two ways; either by a one-step pathway directly from the cytosol, or a two-step pathway which includes transportation into the periplasm via the Sec or Tat pathways before release into the ECM (Robinson & Bolhuis, 2004; Papanikou, Karamanou & Economou, 2007). Bacteria encode multiple types of secretion system, with more being discovered through bioinformatics (Abby *et al.*, 2016). Although more are being found, six classical secretion system types in gram-negative bacteria are well elucidated in the literature due to their high conservation throughout multiple bacterial genera (Figure 1.12) (Costa *et al.*, 2015; Filloux, 2022). However with the rapid expansion of the number of systems being identified, the nomenclature is being called into question.

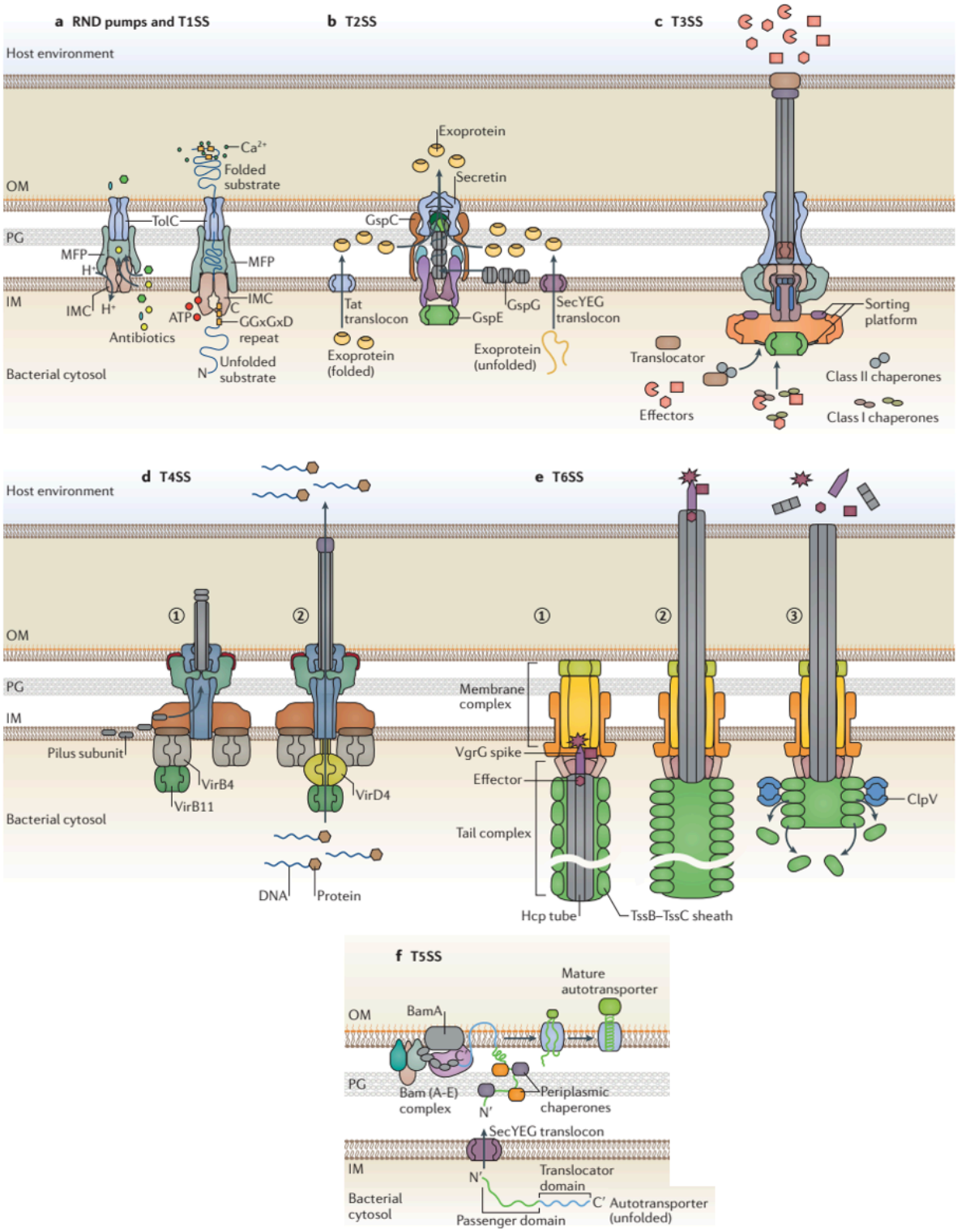


Figure 1.12: Gram-negative classical bacterial secretion systems. Six classical secretion systems are encoded by gram-negative bacteria. Types I – IV are outlined above. Figure adapted from (Costa *et al.*, 2015)**.**

Bacteria interact via multiple complex mechanisms which can be contact dependent. Bacterial cell-cell contact was first described in 1946 upon discovery of bacterial conjugation (Lederberg & Tatum, 1946). Since then, research has expanded the range of contact mechanisms crucial for bacterial survival. Secretion systems are major players ensuring survival by mediating host cell manipulation, nutrient scavenging, defence and competition (Abby *et al.*, 2016). Systems which actively secrete proteins upon direct contact are often involved in bacterial warfare with microbial and host cells (Granato, Meiller-Legrand & Foster, 2019), but can also be utilised in cooperative behaviours (Garcia *et al.*, 2016a) between cells and their environment. Both roles are crucial in pathogenesis and long-term establishment within a niche and are frequently associated with the Contact Dependent Inhibition (CDI) (Aoki *et al.*, 2010; Mercy *et al.*, 2016) and Type Six Secretion Systems (T6SS) (Chen *et al.*, 2015). The systems encoded differ between gram-positive and -negative bacteria due to their function and complexity. Export in gram-positive bacteria is sufficient via the Sec or Tat export pathways, however due to the additional membrane in gram-negative bacteria they require more complex machinery to achieve the same result. These systems are highly conserved amongst gram-negative bacteria and are tightly regulated due to their highly energy expensive nature (Green & Mecsas, 2016).

1.5.1 The type I secretion system (T1SS)- an ABC autotransporter

Considered the simplest representation of bacterial secretion, T1SS is a one-step secretion mechanism associated with ABC transporters which span the entirety of the gram negative cellular envelope (Figure 1.13) (Symmons *et al.*, 2009). First discovered in 1979, this mechanism is utilised for efflux of unwanted compounds and is linked closely to many

acquired mechanisms of antibiotic resistance (Noegel *et al.*, 1979; Greene *et al.*, 2018). Most closely related to the resistance-nodulation and division (RND) transporters, it is comprised of three components; the IM ABC transporter and 'membrane fusion protein' coupled with a β-barrel homotrimer which forms a gated channel between the cytoplasm and extracellular environment, and finally an OM protein allowing access out of the cell (e.g. TolC (Figure 1.13)) (Seeger *et al.*, 2006). T1SSs are found in a large proportion of gram-negative bacteria and move effectors involved in intoxication, adhesion, and nutrient acquisition where they reach their folded mature state once secreted into the ECM. Unique to this system, proteins are not associated with Sec signal peptides and instead utilise a C-terminal non-cleaved target signal.

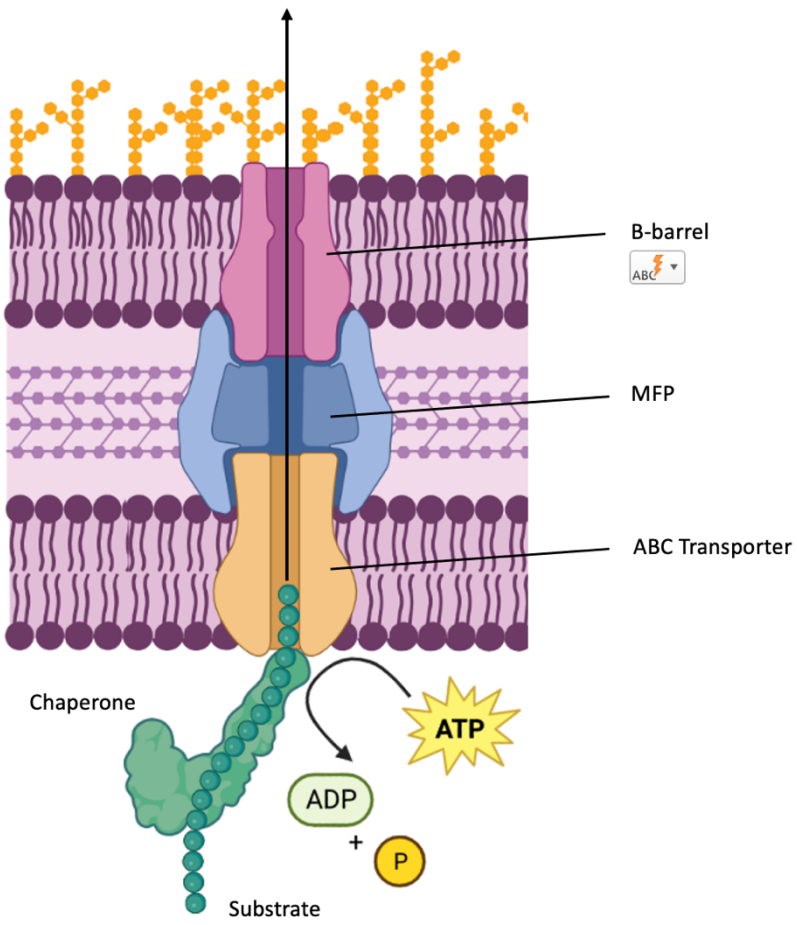


Figure 1.13: The type I secretion system. Schematic representation of T1SS consisting of ABC transporter, IM channel and OM secretin, utilised to secrete substrates.

Initially identified by secretion of hemolysin A toxin HlyA in *E. coli* (Mackman *et al.*, 1985), many toxins have been linked to this system between various genera. T1SSs have been associated with other virulence mechanisms in a broad range of bacteria such a *V. cholerae* and *Serratia marcescens* by secreting MARTX and HasA hemophores,

respectively (Létoffé, Redeker & Wandersman, 1998; Dolores *et al.*, 2015). These toxins are utilised to traverse various mucosal barriers whilst damaging cells as a mechanism of immune evasion. A promiscuous system, there is no underlying genetic predetermination for toxin excretion via this system as it has been demonstrated to secrete proteins from other bacteria in *E. coli* such as CyaA from *Bordetella pertussis* (Kanonenberg *et al.*, 2018). Present in *P. aeruginosa*, it is utilised in immune evasion during infection via the secretion of an alkaline protease AprA. This protease has multiple functions including degradation of antigenic portions of the flagella and cytokines interferon-γ and tumour necrosis factor α (Parmely *et al.*, 1990; Bardoel *et al.*, 2012). Additionally, *P. aeruginosa* utilises iron acquisition protein HasAp which acts in haem acquisition in a TonB-dependent manner but also plays an important role in virulence during infection (Duong *et al.*, 2001; Létoffé *et al.*, 2022).

1.5.2 The type II secretion system (T2SS) and two-step secretion

The classical representation of two-step secretion is defined by the T2SS that is generally found in *Proteobacteriaceae* and *Bacteroidetes* (Denise, Abby & Rocha, 2019). Situated across both membranes, it transports folded proteins from the periplasm to the ECM (Figure 1.14). Evolutionarily linked to the type IV pilus, the T2SS is an intricate protein complex consisting of up to 15 proteins linked to four main structures: the OM complex, IM platform, secretion ATPase and pseudopilus (Naskar *et al.*, 2021). The two-step pathway is ATP-dependent where ATP hydrolysis creates a helical pilus-like structure in the periplasmic space which is anchored to the IM (Sauvonnet *et al.*, 2000). Effectors are exported into the periplasm via the Sec and Tat pathways before secretion (Korotkov, Sandkvist & Hol, 2012). Because of the diversity in

IM export pathways, effectors associated with T2SS have broad specificity with an array of functions linked to both virulent and avirulent mechanisms.

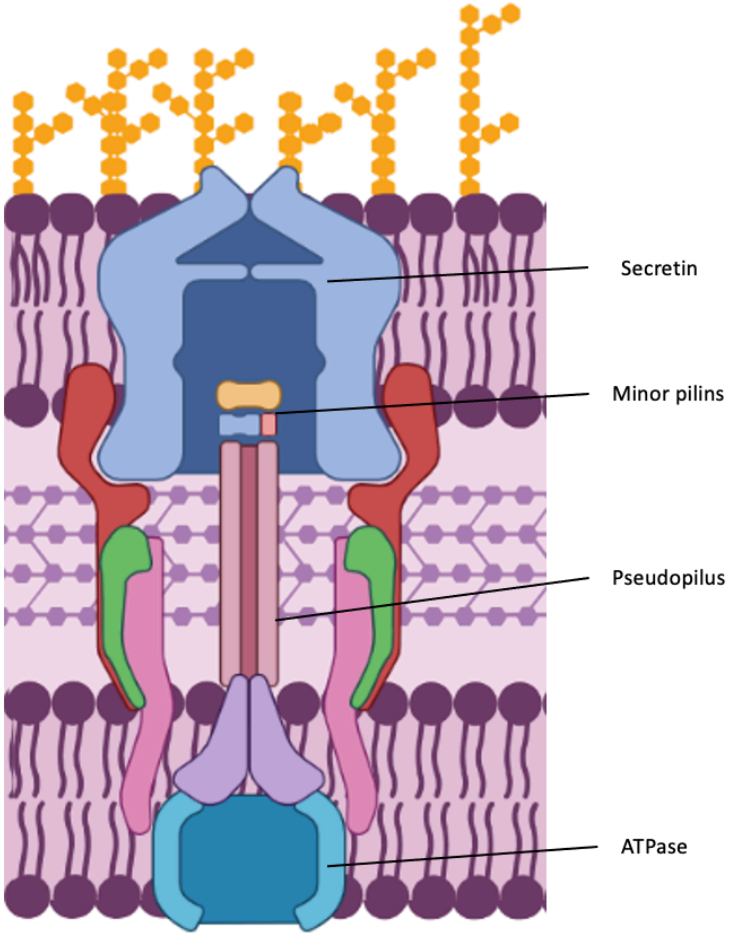


Figure 1.14: The type II secretion system. Schematic representation of T2SS consisting of the secretin, pseudopilus, minor pilins and ATPase to secrete substrates.

Although it remains unclear, the excretion mechanism is thought to be linked to pseudopili retraction which pushes the substrate through the OM channel of the system in an ATP-dependent manner (Green & Mecsas, 2016). It is a key virulence determinant in many pathogens such as *Acinetobacter baumanii*, *Klebsiella pneumoniae* and most importantly for this thesis *P. aeruginosa*, particularly during pulmonary infections (Jyot *et al.*, 2011; Tomás *et al.*, 2015; Elhosseiny & Attia, 2018). T2SS in *P. aeruginosa* is linked to lethality in *in vivo* mice experiments due to the secretion of toxins such as exotoxin A, type IV protease and lipolytic enzymes (Cianciotto, 2005; Jyot *et al.*, 2011). Effector diversity links to *P.aeruginosa* ability of to adapt to hostile niches in the environment and human host and is an example of its flexible mosaic genome (Stover *et al.*, 2000).

1.5.3 The type III secretion system (T3SS) injectosome

One of the most successful secretion systems, the T3SS is a macromolecular complex known as the 'injectosome' which translocates effectors in a one-step mechanism into the ECM and directly into host cells (Figure 1.15) (Schraidt & Marlovits, 2011). Comprised of nine core proteins, eight of which are shared with the flagella, and 25-30 accessory proteins- it encompasses three major subunits: a basal body, needle-like filament and the translocon (Deng *et al.*, 2017). This complex spans both membranes and has a hollow core to enable protein translocation in its unfolded state, where the needle tip is utilised to sense contact with the host (Radics, Königsmaier & Marlovits, 2014; Green & Mecsas, 2016; Filloux, 2022). As a result, these systems are associated with gram-negative bacteria and utilised in trans-kingdom interactions essential in bacterial pathogenesis.

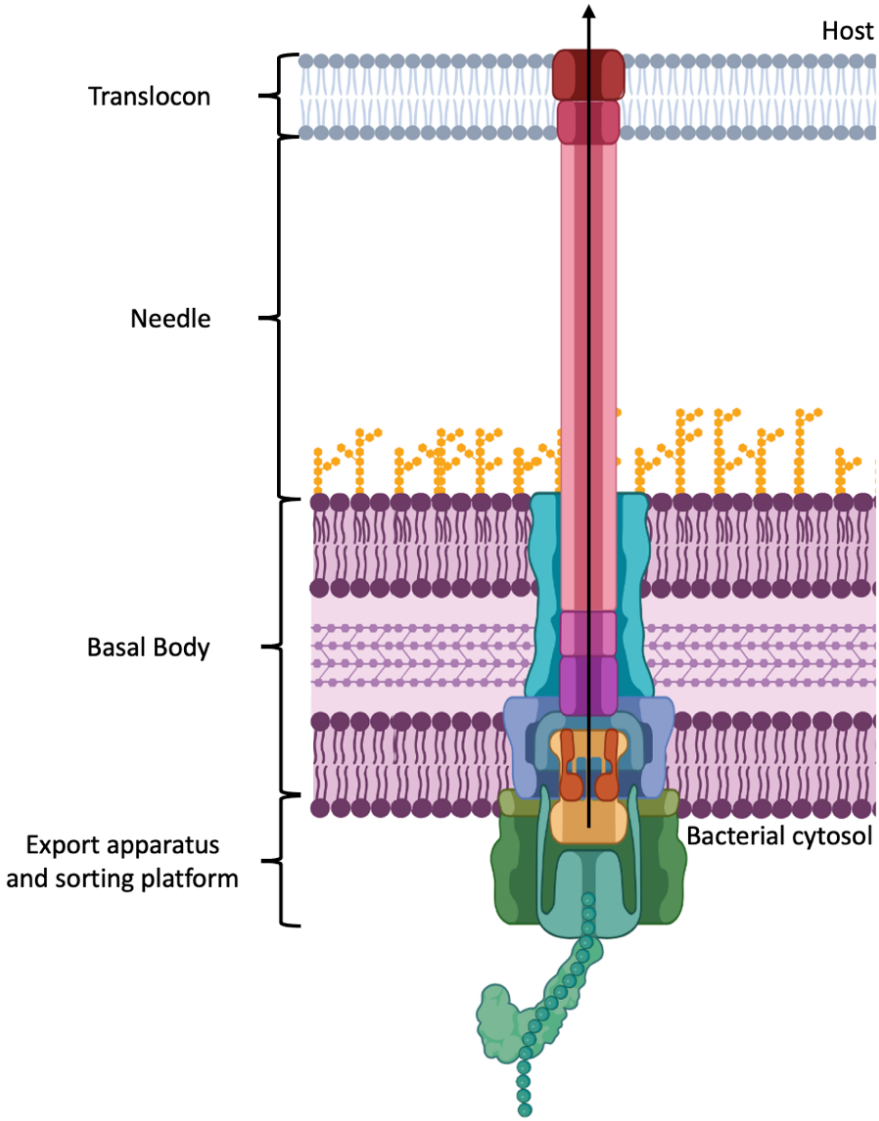


Figure 1.15: The type III secretion system. Schematic representation of T3SS consisting of the export/sorting platform, basal body needle and translocon used to secrete substrates.

Needle proteins bind to the inner rod protein of the basal body to induce polymerisation which is finally capped with a tip protein utilised in docking to target cells (Kuhlen *et al.*, 2018). This tip is crucial in the insertion and formation of the translocation pore into the host membrane to enable effector secretion through the needle and into host cells. The complex includes a sorting platform- an ATP-dependent gate which controls the movement of effectors into the needle subunits (Lara-Tejero *et al.*, 2011). Based on *Yersinia* spp. studies, the ATPase is thought to recognise effector protein N-terminal signal peptides (Sorg, Blaylock & Schneewind, 2006). Proteins are then threaded through the basal body inner rod and needle in their unfolded state. The unfolded protein effectors and needle subunits are both controlled by specialised chaperone proteins which keep proteins in a translocation-competent state and prevents unproductive polymerisation of the needle proteins, respectively (Bennett & Hughes, 2000; Stebbins & Galán, 2001; Kuhlen *et al.*, 2018).

P. aeruginosa encodes a T3SS which utilises four effectors for host manipulation via targeting the epithelial and macrophage cytoskeleton (Jouault, Saliba & Touqui, 2022). The four effectors deployed by the T3SS are: ExoS, ExoT, ExoU and ExoY (Hauser, 2009; Sawa *et al.*, 2014). Largely encompassing GTPase, phospholipase and adenylyl cyclase functions they are linked to rapid host cell apoptosis indicating a major role in pathogenesis (Hauser, 2009). This system is tightly regulated via c-di-GMP due to its cytotoxicity via and has been demonstrated to affect the innate immune response by modulating production of IL-1β and effecting lung damage upon secretion (Jouault, Saliba & Touqui, 2022). Despite a small effector repertoire, the highly potent effectors provide *P. aeruginosa* with a selective advantage during infection.

1.5.4 The type IV secretion system (T4SS) sex pilus

The T4SS is one of the few classical secretion systems which *P. aeruginosa* does not possess (Filloux, Hachani & Bleves, 2008). Utilised for conjugation of substrates and genetic material, they are also used for targeting both prokaryotic and eukaryotic cells to deliver effector proteins (Costa *et al.*, 2021). Another transmembrane complex which spans both membranes, it is largely associated with gram-negative bacteria, but recent evidence indicates deployment by gram positives such as *Enterococcus faecalis* (Kohler *et al.*, 2017; Grohmann *et al.*, 2018). Similarly to the T3SS, direct transfer into the cytoplasm of a neighbouring cell is achieved through the ability to span an additional membrane. All T4SSs are evolutionarily related to ancestral DNA conjugation systems, evolved to secrete additional substrates- sharing structural components and mechanisms. However, the T4SS superfamily functions are subdivided into two major subfamilies, those that mediate conjugation and DNA transfer and those that facilitate macromolecular effector translocation (Costa *et al.*, 2021). They remain a concern due to their role in dissemination of AMR (Boudaher & Shaffer, 2019) and mobile genetic elements (MGEs) (Juhas, 2015). Additionally they enable interkingdom DNA and peptidoglycan transfer (Grohmann *et al.*, 2018; Bleves, Galán & Llosa, 2019; Cover, Borden Lacy & Ohi, 2020).

A subset can secrete DNA and substrates into the ECM (Stingl *et al.*, 2010; Costa *et al.*, 2021). Due to this and the evidence for substrate secretion post-Sec mediated translocation from the cytosol in bacteria such as *Bordetella pertussis*, it is a point of debate whether they comprise a one or two-step system (or more likely they are both depending on the system) (Alvarez-Martinez & Christie, 2009). To date, the only *Pseudomonas* species shown to encode

a T4SS is *P. putida*, which mediates interbacterial competition of other plant-associated gram negatives. It does this via a rare T4bSS expressed by intracellular pathogens to deliver toxic effectors (Purtschert-Montenegro *et al.*, 2022). This outlines a new mechanism for T4SSs and shows a further evolutionary divergence in this class of secretion systems. As the CDI and T6SSs are the focus of this thesis, they are discussed in sections 1.6 and 1.7 respectively

1.5.5 The non-classical secretion systems

Whilst the similarities with T1-T4SSs with other mechanisms appear to indicate evolutionary divergence from conserved mechanisms, 'non-classical' secretion systems hint at evolution of mechanisms specifically pertaining to a subset of bacteria (Green & Mecsas, 2016). Deemed 'non-classical' as they do not adhere to the classification rules defined by gram positive and negative membrane categorisations, their identification is challenging perceptions of secretion in bacteria. To date, 15 secretion systems have been identified but for many the question remains whether they truly represent secretion (Filloux, 2022).

An example of this is the Type VII Secretion System (T7SS)- originally found in *Mycobacterium tuberculosis*, whose classification is weakly gram positive (Stanley *et al.*, 2003). This system was shown to enable substrate transport across an additional layer of the cell envelope known as the mycomembrane- akin to the OM but enriched with mycolic acids and phenolic glycolipids. Later identified as a key virulence factor via bioinformatics in *S. aureus*, it is utilised to export toxic substrates into the ECM (Ulhuq *et al.*, 2020; Gorasia, Veith & Reynolds, 2020). The presence in *S. aureus* and transportation across the membrane in a similar manner to the Sec or Tat pathways has created controversy within the field as to whether this represents a

true secretion system. As the exact translocation mechanism is poorly understood this controversy is yet to be resolved. It is also unclear if interbacterial competition by this system requires proximity or direct physical contact for growth inhibition.

Another example is the Type IX Secretion System (T9SS), exclusive to the Bacteroidetes which is utilised in transportation of surface-adhered proteins. Localised to the IM with 12 OM associated proteins, it secretes effectors with various functions such as proteases and adhesins (Gorasia, Veith & Reynolds, 2020). It has a dual function in gliding motility, where T9SS secretes the major adhesins for this mechanism of movement (Sato *et al.*, 2010; McBride, 2019). As these substrates are surface associated, it is proposed to be involved in effector release via OM vesicles as the terminal branch of the secretion machinery (Filloux, 2022). However, the structural organisation and exact secretion function is yet to be confirmed. The T7SS and T9SS therefore highlight a gap in our understanding and challenges the current rules surrounding secretion system definitions and classification of newly discovered systems in nomenclature.

1.6 The type V secretion system (T5SS) and contact dependent inhibition (CDI) systems

T5SS proteins have a diverse range of functions from general secretion, export to the surface of bacteria, and mediating virulence, cooperative and competitive bacterial behaviours. Originally identified in *Neisseria gonorrhoea* as mediating the secretion of IgA protease (Halter, Pohlner & Meyer, 1984) they are amongst the smallest secretion system structures. Originally classified as an autotransporter, they involve proteins which sit extracellularly and enable the bacteria to interact with its immediate environment. These involve a β-barrel

structure usually consisting of 12 β-strands that act as an OM pore to enable anchoring of the system to the outer leaflet of the OM or be subsequently released into the ECM (Kajava *et al.*, 2001). It is a classic example of two-step secretion which utilises the Sec translocon for substrate transport into the periplasmic space before secretion via the T5SS apparatus (Drobnak *et al.*, 2015). Many T5SSs are comprised of an individual polypeptide chain, whilst others have distinct co-localised genes (Meuskens *et al.*, 2019). Compared with other gram negative secretion systems, these do not act in an ATP-dependent manner and only traverse the OM. It was therefore classified as an autotransporter due to its self-sufficiency in effector secretion. However, they require multiple accessory factors to enable them to traverse the bacterial cell envelope to situate in the OM in their correct conformational state.

The discovery of T5SSs was the first challenge to secretion system classification as it requires both Sec and BAM systems for transport and insertion into the OM respectively (Leyton *et al.*, 2014; Drobnak *et al.*, 2015). An encoded N-terminal signal peptide enables translocation of the nascent polypeptide through the Sec machinery as previously described in 1.1.1. It subsequently uses chaperones such as Skp to transport proteins to the OM before BAM insertion of the β-barrel occurs. The β-barrel creates a channel for the remainder of the protein, known as the passenger domain, to pass through to the ECM (Ruiz-Perez *et al.*, 2009; Wagner *et al.*, 2009). T5SS classes diverge from this point, where the two most common subcategories T5aSS and T5bSS have different gene organisation. The T5aSS system is produced as a single polypeptide chain whilst T5bSS (initially denoted TPS) have separate genes encoding the β-barrel and passenger, generically labelled TpsB and TpsA respectively (Meuskens *et al.*, 2019). Once exported, the passenger either remains attached to the β-barrel or is released into the ECM. T5SSs do not encode an ATPase, due to the physiology of

the periplasm and OM which lack ATP and is too leaky for the potentiation of an ion gradient (Klauser, Pohlner & Meyer, 1993). Therefore the generally accepted export pertains to the Brownian ratchet model where the intrinsic subunit folding properties in addition to stabilisation of TpsB β-hairpins prevent the protein from re-entering the periplasm once secreted (Henderson *et al.*, 2004; Choi & Bernstein, 2010; Yuan *et al.*, 2018). An additional proposition involves an asymmetric charge distribution to drive protein export (Kang'ethe & Bernstein, 2013). The T5SS has been subcategorization into six subtypes based on the structure/domain organisation of the protein/proteins (Figure 1.12).

As these systems encode diverse functions important in pathogenesis, this is a virulence factor that is highly conserved in 62% of gram-negative bacteria and is particularly associated with pathogenic strains involved in human infection (Abby *et al.*, 2016). A subset of T5bSSs have been shown to play roles in interbacterial competition called Contact Dependent Inhibition (CDI) systems. Discovered in *E. coli* in 2005, they have since been linked to pathogenesis (Aoki *et al.*, 2005; Anderson, Garcia & Cotter, 2012; Melvin *et al.*, 2017; Roussin *et al.*, 2019). *P. aeruginosa* is known to encode autotransporters which encode β-barrel complexes conserved across gram-negative bacteria but have different passenger domain functions. An example of this is the esterase EstA- a membrane-bound autotransporter associated with rhamnolipid production and biofilm formation (Wilhelm *et al.*, 2007). *P. aeruginosa* also encodes T5bSSs with roles in host cell manipulation via the LepA protease activation of NFκB (Kida *et al.*, 2008), biofilm maturation utilising the CDR system (Reichhardt *et al.*, 2018), and interbacterial competition through CDI systems (Mercy *et al.*, 2016). The many T5SSs encoded by *P. aeruginosa* suggest they provide a range of functions; from promoting biofilms, attachment, and acting as proteases, to aid in successful niche

colonisation. However, to date these systems remain largely uncharacterised *in vitro* and require further validation to infer their scope in human infection. Due to their highly conserved nature, the presence and activity of these systems particularly in clinical strains may provide a novel target for designing new therapies or may be harnessed for the prevention of chronic colonisation of pathogens such as *P. aeruginosa.*

1.6.1 The T5SS subtypes and classification

The T5SS has six subclasses Va to Vf due to the domain organisation and subsequent structural features each system possesses (Figure 1.16). These systems often have disparate functional properties within each subclassification that can be diverse, pertaining to enzymes, adhesins and even bacterial-derived toxins. Whilst most subclasses have been structurally characterised, two (T5dSS and T5fSS) have not yet had the translocator domains elucidated. All subclasses have a β-barrel domain that sits in the OM and an associated passenger domain or protein. (Meuskens *et al.*, 2019).

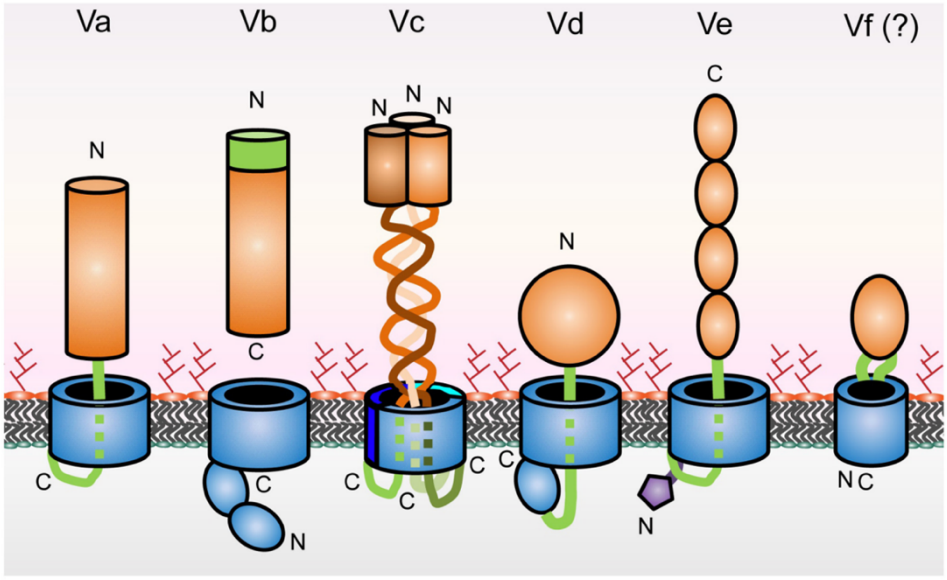


Figure 1.16: Classes of the Type V bacterial secretion systems. Six subtypes of the T5SS are encoded by gram-negative bacteria. Types a-f are outlined in section 1.6.1. Figure reproduced from (Meuskens *et al.*, 2019).

As previously described, the classical autotransporter subclass of the T5SS is the T5aSS which is predicated on one single large polypeptide encoded by a single gene. They consist of a C-terminal 12-stranded β-barrel domain that anchors an N-terminal passenger domain that mostly consists of β-helix folds and bears the functional domain (Emsley *et al.*, 1996). These have been shown to be important in pathogen virulence and are encoded in *P. aeruginosa* such as the previously described EstA lipase system (Henderson *et al.*, 2004).

Differing from the T5aSS is the T5bSS which consists of two polypeptides co-encoded within a single operon and classified as a TPS system as a result (Figure 1.13) (Guérin *et al.*, 2017). The β-barrel, generally labelled TpsB, is a 16-stranded protein with an α-helix that blocks the pore in the inactive state or sits in the periplasm during secretion, followed by two PORTA domains which mediate protein-protein interactions (Kajava *et al.*, 2001). These PORTA domains facilitate the docking of TpsB and TpsA that allows transport of the TpsA to the ECM. This can either remain anchored to the OM or, in most cases, is released into the ECM (Meuskens *et al.*, 2019). Some passenger proteins self-cleave or are cleaved to form the mature protein (Guérin *et al.*, 2017). *P. aeruginosa* is known to encode many of these systems which are involved in biofilm formation such as the CdrAB system (Reichhardt *et al.*, 2018)

The T5cSS also known as trimeric autotransporters have similar structures to T5aSSs, encoding a 12-stranded β-barrel, but forms complex trimeric structures of three subunits with four β-strands each which intertwine to form the β-barrel structure (Figure 1.16) (Hoiczyk *et al.*, 2000). Additionally, there are three secreted passenger domains which intertwine their α-helical coiled-coil and β-rich domains using connector regions to form a lollipop-like stalk and globular head structure (Nummelin *et al.*, 2004; Meng *et al.*, 2006).

T5dSS is a more recent addition to the classification system, which comprises a T5aSS and T5bSS hybrid. Encoding a single polypeptide consisting of a 16-stranded C-terminal β-barrel which mimics that of the T5bSS, it differs through the possession of only a single PORTA domain (Salacha *et al.*, 2010). Additionally, the passenger domain adopts the α/β hydrolase fold that appears to only be associated with lipase or esterase functions (Emsley *et al.*, 1996; Da Mata Madeira *et al.*, 2016). *P. aeruginosa* encodes an example of this- the PlpD system which uses a lipolytic protein from the patatin-like protein (PLP) family and is particularly prevalent amongst pathogenic environmental bacterial species (Salacha *et al.*, 2010).

T5eSS are known as inverse autotransporters due to their similarity to T5aSS with the 12-stranded β-barrel and single secreted attached passenger with an inverted domain order of the β-barrel situated at the N-terminal (Oberhettinger *et al.*, 2012). The passenger adopts Ig-like or lectin-like folds with intimin and invasion functions. Some systems possess an additional periplasmic domain for enhanced peptidoglycan interactions for anchoring during receptor binding interactions and host cell invasion (Leo *et al.*, 2015).

Finally, the newest addition, the T5fSS, is unusual (Grijpstra *et al.*, 2013). They are 8-stranded β-barrels with an α-helical passenger extending from one of the extracellular loops. To date, this system has been solely associated with *Helicobacter pylori* which encodes the Hop adhesin proteins (Coppens *et al.*, 2018). However, relatively little is known about these systems and much remains to be investigated.

1.6.2 The T5bSS CDI systems

A subclass of the T5bSS is the Contact Dependent Inhibition or CDI systems (Aoki *et al.*, 2005). Originally identified by Aoki *et al.* in 2005, these systems were found to play a role in interbacterial competition in *E. coli* from a particularly pathogenic strain EC93 which dominated the gut environment of a rat. These systems are called CDI as they require direct contact with a neighbouring cell for toxin release to kill or inhibit its growth as a form of interbacterial competition. Widely encoded throughout gram-negative bacteria, these systems are categorised into the '*Burkholderia*-type' (Anderson, Garcia & Cotter, 2012) or '*E. coli*-type' secretion systems (Aoki *et al.*, 2010). These systems are formed of three genes which encode three proteins (Figure 1.17). The two structural proteins encompass an OM β-barrel (CdiB) and passenger protein (CdiA) which pertain the classic features of the T5bSS. The passenger C-terminal constitutes the functional domain which exhibits antibacterial toxic properties (Mercy *et al.*, 2016; Cuthbert, Hayes & Goulding, 2022). The final gene encodes an 'immunity' protein (CdiI) to prevent autoinhibition or killing of kin upon translocation of the toxin into a neighbouring sister cell (Aoki *et al.*, 2010; Poole *et al.*, 2011).

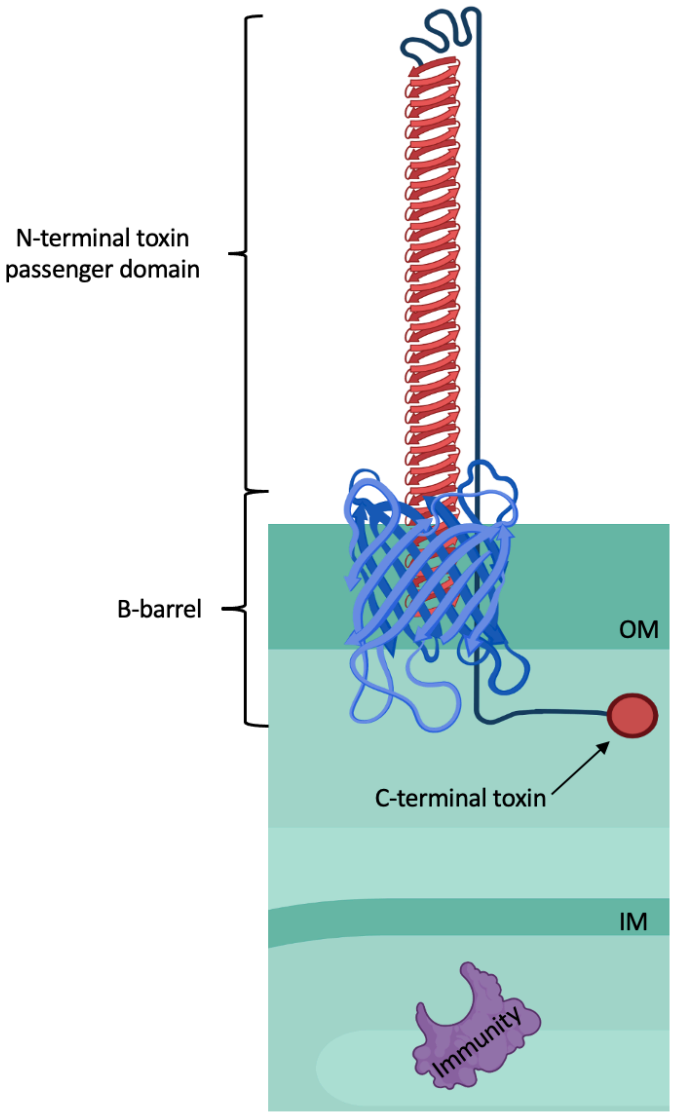


Figure 1.17: The type Vb secretion system. Schematic representation of T5bSS consisting of the TpsB OM β-barrel protein, TpsA with an N-terminal toxin passenger domain and the C-terminal functional domain. A subclass of the T5bSS is termed the CDI systems; CdiB, CdiA, and CdiI immunity.

The categorisation of the two CDI types is based on the operon's organisation. *Burkholderia*-type systems are predicated on the BcpAIOB systems which are comprised of four genes: *bcpA, bcpI, bcpO and bcpB*, from 5' to 3' end (Anderson, Garcia & Cotter, 2012). *E. coli*-type systems differ in gene organisation and are predicated on the *cdiBAI* operon which is comprised of three genes: *cdiB, cdiA and cdiI*, going 5' to 3' end (Aoki *et al.*, 2010). BcpB/CdiB are the 12-stranded β-barrel, BcpA/CdiA denote the passenger which encodes a toxin C-terminal antibacterial effector domain, and BcpI/CdiI represent the immunity genes. *Burkholderia*-type systems have an additional BcpO gene, although the function of this gene remains unknown. The *Burkholderia*-type systems also follow a similar operon organisation as the a-c T5SSs with the β-barrel situated at the C-termini, however CDI have the opposite organisation and are more like T5eSS which has been a topic of debate in the field as to its proper classification as a result. However, as these systems are structurally like the T5bSS, they remain classified as such.

P. aeruginosa only encodes the '*E.coli*-type' system and bioinformatics studies have identified that they generally encode two CDI systems (Mercy *et al.*, 2016; Allen & Hauser, 2019). These proteins have been shown to have a highly conserved N-terminal CdiB which gradually becomes more variable in sequence identity towards the C-terminal toxin which pertain different functions both between systems within an individual substrain as well as between homologous systems found between substrains of the same species. The structure, outlined in Figure 1.18, consists of a large β-barrel encoded by the CdiB which is a 16-stranded structure that is a member of the Omp85 superfamily (Gentle *et al.*, 2004; Heinz & Lithgow, 2014). The β-barrel L6 loop interacts with the passenger protein's TPS domain to export the β-helical polypeptide passenger domain (Ruhe *et al.*, 2013). The passenger contains multiple FHA repeats domains, known as filamentous haemagglutinin which is a major adhesin (Chevalier *et al.*, 2005). This passenger domain loops out into the ECM and sits ~33 nm from the cell surface (Kajava *et al.*, 2001) and is thought to be exported through protein folding or asymmetric charge distribution (Meuskens *et al.*, 2019). On the extracellular surface situated between the two FHA domains named Fha1 and Fha2 is a receptor binding domain (RBD) and YP domain (Aoki *et al.*, 2010). The RBD is utilised for direct binding to receptors such as the BamA on neighbouring cells via the L6/L7 loop to facilitate kin recognition whilst the YP domain is used to block the C-terminal end encoding the toxin into the periplasm (Ruhe *et al.*, 2013, 2018). Other receptors besides BamA have been associated with RBDs such as the OmpC-OmpF, Tsx nucleoside porin and lipopolysaccharides (Ruhe *et al.*, 2017), however the OM receptors utilised by these systems in *P. aeruginosa* are yet to be elucidated.

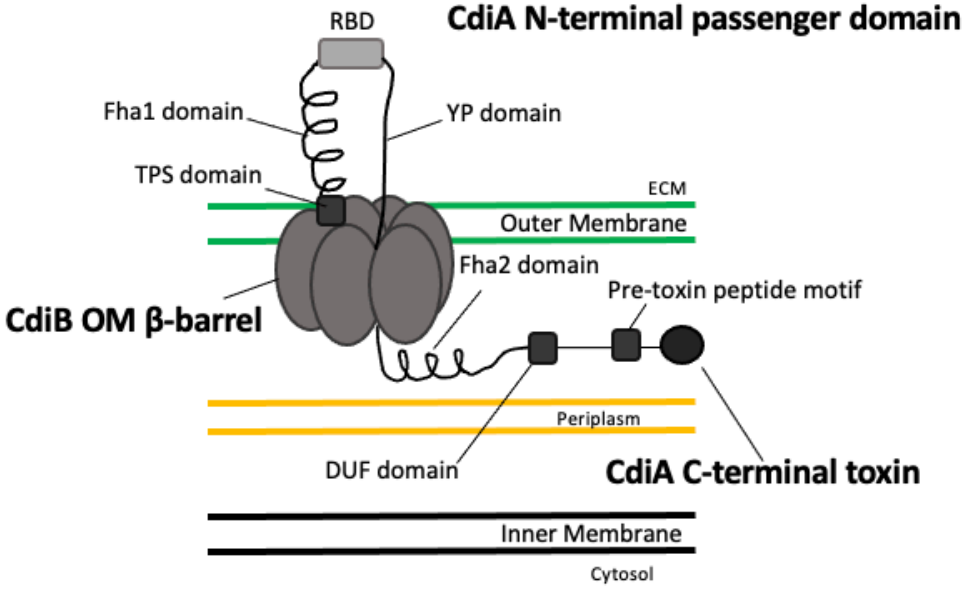


Figure 1.18: The CDI proteins and their domains. Schematic representation of CDI domains consisting of the TPS, Fha1, RBD, YP, Fha2, DUF and pre-toxin peptide motif from N- to C-termini.

After the Fha2 domain is a DUF domain followed by a pre-toxin peptide motif (PTPM). This signals the end of the passenger domain and start of the toxic effector- a common feature in bacterial-derived toxins such as those associated with the T6SS (Wood *et al.*, 2019). *P. aeruginosa* encodes conserved PTPMs that can be classified into 5 types for the CDI system: WVHN, VENN, LYVT, DAMV and NEALV, class one to five respectively (Mercy *et al.*, 2016). In general PTPMs are thought to work in concert with RBDs to determine toxic effector preferential entry mechanisms. The C-terminal toxins have disparate functions and to date have been shown to target cytoplasmic mechanisms (Aoki *et al.*, 2010; Morse *et al.*, 2012; Beck *et al.*, 2014). The high sequence variability at this region is driven by the presence of a genetic hotspot which results in high genetic turnover through acquisition of new genetic material or homologous recombination (HR) (Hayes *et al.*, 2014; Arenas *et al.*, 2013; Koskiniemi *et al.*, 2014). The toxin itself has an N- and C-terminal which are attached by flexible linker peptides and can recombine creating further sequence variation (Guerin *et al.*, 2020). To date, ~50% identified bioinformatically have no discernible function (Allen & Hauser, 2019). The most frequently observed functions pertain homology to DNA and RNA

targeting enzymes with growth inhibitory properties (Cuthbert, Hayes & Goulding, 2022). Downstream of these systems orphan toxins can be found which are often flanked by transposable elements and lack signal peptides which provide a reservoir for HR (Poole *et al.*, 2011).

Finally, the third component of CDI systems encoded directly downstream of the toxin domain is the small *cdiI* immunity gene. When expressed CdiI proteins are typically situated within the cytosol. As these toxins are antibacterial, the immunity is essential in preventing autoinhibition (Aoki *et al.*, 2005). It achieves this by cognate binding to the toxin to neutralise its toxic activity (Mercy *et al.*, 2016). Like the toxin, these immunities are highly variable and specific to their associated toxin and many of the exact structures and functions are unknown. These toxin-immunity modules are highly specific and are often not shared between strains even within the same species (Allen & Hauser, 2019). The CDI systems have clear roles in kin recognition and interbacterial competition as the presence of the immunity when the toxin is deployed in a neighbouring sister cell prevents the killing , whilst providing a toxic effect in a non-sister cell.

1.6.3. The mechanistic deployment of the CDI systems- a molecular spear for bacterial warfare

Although the exact mechanism of action is yet to be understood, much is known about the delivery of the CDI system (Figure 1.19). To date, it has been shown that the RBD binds to a neighbouring cell receptor (Ruhe *et al.*, 2017). It is thought that this contact results in receptor-induced folding which elongates the filament and applies force directly to the Fha2 domain. This allows the YP domain to be released from the CdiB to allow the translocation of

the periplasmic Fha2 and C-terminal toxin domains out of the cell where it is targeted to an OM protein on the neighbouring cell. These have been show to associate with the OmpT protease extracellularly-oriented active site (Ruhe *et al.*, 2018). From here, the toxin is imported via an unknown mechanism, perhaps driven by protein folding. A C-terminal region longer than the toxin domain then interacts with IM proteins involved in metabolite transport such as PtsG, MetI, YciB, FtsH and more recently GltJK (Willett *et al.*, 2015a; Bartelli *et al.*, 2019; Myers-Morales *et al.*, 2021). This allows transport of the C-terminal portion of the C-terminal toxin into the cell via terminal cleavage of its N-termini, which is thought to cleave at multiple points depending on the CdiA, but the mechanism is unclear. Entry into the cytosol is then facilitated via the proton-motive force or electrochemical gradients (Cascales *et al.*, 2007; Hayes *et al.*, 2014). Upon entry, additional prey cytoplasmic factors may activate or enhance toxin activity e.g. CysK sulfhydrylase and translation elongation factors EF-Tu and EF-Ts enable toxin activation through binding to enable toxin stabilisation (Johnson *et al.*, 2016; Jones *et al.*, 2017).

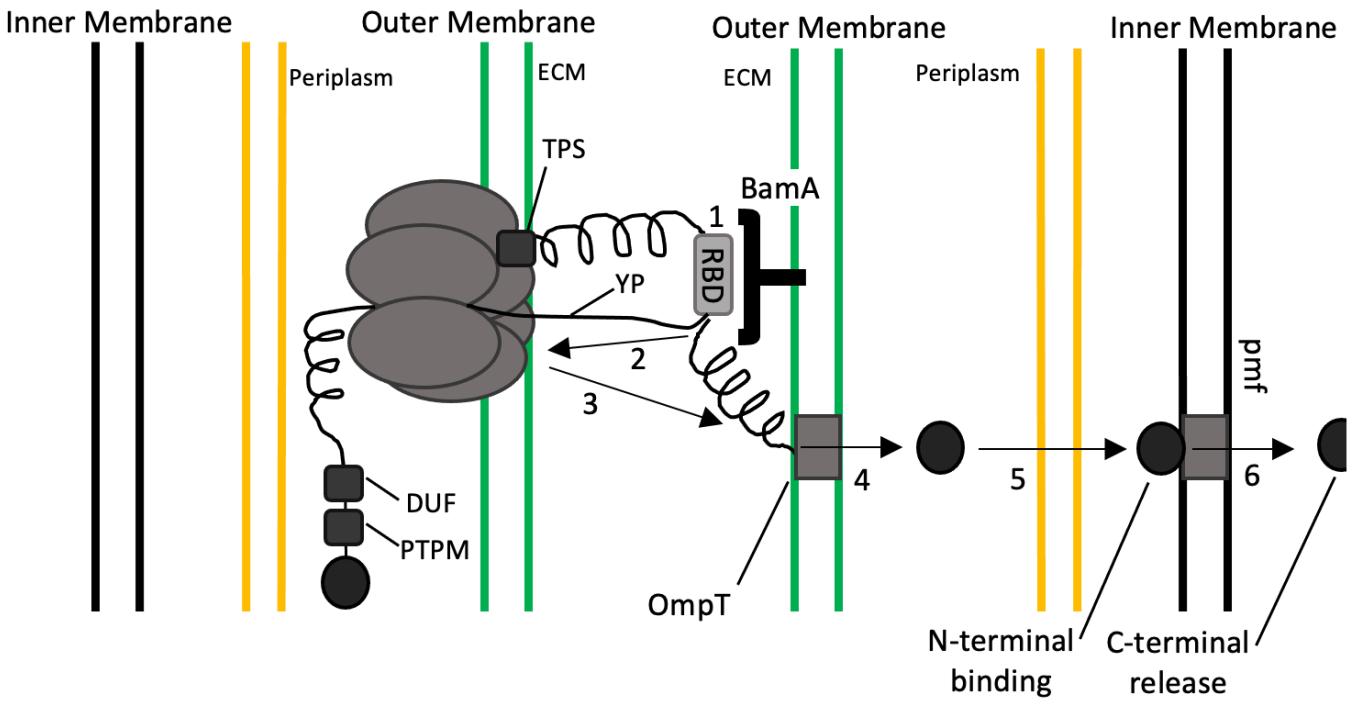


Figure 1.19: Mechanistic deployment of the CDI system effectors. Schematic representation of the deployment of CDI in a six-step toxin delivery mechanism. (1) RBD site binds BamA on neighbouring cell (or another cell surface receptor) (Ruhe *et al.*, 2017). (2) Receptor-induced folding elongates the filament and applying force on Fha2. (3) YP released from CdiB allows C-terminal and periplasmic Fha2 translocation to the target membrane. (4) Associating with OM OmpT protease's extracellularly orientated active site (may use PTPMs to cleave CdiA-CT allowing OM translocation) through unknown mechanisms (Ruhe *et al.*, 2018). (5) CdiA-CT two domains (N-/C-terminal) are attached by flexible peptide linkers where CdiA-CT N-terminal binds specific receptors e.g., PtsG/MetI/YciB/FtsH metabolite transporters, in the inner membrane for cytoplasmic translocation. (6) Through an unknown mechanism, C- terminal cleavage from the N-terminal facilitates entry into cytoplasm using the proton-motive force and electrochemical gradients (Aoki *et al.*, 2010; Willett *et al.*, 2015a, 2015b).

CDI toxins have been shown to utilise a variety of DNase, RNase and pore-forming functions (Cuthbert, Hayes & Goulding, 2022). However, due to their low sequence and structural homology with other known protein domains, the range of their functions is unknown. The original CDI system identified by Aoki *et al.* in 2005 was shown to encode a pore forming toxin

that dissipates the pmf (Morse *et al.*, 2015). Since the discovery of the system, DNase enzymes are also commonly found such as in *E. coli* EC869 which results in anucleate target cells (Morse *et al.*, 2012). More frequently identified are RNase enzymes, such as those found in the *E. coli* EC3006, and *Enterobacter cloacae* encoded CDI. *E. coli* EC3006 encodes a tRNase which specifically cleaves $tRNA_1^{Ile}$ whilst *E. cloacae* encodes a 16S rRNase (Morse *et al.*, 2015)(Willett *et al.*, 2015b). The functional disparity even between *E. coli* strains outlines their importance in strain evolution and niche colonisation by facilitating bacterial competition.

Much of the mechanisms remain unclear at the molecular level and the exact mechanism of toxin import in *P. aeruginosa* is yet to be determined. However, as the mechanism is predicated on receptor binding and so few receptors have been linked with CDI interaction, this narrows the target range due to the requirement for specific receptors to initiate the mechanism and allows for kin recognition. For this reason CDI have been almost exclusively associated with interbacterial competition, however much is yet to be understood about whether receptor homology between strains and species facilitate intrabacterial competition via the CDI. An alternative mechanism proposed is through the utilisation of contact dependent signalling (CDS), where low level toxin activity or formation of the toxin-immunity complex in a neighbouring kin cell can result in altering gene expression to bring about a group mediated response as an alternate mechanism to QS. This has been demonstrated in *Burkholderia thailandensis*, however it is yet to be demonstrated in other bacteria (Garcia *et al.*, 2016a). The disparity in the genetic organisation of the *Burkholderia*-type CDI system compared with the *E. coli*-type, with the addition of the *bcpO* gene may mean this role is specific to the former system type, however this is yet to be determined.

Other roles besides interbacterial competition have been associated with CDI systems. As several have been identified to have a role in biofilm formation and cellular aggregation in *B. thailandensis* (Garcia *et al.*, 2013; Majerczyk *et al.*, 2014)*, E. coli* (Ruhe *et al.*, 2013) and *P. aeruginosa* (Mercy *et al.*, 2016; Melvin *et al.*, 2017), this may be a conserved feature between CDI systems and their homologues such as the CdrAB systems, which has previously been shown to play a role in biofilm maturation and structure formation (Reichhardt *et al.*, 2018). Therefore these additional functions indicate that these systems facilitate infection establishment, particularly in a polymicrobial environment which harbours many competitors pre-colonising that niche, whether from the native microbiota or in the case of CF other pathogens. As these systems appear to be present in a range of CF *P. aeruginosa* isolates and have been associated with early chronic infection stages in differentiated CF bronchial epithelium (Melvin *et al.*, 2017), the ramification of these systems in influencing both bacterial competitive and cooperative behaviours is only now beginning to be explored.

1.7 The type VI secretion system (T6SS) molecular harpoon

The T6SS is a classical one step mechanism utilised for a variety of functions involved in interbacterial competition and nutrient acquisition and plays a crucial role in virulence by various pathogens during infection. Originally identified in *V. cholerae* and *P. aeruginosa* in 2006 (Mougous *et al.*, 2006; Pukatzki *et al.*, 2006), it was shown to play an important role for cytotoxicity and mediating host interactions respectively. Spanning the entirety of the gram negative cell envelope, the T6SS has structural homology to bacteriophage needle and spike proteins (Basler *et al.*, 2012). This similarity indicates a highjacked phage system utilised by bacteria to secret out of the cell and provides a selective advantage to the bacterium. The

most recent classical system to be discovered, it is utilised to translocate protein effectors across the cell envelope into the ECM or directly into neighbouring cells via a contractile transmembrane structure. The T6SS structure is comprised of three main subunits: the baseplate, membrane and sheath complex (Cherrak *et al.*, 2019). Conserved in 25% of gram-negative bacteria (Bingle, Bailey & Pallen, 2008) the association with pathogenic and non-pathogenic bacteria suggests these systems provide a competitive advantage for invading new niches and outcompeting other microbes (Serapio-Palacios *et al.*, 2022) as well as providing a mechanism to evade the host immune response for infection tolerance (Lung *et al.*, 2022). However, due to its highly energy expensive mechanism, it is tightly regulated at a transcriptional and post-transcriptional level (Basler, 2015; Allsopp *et al.*, 2017, 2022).

The T6SS punctures through neighbouring membranes to deploy their protein effectors directly into neighbouring cells. Many of these effectors have enzymatic activity and act as bacterial-derived anti-bacterial toxins but have also been shown to encode anti-eukaryotic and trans-kingdom functions (Hernandez, Gallegos-Monterrosa & Coulthurst, 2020). The structure of the T6SS is complex, requiring multiple proteins with specific functions encoded within operons containing 13 core genes (Zoued *et al.*, 2014). Additional orphan genomic islands are encoded throughout the genome and contribute to the variability in spike complex and effectors utilised by the system (Allsopp *et al.*, 2017). The ability of this system to be employed as a virulence mechanism against eukaryotic cells has been identified (Hachani, Wood & Filloux, 2016; Trunk *et al.*, 2018) although it is primarily considered an anti-bacterial mechanism (Russell *et al.*, 2012; Cherrak *et al.*, 2019). Like the CDI system, a subset of the toxins have antibacterial activity and are encoded alongside an immunity, neutralising toxic activity via cognate binding to prevent autoinhibition (Russell, Peterson & Mougous, 2014).

Anti-eukaryotic toxins do not require encoded immunities, except for trans-kingdom effectors.

The T6SS has four subtypes which are associated with different bacterial genera. Deemed T6SS$^{i\text{-}iv}$ they vary in their structure and are associated with *Proteobacteriaceae* (i), *Thiotrichales* (ii), *Bacteroidetes* (iii), and *Amoebophilus asiaticus* (iv) respectively (Mougous *et al.*, 2006; De Bruin, Ludu & Nano, 2007; Russell *et al.*, 2014a; Böck *et al.*, 2017). Within *Proteobacteriaceae*, bacteria tend to encode multiple subtypes of the system, including *P. aeruginosa* which encodes three, however nomenclature for these systems has changed since their initial discovery. Originally deemed HSI to HSIII for Hcp Secretion Island I to III by Mougous *et al.* in 2006, they were later reclassified as the H1- to H3-T6SS in 2010 (Hood *et al.*, 2010). Like the CDI system, the T6SS is another contact dependent system. Unlike other pathogens, *P. aeruginosa* deploys these systems in a retaliatory fashion compared with bacteria such as *V. cholerae* which is antagonistic in its utilisation of the T6SS (Basler, Ho & Mekalanos, 2013). The prevalence of these systems in *P. aeruginosa* strains, particularly in clinical isolates, shows a great diversity in effector arsenals (Robinson *et al.*, 2023). As *P. aeruginosa* has been well characterised in dominating the CF lung environment and inducing a decline in diversity of the other microbes within the polymicrobial community (Flight *et al.*, 2015), the prevalence of both the CDI and T6SS may indicate that these systems play a role in this. Although this theory is promising in explaining the antagonistic dynamics of *P. aeruginosa,* and T6SS plays a role in virulence in *in vivo* infection models (Lesic *et al.*, 2007; Sana *et al.*, 2012), much is left to be elucidated to understand their role in CF infection.

1.7.1 The T6SS core operons and orphan islands

P. aeruginosa encodes three T6SSs, termed the H1-, H2- and H3-T6SSs that are encoded by three separate core clusters. Within these core clusters there is an observable variability in structure of the operon and genetic composition facilitating the utilisation of variable functions (Figure 1.20). Expression is readily enhanced via the deletion of the gene encoding the RetS kinase sensor which is a two-component system involved in sensing environmental signals such as membrane damage (Goodman *et al.*, 2009). Historically T6SSs were identified by the presence of Hcp and VgrG genes, but further studies indicated these systems formed multimeric protein complexes which hinted at a more complex molecular structure. This suggested a role for these proteins in the structural complex of the system instead of acting as effector proteins. Further elucidation of the genomic regions identified complex operons encoding multiple genes all contributing to system deployment. Conserved in more that 25% of gram-negative bacteria, they all share 13 core components despite their variation between and within various species (Russell *et al.*, 2014b; Allsopp *et al.*, 2020). These core components make up the structure of the secretion apparatus, whilst effector encoding genes are auxiliary and are found within the core cluster or in additional orphan islands spread throughout the genome (Allsopp *et al.*, 2017). Additionally, orphan islands can encode accessory proteins such as adaptors for effector association with the needle complex tip (Bondage *et al.*, 2016).

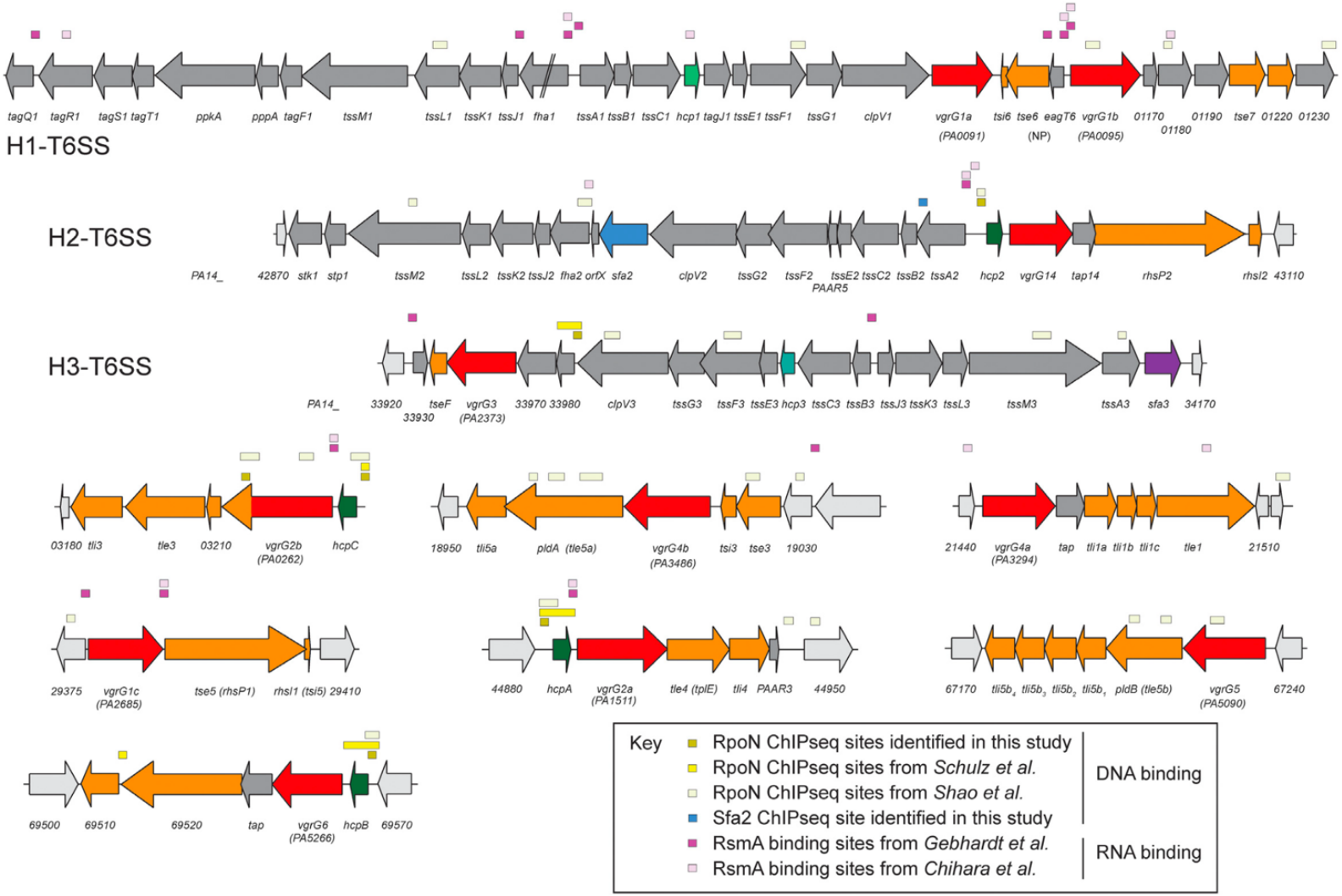


Figure 1.20: The type VI secretion system. Schematic representation of T6SS consisting of the membrane complex (TssJLM), baseplate (TssEFGK), Sheath (TssBC), Hcp tube, VgrG trimer and PAAR tip.

The T6SS structure is comprised of three subcomplexes and is outlined in Figure 1.21. The membrane complex is formed by TssJ, TssL and TssM proteins. Homologous to T4SS envelope-associated proteins IcmF and DotU (Schroeder, 2017), these were some of the first identified structural components of the system. This enabled T6SS evolution by enabling anchoring of the phage tail-like proteins to the bacterial cell membranes for firing out of the cell. TssM and TssL are components of the transmembrane complex and are associated with TssJ which recruits IM proteins during T6SS apparatus assembly (Durand *et al.*, 2015). It does so through the orientation of TssJ which faces the periplasm and interacts with the TssM periplasmic domain via the β1-β2 conserved loop (Felisberto-Rodrigues *et al.*, 2011; Robb *et al.*, 2013). TssM is then able to interact with the cytoplasmic domain of TssL and oligomerise where TssL then dimerises its cytoplasmic domain- an essential step in the correct assembly of the T6SS. The TssL C-terminal peptidoglycan binding motif is crucial for stable anchoring of the complex to the membrane (Durand *et al.*, 2015). This creates a pore in the membrane which is linked to the second structure associated with the membrane complex, the baseplate.

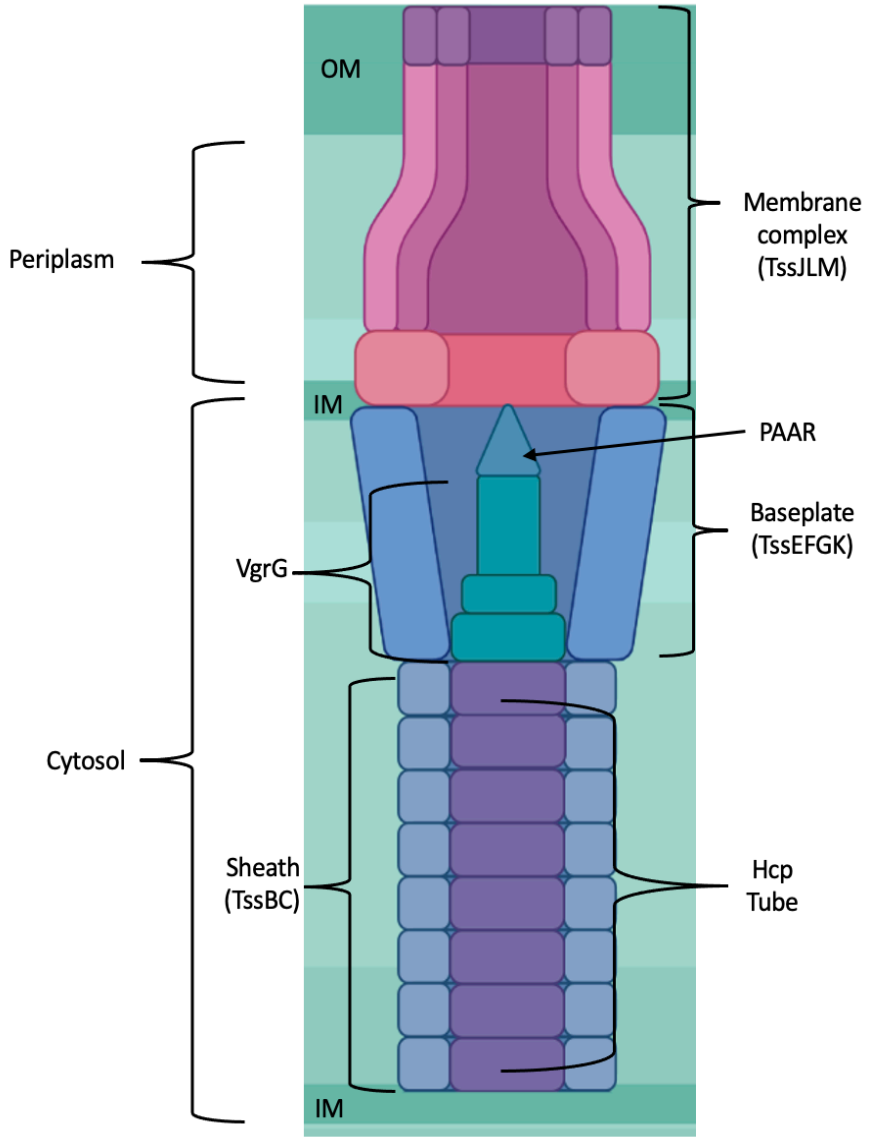


Figure 1.21: Core clusters and orphan islands of the type VI secretion system. Three core clusters H1-, H2-, and H3-T6SS and multiple orphan islands in PA14 are outlined above. Figure reproduced from (Allsopp *et al.*, 2022).

The baseplate is comprised of the TssF, TssG, TssK, TssE and TssA proteins and is situated at the IM portion of the membrane complex. It is required for the formation of the Hcp tube as well as mediating its translocation through the TssM pore. The baseplate also shows homology to T4 bacteriophage proteins. TssE was the first to be associated with the baseplate structure through its structural homology to T4 phage baseplate protein gp25 and indicated a complex structure for the system (Lossi *et al.*, 2011). Since the discovery of TssE homology, other components have T4 phage homology such as TssK with gp8/gp10 protein similarity which indicates a TssK trimer bridges the baseplate to the membrane components based on this structural homology (Taylor *et al.*, 2016; Nguyen *et al.*, 2017). TssF and TssG interact with

TssE, where TssG acts as an adaptor that interacts with TssK, whilst two TssF subunits interact with TssE to form the baseplate wedge (Park *et al.*, 2018). Meanwhile, TssA plays an essential role in assembly of the baseplate and sheath-tube. Further homology of TssA is observed with phage protein gp6 and forms a ring-shaped complex associated at the distal end of the sheath (Santin *et al.*, 2018; Bernal *et al.*, 2021).

The sheath, connected to the baseplate, is a contractile tube comprised of polymerised TssB and TssC heterodimers. The polymerised sheath structure forms a helical conformation which wraps around the Hcp tube in a high energy state and provides a collapsible structure that provides the force required for firing in a similar way to R-type pyocins from phage (Salih *et al.*, 2018). Internally, an additional tube complex comprised of Hcp proteins which form hexameric rings encompasses the structural 'harpoon-like' component fired externally from the cell (Douzi *et al.*, 2014; Mougous *et al.*, 2006). This tube is capped with a VgrG trimer and cone-like PAAR forming the sharp spike complex tip (Pukatzki *et al.*, 2007; Shneider *et al.*, 2013). VgrG interacts with the first hexameric Hcp via its flat proximal end which docks the tip to the harpoon sheath (Mougous *et al.*, 2006). *P. aeruginosa* possesses 10 and 8 gene variants to date of VgrG and PAAR proteins which are interchangeable for the association with different protein effectors (Hachani *et al.*, 2011; Wood *et al.*, 2019).

1.7.2 A nano-harpoon apparatus- the mechanism of T6SS deployment in P. aeruginosa

Upon the induction of membrane damage from antagonistic interactions with other bacterial cells, the attacked bacteria will sense the stress, relaying the signal via a signal transduction pathway to induce the expression of the T6SS core clusters involved in interbacterial

competition and retaliation (Figure 1.22) (Basler, Ho & Mekalanos, 2013). In *P. aeruginosa* this is via the Gac/Rsm pathway which will be discussed in 1.8 of this chapter. The membrane complex inserts into the membrane near the site of damage before the baseplate and sheath complex formation occurs (Stolle *et al.*, 2021). Polymerisation of the TssB-TssC heterodimer sheath is initiated at the distal end which is primed by TssA in the baseplate and assembles until it reaches the membrane of the cell opposite the site of assembly (Vettiger *et al.*, 2017). The sheath is then capped by TssA at the distal end which is thought to stabilise the elongated sheath by converting it from a high to low energy state which enables contraction from the baseplate within <2 ms (Basler *et al.*, 2012; Zoued *et al.*, 2016; Bernal *et al.*, 2021). This is a highly energy expensive mechanism and has been predicted to release ~1600 molecules of ATP worth of energy upon collapse to propel the harpoon out of the cell at an incredible rate of 100-800 µm/s (Basler, 2015). Upon firing, there is a release of roughly 100 Hcp proteins into the ECM (Lin *et al.*, 2019) and this is thought to contribute to inflammation, however this is yet to be determined in *P. aeruginosa* (Mougous *et al.*, 2006; Suarez *et al.*, 2010; Zhou *et al.*, 2012).

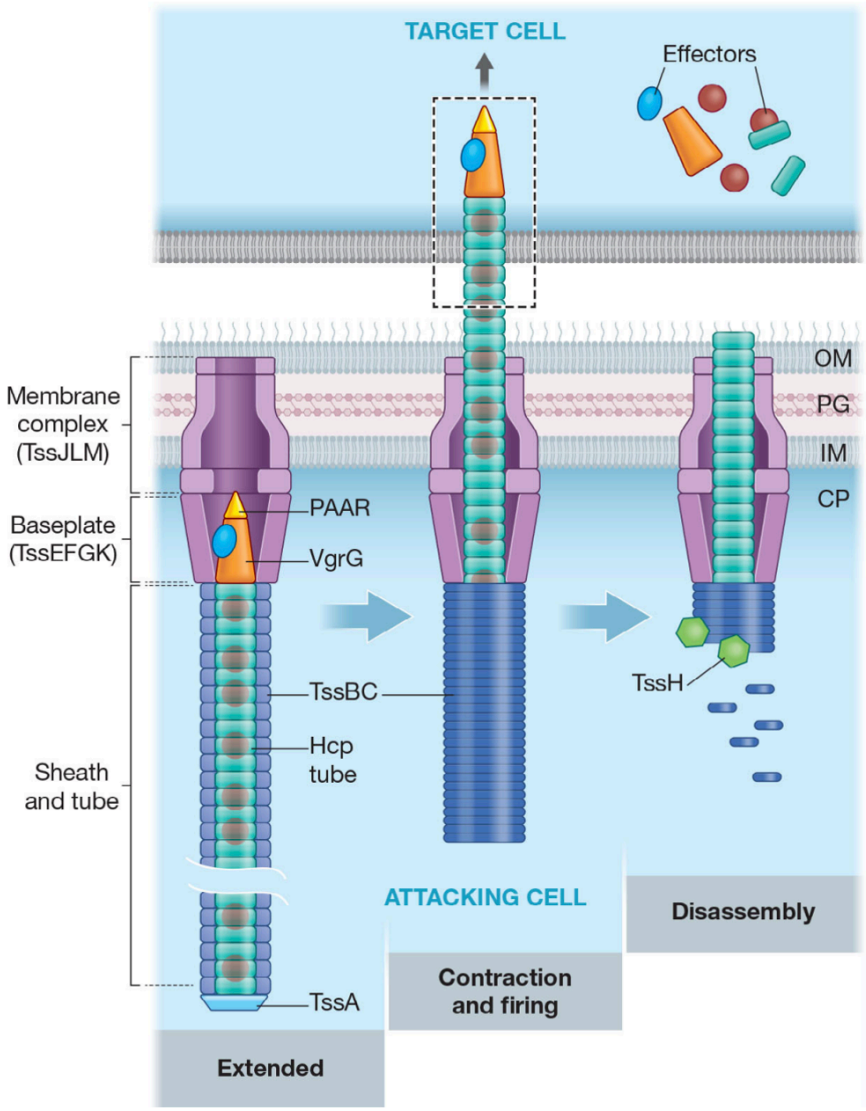


Figure 1.22: Mechanistic deployment of the T6SS system. The cycle of assembly, firing from extended state to contraction and finally disassembly is outlined above. Figure adapted from (Hernandez, Gallegos-Monterrosa & Coulthurst, 2020).

Post-firing an additional protein from the core cluster known as ClpV is utilised in recycling the components to enable subsequent firing events, which can be disassembled and reassembled at new sites on the membrane (Basler, Ho & Mekalanos, 2013; Stolle *et al.*, 2021). ClpV is an AAA$^+$-ATPase which interacts with the exposed TssC N-terminus (Pietrosiuk *et al.*, 2011), which is only exposed in the collapsed sheath state. This releases the contractile sheath subunits into the cytosol for recycled use in further apparatus assemblies by replenishing the cytoplasmic pool of TssB/TssC (Bönemann *et al.*, 2009; Pietrosiuk *et al.*, 2011; Basler *et al.*, 2012). Although many subunits of the T6SS have high homology to bacteriophage, ClpV is a unique features for bacteria- required due to the multiple assembling and disassembling cycles. This process can utilise accessory proteins, observed in *P.*

aeruginosa T6SS subtype H1, which employs TagJ to recruit ClpV to enhance the rate of disassembly for rapid succession of further firing (Förster *et al.*, 2014).

1.7.3 Transkingdom interactions and bacterial warfare

T6SS firing is used to deploy effectors into neighbouring cells in a contact-dependent competitive mechanism. These effectors can vary between strains which is seen throughout various bacterial genera such as *P. aeruginosa, Vibrio fischeri and Campylobacter jejuni* (Robinson *et al.*, 2021; Suria *et al.*, 2022; Robinson *et al.*, 2023). As previously outlined, *P. aeruginosa* encodes multiple VgrG and PAAR which associate with different effectors which have a range of functions. These effectors are specific and associate with a single subtype of the T6SS, H1- to H3-, where multiple effectors can be deployed simultaneously to enhance the effectiveness of the firing event. This is to ensure the energy expensive mechanism has maximal effect for its cost. Effectors for the T6SS are categorised into two subtypes: specialised and cargo (Figure 1.23) (Hernandez, Gallegos-Monterrosa & Coulthurst, 2020). Specialised effectors are accurately named due to their specific association with the tip complex via covalent links. The close association with the tip complex means these can be designated homologues of evolved Hcp/VgrG/PAAR proteins due to links with the structure of the tip which additionally have effector function capabilities. Cargo effectors however are non-covalently bound to the system, often associating with the internal Hcp tube, although some associate with the VgrG or PAAR and sit on the outside surface of the tip complex.

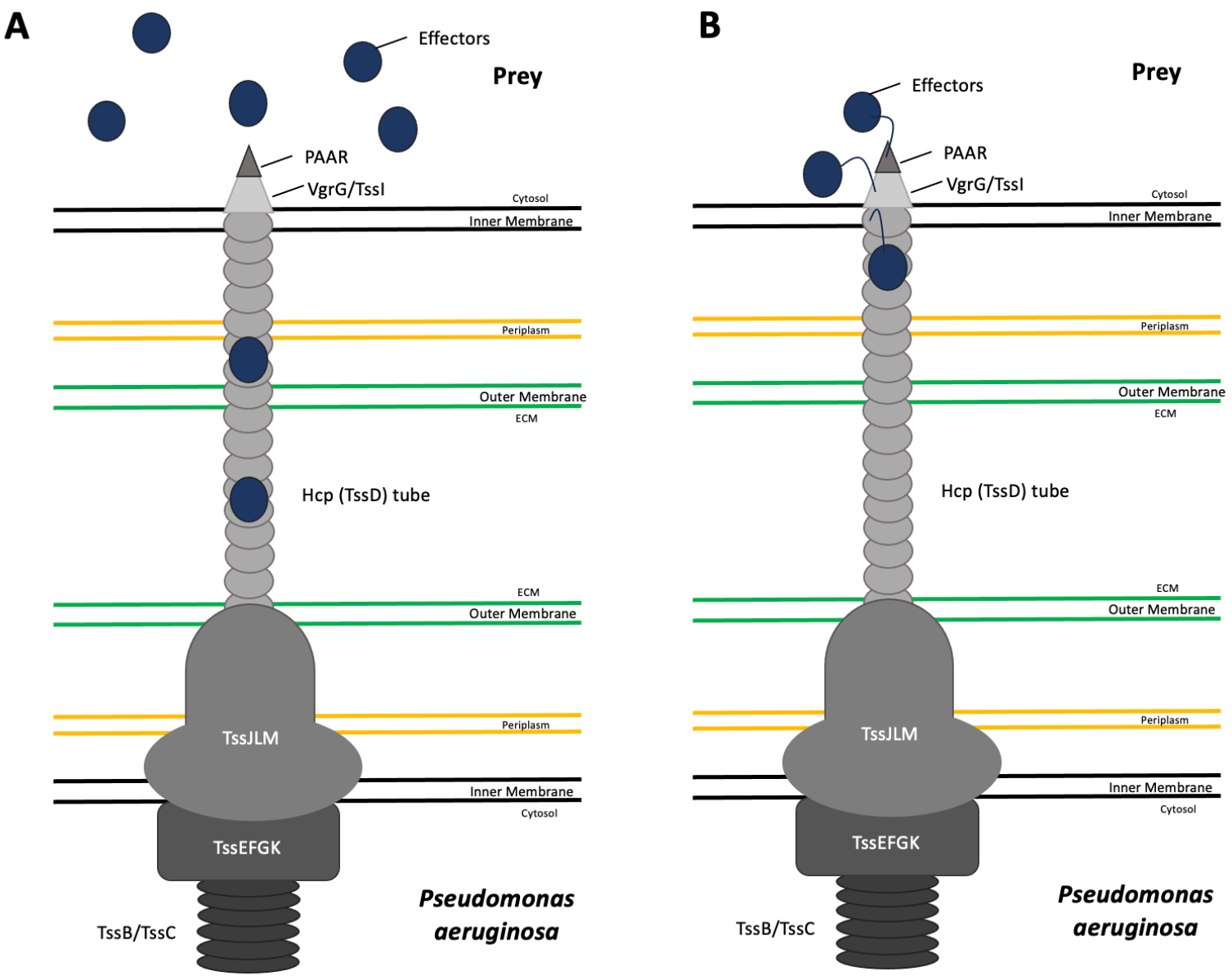


Figure 1.23: Mechanistic deployment of the T6SS system. (A) Cargo effectors, (B) Specialised effectors. Cargo effectors are non-covalently bound to the T6SS needle proteins, whilst specialised effectors have additional toxic domains that are extensions of VgrG, PAAR or Hcp proteins.

P. aeruginosa utilises the H1-T6SS for interbacterial competition, the H2-T6SS for anti-bacterial and anti-eukaryotic functions and uses the H3-T6SS for nutrient scavenging (Mougous *et al.*, 2006; Sana *et al.*, 2012; Sana, Bleves & Berni, 2016). Therefore, different types of effectors are associated with each system depending on their target. These have been grouped into four families designated Tae, Tge, Tle and Tde based on their respective amidase, glucosidase, lipase, and DNase functions. As the H1-T6SS is anti-bacterial, it largely encodes toxin-immunity modules such as those previously described for the CDI system. Commonly associated with Tse1-3, these were the first three antibacterial effectors associated with the H1-T6SS in *P. aeruginosa* (Hood *et al.*, 2010). Tse1 and Tse3 encode peptidoglycanase activity and are injected into the periplasmic space to disrupt the peptidoglycan layer (Russell *et al.*, 2012). Here Tse1 specifically cleaves the γ-D-glutamyl-l-meso-diaminopimelic acid amide bond (Benz *et al.*, 2012), whilst Tse3 cleaves the β-1,4-linkage of the peptidoglycan subunits N-acetylmuramic acid and acetylglucosamine (Lu *et al.*, 2013). Tse2 is a cytoplasmic toxin which targets the cytoplasm inducing a quiescent state in an NAD-dependent manner but the exact mechanism of intoxication remains unknown (Li *et al.*, 2012; Robb *et al.*, 2016). Since their discovery, a further five Tse effectors have been identified. Tse4 encodes a lytic transglycosylase which can target both gram-positive and negative bacteria (Le *et al.*, 2021), Tse5 is a pore-forming toxin (González-Magaña *et al.*, 2022), Tse6 encodes a $NAD(P)^+$-glycohydrolase (Whitney *et al.*, 2015), Tse7 is a DNase (Pissaridou *et al.*, 2018) and finally Tse8 targets the transamidosome (Nolan *et al.*, 2021).

The H2-T6SS is linked with anti-bacterial and anti-eukaryotic activity in *P. aeruginosa*. Most associated with the Tle effector class, it encodes a eukaryotic-like phospholipase D effector called PldA. PldA degrades phosphatidylethanolamine- a key component of the bacterial

membrane (Russell *et al.*, 2013). PldA and a second phospholipase D effector PldB are also involved in *P. aeruginosa* invasion into host cells by targeting the PI3K/Akt pathway (Kierbel *et al.*, 2005; Jiang *et al.*, 2014), and requires the respective VgrG4b and VgrG5 for export (Wettstadt *et al.*, 2019). It also possesses a Tle effector Tle4 (or TplE) which encodes a phospholipase function which alongside PldA/PldB has been deemed a 'trans-kingdom effector' (Bleves, 2016; Jiang *et al.*, 2016). Additionally, the VgrG2b effector encodes a zinc-metallopeptidase which interferes with cell division through the induction of membrane blebbing (Wood *et al.*, 2019). The H2-T6SS has the broadest target range where it is additionally utilised in copper acquisition to provide a selective advantage in growth as copper utilisation occurs by multiple enzymes associated with various crucial intracellular functions such as the NADH dehydrogenase (Festa & Thiele, 2011; Han *et al.*, 2019). It also secretes the molybdate binding protein ModA which transports molybdenum ions through OM receptor IcmP for adaptation to anaerobic environments (Wang *et al.*, 2021).

Unlike the H1- and H2-T6SS, relatively little is understood about the H3-T6SS which is not readily expressed under laboratory conditions, making its function difficult to dissect. To date it has been linked to iron acquisition- a crucial function for virulent bacteria. It secretes the effector TseF which is incorporated into OM Vesicles (OMVs) through direct binding to the PQS quinolone QS signal. Remarkably, it facilitates uptake of these iron-containing OMVs via the OprF porin FptA receptor and is utilised in both cell signalling and siderophore-based functions (Lin *et al.*, 2017). Most recently it has also been linked to combatting H_2O_2 stress through RpoS regulation which inhibits quinolone signal PQS in iron-rich conditions and in turn regulates the expression of the H3-T6SS structural genes and *tseF* (Lin *et al.*, 2023).

The range of functions these systems provide increases the likelihood that they are used in highly hostile environments such as in the CF lung and that they provide a selective advantage to the pathogen by providing hostile takeover factors utilised in establishing and maintaining chronic infection. As the CDI systems have shown a role in the colonisation of CF epithelia (Melvin *et al.*, 2017), this indicates the T6SSs may be utilised by the bacteria for the dominance of the polymicrobial community and control of the diversity observed in patients during disease progression upon acquisition of the infection (Flight *et al.*, 2015). However, this is yet to be determined *in vivo* for *P. aeruginosa*, therefore there is much left to learn about the role these systems play in CF infection.

1.8 Regulation networks and controlling bacterial phenotypes

Due to the complexity of bacterial responses to stimuli from their environment, various virulence determinants are regulated at the transcriptional, post-transcriptional and post-translational levels. Particularly with the secretion systems which are highly energy expensive and potent, these are tightly regulated for the cost-benefit of expressing these systems. Virulence factors are often coregulated under an overarching gene network which is able to coordinate a change in bacterial phenotype, such as the motile-sessile switch (Li *et al.*, 2017), to bring about a response during various phases of infection. These overarching regulation networks control multiple virulence mechanisms and are often controlled via two-component systems (TCS) (Gao *et al.*, 2020). For the motile-sessile switch in *P. aeruginosa*, this is controlled by the Gac/Rsm signal transduction cascade which is considered a global regulation network (Martínez-Granero *et al.*, 2012). These are some of the most important tools in the bacteria's arsenal as it allows adaptation to the immediate environment through sensing and

transmitting through a relay cascade to bring about a global response (Stock, Robinson & Goudreau, 2000; Gao, Mack & Stock, 2007).

TCSs generally encompass the transfer of a phosphoryl molecule between two components such as a histidine kinase which contains the sensory domain, of which the response is then relayed through its associated response regulator protein which contains the regulation domain (Gao & Stock, 2009). These TCS are broadly found within bacteria, archaea and some eukaryotes (Wuichet, Cantwell & Zhulin, 2010). TCS control crucial functions in many branches on the tree of life by regulating the mechanisms in response to the environment. The variation in lifestyles and broad host range observed by *P. aeruginosa* confers an additional need for a controlled response which is flexible and encompasses multiple input stimuli to trigger the expression of the correct virulence factors in retaliation.

Due to its complex lifestyle, *P. aeruginosa* possesses a multitude of complex networks which is multi-layered for efficient utilisation of its many virulence factors. These networks are yet to be understood in their entirety due to differences observed in clinical isolates through changes in these regulation networks upon adaptation to various niches such as those found in the CF lung. This adds an additional layer of complexity to understanding these pathways, and much work is required to elucidate their relationships to observed responses and phenotypes at a cellular level. However, many of the important regulation pathways for these systems will be conserved. The differences between clinical and lab strains therefore gives insight into how and when bacteria switch on specific virulence factors which can be useful in combatting these infections. This inherent flexibility and ability to sense and adapt to multiple stimuli is utilised by *Pseudomonas* in the CF lung which enhances the inherent difficulty of

removing the infection once established in the lungs. Therefore understanding the interplay of these pathways with the expression of virulence determinants is crucial in elucidating *P. aeruginosa* adaptability to the CF environment during various stages of infection.

1.8.1 The post-transcriptional Gac/Rsm regulation pathway

The Gac/Rsm pathway is the most well resolved in its role in regulating the secretion systems, biofilm and motility at a post-transcriptional level and a major focus of this thesis and will therefore be discussed first. GacS/GacA is a well-characterised global regulator TCS which feeds into the Rsm signal cascade pathway and is primarily associated with the motile-sessile switch. However, it controls many additional roles such as the production of QS molecules, secondary metabolites and antibiotic resistance (Figure 1.24) (Latour, 2020; Song, Li & Wang, 2023). GacS comprises the membrane bound sensor kinase whilst GacA comprises the response regulator (Rich *et al.*, 1994; Yan *et al.*, 2018), which are regulated by sensor kinase RetS and LadS for GacS repression and activation respectively (Ventre *et al.*, 2006). RetS represses the Gac/Rsm network by directly interacting with the H1 domain to prevent autophosphorylation (Goodman *et al.*, 2004, 2009; Ali-Ahmad *et al.*, 2017). Alternatively LadS activates GacS via phosphorelay and is activated through calcium sensing in the periplasm (Ventre *et al.*, 2006; Chambonnier *et al.*, 2016; Broder, Jaeger & Jenal, 2016).

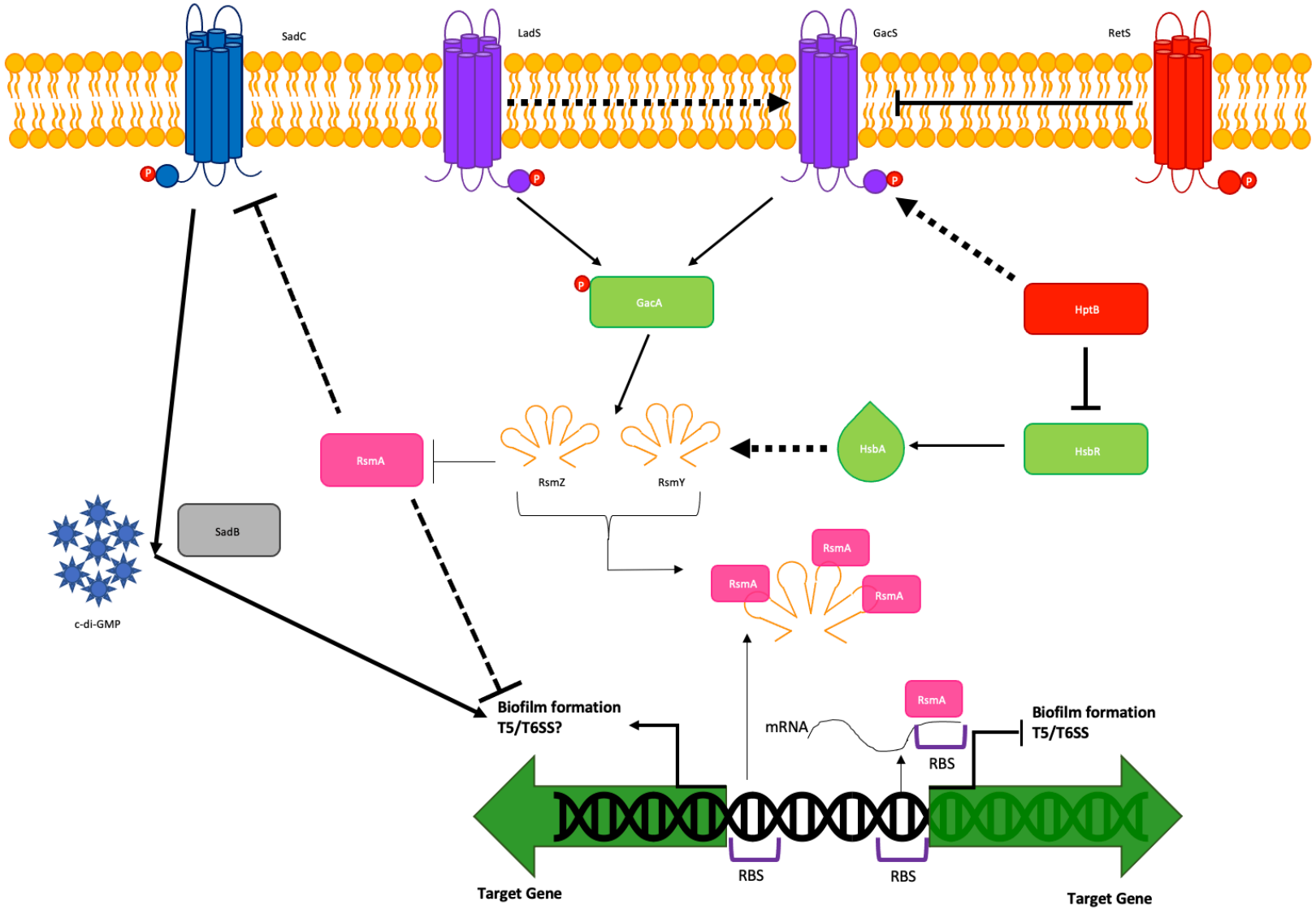


Figure 1.24: The Gac/Rsm global regulation pathway. Schematic representation integrated Gac/Rsm pathway with cyclic di-GMP for regulation of phenotypes and mechanisms associated with the motile-sessile switch.

GacA activation induces the expression of small regulatory non-coding RNAs (sRNA) *rsmY* and *rsmZ* (Brencic *et al.*, 2009). RsmY and RsmZ form stem loop structures and are composed of GGA motifs known to enable binding to a secondary global post-transcriptional regulator RsmA (Valentini *et al.*, 2017). RsmA is an RNA binding protein from the Rsm/Csr pathway and is a direct regulator of gene expression (Vakulskas *et al.*, 2015). RsmA regulates translation and acts by binding to the GGA motifs often overlapping the ribosomal binding sites (RBS) and negatively regulate specific genes by preventing translation (Brencic *et al.*, 2009). RsmA is an activator of the motile and a repressor of the sessile phenotype (Francis *et al.*, 2017). To induce the switch to a sessile lifestyle and activate the sRNAs, GacA is phosphorylated by LadS or GacS (Ventre *et al.*, 2006) where it binds the GacA box palindromic sequences upstream of *rsmYZ* genes to activate transcription (Brencic *et al.*, 2009; Humair, Wackwitz & Haas, 2010). RsmYZ directly interacts with RsmA via preferential binding sites to sequester it from the nascent mRNA allowing translation to occur (Janssen *et al.*, 2018).

The HptB/HsbR system is linked to this pathway, where HptB counteracts GacS repression by interacting with RetS upon phosphorylation. This in turn phosphorylates HsbR, a dual phosphatase and kinase, which regulates the phosphorylation state of anti-anti-sigma factor HsbA. HptB and HsbA both converge on RsmY, controlling intracellular availability and therefore expression of motility genes (Moscoso *et al.*, 2014). The SadBC system also converges with RsmA which is involved in c-di-GMP production which plays a role in the phenotype regulation as previously described in 1.7.2 (Martínez-Granero *et al.*, 2012).

The Gac/Rsm regulatory network has been linked to many virulence mechanisms in *P. aeruginosa* infection. This includes CF specific links via *in vivo* mouse acute infection models

(Jander, Rahme & Ausubel, 2000). Specifically it has been linked to the regulation of both the CDI and T6SSs and negatively regulates their expression post-transcriptionally (Mercy *et al.*, 2016; Allsopp *et al.*, 2017). Therefore it plays a crucial role in interbacterial competition and the expression of competitive secretion systems. As Gac/Rsm is associated with the regulation of QS molecules such as N-acyl homoserine lactone (AHL) (Kay *et al.*, 2006) which are crucial in the expression of other virulence determinants associated with chronic infection such as biofilm formation, it shows a complex interplay of regulation networks to switch to chronic infection. Isolates from CF patients are often found to have pathoadaptive mutations within the GacS network which enhance colonisation and mucoid phenotype induction upon chronic infection initiation, such as *ladS* mutation in *P. aeruginosa* strain PA14 (Mikkelsen, Mcmullan & Filloux, 2011; Cramer *et al.*, 2011; Marvig *et al.*, 2014). This outlines the fine tuning of these networks controls the phenotypes observed in patients, aided through the transcriptional regulation of these systems, and are outlined within the section below.

1.8.2 Sigma factors and enhancer binding proteins in transcriptional regulation

The first level of regulation associated with secretion systems is at the transcriptional level, which is yet to be fully elucidated. To date, far more is known about the transcriptional regulation of the T6SS whilst that of the CDI system in *P. aeruginosa* remains unknown. Transcriptional regulation occurs at the promotor site of a gene where the transcription initiation complex forms to induce gene expression via open complex formation. This involves an RNA polymerase (RNAp) and sigma factors (Bush & Dixon, 2012; Chen, Boyaci & Campbell, 2021). Upon promotor recognition, loading of single stranded DNA into RNAp occurs in an ATP-dependent manner for some sigma factors such as RpoN (Sharma *et al.*, 2014). Some

sigma factors requires additional factors for transcription initiation such as enhancer binding proteins which interact via conserved motifs (Zhang *et al.*, 2009; Gao *et al.*, 2020). *P. aeruginosa* has >25 sigma factors although it is yet to be determined which are involved in the regulation of the T6SS (Potvin, Sanschagrin & Levesque, 2008).

The first regulator of *P. aeruginosa* T6SSs is the global repressor histone-like nucleoid structuring (H-NS) protein homologue MvaT. MvaT is thought to be a negative regulator of T6SS due to the ability to bind to T6SS coding regions, facilitating chromosomal supercoiling through the recognition of AT-rich regions in the 5' end of these regions (Dorman, 2004; Castang *et al.*, 2008). In addition to the supercoiling, these systems appear temperature sensitive where the H2-T6SS is upregulated at 25 °C where H1- and H2-T6SS can also be expressed at 37 °C in PA14, but this differs in PAO1 where only H2-T6SS is expressed at 25 °C (Wurtzel *et al.*, 2012; Allsopp *et al.*, 2017). This suggest that these systems are differentially regulated to provide different roles during colonisation and infection.

T6SS is regulated by the transcription factor AmrZ which is linked to the well characterised Gac/Rsm pathway outlined in the previous section. AmrZ is utilised to fine tune the expression of T6SSs compared with the post-transcriptional regulator RsmA which modulates all associated T6SS mRNAs, upregulating H1- and H3-T6SS and downregulating H2-T6SS (Allsopp *et al.*, 2017). AmrZ is itself regulated by PhoB where it can directly bind to the *fleQ* promoter for inhibition of H1-T6SS expression via c-di-GMP (Zhou *et al.*, 2022). AmrZ has additionally been linked to the motile-sessile switch through controlling the expression of biofilm genes where it positively regulates both twitching motility and *alg* operon expression to control levels of Psl production (Jones *et al.*, 2013).

The major transcriptional regulator associated with the T6SS is sigma factor RpoN. Also known as the major alternative sigma factor, RpoN was initially linked to nitrogen metabolism, but many studies are now associating it with the regulation of surface expressed proteins and other virulence factors (Buck *et al.*, 2000; Francke *et al.*, 2011; Riordan & Mitra, 2017; Shao *et al.*, 2018). Most commonly linked to the expression of flagellar operon, it is required for a range of bacterial virulence factors in both plant and animal models (Hendrickson *et al.*, 2001). It is utilised for open complex formation by the polymerase complex and requires additional proteins known as enhancer binding proteins (EBPs) such as FleQ to activate RpoN and enable the expression of flagellar genes (Figure 1.25) (Dasgupta *et al.*, 2003). In *P. aeruginosa* RpoN influences expression of the H2- and H3-T6SS (Bernard *et al.*, 2011; Sana *et al.*, 2013; Shao *et al.*, 2018). Other enhancer binding proteins such as Sfa2 have been reported to be involved in expressional repression of H2-T6SS in regard to RpoN (Sana *et al.*, 2013), however work I contributed to that is presented in Chapter 7 and now a published study challenges this observation as only one identified EBP was shown to contribute to regulation.

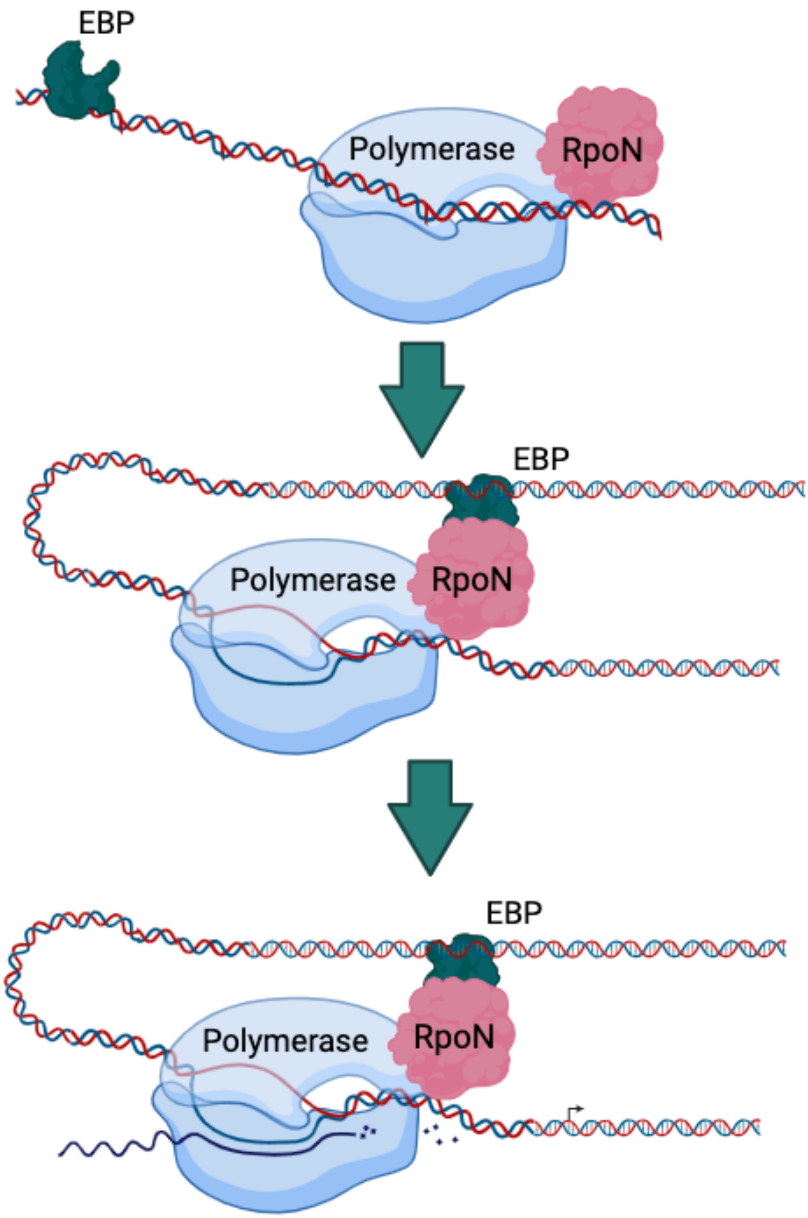


Figure 1.25: RpoN transcription initiation through the utilisation of enhancer binding proteins. RpoN major alternative sigma factor binds to the polymerase associated with the promotor region of a gene of interest in the DNA. EBPs bind upstream and induce DNA bending before associating with RpoN. Association initiates open complex formation and therefore initiates transcription via the polymerase.

In addition to these transcriptional regulators, other regulators which have been linked to the expression of the T6SSs as well as to the motile-sessile switch is through QS. *P. aeruginosa* encodes three QS systems which are interlinked (Figure 1.9); Las and Rhl named due to their historic discovery in controlling elastase and rhamnolipid production respectively (Gambello & Iglewski, 1991; Ochsner & Reiser, 1995). This also controlled by the PhoB-PhoR TCS which in itself upregulates the H1- and H3-T6SSs (Bains, Fernández & Hancock, 2012). Due to their role in the regulation of virulence factors, QS systems and particularly the *lasR* gene are regularly found with inactivating mutations in CF chronic isolates from adaptation to the lungs (Hoffman *et al.*,

2009). Studies have identified the H2- and H3-T6SSs to be controlled by the Las and Rhl QS systems (Lesic *et al.*, 2009).

For CDI systems, in *A. baumanii* PhoB is a suggested transcriptional regulator which acts through differential phosphate levels. This could be utilised in *P. aeruginosa* as PhoB has previously been characterised to play a role in the expression of the T5SS/TPS genes *tspA/tpsB* (Faure *et al.*, 2013). An additional regulator proposed in *P. aeruginosa*, BfmR, negatively regulates the CDI as well as showing roles in T6SS regulation (Krasauskas *et al.*, 2019; Perez Mora *et al.*, 2023). As overlapping regulators have been observed between the CDI and T6SS at a post-transcriptional level in *P. aeruginosa*, they may be coregulated for a coordinated response. Although BfmR has not been implicated in transcriptional T6SS regulation in *P. aeruginosa*, it may be an important regulator in the motile-sessile switch as it controls the expression of various genes such as *phzA1* for pyocyanin production and biofilm formation and cell death through QS regulation alongside PhoB (Huang *et al.*, 2019; Fan, Cao & Lan, 2021). Although this indicates an overlap in regulation between the two systems, little evidence besides a role for RsmA has been elucidated *in vitro* (Mercy *et al.*, 2016).

Other CDI homologues such as the CdrAB system have their transcriptional regulation linked to c-di-GMP. For LapA secretion (as previously discussed in 1.7.2), c-di-GMP controls transcription by binding to FleQ which in turn interacts with sigma factor RpoS and induces the synthesis and subsequent expression of the protein (Martínez-Gil, Ramos-González & Espinosa-Urgel, 2014). As c-di-GMPs have extensively been shown to have a role in the motile-sessile switch, control of expression of other CDI homologues could indicate these systems are co-regulated and therefore may play an important role upon colonisation and chronic

infection establishment. This is supported by the T6SS regulator AmrZ, which has been linked to T5SS *cdrA* regulation which when expressed has also been shown to play a role in biofilm maturation (Jones *et al.*, 2014; Reichhardt *et al.*, 2018). Therefore this indicates AmrZ may be a major general regulator in secretion systems but is yet to be validated experimentally.

1.8.3 Post-translational regulation and other networks for virulence factor interplay

The final level of regulation is at the post-translational level. To date, no post-translational regulation has been determined for the CDI systems. Several *Proteobacteriaceae* have been found to contain an additional gene in the CDI operon CdiC which currently has an unknown function but has been proposed to be involved in CdiA generation and/or post-translational modification (Ruhe *et al.*, 2013; Ogier *et al.*, 2016). Looking more broadly at T5SSs, several have been shown to require cleavage for full activity such as NalP in *N. meningitidis* (Roussel-Jazédé *et al.*, 2010), or glycosylated such as AIDA-I from *E. coli* (Benz & Schmidt, 2001). To date this has not been shown to be a feature of CDI systems, but such post-translational modification could occur.

Due to the requirement of the Sec translocation pathway outlined above in 1.1.1, post-translational modifications may occur co-translationally during export due to the protection of the nascent chains by the chaperone proteins which could facilitate modification (Hoffmann, Bukau & Kramer, 2010; Bruel & Genevaux, 2014). As these proteins can additionally be targeted post-translationally to the Sec machinery, there may be mechanisms allowing post-translational regulation and modification via both Sec translocon mediated

pathways (Dautin, 2021). However, this remains conjecture and much research is required to validate any post-translational regulation of the CDI systems.

For the T6SS, much more is understood about its post-translational modification. In *P. aeruginosa*, the H1-T6SS is controlled by the antagonistic activity of the serine-threonine kinase PpkA and phosphatase PppA. Both proteins are encoded in the H1-T6SS core cluster. They act by controlling the phosphorylation state of Fha1 protein and therefore ClpV-mediated sheath disassembly (Figure 1.26) (Mougous *et al.*, 2007). PpkA autophosphorylation is induced by the TagRSTQ transmembrane signalling complex directly through TagR upon sensing environmental signals through the TagQ-TagTS complex (Hsu, Schwarz & Mougous, 2009; Casabona *et al.*, 2013). This recruits Fha1 which becomes phosphorylated and co-localises ClpV1 and is known as threonine phosphorylation (TPP) dependent regulation (Mougous *et al.*, 2007; Silverman *et al.*, 2011). Membrane targeting antibiotics, T6SS attack and conjugative pili stimulate this pathway to initiate counterattack (Basler, Ho & Mekalanos, 2013; Basler, 2015). This adds an additional level of regulation for the activation of the H1-T6SS, however the utilisation of a similar system by the H2- and H3-T6SSs is yet to be determined. The H2-T6SS encodes a phosphatase and kinase called *stp1* and *stk1* respectively, as well as encoding *fha2* and indicates that this may be utilised for this system but is yet to be validated *in vitro* (Mukhopadhyay *et al.*, 1999).

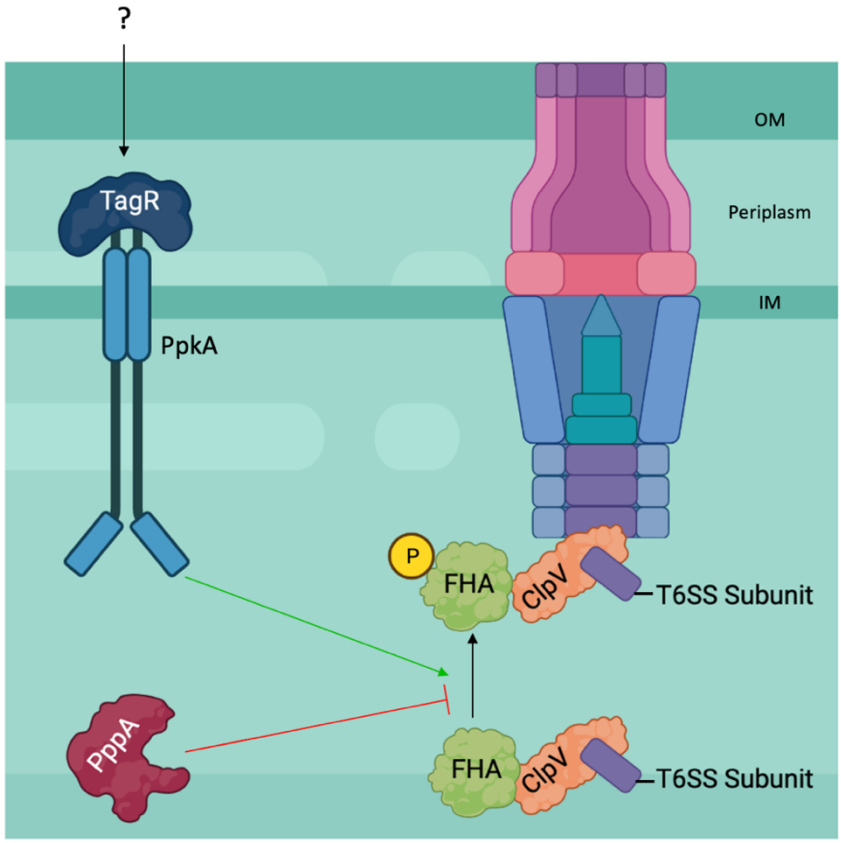


Figure 1.26: The threonine phosphorylation (TPP) post-translational regulation of the T6SS. Schematic representation of the posttranslational regulation of the T6SS via the PpkA kinase and PppA phosphatase.

Although TagRSTQ is conserved in other bacteria such as *Serratia marcescens*, it is not a ubiquitous regulation system (Ostrowski *et al.*, 2018). *Agrobacterium tumefaciens* does not show Fha phosphorylation but instead phosphorylates TssL which in turn recruits Fha and induction of TssM-mediated ATP hydrolysis for activation (Lin *et al.*, 2014). The disparity in regulation of the systems between bacteria outlines their adaptability. In addition to the TPP system, regulation is also induced by TagF which is independent of TPP. TagF also activates H1-T6SS but represses secretion upon overexpression, however the exact method of induction remains to be elucidated (Silverman *et al.*, 2011).

Due to the energy expensive nature of the T6SS and limiting aggression when it would not be advantageous, the use of other currently uncharacterised mechanisms of post-transcriptional regulation is likely. Due to the many environmental signals which integrate for the regulation of the T6SS, controlling regulation pathways may be disparate to express the system in a

stimuli-dependent manner. The differences in the regulation at all levels between the various T6SSs supports this idea. The additional co-regulation of both the CDI and T6SS through the Gac/Rsm pathways indicates these systems are similarly suppressed in prosperous conditions. However, more work is required to determine the extent of this co-regulation and if they share more regulators. This is especially the case for CDI systems where little is understood about their regulation. Understanding the regulator mechanisms of these systems would be beneficial in elucidating environmental signals that control the expression of one system subtype versus another.

1.9 Project overview and aims

P. aeruginosa is a highly versatile organism which is successful at colonising a multitude of niches, attributed to its large and highly mosaic genome (Moradali, Ghods & Rehm, 2017; Robinson *et al.*, 2023). A common agent in nosocomial infections often being multidrug resistant means that a better understanding of its colonisation mechanisms and new therapies are required to combat its prevalence in the population (WHO, 2017). Mounting evidence shows that contact dependent killing systems such as the CDI and T6SS have clear roles in interbacterial and interstrain competition that can have roles in virulence through clearing bacteria and for successful colonisation and dominance of host niches (Mercy *et al.*, 2016; Hachani *et al.*, 2014). Moreover, both the CDI and T6SS have been shown to have direct roles in virulence in animal models (Sana *et al.*, 2012; Melvin *et al.*, 2017; Allen *et al.*, 2020; Bernal *et al.*, 2021). As the CDI systems to date have mostly been outlined both *in vitro* and *in vivo* in *E. coli*, identifying and validating these systems in *P. aeruginosa* will enable us to infer the importance of their role in pathogen dominance in the CF airways. The high

conservation of these systems within gram-negative bacteria (Abby *et al.*, 2016; Allsopp *et al.*, 2020) suggests they could be exploited in the future as targets for new therapies. Further characterisation of these systems in *P. aeruginosa* strains will enhance our understanding of infection mechanisms in conditions such as cystic fibrosis where *P. aeruginosa* is responsible for the largest burden to patient health, life span and quality of life. The hypotheses of my study are:

1. *P. aeruginosa* encodes multiple CDI systems with diverse toxicities
2. These CDI systems are functional inducing bacterial intoxication which is specific due to their unique toxin-immunity modules
3. CDI systems play a role in interbacterial competition and cooperation and therefore influence the ability of *P. aeruginosa* to colonise a niche and control of the polymicrobial community in CF
4. A functional tool such as antibodies can be generated and used to study the presence and activity of the systems *in vitro*
5. Expression of the CDI and T6SS are regulated at multiple levels through specific and overlapping mechanisms

I will investigate these hypotheses through the following aims:

1. Engineer deletion mutants of the CDI systems in *P. aeruginosa* (Chapter 3 and 4)
    a. Identify and characterise the systems encoded in *P. aeruginosa* strain PA14 via bioinformatics analysis
    b. Engineer mutants in PA14, *rsmA*, *rsmA*H123 and H123 backgrounds

c. Clone toxin-immunity modules into inducible vectors to validate via expression, western blot analysis and co-immunoprecipitation assays

2. Generate specific antibodies against conserved CdiA regions of the two CDI systems in *P. aeruginosa* (Chapter 5)

   a. Identify system conserved protein regions, cloning corresponding encoding regions into inducible vectors
   b. Use western blot analysis to confirm expression
   c. Purify proteins using on-column streptactin resin
   d. Send purified proteins to Eurogentec to generate rabbit polyclonal antibodies

3. Perform bacterial competition and cooperation assays using constructed mutants to evaluate the systems' roles in (Chapter 6):

   a. Interbacterial competition
   b. Interbacterial cooperation e.g. motility and biofilm formation
   c. Intrabacterial competition using other common CF pathogens

4. Characterise *rsmA*, *rpoN*, *sfa2* and *sfa3* mutants for altered T6SS expression and impact on biofilm and motility and the role of *rpoN* and *rsmA* in CDI expression (Chapter 7)

   a. Perform H2-T6SS and H3-T6SS *lacZ* promoter assay
   b. Perform biofilm and motility assays
   c. Utilise a previously generated transcriptomics dataset by the Allsopp group to identify expression of CDI in *rpoN* and *rsmA* mutant strain backgrounds

2. Materials and methods

2.1 Bacteria

Bacterial strains were drawn from the Allsopp collection at Imperial College London (Allsopp *et al.*, 2017).

Table 2.1: *Pseudomonas* strains and strain background deletion mutant constructs

Bacteria	Strain	Vector	Mutation	Origin
E. coli	CC118λPIR	pKNG101	-	(De Lorenzo *et al.*, 1990)
E. coli	CC118λPIR	-	-	(De Lorenzo *et al.*, 1990)
PA14	-	-	-	(Rahme *et al.*, 1995)
PA14	-	-	*rsmA*	(Allsopp *et al.*, 2017)
PA14	-	-	*rsmA*H123	Allsopp lab repository
E. coli	CC118λPIR	pKNG101	*rsmA*	Allsopp lab repository
E. coli	pRK2013	-	-	(Figurski & Helinski, 1979)
E. coli	CC118λPIR	pKNG101	ΔCDI^{00510}	This project
PA14	-	-	ΔCDI^{00510}	This project
PA14	-	-	*rsmA*H123 ΔCDI^{00510}	This project
PA14	-	-	*rsmA* ΔCDI^{00510}	This project
E. coli	TOP10	pCR BluntII-TOPO	ΔCDI^{00510}	This project
PA14	-	mini-CTX:*lacZ*	-	Allsopp lab repository
PA14	-	mini-CTX:*lacZ*	*rsmA*	Allsopp lab repository
E. coli	CC118λPIR	pKNG101	ΔCDI^{32790}	This project
PA14	-	-	*sfa2*	(Allsopp *et al.*, 2022)
PA14	-	-	*sfa3*	(Allsopp *et al.*, 2022)
PA14	-	-	*rpoN*	Allsopp lab repository
PA14	-	-	*rsmAsfa2*	(Allsopp *et al.*, 2022)
PA14	-	-	*rsmAsfa3*	(Allsopp *et al.*, 2022)

PA14	-	-	*rsmArpoN*	(Allsopp *et al.*, 2022)
PA14	SMC 232	-	-	(Limoli *et al.*, 2019)
PA14	SMC 3782	-	*pilA*	(Limoli *et al.*, 2019)
PA14	SMC 5845	-	*flgK*	(Limoli *et al.*, 2019)
PA14	SMC 6595	-	*flgKpilA*	(Limoli *et al.*, 2019)
PA14	-	-	ΔCDI^{32790}	This project
PA14	-	-	*rsmA* ΔCDI^{32790}	This project
PA14	-	-	*rsmA*H123 ΔCDI^{32790}	This project
E. coli	CC118λPIR	pKNG101	*rsmA*	This project
PA14	-	-	ΔCDI^{00510}ΔCDI^{32790}	This project
PA14	-	-	*rsmA* ΔCDI^{00510}ΔCDI^{32790}	This project
PA14	-	-	*rsmA*H123 ΔCDI^{00510}ΔCDI^{32790}	This project
PA14	-	-	H123	This project
PA14	-	-	H123 ΔCDI^{32790}	This project
PA14	-	-	H123 ΔCDI^{32790}	This project
PA14	-	-	H123 ΔCDI^{00510}ΔCDI^{32790}	This project
E. coli	TOP10	pET29a:*amrZ*	-	(Allsopp *et al.*, 2017)
E. coli	TOP10	-	-	Invitrogen
PA14	-	-	*rsmA*H123 ΔCDI^{00510}	This project
E. coli	TOP10	pCR BluntII-TOPO	Antibody System 1	This project
E. coli	TOP10	pCR BluntII-TOPO	Antibody System 2	This project
PA14	-	-	*retS*	(Goodman *et al.*, 2004)
E. coli	TOP10	pET29a	Antibody System 1	This project
E. coli	TOP10	pET29a	Antibody System 2	This project
E. coli	TOP10	pRL662	-	(Hachani *et al.*, 2014)
PA14	-	-	*rpoN*	(Allsopp *et al.*, 2017)
PA14	-	-	A2tc	(Allsopp *et al.*, 2017)
PA14	-	-	A2tc *rsmA*	(Allsopp *et al.*, 2017)
PA14	-	-	A2tc *rsmArpoN*	(Allsopp *et al.*, 2017)
PA14	-	-	B3tc	(Allsopp *et al.*, 2017)

PA14	-	-	B3tc *rsmA*	(Allsopp *et al.*, 2017)
PA14	-	-	B3tc *rsmArpoN*	(Allsopp *et al.*, 2017)
E. coli	TOP10	pCR BluntII-TOPO	General Ab	This project
PA14	-	mini-CTX:plac*rpoN*	B3tc *rsmA*	(Allsopp *et al.*, 2017)
PA14	-	mini-CTX:plac*rpoN*	B3tc *rsmArpoN*	(Allsopp *et al.*, 2017)
E. coli	TOP10	pCR BluntII-TOPO	General Ab	This project
E. coli	-	mini-T7:GFP	-	Allsopp lab repository
PA14	-	mini-T7:GFP	-	This project
PA14	-	mini-T7:GFP	ΔCDI^{00510}	This project
PA14	-	mini-T7:GFP	ΔCDI^{32790}	This project
PA14		mini-T7:GFP	ΔCDI^{00510}ΔCDI^{32790}	This project
PA14	-	mini-T7:GFP	*rsmA*	This project
PA14	-	mini-T7:GFP	*rsmA* ΔCDI^{00510}	This project
PA14	-	mini-T7:GFP	*rsmA* ΔCDI^{32790}	This project
PA14	-	mini-T7:GFP	*rsmA* ΔCDI^{00510}ΔCDI^{32790}	This project
PA14	-	mini-T7:GFP	*rsmA*H123	This project
PA14	-	mini-T7:GFP	*rsmA*H123 ΔCDI^{00510}	This project
PA14	-	mini-T7:GFP	*rsmA*H123 ΔCDI^{32790}	This project
PA14	-	mini-T7:GFP	*rsmA*H123 ΔCDI^{00510}ΔCDI^{32790}	This project
PA14	-	mini-T7:GFP	H123	This project
PA14	-	mini-T7:GFP	H123 ΔCDI^{00510}	This project
PA14	-	mini-T7:GFP	H123 ΔCDI^{32790}	This project
PA14	-	mini-T7:GFP	H123 ΔCDI^{00510}ΔCDI^{32790}	This project
E. coli	TOP10	pBBR1-MSC3	Beta AB His	This project
E. coli	TOP10	pBBR1-MSC3	Beta AB Strep II	This project
E. coli	BL21	pET29a	Antibody 1	This project
E. coli	TOP10	pCR BluntII-TOPO	General Antibody (codon optimised)	This project
E. coli	TOP10	pCR BluntII-TOPO	Antibody 2 (codon optimised)	This project

E. coli	BL21	-	-	Invitrogen
E. coli	BL21	pET29a	-	This project
E. coli	BL21 (Rosetta)	-	-	Invitrogen
E. coli	TOP10	pBAD33	-	ThermoFisher
E. coli	TOP10	pNDM220	-	ThermoFisher
E. coli	TOP10	pET29a	General Antibody (codon optimised)	This project
E. coli	TOP10	pET29a	Antibody 2 (codon optimised)	This project
E. coli	TOP10	pET29a	Antibody 2 (codon optimised)	This project
E. coli	TOP10	pCR BluntII-TOPO	CDI^{00510} toxin	This project
E. coli	TOP10	pCR BluntII-TOPO	CDI^{32790} toxin	This project
E. coli	TOP10	pCR BluntII-TOPO	CDI^{00510} immunity	This project
E. coli	BL21	pET29a	General Antibody (codon optimised)	This project
E. coli	BL21	pET29a	Antibody 2 (codon optimised)	This project
E. coli	BL21 (Rosetta)	pET29a	Antibody 2 (codon optimised)	This project
E. coli	TOP10	pCR BluntII-TOPO	CDI^{32790} Immunity	This project
E. coli	TOP10	pET29a	Antibody 1 His tagged	This project
E. coli	BL21	pET29a	General Antibody His tagged	This project
E. coli	BL21	pET29a	Antibody 1 His tagged	This project
E. coli	TOP10	pBAD33	CDI^{00510} Immunity	This project
E. coli	TOP10	pBAD33	CDI^{32790} Immunity	This project
E. coli	TOP10	pNDM220 and pBAD33	CDI^{00510} Toxin and Immunity	This project
E. coli	TOP10	pNDM220 and pBAD33	CDI^{32790} Toxin and Immunity	This project

E. coli	TOP10	pNDM and pBAD	-	This project
E. coli	TOP10	pNDM and pBAD	CDI^{00510} Toxin and Immunity	This project
E. coli	TOP10	pNDM	CDI^{32790}	This project
E. coli	TOP10	pNDM	CDI^{00510}	This project
E. coli	TOP10	-	*rsmF*	Allsopp lab repository
E. coli	TOP10	-	*rsmArsmF*	Allsopp lab repository
E. coli	TOP10	pNDM	CDI^{00510}	This project
E. coli	TOP10	pNDM and pBAD	CDI^{00510}	This project
E. coli	TOP10	pNDM	CDI^{32790}	This project
E. coli	TOP10	pNDM and pBAD	CDI^{32790}	This project
E. coli	TOP10	pNDM and pBAD	Toxin (CDI^{00510}) Immunity (CDI^{32790})	This project
E. coli	TOP10	pNDM and pBAD	Toxin (CDI^{32790}) Immunity (CDI^{00510})	This project
E. coli	TOP10	pBBR-MCS5	-	This project
E. coli	CC118λPIR	pBBR-MCS5	-	This project
PA14	-	pBBR-MCS5	$\Delta CDI^{00510}\Delta CDI^{32790}$	This project
S. aureus	USA300	-	-	(McDougal *et al.*, 2003)
B. cenocepacia	AU1054	-	-	(Chen *et al.*, 2001)

2.2 Media

Analytical-grade media ingredients obtained from ThermoFischer and Sigma UK were prepared as follows. Sterilisation through autoclaving (138 kPa, 120 °C for 20 mins), cooling to 50 °C for agar-based media. Overnight bacterial cultures and transformation growth cultures used Lysogeny broth (LB) (Table 2.2) (2.9-2.10). Strain cultures, three partner conjugation, 'pick and patch' protocols and competition assays used LB agar (Table 2.3) (2.12-

2.13). Three partner conjugations used Vogel-Bonner media (VBM), for VBM agar, and sucrose agar (Tables 2.4-2.6). Biofilm production assays used crystal violet (Table 2.7). Intrabacterial competition utilised BCSA (Table 2.8). β-galactosidase assays were conducted using tryptone soy broth (TSB) (Table 2.9). Various conjugation and transformation steps required antibiotics listed in Table 2.10.

Table 2.2: Components for making 1L of LB broth

LB Broth	Media Component (per litre)		
	NaCl	Yeast Extract	Tryptone
Weight (g)	10	5	10

Table 2.3: Components for making 1L of LB agar

LB Agar	Media Component (per litre)			
	NaCl	Yeast Extract	Tryptone	Agar
Weight (g)	10	5	10	15

Note: to make 5-bromo-4-chloro-indolyl-β-D-galactopyranoside (X-gal) plates add 100 µg/ml to make a final concentration of 0.1 µg/ml

Table 2.4: Components for making 1L of VBM X10 stock

Vogel-Bonner Media	Media Component (per litre)			
	$MgSO_4.7H_2O$	Anhydrous Citric Acid	K_2HPO_4	$(NH_4)NaHPO_4$
Weight (g)	2	20	100	35

pH must be normalised to pH 7 and filter sterilised

Table 2.5: Components for making 1L of Vogel-Bonner agar

Vogel-Bonner Agar	Media Component (per litre)		
	VBM x10 stock	2% Agar	Streptomycin (Sm100 mg/ml)
Volume (ml)	113.6	886.4	10

Table 2.6: Components for making 1L of 20% Sucrose agar media

Sucrose Agar	Media Component (per litre)	
	Sucrose	LB Agar
Volume (g or ml)	333.3	666.7

Table 2.7: Components for making 1L of 0.1% Crystal Violet solution

Crystal Violet Solution	Media Component (per litre)
	Crystal Violet powder
Weight (g)	1

Table 2.8: Components for making 1L of *Burkholderia cepacia* Selective Agar

BCSA Agar	Media Component (per litre)											
	Peptone	Yeast	Sodium pyruvate	Potassium dihydrogen phosphate	Disodium hydrogen phosphate	Bile salts	Ammonium sulphate	Magnesium sulphate	Ammonium ferrous sulphate	Phenol red	Crystal Violet	Agar
Weight (g)	5	4	7	4.4	1.4	1.5	1	0.2	0.01	0.02	0.001	12

Note: BCSA selective supplement is required to ensure selection composed of polymyxin B (75,000 IU/L), gentamycin (2.5 mg/L) and ticarcillin (50 mg/L).

Table 2.9: Antibiotics used for media and bacterial growth maintenance of vectors

Tryptone Soy Broth	Media Component (per litre)				
	Pancreatic digest of casein	Enzymatic digest of soya bean	Sodium Chloride	Dipotassium hydrogen phosphate	Glucose
Weight (g)	17	3	5	2.5	2.5

Table 2.10: Antibiotics used for media and bacterial growth maintenance of vectors

Antibiotics	Final Concentration (µg/ml)
Ampicillin	50
Kanamycin	50
Chloramphenicol	15/30
Streptomycin	50
Gentamycin	50
Tetracycline	15

Note: chloramphenicol is made using DMSO not ddH_2O

2.3 Primers

Cloning primers were designed using Benchling (biology software 2020), produced by Sigma (Table 2.11). To construct deletion mutants using stepwise cloning (2.8-2.11) and were sent with miniprepped plasmid constructs/PCR products for Eurofins Sanger sequencing.

Table 2.11: Oligonucleotides

Primer Number	Oligomer Name	F/R	*Pseudomonas* Strain/Vector	Sequence 5'-3'
1	CDI Primer 1	F	UCBPP-PA14_00510	TAGTAGGATCCCGCCGCCAAGCCCTGTG
2	CDI Primer 2	R	UCBPP-PA14_00510	ACCCAGCCTGAGAGCCACGAGTTCATTCCTT
3	CDI Primer 3	F	UCBPP-PA14_00510	GTGGCTCTCAGGCTGGGTCCTCTTCTTTAG
4	CDI Primer 4	R	UCBPP-PA14_00510	TAGTATCTAGACTCCAGTATTACCGCCCCCCTATCC
5	CDI Primer 5	F	UCBPP-PA14_00510	CACCCTGGAAACCTGTCCAC

6	CDI Primer 6	R	UCBPP-PA14_00510	GCCTCCCCTGCTTAGAAA
7	UpKn	F	pKNG101	CATATCACAACGTGCGTGGA
8	RpKn	R	pKNG101	CTCATCAGTGAAATCCAGGG
9	M13F	F	pCR BluntII-TOPO	TGTAAAACGACGGCCAGT
10	M13R	R	pCR BluntII-TOPO	CAGGAAACAGCTATGACC
11	CDI Primer 1	F	UCBPP-PA14_32790	TAGTAGGATCCGCTACTCCAACGCCCTG
12	CDI Primer 2	R	UCBPP-PA14_32790	TCAATGCTGGCTAGAACGCAACATCCG
13	CDI Primer 3	F	UCBPP-PA14_32790	CGTTCTAGCCAGCATTGAAAAGCCCCG
14	CDI Primer 4	R	UCBPP-PA14_32790	TAGTATCTAGACTGTCCCCTTTATTCACCCTTTA
15	CDI Primer 5	F	UCBPP-PA14_32790	GCTCGGTCAAGGATGCG
15	CDI Primer 6	R	UCBPP-PA14_32790	AACTTGTTGGCGTTCTGAC
16	CDI Primer Toxin	F	UCBPP-PA14_00510	TAGATGGTACCTTCACACAGGAAACAGCTATGGACTACAAAGATGAC GACGATAAAAGCCTCGTCGGTGAAAAGATCTTC
17	CDI Primer Toxin	R	UCBPP-PA14_00510	TAGATCTCGAGTCAGTCAATAAACCCTTTAAAAGTTCCATCTAG
18	CDI Primer Toxin	F	UCBPP-PA14_32790	CGACTACTCCGGGGGTTGTTAAGTG
19	CDI Primer Toxin	R	UCBPP-PA14_32790	TAGATCTCGAGTCACTTAACAACCCCCGGAGTAGTCG
20	CDI Primer Immunity	F	UCBPP-PA14_00510	TAGATTCTAGATTCACACAGGAAACAGCTATGAAAGAATTATTTGAA GTGATTTTTGAGGGTG
21	CDI Primer Immunity	R	UCBPP-PA14_00510	TAGATCTGCAGTCACTTTTCGAACTGCGGGTGGCTCCAAAGAAGAGG ACCCAGCCTGTTGTTAG
22	CDI Primer Immunity	F	UCBPP-PA14_32790	TAGATTCTAGATTCACACAGGAAACAGCTATGAAATTAATTGGAAGC CTTGCGGAG
23	CDI Primer Immunity	R	UCBPP-PA14_32790	TAGATCTGCAGTCACTTTTCGAACTGCGGGTGGCTCCAATGCTGACGT GCTAAATCAAGAGCAAC

24	General Antibody Strep tag	F	UCBPP-PA14_00510/ UCBPP-PA14_32790	CATAATGCAGGCCGGCAG
25	General Antibody Strep tag	R	UCBPP-PA14_00510/ UCBPP-PA14_32790	CTCGAGTCACTTTTCGAACTGCGGGTGGCTCCAGCTGGCCAGCAGGC
26	Antibody 1 Strep tag	F	UCBPP-PA14_00510	CATATGCGCAACCTTTCCGGG
27	Antibody 1 Strep tag	R	UCBPP-PA14_00510	CTCGAGTCACTTTTCGAACTGCGGGTGGCTCCAGGTCAGCGGCACGACC
28	Antibody 2 Strep tag	F	UCBPP-PA14_32790	CATATGCTTTTCGAACTGCGGGTGGCTCCAGGCAGTGACGCAAGTGGC
29	Antibody 2 Strep tag	R	UCBPP-PA14_32790	CATATGTCAGCTGGGCACGCCCTC
30	General Antibody Strep tag	F	UCBPP-PA14_00510/ UCBPP-PA14_32790	CTTTAAGAAGGAGATATACATATGCATCATCATCATCATCACGCTGCACAGGCC
31	General Antibody Strep tag	R	UCBPP-PA14_00510/ UCBPP-PA14_32790	GTTGTCCAGGCTGCCGGCCTGTGCAGCGTGATGATGATGATGATGCATATGTAT
32	Antibody 1 Strep tag	F	UCBPP-PA14_00510	CCGCTGACCCATCATCATCATCATCACTAGCTCGAGCACCACCACCACCACCAC
33	Antibody 1 Strep tag	R	UCBPP-PA14_00510	GGTGCTCGAGCTAGTGATGATGATGATGATGGGTCAGCGGCACGACCACCGAAAC
34	T7 Promoter	F	pET29a	TAATACGACTCACTATAGGG
35	T7 Terminator	R	pET29a	GCTAGTTATTGCTCAGCGG
36	pNDM220F	F	pNDM220	CGACGTTCCTGTCCACGGTA
37	pNDM220R	R	pNDM220	GGAATTTATGCGGTGTGAAATACCGCA
38	pBADF	F	pBAD33	ATGCCATAGCATTTTTATCC
39	pBADR	R	pBAD33	GATTTAATCTGTATCAGG

2.4 Low temperature storage of bacterial cultures

All overnight cultures were in LB or TSB broth, incubated overnight (150 RPM shaking, 37 °C). Adding 750 μl culture to 750 μl sterile 80% glycerol made -80 °C stocks stored in cryovials for long term storage.

2.5 Bioinformatic analysis of T5SS CDI operons for immunity protein and conserved sequence identification

2.5.1 Putative immunity identification through small ORF analysis

Two T5SS CDI sequences in PAO1 and PA14 were uploaded into Benchling. Annotated putative and known genes identified open reading frames (ORFs) and additional small downstream ORFs using NCBI ORFfinder and VectorNTI. ORF ribosomal binding sites (RBS) (-18 to +18 of sequence) were tested using a Kolaskar calculator, identifying those likely to be expressed or encode putative immunities. Protein sequences were then loaded into software (Table 2.12) to predict functions.

Table 2.12: Online bioinformatics tools used for small ORFs function identification

Bioinformatics Tool	Features	Reference
Benchling	Cloud-based informatics for genetics bioprocessing; primer design, sequence alignment	Biology Software 2019
ORF finder	DNA sequence search for putative protein coding sequences based on start codons	Wheeler *et al.*, 2003

VectorNTI	DNA and protein sequence for bioprocessing; sequence alignment, putative ORF identification	Invitrogen
NCBI Blast	DNA sequence comparison to database of genetic sequences	Johnson *et al.*, 2008
SMART Bioinformatics	Protein database for identifying roles of putative protein sequences	Letunic and Bork, 2017
NCBI Cdd Domain Search	Multiple sequence alignment of well annotated genes	Lu *et al.*, 2020
Phobius	Transmembrane topology prediction with signal peptide prediction	Madeira *et al.*, 2019
Signal P	Signal peptide prediction	Almagro Armenteros *et al.*, 2019
TMpred	Membrane spanning protein region prediction; helices, orientation	Ikeda *et al.*, 2003
Phyre2	Protein folding recognition server for protein modelling, prediction and analysis	Kelley *et al.*, 2015

2.5.2 Phylogenetic analysis of toxin genes from P. aeruginosa CDI systems

Phylogenetic relatedness was determined using CDI toxin sequences from PA14 and PAO1, obtained from www.pseudomonas.com. Each system's orthologues were also obtained to determine relatedness between systems between *P. aeruginosa* strains. Analysis was conducted in MEGA, after ClustalW sequence alignment, using Table 2.13 settings (Kumar *et al.*, 2018).

Table 2.13: MEGA settings for phylogenetic analysis from ClustalW toxin sequence alignment

MEGA Setting	Nucleotide Settings	Amino Acid Settings
Clustering method	Maximum likelihood	Maximum likelihood
Distance matrix model	Tamura-Nei	Jones-Taylor-Thornton
Substitutions to include	Nucleotide	Amino Acid (Bacterial Plastid)

Rates among sites	Gamma distribution (Coeff. 2)	Gamma distribution (Coeff. 2)
Bootstrapping replicates	1000	1000
Missing Data	Use all sites	Use all sites
Heuristic ML method	Nearest neighbour interchange	Nearest neighbour interchange
Initial tree produced from ML	Neighbour joining	Neighbour joining

2.5.3 Phylogenetic analysis of T5SS CDI toxin gene orthologues in P. aeruginosa and other Pseudomonas species

Phylogenetic relatedness between different *Pseudomonas* species was determined using toxin orthologues, obtained from www.pseudomonas.com. Using 2.5.2 methods and Table 2.14 MEGA settings, evolutionary relationships between species were determined to ascertain system evolutionary dynamics and potential horizontal gene transfers (HGT).

Table 2.14: MEGA settings for phylogenetic analysis from ClustalW toxin sequence alignment

MEGA Setting	Chosen Setting
Clustering method	Maximum likelihood
Distance matrix model	Tamura-Nei
Substitutions to include	Nucleotide
Rates among sites	Gamma distribution
Bootstrapping replicates	1000
Missing Data	Use all sites
Heuristic ML method	Nearest neighbour interchange
Initial tree produced from ML	Neighbour joining

2.6 Primer design for mutator fragment construction

Primers were designed using Benchling (Table 2.10) to perform cloning (2.8-2.11). CDI sequences loaded into Benchling distinguishing *cdiB* to putative *cdiI* sequence regions (identified using ORF finder). Primers 2 and 3 were designed using start/stop codon, with primer 1 ~500 bp upstream of primer 2 and primer 4 ~500 bp downstream of primer 3. Primers 5 and 6 were designed ~250 bp upstream/downstream of primers 1 and 4, respectively (Figure 2.1) (Vasseur *et al.*, 2005). Primer locations were optimised using melting temperatures (Tm) and secondary structure ΔG minimum homodimer values (kcal), designing similar Tm values and ΔG values ~2-6 kcal.

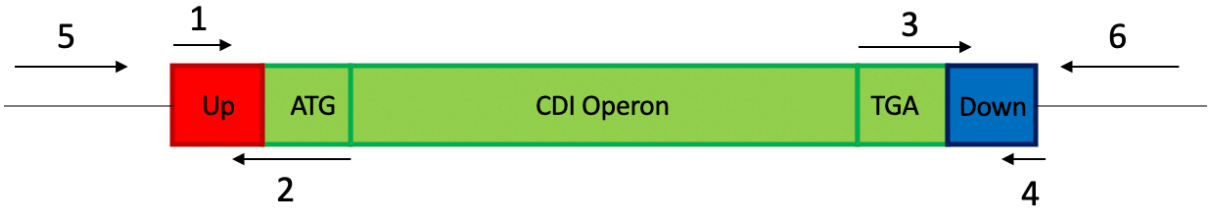


Figure 2.1: Primer positions and orientations. Primers designed for cloning deletion mutator fragment into *Pseudomonas* are represented above.

2.7 Gene deletion mutator fragment construction through PCR amplification

2.7.1 PCR for cloning CDI genes and screening constructed transformant colonies

Genomic and plasmid vector DNA was purified using Qiagen DNeasy Blood and Tissue® and QIAprep Spin Miniprep® kits, respectively. Cloning PCR amplification used KOD hot start high-fidelity components (Table 2.15). Master-mix aliquoted 48.5 µl into PCR tubes. 1.5 µl PA14 genomic DNA (20 ng/µl) enabled upstream/downstream DNA amplification (Allsopp *et al.*,

2017) using primer pairs 1 and 2, 3 and 4 respectively (Table 2.11). QIAquick® PCR purification kit protocol then purified PCR products. Overlap PCR for mutator fragment generation used primers 1 and 4, with upstream/downstream fragments as the mutator template (Table 2.16). Table 2.17 PCR protocol repeats steps 2 to 4 30 times. Cloning of other genes from the operon also used this method.

Table 2.15: PCR components for making 50 μl final volume sample for DNA amplification

	MilliQ	5M Betaine	10X KOD Buffer	$MgSO_4$	Forward Primer	Reverse Primer	DNA	dNTPs	KOD pol
Volume (μl)	26.5	10	5	2	1.5	1.5	1.5	1	1

Table 2.16: PCR components for making 50 μl final volume sample for overlap amplification

	MilliQ	5M Betaine	10X KOD Buffer	$MgSO_4$	Forward Primer	Reverse Primer	DNA Upstream	DNA Downstream	dNTPs	KOD pol
Volume (μl)	26	10	5	2	1.5	1.5	1	1	1	1

Table 2.17: PCR cycle step protocol for DNA fragment amplification

Step	Temperature (°C)	Time (secs)
1	95	120
2	94	20
3	58	30
4	68	60 /kb
5	68	600

2.7.2 Agarose gel electrophoresis of cloning/colony PCR products

PCR product visualisation used agarose gel electrophoresis. Using the ratio (10 ml 0.5x TBE : 0.1 g agarose powder), agarose gel solutions were microwaved ~1 min 30 secs until agarose powder dissolved. Molten agar was cooled by running duran under cold water, SafeView was added using the ratio (10 ml of gel : 1 µl) to DNA visualisation. Gel was poured, left for 20 mins to set, before loading into buffer filled electrophoresis apparatus. Samples were loaded into wells using the ratio (5 µl PCR product : 2 µl loading dye) with 4 µl of 2 log ladder. Electrophoresis at 80 Volts was conducted for 40 mins before MultiDoc-It digital imaging system visualisation.

2.8 Ligation of mutator fragment into plasmid vectors in *Escherichia coli*

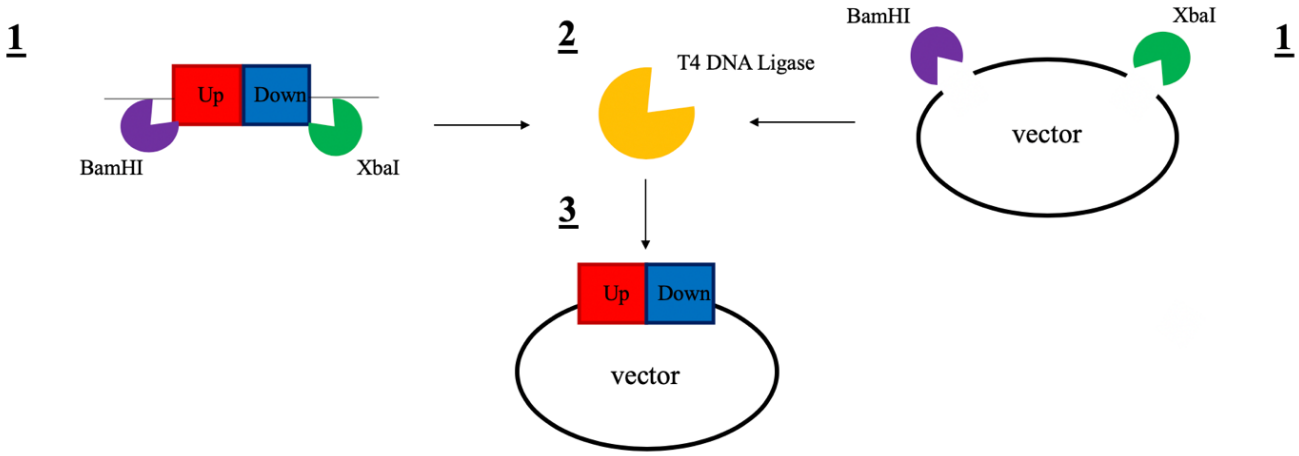


Figure 2.2: Mutator fragment insertion into plasmid vector. (1) Restriction digest, (2) plasmid ligation, (3) Transformation. Cloning mutator fragment into vector plasmid after construction of mutator fragment in 2.8.

2.8.1 Restriction digest of PCR products and vector

PCR products and final (or pCR BluntII-TOPO) vectors were digested using restriction enzymes (Figure 2.2). Using Table 2.18 components, digests were incubated at 37 °C (based on New England BioLabs enzyme reaction temperatures) for 2-8 hrs. Digests where PCR cleaned up or gel electrophoresis and gel extraction was conducted.

Table 2.18: Components for making a 50 µl final volume sample for double enzyme digest of mutator fragment or vector DNA

	Enzyme 1	Enzyme 2	10X Buffer	MilliQ	DNA
Volume (µl)	1	1	2	y	x

For DNA digestions 1000 ng or 2000 ng of vector DNA was cut.

2.8.2 Ligation of restriction digest products

Digested final vector and mutator inserts were ligated using Table 2.19 components, incubating the reaction at 16 °C overnight mixing digested insert DNA with digested vector DNA (Figure 2.2). Ligated plasmids were transformed into chemically competent cells.

Table 2.19: Components for making 20 µl final volume sample for mutator fragment ligation into pKNG

	Insert	pKNG	Ligase	X10 Buffer
Volume (µl)	x	y	1	2

Using a ligation calculator, ratio of insert to vector volumes were calculated based on the size of the vector and insert and the concentration of DNA produced from the restriction digest and PCR clean up.

2.9 Chemically competent cell production for transformations

E. coli strains (Top10/CC118λPIR/BL21) were grown in 5 ml LB cultures overnight (Tu *et al.*, 2005). Culture OD_{600} was taken before inoculating fresh media to OD_{600} = 0.1. Bacteria were incubated at 37 °C until OD_{600} = 0.6 and cooled on ice. Next, cultures where centrifuged for 10 mins (4000 RPM, 4 °C), supernatant was discarded, resuspending pellet in 25 ml filter-sterilised ice cold $CaCl_2$. The wash step was repeated prior to a 20 min incubation on ice. Cells were centrifuged for 10 min to pellet followed by a 30 sec centrifugation to remove supernatant remnants. Cells were resuspended in 1 ml 50 mM $CaCl_2$ with 15% glycerol, aliquoting 100 μl before -80 °C storage.

2.10 Transformation into vectors and competent strains

Transformation into competent cells was achieved by mixing ligated vectors with chemically competent cells for 10 mins. Heat shock at 42 °C for 1 minute followed by recovery on ice for 2 mins enabled vector uptake. Finally, 1 ml LB added for recovery, where it was incubating at 37 °C at 175 RPM for 1 hr. Bacteria were then spread plated onto agar with any required selection agents such as antibiotics. If no colonies grow upon ligation and transformation into the final vector, pCR BluntII-TOPO vector was used (Table 2.20). Using 2.9.1-2.9.2 protocol, pCR BluntII-TOPO-mutator/cloned gene was miniprepped to extract plasmid DNA before restriction digestion, ligation into final vector and transformation into competent cells. For pKNG-mutator (Figure 2.3), ligation enabled transformation from donor strain *E. coli* CC118λPIR via three partner conjugation, resulting in PA14 genomic integration and construction of whole system deletion mutants (Vasseur *et al.*, 2005).

Table 2.20: Components for making 6 µl final volume sample for mutator fragment ligation into pCR BluntII-TOPO

	Insert	pCR BluntII-TOPO	MilliQ	Salt Solution
Volume (µl)	2	1	2	1

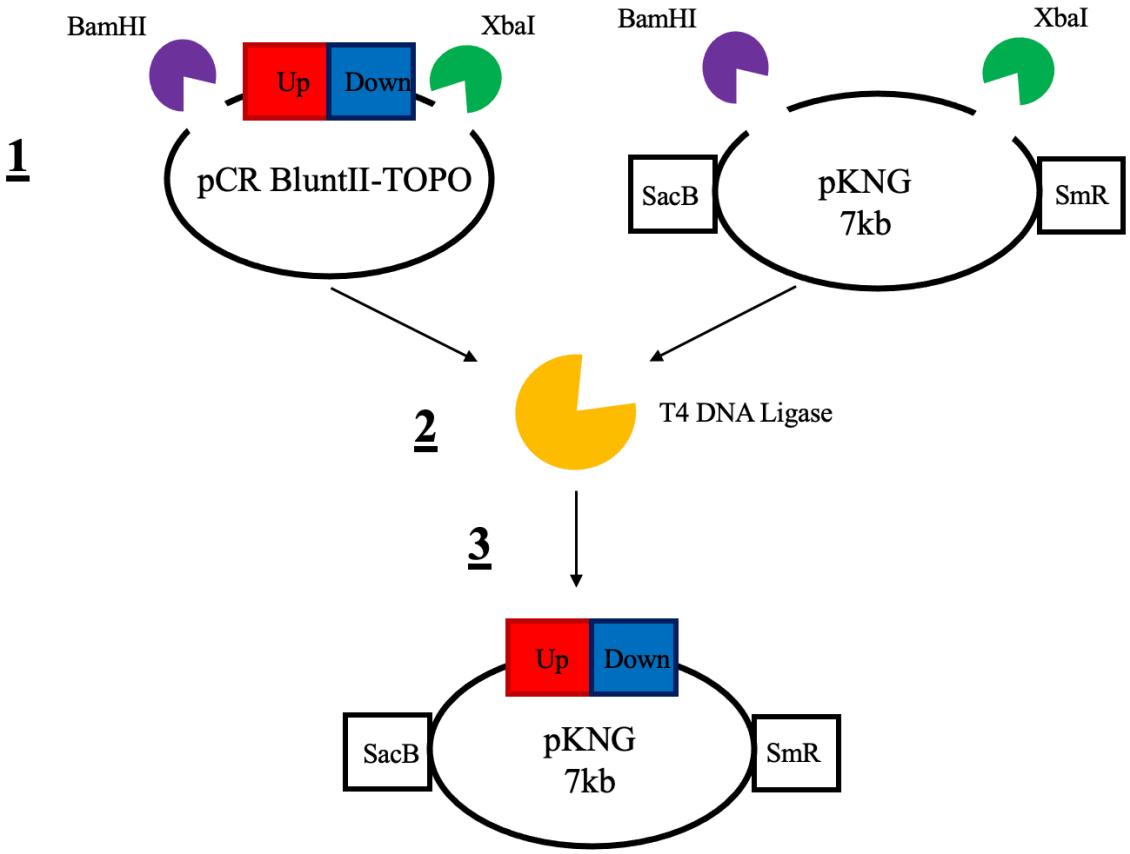


Figure 2.3: Mutator fragment insertion into pKNG. (1) Restriction digest, (2) pKNG ligation, (3) Transformation. Cloning mutator fragment into *Pseudomonas* replicating plasmid after insertion into cloning vector in 2.9. Note: genes in pKNG important for conjugation in 2.12 are illustrated above.

2.11 Screening isolates through colony PCR

Colony PCR for the desired amplicons was conducted using Table 2.21 components. Master mix aliquoted 18 µl into PCR tubes, adding 2 µl colony water from each isolate for

amplification (Allsopp *et al.*, 2017). Primers used were reliant on vector. Table 2.22 PCR protocol repeats steps 2 to 4 30 times.

Table 2.21: PCR components for making 20 μl final volume sample for DNA amplification

	MilliQ	Taq Buffer	Forward Primer	Reverse Primer	DNA	dNTPs	DMSO	Taq pol
Volume (μl)	12	2	1	1	2	1	0.6	0.4

Table 2.22: PCR cycle step protocol for DNA fragment amplification

Step	Temperature (°C)	Time (secs)
1	95	300
2	95	30
3	55	30
4	72	60 /kb
5	72	600

2.12 Three partner conjugation for transfer of gene deletion plasmids into *P. aeruginosa* strains

Overnight cultures of; receiver (PA14), helper (pRK2013) and donor (CC118λPIR with mutator-pKNG101) strains were incubated overnight with shaking. The next day, 100 μl receiver strain aliquots were incubated at 43 °C for 2 hrs, inactivating *P. aeruginosa* restriction modification systems. Simultaneously, 20 μl spots of helper and donor strains on LB agar plates (separately and overlaid) were incubated at 37 °C for 2 hrs. Next, 40 μl receiver strain overlaid helper/donor spot and was incubated for 4 hrs at 37 °C (Figure 2.4). Spots were collected using sterile loops and resuspended in LB broth (outlined Figure 2.5). Colonies were

first screened for chromosomal mutator insertion using primers 5 with 7 and primer 6 with 8, confirming integration (Figure 2.1). Next, sucrose counter selection was used to induce pKNG to recombine out leaving the mutator fragment behind. Screening then confirmed CDI deletion using primers 5 and 6 (Figure 2.1), encoded externally to the mutator fragment (Vasseur *et al.*, 2005).

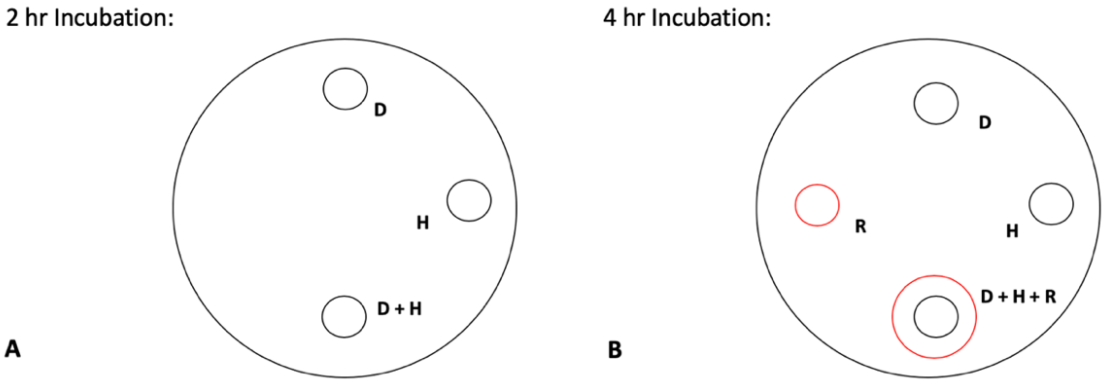
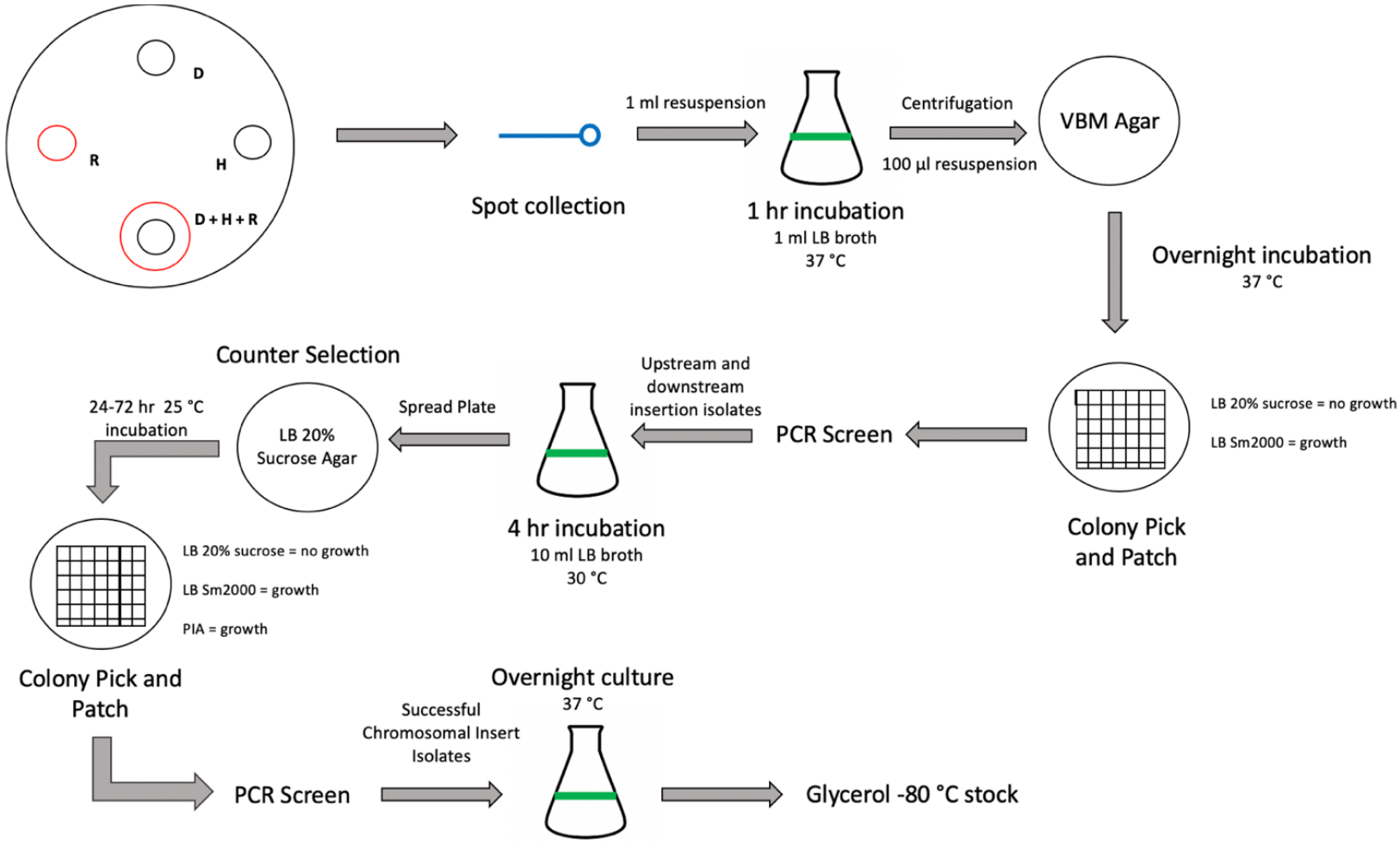


Figure 2.4: Strain spotting on LB agar for conjugation incubation. (A) 2 hrs incubation, (B) 4 hrs conjugation incubation using all three strains

Figure 2.5: Culture processing for three partner conjugation. Mutator fragment selection was enabled by patching colonies onto LB 20% sucrose and Streptomycin 2000 agar plates, removing sucrose resistant colonies and preventing mutagenic VBM action on *Pseudomonas*. Colonies with successful second recombination event are Streptomycin sensitive through pKNG101 excision and constrain either mutator deletion fragments or the WT alleles.



2.13 Inter and intrabacterial killing assays

WT killing of ΔCDI strains evaluated CDI roles in bacterial competition (Allsopp *et al.*, 2017). Attacker (WT) and prey (mutant) cultures were inoculated in 5 ml LB in 50 ml conical flasks and incubated overnight. Attacker and prey strains were mixed using the method outlined in Figure 2.6. A 10^{-8} dilution series was made (270µl LB : 30 µl bacteria) using input cultures before spotting 20 µl of each dilution in triplicate onto 8 x 8 gridded selective LB agar plates to assess prey survival. LB plates were dried after spotting dilutions and incubated at 37 °C overnight.

After 5/24 hrs incubation, spots collected in eppendorfs were resuspended in 1 ml LB by vortexing. A second 10^{-8} dilution series was made using output cultures spotting in triplicate on 5-bromo-4-chloro-indolyl-β-D-galactopyranoside (X-gal) LB agar or selective media as required. Input and output plates were incubated upward facing at 37 °C overnight before colonies were counted and spot ratios calculated to determine prey survival. One version of the assay conducted within this thesis used GFP-tagged strains and had additional steps where the 10^{-2} spot was resuspended in 1 ml PBS before plating in a Corning black 96 well clear bottom plate using the FLUOstar Omega to measure levels of fluorescence of the samples to determine prey survival.

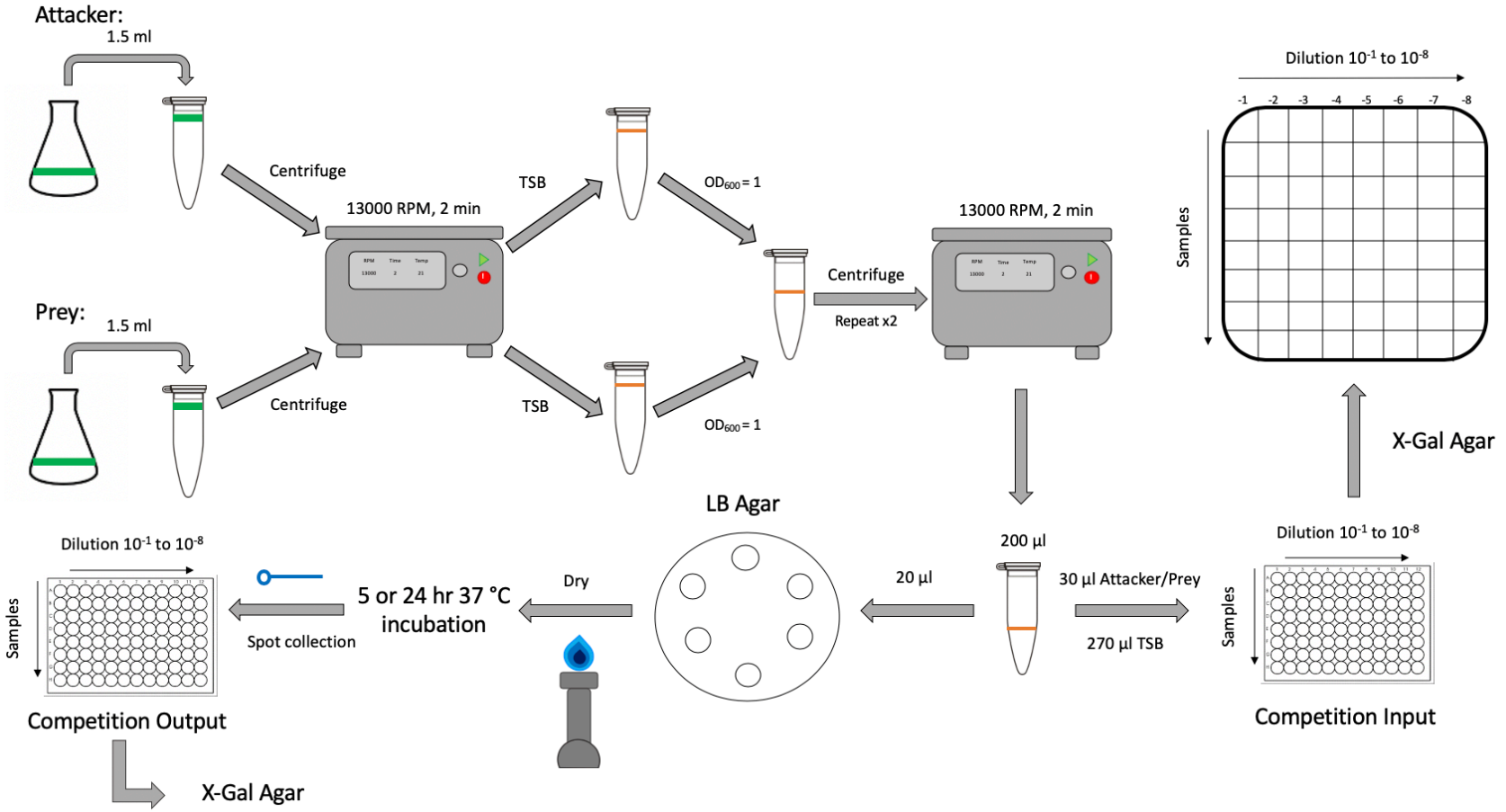


Figure 2.6: Culture processing for competition assays. Overnight culture processing and mixing of attacker and prey strains were used for producing input and output competition cultures. Attackers and prey are differentiated on selective e.g. X-gal plates, attacker and prey will be differentially selected via antibiotics or exhibit differences in colour (e.g. *lacZ* attacker blue and prey white). Colony counts enable attacker/prey ratios and competitive index to be calculated. 5 and 24 hrs incubations and 1:1 and 1:5 attacker:prey ratios were trialled to optimise experimental methodology to ensure true competitive abilities are assessed by determining the optimal window of time to observe the competitive effect.

2.14 Determining biofilm production of CDI mutants

WT and ΔCDI biofilm production evaluated CDI role in biofilm formation (Pardee, 1959; O'Toole & Kolter, 1998). Overnight cultures were processed using Figure 2.7 method. Using clear 96 well plates (Corning™ Falcon™), six 200 µl replicates of each strain were inoculated per plate. Six 200 µl sterile media replicates were negative controls (Figure 2.8). Plates were left static for 24 hrs at 37 °C. Randomised 96 well format was used for final assay where six repeats were spread over three 96 well plates to ensure every strain was at a different location within the plate and surrounded by different strains in every well. I also filled every surrounding well with media to further reduce edge effects.

Biofilm biomass was determined using Figure 2.7 method. Plate submerging in sterile purified water post well-washing removed biofilm from plate exterior. Biofilms staining using crystal violet (Table 2.7) was left for 15 minutes before washing and plate submerging in sterile purified water. Ethanol was added and left for 15 minutes to solubilise crystal violet, before shaking on Bio-Rad plate shaker (500 RPM for 1 min). Well absorbances were read at 600 nm using a FLUOstar Omega plate reader.

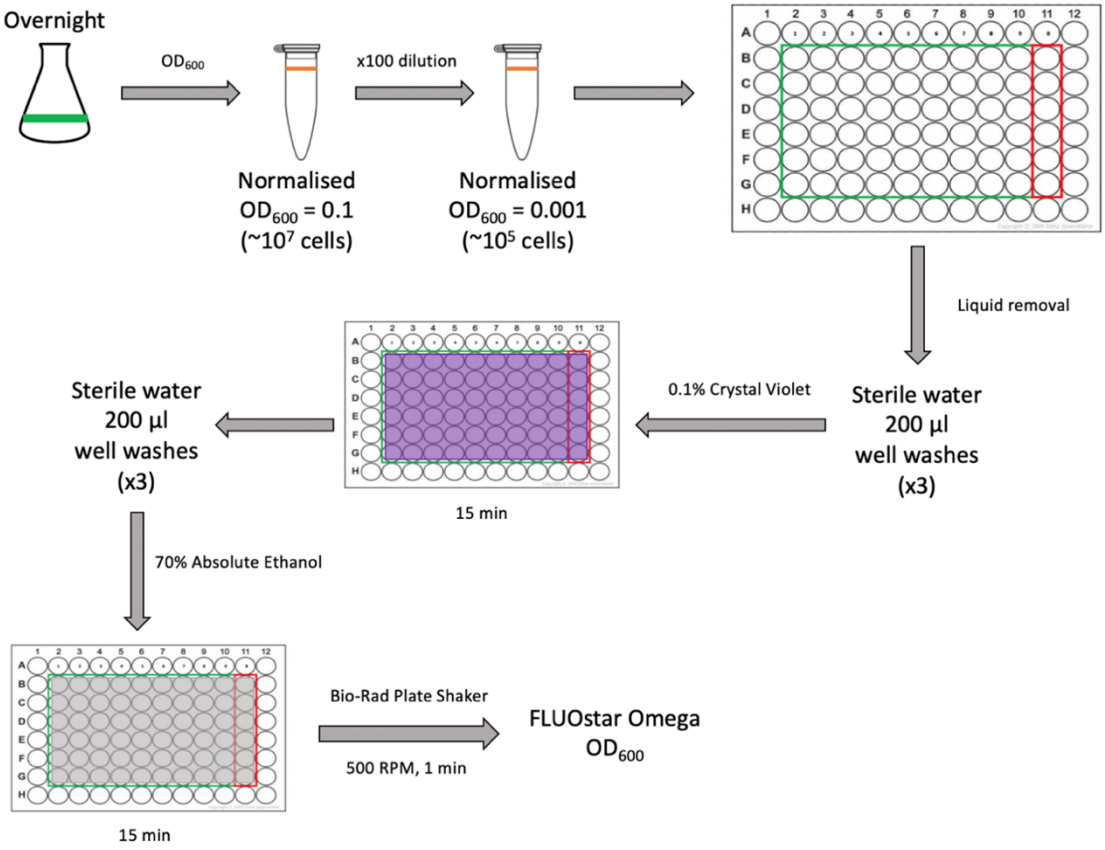


Figure 2.7: Culture processing for biofilm biomass production assay. Overnight culture processing was used to make OD_{600} = 0.001 starting cultures for biofilm production. Crystal violet absorbance is proportional to the biomass present within each well, quantifying the amount produced within 24 hrs.

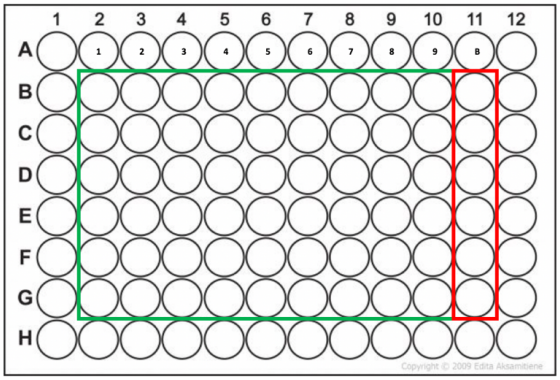


Figure 2.8: Biofilm assay 96 well plate layout representation. Columns 1-9, individual strain. The six repeats are down each column from row B-G. Column B represents blank replicates as a negative control. Subtracting average blank well absorbance to each well produces final absorbance readings. Random well format was also conducted with strains arranged in wells surrounded by different strains in each instance, interspersed by blank wells.

2.15 Determining motility of CDI mutants

2.15.1 Determining swimming motility of CDI mutants

I evaluated WT and ΔCDI strains for swimming motility to evaluate if there is any impact of deletion of the CDI on flagellar-based motility. Overnight cultures were grown to exponential growth phase before inoculation. Agar plates were poured and left to dry in the hood for 20 mins, prior to inoculation. Motility plates where inoculated using a sterile metal probe, on 20 ml plates of tryptone agar (0.3%) (Chow *et al.*, 2011). Three replicates per strain were inoculated and stacked together before placement into a plastic container (with the lid cracked open to allow oxygen replenishment) then left static in the dark for 24 hrs at 37 °C.

After incubation, images of plates were taken to quantify swimming by area migrated over 24 hrs (Figure 2.9). Area was measured using ImageJ software (Schneider, Rasband & Eliceiri, 2012). Image was converted to 8-bit before calibrating the scale from the inclusion of a ruler situated next to the plate in the image. Area was measured using the functions in the toolbar to isolate the motility area before selecting the measure function. Outputs were tabulated and averaged over three biological repeats.

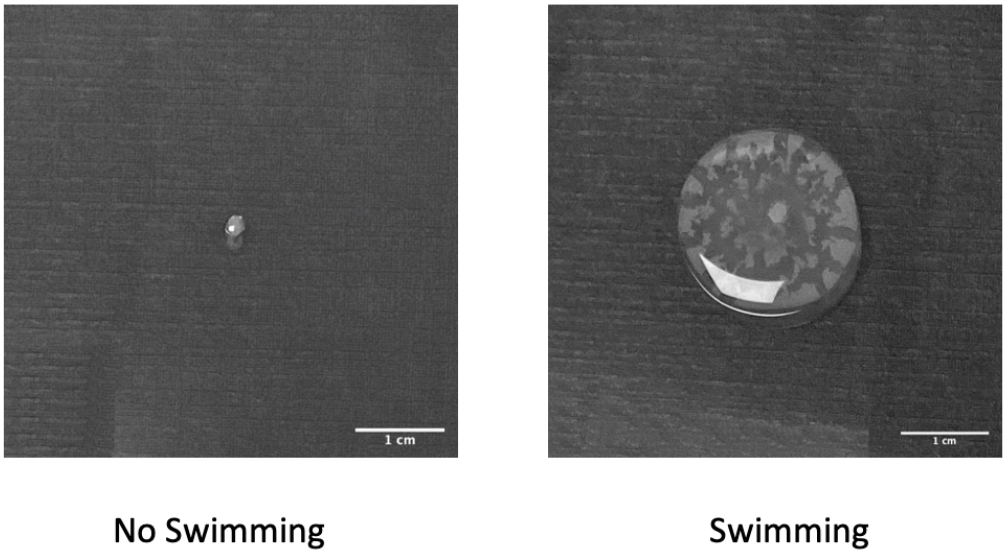


Figure 2.9: Swimming motility on low agar plates. Representative images of non-motile and swimming motility phenotypes observed which were measured to determine area moved over 24 hrs.

2.15.2 Determining swarming motility of CDI mutants

I evaluated WT and ΔCDI strains for swarming motility to evaluate if there is any impact of deletion of the CDI on group-mediated motility (O'May & Tufenkji, 2011). Agar plates were poured and left to dry on the bench for 4 hrs, prior to inoculation. Overnight cultures were grown to exponential growth phase before inoculation, using a sterile metal probe, on 20 ml plates of LB agar (0.225%) (Alsohim *et al.*, 2014). Three replicates per strain were inoculated and stacked together before placement into a plastic container (with the lid cracked open) then left static in the dark for 24 hrs at 37°C.

After incubation, images of plates were taken to quantify swarming by area migrated over 24 hrs as described above in 2.15.1 (Figure 2.10). Outputs were tabulated and averaged over three biological repeats.

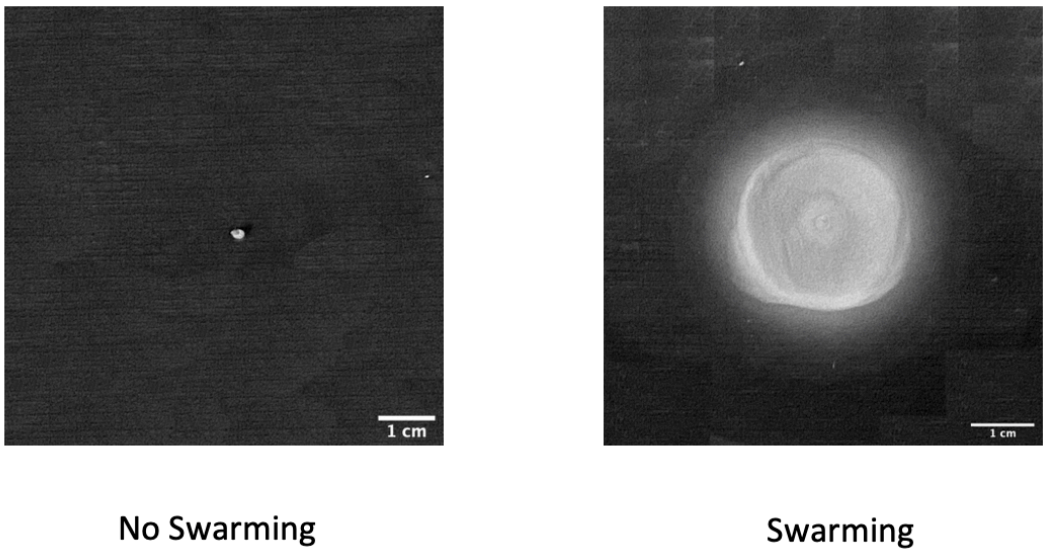


Figure 2.10: Swarming motility on low agar plates. Representative images of non-motile and swarming motility phenotypes observed which were measured to determine area moved over 24 hrs.

2.16 Determining growth rates of CDI mutants

Effect of the deletion of CDI systems on fitness was determined via growth rate. Overnight cultures were grown to exponential growth phase before inoculation. Using clear 96 well plates (Corning™ Falcon™), three 200 µl replicates of each strain were inoculated at OD 0.001. Three 200 µl sterile media replicates were negative controls. Plates were left in the FLUOstar Omega static for 24 hrs at 37 °C with shaking for 30 s before reading at 15 min intervals at OD_{600}.

2.17 Toxin-immunity module cloning, plus validation via growth rate and agar plate induction

The functionality of the CDI encoded toxin-immunity modules were evaluated via growth rate and agar plate survival upon induction of expression of each protein (Hachani *et al.*, 2014). Toxins were cloned into pNDM220 vector where expression was controlled under an isopropyl β-D-1-thiogalactopyranoside (IPTG) inducible promotor. Immunities were cloned into pBAD33 vector where expression was controlled under an arabinose inducible promotor. *E. coli* strains were constructed which contained both vectors due to inherent toxicity and inability to obtain transformant strains containing pNDM harbouring the toxins alone.

Growth rate assays were conducted by initially growing strains in overnight cultures at 37 °C and 175 RPM. Strains were subcultured to OD_{600} 0.1 and grown for a further 2hrs before addition of the inducer. A non-induced strain control was used to determine baseline growth rate, whilst inducers were added in flasks with IPTG alone, arabinose alone and IPTG and arabinose together to individually express each protein as well as both proteins together to determine ability to cause bacterial intoxication and recovery from intoxication upon subsequent expression of the immunity. After induction, strains were grown for a further 6 hours, where OD_{600} readings were taken at each hour for the entire 8 hr experimental time course.

In tandem with the growth rate, directly from the overnight cultures the OD was again normalised to OD_{600} 0.1. A dilution series to 10^{-8} was then conducted before spotting onto agar plates which contained the various inducers in the same manner as the growth rate

assay. After overnight growth, colonies were counted to calculate CFU to determine strain survival upon induction of each strain. This assay was also repeated with *E. coli* strains constructed to contain the toxin of one system (e.g. *cdiA*-CT^{00510}) and the immunity of the opposite system (e.g. *cdiI*^{32790}) to determine the specificity of these modules in enabling recovery from intoxication.

2.18 SDS-PAGE and western blot analysis

2.18.1 SDS-PAGE and semi-dry transfer

Upon collection of various samples from the assays outlined above in sections 2.18-2.19, samples were heat treated to denature proteins for separation via SDS-PAGE. SDS-PAGE utilised 15% polyacrylamide gels and were run for 80 V for 30 mins, 100 V for 30 mins and 150 V for 55 mins. Gels were prepared using Bio-Rad Mini-PROTEAN® handcast systems with 10 well combs. Electrophoresis was conducted using Tris-glycine-SDS (TGS) buffer (0.3% (w/v) Tris, 1.44% (w/v) glycine and 0.01% (w/v) SDS). The ladder utilised as a molecular weight guide was the 10-250 kDa Bio-Rad Precision Plus Protein™ Kaleidoscope™ Prestained Protein Standard. Samples were analysed via Coomassie staining (0.5% (w/v) Coomassie Brilliant Blue, 40% (v/v) methanol, 10% (v/v) acetic acid, 49.5% (v/v) ddH_2O) or via western blot analysis.

Western blot transfer used either Bio-Rad Trans-Blot® Turbo Midi 0.2 µm Nitrocellulose Transfer Packs or Amersham™ Protan™ 0.2 µm nitrocellulose membrane with Whatman filter paper with transfer buffer (TB) (10% (v/v) TGS buffer, 20% (v/v) ethanol, 70% (v/v) ddH_2O). Gels were placed on the nitrocellulose and inserted between six layers of filter paper on each side of the nitrocellulose-gel composite. Transfer was conducted using the Bio-Rad Trans-

Blot® Turbo Transfer System at 25 V, 1 A for 30 mins. Nitrocellulose was then transferred to square petri dishes where they underwent blocking for 2 hrs using tris-buffered saline solution (TBST) (20% (v/v) ethanol, 10% (v/v) TGS buffer, 70% (v/v) ddH_2O, 0.1% (v/v) Tween20) with either 5% Bovine Serum Albumin (BSA) or 5% Skimmed Milk (SM).

Primary antibody (anti-his/anti-strep/anti-flag) was added for overnight incubation which was made up in the 5% BSA/SM and added at a ratio of 1:5000 for His and Strep, or 1:10000 for Flag. In the morning, three 5 min washes with TBST were used before secondary anti-rabbit antibody at 1:5000 ratio in 5% BSA/SM was added and left to incubate for 1 hr. Three 5 min washes were repeated with TBST before visualisation.

Visualisation was conducted using the Bio-Rad ChemiDoc MP Imaging System to take both colorimetric and chemiluminescent images of the nitrocellulose blots, as well as Coomassie images of the SDS-PAGE gels. Nitrocellulose visualisation was achieved by adding ~1 ml of Immobilon® Forte Western HRP Substrate directly onto the nitrocellulose and incubated for 2 mins.

2.18.2 Tris-Acetate electrophoresis and wet transfer

An alternative for SDS-PAGE was utilised for validating the antibodies generated from the conserved *cdiA* regions- NuPAGE™ Tris-Acetate 3-8% Gels (Invitrogen) and wet-transfer. Due to the large size of the CdiA proteins (~300-550 kDa) difficulty visualising via conventional SDS-PAGE gel and western blot method was observed. An alternative for SDS-PAGE was utilised for validating the antibodies generated from the conserved *cdiA* regions- NuPAGE™ Tris-Acetate 3-8% Gels (Invitrogen) and wet-transfer.

Here, gels were run in the Invitrogen™ XCell SureLock Mini-Cell using the NuPAGE™ Tris-Acetate Running Buffer, run at 100 V for 1 hr. Wet transfer was then conducted using Amersham™ Protan™ 0.2 µm nitrocellulose membrane with Whatman filter paper and TB at 4 °C in Bio-Rad Trans-Blot® Cell at 30 V for 30 min, 35 V for 1 h, 40 V for 1 h, 50 V for 1 h, and then 65 V for 4 h. Blocking and antibody exposure the same as outlined above in 2.20.1.

2.19 Protein purification for toxin-immunity validation and antibody production

Recombinant proteins for both toxin-immunity modules and conserved CdiA regions for antibody production were purified here based on His and Strep tags incorporated in the cloning steps. Briefly, *E. coli* strains containing the expression vectors encoding these recombinant proteins were grown overnight at 37 °C at 175 RPM. Strains were subcultured to OD_{600} 0.1 and grown shaking at 37 °C for two hours before adding the inducer. Strains were then grown for a further 5 hours before spinning sample down to a pellet and storing at -80 °C.

For purification, pellets were stored at -80 °C were thawed on ice, before resuspending in 3-5 ml of Buffer W (100 mM Tris/HCl, pH 8.0 150 mM NaCl, 1 mM EDTA) containing proteinase inhibitor and lysozyme depending on pellet size. Sonication at 40% for 140 s with 5 s on-off intervals allowing cell lysis for protein purification. Suspension was then centrifuged at 15,000 RPM for 15 mins to separate soluble fraction containing proteins of interest. Supernatant was then collected for running through the resin-column. Resin column with 1 column volume (CV) was prepared with either TALON® His or Strep-Tactin® Sepharose® Strep resin and

equilibrated with Buffer W, which either required gravity or centrifugation for purification dependent on pellet size and resuspension volume.

Soluble fraction was run through the column to enable binding of the tagged protein to the resin. This is then washed 3-9 times with 2x CVs to remove any non-bound proteins in the soluble fraction. Elution occurs by adding 0.5 CVs of Buffer E (100 mM Tris/HCl, pH 8.0 150 mM NaCl, 1 mM EDTA, 2.5 mM desthiobiotin) 3 times to collect the bound protein. For each step from whole cell lysate, lysate, pellet, soluble, washes and elution steps, SDS-polyacrylamide gel electrophoresis (SDS-PAGE) samples were collected and resuspended in Laemmli sample buffer (4% (v/v) glycerol, 2% (w/v) sodium dodecyl sulfate (SDS), 60 mM Tris-HCl pH 6.8, 5 % (v/v) β-mercaptoethanol and 0.002% (w/v) bromophenol blue) to evaluate purification via western blot analysis.

For antibody production, upon collection of the purified proteins, the buffer needed to be equilibrated via dialysis before sending off to Eurogentec for antibody production. This was due to the high concentration of urea present in the purification buffer of the general and antibody 1 specific recombinant proteins produced. To do this, elution samples containing the purified protein were mixed and added to SnakeSkin™ dialysis tubing. Upon clamping the SnakeSkin™ closed, samples were floated in separate 2 L of Buffer W and left overnight to dialyse at 4 °C rotating at 30 RPM. The next day, samples were collected, and concentration was determined using a Nano drop spectrophotometer. Aliquots of each sample were made up to a concentration of 0.5 mg/ml and stored at -80 °C before sending off to Eurogentec for antibody production in rabbits.

2.20 Protein pull down for toxin-immunity validation

To evaluate ability for toxin-immunity modules to interact via cognate binding, protein pull-down was conducted (Mercy *et al.*, 2016). Methods mimic those outlined in 2.18 for sample collection and cell lysis. The pull-down however differs in that the strains containing both toxins and immunities in separate expression vectors are both induced. This is due to the inherent toxicity of both the toxins under study which prevents production of detectable levels of toxin via western blot analysis due to cell death or cessation of growth.

Immunities are Strep tagged, whilst toxins are flag tagged. Therefore the soluble fraction was run through a Strep resin column via centrifugation. Once all soluble fraction was passed through the column, samples were washed 9 times before the resin was collected and resuspended in SDS-PAGE Laemmli sample buffer. Soluble, wash steps and resin samples were used to conduct western blot analysis to determine direct binding of toxins and immunities via the detection of co-purification of the toxin with the immunity.

2.21 Site-directed mutagenesis for protein tag replacement

Due to the inability to purify the recombinant proteins of the conserved *cdiA* regions to produce a general antibody and system type 1 specific antibody, site-directed mutagenesis was conducted to replace the Strep tag on the proteins with a His tag (Edelheit, Hanukoglu & Hanukoglu, 2009). This would enable purification due the ability to utilise higher concentration buffers to ensure the proteins would remain in the soluble fraction instead of the pellet fraction.

To do this, vectors containing the conserved *cdiA* sequence were utilised at 5 ng/µl, where primers were designed to overlap both sides of the vector either side of the tag but include a His tag sequence instead of the Strep tag sequence which is within the template (Figure 2.11). Cloning PCR protocol was utilised for this where primers would clone the new His tag into the region of interest but also replicate the entire plasmid. To remove template DNA with Strep tag, DpnI mediated digest was conducted in the PCR tubes at 37 °C for 3 hrs. Transformation into competent TOP10 cells completed the process.

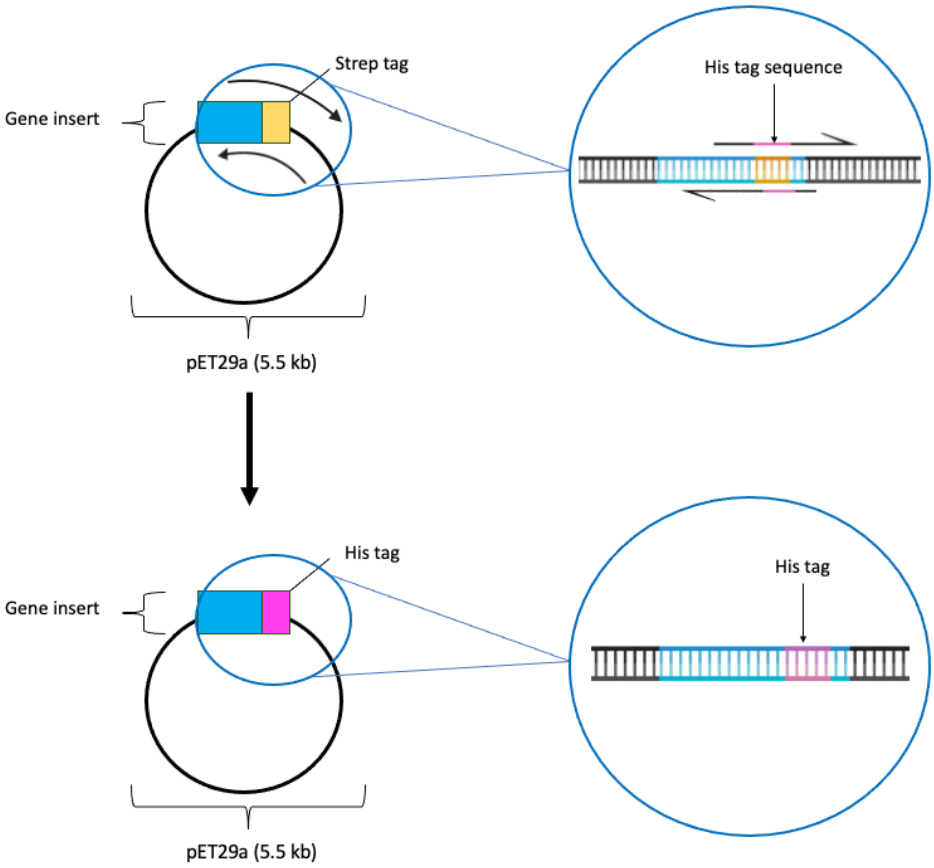


Figure 2.11: Site-direct mutagenesis for protein tag exchange. Schematic representation of direct mutagenesis utilises overlapping primers with Strep tag replacement by His tag sequence and subsequent replication of the entire plasmid.

2.22 Determining regulation control of T6SS via β-galactosidase expression assay

To evaluate the role RpoN plays in the expression of the H2- and H3-T6SSs, β-galactosidase assay was conducted using *lacZ* transcriptional fusions (Allsopp *et al.*, 2017). Bacterial strains

were grown overnight at 37 °C and 175 RPM in TSB. Strains were subcultured to OD_{600} 0.1 and grown until culture reached mid-log phase at OD_{600} 1 before collecting the cell pellet. Pellet was then resuspended in Z-buffer (Na_2HPO_4 0.06M, NaH_2PO_4 0.04M, KCl 0.01M, $MgSO_4$ 0.001M, β-mercaptoethanol 0.05M) before permeabilising cells with 50 µl 0.1% SDS and 100 µl chloroform and vortexing for 2 mins at 2000 RPM for phase separation to occur. Sample was left to settle for 2 minutes before lysate collection which was added to a 96-well Falcon plate. Z-buffer was used as a control with three wells per sample/control used. To start the conversion of lactose to galactose and glucose, 180 µl of Z-buffer was added to 20 µl of cell lysate. Then 40 µl of ortho-nitrophenyl-β-galactoside (4 mg/ml) was added and incubated at 28 °C for 15 mins. Reaction was stopped using 100 µl 1 M Na_2CO_3 stop solution. Samples were read at both 405 and 540 nm in the FLUOstar plate reader before calculation of activity in Miller units using the β-galactosidase equation below.

$$\beta - \text{galactosidase activity} = \frac{1000 \text{ x } \text{OD405} - \text{OD540}}{\text{Time(mins)} \text{ x volume of cells in assay } (0.02) \text{ x } \text{OD600}}$$

2.23 Statistical analyses

PRISM 9 (Software, USA) was used to run One-Way parametric ANOVAs on biofilm, motility and killing assay data. Two-Way parametric ANOVAs were conducted on toxin-immunity validation CFU counts. Tukey's post-hoc tests determined statistical significance between toxin and immunity induced strains during toxin-immunity module validation (Lee & Lee, 2018). Šídák's post-hoc tests determined statistical significance in biofilm biomass production, motility, killing capacity (Holm, 1979).

3. Bioinformatic analysis of CDI operons to investigate the putative functions of CDI systems in *P. aeruginosa* PA14 and PAO1

3.1 Introduction

In 2005, research carried out on the dominant pathogen from the gut flora of a rat gave rise to the discovery of a subset of T5SSs known as Contact Dependent Inhibition (CDI) systems (Aoki *et al.*, 2005). The *E. coli* strain isolated, denoted EC93, was analysed in the study conducted by Aoki *et al.* which defined three genes that mediated contact-dependent killing, leading to dominance over the gut flora. The CdiBAI, analogous with T5bSS, highlighted a new subset of T5bSS specifically associated with growth inhibition of neighbouring cells as a mechanism of competition (Aoki *et al.*, 2010; Guérin *et al.*, 2017). Since then further analysis has been conducted on the proteins that mediate CDI with various protein domains being identified that are required for the CDI system's mechanism of action. However several of the domains have unknown functions or have yet to be characterised causing the exact structures and role of these domains to remain elusive.

The CDI operons encode highly conserved genes and are activated in close cellular proximity (Meuskens *et al.*, 2019; Klein, Ahmad & Whitney, 2020). *P. aeruginosa* encodes CDI systems known as '*E. coli*-type' due to their genetic arrangement mimicking those originally discovered in *E. coli* (Aoki *et al.*, 2005). So far, it is understood that the CdiB encodes a β-barrel which is inserted into the OM. CdiB acts as a stabiliser for the system and transports the extracellular N-terminal passenger domain of CdiA, interacting through its POTRA domains (Ruhe *et al.*, 2013). The CdiA Fha1 domain, known as the passenger domain, is exported

through CdiB and sits ~33nm from the cell surface (Ruhe *et al.*, 2018). The passenger domain is crucial for facilitating toxin release; however this exact mechanism remains unknown. To fire, CdiA possesses a receptor binding domain (RBD) which binds neighbouring cells to induce a conformational change allowing the release of the C-terminal toxin (Ruhe *et al.*, 2018). The RBDs for '*E. coli* type' systems are classified into; BamA, OmpF/C and Tsx to enable specific binding for targeted release of the C-terminal toxin sequestered in the periplasm (Aoki *et al.*, 2008; Beck *et al.*, 2016; Ruhe *et al.*, 2017). However the exact RBD OM targets in *Pseudomonas* spp. remain unknown.

Encoded after the Fha1 and RBDs is the C-terminal CdiA toxins, also known as CdiA-CTs, which are locked in their sequestered periplasmic conformations by YP domains. YP domains precede the translocation domain, Fha2 domain and pre-toxin peptide motifs (PTPMs)-signalling the end of the passenger domain and the beginning of the toxin (Aoki *et al.*, 2010; Mercy *et al.*, 2016; Allen & Hauser, 2019). It is thought that upon binding to a receptor on a neighbouring cell, either protein folding or asymmetric charge distribution drives a conformational change from the RBD down the YP domain and across the Fha2 to allow export and release of the toxin through the CdiB (Meuskens *et al.*, 2019). The combination of this CdiA-CT and RBD sequence variation is believed to mediate strain specific kin recognition associated with contact-dependent systems (Willett *et al.*, 2015b). However the exact functions of these toxin-immunity modules remain largely unknown, where 18 of 37 (~50%) CdiA-CT domain variations identified in *P. aeruginosa* to date have no known function (Allen & Hauser, 2019). These toxins are encoded directly upstream of immunity genes which protect the cell by preventing autoinhibition or killing of kin through cognate binding to their associated toxin and inhibiting its enzymatic activity (Aoki *et al.*, 2010). This mechanism has

been shown to be specific as closely related immunities do not confer protection to other CDI toxins (Ruhe *et al.*, 2016).

Further downstream of the *cdiBAI* operon is associated with multiple unannotated 'orphan' ORFs which confer CdiA/I sequence homology. As this has been shown to be a recombination hot-spot, these systems are frequently flanked by genes associated with transposable elements such as transposases (Poole *et al.*, 2011; Allen & Hauser, 2019), and represent displaced toxin-immunity modules. This recombination provides a genetic reservoir to give rise to novel toxin-immunity modules through HR from these downstream regions or from acquired novel DNA (Arenas *et al.*, 2013; Koskiniemi *et al.*, 2014).

A relatively recent discovery in contact-dependent mechanisms, the T5SS was not identified in *P. aeruginosa* until 2007 (Wilhelm *et al.*, 2007). It is now widely accepted that *P. aeruginosa* encodes two CDI systems (Van Ulsen *et al.*, 2014), however most research to date has focussed on lab strain PAO1. The first focussed study in *P. aeruginosa* was by Mercy *et al.* in 2016, where they defined a role of the two PAO1 encoded CDI systems in competition under laboratory conditions. This study in combination with that conducted by Allen *et al.* in 2019 highlighted that many *P. aeruginosa* strains associated with human infection contain CDI systems. Additionally, Mercy *et al.* outlined that *P. aeruginosa* PA14 encodes at least one CDI system. The PA14 strain background is commonly associated with cystic fibrosis pulmonary infection (Cramer *et al.*, 2011). However, much of the characterisation of the presence, genomic arrangement and functionality of these systems including identification of the immunities is yet to be elucidated in this commonly used prototypical strain. In this chapter I have performed a close inspection of the components or the PA14 CdiBAI system as well as its domains and motifs to better understand CDI systems in *P. aeruginosa*.

3.2 Aims of this study

From the current literature I have one major hypothesis to address within this chapter:

P. aeruginosa strain PA14 encodes two CDI systems that are homologous to those found in PAO1 but differ in their putative C-terminal toxic function.

This chapter summarises research conducted to expand the genomic and proteomic understanding of the CDI systems in *P. aeruginosa* PA14 through addressing the following aims:

1. Identification of the genomic locations of CDI systems in *P. aeruginosa* PA14
2. Determination of the homology of CDI operon genes and domain structures to the systems from *P. aeruginosa* PAO1
3. Identification of putative *cdiI* genes and bioinformatic prediction of their functions through small ORF analysis
4. Determination of the phylogenetic relatedness of CDI systems in *Pseudomonas* spp.
5. Identification of conserved genomic regions between genetically distinct and homologous CDI systems

3.3 Results

3.3.1 Identification and bioinformatic analysis of T5SS CDI operons in P. aeruginosa

Previously, CDI systems identified in *P. aeruginosa* PAO1 were analysed and demonstrated to play a role in interbacterial competition (Mercy *et al.*, 2016). The study conducted by Mercy *et al.* built upon the current literature around CDI systems in *Pseudomonas* spp. suggesting *P. aeruginosa* strains encode two CDI systems (Van Ulsen *et al.*, 2014). Using the PAO1 genes outlined in Mercy *et al.* 2016, *in silico* analysis was performed to compare these sequences against the Pseudomonas.com search engine to identify any PAO1 CDI homologs in PA14 through database hits. Using the CdiA sequences for each system type, two systems homologous to those in PAO1 and their gene designations were identified in PA14.

PAO1 system 1 (PA0041) was shown to encode a homologous system in PA14 which was identified as PA14_00510 based on chromosomal location. PAO1 system 2 (designated PA2462) homologous system in PA14 was identified as PA14_32790. Both operons are outlined in Figure 3.1. Identification of the PA14 systems utilised the PAO1 *cdiA* sequences due to their size and the understanding that the 5' end has high sequence identity between strains. To confirm the genes identified pertained CDI systems, the first gene in the operon *cdiB* which is encoded directly upstream of *cdiA* was identified through sequence homology to those in PAO1. This confirmed that each system in PA14 demonstrates the *cdiBAI* genetic structure conserved in '*E. coli* type' T5bSS that are associated with CDI (Guérin *et al.*, 2017). This supports current literature and confirms my hypothesis that CDI systems in *P. aeruginosa* retain this *cdiBAI* genetic structure. From this point these systems will be denoted CDI^{00510} and CDI^{32790} from PA14, CDI^{0041} and CDI^{2462} from PAO1.

Using SMART bioinformatics tool, these systems in PA14 also exhibited similarities in putative function in genes upstream and downstream of the operons to the CDI genome location in PAO1 (Figure 3.1 and Table S1). All four retained a pattern of the putative subcellular localisation of each functional gene. From 5' to 3' this consisted of a membrane based region followed by an extracellular gene, another membrane based region and finally ending in an exotoxin. The retention of the gene order and functional characteristics of the CDI operons in PA14 compared to those in PAO1 confirm these systems are T5bSSs as they contain all the markers of a CDI operon. Having studied the general genomic characteristics of these systems in PA14, the sequences downstream of each CdiA-CT were studied to identify putative *cdiI*s and their predicted domain functions using the various software and bioinformatics tools outlined in Table 2.12 from Chapter 2.5.1.

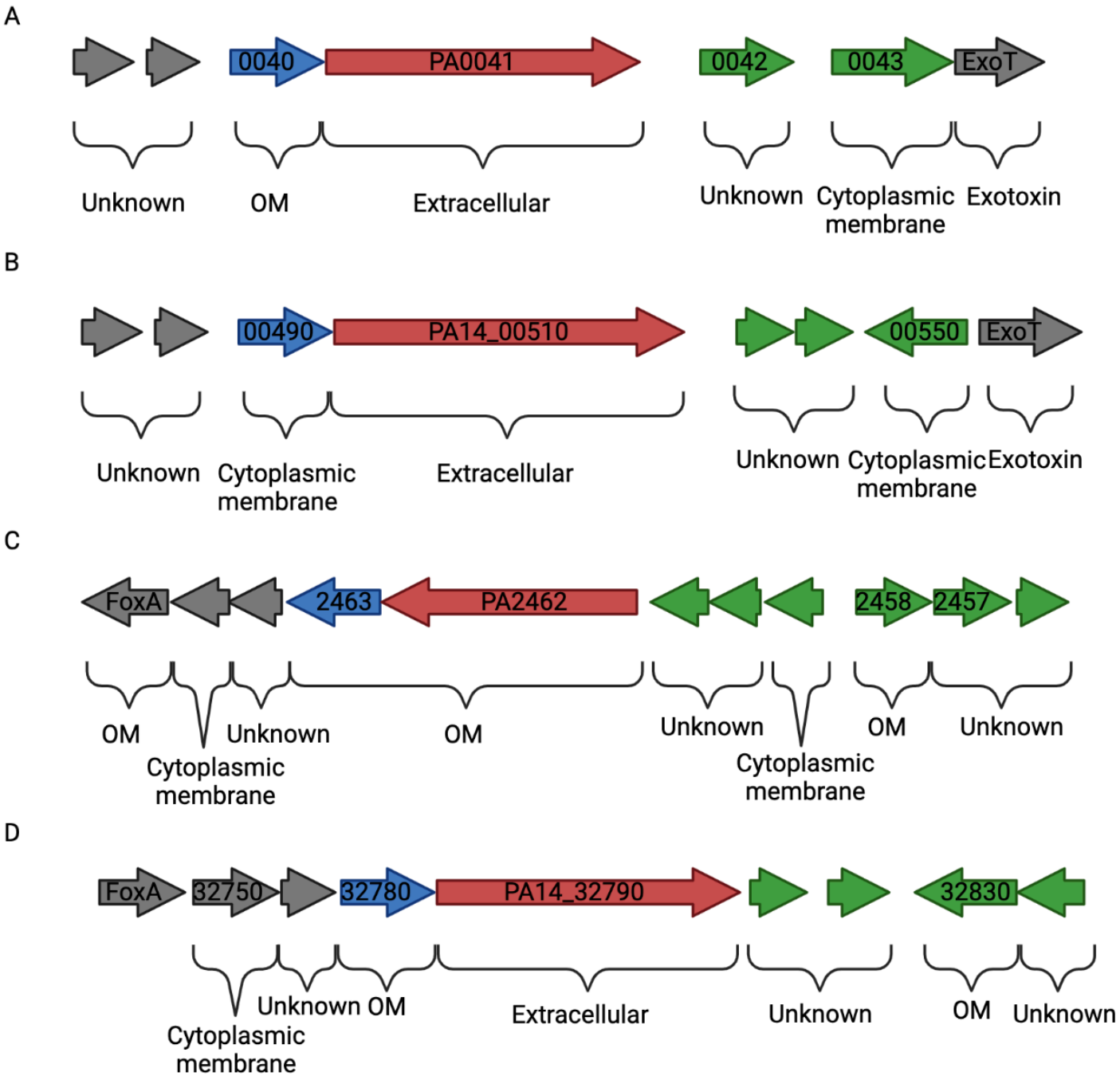


Figure 3.1: CDI operons in PAO1 and PA14. (A) PAO1 CDI^{0041} system 1, (B) PA14 CDI^{00510} system 1, (C) PAO1 CDI^{2462} system 2, (D) PA14 CDI^{32790} system 2. Operons constructed from sequence information from www.pseudomonas.com. Note: Systems A and B, and C and D are homologous systems between PAO1 and PA14. *cdiB* (PA0040/PA14_00490/PA2463/PA14_32780), *cdiA* (PA0041/PA14_00510/PA2464/PA14_32790). Note: blue arrows signify CdiB encoding genes, red arrows signify CdiA encoding genes. Green arrows indicate genome region explored for *cdiI*, whilst grey arrows signify other genes within the genomic location of the CDI operons.

3.3.2 Comprehensive in silico identification orphan-immunity pairs and unannotated putative immunity genes through small ORF analysis

Genes encoding immunity proteins are important in preventing autoinhibition and killing of neighbouring kin by cognate binding to toxins to neutralise their activity (Aoki *et al.*, 2010). *cdiI* genes are very small with low sequence identity, therefore unless identified via other means they aren't labelled as putative genes, instead appearing to reside within uncharacterised regions of the genome. As the region downstream of *cdiA* has many putative ORFs as it is a HR hotspot (Ruhe *et al.*, 2016), this provides a genetic reservoir. Therefore *cdiI* identification in the PAO1/PA14 CDI systems requires in depth analysis of these ORFs. In a previous study, Mercy *et al.* identified *cdiI* for both CDI systems from PAO1. To identify the unknown *cdiI*s for systems CDI^{00510} and CDI^{32790}, ORF prediction software and manual investigation was conducted here from the genome region ~500 bp downstream of each *cdiA*. Downstream analysis can outline orphan domains encoding toxic functions previously utilised by these systems, indicating system evolution and previous CDI targets based on these genetically decayed regions

ORF finder, Vector NTI software and manual investigation were used to identify multiple small ORFs. As part of the manual investigation, 18 bp upstream and downstream of the start codon of each ORF was input into a Kolaskar calculator to calculate the likelihood of expression. Any ORFs with a Kolaskar value ≥ 25 indicated expression would occur by identifying Shine-Dalgarno sequences, and these were analysed further to identify their putative functions to determine which ORF pertained the *cdiI*. Although Mercy *et al.* previously identified a *cdiI* for CDI^{0041} and CDI^{2462}, the downstream sequence for these systems were analysed alongside those from PA14 using the same method to validate their finding. The

identification of the *cdiI* for each system was crucial for distinguishing the regions of the entire *cdiBAI* operon. This was essential for the construction of deletion mutants for subsequent experiments into CDI functionality. Protein domain prediction tools were then used (Table 2.12 in 2.5.1) to conduct a functional analysis of these proteins.

Multiple downstream ORFs with Kolaskar scores ≥ 25 are outlined in the annotated genomic region for each system (Figure 3.2 and Table S2). From this, the downstream ORF organisation of CDI^{0041}/ CDI^{00510} was shown to support the homology observed in Figure 3.1. These annotated and putative ORFs were then used to query sequence databases e.g. BLAST to elucidate potential functions. CDI^{0041}/CDI^{00510} showed fewer conserved predicted functions directly downstream of the *cdiA* at the 5' end (CDI^{0041} ORF predicted to be involved in anaerobic energy transfer and membrane modification, whilst the ORF downstream of $cdiA^{00510}$ may be associated with quorum sensing and membrane modification) and higher levels of homology closer towards the 3' end (e.g. predictions of signal transduction and DNA modelling/modification functions, followed by an ExoT- commonly involved in T3SSs) of this downstream region. This re-enforces the concept that variation exists within these regions between strains. As some of these predicted functions suggest roles for putative toxins with intracellular membrane targeting in prey cells, this supports current literature which shows CDI toxins have intracellular targets (Aoki *et al.*, 2009; Willett *et al.*, 2015b).

The homology and functional organisation of CDI^{2462}/CDI^{32790} is more variable. However CDI^{2462}/CDI^{32790} DNA regions do encode recognised secondary CdiA/I domains. Downstream of $cdiA^{2462}$ ORFs have predicted homology to genes involved in anaerobic energy transfer, chemoreceptors, and nutrient scavenging toxins. This suggests the previous roles of these putative toxins may have involved blocking prey cell response to or retrieval ability of

nutrients within its environment. Finally, downstream of *cdiA*^{32790} ORFs have predicted homology to genes predicted to be involved in OM structure and its enzymatic alteration. Interestingly it additionally encoded ORFs directly upstream of secondary CdiA/I domains that had homology to ABC transporter genes which looks like a genetically decayed/displaced *cdiB*. Additionally, a 3' end ORF encodes a putative *tonB* gene. TonB is coupled with ABC autotransporters in TPS systems, and is associated with iron acquisition (Andrews, Robinson & Rodríguez-Quiñones, 2003). This supports homology observed CDI^{32790} ORF functionality and may suggest a common ancestor with a role in nutrient acquisition whereupon HR events after strain divergence gave rise to evolutionarily different CDI systems evolved for offence.

This analysis highlighted variations in putative functions that suggests a specificity to system type and strain. This supports my hypothesis that these systems maintain the '*E. coli* type' *cdiBAI* organisation, as well as the retention of domain organisation between homologous systems. This also supports the literature indicating that these systems are specific at individual strain level (Ruhe *et al.*, 2013) and has built upon our current understanding of the organisation of the orphan region downstream of *cdiA*. The presence of transposable elements in CDI^{0041} supports the idea that this region acts as a hotspot, not just for HR but by acquiring genes via the insertion of transposable elements. From these analyses of the downstream ORFs, the *cdiI* for each system was identified (CDI^{0041}-ORF6, CDI^{00510}-ORF54, CDI^{2462}-ORF132, CDI^{32790}-VectorNTI). These ORFs were picked based on their proximity to the *cdiA*-CT 3' end, function and Kolaskar value (Table 3.1). Whilst the immunities outlined in the Mercy *et al.* 2016 study were shown to be functional, it is likely a longer ORF with 57 additional amino acids for *cdiI*^{0041}, and a different ORF starting 30 amino acids downstream

of the end of *cdiA*^{2462} are more likely the true immunities. Further domain analysis using SMART bioinformatics was used on the selected immunity ORFs.

ORF6 (CDI^{0041}) identified homology to zinc ribbons and rubredoxin. Zinc ribbons are involved in processes such as protein folding and assembly (Malgieri *et al.*, 2015), whilst rubredoxin acts as a protein carrier and responds to oxidative stress (Li & Ni, 2019). As the function of this ORF is associated with toxin neutralisation through binding and is near the *cdiA*-CT, this ORF was identified as likely encoding *cdiI*^{0041}. Therefore, this is the more likely ORF as this is a more comprehensive analysis compared to that outlined in Mercy *et al.* 2016.

ORF132 (CDI^{2462}) identified homology to a sulfate permease and N-6 DNA methylase. APC superfamily sulfate permeases are secondary substrate transporters (Marietou *et al.*, 2018). N-6 DNA methylases are found in bacterial restriction-modification systems, protecting prokaryote DNA against restriction enzyme induced degradation via adenine methylation (Cheng, 1995). As ORF132 is associated with substrate transport, substrate editing via methylation, and is near the *cdiA*-CT, this ORF was identified as likely encoding *cdiI*^{2462} compared to that outlined in Mercy *et al.* 2016. The analysis of ORF132 suggests it might have a role in protein binding which as immunities act via cognate binding is supportive that this is the associated immunity.

ORF54 (CDI^{00510}) identified homology to AgrD and Pox_P35. AgrD from *S. aureus* is associated with production of exoproteins involved in virulence (Dufour *et al.*, 2002). Pox_P35 is associated with the poxvirus envelope involved in target cell attachment (Massung *et al.*, 1993). As ORF54 is in proximity to *cdiA*-CT, this ORF was identified as likely encoding *cdiI*^{00510}. However, its predicted function does not tell us much about its function besides an

association with attachment and substrate transport, but the level of homology is weak limiting this interpretation.

Finally ORFVectorNTI (CDI^{32790}) identified homology to SCOP domain and AXN. SCOP domains have no identified function (Murzin *et al.*, 1995). Using NCBI BLAST to query this SCOP, ~70% homology to *Stenotrophomonas maltophilia* was observed. AXN are calcium-dependent membrane-binding proteins from the eukaryotic cell cycles (Schloer, Pajonczyk & Rescher, 2018). As the ORFVectorNTI is associated with metal-dependent membrane binding, and it is near the *cdiA*-CT, this ORF was identified as likely encoding *cdiI*^{32790}.

The predicted functions of ORF6, ORF54, ORF132, and ORFVectorNTI further support the notion of toxin-immunity cognate binding through active site protection/blocking. However initial queries in various online bioinformatics tools indicated no predicted functions or functional/structural domain homology (Figure 3.3). This suggest these proteins are novel, supporting current literature, but could also belong to a class of unidentified protein or function (Mercy *et al.*, 2016; Allen & Hauser, 2019). This is common for immunity proteins due to their high variability and specificity to their associated toxin as genes encoding the toxin/immunity pair are acquired together.

Analysis conducted by MRes student Madeleine Humphrey at a later date identified *cdiI*^{00510} had 100% structural homology with *cdiI* from *P. aeruginosa* PABL017 using Phyre2 (Allen *et al.*, 2020) suggesting *cdiI*^{00510} encodes an anti-tRNase immunity. However no putative functions were found for other immunities at this time. I conducted further analysis on these four immunities later to support her findings and determine whether their functions and/or domains had been elucidated through updated database searches. This final analysis

supported Madeleine's finding that *cdiI*^{00510} had 100% sequence identity to CdiI^{PABL017} . Further BLASTp searches showed high identity to an *Enterobacter cloacae* gene, which upon amino acid alignments, showed 99% sequence identity (Table 3.2). As this new database search identified additional homologies to genes from other bacteria, I re-analysed the other immunities via structural analysis using Phyre2.

Analysis indicated *cdiI*^{32790} structural homology to a *Klebsiella pneumoniae* toxin-antitoxin system with a SpoVT-AbrB domain. SpoVT enables transcriptional regulation of endospore formation in *Bacillus subtilis* (Ramirez-Peralta *et al.*, 2012), whilst AbrB is an AMR protein B transition state regulator (Robertson *et al.*, 1989). Aligning the *Klebsiella* immunity with *cdiI*^{32790} showed 40% sequence coverage (Table 3.2). The high sequence coverage indicates the CDI^{32790} toxin-immunity is similar to this *Klebsiella* toxin-antitoxin. Literature searches showed this toxin-antitoxin system is synonymous to the MazF/MazE toxin-immunity system in *Enterobacteriaceae* and other *Klebsiella* strains and encodes an endoribonuclease (Jin *et al.*, 2021). Blasting this *Klebsiella* immunity identified sequence homology to *Klebsiella pneumoniae* and *E. coli* which, upon sequence alignment showed a 46% and 35% sequence identity respectively (Table 3.2). This supported the literature indicating this toxin system is found in the *Enterobacteriaceae* family (Aizenman, Engelberg-Kulkat & Glaser, 1996). Blasting *cdiI*^{32790} showed high percentage identity to *Stenotrophomonas maltophilia* (76%), supporting previous BLAST results, and *Achromobacter xylosoxidans* (51%). Upon sequence alignment it showed a 73% and 39% sequence coverage to *Stenotrophomonas* and *Achromobacter* respectively (Table 3.2). Therefore the conclusion is that *cdiI*^{32790} is an anti-endoribonuclease.

Next analysis was conducted on *cdiI*^{2462}, which identified homology to an ATP-dependent RNA helicase. However, sequence alignment showed only 2% sequence identity (Table 3.2). As no

other domain hits were outlined, I could not conclude its function. The novelty of this sequence supports the literature indicating *cdiI* have high sequence variability (Morse *et al.*, 2015).

Finally, analysis on *cdiI*^{0041} showed high percentage coverage to a rubredoxin-like binding protein from *P. aeruginosa* designated *alkT* (van Beilen, Wubbolts & Witholt, 1994). Upon sequence alignment, *cdiI*^{0041} showed 15% coverage to *alkT* (Table 3.2). However, blast indicated 100% sequence identity with *Eggerthia catenaformis*, a gram-positive bacteria. Sequence alignments confirmed a 99% sequence homology based on one amino acid addition in *Eggerthia* indicating *cdiI*^{0041} is found in gram-positive bacteria and may be present in a different secretion system such as the T7SS as gram-positive bacteria do not encode T5SSs. CDI systems have not yet been implicated in interactions with gram-positive bacteria. As no other domain hits were identified, I could not conclude it function.

Having performed an initial search on the full operon, the domains within the *cdiB/cdiA* were then further queried against online sequence databases to evaluate putative domain function predictions using the various software programmes outlined in Table 2.12 in 2.5.1.

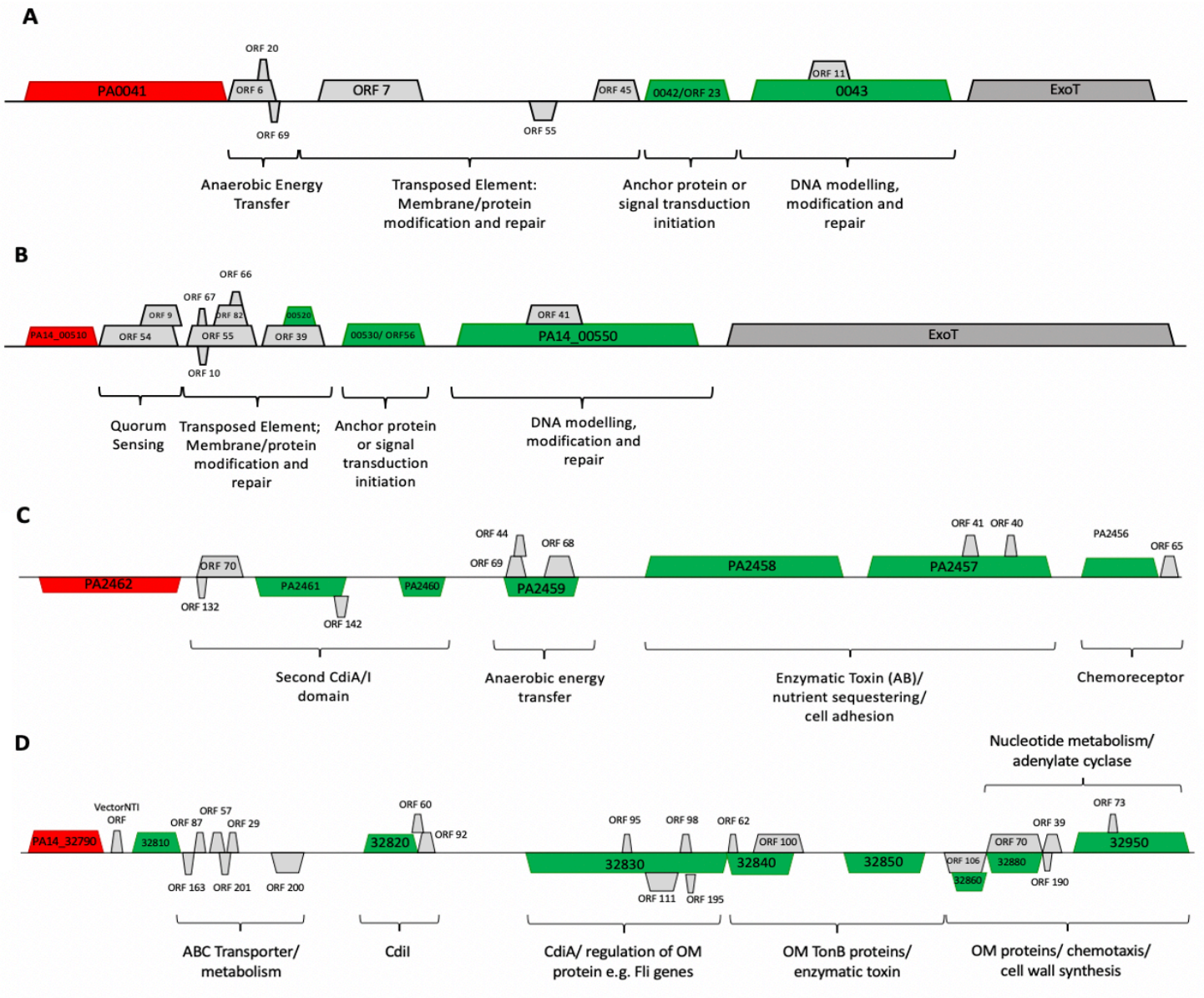


Figure 3.2: Small ORFs of toxin-Immunity regions downstream of CDI operons in PAO1 and PA14. (A) PAO1 CDI^{0041} system 1, (B) PA14 CDI^{00510} system 1, (C) PAO1 CDI^{2462} system 2, (D) PA14 CDI^{32790} system 2. Operons constructs from sequence information from using bioinformatics programmes in Chapter 2 Table 2.12. Genes were identified using ORFfinder and VectorNTI, where the forward strand are represented above the line, whilst reverse strand genes are represented below, with gene functions indicated. Note: Systems A and B, and C and D are homologous systems between PAO1 and PA14.

Table 3.1: Kolaskar values for expression likelihood of immunity ORFs for PA14 and PAO1 CDI systems

CDI System	ORF	Kolaskar Value
PA0041	VectorNTI	33
PA14_00510	6	28
PA2462	132	28
PA14_32790	54	30

*Note Kolaskar value above 25 means ORF is likely expressed, above 25 increases likelihood

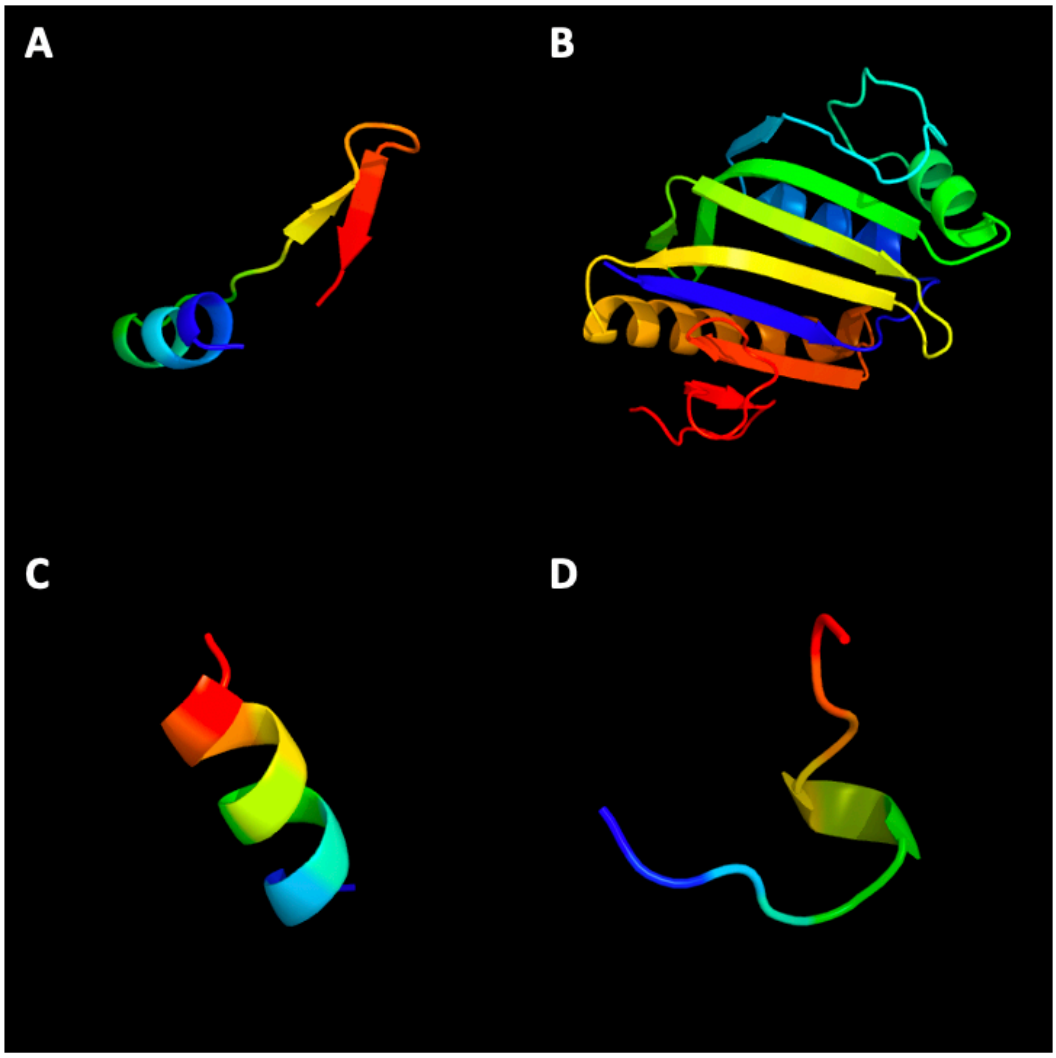


Figure 3.3: Phyre2 analysis of CdiI from CDI systems in PAO1 and PA14. (A) PAO1 CdiI^{0041} ORF6, (B) PA14 CdiI^{00510} ORF54, (C) PAO1 CdiI^{2462} ORF132, (D) PA14 CdiI^{32790} VectorNTI ORF. Analysis of CdiI immunities from CDI systems in different strains highlights their variability in size and structure indicating disparate functional mechanisms utilised for toxin neutralisation. **(A)** PAO1 CdiI^{0041} indicates immunity identified as homologous to OB-fold. Structure showed 89.5% confidence in nucleic acid-binding protein homology with only 31% coverage (26 residues) and 27% identity to template. **(B)** PA14 CdiI^{00510} indicates immunity identified as homologous to *P. aeruginosa* CdiA/I. Structure showed 100% confidence in chain B immunity homology with 100% coverage (155 residues) and 97% identity to template. **(C)** PAO1 CdiI^{2462}

indicates immunity identified as homologous to *S. cerevisiae* Dpb5. Structure showed 24.2% confidence in hydrolase homology with only 34% coverage (12 residues) and 33% identity to template. **(D)** PA14 CdiI^{32790} indicates immunity identified as homologous an uncharacterised hydrolase protein from *Klebsiella pneumoniae* toxin-antitoxin complex. Structure showed 72.9% confidence in hydrolase component homology with only 10% coverage (11 residues) and 18% identity to template. Note: rainbow colours indicate N to C terminus.

Table 3.2: Percentage sequence identity of toxins based on bioinformatics software based database hits and UGENE sequence alignments

Immunity	Result Identified Via	Homologous Bacterial Species	Bacterial Strain	Identified Gene	Percentage Sequence Identity	Alignment Matrix Used	Alignment Percentage Sequence Homology
PA14_00510	Allen *et al.* 2020	*Pseudomonas aeruginosa*	PABL017	CdiI	-	MUSCLE	100%
	NCBI blastp	*Enterobacter cloacae*	e403	N/A	100%	MUSCLE	99%
PA14_32790	Phyre2	*Klebsiella pneumoniae*	MGH 78578	Toxin	72.9%	MUSCLE	46%
	Klebsiella pneumoniae RCSB PDB	*Escherichia coli*	K12	MazE	-	MUSCLE	37%
	NCBI blastp	*Stenotrophomonas maltophilia*	40324	-	75%	MUSCLE	73%
	NCBI blastp	*Achromobacter xylosoxidans*	85698	-	51%	MUSCLE	39%
PA0041	Phyre2	*Pseudomonas aeruginosa*	PAO1	PA5349	31%	ClustalW	15%
	NCBI blastp	*Eggerthia catenaformis*	MAR1	-	100%	MUSCLE	99%
PA2462	Phyre2	*Saccharomyces cerevisiae*	ATCC 204508	-	24.2	MUSCLE	2%

3.3.3 Determining CDI operon genetic and protein structure homologies through in silico analysis

Many domains within the *cdiBAI* operon associated with its structure have been elucidated. As the CDI system is only composed of three genes, this domain analysis has played a crucial role in elucidating its rudimentary mechanism of action. Studies by Ruhe *et al.* and Willett *et al.* in 2015 and 2018 respectively identified domains including TPS (which facilitate extracellular N-terminal CdiA release), and YP (which keep the toxin periplasmically sequestered). From this a general domain structure within the '*E. coli* type' *cdiA* has now been accepted and has been extrapolated in part to the CDI systems in *P. aeruginosa* (Allen & Hauser, 2019). Using the CDI systems identified in 3.3.1, further analysis on CDI in PAO1 and PA14 was used to elucidate protein domains within each CDI gene to determine whether domain retention occurs with other *Pseudomonas* and non-*Pseudomonas* CDIs to infer potential protein functions. This was also used to identify similarities between homologous systems in domain layout and functionality.

3.3.3.1 CdiB outer membrane β-barrel

Each system and their homologue were identified to have a conserved CdiB β-barrel region and Sec signal peptide with 100% confidence in structural homology based on Phyre2 analysis (Figure 3.4). CdiB in homologous systems CDI^{0041} and CDI^{00510} retained a TpsB2/ShlB/FhaC/HecB hemolysin secretion/activation domain at position 27 followed by a POTRA domain at position 53, with SCOP and Pfam:POTRA domains further downstream. CdiB in homologous systems CDI^{2462} and CDI^{32790} maintained similar domain homology to CDI^{0041} and CDI^{00510} but at slightly different positions (30 and 57 respectively).

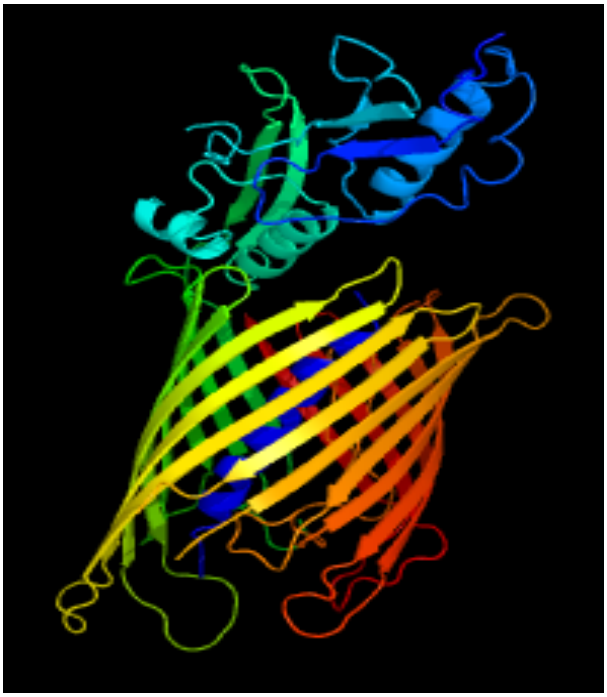


Figure 3.4: Phyre2 PA14 CdiB^{00490} analysis. Analysis of CdiB genes for each system in both PAO1 and PA14 indicates conserved an Omp185 16-strand β-barrel structure identified as homologous to the TpsB OM transporters. PA14 CdiB^{00490} indicated here is representative of CdiB structure. CdiB^{00490} structure showed 100% confidence in chain A FhaC homology, indicating protein transport functions. Note: rainbow colours indicate N to C terminus.

Interestingly CDI^{2462}/CDI^{32790} CdiA domains differed from CDI^{0041}/CDI^{00510} at the C-terminus, replacing the UBA_e1_C ubiquitin binding and DEATH apoptotic associated domains with the DNAG_DnaB_bind DNA binding and FCD N-terminal effector binding domains. Ubiquitin binding domains are associated with ubiquitin attachment, with UBA_e1_C encoding the Ubiquitin-activating enzyme E1 C-terminus (Lee & Schindelin, 2008). This enzyme is involved in ATP-dependent activation of ubiquitin (Rytkönen & Holden, 2007) and requires protein-protein interactions which may aid CdiA-CdiB interactions. DEATH domains are part of effector-associated α-helical adaptor domains which mediate interactions between effector and signalling domains (Kaur *et al.*, 2021). These domains, situated near the gene 3' end and surrounded by POTRA domains suggests a different mechanism of action for the stability of the extracellular N-terminal CdiA. The DNAG_DnaB_bind domain is found in DnaG primases required for DnaB DNA helicase interactions for RNA synthesis (Oakley *et al.*, 2005). FCD N-terminal effector binding domain is a ligand binding domain from GntR-like bacterial transcription factors associated with sugar biosynthesis operons (Zheng *et al.*, 2009;

Suvorova, Korostelev & Gelfand, 2015). Together these domains indicate the CdiB C-terminal of all systems may be associated with the specific binding between the toxin passenger and CdiB. Although slight differences in domains between homologous systems exist, the structure is highly conserved supporting the current literature (Aoki *et al.*, 2005; Baud *et al.*, 2014). This analysis supports my hypothesis that PA14 shares domain organisation to the homologous systems in PAO1.

3.3.3.2 CdiA toxin passenger domain and C-terminal toxin

Analysis and alignment of N-terminal *cdiA* passenger domains showed high conservation with a gradual loss of homology and percentage identity between strains from the 5' to 3' end. This supports previous work by Aoki *et al.* in 2010 which showed divergence occurring after the pre-toxin peptide motif. Based on previously studies, CdiA encode domains; TPS, Fha1, RBD, YP, Fha2, PTPM and a C-terminal toxin, from 5' to 3' end (Faure *et al.*, 2014; Willett *et al.*, 2015b; Ruhe *et al.*, 2018; Allen & Hauser, 2019) (Figure 3.5). Further protein domain analysis of these systems in PAO1 and PA14 are outlined in Figure 3.6 and described below.

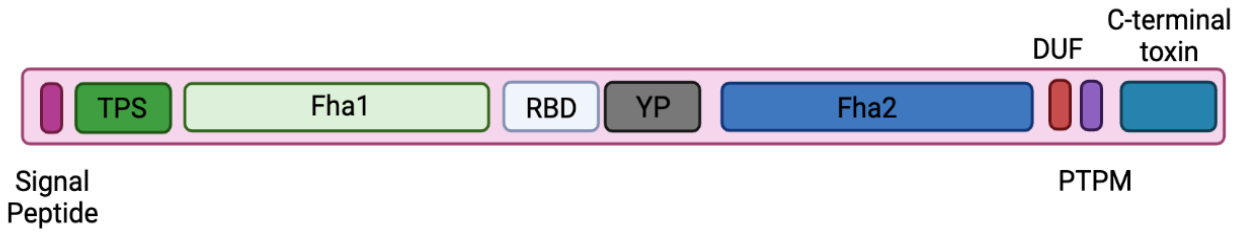


Figure 3.5: Domains of CdiA proteins in *E. coli* type CDI systems in *Pseudomonas* spp. Analysis conducted in the studies Faure *et al.*, 2014, Willett *et al.*, 2015, Ruhe *et al.*, 2018 and Allen & Hauser, 2019 outlined this general domain organisation for CdiA.

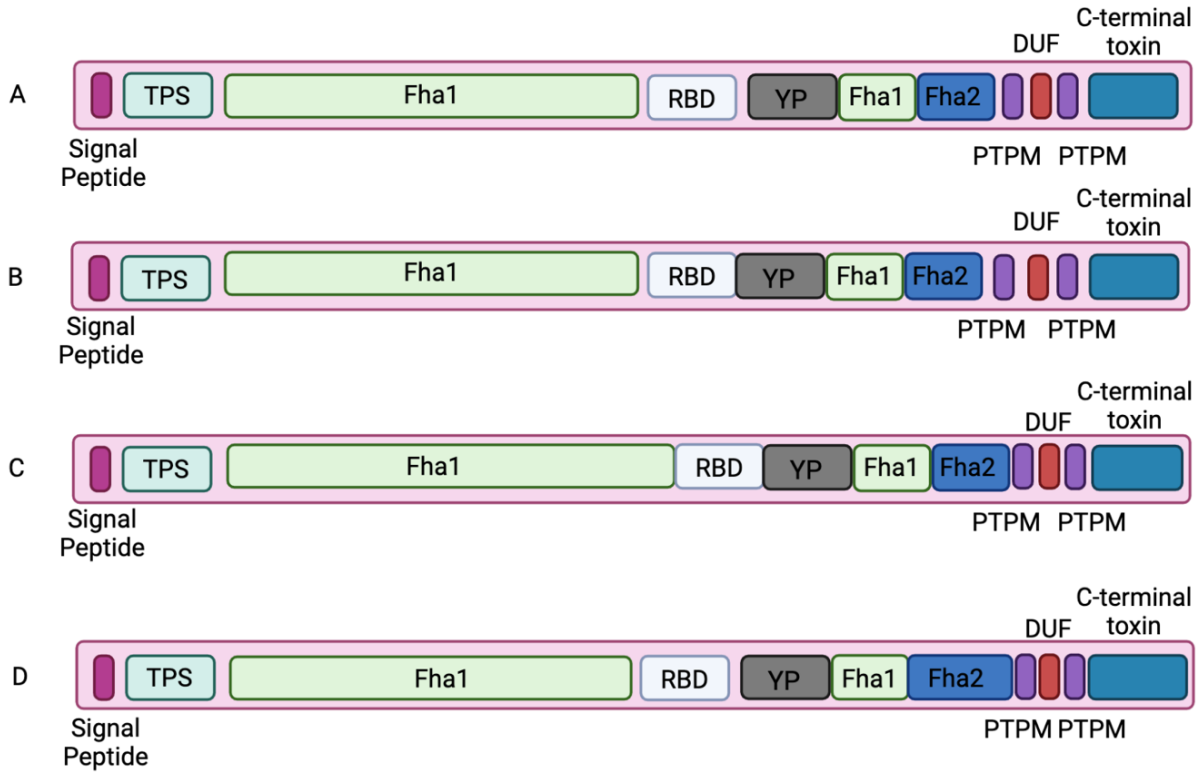


Figure 3.6: Domains of CdiA proteins in CDI systems within *P. aeruginosa* strains PAO1 and PA14. Analysis of CdiA domain structures from homologous CDI systems in different strains highlights the conserved nature of the N-terminal and the variability of the C-terminal. (A) PAO1 CdiA^{0041} domain analysis indicates it encodes two PTPMs of different classes (IV and V respectively) and a DUF domain prior to the C-terminal toxin. (B) PA14 CDI^{00510} domain analysis indicates it encodes a DUF domain and a class V PTPM prior to the C-terminal toxin. (C) PA01 CDI^{2462} domain analysis indicates it encodes a DUF domain and a class IV PTPM prior to the C-terminal toxin. (D) PA14 CDI^{32790} domain analysis indicates it encodes a DUF domain and a class IV PTPM prior to the C-terminal toxin.

All CdiA encoded a signal peptide, confirming extracellular translocation in line with T5SS/CDIs, and were associated with the Sec translocation pathway. This supports the literature showing CdiA translocation occurs via the Sec pathway (Desvaux *et al.*, 2007; Papanikou, Karamanou & Economou, 2007). The TPS directly downstream of the signal peptide in each system consisted of POTRA domains, whilst Fha domains consisted of filamentous haemagglutinin repeats.

RBDs are variable and enable CdiA classification into three types based on the receptors they bind. To date these have been identified in *E. coli* (BamA, OmpC/F and Tsx (Aoki *et al.*, 2008; Beck *et al.*, 2016; Ruhe *et al.*, 2017)), however they are yet to be identified in *Pseudomonas* spp. All RBDs here were situated between Fha repeat domains Fha1 and Fha2, and contain domains associated with PRK15319 fibronectin-binding autotransporter adhesin ShdA domain which mimics heparin binding (Kingsley *et al.*, 2004). Despite these similarities, identifying cognate receptors is not currently achievable via bioinformatic analysis (Allen & Hauser, 2019).

YP domains are situated next to RBDs, therefore these regions were elucidated using the sequences outlined in the 2019 Allen and Hauser study supplementary material Figure S1. Allen and Hauser classified RBD/YP domains, denoting them *rbdA*-*rbdE* based on amino acid conservation. Homologous systems CDI^{0041}/CDI^{00510} YP domains aligned the CdiA1_rA_V sequence, indicating their RBD/YP are synonymous to the *rdbA* classification. However the CDI^{2462}/CDI^{32790} homologous systems did not have homologous RBD/YP domain classifications, indicating these systems likely bind different receptors. CDI^{2462} YP aligned the CdiA2_rB_V sequence, indicating its RBD/YP is synonymous to the *rdbB* classification. Finally CDI^{32790} YP domains aligned closely to both CdiA2_rD_V and CdiA2_rE_V, which have high sequence identity. Further alignments using MUSCLE outlined small nucleotide differences between CdiA2_rD_V and CdiA2_rE_V and showed CDI^{32790} YP aligned to CdiA2_rE_V with 100% sequence identity, indicating its synonymity to the *rdbE* classification. This analysis outlines three RBD domains indicating three binding mechanisms or receptors are utilised.

Next the pre-toxin peptide motifs (PTPMs) were identified based on classes outlined in Mercy *et al.* 2016 to determine the separation point between the toxin passenger and toxin

domains. The amino acid sequences of all four CdiA were queried. Contrary to the literature indicating CdiA encode one PTPM (Mercy *et al.*, 2016; Allen *et al.*, 2020), all four systems were shown to encode two PTPMs. Downstream of Fha2 domains, a class IV DAMV motif followed by a domain of unknown function (DUF) domain and finally a class V NEALV were outlined before the toxin encoded region. The exception to the upstream DAMV motif was in *cdiA*^{00510} which encoded an amino acid derivative of DAMV- replacing alanine with valine. However it remains grouped as class IV as it is a DAMV sequence homologue which was noted in the sequences from 2019 Allen and Hauser Figure S1. The presence of two PTPMs could suggest expression of two toxins or previous recombination events leading to a longer CT and two PTPMs. However the presence of DUF domains between these PTPMs may indicate a role in CDI mechanism of action such as toxin import, potentially acting as a translocation domain (TD). Therefore the sequence between PTPMs for each system was analysed.

Comparing DUF domain sequences, they retained 100% homology of 168 amino acids between all systems. However, looking further at these sequences identified that DUF domains are not encoded directly downstream from DAMV but are preceded by a run of amino acids of differing lengths (Figure 3.7). Analysing these lengths between systems showed CDI^{2462}/CDI^{32790} had 100% homology in these sequences. In contrast, CDI^{0041}/CDI^{00510} shared no sequence homology to each other or CDI^{2462}/CDI^{32790}. Comparing this CDI^{2462}/CDI^{32790} sequence to the other systems showed that the first ~50 amino acids after DAMV were highly conserved with a small number of amino acid changes in each sequence of CDI^{0041}/CDI^{00510}. The 3’ end of these sequences directly preceding the DUF domain were more variable with low homology. This supports the idea that this region could be used for toxin import as this sequence may be specific when targeting membrane proteins of prey

cells. If so, this may suggest CDI^{2462}/CDI^{32790} use the same IM import mechanism and potentially have a common ancestor. Using NCBI BLAST, potential donors/shared targets were identified for these systems and revealed sequency identity of each CDI to those encoded by different bacterial species, further supporting this idea.

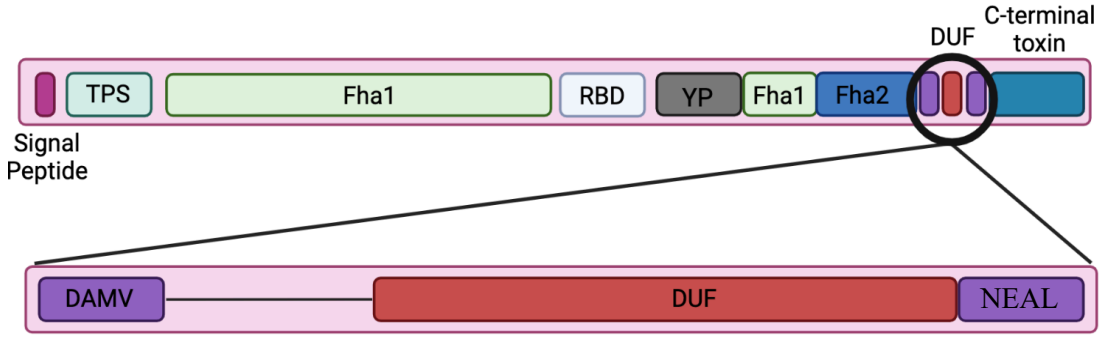


Figure 3.7: DUF domain situation in C-terminal CdiA from *P. aeruginosa* CDI systems. Analysis of CdiA domains situated between the two identified PTPMs highlights the conserved nature of the DUF domain and the variability of the sequence preceding the NEALV C-terminal PTPM. This sequence showed no domain homology to other known proteins uploaded to currently available databases, or sequence homology to the other CDI systems. This suggests a specificity mechanism in toxin import.

CDI^{0041} DUF showed 100% identity to *Acinetobacter baumanii* and *Salmonella enterica* (serovar Typhimurium), and 93% identity with *Listeria monocytogenes* (58%, 58% and 56% coverage respectively). CDI^{00510} DUF showed 100% identity to *Enterobacter cloacae* and *Acinetobacter baumanii* (98% coverage for each). These BLAST results were interesting as hits identified virulent bacteria from severe human infections, many associated with CF. Phyre2 indicated CDI^{00510} also had 24% identity with Tse6, a known T6SS NAD/NADPase (Whitney *et al.*, 2015). Gene alignments with Tse6 indicated 34% sequence identity (Table 3.3). Finally BLAST results for CDI^{2462}/CDI^{32790} shared sequence showed 100% identity to *Pseudomonas fluorescens* and *Acinetobacter baumanii*, and 98% identity to *Streptococcus dysgalactiae* and *E. catenaformis* (52%, 52%, 54% and 51% coverage respectively). This was interesting as *S.*

dysgalactiae and *E. catenaformis* are both gram-positive bacteria. CDI systems have not been documented to be used against gram-positive bacteria. The high sequence identity to other bacteria associated with human infections may suggest they are used in other polymorphic toxin systems or toxin/antitoxin systems (Zhang *et al.*, 2012; Allsopp *et al.*, 2020).

Table 3.3: Percentage sequence identity of region upstream second PTPM compared to Tse6 based on MUSCLE genome alignment

	PA14_01140_Tse6
PA14_01140_Tse6	100%
PA14_00510_DUF_upstream	34%

Next C-terminal toxin domains were queried to determine their putative functions. PA14 toxins showed almost no sequence identity to PAO1 toxins and had little homology to other identified database proteins from NCBI tBLAST and BLASTp. However, Phyre2 protein function predictions indicated putative DNA/RNA enzyme functions (Figure 3.8). This lack of homology to database proteins supports the idea HR gives rise to novel toxins (Zhang *et al.*, 2012; Allsopp *et al.*, 2020). This theory was further supported by initial analysis of small downstream orphan ORFs which were shown to encode additional functional enzymatic domains.

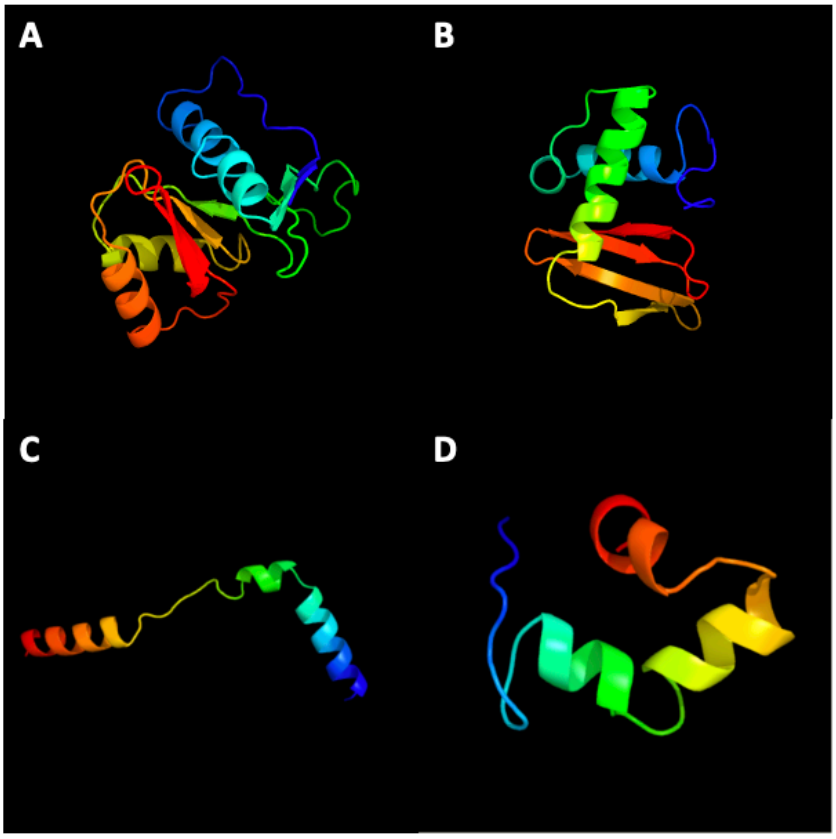


Figure 3.8: Phyre2 analysis of CdiA-CT from homologous CDI system PAO1^{0041} and PA14^{00510}. Analysis of CdiA-CT toxins from homologous CDI systems in different strains highlights their variability. C-terminal toxin domains were identified using pre-toxin peptide motifs. **(A)** PAO1 CdiA^{0041} indicates toxin identified as homologous to *B. pseudomallei* CdiA. Structure showed 99.9% confidence in chain A hemolysin homology but with only 20% coverage (128 residues) and 20% identity to template. **(B)** PA14 CdiA^{00510} indicates toxin identified as homologous to *P. aeruginosa* CdiA. Structure showed 100% confidence in chain A hemagglutinin homology. With 27% coverage aligning (92 residues) and 97% identity to template. **(C)** PAO1 CdiA^{2462} indicates toxin identified as homologous to glycosyltransferase from *B. subtilis*. Structure showed 46.3% confidence in chain A transferase homology. With 6% coverage aligning (43 residues) and 16% identity to the template. **(D)** PA14 CdiA^{32790} indicates toxin identified as homologous to *S. marcescens* CdiA. Structure showed 80.9% confidence in chain C toxin homology but with 6% coverage (37 residues) and 24% identity to template. Note: rainbow colours indicate N to C terminus.

Initial analysis was unable to identify putative functions due to the lack of structural identity to database entries. Analysis conducted by MRes student Madeleine Humphrey at a later date identified CdiA-CT^{00510} encodes a trans-kingdom tRNase effector via alignment with CdiA^{PABL017} (Allen *et al.*, 2020) which had 100% sequence homology. Madeleine also identified a putative function for CdiA-CT^{32790} as an acetyltransferase due to the presence of an ArgJ-like domain involved in arginine biosynthesis (Marc *et al.*, 2000). After this I conducted further

analysis to support her findings and determine whether toxic functions could be elucidated through updated database searches. This final analysis supported this finding and additionally showed 100% sequence identity with *Acinetobacter baumanii* and *Enterobacter cloacae*- further supporting the claim of its trans-kingdom nature (Table 3.4).

Table 3.4: Percentage sequence identity of toxins based on NCBI BLASTp hits and UGENE sequence alignments

Toxin	Result Identified Via	Homologous Bacterial Species	Bacterial Strain	Identified Gene	Percentage Sequence Identity	Alignment Matrix Used	Alignment Percentage Sequence Homology
PA14_00510	Allen *et al.* 2020	*Pseudomonas aeruginosa*	PABL017	CdiA	-	MUSCLE	100%
	NCBI blastp	*Acinetobacter baumanii*	4300STDY7045804	-	100%	ClustalW	100%
	NCBI blastp	*Enterobacter cloacae*	e403	-	100%	ClustalW	100%
PA14_32790	PA14_32790 Immunity Phyre2	*Klebsiella pneumoniae*	MGH 78578	MazF	-	ClustalO	15%
	NCBI blastp	*Acinetobacter baumanii*	4300STDY7045804	-	98%	ClustalW	67%
	NCBI blastp	*Streptococcus dysgalactiae* subsp. *equisimilis*	NCTC 11565	-	99%	ClustalW	71%
	HHpred	*Escherichia coli* O157:H7 str. EC869					
PA0041	Phyre2	*Burkholderia pseudomallei*	1026a	-	100%	ClustalO	12%
	NCBI blastp	*Acinetobacter baumanii*		-	100%	ClustalO	100%
	NCBI blastp	*Salmonella enterica* subsp. *enterica* serovar *Thyphimurium*	590494	-	100%	ClustalO	82%
PA2462	Phyre2	*Bacillus subtilis*	168	Bs-YijC	50.8%	ClustalO	41%
	NCBI blastp	*Acinetobacter baumanii*	4300STDY7045804	-	100%	MUSCLE	79%

Further analysis of CdiA-CT^{32790} indicated the ArgJ-like domain identified by Madeleine lay within the DUF domain between the two PTPMs based on InterPro alignments and was unlikely to be the function of the toxin (Figure 3.9). Therefore another round of database searches was used. Based on database hits and high sequence identity to *cdii*^{32790} immunity to *Klebsiella pneumoniae* MazE, alignment of MazF toxin from the *Klebsiella* toxin-antitoxin system was conducted, identifying 15% sequence identity (Table 3.4). Further NCBI BLASTs identified high sequence identity to *Streptococcus dysgalactiae* and *Acinetobacter baumannii* (71% and 67% sequence identity respectively), however these were from uncharacterised genes (Table 3.4). A SMART bioinformatics domain search indicated the presence of two potential domains encoding an endonuclease or alanine dehydrogenase (Delforge *et al.*, 1993; Bruner, Norman & Verdine, 2000). A final search by MRes student Nicholas Yuen identified 98.66% probability and further sequence alignments indicated 62% sequence identity to CdiA tRNase from *E. coli* O157:H7 (Wang *et al.*, 2022). Therefore the conclusion is the PA14 CdiA toxins are likely tRNases.

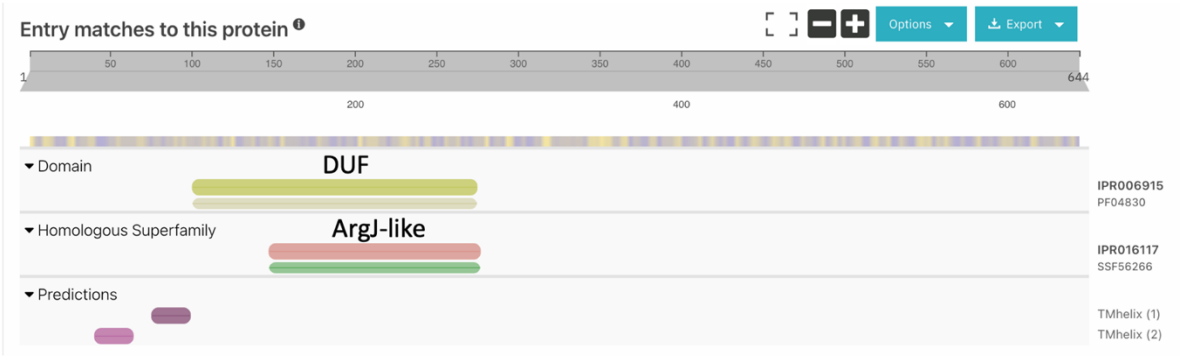


Figure 3.9: InterPro ArgJ-like domain alignment to C-terminal DUF domain of CdiA in *P. aeruginosa* CDI systems. Analysis of ArgJ-like domain identified by Madeleine Humphrey in her MRes thesis, where she indicated that this toxin function was a putative acetyltransferase. Alignment to the DUF domain indicates that this is not the function of the C-terminal toxin but may be a conserved aspect to the DUF domain which remains an unidentified domain. This could have implications in toxin import.

With this newly identified function, CdiA-CT^{00410} and CdiA-CT^{2462} analysis was repeated. SMART domains and InterPro identified the presence of an EndoU domain for CdiA-CT^{2462} which encodes a U-specific nuclease for cleaving single stranded RNA (Michalska *et al.*, 2018). BLAST showed 99% coverage to EndoU encoded in *P. fluorescens* and *A. baumanii,* 87% coverage to *Achromobacter animicus*, and 86% coverage to *Yersinia enterocolitica,* highlighting the use of this domain in many virulent bacteria (Table 3.4). A maximum-likelihood phylogenetic tree determined genetic relatedness of these EndoU (Figure 3.10) which indicated CdiA-CT^{2462} was closely related to *A. baumanii* and *P. fluorescens*. As *A. baumanii* was more closely related a direct alignment of the sequence with CdiA-CT^{32790} EndoU domain was conducted, showing 79% sequence identity (Table 3.4). Phyre2 analysis identified structural homology to a *Bacillus subtilis* glycosyltransferase. Aligning these sequences showed 41% sequence identity (Table 3.4). As glycosyltransferases are associated with catalysing glycosidic bond formation and have been shown to have a role in CDI transport (Lairson *et al.*, 2008; Dautin, 2021), CdiA-CT^{2462} may have GTase function.

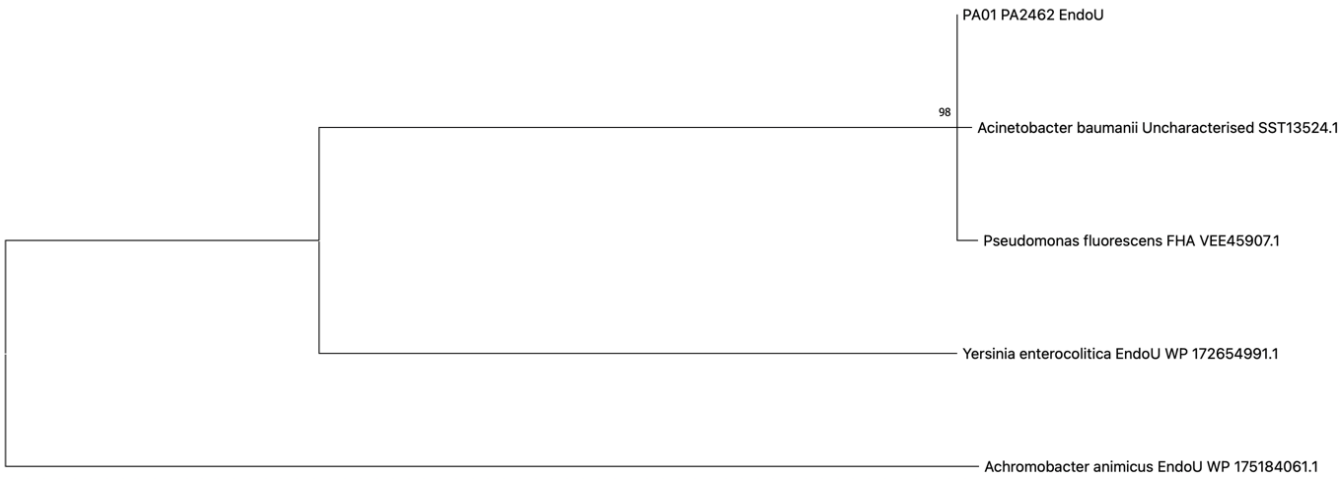


Figure 3.10: Maximum-Likelihood phylogenetic tree of BLAST results homologous to PA2462 using amino acid sequence alignments. CDI toxin MegaX alignments were used to produce a phylogenetic tree through UGENE using the settings outlined in Table X for the sequences highlighted via BLAST to have high homology to PA2462 EndoU domain. Inference of evolutionary history was achieved using Maximum-Likelihood method and Jones-Taylor-Thornton model using 1000 bootstrap replicates. Using discrete Gamma distribution, evolutionary rate differences were modelled among all sites including codon positions +1,+2, +3 and noncoding.

Finally, CdiA-CT^{0041} Phyre2 analysis identified high structural homology to a CdiA toxin from *Burkholderia pseudomallei*, however upon sequence alignment only 12% sequence identity was observed (Table 3.4). Using InterPro, a tRNA-specific ribonuclease domain was observed. BLAST analysis identified high sequence homology to *A. baumanii* (99%) and *Salmonella enterica* (77%) (Table 3.4). Upon alignment *A. baumanii* and *S. enterica* had 100% and 82% sequence identity respectively. Although these domains remain functionally uncharacterised, the conclusion via domain hits is that CdiA-CT^{0041} is likely a tRNAse.

The analysis supports my hypothesis that PA14 shares domain organisation to PAO1 homologous systems and has built upon current literature regarding the domains and their organisations in *cdiA*. Having identified the whole CDI operons, further analysis was conducted to understand the phylogenetic relatedness of these systems to each other and to others found throughout *Pseudomonas* spp. genera.

3.3.4 Determining phylogenetic relatedness of CDI systems in Pseudomonas species

Previous research has shown that gram-negative bacteria which utilise CDI systems have been found to encode two genetically distinct systems within their genomes (Aoki *et al.*, 2005; Mercy *et al.*, 2016). Many studies have outlined the genetic variability of CDI systems, particularly at the *cdiA* 3' toxin domain, which is evident at the strain level (Allen & Hauser, 2019). The CDI operon 5' end, encoding the *cdiB*, is highly conserved with a gradual loss in conserved sequence identity between strains moving towards the CDI operon's 3' end. HR occurs at high rates in these regions as the C-terminal toxin domain is situated within a recombination hotspot. The presence of these hotspots allows rapid evolution of novel toxin modules. These recombination events can occur through DNA acquisition and can suggest exchange of genetic material between species (Ruhe *et al.*, 2016). Therefore it is important to determine the *cdiA* genetic relatedness as this can indicate evolutionary distances between strains and other *Pseudomonas* species.

Using UGENE and MegaX, DNA and amino acid alignments were conducted to create Maximum-Likelihood phylogenetic trees. As *cdiB* is highly conserved, analysis was conducted on full length *cdiA* gene sequences to determine toxin passenger domain relatedness. Figure 3.11 outlines the genetic relatedness between the systems found within PAO1 and PA14. Interestingly the DNA alignment showed that *cdiA*^{2462} appears analogous to *cdiA*^{00510} instead of its homologue *cdiA*^{32790}. *cdiA*^{32790} appears the most distantly related, residing outside the clade. Amino acid alignment showed a different tree structure with CdiA^{0041}/CdiA^{00510} homologous systems clustering within the same clade and separately from the other two systems whilst CdiA^{32790} continues to appear the most distantly related. The differences in

these results highlight the importance of not only doing DNA alignments. However as with all alignments, the use of a small subset of sequences is less reliable in accurately building phylogenetic trees. Therefore the next step was to determine *cdiA* phylogenetic relatedness within *P. aeruginosa* clonal lineages to increase result validity.

Figure 3.12 outlines *cdiA* genetic relatedness between *P. aeruginosa* strains PAO1, PA14, PAK and PA7. This new analysis identified *cdiA*^{2462} as the most distantly related compared to all *cdiA* homologues found within *P. aeruginosa* strains using DNA sequences. It also highlights *cdiA* formation of strain-based clades, with clade 1 (*cdiA*^{0041} and *cdiA*^{PA7}) as the exception. Like Figure 3.11, trees using amino acid sequences had clades inconsistent with those constructed from DNA sequences where CdiA^{2462}/CdiA^{32790} and CdiA^{PAK} clade together. However homologous systems CdiA^{0041}/CdiA^{00510} cluster separately with CdiA^{0041} appearing analogous to CdiA^{PA7}. Discrepancies between DNA and amino acid alignments meant a more accurate phylogenetic tree was required. Here *Pseudomonas* spp. *cdiA* relatedness was determined.

Figure 3.13 outlines *cdiA* genetic relatedness within *Pseudomonas* spp. Using all homologues identified through the Pseudomonas.com database, DNA and amino acid alignments were conducted. This final analysis reconfirmed *cdiA* formation of strain-based clades. All the *P. aeruginosa* strains were found within a single major clade except for *cdiA*^{2462} which was the most distantly related. Analysis showed that the homologous systems within the *P. aeruginosa* strains tended to cluster together and separates into two subclades. This sub-clading and phylogenetic relatedness suggests HGT of ancestor *cdiBAI* operons occurs between strains before system diversification and was consistent between DNA and amino acid sequence alignments. Validity of strain phylogenetic relatedness was improved between

DNA and amino acid alignments by inclusion of more sequences. This resolution is lost in other subclades, which may be due to their underrepresentation in addition to unidentified systems within the Pseudomonas.com database. Having outlined CDI phylogenetic relatedness, analysis was used to identify conserved extracellular CdiA regions between systems.

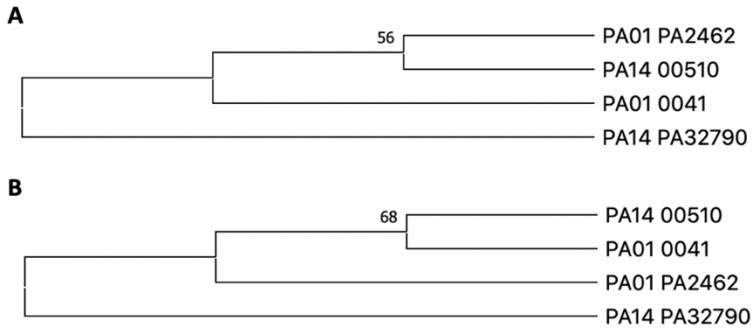


Figure 3.11: Maximum-Likelihood phylogenetic trees of CDI toxins in PAO1 and PA14 using DNA and amino acid sequence alignments. (A) DNA alignment, (B) amino acid alignment. CDI toxin ClustalW alignments were used to produce phylogenetic trees through MEGAX using the settings outlined in Table X for the two systems in PAO1 and PA14. Inference of evolutionary history was achieved using Maximum-Likelihood method and Tamura-Nei model using 1000 bootstrap replicates. Using discrete Gamma distribution, evolutionary rate differences were modelled among all sites including codon positions +1,+2, +3 and noncoding.

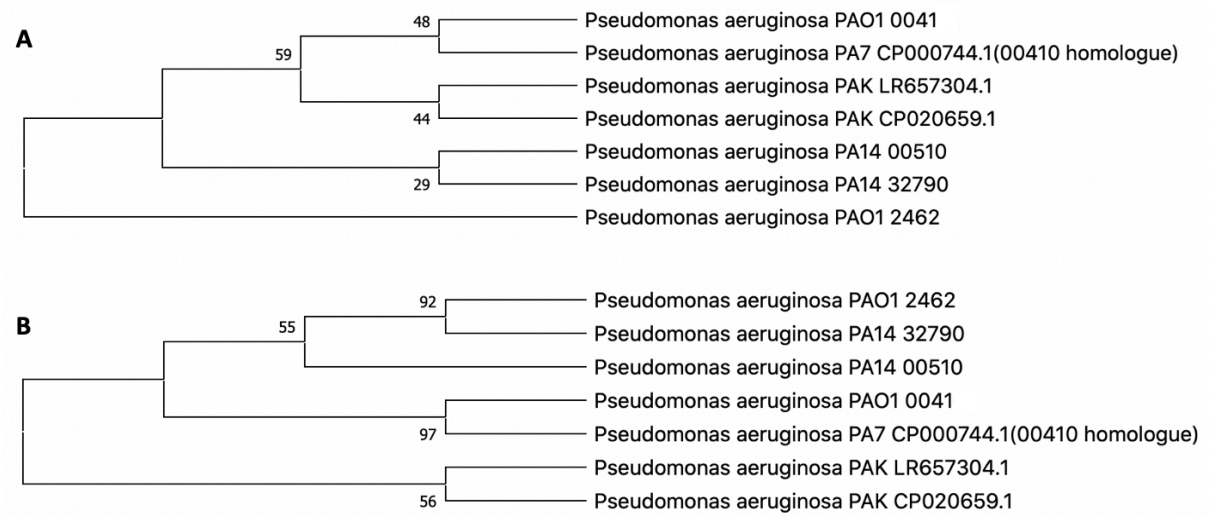


Figure 3.12: Maximum-Likelihood phylogenetic trees of CDI toxins in *P. aeruginosa* clonal lineages using DNA and amino acid sequence alignments. (A) DNA alignment, (B) amino acid alignment. CDI toxin ClustalW alignments were used to produce phylogenetic trees through MEGAX using the settings outlined in Table X for the two systems the *P. aeruginosa* clonal lineages.

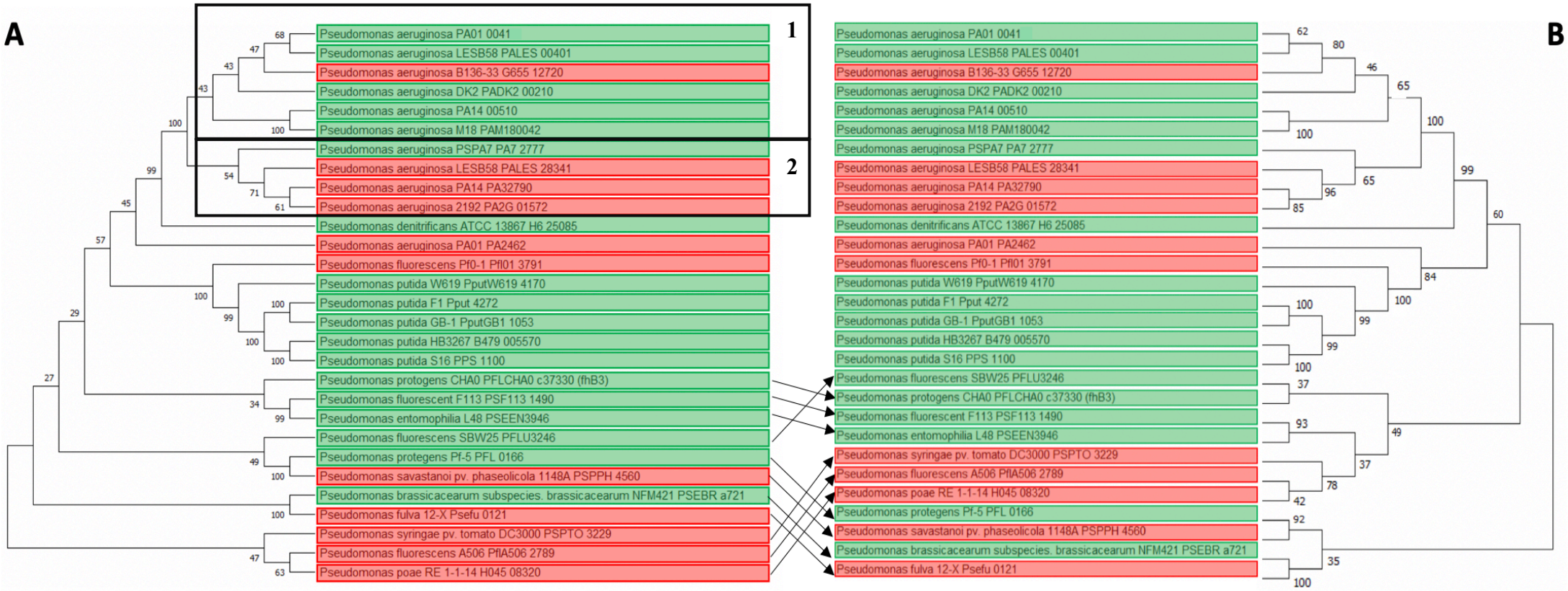


Figure 3.13: Maximum-Likelihood phylogenetic trees of all CDI toxin homologues from *Pseudomonas* spp. using DNA and amino acid alignments. (A) DNA alignment, (B) amino acid alignment. Tree A (1) *P. aeruginosa* clade 1, (2) *P. aeruginosa* clade 2. CDI toxin ClustalW alignments were used to produce phylogenetic trees through MEGAX using the settings outlined in Table X for all systems in *Pseudomonas* spp. Note: type 1 systems homologous to PAO1 CDI^{0041} are indicated in green, where type 2 systems homologous to PA14 CDI^{00510} are indicated in red.

3.3.5 Identification of conserved regions specific to P. aeruginosa PA14 CdiA proteins to enable cloning into inducible vectors for recombinant protein expression

The CdiA toxin passenger domain is situated extracellularly from the bacterium and is a good candidate for an immunogenic protein due to its size and distance it protrudes from the cell (Ruhe *et al.*, 2018). It is well noted within literature that CdiA N-terminals are more conserved with a gradual loss of genetic identity towards the C-terminal toxin domain (Aoki *et al.*, 2010). From previous studies and the bioinformatic analysis outlined in this PhD, it has been shown that the toxin passenger domain of CdiA contains conserved domain organisation and sequences within their N-termini (Allen & Hauser, 2019). These conserved regions suggest regions exist within the extracellular passenger domain that are conserved between all systems, and some are specific to each homologous system type. To establish the presence and activity of CDI systems under different conditions in both laboratory strains, identification of these conserved regions would enable engineering of recombinant proteins which could be expressed and purified to challenge rabbits to produce specific antibodies against the CDI systems for future experiments screening clinical strains from CF patients.

Using UGENE and MegaX, amino acid alignments were created of the CdiA-NTs of each system to identify regions of conserved sequence (Figure 3.14). As these antibodies would be used to identify the presence and activity of CDI systems in different *P. aeruginosa* strains, the sequences included in the alignment covered the N-termini through to the first PTPMs and did not include the C-terminal variable toxin region. The CdiB was not chosen for recombinant protein construction as this OM β-barrel is highly conserved in other TPS systems encoded

throughout the genome and was therefore unsuitable for this construct. CdiA is also a much larger protein and provides more potential antigenic targets.

From these alignments, conserved regions were blasted to determine similarity to other sequences found throughout the PA14 genome to indicate if any cross-reactivity with an antibody made using these regions could occur. From the BLAST results, the conserved regions which showed low or no percentage identity to the rest of the genome were then analysed further. These regions were aligned with the sequences from other T5SSs present in the genome of PA14 or other *P. aeruginosa* TPS systems identified by MRes student Madeleine Humphrey to determine their specificity to CDI systems only (Table 3.5). From these alignments, the longest $CdiA^{00510}$, $CdiA^{32790}$ and $CdiA^{00510/32790}$ amino acid sequence stretches with the fewest matches to the other T5SSs encoded within the genome were selected (Table 3.6). The conserved region for each system was chosen based the best overall lowest number of matching amino acid stretches under 5 amino acids. This identified our conserved regions of interest to create three recombinant proteins: general, system type one (homologous to CDI^{00510}) and system type two (homologous to CDI^{32790}). Primers were then designed to amplify the DNA encoding them for antibody production, outlined in Chapter 6.



Figure 3.14: CdiA toxin passenger domain alignment between homologous systems to identify conserved domain regions. Analysis of N-terminal toxin passenger domain were used to identify regions conserved sequences. This was used in order to identify regions suitable for cloning to purify and send for antibody production with Eurogentec. This figure is a representation of this alignment between homologous systems $CdiA^{2462}$ and $CdiA^{32790}$.

Table 3.5: T5SS and TPS systems identified by Madeleine Humphrey during PAO1 and PA14 genome searches

***Pseudomonas aeruginosa* Strain**	**System Type**	**TpsB**	**TpsA**
PAO1	PdtB/PdtA	PA0692	PA0690
	CupB5	-	PA4082
	LepB/LepA	PA4540	PA4541
	CdrB/CdrA	PA4624	PA4625
PA14	Hypothetical	PA14_55380	PA14_55400
	Hypothetical	PA14_58890	PA14_58900
	Hypothetical	PA14_61190	PA14_61200
	CupB5	-	PA14_11100

Table 3.6: Maximum amino acid sequence identity stretches between TpsA found throughout the genome compared to *P. aeruginosa* CdiB

System Type	Aligned System	Aligned System Selection	Consensus Positions (%)	Identity Positions (%)	Maximum Amino Acid Stretch Matching Aligned System Sequence
General (PA0041$_{1520-1829}$)	PA14_00510	1520-1829	99.7	99.7	1
	PA0041	1520-1892	100	100	0
	PA14_32790	2983-3292	99.7	99.7	1
	PA2462	3398-3707	99.7	99.7	1
	PA14_58900	767-1087	30.2	17.8	3
	PA14_11100	595-957	33.6	17.9	3
	PA14_61200	179-495	29.3	15.1	2
	PA14_55400	255-584	30.9	17.9	2
System 1 (PA0041$_{1968-2217}$)	PA14_00510	1968-2217	100	100	-
	PA0041	1968-2217	100	100	-
	PA14_32790	3431-3629	30.9	16	3
	PA2462	3846-4123	32	16.9	3
	PA14_58900	1048-1304	27.6	12.8	2
	PA14_11100	688-947	31	18.1	3
	PA14_61200	263-524	28.6	14.9	3
	PA14_55400	3822-4079	26.4	15.5	4
System 2 (PA14_32790$_{1001-1526}$)	PA14_00510	863-1068	34	17	2
	PA0041	2903-3108	32.5	16.5	3
	PA14_32790	3798-4003	100	100	-
	PA2462	4218-4423	98.5	99.6	-
	PA14_58900	1063-1278	29.2	18.1	3
	PA14_11100	744-960	30.4	14.1	5
	PA14_61200	448-653	30.1	16	2
	PA14_55400	328-540	32.4	14.1	4

3.4 Discussion

CDI systems have previously been described in *P. aeruginosa* and associated with contact dependent killing of competing strains (Aoki *et al.*, 2005; Mercy *et al.*, 2016). The results presented in Chapter 3 of this thesis outline the characterisation of CDI operons, their domains and putative functions within the genome of *P. aeruginosa* PA14 and PAO1. The relatedness of CDI systems between species as well as regions conserved between and within CDI types were also elucidated. Here I demonstrate that *P. aeruginosa* PA14 encodes two CDI systems synonymous to '*E. coli* type' T5bSSs which are more conserved at the 5' end and gradually lose sequence conservation towards the 3' end. I also demonstrate that the C-terminal toxins have disparate putative functions even compared to their homologous systems in PAO1. Finally I outline the phylogenetic relatedness of these systems, highlighting the clading of genetically synonymous systems within both the *Pseudomonas* spp. and *P. aeruginosa* strains, whilst identifying the conserved sequence regions within and between each system type. Elucidating the genetic structure of these systems provides insights into their benefits in bacterial survival and colonisation, driving acquisition and conservation within bacterial genomes. This characterisation has highlighted specific putative functional roles in bacterial competition, where strain diversity may indicate the potential use of these systems in inter-*Pseudomonas* competition.

3.4.1 Does the genome of P. aeruginosa PA14 contain multiple CDI systems?

As *P. aeruginosa* has previously been shown to act competitively using other systems such as the T6SS (Ho, Dong & Mekalanos, 2014) it is reasonable to think that bacteria use other alternative means for competition to ensure its survival. Therefore identifying the presence of CDI systems within a genome assesses the bacteria's ability to successfully compete with other bacteria in their immediate environment (Aoki *et al.*, 2005). The work conducted by Mercy *et al.* in 2016 outlined a more in depth study on CDI systems in *P. aeruginosa* than previously conveyed in the literature. Their study included the identification of the presence of CDI systems in other *P. aeruginosa* strains. Elucidating these systems in different strains is important in understanding whether they play a role in infection in CF. This will improve our understanding of the potential mechanisms used in the dominance and decline in diversity of the polymicrobial community or inter-*P. aeruginosa* strain succession that leads to reduced lung function observed in patients with this condition.

Using the CDI system genome locations in PAO1, outlined by Mercy *et al.*, two CDI systems were successfully identified in PA14 for this study (Figure 3.1). As CDI system identification within many strains of *Pseudomonas* spp. is limited, the PAO1 *cdiA* gene sequence comparison was key in identifying PA14 homologues through the Pseudomonas.com database. *cdiA* sequences encompassed a more specific search for CDI genomic presence and position as the largest gene which is conserved within the operon and therefore more likely to return promising database hits. This is the first study to outline two CDI systems in *P. aeruginosa* PA14 and supports previous work indicating that bacteria encode two CDI systems within their genomes (Aoki *et al.*, 2010).

Analysis of the genes immediately upstream of the putative *cdiA*s identified confirmed the presence of OM β-barrel hits, further supporting the indication those genome regions give rise to T5bSS CDI systems, based on findings outlined in the current literature (Filloux, 2011). Further analysis of *cdiA* indicated domain organisation and cellular localisation similarities, with a gradual loss in homology from 5' to 3' end. Although the putative functions of the toxins were disparate, this analysis suggested they all have cellular targets. This similarity in domain organisation and toxin target localisation mirrors the findings observed in previous studies (Allen & Hauser, 2019). If these systems are active within clinical strains, this could be an important mechanism driving competition, dominance, and control of the polymicrobial community in CF pulmonary infection. However a more in depth study was required for understanding putative domain functions to elucidate structures and potential mechanisms of action. Furthermore, *cdiI* genes were not able to be discerned through this initial screen of the genome, which was required for elucidating the CDI operon. As *cdiI*s are composed of very small ORFs, bioinformatics software during genome reconstruction after sequencing would not assign them as putative genes with genome number designations. Multiple ORFs are present between genes throughout the genome therefore an in depth manual study of the downstream region of *cdiA* was required for *cdiI* identification by determining ORF likelihood of expression, proximity to *cdiA* 3' end and putative functions and discussed below.

3.4.2 Do downstream small ORFs encode putative immunities and toxin/immunity modules?

Immunity proteins are expressed in conjunction with CdiA proteins to cognate bind and neutralise their toxic effect, preventing autoinhibition and killing of kin (Aoki *et al.*, 2010). However as these genes are so small, they are difficult to discern. Using ORF finder/VectorNTI

and a Kolaskar calculator, putative ORFs were identified by discerning ORFs downstream of each CdiA likely to be expressed, their position and finally screening each ORF bioinformatically for predicted protein functions or domains (Figure 3.2). Previous literature has outlined that immunities are encoded directly downstream of their cognate toxins (Aoki *et al.*, 2010), therefore narrowing the search to ORFs identified as 'potentially expressed' encoded directly downstream of each *cdiA*. Although Mercy *et al.* had previously identified immunities for CDI^{0041} and CDI^{2462}, these system were included to validate the immunities previously identified. My analysis contradicted Mercy *et al.* as it suggests part of the 3' end of $cdiI^{0041}$ was missed, whilst the true $cdiI^{2462}$ was located 92 bp downstream (from the start of immunity) when compared to the genome locations outlined in the paper and may be a reason for the problems encountered in functional validation of the toxin-immunity modules. As the immunities outlined appear the likely immunity for each system, those identified in PA14 were validated by cloning and construction of whole system deletion mutants (WSDMs) outlined in Chapter 4 of this thesis.

No conserved sequences were identified from initial ORF analysis between each other or the rest of the genome (Figure 3.3), supporting literature outlining toxin-immunity specificity (Poole *et al.*, 2011). However, MRes student Madeleine Humphrey identified the CDI^{00510} tRNAse immunity later via alignment with the toxin-immunity complex outlined in Allen *et al.* 2020. Additionally NCBI BLASTp of $cdiI^{00510}$ identified a 99% sequence identity to *Enterobacter cloacae*. Upon conducting a Phyre2 and BLASTp validation search on each immunity prior to write up, I was able to identify high percentage identity to sequences found within other bacterial genera outlined in Table 3.2 that show some conservation and presence in other bacterial species.

Phyre2 analysis of *cdiI*^{32790} yielded a strong hit to the known MazFE endoribonuclease toxin-immunity module from *Klebsiella pneumoniae* (Jin *et al.*, 2021). Upon manual sequence alignment this showed a 46% sequence identity- high for an immunity. This suggested that CDI^{32790} toxin-immunity module may encode an endoribonuclease toxin-antitoxin module synonymous to MazFE in *K. pneumoniae* which did not support the literature outlining toxin-immunity module specificity. BLASTp and alignment of *cdiI*^{32790} indicated a 73% and 39% sequence identity respectively to *Stenotrophomonas maltophilia* and *Achromobacter xylosoxidans*. The percentage identity with *Stenotrophomonas* and *Achromobacter* is interesting as they are bacteria associated with CF infection (Marra *et al.*, 2020; Marsac *et al.*, 2021). Sharing immunities between these bacteria may support the idea that *P. aeruginosa* strains control polymicrobial community dynamics and presence of different genera in CF based on these shared immunities (Bisht, Baishya & Wakeman, 2020).

Phyre2 analysis of *cdiI*^{0041} indicated 31% match to *P. aeruginosa* PAO1 gene- PA5349, which showed 15% sequence identity upon sequence alignment. Checking the surrounding genome region determined PA5349 was not within a previously identified or putative CDI/TPS system. Therefore this conserved region suggests the toxin-immunity module domain may undergo similar interactions or pertain a similar function to PA5349. BLASTp search and gene alignment indicated 99% sequence identity to an uncharacterised gram positive *Eggerthia catenaformis* gene. This may indicate that; *Eggerthia* can survive *P. aeruginosa* by encoding an immunity against CdiA-CT^{0041}, PAO1 communicates via CDS with gram positives or this immunity is encoded in a gram positive associated T7SS (Meuskens *et al.*, 2019). This high identity to a gram positive is interesting as no studies outline CDI in competition or cooperation with gram-positive bacteria. An alternative explanation is that this domain is

used as a polymorphic toxin domain that can be shared in different competition systems (Zhang *et al.*, 2012; Allsopp *et al.*, 2020). Finally, Phyre2 analysis of *cdiI*^{2462} indicated 24.2% identity to an uncharacterised *Saccharomyces cerevisiae* gene, however upon alignment this identity dropped to only 2%. BLASTp analysis showed no homology to any other database sequences, though this shows the potential power of the Phyre2 analysis as its hits are based on structural homology. The novelty of this immunity sequence could be due to a recombination event to give rise to a new interaction domain for toxin neutralisation or is similar in structure to other proteins with unidentified functions that have not yet been elucidated and/or uploaded into protein structural databases to enable identification.

The analysis of *cdiI*^{2462} supports my hypothesis and the current literature indicating that immunity sequences and their protein structures are novel (Mercy *et al.*, 2016; Allen & Hauser, 2019). However the strong Phyre2 hits and identity of the other three immunities refutes this claim and expands our current understanding of CDI immunities. The sharing of toxin-immunity modules between different bacteria would enable *P. aeruginosa* to control the presence of different genera and *P. aeruginosa* strains for strain succession within the polymicrobial community in CF. If this is the same in clinical strains, it may indicate why bacterial diversity within the lung declines as *P. aeruginosa* infection progresses (Flight *et al.*, 2015), through competition with those that do not encode the immunities and communication with those that do. This has been shown to occur between *P. aeruginosa* and *B. cepacia* (Perault *et al.*, 2020), as well as in other areas of polymicrobial research such as the gut microbiome with the T6SS (Ross *et al.*, 2019a) and is therefore a feasible mechanism for dominance in CF pulmonary infection. However this would require a more in depth study of function to understand whether *P. aeruginosa* undergoes CDS like *Burkholderia* (Ocasio &

Cotter, 2019). If this could be shown it would elucidate the dynamics of strain acquisition, integration, and dominance via CDI in polymicrobial environments, however this would require more functional analysis outside the scope of this project.

Analysis of the region ~500 bp downstream of each CDI system outlined that no clear putative functions could be deduced beyond a broad suggestion of potential involvement with a variety of membrane and DNA remodelling functions (Figure 3.2). However, identifying transposable elements and *cdiA/I* modules through BLAST analyses supports the literature showing that the regions downstream of *cdiA* undergo high rates of HR and gene acquisition (Poole *et al.*, 2011; Allen & Hauser, 2019). Whilst 3' end variability shows little strain homology, downstream functional orphan structures are retained between homologous systems suggesting a shared ancestor. System 1 (CDI^{0041}/CDI^{00510}) orphan ORFs share order and signal transduction, DNA modification and transposed membrane/protein modification functions. System 2 (CDI^{2462}/CDI^{32790}) orphan ORFs share a secondary *cdiA/I* region between strains. No homology between system 1 and 2 beyond *cdiBAI* architecture was observed.

Orphan homology combined with the presence of transposable elements suggests these regions may exhibit *cdiA* toxin domain 'fossil records' whilst providing genetic reservoirs for recombination. Therefore, understanding domain functions in the future may provide insight into their specific roles in bacterial competition. Due to the inability to assign clear putative functions to many genes in these systems, this analysis can only proceed with further domain and function identification to elucidate the potential mechanisms of these genetically decayed regions. The downstream region highlights disparity in identity between homologous strains and stipulates the novelty observed in each C-terminus even between homologous

systems. One experimental approach that could be performed to validate this is genetically engineering the *cdiA* toxin domain with these ancestral domains. This strain and system specificity may play a role in invasive strain fitness within polymicrobial communities. I will discuss how this plays into genetic relatedness between systems in 3.4.4.

3.4.3 Do CDI operon structures and genes have homology?

P. aeruginosa encodes '*E. coli* type' CDI systems which have been shown to have a similar operon structure and homology both within and between its species (Mercy *et al.*, 2016). Therefore identifying CDI- associated domains builds a picture of its structure and potential mechanism of action. However this relies heavily on online databases and is limited by known or identified domains. Previous studies have identified *cdiB* conservation as well as *cdiA* passenger domain structure (Aoki *et al.*, 2010). Therefore identifying the domains, particularly those associated with the CdiA, will enable the classification of each system based on groups outlined from previous studies in the literature (Allen & Hauser, 2019). The gradual loss of sequence identity towards the C-terminal end and RBD classification has been shown to contribute to inter-strain variation (Mercy *et al.*, 2016). Therefore outlining the domain classifications and putative toxin functions in the PAO1 and PA14 CDI systems may indicate whether these systems would have similar targets. Identifying these domains may provide insight into the interstrain competition observed within the CF lung.

Using online bioinformatics programmes outlined in Table 2.12 in 2.5.1, the *cdiB* and *cdiA* domains were determined to highlight similarities and differences between homologous strains. As expected, *cdiB* was more highly conserved than *cdiA*, where *cdiA* showed

similarities in domain CdiA-NT structure between systems and strains. I discerned 100% structural homology between encoded CdiB proteins from homologous systems using Phyre2 (Figure 3.4). This suggests *cdiB* is conserved in *P. aeruginosa* CDI systems, supporting the current literature outlining conservation based on their role in export (Henderson *et al.*, 2004; Gentle, Burri & Lithgow, 2005). However CdiB domain variation between different system types may indicate different mechanisms for toxin passenger deployment. This variation in mechanism may have evolved based on the exported substrates. The high *cdiB* conservation between strains identifies a potential target for novel therapeutic treatment development to either block or disable CdiB pore formation or PORTA domains to prevent interbacterial competition.

Next, *cdiA* analysis highlighted signal peptides and hemagglutinin repeats. Based on the Allen *et al*. 2019 study, I was able to show deviations in all PA14 and PAO1 systems from the general CDI domain structure they outlined (Figure 3.5) through a more in depth analysis (Figure 3.6). Unfortunately RBD target domains in this study could not be identified through a bioinformatic approach and could not be classified within this study, synonymous to Allen *et al*. However, YP domains were classified based on the *rdbA-rdbE* classes outlined in Allen *et al.* which could suggest RBD classification type as YP are situated directly downstream of RBDs. Interestingly these PAO1/PA14 systems encoded three different YP domain classes, suggesting disparity in RBD targets and indicates interstrain variation in competition and likely toxin entry. YP domains exhibited 100% sequence identity between CDI^{0041}/CDI^{00510}, and were therefore classified *rdbA*, which may indicate their use for interstrain competition between PAO1 and PA14 based on the high degree of similarity between their interaction domains. This could allow the toxins from one strain to enter the other.

PTPM analysis identified two PTPMs within the *cdiA* 3' end. This contradicts the literature which only outlines one PTPM (Allen & Hauser, 2019). PTPMs indicate the beginning of toxin domains in both the CDI and T6SS (Zhang *et al.*, 2012; Mercy *et al.*, 2016), therefore previous studies may have picked the PTPM closer to the C-terminal for this reason (Allen & Hauser, 2019). However the presence of two suggests either two separate functional domains required for import, the ability to express two separate toxins from a single system or outlines a signal peptide left by a previous ancestral HR event (Van Ulsen *et al.*, 2014). However, the regions between the PTPMs suggested this was not the case. The 3' end of each downstream PTPM clearly indicated the start of the active toxin domains. However amino acid sequences between the two PTPMs suggests a separate function, due to the presence of a small sequence between the upstream PTPM and the DUF 5' end (Figure 3.7). Based on BLAST, sequence identity to different bacterial species was high and indicated these sequences may be part of the CDI import mechanism which is not currently fully elucidated. The upstream PTPM may signal the start of the toxin region, which is imported into a neighbouring cell with the active C-terminal toxin, whilst the downstream PTPM may signal where the active C-terminal toxin domain breaks off from the N-terminal domain that binds to an IM protein enabling import into the cytoplasm (Cascales *et al.*, 2007; Hayes *et al.*, 2014; Willett *et al.*, 2015a; Bartelli *et al.*, 2019; Myers-Morales *et al.*, 2021). To identify if it is used for IM protein binding, a more in depth bioinformatic analysis of sequence similarities to other proteins which are imported through the IM as well as functional assays would be required, and this is not within the scope of this study.

The CDI^{00510} DUF-associated sequence had homology to Tse6 (Table 3.2), a characterised NAD/NADPase intracellular toxin (Whitney *et al.*, 2015). Although only 34% aligned to Tse6,

homology with this T6SS effector and 100% identity to T6SS-encoding *E. cloacae* and *A. baumanii* genes is interesting (Lewis *et al.*, 2019; Soria-Bustos *et al.*, 2020). This T6SS effector identity may suggest HR with T6SS clusters, evolving into the currently encoded toxin through subsequent HR events. This high percentage identity to these two bacteria, which are both associated with CF infection (LiPuma, 2010; Rocha *et al.*, 2018) (although not major contenders in the frequency of causing chronic pulmonary infection) suggests that this effector may have a trans-genera function but this is yet to be elucidated. The CDI^{0041} DUF-associated sequence had homology to *Acinetobacter baumanii, Salmonella enterica* (100%) and *Listeria monocytogenes* (93%) but no homology was observed using Phyre2 hits. This sequence identity supports the hypothesis that these systems are widespread throughout gram-negative bacteria (Henderson & Nataro, 2001; Dautin, 2021), and particularly associated with invasive pathogens. The CDI^{2462}/CDI^{32790} DUF-associated sequence had 100% homology with top BLAST results to gram-positive bacteria. However, CDI systems have not been shown to be utilised against gram-positive bacteria. If *P. aeruginosa* can use CDI systems against gram-positive bacteria, this is further evidence of their role in controlling the CF polymicrobial community as these systems could enable outcompeting of gram positives associated with chronic infection, such as *Staphylococcus aureus* (Orenti *et al.*, 2021).

CdiA-CT analysis indicates putative toxins involved in DNA/RNA modification. This supports the current literature outlining CDI toxins with intracellular targets (Aoki *et al.*, 2009; Willett *et al.*, 2015b). CdiA-CT^{0041} could not be elucidated, however the putative functions of the other toxins fall within the hydrolase enzyme family but are different even between homologous systems (Figure 3.8). This further supports the literature highlighting CDI toxin specificity (Allen & Hauser, 2019). Outlined in Madeleine Humphrey's MRes thesis, CdiA-

CT^{00510} has 100% sequence homology with a trans-kingdom tRNase identified by Allen *et al.* in 2020 and was reconfirmed by my analysis. A trans-kingdom effector domain suggests these systems may undergo competition with fungi and other eukaryotic cells. This would further support the notion these systems influence the polymicrobial community in CF and possibly potentiate pulmonary exacerbations during these competition events through interactions with the host. Analysis of the other toxins is outlined in Table 3.4 and discussed below.

CdiA-CT^{00510} showed high sequence identity with *Acinetobacter baumanii* and *Enterobacter cloacae*. This similarity to *A. baumanii* is interesting as it is also associated with CF pulmonary infection (Jenkinson *et al.*, 2021). Additionally, similarity to gut-associated *E. cloacae* shows toxins are present in bacteria from diverse niches within the human body, as well as being a widespread competitive mechanism utilised by gram-negative bacteria for intermicrobial competition in polymicrobial environments. CdiA-CT^{32790} showed high sequence identity with *Acinetobacter baumanii* and *Streptococcus dysgalactiae* (67% and 71% respectively) which are both associated with CF and upper respiratory infections (Oppegaard *et al.*, 2017; Jenkinson *et al.*, 2021). This is very high sequence identity and indicates other bacterial species encode a similar toxin which may be associated with unidentified CDI systems and supports recent claims of potential HGT of CDI (Cuthbert, Hayes & Goulding, 2022). SMART bioinformatics identified an EndoU domain indicating a ribonuclease with either DNase or RNase function. HHpred analysis by MRes student Nicholas Yuen supported this finding through a hit against an *E. coli* O157:H7 CdiA tRNase with 62% sequence identity upon alignment. As the putative function of this toxin is also a tRNase it supports the current literature which indicates CDI toxins have intracellular targets (Aoki *et al.*, 2009; Willett *et al.*, 2015b). InterPro analysis of CdiA-CT^{0041} indicated homology to a tRNase-specific ribonuclease

from *Burkholderia pseudomallei*, however the paper outlining this toxin had been redacted and I was therefore unable to check the amino acid alignment. SMART domains also identified a ribonuclease domain, suggesting the function of the toxin is tRNase. High sequence homology was also observed with *Acinetobacter baumanii* and *Salmonella enterica*, bacteria which are associated with CF/other human polymicrobial environments. Finally, InterPro analysis of CdiA-CT^{2462} identified an EndoU domain which supports the Mercy *et al.* findings. High percentage identity to *Acinetobacter baumanii* was observed and many other gram-negative bacteria. The Maximum-Likelihood phylogenetic tree constructed based on these sequence hits (Figure 3.10) identified *P. fluorescens* and *Acinetobacter* were closely related. The identity to *Achromobacter animicus* which is an emerging CF pathogen was interesting as well as the fact that it was the most distantly related of all the species present within this analysis (Vandamme *et al.*, 2013) and could be an indicator of divergent evolution from an acquired CDI system.

The analysis on these toxins outlined here refutes the current literature that indicates that toxin-immunity complexes are novel in CDI systems as high percentage sequence identities were observed in other genomes in different bacterial genera. This is supported by the analysis conducted on the immunities in 3.3.2. Interestingly, there appeared to be some shared functional domains between the toxins and immunities suggesting domains are complementary to enable toxin neutralisation. If this is the case, toxin functions may be identified bioinformatically in the future. The lack of functional domain identity to determine toxin functions may be overcome through the development of bioinformatics tools and databases for protein structures to increase their accuracy and information available. In addition more domains require identification *in vitro* which could confirm the idea that DNase

toxins may be more bactericidal in competitive interactions due to their potency, whereas tRNase toxins may be more bacteriostatic through preventing translation initiation.

The analysis conducted here supports my hypothesis that homologous systems encode toxins with similar functions as CdiA-CT^{0041}/CdiA-CT^{00510} are likely tRNase toxins. However, it also refutes my hypothesis as CdiA-CT^{2462}/CdiA-CT^{32790} toxins had disparate functions. The toxicity and functions of the PA14 encoded toxins will be investigated experimentally in Chapter 6. As these systems showed both a degree of conservation and complete disparity in identity even between homologous systems, it can be difficult to determine the genetic relatedness between systems when looking at *cdiA* sequences which I discuss in 3.4.4.

3.4.4 Are CDI systems in P. aeruginosa closely related to those found within other Pseudomonas species?

CDI systems are highly conserved and found throughout gram-negative bacterial species but there are two classes of CDI systems identified (Aoki *et al.*, 2010; Anderson, Garcia & Cotter, 2012). *P. aeruginosa* has previously been shown to encode two '*E. coli* type' CDI systems (Van Ulsen *et al.*, 2014), therefore understanding the phylogeny of these systems can provide potential insight into inter-*Pseudomonal* and interstrain interactions based on the homology/conservation of these systems. However, as these systems are not well defined or characterised, particularly within different strains and species of *Pseudomonas*, identification of homologues using the Pseudomonas.com database was crucial in outlining genomic links between strains and their systems. Previous work by Allen *et al.* in 2019 focussed on comparative genomics of the CdiA domains and its C-terminal toxin, therefore building a

phylogenetic tree based on the entire CdiA was used here to classify CDI system homologues between species whilst accounting for diversification in the *cdiA* 3' end. Understanding system genetic clading of various lab strains of different genetic lineages could shed light on dominance of specific *P. aeruginosa* strains in the CF lung. Strain displacement and dominance could be aided by genetically distinct systems which provides a fitness advantage, which may be a major factor in the control of the polymicrobial community.

This analysis (Figure 3.12) identified CDI^{0041} as the most distantly related system from *P. aeruginosa* strains and was found to clade with the PA7 TPS system, where homologous systems CDI^{2462}/CDI^{32790} cladded together. This tree indicates that these systems are more closely related at the amino acid level than CDI^{0041}/CDI^{00510}. Using the *cdiA* of all homologues for both systems found within genomes of different *Pseudomonas* species from the Pseudomonas.com database (Figure 3.13), outlined clustering based on homologous system type and species in *P. aeruginosa*. The analysis conducted here supports my hypothesis that PA14 contains conserved genetic regions due to the close alignment of the CdiA-NT. This suggests that the systems in *P. aeruginosa* appear to stem from a common ancestor. It was also able to identify that the most genetically distant system within the *P. aeruginosa* species was $CdiA^{2462}$ and suggests that this may have been introduced by a genetic transfer event, most likely conjugation, from another species (Wäneskog *et al.*, 2021). Identifying the genetic dynamics and clustering of these systems in *P. aeruginosa* strains enables a more in depth look at conserved regions within the CdiA-NT, which will be discussed in 3.4.5.

3.4.5 Are there conserved regions in CDI systems that could enable identification of presence and activity of each system type?

As CDI systems have been shown to be highly conserved in gram-negative bacteria (Aoki *et al.*, 2010), it is logical to assume these systems must have some homology in regions of the CdiA-NT. Allen *et al.* in 2019 suggested that the similarity between domains, particularly in CdiA-NT suggests parity in their structural architecture. Therefore these systems may share domains which could allow identification of their presence and activation status through their expression on the extracellular surface. Identifying these regions would enable isolation of these antigens, through the production of recombinant proteins, for antibody production. This would allow us to test for these systems within clinical strains isolated from CF patients to determine if they are active and indicate that these systems may be important drivers in pulmonary infection in these patients.

The N-terminal of each CDI was studied for conserved regions (Figure 3.14) which was successful. As these systems have high homology to other TPS found throughout the genome, the key was to identify regions conserved between/within homologous systems which were specific to these genetically distinct T5bSS that are not also found in other systems.

Initial alignments between all T5bSSs encoded in PAO1/PA14 identified conserved regions found only between homologous systems throughout other *P. aeruginosa* species to produce a 'General' antibody. From the analysis conducted in 3.3.4, showing clading of homologous systems, two regions were identified which were specific to each homologous system type to produce two antibodies designated 'System Type 1 (ST1)' and 'System Type 2 (ST2)'

antibodies. ST1 was specific to the CDI^{0041}/CDI^{00510} homologous systems, whilst ST2 was specific to the CDI^{2462}/CDI^{32790}. Aligning these regions with other T5SS identified throughout *Pseudomonas* spp. genomes to confirm antigenic specificity was successful, enabling me to narrow down regions to those with a minimum overlap of five amino acids between the sequences and other T5SSs and TPS encoded within *Pseudomonas* spp. (Table 3.5). The identity of conserved domains within the CDI supports my hypothesis and previous studies on CdiA domain conservation (Allen & Hauser, 2019). The cloning of these regions and isolation of the subsequent recombinant proteins produced through this cloning will be discussed in Chapter 5 of this thesis.

3.5 Conclusions

The main conclusions associated with the genomic, downstream ORF and phylogenetic analysis are as follows:

1. *P. aeruginosa* PA14 contains two CDI systems homologous to those found in PAO1 strains
2. They retain the conserved *E. coli* type *cdiBAI* genomic structure
3. N-terminal *cdiB* is highly conserved whilst the *cdiA* C-terminal is variable
4. CDI^{0041}/CDI^{00510} have high homology in genomic organisation and function
5. CDI^{2462}/CDI^{32790} do not have high homology in genomic organisation and function
6. Immunities have little homology in structural/functional domains
7. *cdiI*^{0041} had no discernible structure or function but showed high sequence identity to gram-positive bacteria
8. *cdiI*^{00510} appears to have anti-tRNase function, as CdiA-CT^{00510} is a tRNase toxin

9. *cdiI*^{2462} has no discernible structure/function indicating a potential novel immunity
10. *cdiI*^{32790} appears to have anti-endoribonuclease function
11. CdiA-CT^{0041} and CdiA-CT^{00510} toxins appear to have tRNase function
12. CdiA-CT^{2462} toxin appears to have GTase function
13. CdiA-CT^{32790} toxin appears to have tRNase function
14. *cdiA*^{2462} appears most distantly related to *cdiA* in other *P. aeruginosa* when compared with other *Pseudomonas* spp. genomes
15. Homologous system types appear to phylogenetically cluster together
16. CdiA-NT share homologous regions between and within system types

Therefore, these results presented in Chapter 3 reveal links in genomic and domain structures of the CDI systems, as well as their functions, in genetically distinct laboratory strains of *P. aeruginosa*. Similarities and differences in domains and functions between homologous and non-homologous systems show the unique nature of CDI and support the inter- and intrastrain variation observed. So, the final step was to consider whether these results supported or refuted the hypotheses proposed at the beginning of this chapter.

Hypothesis 1: *P. aeruginosa* PA14 encodes two CDIs that retain '*E. coli* type' *cdiBAI* genetic organisation. **This was accepted.**

Hypothesis 2: These CDI systems share homology in domain organisation with those found in *P. aeruginosa* strain PAO1. **This was accepted.**

Hypothesis 3: The putative CdiI immunities share no sequence homology to other known genes or protein domains. **This is unclear as immunities shared no sequence or domain homology to each other but have high sequence identity to genes from other bacterial genera. This identity refutes previous claims of the immunity novelty, suggesting toxin-immunity modules could be shared between genera.**

Hypothesis 4: The putative CdiA-CT toxin for these systems have different functions. **This is unclear as the homologous systems (CDI^{00510}/CDI^{32790}) in PA14 encode putative tRNase functions although they are genetically distinct. This was not observed in PAO1 which may be due to the phylogenetic distance between systems. Therefore further bioinformatics work is required between homologous system types to determine if this is a common trait.**

Hypothesis 5: These systems encode conserved regions which can be exploited to produce antibodies against the CDI systems in future experiments. **This was accepted.**

The ability to show the homology between these systems will enable any results conducted throughout the rest of this thesis to be synonymous with the general action of other homologous CDI systems encoded either throughout the *Pseudomonas* genera or in clinical strains which are currently uncharacterised. This is a prerequisite that will inform results which can be linked to our understanding of clinical outcome with chronic *P. aeruginosa* infection in CF.

4. CDI system activity in *P. aeruginosa* strain PA14

4.1 Introduction

It is well established both in the literature and within this thesis that *P. aeruginosa* strains encode two T5bSSs, denoted CDI^{00510} and CDI^{32790} for systems encoded in PA14 (Aoki *et al.*, 2010; Van Ulsen *et al.*, 2014; Mercy *et al.*, 2016; Melvin *et al.*, 2017). Although T5bSS systems have been identified throughout the genus, it remains to be seen whether many of the systems confer **C**ontact **D**ependent **I**nhibition (CDI). To date, most research on CDI systems in *P. aeruginosa* has been conducted on the reference strain PAO1, where studies have shown a role for CDI in pathogenesis both *in vitro* and *in vivo* (Mercy *et al.*, 2016; Melvin *et al.*, 2017).

The study conducted by Mercy *et al.* in 2016 constructed deletion mutants to evaluate the change in bacterial competitive capabilities in the absence of these systems. Although the study was able to characterise the operons in PAO1, validate the functional toxin-immunity modules and determine a role for these systems in competition, it was unable to identify the mechanism of action for the encoded toxins and whether both immunities cognate bind the toxins through direct interactions. The study did however support the literature which indicates that these toxins pertain intracellular targets, as the encoded effectors appeared highly toxic in this study due to the difficulties the authors experienced in cloning and expression of the toxins through inducible vectors.

The study conducted by Melvin *et al.* shortly after in 2017 supported these findings for their role in interbacterial competition via an encoded RNase toxin. They additionally added to the literature of the known roles of CDI in acute virulence using both lettuce and *Galleria*

mellonella models indicating their importance in infection. The study also outlined differences in expression of other known virulence factors such as cyanide production and swarming motility and divulges a larger scope in virulence factor interplay with these systems.

Genomic analysis outlining the high conservation and retention of these systems in virulent strains indicates CDI systems are virulence determinants which suggests they are expressed and evolutionarily important in strain survival (Allen & Hauser, 2019; Allen *et al.*, 2020). The discovery in the Allen *et al.* study in 2020 showed CDI from *P. aeruginosa* blood isolates also contribute to virulence through *in vivo* mouse models via a trans-kingdom tRNase effector, suggesting a much wider application of these systems in virulence and competition by virulent bacterial strains in various niches such as polymicrobial communities.

However, other organisms have demonstrated that these systems may also be used cooperatively in a mechanism called **C**ontact **D**ependent **S**ignalling (CDS) (Garcia *et al.*, 2016a). CDS enables crosstalk between strains as an alternative to quorum sensing through the formation of the toxin-immunity complex which may influence transcriptional control of genes involved in group-mediated responses. This has not been shown for *P. aeruginosa*.

A handful of studies have found putative functions for CDI toxins in *Pseudomonas* spp. suggesting these systems target highly conserved intracellular functions such as DNA structure, transcriptional regulation and translation (Willett *et al.*, 2015a; Ocasio & Cotter, 2019; Wang *et al.*, 2022). This mirrors what is found across Gram-negative bacteria with nucleases being particularly prevalent (Iyer *et al.*, 2011; Zhang *et al.*, 2012; Roussin *et al.*, 2019). However, many of these putative functions still require experimental validation. Although the putative function of the toxins found in CDI systems throughout the

Pseudomonas spp. have been elucidated bioinformatically (Allen & Hauser, 2019), many of these systems have not had their downstream cognate immunities outlined. This is due to the difficulty in identifying the exact downstream ORFs conferring immunity as bioinformatics gene designation functions in various platforms do not recognise the ORFs pertaining to the encoded immunities due to their small size, overlapping start codons, alternative start codon usage and weak ribosomal binding sites. Therefore, experimentally validating the function of these putative toxins as well as any identified immunities in rescuing survival after toxin expression would enhance our understanding of the systems, informing future studies in toxin-immunity complex identification both bioinformatically and experimentally. This would expand our understanding of these systems contextually in conditions associated with virulent bacteria such as *P. aeruginosa* in CF polymicrobial communities.

4.2 Aims of this study

From the current literature and based on the *in silico* results outlined in Chapter 3 of this thesis, I have four major hypotheses to address in this chapter:

1. The operons identified in Chapter 3 of this thesis encode functional CDI systems
2. The removal of each CDI operon has no effect on bacterial fitness
3. Both CDI systems in *P. aeruginosa* PA14 encode functional toxin-immunity modules
4. The CdiA-CT^{00510} and CdiA-CT^{32790} are tRNase encoding effectors

This chapter summarises research conducted to expand the genomic and functional understanding of the CDI systems in *P. aeruginosa* PA14 through addressing the following aims:

1. Generating strain background PA14 H123
2. Constructing whole system deletion mutants of both *cdiBAI*^{00510} and *cdiBAI*^{32790}
3. Engineer the inducible vector pNDM220 to harbour *cdiA*-CT^{00510} or *cdiA*-CT^{32790} for expression in *E. coli*
4. Engineer the inducible vector pBAD33 to harbour *cdiI*^{00510} or *cdiI*^{32790} for expression in *E. coli*
5. Determining whether each toxin-immunity pair encodes functional effector-anti-effector modules

4.3 Results

4.3.1 Mutant strain background engineering

The complexity of competitive systems in their structure and function means they require tight regulation at the transcriptional, post-transcriptional and post-translational levels (Mercy *et al.*, 2016; Wang, Brodmann & Basler, 2019; Allsopp *et al.*, 2022). Previously it has been shown that the post-transcriptional regulator RsmA (Goodman *et al.*, 2004) negatively regulates the expression of the CDI (Mercy *et al.*, 2016) and T6SSs (Mougous *et al.*, 2006; Allsopp *et al.*, 2017). Therefore the *rsmA* strain is used as a standard strain background for experimental studies looking at the role of RsmA in the expression of competitive systems.

P. aeruginosa encodes three T6SSs (H1-, H2-, H3-T6SS) in its genome (Mougous *et al.*, 2006; Allsopp *et al.*, 2020). Research aimed at understanding the expression and function of the T6SSs in *P. aeruginosa* has utilised mutants with a combination of systems and their regulators deleted from the genome (Allsopp *et al.*, 2017) to remove potential influences on

the competitive effect observed, ensuring results only pertain to the system of interest. Therefore, to study the role of CDI systems and their identified regulators in interbacterial competition, the creation of strain backgrounds with various competitive systems and their regulators deleted was required.

Genetic backgrounds PA14, PA14 *rsmA* and PA14 *rsmA*H123 were available from the Allsopp lab -80°C stores pre-dating the commencement of this PhD (Figure 4.1). PA14 represents the WT background with all systems and its regulation pathways intact. PA14 *rsmA* strain would remove post-transcriptional regulation of the systems and was expected to increase the expression of both CDI and T6SS in this background. Finally, PA14 *rsmA*H123 would remove both post-transcriptional regulation and inactivate all three T6SSs, eliminating these as confounding factors on any competitive effect observed.

To complete the strain background panel I created the final genetic background PA14 H123 (Figure 4.1). To do this, *rsmA* was reintroduced into the genome of PA14 *rsmA*H123 via a vector pKNG101 three-partner conjugation assay (outlined in 2.12). Colonies were PCR screened to confirm successful reinsertion of *rsmA* into the genome (Figure 4.2). Based on the results in Figure 4.2 colonies 1, 5 and 8 were sent for sequencing via Eurofins SupremeRun Tube Sanger sequencing to verify *rsmA* insertion and confirm no mutations had accumulated. From the sequencing results, colonies 1 and 8 showed 100% sequence identity indicating successful insertion into the genome (Figure 4.3). These colonies were then stocked and used in subsequent experiments to represent the H123 strain background.

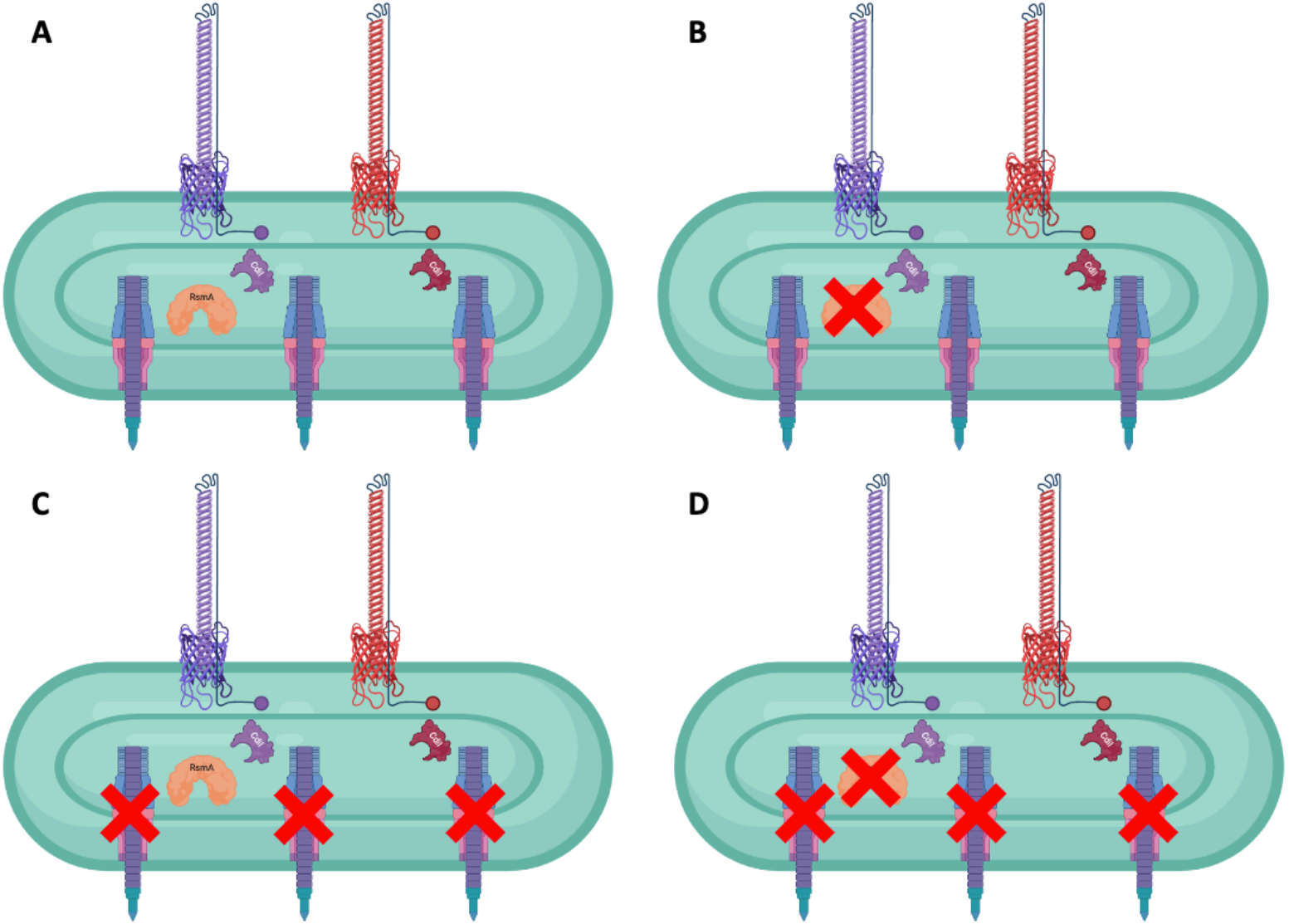


Figure 4.1: *P. aeruginosa* strain backgrounds for CDI mutant production. *P. aeruginosa* strains were required to produce CDI mutant strains for future assays in these four backgrounds. (A) PA14 WT contains all five competition systems and *rsmA* post-transcriptional regulation. (B) *rsmA* strains contains all five competition systems but has the post-transcriptional regulation removed. (C) *rsmA*H123 has the three T6SSs H1-/H2-/H3- and post-transcriptional regulation inactivated. (D) H123 has the three T6SSs H1-/H2-/H3- removed only.

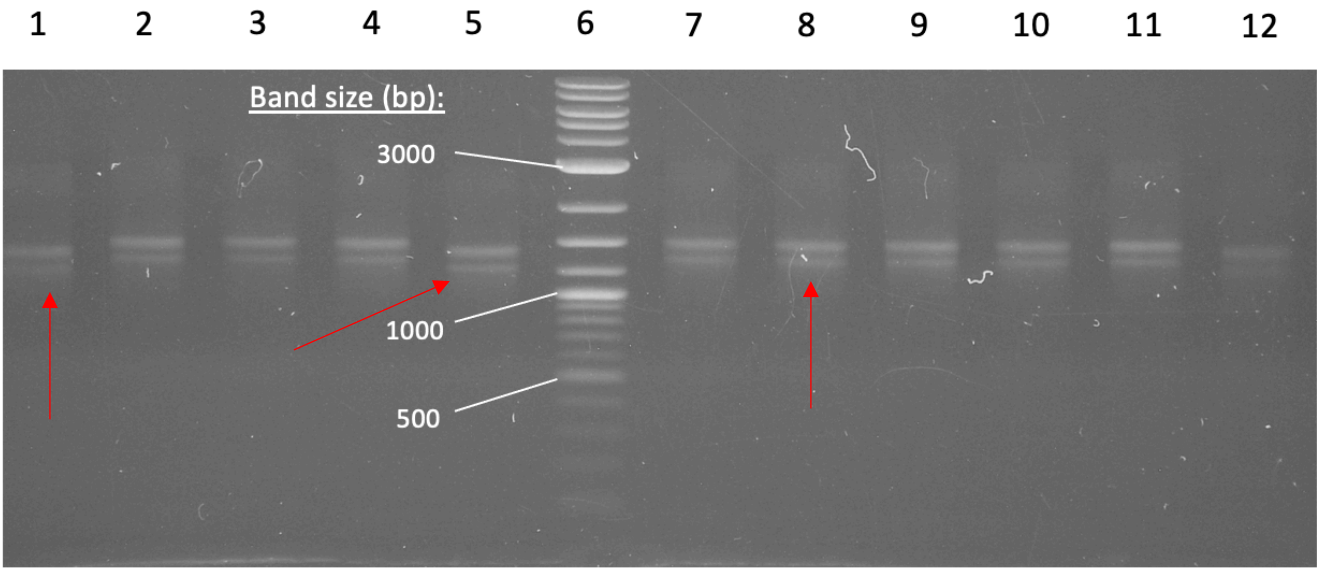


Figure 4.2: PCR confirmation of successful *rsmA* repair on the chromosome of *P. aeruginosa* PA14. Gel electrophoresis imaging shows results of PCR products of *rsmA* amplification from insertion into PA14 via three partner conjugation. Lane (1-5 and 7-12) colonies screened (primers found in 2.3 Table 2.11), Lanes 1, 5 and 8 show successful reinsertion of *rsmA* at 1400 bp (indicated by red arrows) compared with Lanes 2 - 4 or 7, 9-12 when compared against the DNA ladder.

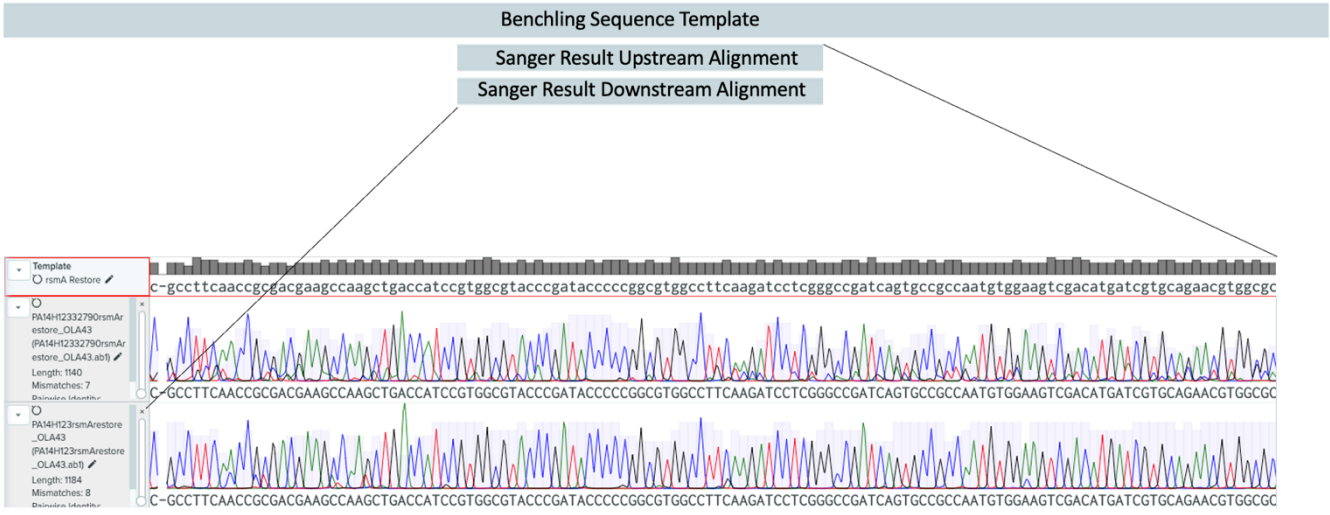


Figure 4.3: Sequence alignment confirming successful chromosomal reinsertion of *rsmA* . Grey coloured bars represent exact sequence of *rsmA*. Second and third lines show sequencing chromatograms that confirm the presence of the WT *rsmA* sequence. Absence of red colouring of the grey bars indicates no mutations accumulated within the fragment during insertion.

4.3.2 CDI system deletion mutant engineering from in silico characterisation of CDI operons

CDI systems have been associated with interbacterial competition in multiple bacteria, including various species and strains of *Pseudomonas* (Aoki *et al.*, 2010; Mercy *et al.*, 2016). In the Mercy *et al.* study in 2016, whole system deletion mutants (WSDMs) were created for *P. aeruginosa* strain PAO1 homologous systems. To date no experimental studies have attempted to study CDI systems in PA14. Therefore, to study the role of CDI systems in interbacterial competition, engineering WSDMs in the four strain backgrounds (Figure 4.1) was required. Based on the CDI operons outlined in Chapter 3 of this thesis, I generated WSDMs for use in subsequent experiments in Chapter 6 of this thesis, determining the role of CDI in competitive and cooperative interactions.

Using genomic DNA, mutator fragments were created by amplifying the upstream and downstream regions directly flanking the CDI operons. Splice overlap PCR created a mutator fragment that was cloned into pKNG101 prior to a three partner conjugation for insertion into the genome resulting in the creation of the deletion mutants. This process was used to create mutants in all four genetic backgrounds (PA14, *rsmA, rsmA*H123 and H123) which had the CDI^{00510}, CDI^{32790} or both CDI deleted (Figure 4.4). This formed a panel of 16 strains.

Here I detail a representative example for deletion of $cdiBAI^{00510}$. Initially, I designed primers to amplify genome regions flanking the operon- directly upstream of *cdiB* and downstream of *cdiI*. Each primer encoded a 'tail' for overlap PCR and mutator fragment production (Figure 4.5). Amplification of these sequences and subsequent overlap PCR produced the final mutator fragment (Figure 4.6). Restriction digest and ligation into the pKNG101 vector followed before transformation into competent *E. coli* CC118λPIR cells (Figure 4.7).

Constructs were confirmed via sequencing (Figure 4.8). Three partner conjugation was used to transfer pKNG101::mutator-fragment vectors from CC118λPIR into PA14. Conjugants where plated on SM2000 plates to select for pKNG101::mutator-fragment integration and confirmed by PCR (Figure 4.9). Counterselection forcing pKNG101 out of the chromosome enabled successful replacement of the mutator fragment, demonstrated by PCR (Figure 4.10) and confirmed via sequencing (Figure 4.11).

After the creation of all mutants in each strain background, the final step was to determine whether CDI deletion impacted strain fitness. Therefore, a growth rate assay was conducted as a measure of fitness when compared with PA14 WT (Figure 4.12). From this analysis, growth of all mutants was unaffected with CDI deletion although a slightly longer lag phase was noted in the *rsmA* strains. Having created the WSDMs, the toxins and immunities from each system were cloned into inducible vectors to validate their putative functionality.

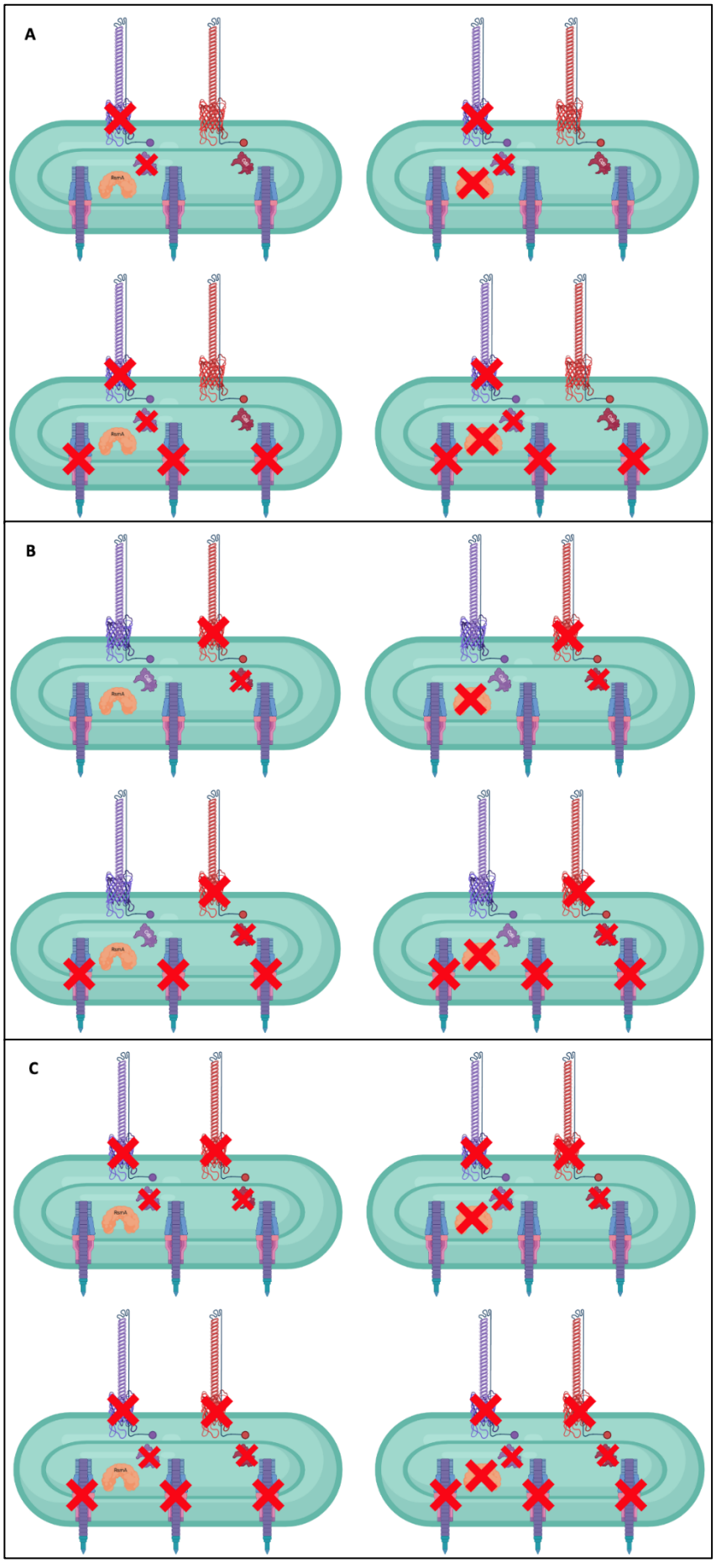


Figure 4.4: CDI mutant strains generated. (A) Illustration of each strain background from Figure 1 with the *cdiBAI*^{00510} system deleted. (B) Illustration of each strain background with the *cdiBAI*^{32790} system deleted. (C) Illustration of each strain background with both *cdiBAI*^{00510} and *cdiBAI*^{32790} systems deleted.

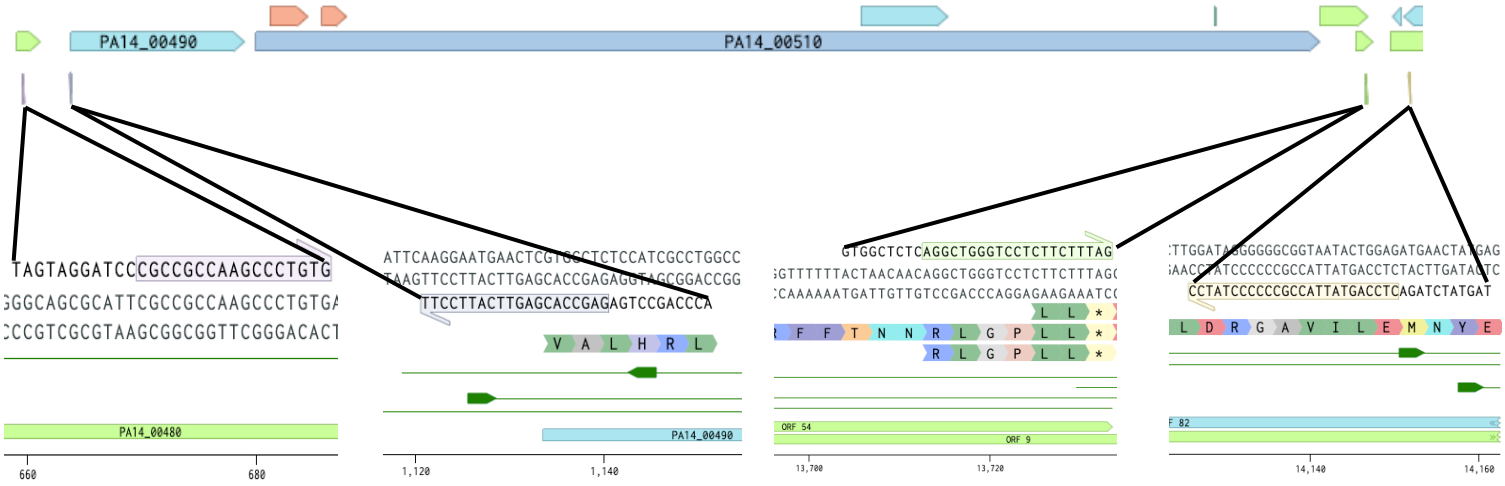


Figure 4.5: Primers for amplification of PA14 *cdiBAI*^{00510} upstream and downstream fragments. Primers were designed to amplify the regions directly flanking upstream and downstream of each CDI operon. The above primers represent those designed for CDI^{00510} mutator fragment creation. Primers 2 and 3 had designed overlapping tails for mutator fragment creation via overlap PCR for deleting this operon form the genome.

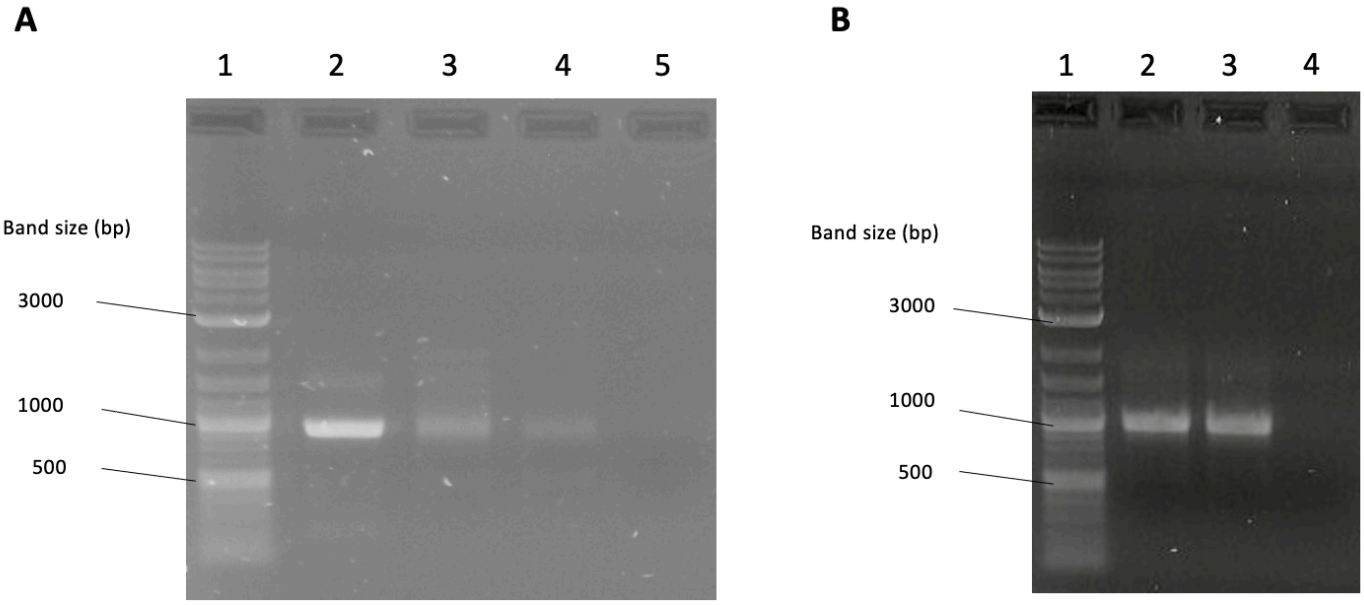


Figure 4.6: Splice overlap PCRs of PA14 *cdiBAI*^{00510} and *cdiBAI*^{32790} upstream and downstream fragments. (A) Lanes 2-4 indicate successful overlap and amplification of CDI^{00510} overlap fragment. Lane 5 indicates negative water control. (B) Lanes 2 and 3 indicate successful overlap and amplification of CDI^{32790} overlap fragment. Lane 4 indicates negative water control. Note: 2-log ladder was used (and on every gel in this thesis unless otherwise stated).

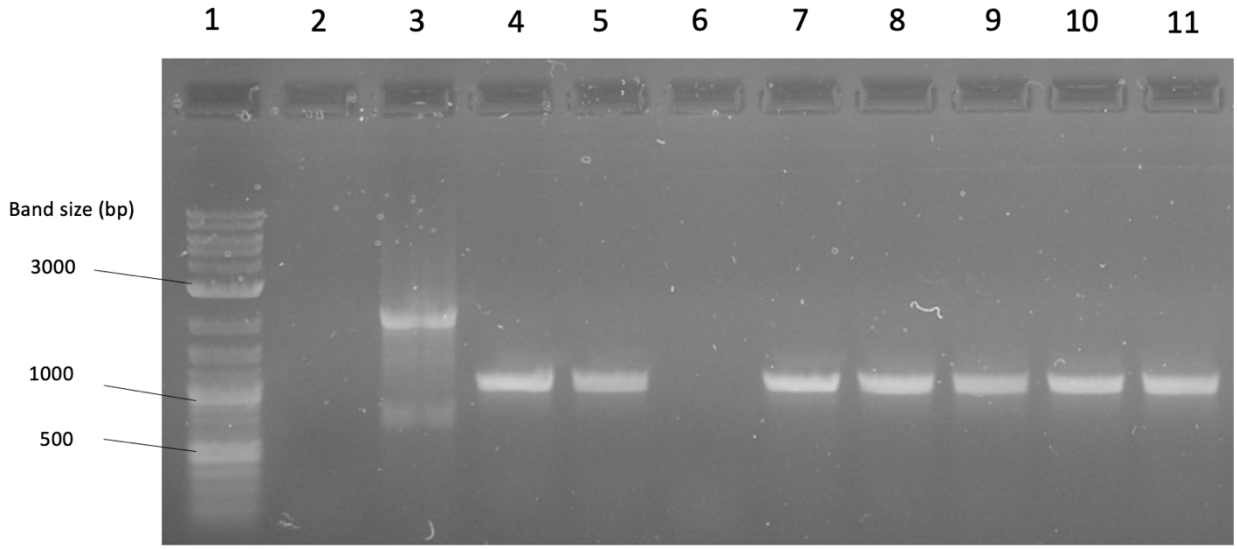


Figure 4.7: Successful generation of pKNG101*cdiBAI*^{00510} mutator confirmed by PCR screening. Transformants grown and selected on SM50 agar were screened via PCR to determine successful insertion of mutator fragments into pKNG101. Gel shows PCR results using pKNG101 vector primers UpKn and RpKn, with lanes 4, 5 and 7-9 exhibiting a band matching the predicted 1200 bp. Lane 3 pertains the empty pKNG101 positive control and lane 2 the negative water control.

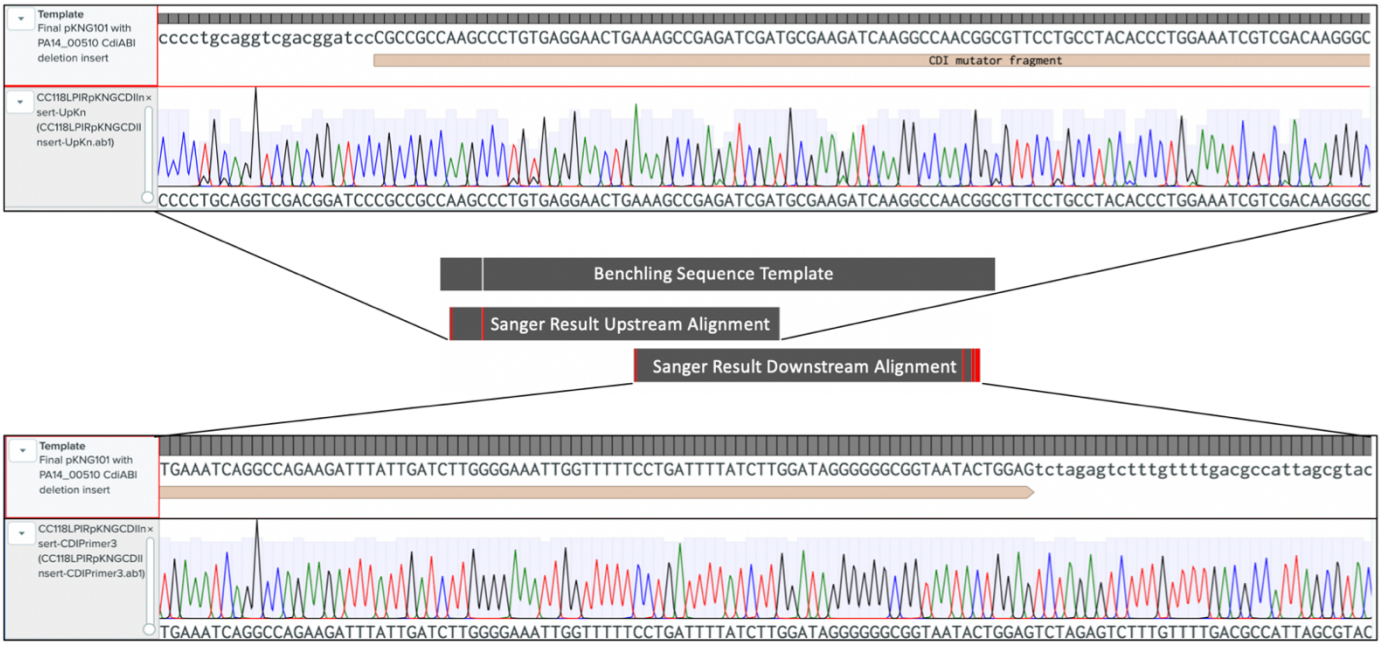


Figure 4.8: Sequencing alignment confirming successful construction of pKNG101cdi*BAI*^{00510} Alignment of the sequence results was created comparing it to the *in silico* designed strategy to confirm successful insertion into pKNG101. Note: clean sharp chromatogram peaks indicate high quality sequence output. Grey rectangles in the centre represents sequence alignments and indicates exact sequence homology to the template.

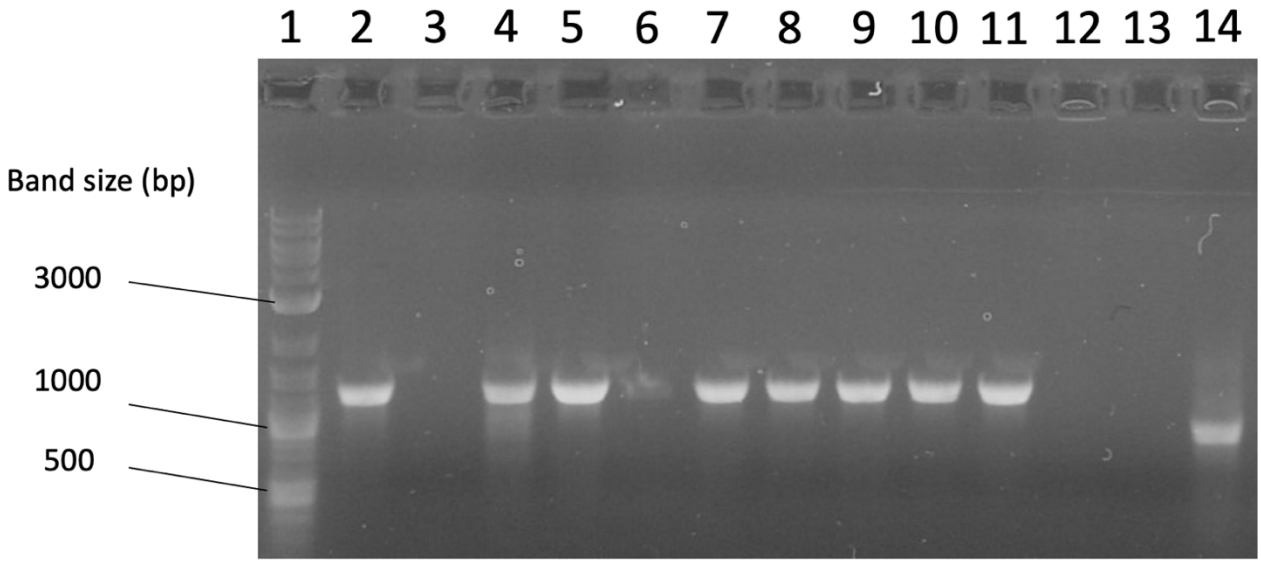


Figure 4.9: PCR amplification confirming successful insertion of pKNG101*cdiBAI*^{00510} mutator into PA14. Transformants grown and selected on VBM SM2000 agar were screened via PCR to determine successful insertion of pKNG101::ΔCDI^{00510} into chromosomal DNA. Using designed primer 5 and pKNG vector primer RpKn, lanes 2-9 represent colonies screened. Lane 13 pertains the negative water control and lane 14 representing the empty pKNG101 positive control. Note: no amplification in lanes 3 and 12 indicate either no pKNG101::ΔCDI^{00510} chromosomal insertion or insertion in the opposite (primer 6 and UpKn) orientation in the chromosome.

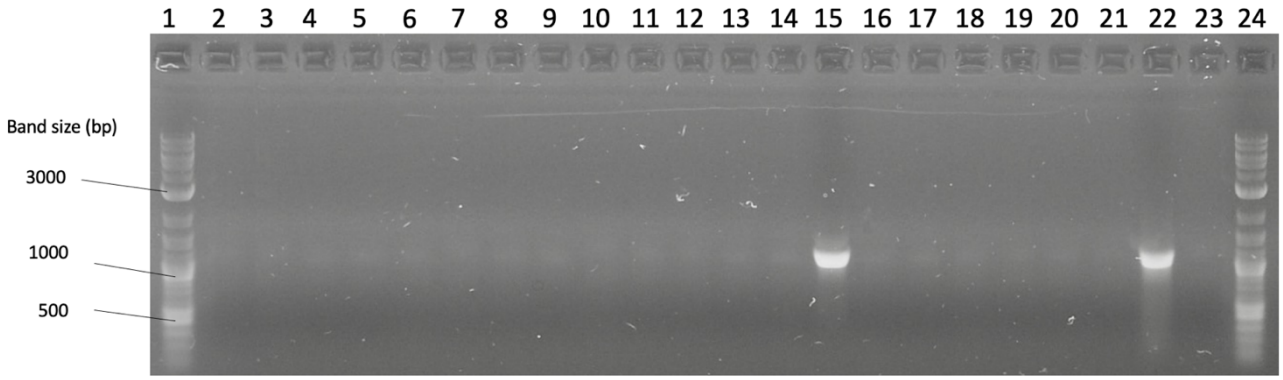


Figure 4.10: PCR amplification of successful PA14 Δ*cdiBAI*^{00510} mutant construction in the PA14 background. Colony PCR confirms CDI^{00510} deletion in the chromosome in PA14 WT strain. Lanes 2-21 represent colonies screened using designed primers 5 and 6, with lane 22 representing the mutator PCR mutator fragment utilised as positive control and lane 23 representing the negative water control. Note: Lane 14 shows successful replacement of WT CDI operon by mutator fragment insertion.

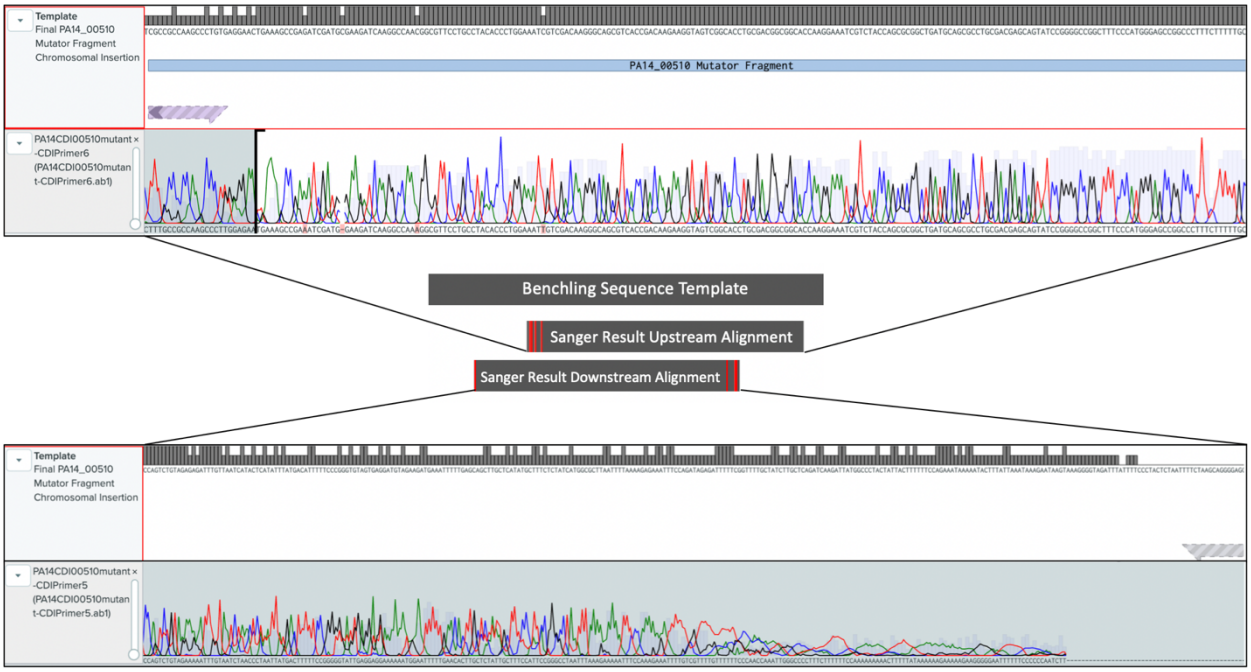


Figure 4.11: Sequencing alignment confirming successful construction of PA14 Δ*cdiBAI*^{00510}. Transformants with a band at the approximate relative fragment size were sent for sequencing to confirm successful insertion of mutator fragment into PA14 chromosomal DNA and removal of CDI WT operon. Sequence results were aligned to the *in silico* designed strategy. Note: clean sharp chromatogram peaks indicate high quality sequence output. Grey bars represent sequence alignments and indicates exact sequence homology to template.

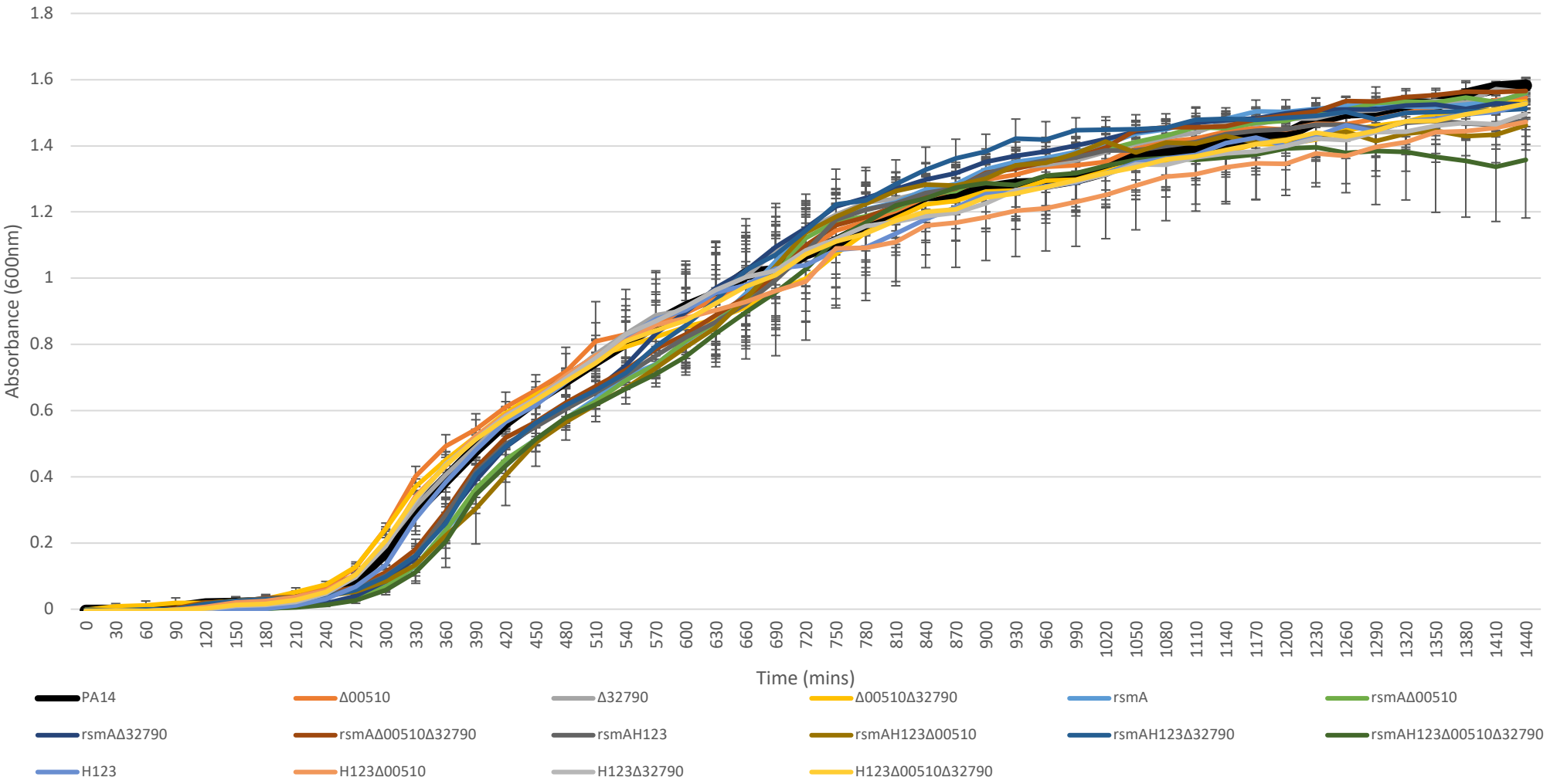


Figure 4.12: CDI mutations in all *P. aeruginosa* strain backgrounds have no significant impacts to growth rate. Graph showing growth rates of each strain over 24 hrs. Average absorbance of three replicates for each growth rate and standard error are indicated above. A One-Way ANOVA was performed between strains at each time point, non-significant to *P < 0.05.

4.3.3 Cloning of CDI toxin and immunity pairs into inducible vectors

CDI systems have been shown to encode toxins with enzymatic activities that target intracellular substrates such as those involved in transcription and translation (Dautin, 2021; Wang *et al.*, 2022). Although many putative toxin functions have been identified, most are yet to be validated experimentally, and is the case for CDI toxins in *P. aeruginosa.* As the toxins associated with the two CDI systems in PA14, discerned in Chapter 3 of this thesis, were identified to have a defined putative tRNase function with a high level of confidence, isolating these toxin-immunity pairs was crucial to experimentally validate their functions. Here the toxins and immunities were cloned into separate expression vectors to control expression separately to determine if these toxins induce bacterial intoxication, if the immunity could recover strains from intoxication, and to validate their functions as putative tRNase enzymes.

Based on in depth *cdiA* domain analysis which outlined the PTPMs, toxin domains, and *cdiI* ORFs (Chapter 3), primers were designed by MRes student Madeleine Humphrey. Primers enabled cloning of each toxins from the upstream PTPM and immunities (*cdiA*^{00510}, *cdiA*^{32790}, *cdiI*^{00510} and *cdiI*^{32790}) into the expression vectors pNDM220 and pBAD33, respectively. These primers were designed to add DNA encoding a Flag tag (toxins) or StrepII tag (immunities) (Figure 4.13) during amplification. Upon induction and protein expression, protein pull-down assay was used to determine whether direct binding of the toxins and immunities could be validated using these tags. Amplified toxin and immunity genes were first ligated into high efficacy vector pCR Blunt II- TOPO, transformed into competent *E. coli* TOP10 cells (Figure 4.14) and sequence confirmed (Figure 4.15). Restriction digestion and ligation into expression vectors pBAD33 (immunity) (Figure 4.16) and pNDM220 (toxin) (Figure 4.17) was then sequence confirmed (Figure 4.18 and 4.19). Cloning of both immunities into pBAD33 was

conducted by MRes student Nicholas Yuen. Due to difficulties experienced cloning and transforming toxins directly into pNDM220, immunities were first cloned into pBAD33 before competent *E. coli* TOP10 cells containing the induced immunity were produced (method 2.9). Amplification of toxin sequences was followed by ligation directly into the pNDM220 before transformation into *cdiI*$^{+}$ *E. coli* TOP10 competent cells (p*cdiI*^{00510} or p*cdiI*^{32790}). Transformation of *cdiA*^{00510}/*cdiA*^{32790} in pNDM220 was successful and validated via PCR (Figure 4.18) and sequencing (Figure 4.19), overcoming this challenge. These vectors were designated p*cdiA*-CT^{00510}, p*cdiA*-CT^{32790}, p*cdiI*^{00510} and p*cdiI*^{32790}. Final transformants were *cdiA*$^{+}$*cdiI*$^{+}$ strains (Figure 4.20). Having created these strains, the functionality and specificity of these pairs was determined.

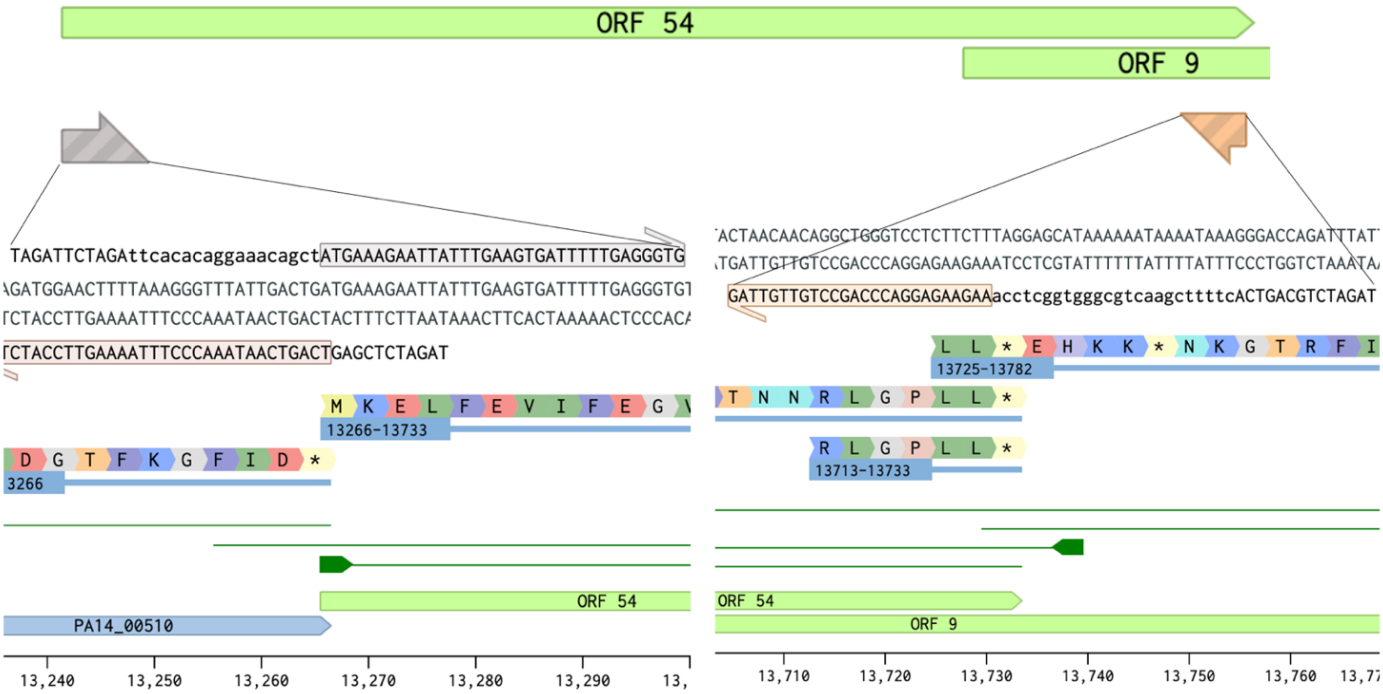


Figure 4.13: Primers for amplification of PA14 CDI^{00510} *cdiI* genes. Primers designed to amplify *cdiI* regions directly downstream of each *cdiA* gene above represent those for CDI^{00510} *cdiI*. Forward primers incorporate the DNA encoding a StrepII tag.

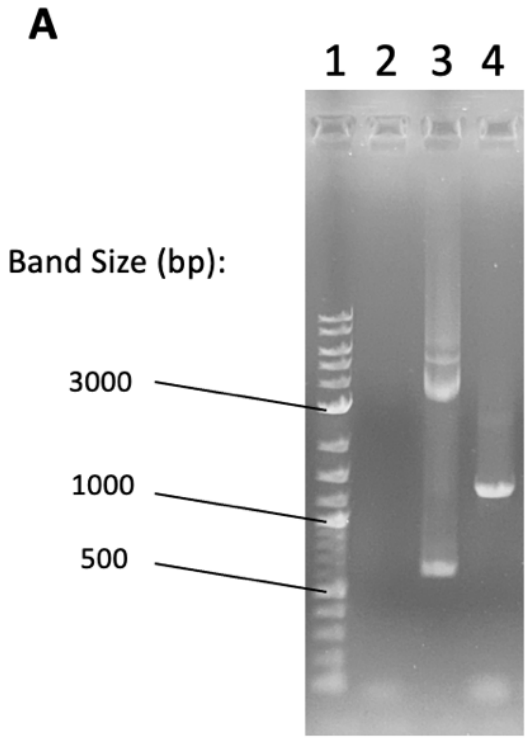
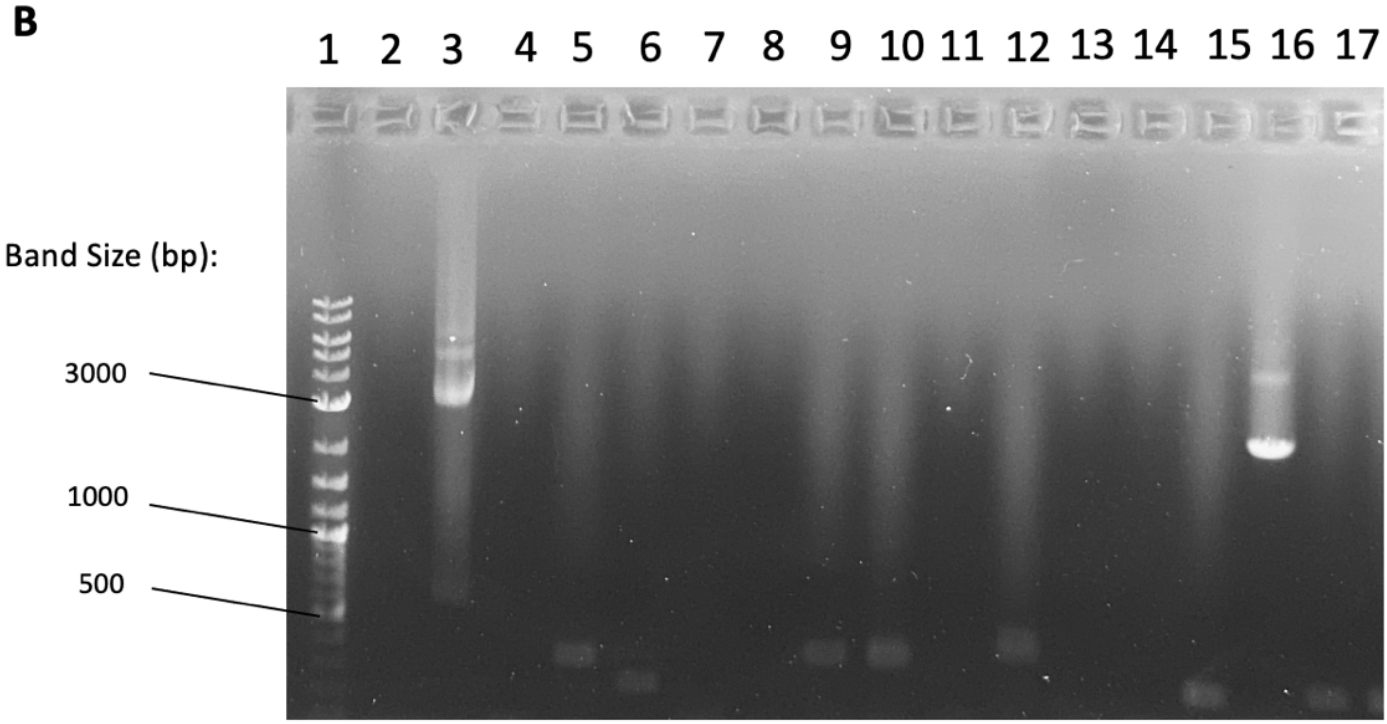


Figure 4.14: PCR amplification of successful insertion of cloned *cdiI*^{00510} or *cdiI*^{32790} into pCR Blunt II-TOPO. Transformants were screened to determine successful pCR BluntII-TOPO::*cdiI* construction. (A) Lane 4 indicates successful insertion of *cdiI*^{00510}. Lane 2 indicates negative water control, whilst lane 3 indicates positive control. (B) Lane 16 indicates successful insertion of *cdiI*^{00510}. Lane 2 indicates negative water control, whilst lane 3 indicates positive control.



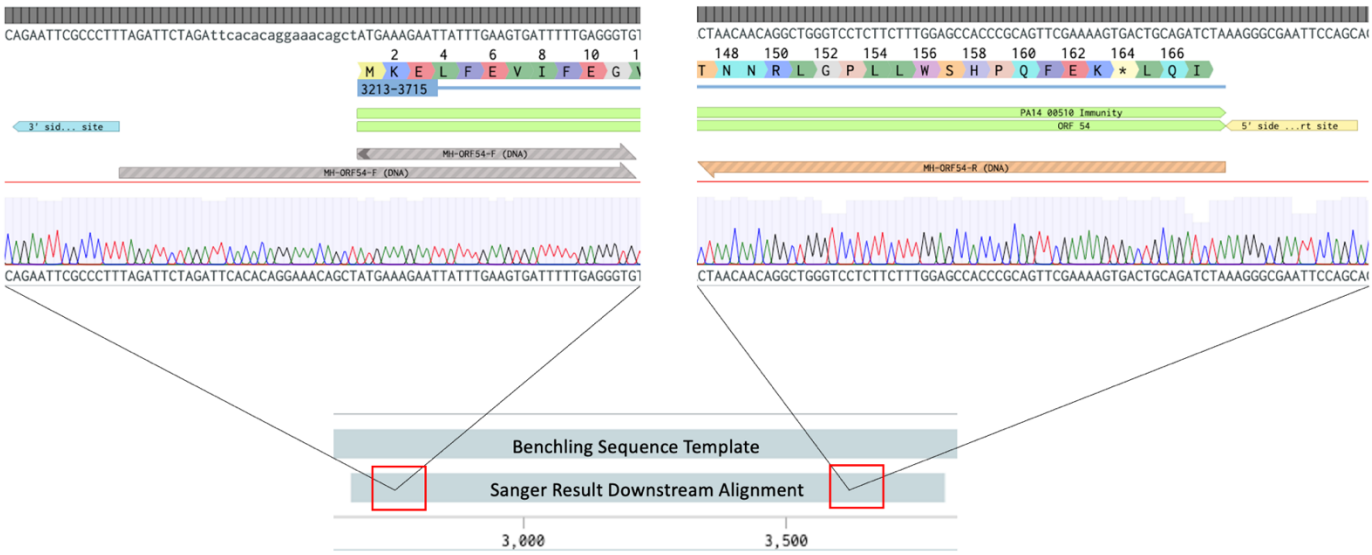


Figure 4.15: Sequencing alignment confirming successful construction of pCR Blunt II-TOPO-*cdil*^{00510}. Sequencing with vector primers confirm successful insertion and lack of errors of *cdil*^{00510} in pCR BluntII-TOPO.

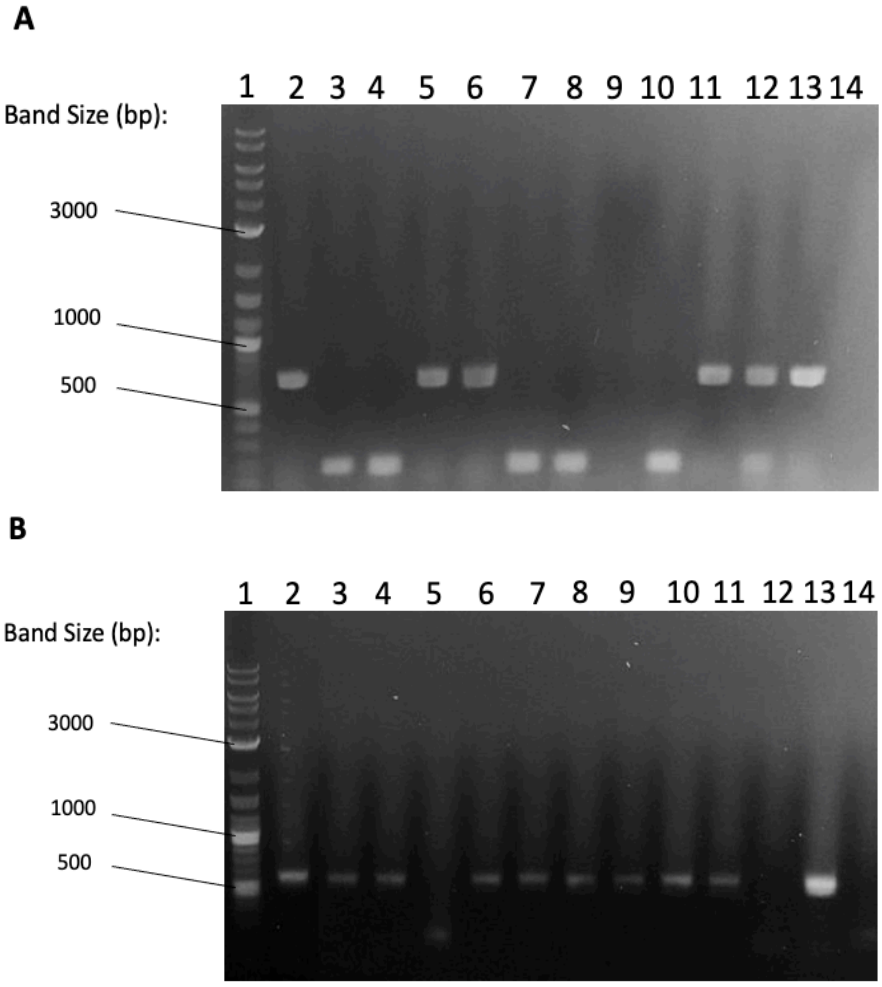


Figure 4.16: Amplification of successful insertion of cloned *cdil*^{00510} and *cdil*^{32790} into expression vector pBAD33. Transformants isolated were screened to determine successful construction of pBAD33::*cdil.* (A) Lane 4 indicates successful insertion of *cdil*^{00510}. Lane 2 indicates negative water control, whilst lane 3 indicates positive control. (B) Lane 16 indicates successful insertion of *cdil*^{00510}. Lane 2 indicates negative water control, whilst lane 3 indicates positive control.

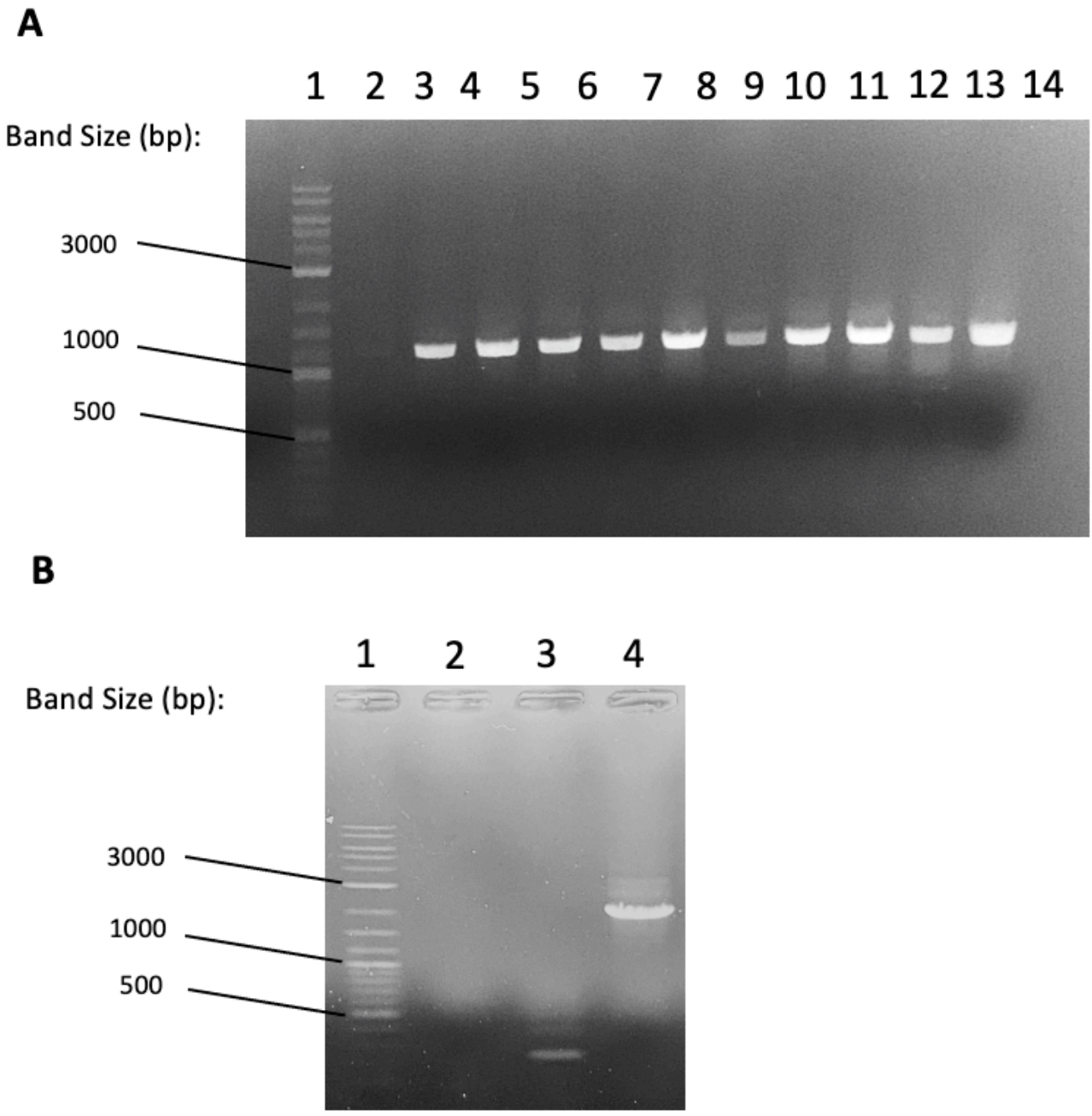


Figure 4.17: Amplification of successful insertion of cloned *cdiA*^{00510} and *cdiA*^{32790} into expression vector pNDM220. Transformants isolated were screened to determine successful construction of pNDM220::*cdiA.* (A) Screening of p*cdiA*^{00510} transformants with lanes 3-12 indicating successful insertion of *cdiA*^{00510}. Lane 14 indicates negative water control, whilst lane 14 indicates positive control. (B) Screening p*cdiA*^{32790} transformants with lane 16 indicates successful insertion of *cdiA*^{00510}. Lane 2 indicates negative water control, whilst lane 3 indicates positive control.

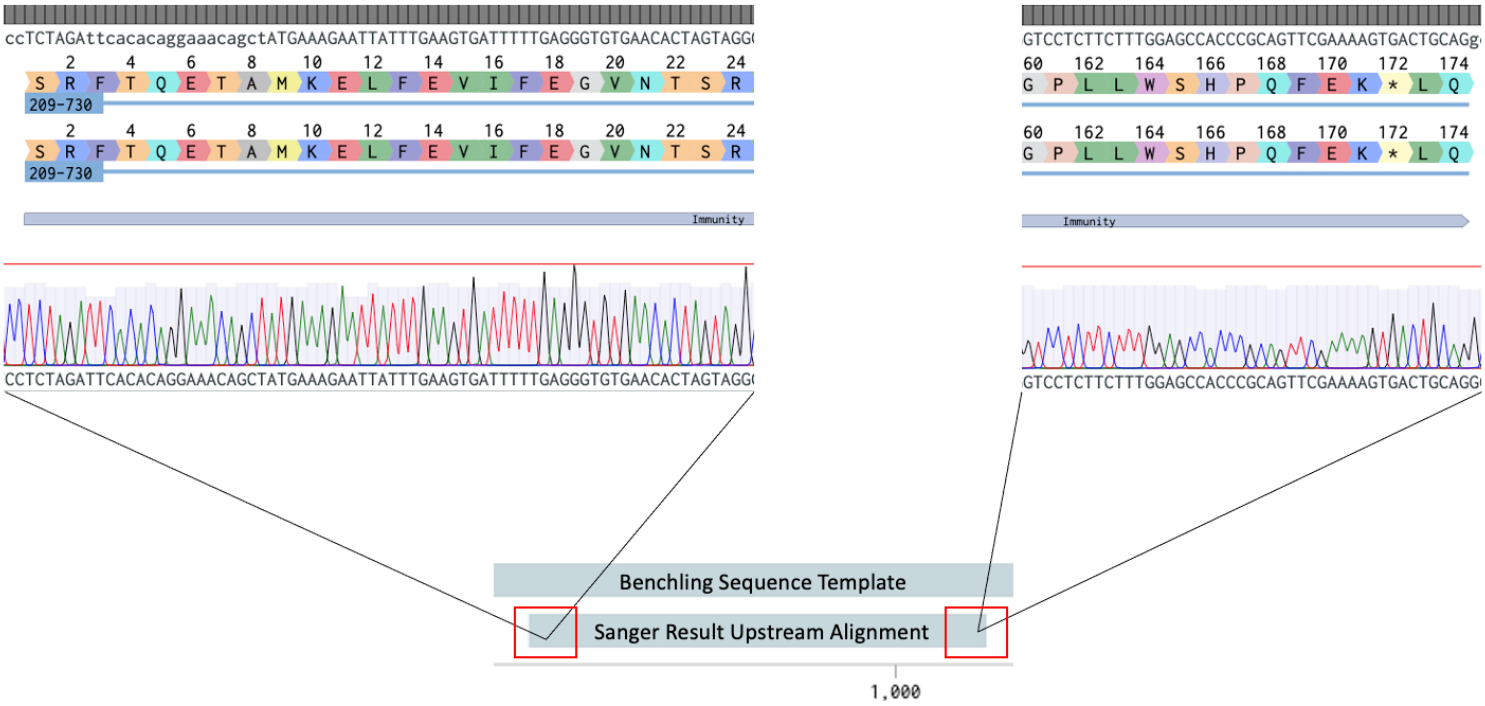


Figure 4.18: Sequencing alignment confirming successful construction of p*cdiI*^{00510}. Sequencing with vector primers confirm successful insertion and lack of errors of *cdiI*^{00510} in pBAD33.

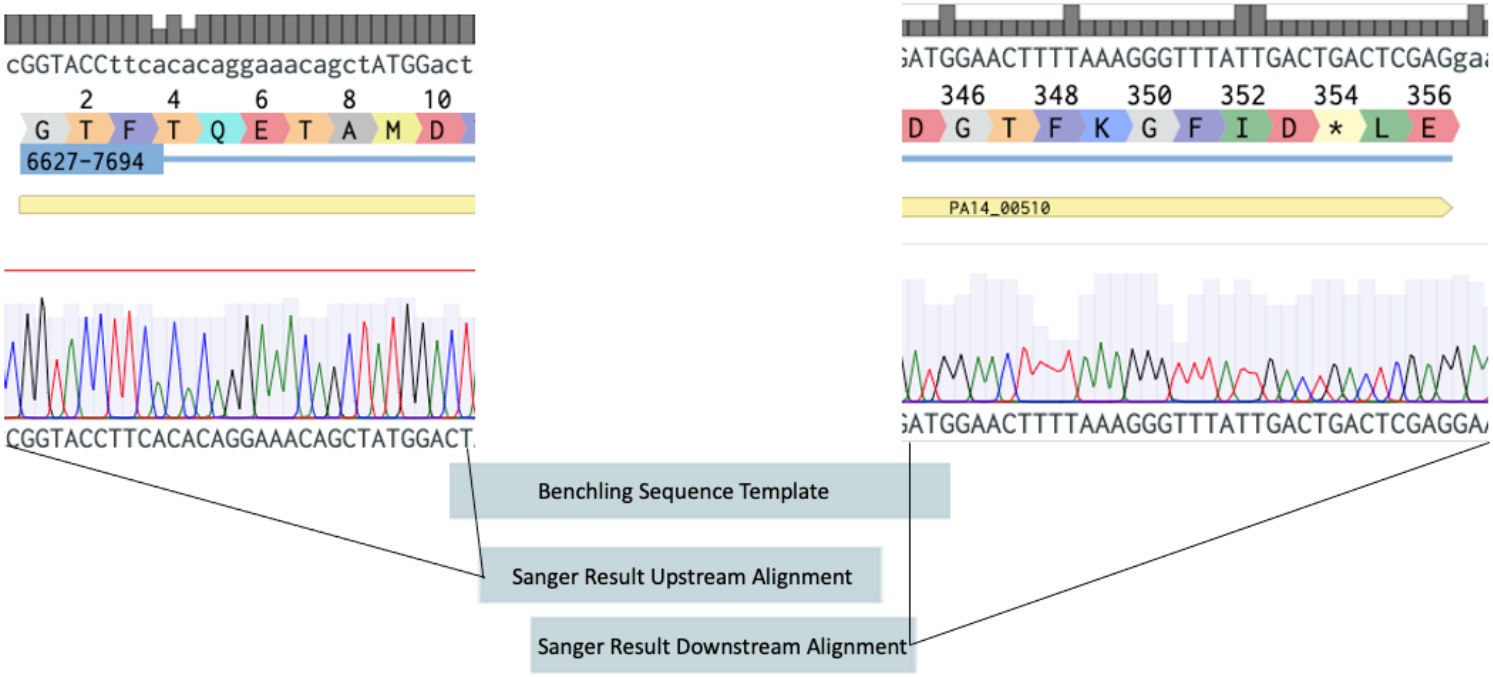


Figure 4.19: Sequencing alignment confirming successful construction of p*cdiA*^{00510}. Sequencing with vector primers confirm successful insertion of *cdiA*^{00510} and lack of errors in pNDM220.

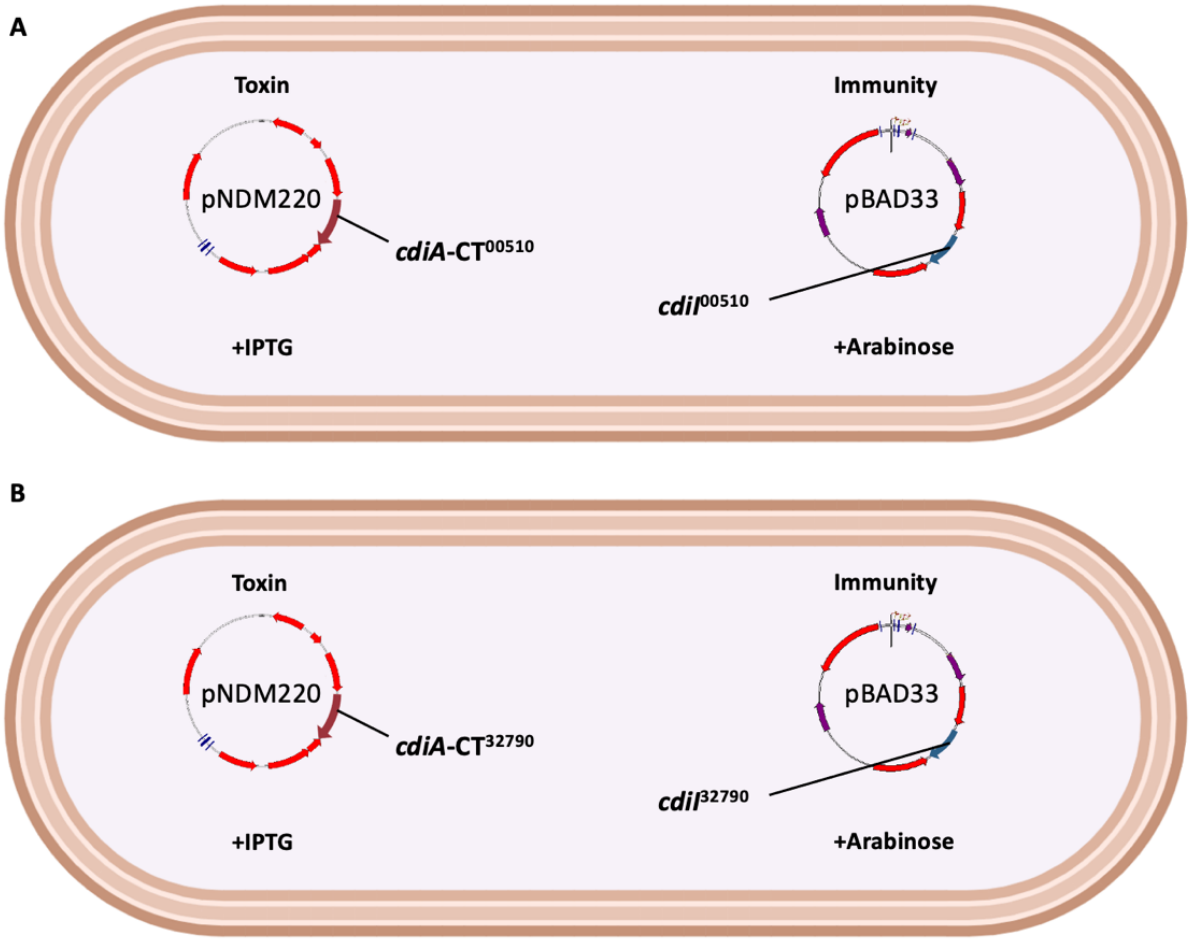


Figure 4.20: Model of *Escherichia coli* BL21 strains with cloned toxin-immunity pairs from CDI systems. *E. coli* strains containing toxin-immunity pairs cloned into expression vectors were required to validate expression and activity *in vitro*. Toxins and immunities were cloned into separate vectors pNDM220 and pBAD33, respectively. (A) *E. coli* TOP10 containing cloned CDI^{00510} toxin and immunity. (B) *E. coli* TOP10 containing cloned CDI^{32790} toxin and immunity.

4.3.4 CdiA^{PA14_00510} and CdiA^{PA14_32790} encode functional toxin-immunity pairs

Research to date has confirmed CDI encode intracellular toxins which target central cell components, and that immunities directly interact via cognate binding to neutralise the toxin's function (Ruhe *et al.*, 2013; Hayes *et al.*, 2014). Here I sought to determine whether the CDI putative toxin-immunity pairs from PA14 are functional and specific. Using strains constructed in 4.3.3; time course induction assays, western blot analysis and protein pull-down was conducted to validate the CDI toxin-immunity pairs under study in this thesis.

Expression assays were conducted to investigate if the toxin-immunity pairs identified in Chapter 3 were functional. Initially, a selective agar spot plate method was used to determine inducer concentrations required for toxins and immunity expression. From this, the concentrations were found to be 0.1 mM IPTG and for toxin and 0.2% arabinose for immunity induction sufficient for recovery from intoxication. Once inducer concentrations were determined, the selective agar spot plate assay was conducted. This showed induction of both toxins *cdiA*-CT^{00510} (Figure 4.21) and *cdiA*-CT^{32790} (Figure 4.22) incited significant reduction in *E. coli* CFU whilst subsequent immunity induction recovered CFU. From this a time course growth assay was conducted in flasks to evaluate intoxication and immunity recovery capabilities (Figure 4.23). These results show a large growth reduction after immunity induction, indicating the immunity expression is energy expensive. Further growth reduction is observed after toxin induction which plateaus directly after 2 hr induction for *cdiA*-CT^{00510} (Figure 4.23a) indicating an immediate intoxication effect on bacterial growth. Reduction is also observed for *cdiA*-CT^{32790} (Figure 4.23b), however growth does not plateau for a further 2 hrs post-induction indicating intoxication is not immediate as seen with *cdiA*-CT^{00510} and

therefore may have a disparate mechanism of action. Subsequent immunity expression recovered growth rate to immunity induced levels alone.

To quantify the growth rate disparity, area under the curve (AUC) of each growth rate was calculated for each assay repeat (Figure 4.24). Significant growth rate reduction was observed upon toxin expression. Significant growth rate recovery was observed with additional induction of the paired immunity. This was also reflected in the doubling times observed (Figure 4.25). Inducing the *cdiA*-CT^{00510} toxin (Figure 4.25a) resulted in an increased doubling rate of 24.82 hrs compared with 3.98 hrs upon immunity induction alone. Inducing the *cdiA*-CT^{32790} toxin showed a smaller increase in doubling rate of 5.95 hrs compared with 3.61 hrs when the immunity was induced alone. To confirm toxin-immunity pairs were expressed during induction, paired samples were collected from the time course induction assay to conduct western blot analysis (Figure 4.26). As both toxins and immunities were confirmed to be expressed, we can conclude that both CDI systems from PA14 encode functional toxin-immunity pairs.

After validating toxin-immunity pair functionality, their specificity was also evaluated via the spot plate assay. *E. coli* BL21 strains were constructed with the opposite toxin and immunities from the two systems (Figure 4.27). The spot plate assay indicated recovery from intoxication by immunities is specific as CFU for *cdiA*-CT^{00510} (Figure 4.28) and *cdiA*-CT^{32790} (Figure 4.29) was not recovered upon inducing the expression of the opposite immunity. After validating toxin-immunity pair functionality and specificity, direct interaction was determined using a protein pull-down assay and evaluated via western blot analysis (Figure 4.30). This indicated both toxins directly bind to their respective immunities confirming cognate binding as a mechanism for toxin neutralisation. Due to time constraints toxin function was not validated.

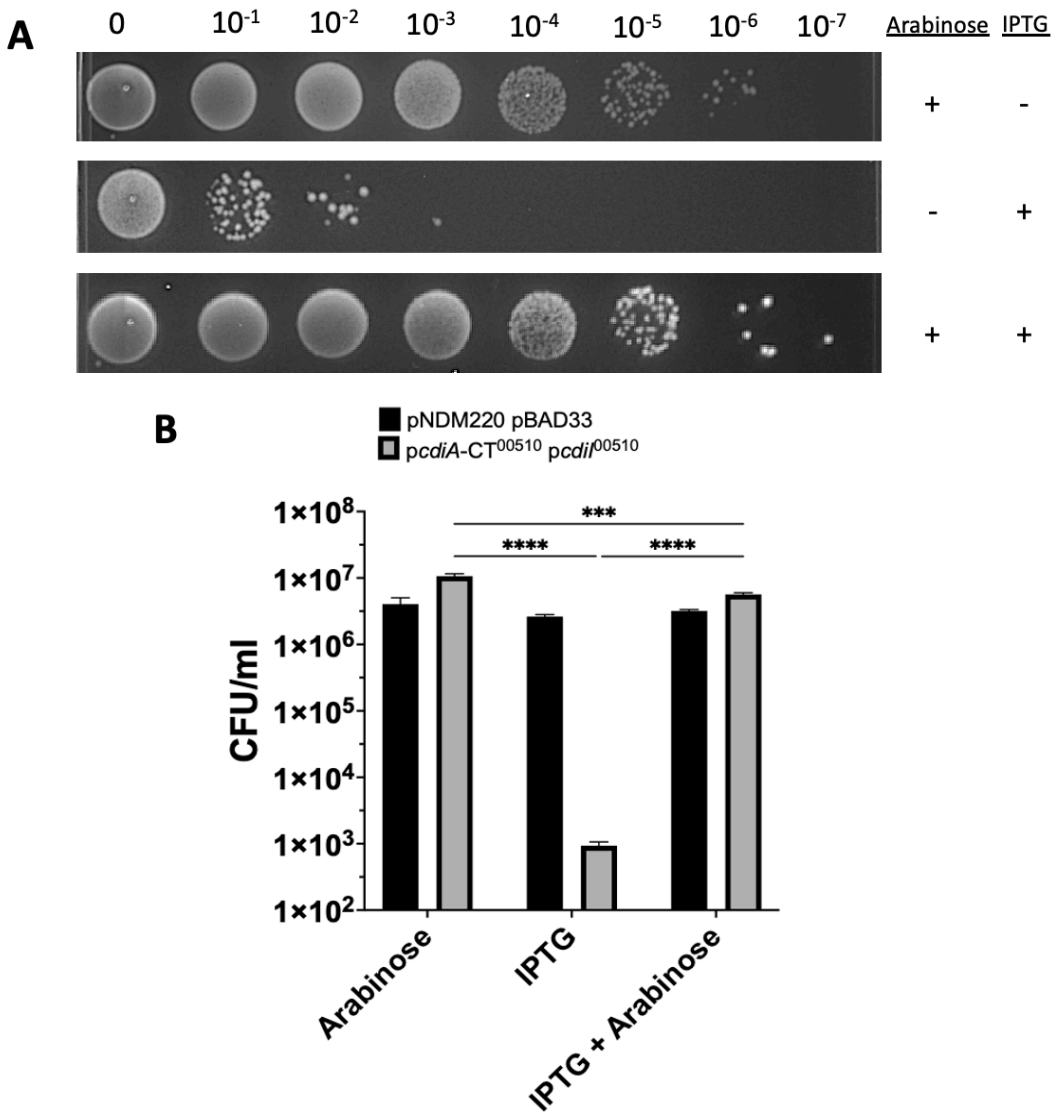


Figure 4.21: *cdiAI*^{00510} encodes a functional toxin-immunity pair which induces both bacterial intoxication and recovery when expressed in *E. coli* BL21. BL21 containing both p*cdiA*-CT^{00510} and p*cdiI*^{00510} was used to create a dilution series which was plated onto selective agars containing Amp50 and Cm30, with either no inducers or the addition of either IPTG to induce p*cdiA*-CT^{00510}, arabinose to induce p*cdiI*^{00510}, or both. Colony counts after overnight incubation determined toxin-immunity pair functionality. (A) Large reduction in survival is observed with CdiA^{00510} induction. Additional immunity induction recovers survival. (B) Quantification of A using CFU calculations confirms a 5- fold reduction in bacterial survival upon toxin induction. Reduction is completely ameliorated with additional immunity induction. A Two-Way ANOVA was performed on average CFU for each strain, statistically significant to ****P<0.0001. Post-hoc statistical significance of induced strains was compared using Tukey's test (n=3).

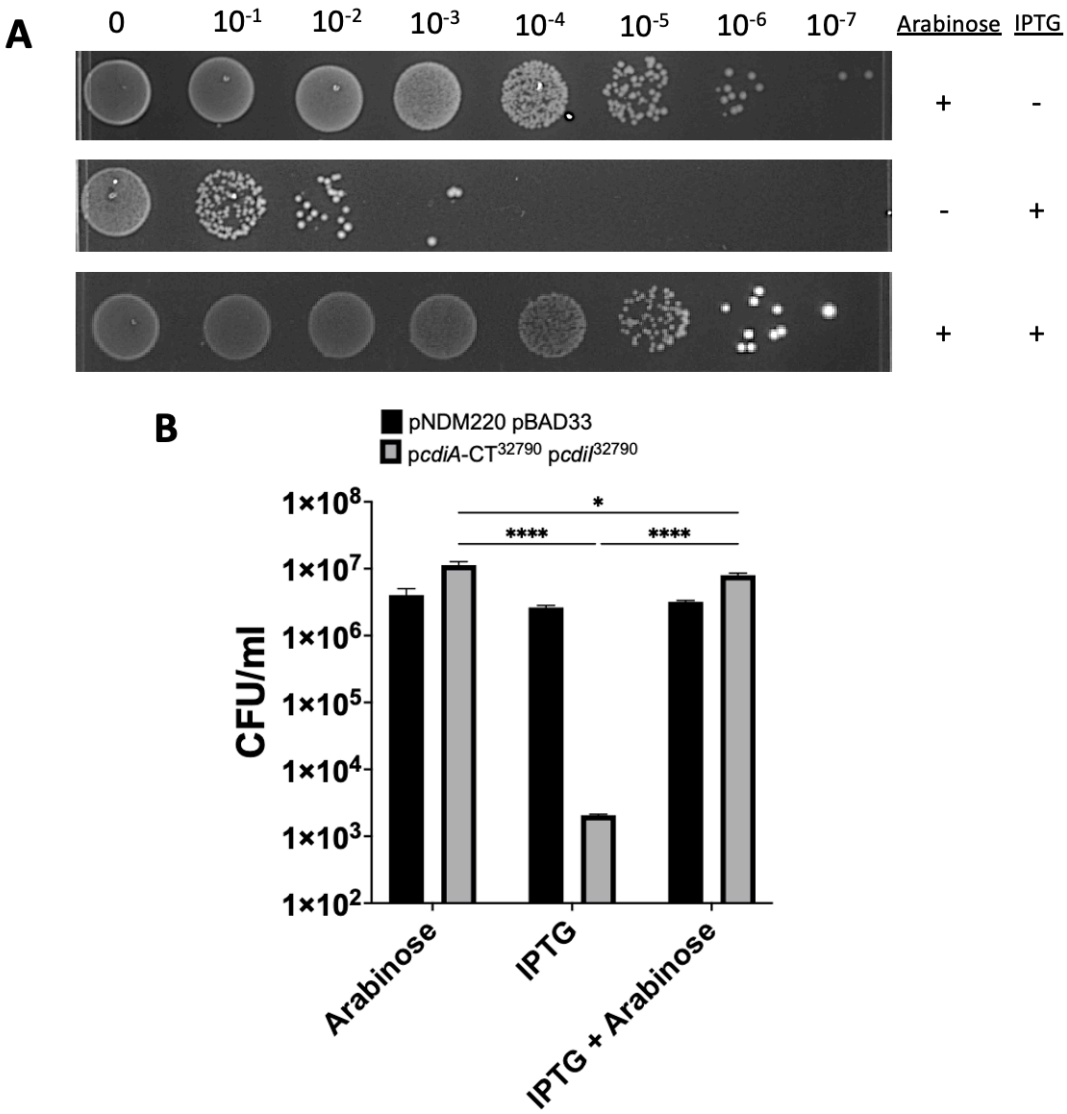


Figure 4.22: *cdiAI^{32790}* encodes a functional toxin-immunity pair which induces both bacterial intoxication and recovery when expressed in *E. coli* BL21. BL21 containing both p*cdiA*-CT^{32790} and p*cdiI*^{32790} was used to create a dilution series which was plated onto selective agars containing Amp50 and Cm30, with either no inducers or the addition of either IPTG to induce p*cdiA*-CT^{32790}, arabinose to induce p*cdiI*^{32790}, or both. Colony counts after overnight incubation determined toxin-immunity pair functionality. (A) Large reduction in survival is observed with CdiA^{32790} induction. Additional immunity induction recovers survival. (B) Quantification of A using CFU calculations confirms a 3.7- fold reduction in bacterial survival upon toxin induction. Reduction is completely ameliorated with additional immunity induction. A Two-Way ANOVA was performed on average CFU for each strain, statistically significant to ****P<0.0001. Post-hoc statistical significance of induced strains was compared using Tukey's test (n=3).

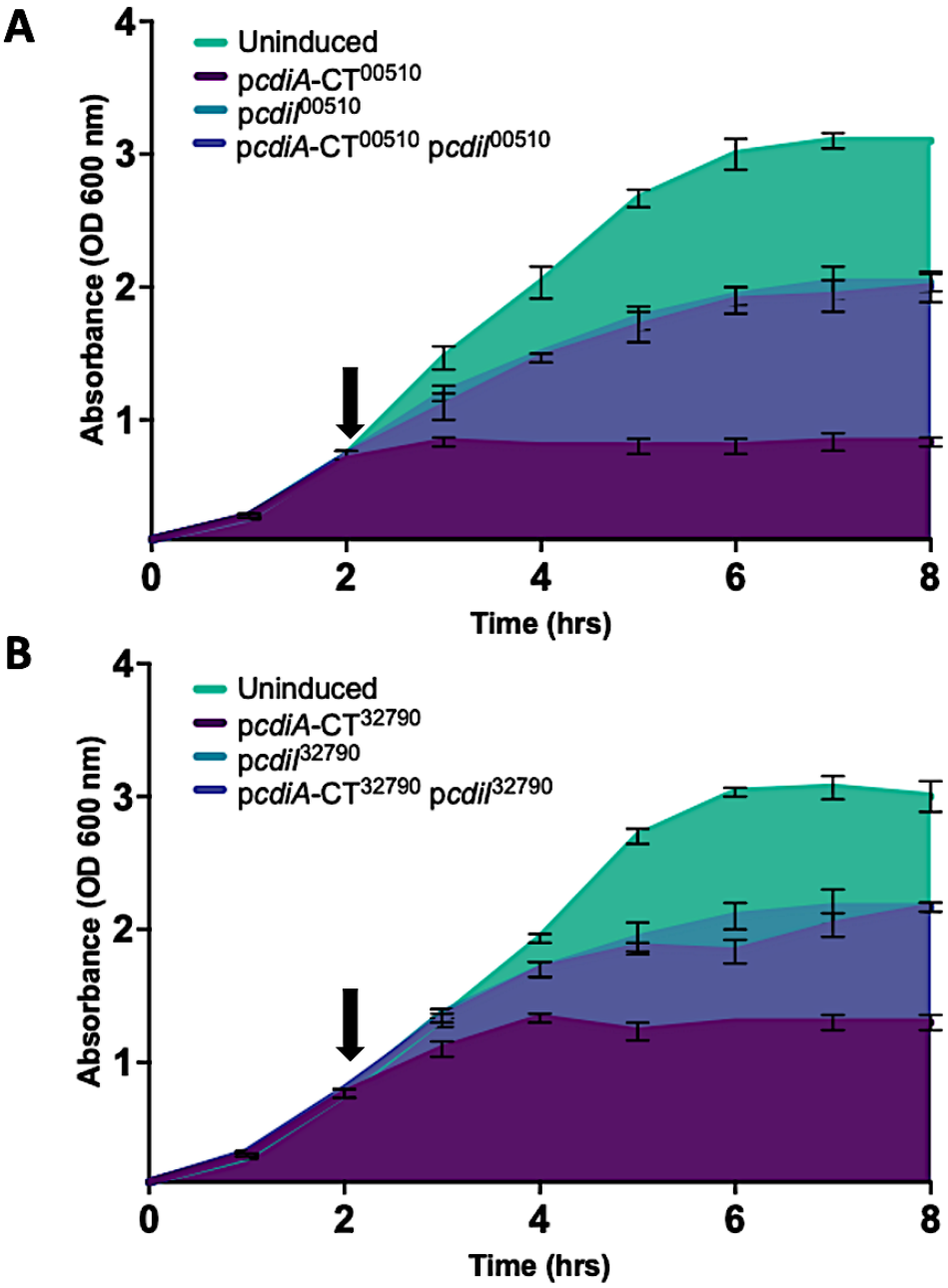


Figure 4.23: Liquid growth assays confirm CdiAI^{00510} and CdiAI^{32790} are functional toxin-immunity pairs. *E. coli* BL21 strains containing both p*cdiA*-CT and p*cdiI* expression vectors were used to determine the effect of toxin-immunity pair expression on growth rate. OD_{600} readings were taken at each hour. Black arrows indicated induction time point. (A) Immediate cessation in growth rate is observed upon induction of p*cdiA*-CT^{00510}. With additional induction of p*cdiI*^{00510}, survival is recovered to p*cdiI*^{00510} induced alone levels. (B) Reduction in growth rate is observed upon induction of p*cdiA*-CT^{32790} between hours 2 - 4. Cessation in growth rate is then observed from hour 4. With additional induction of p*cdiI*^{32790}, survival is recovered to p*cdiI*^{32790} induced alone levels.

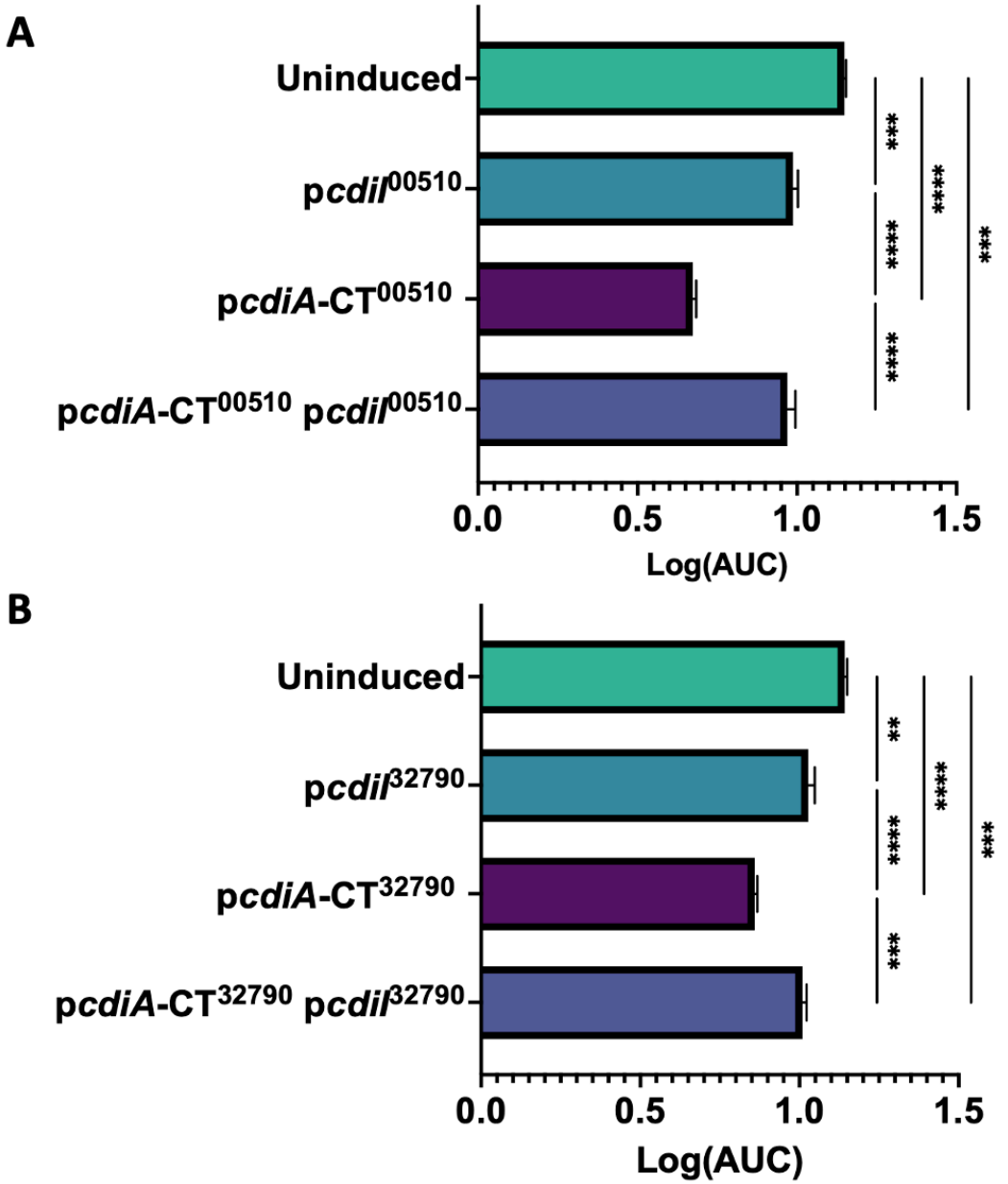


Figure 4.24: Area under the curve parameters calculated from toxin-immunity expression assay growth rates show significant reduction in area during toxin induction when expressed. From growth rate curves from Figure 4.23, Area Under the Curve (AUC) was calculated for each strain using PRISM9. Baseline was set at OD 0.1. (A) Significant decrease in AUC is observed upon induction of p*cdiA*-CT^{00510}. With additional induction of p*cdiI*^{00510}, AUC is recovered to p*cdiI*^{00510} induced alone levels. (B) Significant decrease in AUC is observed upon induction of p*cdiA*-CT^{32790}. With additional induction of p*cdiI*^{32790}, AUC is recovered to p*cdiI*^{32790} induced alone levels. A One-Way ANOVA was performed on AUC for each strain, statistically significant to ****P<0.0001. Post-hoc statistical significance of AUCs was compared using Tukey's test (n=3).

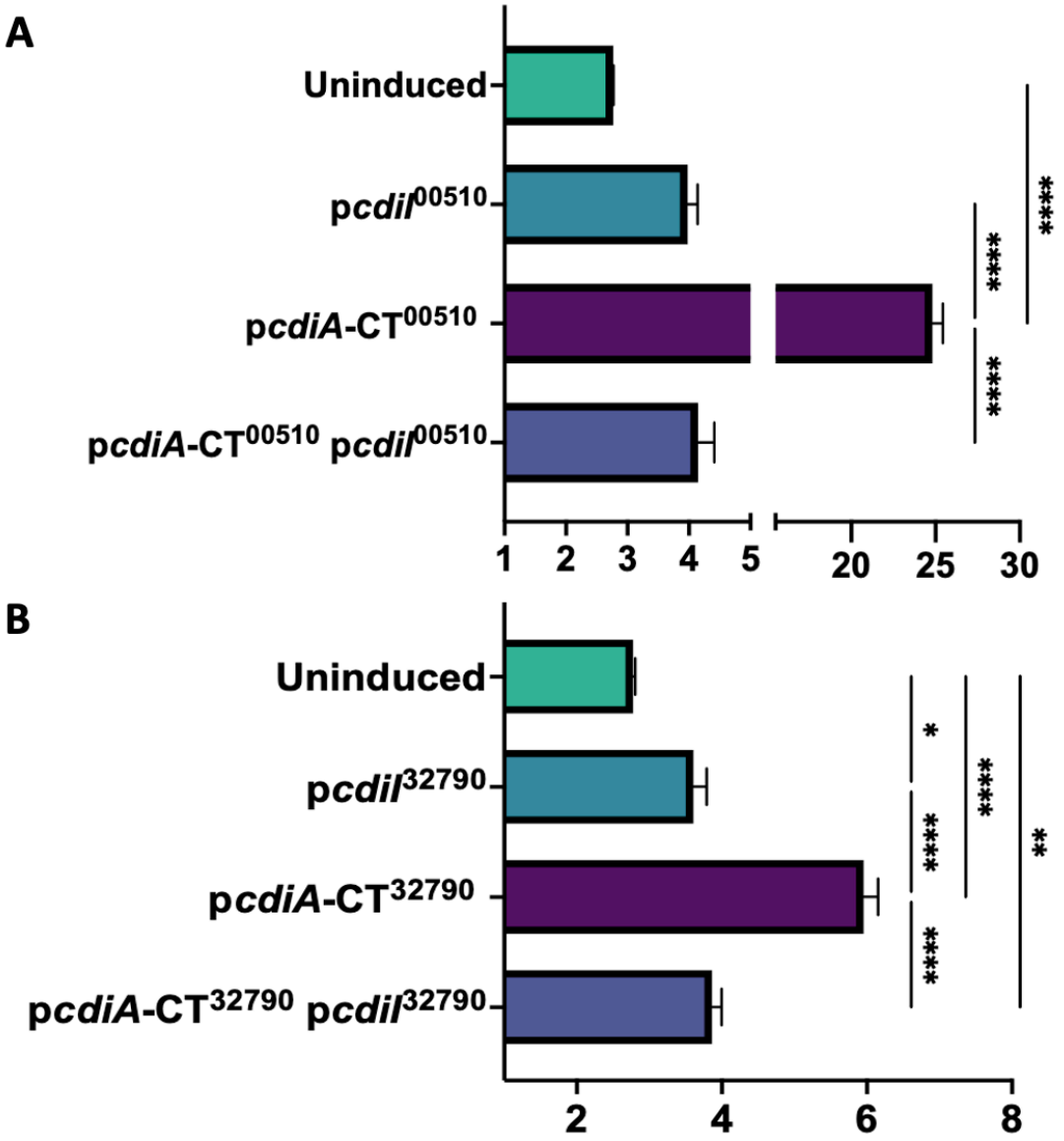


Figure 4.25: Doubling time calculated from toxin-immunity expression assay growth rates show significant increase during toxin induction when expressed. From growth rate curves from Figure 4.23, Doubling Time was calculated for each strain using PRISM9. Doubling time was determined using exponential growth phase 2-6 hrs post-induction. (A) Significant increase in Doubling Time is observed upon induction of p*cdiA*-CT^{00510} to 24.82 hrs. With additional induction of p*cdiI*^{00510}, Doubling Time is recovered to p*cdiI*^{00510} induced alone levels. (B) Significant increase in Doubling Time is observed upon induction of p*cdiA*-CT^{32790} to 5.95 hrs. With additional induction of p*cdiI*^{32790}, Doubling Time is recovered to p*cdiI*^{32790} induced alone levels. A One-Way ANOVA was performed on the Doubling Time for each strain, statistically significant to ****P<0.0001. Post-hoc statistical significance of AUCs was compared using Tukey's test (n=3).

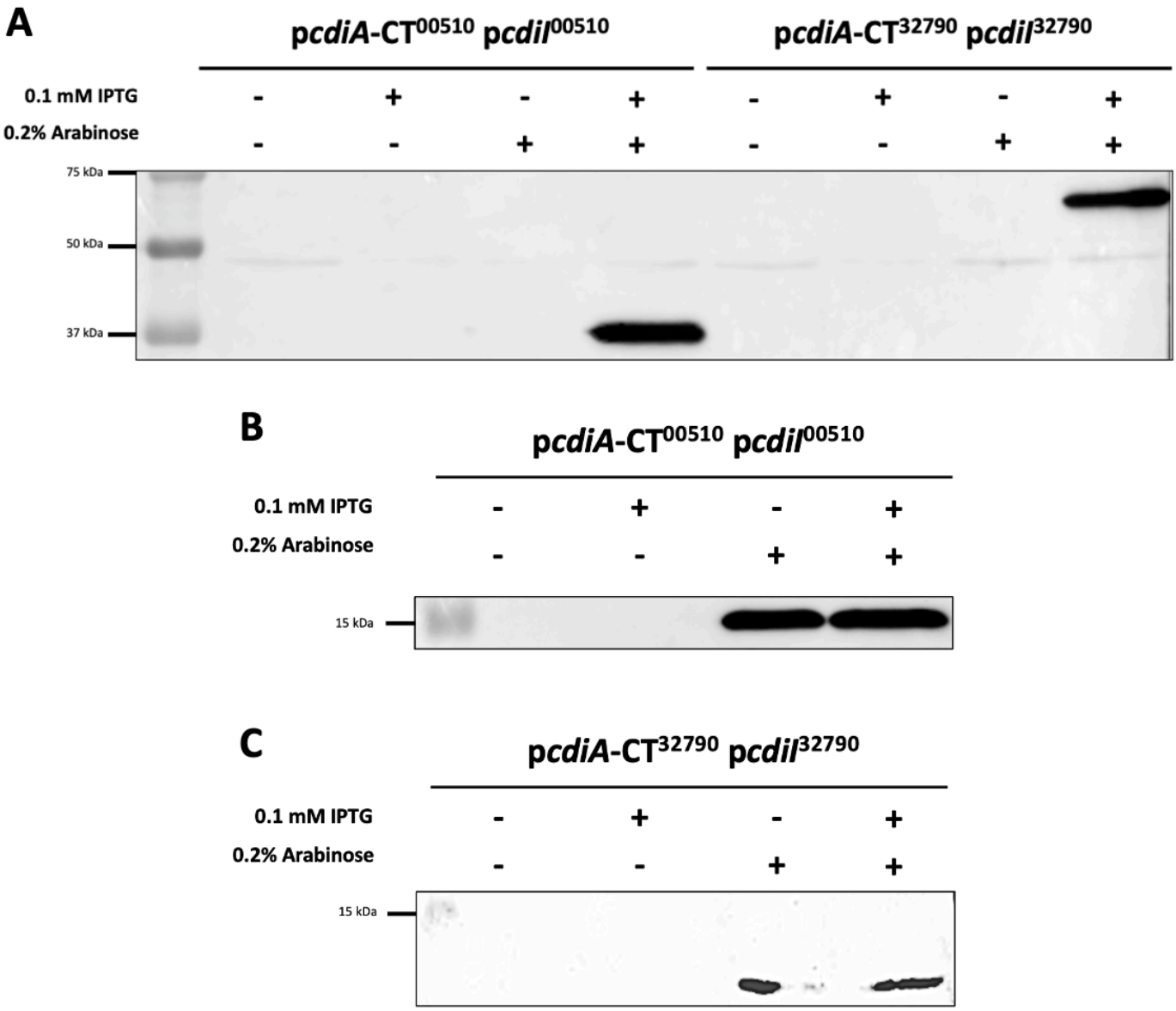


Figure 4.26: Western blot analysis confirms CDI toxin-immunity modules are expressed upon induction. Western blot analysis of paired flask growth samples taken 5 hrs post-induction and normalised to OD 1 showed expression of toxins (Flag tag) and immunities (StrepII tag) from both CDI systems CDI^{00510} and CdiI^{32790}. Uninduced sample was used as a control. Blots confirm both toxins and immunities are expressed but toxins are only detected in the presence of the immunity. Lack of toxin detection when expressed alone likely due to toxic nature and cessation of growth upon induction. Induction using IPTG and arabinose enables expression of cloned toxin and immunities, respectively. (A) CdiA-CT^{00510} size expected at 32.8 kDa and CdiA-CT^{32790} size expected at 69.1 kDa. (B) CdiI^{00510} size expected at 19.6 kDa. (C) CdiI^{32790} size expected at 14.6 kDa.

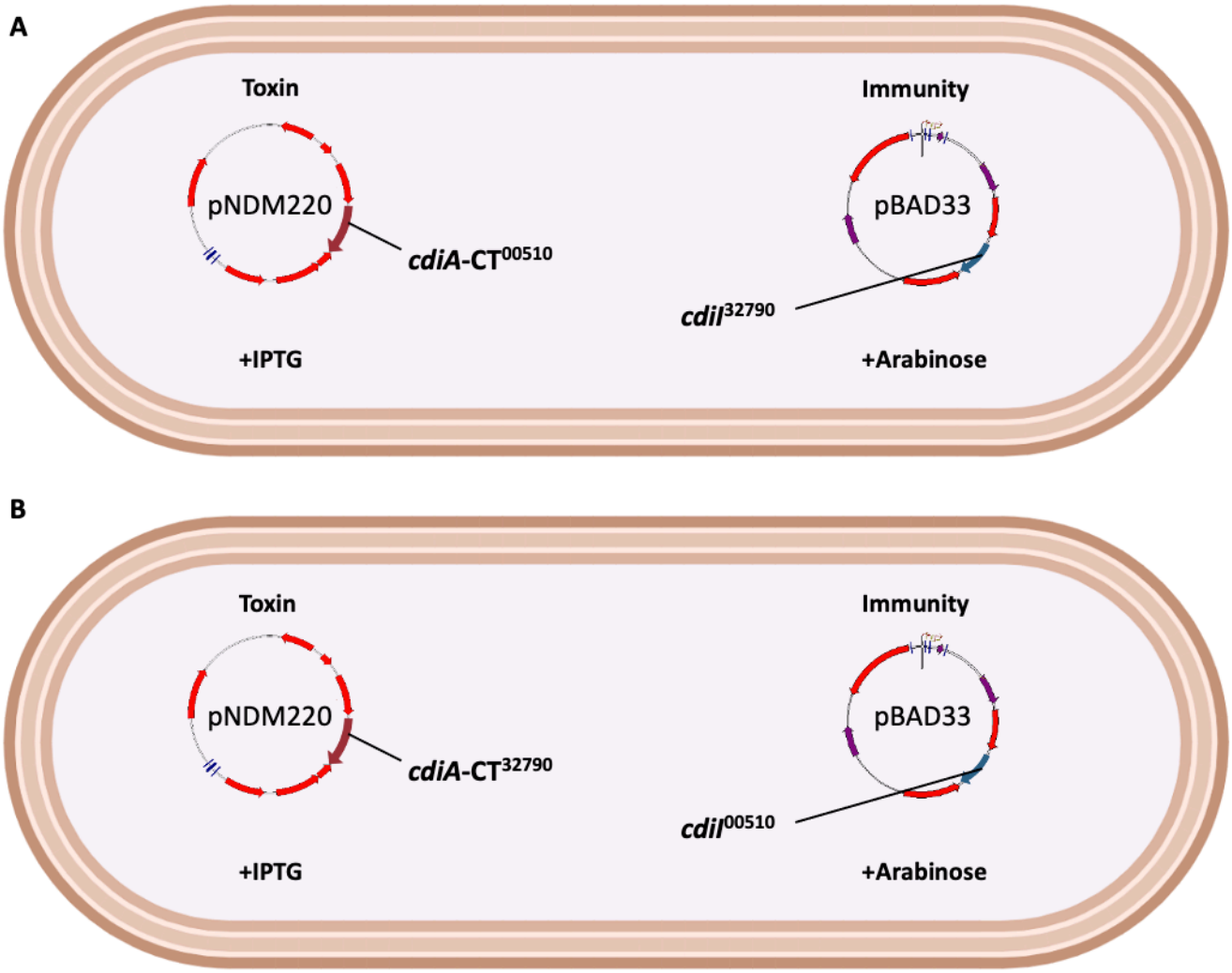


Figure 4.27: Model of BL21 strains with plasmids encoding the unmatched CdiA and CdiI pairs. (A) *E. coli* TOP10 strain contains cloned toxin from CDI^{00510} system and immunity from CDI^{32790} system. (B) *E. coli* TOP10 strain contains cloned toxin from CDI^{32790} system and immunity from CDI^{00510} system.

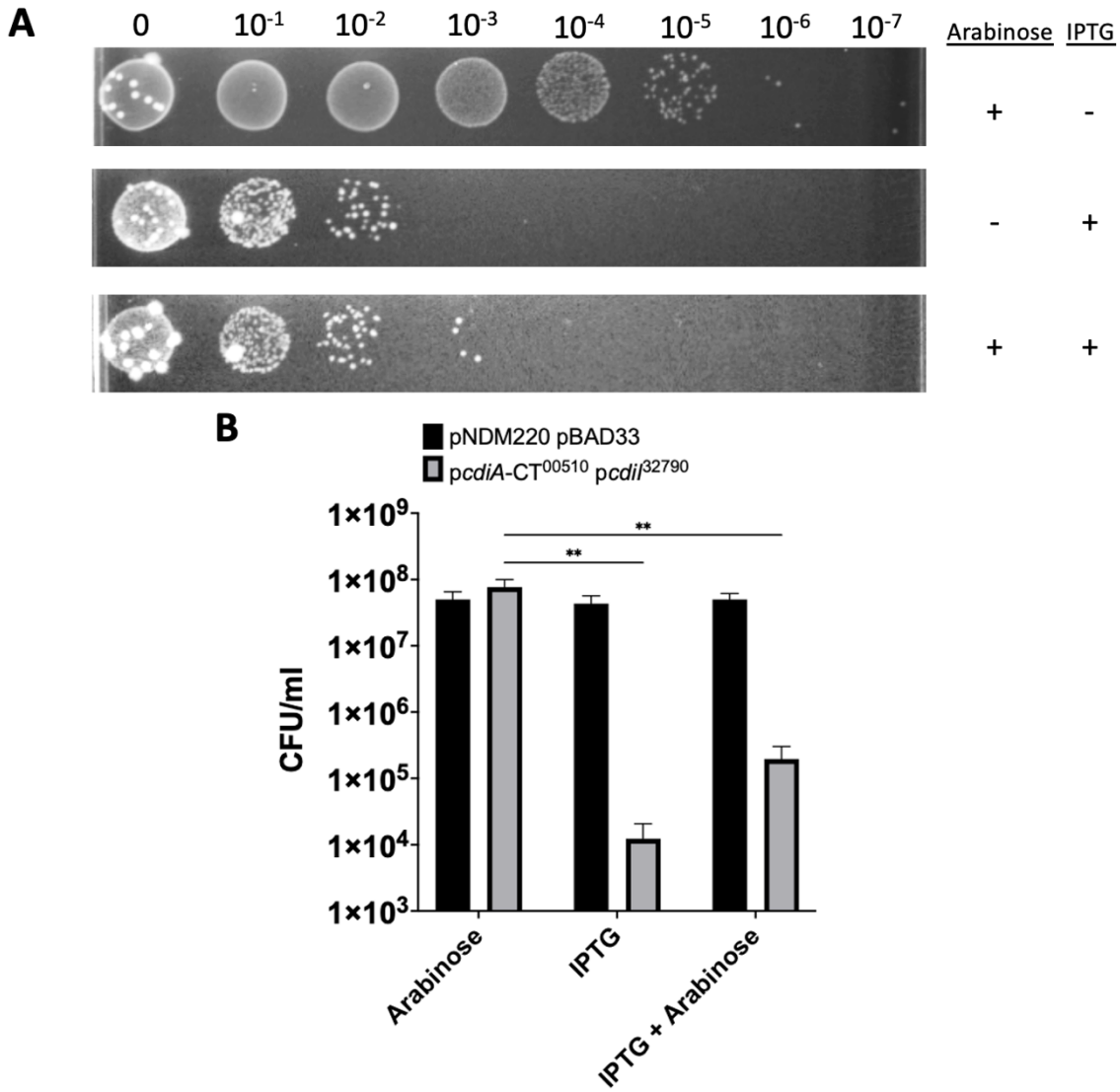


Figure 4.28: CdiI^{32790} does not recover from CdiA-CT^{00510} intoxication. BL21 containing both p*cdiA*-CT^{00510} and p*cdiI*^{00510} was used to create a dilution series which was plated onto selective agars containing Amp50 and Cm30, with either no inducers or the addition of either IPTG to induce p*cdiA*-CT^{00510}, arabinose to induce p*cdiI*^{00510}, or both. Colony counts after overnight incubation determined toxin-immunity pair functionality. (A) Large reduction in survival is observed with CdiA^{00510} induction. Additional immunity induction recovers survival. (B) Quantification of A using CFU calculations confirms a 5- fold reduction in bacterial survival upon toxin induction. Reduction is completely ameliorated with additional immunity induction. A Two-Way ANOVA was performed on average CFU for each strain, statistically significant to ****P<0.0001. Post-hoc statistical significance of induced strains was compared using Tukey's test (n=3).

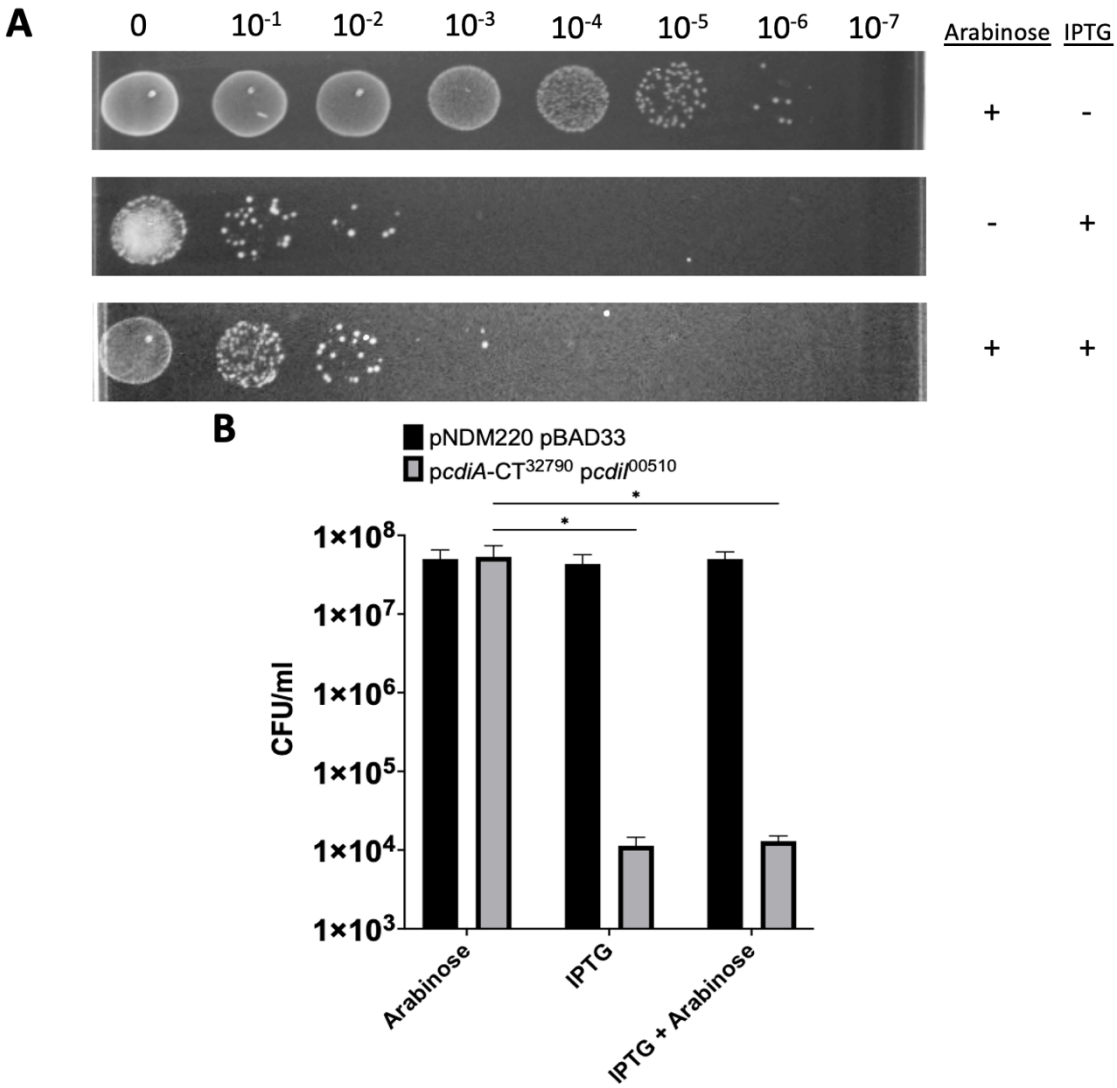


Figure 4.29: CdiI^{00510} does not recover from CdiA-CT^{32790} intoxication. BL21 containing both p*cdiA*-CT^{32790} and p*cdiI*^{32790} was used to create a dilution series which was plated onto selective agars containing Amp50 and Cm30, with either no inducers or the addition of either IPTG to induce p*cdiA*-CT^{32790}, arabinose to induce p*cdiI*^{32790}, or both. Colony counts after overnight incubation determined toxin-immunity pair functionality. (A) Large reduction in survival is observed with CdiA^{32790} induction. Additional immunity induction recovers survival. (B) Quantification of A using CFU calculations confirms a 3.7- fold reduction in bacterial survival upon toxin induction. Reduction is completely ameliorated with additional immunity induction. A Two-Way ANOVA was performed on average CFU for each strain, statistically significant to ****P<0.0001. Post-hoc statistical significance of induced strains was compared using Tukey's test (n=3).

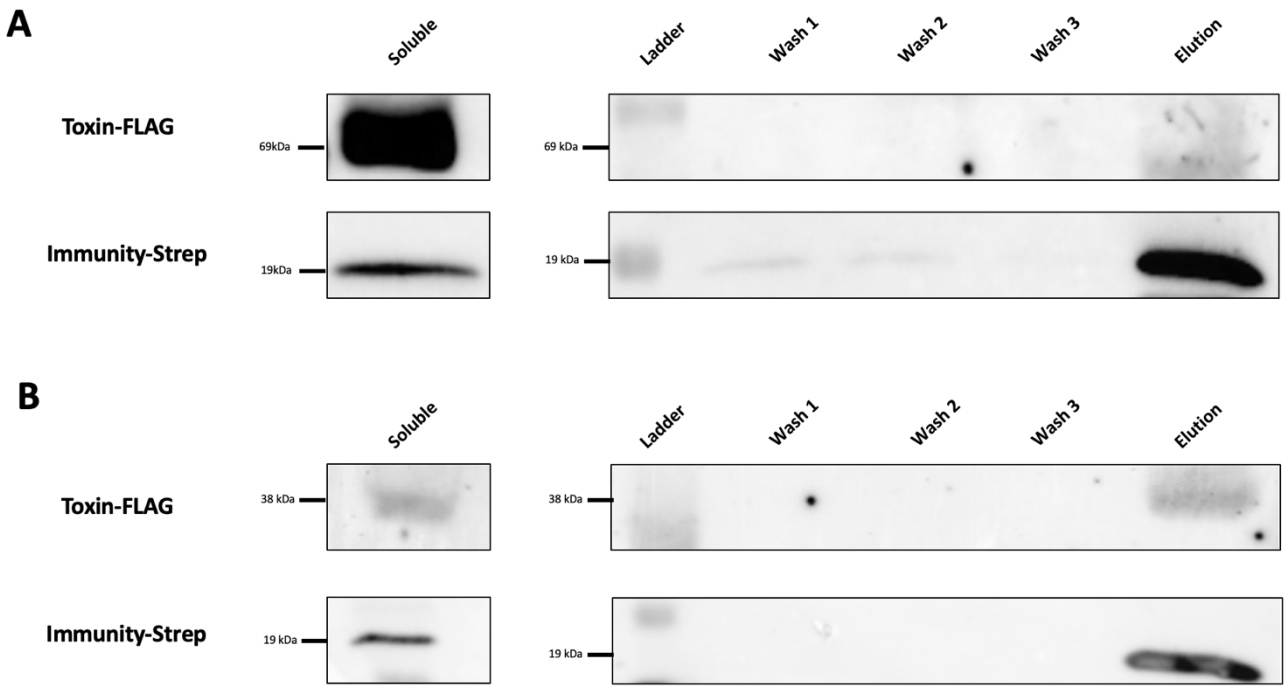


Figure 4.30: Protein pull-down confirms CDI toxin-immunity pairs interact via cognate binding. Western blot analysis of paired flask growth samples taken 5 hrs post-induction showed pull down of toxins (Flag tag) via immunities (StrepII tag) using Strep-Tactin resin from both CDI systems CDI^{00510} and CdiI^{32790}. Induction using IPTG and arabinose enables expression of cloned toxin and immunities, respectively. (A) CdiA-CT^{00510} size expected at 32.8 kDa and CdiI^{00510} expected at 19.6 kDa. (B) CdiA-CT^{32790} size expected at 69.1 kDa and CdiI^{32790} expected at 14.6 kDa.

4.4 Discussion

The activity of CDI systems has previously been described in *P. aeruginosa* and associated with toxins which kill or inhibit the growth of competing bacterial strains (Mercy *et al.*, 2016; Allen *et al.*, 2020). The results presented in Chapter 4 of this thesis outline production of WSDMs for two CDI systems identified in this thesis in *P. aeruginosa* PA14 in four strain backgrounds: PA14, *rsmA*, *rsmA*H123, and H123. I also outline construction of *E. coli* strains containing cloned toxins and immunities and confirm expression of both CDI system toxin and immunity proteins. Finally, I validated toxin-immunity pair functionality, ability to directly interact, and sought to confirm the putative tRNase functions (identified in Chapter 3). Elucidating the functionality of these toxin-immunity modules provides insight into their potential uses and evolutionary importance in enabling bacterial survival in hostile polymicrobial environments driving their high conservation in bacterial genomes.

4.4.1 Can rsmA be restored in PA14 rsmAH123 background?

In molecular biology, to evaluate the function and role of specific genes/systems of interest, it is important to use various genetic backgrounds. These backgrounds remove genes from the genome conferring confounding factors to enable a higher level of clarity when interpreting the results of various assays. Alternatively they remove known regulators for evaluating the interplay of the regulation with function (Gerlai, 2005). To evaluate whether RsmA also controls CDI in PA14, as seen in Mercy *et al.* 2016 in PAO1, I first used PA14 *rsmA*H123 from the Allsopp repository to successfully restore *rsmA* using pKNG101 to create the H123 background (Figure 4.2 and 4.3). This allowed commencement of the WSDM construction. As competition via the T6SSs in *P. aeruginosa* is well documented and to ensure the competitive effect observed in subsequent experiments was solely due to CDI systems, I

constructed my mutant panel in four backgrounds (PA14, *rsmA*, *rsmA*H123, and H123) (Figure 4.1). These four backgrounds would ensure that I was accounting for confounding factors i such as negative regulation via the removal of the post-transcriptional regulator *rsmA* (Goodman *et al.*, 2004), the T6SSs, and a combination of removing both factors. This would enable identification of potential interplay between post-transcriptional regulation and the utilisation of T6SSs during CDI activation. Mutant production in these backgrounds will enable study of the interplay of other genetic and phenotypic factors associated with bacterial competition in *P. aeruginosa* which could help elucidate whether these factors influence activation or repression of certain systems in the presence of a competitor, whether some systems have a more potent effect, are used under different conditions or alternatively against specific competitors. This would identify a potential regulation network for system interplay.

4.4.2 Can whole system deletion mutants of each CDI system in P. aeruginosa strain PA14 be engineered?

Deleting or inactivating the operons is a common method used in molecular biology to determine the role of a particular system in an observed phenotypic trait (Link, Phillips & Church, 1997). Deleting the entire operon of each system was required so the role of CDI in *P. aeruginosa* competition could be evaluated in subsequent competition experiments. CDI systems encode large genes, with operon regions in PA14 spanning ~12-18 kb which makes cloning difficult. Additionally, deletion of immunity genes is typically not possible when toxin encoding genes remain.

Here both systems in each strain background were successfully deleted via three partner conjugation and mutator fragment recombinant selection, including double system deletion mutants to create my strain panel (Figure 4.4 - 4.11). This is the first study to implement the deletion of the entire CDI operons in PA14 as previous studies have focussed on PAO1 or deleting individual toxins/immunities (Mercy *et al.*, 2016; Allen *et al.*, 2020). This did not affect strain fitness (Figure 4.12). These strains will enable study of the role CDI play in interbacterial competition to indicate whether these systems are actively used by the bacteria under lab conditions and therefore might be used in the CF lung environment as a competitive advantage. This would identify other potential virulence factors utilised by *P. aeruginosa* during dominance observed in CF patients outlined in the literature (Flight *et al.*, 2015).

4.4.3 Can the CDI toxins and immunities be cloned into expression vectors in E. coli?

E. coli strains which carry inducible vectors are used to enable controlled expression of particular genes of interest (Figure 4.20) (Deo *et al.*, 2022; Zhang *et al.*, 2022). This is a crucial tool in molecular biology to enhance our understanding of the role proteins from key genes play in virulence. For toxin-immunity modules, this enables experimental validation of genes identified as well as study the toxin's function and is a protocol previously used to study T6SSs effectors (Allsopp *et al.*, 2017). To study PA14 CDI toxin-immunity modules, constructing strains which possess toxins and immunities in separate expression vectors to individually control expression was required to confirm their toxicity. However, cloning toxins is inherently difficult due to their toxic nature, especially as CDI toxin functions target components of the central dogma e.g. DNA and RNA as well as pore-forming functions (Aoki *et al.*, 2010; Zhang *et al.*, 2012; Michalska *et al.*, 2018; Roussin *et al.*, 2019; Wang *et al.*, 2022). Construction of these strains were used to determine proteins expression, intoxication and

subsequent recovery from intoxication, their specificity, as well as their ability to directly interact for toxin neutralisation.

The toxin and immunity genes were successfully cloned into their respective expression vectors- pNDM220 and pBAD33 (Figure 4.13 - 4.19). However, difficulties were experienced during toxin cloning, where no colonies would grow post-transformation. This indicated the toxins have high lethality despite use of tight vectors with lower copy numbers. This supports the concept they encode putative tRNase functions, outlined in Chapter 3, which are highly effective toxins. Therefore, potentially leaky expression may have influenced cloning difficulty, and mirrors difficulties observed in the literature (Goeders & Van Melderen, 2014; Mercy *et al.*, 2016; Li, Hao & Xu, 2017). To overcome this, immunities were cloned into pBAD33 first. Once confirmed, I induced immunities to make competent cells for transformation of pNDM::toxin vectors to overcome any potential leaky expression leading to no cell survival post-transformation (Figure 4.20).

This enabled successful toxin transformation with no sequence errors. As toxins and immunities were under different promoters, pA1/O4/O3 promoter for pNDM220 (Lanzer & Bujard, 1988) driven by IPTG induction and PBAD for pBAD33 (Guzman *et al.*, 1995) driven by arabinose induction, these constructs were differentially expressed. Additionally, induction of both proteins in the same strain decreased the likelihood of confounding factors such as point mutations from possession of the toxin alone which could have off target effects in the encoding cell. Subsequent toxin transformation alone was also successful later. This shows pNDM*cdiA*-CT^{00510} and pNDM*cdiA*-CT^{32790} strains could be generated but where not necessary to confirm toxicity here.

4.4.4 Are the toxin-immunity modules from the CDI systems in P. aeruginosa strain PA14 functional and induce bacterial intoxication?

The use of inducible vectors to study toxicity and recovery of intoxication via expression of immunity proteins has been well documented within the CDI systems' literature (Aoki *et al.*, 2010; Wood *et al.*, 2019; Zhang *et al.*, 2022). Therefore isolating the toxins and immunities in differentially inducible vectors in *E. coli* is an important tool in validation and is a widely accepted strategy in the field (Willett *et al.*, 2015b; Berni *et al.*, 2019). Confirming expression of these proteins upon induction via western blot analysis would ensure the effects observed were due to toxin/immunity expression alone. However, confirming expression can be inherently difficult due to both toxin stability (Goeders & Van Melderen, 2014) and tRNase mechanism of action which shuts down translation and toxin production from stasis or cell death (Wang *et al.*, 2022). These problems are documented in the literature (Li, Hao & Xu, 2017). To confirm module functionality, plate and broth culture expression assays were used.

Both toxins and immunities were found to optimally express under 0.1 mM IPTG and 0.2% arabinose expression respectively, supporting the literature (Wood *et al.*, 2019). CFU assays exhibited clear intoxication for both toxins, showing 5-fold reduction in CFU for p*cdiA*-CT^{00510} (Figure 4.21) and 3.7-fold reduction for p*cdiA*-CT^{32790} (Figure 4.22). The 5-fold reduction in CFU for p*cdiA*-CT^{00510} was also observed during toxin induction from the homologous system in *P. aeruginosa* strain PAO1 in Mercy *et al.* 2016. Upon additional induction of their respective immunities, CFU for each toxin was recovered back to immunity induced alone levels. A Two-Way ANOVA determined changes in CFU for both toxin-immunity modules were statistically significant to ****P<0.0001. Tukey's post-hoc tests for both modules showed a significant decrease in CFU during toxin expression (****P<0.0001) and recovery to immunity

induced levels alone (****P<0.0001). There does appear to be a statistical difference between the immunity induced alone and the toxin-immunity module induced together (CDI^{00510} module ***P<0.001, CDI^{32790} module *P<0.05). This significant difference may be due to the energy expensive nature of this induction which may be enhanced when both proteins are expressed. This confirms $CdiAI^{00510}$ and $CdiAI^{32790}$ are functional.

System functionality was additionally assessed via growth rate assay. This was conducted using the same strains but in liquid culture with induction of expression initiated at 2 hr time point (Figure 4.23). A clear growth rate reduction was observed during immunity induction compared with uninduced strains. As immunity induction is constitutively switched on by the inducer, production might be energy expensive affecting bacterial fitness. Whilst titrating the inducer could reduce this issue, the 0.02% arabinose utilised was the best for expression from the optimisation step (0.00002% – 20% tested). A large reduction in growth rate was observed upon toxin induction alone. The toxin growth rates differ, where p*cdiA*-CT^{00510} immediately ceases growth, whilst p*cdiA*-CT^{32790} exhibits markedly slowed growth over 2 hours post-induction before growth cessation. As these toxins are putative tRNase, this would explain the growth cessation observed. However, the bacteriostatic vs bactericidal effect is unknown and would require further experimentation. This nuance may be attributed to functional differences, which would support Chapter 3 bioinformatics analysis outlining homology to tRNase with different defined functions associated with different bacteria (Allen *et al.*, 2020; Wang *et al.*, 2022). Alternatively, expression levels or intracellular target abundance could alter growth rate. Finally, induction of both toxin and immunity recovered growth rate to immunity induced alone, supporting the CFU assay.

To quantify differences in growth rates, AUC and doubling time were calculated as another measure of growth. AUC was calculated to quantify differences in growth rates, setting a baseline of OD 0.1 (correlating with initial OD). The data was transformed using Log to ensure Gaussian data would optimally fit the model (Figure 4.24) (Gaussian, 1809). A One-Way ANOVA determined a change in AUCs between the different induction conditions was significant to ****P<0.0001, agreeing with CFU significance observed. Tukey's post-hoc tests for both modules showed a significant decrease in AUC for toxin induction (****P<0.0001). AUC of immunity induction was significantly reduced compared with uninduced (CDI^{00510} module ***P<0.001, CDI^{32790} module **P<0.01). Unlike CFU, no difference in AUCs is observed in the immunity induced alone compared with the toxin-immunity module induced together. This test conflicts with significance observed in Figure 4.21 and Figure 4.22. Significance observed in the CFU counts may be due to data robustness which is more closely repeatable than a broth-based assay. In general, this supports CFU results and further confirms PA14 CDI toxin-immunity functionality.

Doubling time quantified changes in growth rate through OD measurement conversion to Log by data transformation (Figure 4.25). The exponential period was identified to occur between 2 and 6 hrs. Doubling time was calculated between these times, using Malthusian growth model (Weil & Wilde, 2014) and constraining Y0 (population starting point) to 0.7, the OD of the cultures at 2 hrs. Doubling time was averaged between repeats and doubling time of p*cdiA*-CT^{00510} and p*cdiA*-CT^{32790} indicated 24.82 hrs and 5.95 hrs, respectively (Figure 4.25). A One-Way ANOVA determined a change in doubling time between different inducers was statistically significant to ****P<0.0001, further agreeing with the CFU assays. Tukey's post-hoc tests for both modules showed a significant increase in doubling time for toxin induction

(****P<0.0001). Doubling time of immunity induction was significantly increased compared with uninduced for CDI^{00510} (*P<0.05). Additionally, doubling time of toxin-immunity module induced together was significantly increased compared with uninduced for CDI^{32790} module alone (**P<0.01). This could indicate expression of CDI^{32790} toxin-immunity module is more energy expensive, which could be attributed to increased toxin and immunity size compared to CDI^{00510}. As doubling time is inversely proportional to AUC, this supports the CFU and AUC analyses. A large difference in doubling time is observed between p*cdiA*-CT^{00510} and p*cdiA*-CT^{32790}. As p*cdiA*-CT^{00510} is over 24 hrs, this exhibits a more potent toxin, whilst p*cdiA*-CT^{32790} may be concentration dependent or exhibits a less potent toxin. This supports the Chapter 3 analyses indicating putative tRNase toxins act via disparate mechanisms. p*cdiA*-CT^{00510} showed 100% sequence homology to a trans-kingdom tRNase identified in Allen *et al*. in 2020 which could explain its potent nature here. Whereas p*cdiA*-CT^{32790} showed 62% sequence identity to a tRNase which interacts with specific tRNAs: $tRNA^{Gln}$, $tRNA^{Asn}$, $tRNA^{Trp}$ and $tRNA_f^{Met}$. This may support my argument for concentration dependency where tRNA cleavage requires a threshold before growth rate ceases. From these results, I can confirm the toxin-immunity modules of the two PA14 CDI systems are functional.

4.4.5 Are the toxin-immunity modules from the CDI systems in P. aeruginosa strain PA14 specific and interact via cognate binding?

As the toxin-immunity modules were found to be functional, expression of both toxins and immunities post-induction was evaluated via western blot analysis (Figure 4.26). This confirmed expression of the immunities, although expression of toxins alone was not apparent. As tRNase effectors shut down cellular translation, the lack of band visualisation could be due to stasis or cell death resulting in no toxin production and therefore no band. As

toxin expression was only observed upon subsequent immunity expression, this suggests the toxin is only visualised upon binding their cognate immunities which may be due to their tRNase function. This indicates these toxin-immunity modules may directly interact through cognate binding which supports current literature (Mercy *et al.*, 2016; Roussin *et al.*, 2019; Nolan *et al.*, 2021). However, this required further validation through a protein pull-down assay.

The next step was to determine whether immunities were specific in their ability to neutralise the toxin's effects or were interchangeable between systems encoded in the same bacterial strain (Figure 4.27). The CFU assay was repeated, using the same inducer concentrations. Again, clear intoxication was observed for both toxins, showing the same 5-fold and 3.7-fold reduction in CFU for p*cdiA*-CT^{00510}(Figure 4.28) and p*cdiA*-CT^{32790} (Figure 4.29), respectively. Induction of the opposite immunity did not recover CFU. A Two-Way ANOVA determined changes in CFU for both toxin-immunity modules were not statistically significant. Tukey's post-hoc tests for both modules showed a significant decrease in CFU during toxin expression (**P<0.01 p*cdiA*-CT^{00510}p*cdiI*^{32790}, *P<0.05 p*cdiA*-CT^{32790}p*cdiI*^{00510}) and toxin and opposite immunity expression (**P<0.01 p*cdiA*-CT^{00510}p*cdiI*^{32790}, *P<0.05 p*cdiA*-CT^{32790}p*cdiI*^{00510}) compared with immunity induced alone. Although increased CFU was observed in p*cdiA*-CT^{00510}p*cdiI*^{32790}, this was not significant. The inability to recover intoxication upon expression of the opposite immunity shows specificity in respect to the encoded immunity, supporting the current literature (Aoki *et al.*, 2010; Mercy *et al.*, 2016). This confirms both toxin-immunity modules from the two CDI systems are specific.

Finally, due to the confirmation these toxin-immunity modules are specific, and the indication they directly interact from previous western blot analyses conducted here, direct interaction

was evaluated. It is well documented in the literature that cognate immunities directly interact with their respective toxins (Ruhe, Low & Hayes, 2020). This was evaluated via a protein pull-down assay using Strep-Tactin® Sepharose® resin to bind immunities to the column and western blot analysis to confirm co-purification of the Flag tagged toxins (Figure 4.30). This confirmed both toxins directly interact with immunities via cognate binding. Due to difficulties experienced when cloning toxins alone, only strains with both toxin and immunity present could be used and therefore a protein pull-down was utilised instead of co-immunoprecipitation. This supports the literature and previous studies on PAO1 CDI toxin-immunity modules (Mercy *et al.*, 2016; Allen & Hauser, 2019; Nolan *et al.*, 2021).

When studying competitive systems identifying toxin functions infers their role in bacterial survival, competition, and evolutionary importance to deduce why these systems are highly conserved and encode certain toxin functions. Due to time constraints of the project, this was not validated here. Work towards toxin function validation was conducted in tandem with CFU assays (Figures 4.21 and 4.22). Colonies which survived toxin induction alone were collected. Three fresh transformants of both $CdiAI^{00510}$ and $CdiAI^{32790}$, alongside four transformants of $CdiA\text{-}CT^{00510}$ and $CdiA\text{-}CT^{32790}$ were also grown on IPTG agar plates. All 16 colonies chosen (two from each transformation) have been sent for sequencing to identify mutations enabling their growth- whether in the toxin's gene itself or downstream but have not been received by the end of this project. However, this will go towards publication. Validating the putative functions identified in Chapter 3 would help outline their functions in *P. aeruginosa* infection in CF. As the toxins identified to be involved in CDS observed in *Burkholderia* were shown to encode a tRNase function, this indicates these systems may also be used in interbacterial cooperation (Garcia *et al.*, 2016a).

4.5 Conclusions

The main conclusions associated with the CDI mutant strain construction, toxin-immunity module cloning, and validation are as follows:

1. Deletion of each CDI system does not negatively impact the fitness
2. Toxin-immunity modules of both CDI^{00510} and CDI^{32790} can be cloned into expression vectors and can produce toxin and immunity proteins upon induction.
3. $CdiAI^{00510}$ and $CdiAI^{32790}$ are functional, where toxins induce bacterial death and immunities recover bacteria from this intoxication.
4. $CdiAI^{00510}$ and $CdiAI^{32790}$ are specific as recovery from intoxication can only occur when the encoded immunity pair is expressed.

Therefore, these results presented in Chapter 4 validate the *in silico* characterisation of the two CDI systems in *P. aeruginosa* strain PA14, the functionality of their toxin-immunity modules and confirms the specificity of the two encoded immunities. The differences in effector toxicity between the two systems encoded within the same strain and lack of cross reaction with the alternative immunity shows that these systems could have different roles when engaging in interbacterial competition/cooperation.

So, the final step was to consider whether these results supported or refuted the hypotheses proposed at the beginning of this chapter.

Hypothesis 1: The operons identified in Chapter 3 of this thesis encode functional CDI systems. **This was accepted.**

Hypothesis 2: The removal of each system operon has no effect on bacterial fitness. **This was accepted.**

Hypothesis 3: Both CDI systems in *P. aeruginosa* strain PA14 encode functional toxin-immunity modules. **This was accepted.**

Hypothesis 4: The CdiA-CT^{00510} and CdiA-CT^{PA14_32790} are tRNase encoding effectors. **To be determined. Strains which survived intoxication have been sent for sequencing. Once assembled, mutations observed whether in the toxin gene itself or throughout the genome will indicate targets of this toxin.**

The ability to delete the two CDI systems identified in Chapter 3 from the genome as well as confirming the activity of the toxin-immunity modules will enable results conducted throughout the rest of the of this thesis to be synonymous to active utilisation of these putative systems in *P. aeruginosa* which are yet to be validated *in vitro*. This is a prerequisite for conducting phenotypic assays determining the role of CDI in cooperative and competitive mechanisms associated with bacterial behaviour and infection pathogenesis.

5. Generation of CDI specific polyclonal mouse antibodies via the production of recombinant proteins from conserved regions of the CdiA extracellular toxin-passenger domain

5.1 Introduction

Since the discovery of the T5SS in *N. gonorrhoea* in 1984 (Halter, Pohlner & Meyer, 1984), they have been shown to play a role in pathogenesis for multiple bacterial species such as *E. coli* (Aoki *et al.*, 2010) and more recently *P. aeruginosa* (Wilhelm *et al.*, 2007). To date, six subtypes of T5SS have been outlined in the literature, a-f, which are structurally and functionally different and are utilised by the bacteria for different physiological functions (Meuskens *et al.*, 2019). The high conservation of T5SSs, equating to 62% of diderm bacteria (Abby *et al.*, 2016), and classification as a virulence determinant indicates their importance in both infection and general survival regardless of their ecological niche (Allen *et al.*, 2020).

After the identification of the subset of T5bSS involved in interbacterial competition called the CDI by Aoki *et al.* in 2005 and the rise in use of genomics and metagenomic studies in the field of bacteriology, many bacterial species have been identified to encode putative CDI systems. These systems maintain high sequence homology in the *cdiB* and the 5' end of *cdiA* genes, before increasing in variability towards 3' end of the gene (Gentle, Burri & Lithgow, 2005; Aoki *et al.*, 2008; Allen *et al.*, 2020). This indicates that conserved portions of CdiA could be exploited to understand the presence and activation status of competitive systems in clinical strains. As CDI systems have been shown to have a role in interbacterial competition

in both *in vitro* and *in vivo* studies (Mercy *et al.*, 2016; Melvin *et al.*, 2017; Allen *et al.*, 2020), as well as being highly prevalent in clinical *P. aeruginosa* strains (Allen & Hauser, 2019), outlining their presence and activity in clinical isolates could be useful to expand our understanding of the role of these systems in bacterial strains. We currently do not know if these systems are expressed and active during human infection. If these systems are highly active in clinical strains, this would support the concept that CDI systems play a role in pathogen dominance during infection and survival of virulent strains during colonisation.

To date, most research conducted on studying these systems experimentally has been based largely on the laboratory strain *P. aeruginosa* PAO1 which has shown that pathogenesis is influenced by the presence of CDI (Mercy *et al.*, 2016; Melvin *et al.*, 2017). These studies show that PAO1 can express its two CDI systems which are involved in interstrain competition under laboratory conditions. Work published in by Allen *et al.* in 2019 and 2020 demonstrated that CDI may be clinically relevant due to their frequency in virulent clinical isolates from blood samples which were shown to play a role in acute mouse infection models. However, the activity and likelihood that these systems play a role in clinical CF *P. aeruginosa* isolates has not been validated experimentally or indirectly from patient samples.

As pathogenesis of *P. aeruginosa* in the CF lung is multifactorial and can be strain specific, I sought to determine if these systems are active in clinical strains associated with CF as a first step in validating their role in *P. aeruginosa* infection. However, currently no tools are available to enable easy detection of these systems experimentally. Many potential methods are exploited by molecular biologists to study the expression of systems in living cells such as protein tags and antibodies (Costa *et al.*, 2014; Allsopp *et al.*, 2017). Developing an easy-to-

use CDI detection method would expand our understanding of the mechanisms utilised by *P. aeruginosa* to dominate the lung and mediate *P. aeruginosa* strain succession or contribute to a decline in diversity of the polymicrobial community which may provide potential future targets for treatments of *P. aeruginosa* infection.

5.2 Aims of this study

From the current literature and based on the *in silico* results outlined in Chapter 3 of this thesis, I have one major hypothesis to address in this chapter:

Both CDI^{00510} and CDI^{32790} are expressed under laboratory conditions and in clinical isolates of *P. aeruginosa*

This chapter summarises research conducted to addressing this hypothesis through the following aims:

1. Cloning conserved CdiA-NT regions identified in Chapter 3 of this thesis
2. Constructing inducible vectors containing the coding regions for expression induction of recombinant proteins
3. Purification of these recombinant proteins via on-column resin gravity purification
4. Sending recombinant proteins to Eurogentec for production of rabbit polyclonal antibodies
5. Validating antibody efficacy in CDI detection via western-blot analysis of PA14 laboratory strains and generated CDI system mutants
6. Screening polyclonal antibodies to determine the expression of CDI systems in clinical isolates from the Personalised Approach to *P. aeruginosa* (PAPA) strain repository

5.3 Results

5.3.1 Cloning conserved CdiA-NT regions enables generation of inducible recombinant protein vectors

A major, widely accepted method of protein detection in bacterial samples is using polyclonal antibodies. Previous research by Allsopp *et al.* in 2017 has shown system specific antibodies are effective in detecting expression of another contact-dependent competition system, the T6SS, in *P. aeruginosa* or indeed the expression of other T5SS secretion systems in pathogenic strains of *E. coli* (Allsopp *et al.*, 2010, 2012). However, no tools currently exist to detect CDI *in vitro* in *P. aeruginosa.* Therefore, producing antibodies against the CDI systems would enable easy identification in laboratory and clinical strains. As the CdiA-NT sits ~33 nm extracellularly from the cell membrane and is a large protein, it provides an ideal antigenic target to exploit (Ruhe *et al.*, 2018).

In Chapter 3.3.5, three conserved regions in the extracellular N-terminal passenger domains were identified. One specific to each of the two CdiA homologous systems and one present in both CdiA proteins but not in other T5bSS or TPS proteins. The DNA encoding these regions was used to design primers to clone these conserved regions into pET29a (Figure 5.1). This process was used to create three strains, each containing one of the pET29a vectors encoding one of the conserved regions (Figure 5.2). Initially primers were designed to enable amplification of these regions where each reverse primer was designed with a tail encoding a Strep-II tag for recombinant protein purification (Figure 5.3). First, amplification of the conserved regions from genomic DNA (Figure 5.4) was followed by ligation into pCR Blunt II-

TOPO and transformation into competent *E. coli* TOP10 cells before confirmation of successful inserts via PCR (Figure 5.5) and subsequent validation via Sanger sequencing (Figure 5.6). For ST1, the conserved sequence was digested out of pCR Blunt II- TOPO, ligated into pET29a (Figure 5.7) and confirmed via Sanger sequencing (Figure 5.8). This method was not successful for the General and ST2 conserved sequences. To overcome this, ThermoFisher GeneArt was used to construct these regions synthetically in pMA-RQ and pMK-RQ, respectively (Figure 5.9). Upon receiving these constructs, the General and ST2 regions were digested out of pMK-RQ, ligated into pET29a (Figure 5.10) and confirmed via sequencing (Figure 5.11).

After confirming successful construction, the next step was to validate the expression of these recombinant proteins. IPTG inducer was added after two hours of growth and strains were grown for a further five hours before SDS samples were taken. Expression was evaluated via western blot analysis, which was successful for all three proteins (Figure 5.12). After confirming recombinant protein expression, the next goal was to purify each protein to serve as antigen doses for injection into rabbits commercially by Eurogentec.

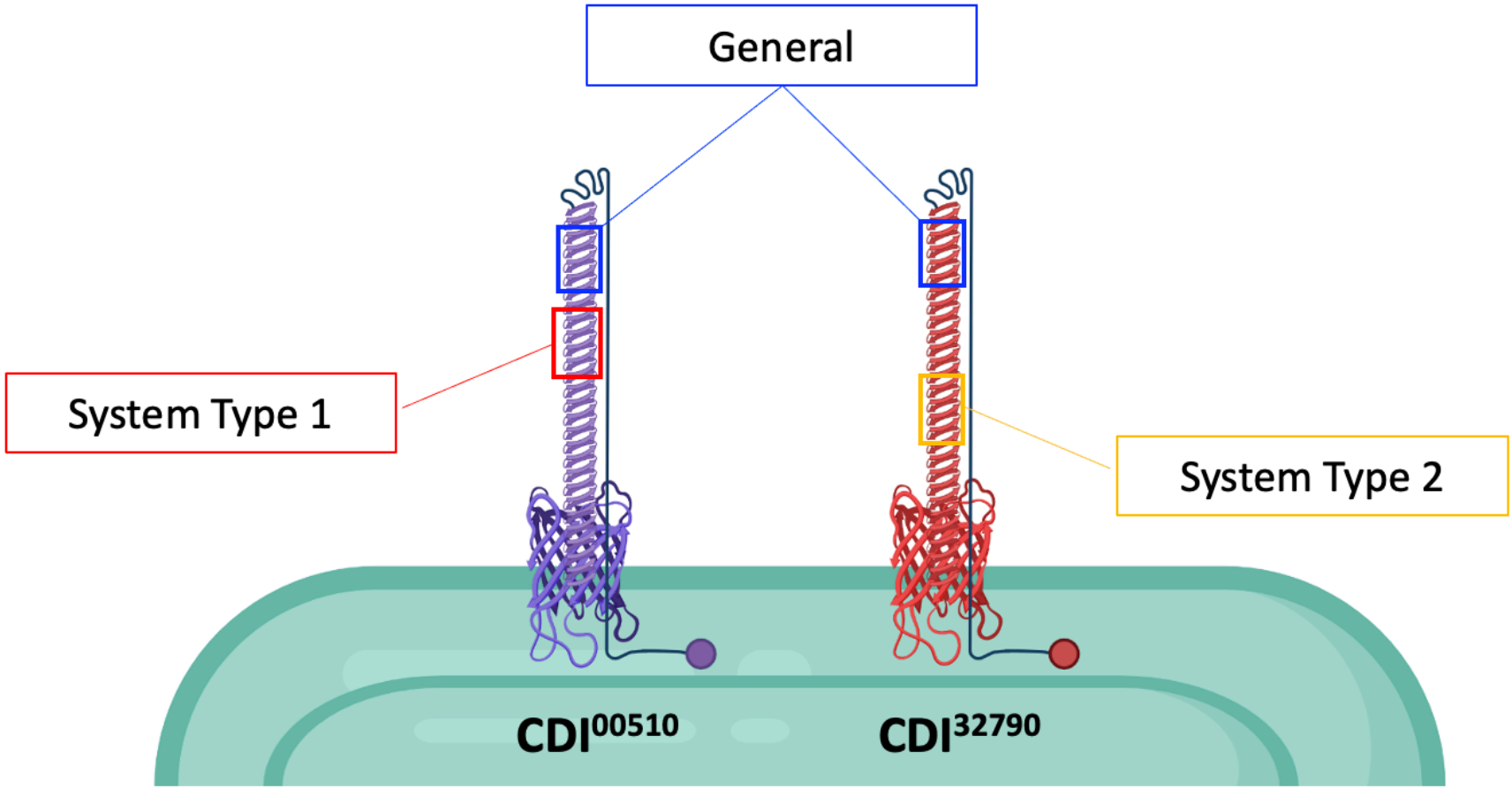


Figure 5.1: Conserved extracellular CdiA-NT regions from *P. aeruginosa* CDI systems. Conserved CdiA-NT regions from CdiA^{00510} and CdiA^{32790} were identified in 3.3.5 of this thesis. Illustration of the three conserved N-terminal regions is highlighted here. The DNA encoding these regions was cloned for subsequent production of recombinant proteins. Recombinant proteins were sent to Eurogentec for antibody production in rabbits.

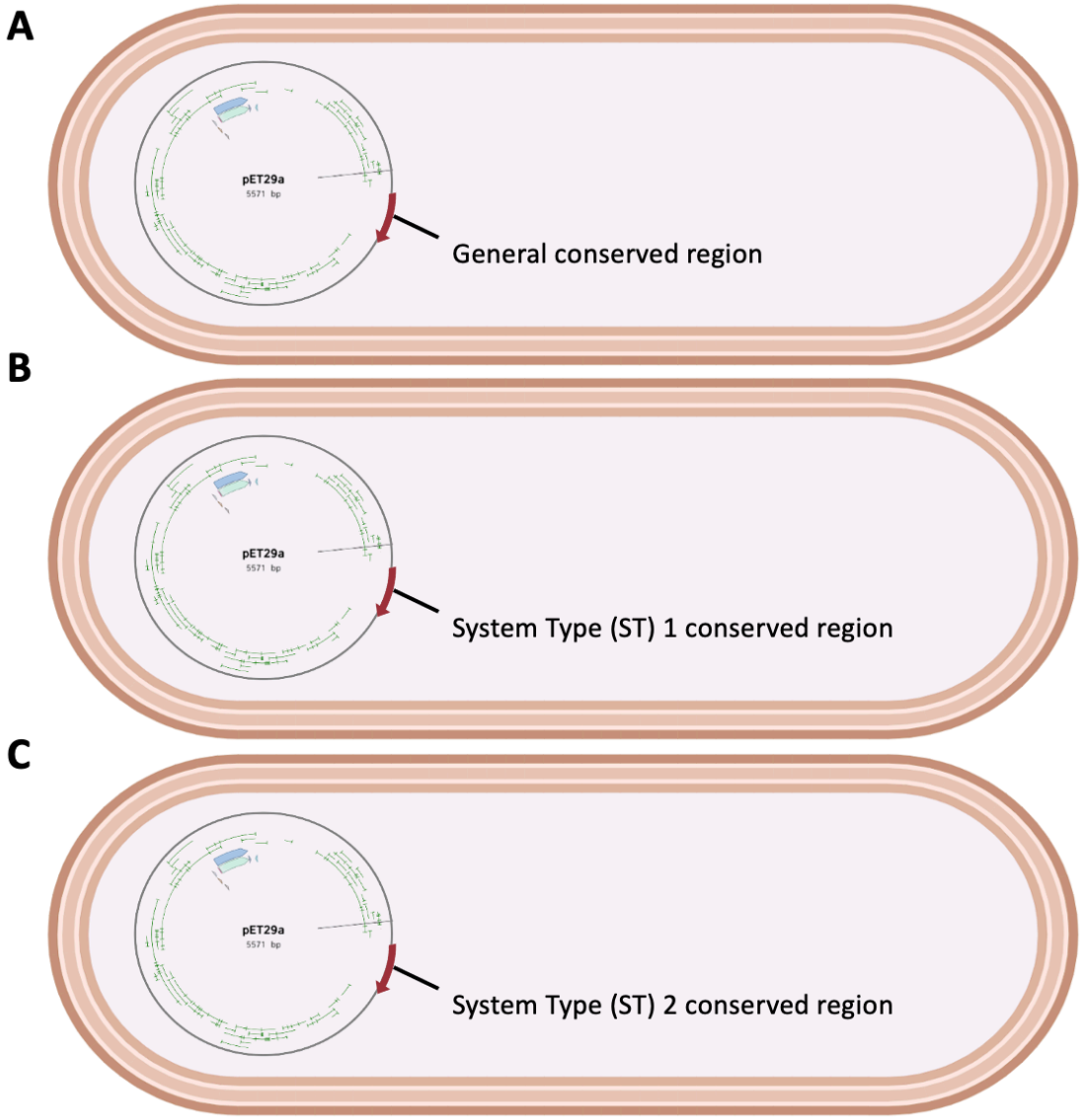


Figure 5.2: Model of *Escherichia coli* BL21 strains with cloned conserved *cdiA* regions from *P. aeruginosa* strain PA14 CDI systems. *E. coli* strains containing the conserved regions cloned into expression vector pET29a were required in order to express the recombinant proteins *in vitro* for purification. (A) General CDI conserved region, (B) System Type 1 (PA14_00510) CDI conserved region, (C) System Type 2 (PA14_32790) CDI conserved region.

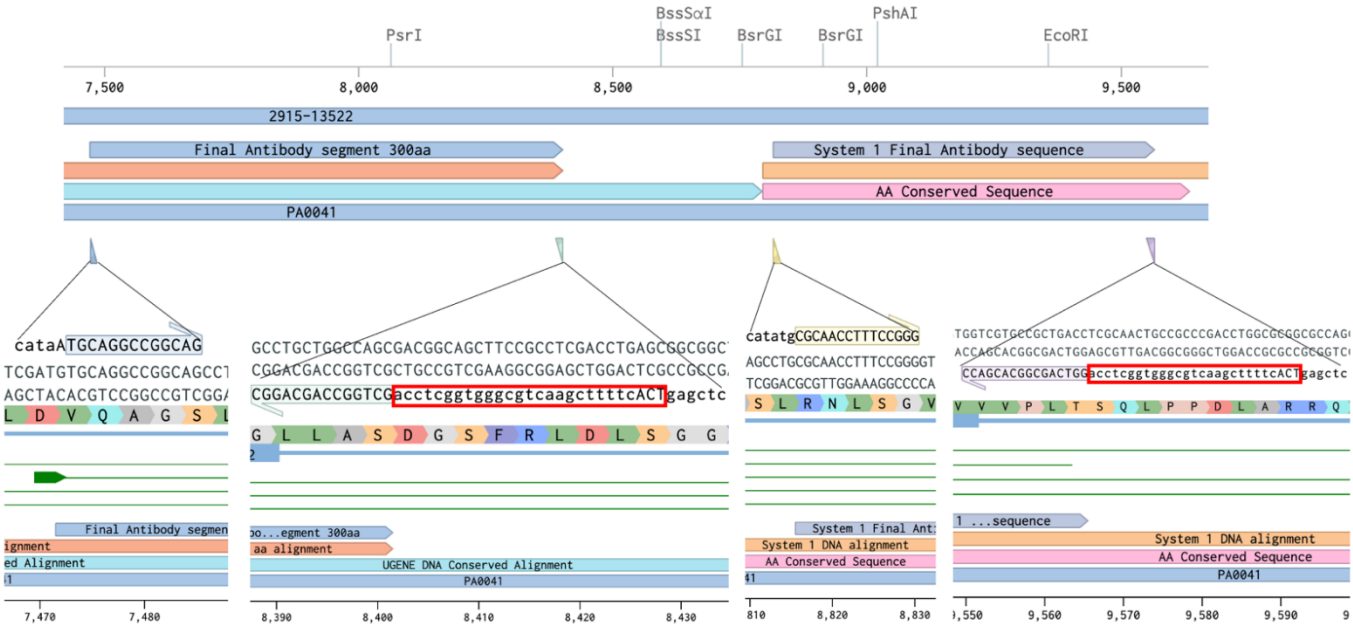


Figure 5.3: Primers for amplification of PA14 CDI General and System Type 1 conserved regions. Primers were designed to amplify the DNA encoding three regions identified. The above primers represent those designed for amplification of the General and System Type 1 conserved regions. Reverse primers were designed to encode a Strep-II tag, indicated by the red boxes, to be used in subsequent recombinant protein purification experiments.

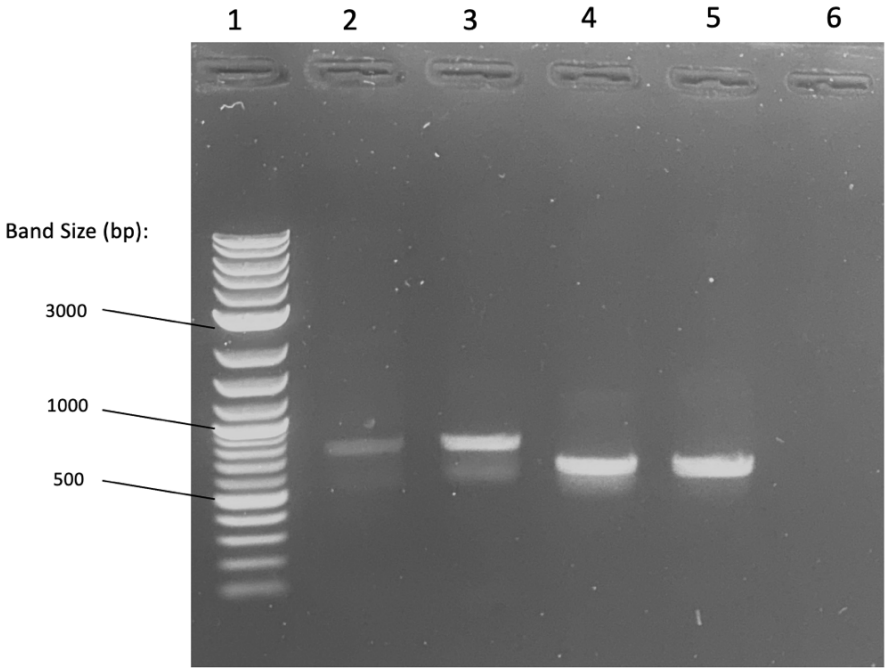


Figure 5.4: PCR of CDI System Type 1 and System Type 2 amplified DNA fragments. Amplified fragments were produced via PCR in order to clone these conserved regions into inducible vectors for subsequent expression and purification of recombinant proteins. Lanes 2-3 indicate successful amplification of System Type 1 conserved region. Lanes 4-5 indicate successful amplification of System Type 2 conserved region. Lane 6 indicates negative water control. Two amplifications of each system type were used due to difficulties in cloning, requiring different annealing temperatures: 45 °C for System Type 1 and 55 °C for System Type 2.

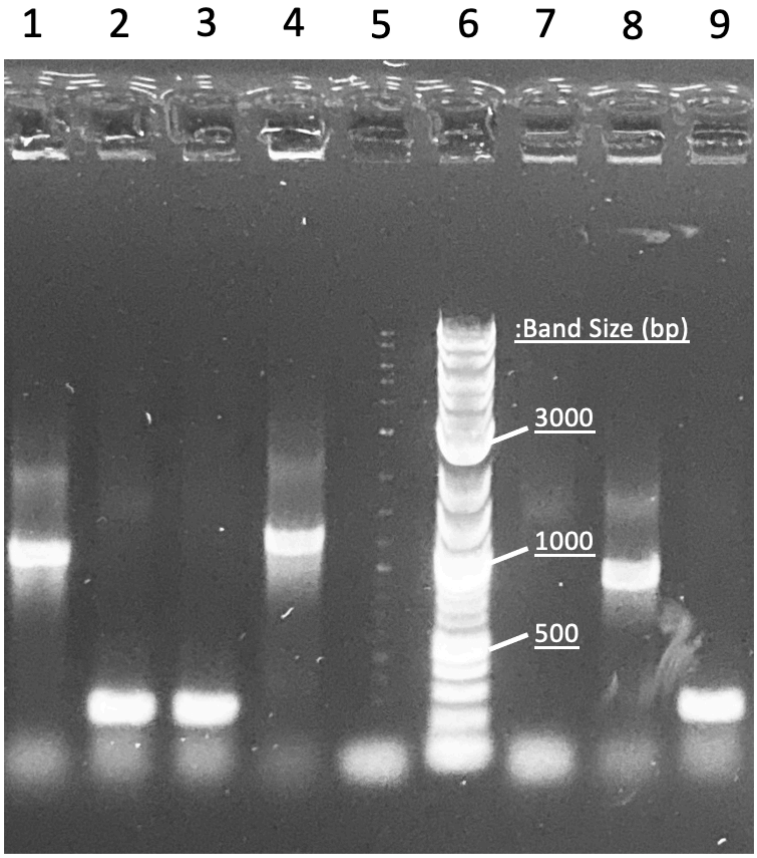


Figure 5.5: PCR confirms successful insertion System Type 1 and System Type 2 DNA fragments into high efficacy intermediary vector pCRBlunt II-TOPO. Colony PCR to determine successful insertion of the cloned regions into the high efficacy vector pCRBlunt II-TOPO. Lanes 1-3 indicate insertions of System Type 1 conserved region. Successful insertion is shown in lane 1. Lanes 7-9 indicate insertions of System Type 2 conserved region. Successful insertion is shown in lane 8. Lane 4 indicates positive control. Lane 5 indicates negative water control.



Figure 5.6: Sequencing alignment confirming successful construction of pCR Blunt II-TOPO-System Type 1. Plasmids from positive isolates in Figure 5.5 where miniprepped and sent for sequencing to confirm error free amplification and successful insertion into pCR Blunt II-TOPO. An alignment of the sequence results was created comparing it to the *in silico* designed strategy. Note: clean sharp chromatogram peaks indicate high quality sequence output. Grey colour of bars represents sequence alignments and indicates exact sequence homology to the template.

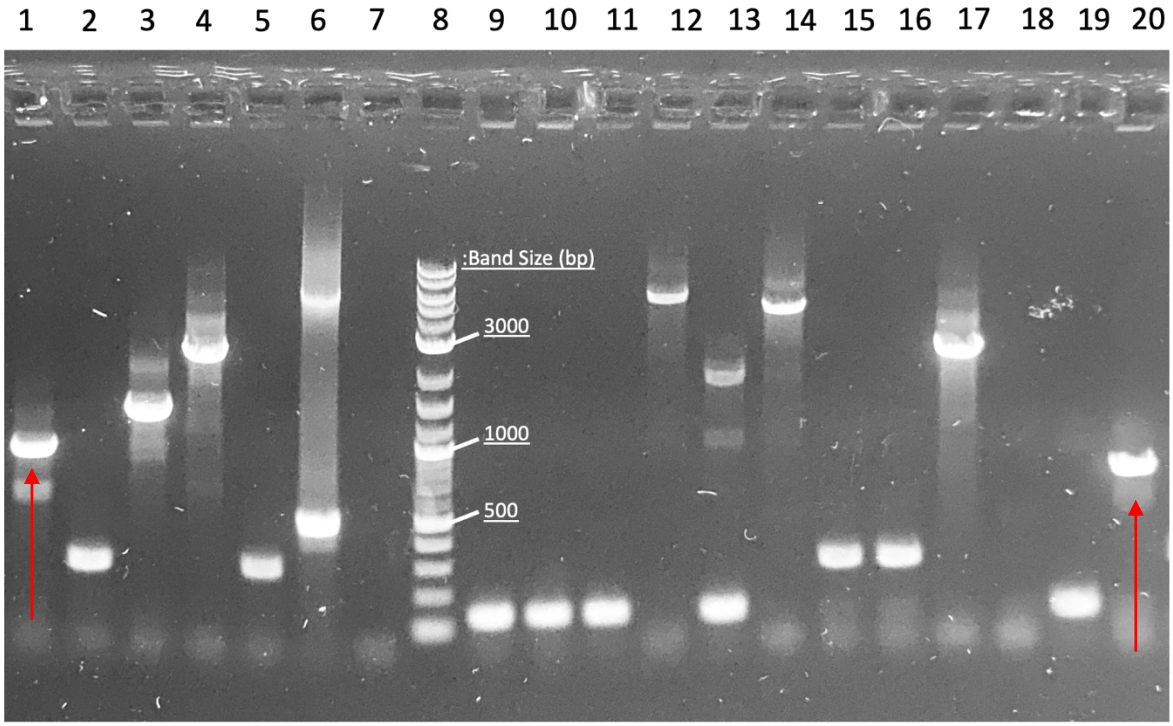


Figure 5.7: PCR confirms successful insertion System Type 1 and System Type 2 DNA fragments into expression vector pET29a. Colony PCR to determine successful insertion of the cloned regions into the expression vector pET29a. Lanes 1-5 indicate insertions of System Type 1 conserved region. Successful insertion is shown in lane 1. Lanes 9-20 indicate insertions of System Type 2 conserved region. Successful insertion is shown in lane 20. Lane 6 indicates positive control. Lane 7 indicates negative water control. Successful insertions are indicated by red arrows.

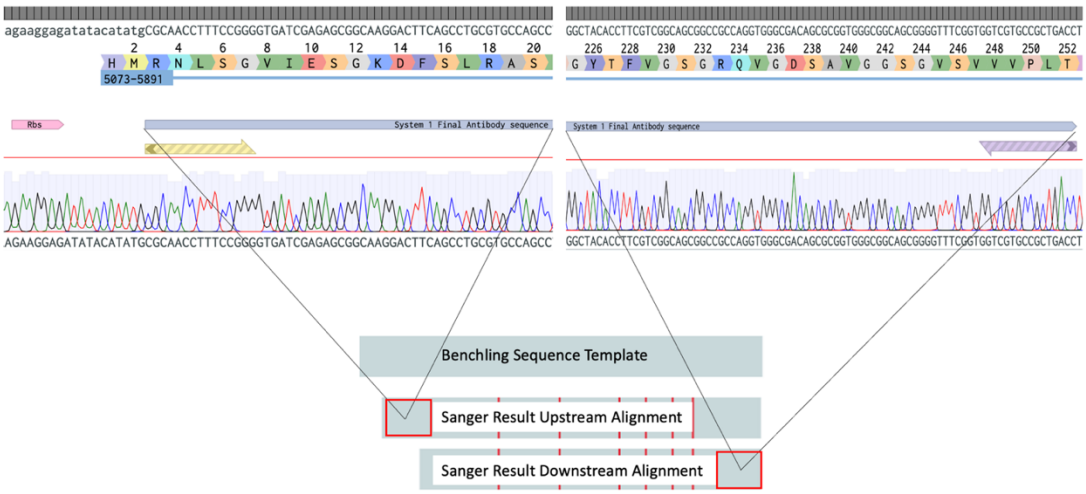


Figure 5.8: Sequencing alignment confirming successful construction of pET29a-System Type 1. Grey coloured bars represent exact sequence of System Type 1 conserved DNA fragment. Second and third lines show sequencing chromatograms that confirm the presence of the sequence. Red colouring of the grey bars indicates single nucleotide mutations accumulated within the fragment during insertion, however these changes were determined to encode the same amino acids and were therefore carried forward.

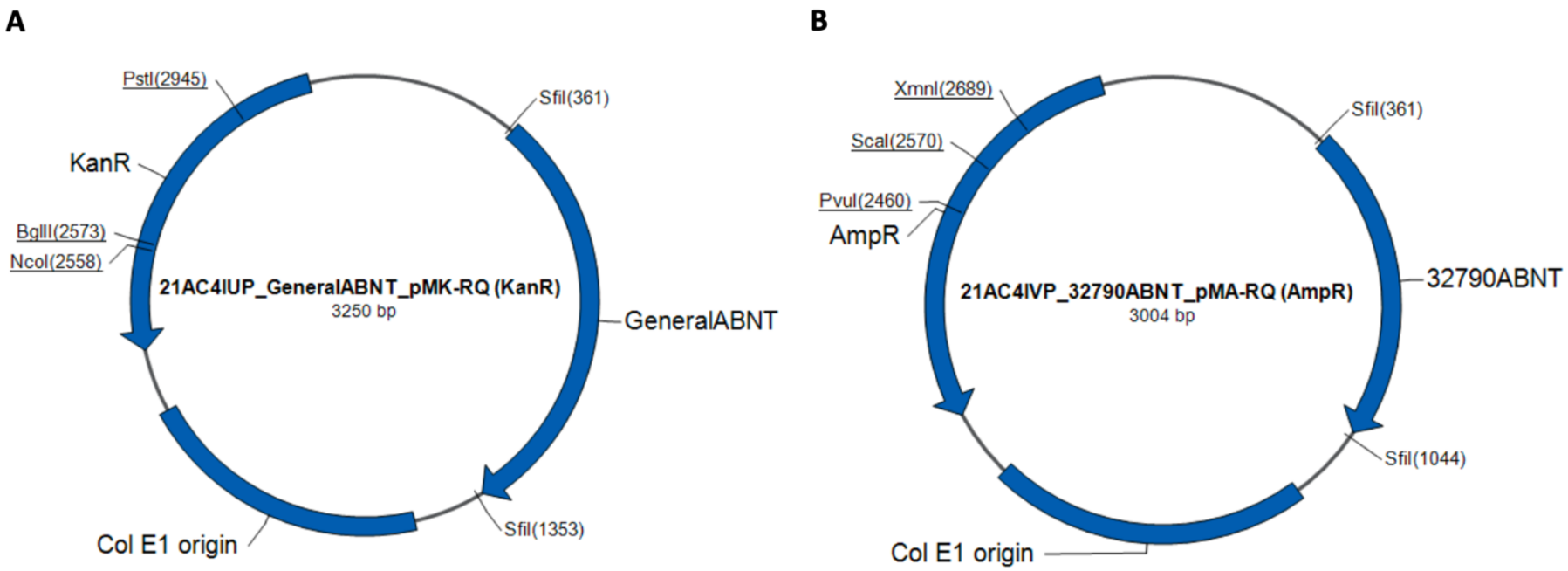


Figure 5.9: GeneArt synthesised vectors with conserved *cdiA* regions from *P. aeruginosa* strain PA14 CDI systems. (A) pMK-RQ contains cloned General conserved region. (B) pMK-RQ contains cloned system type 2 conserved region, genetically derived from CDI^{32790}. Regions were codon optimised and synthesised via ThermoFisher Scientific GeneArt service.

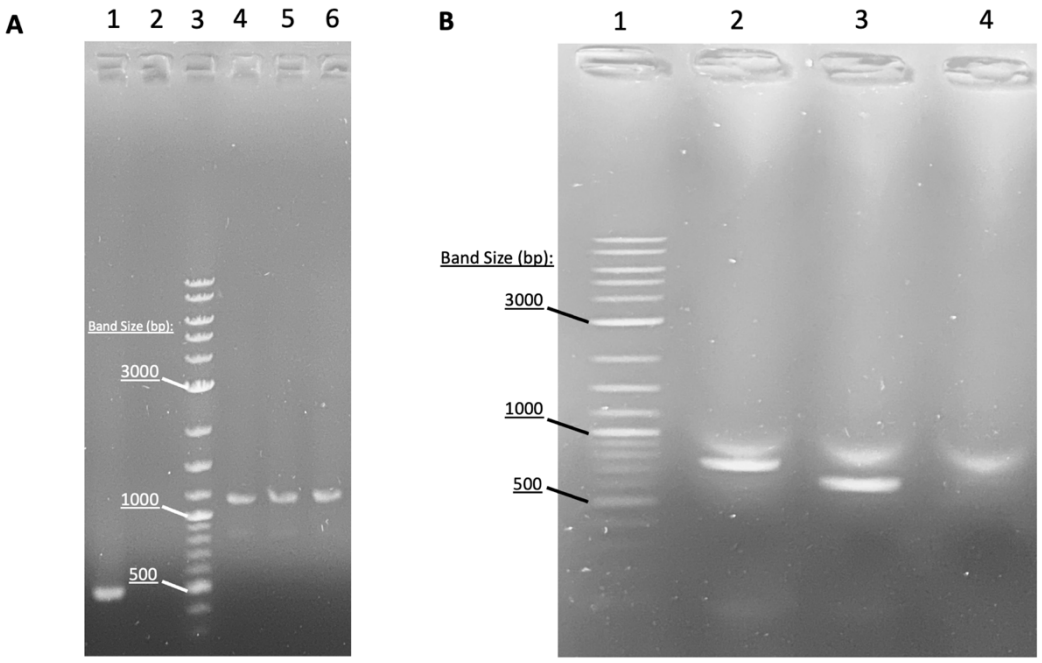


Figure 5.10: PCR confirms successful insertion of codon optimised General and System Type 2 DNA fragments into expression vector pET29a. Colony PCR to determine successful insertion of the cloned regions into the expression vector pET29a. (A) Lanes 4-6 indicate successful insertion of General conserved region. Lane 1 indicates positive empty vector control. Lane 2 indicates negative water control. (B) Lane 2 indicates successful insertion of System Type 2 conserved region. Lane 3 indicates positive empty vector control. Lane 4 indicates negative water control. Note: 2-log ladder was used.

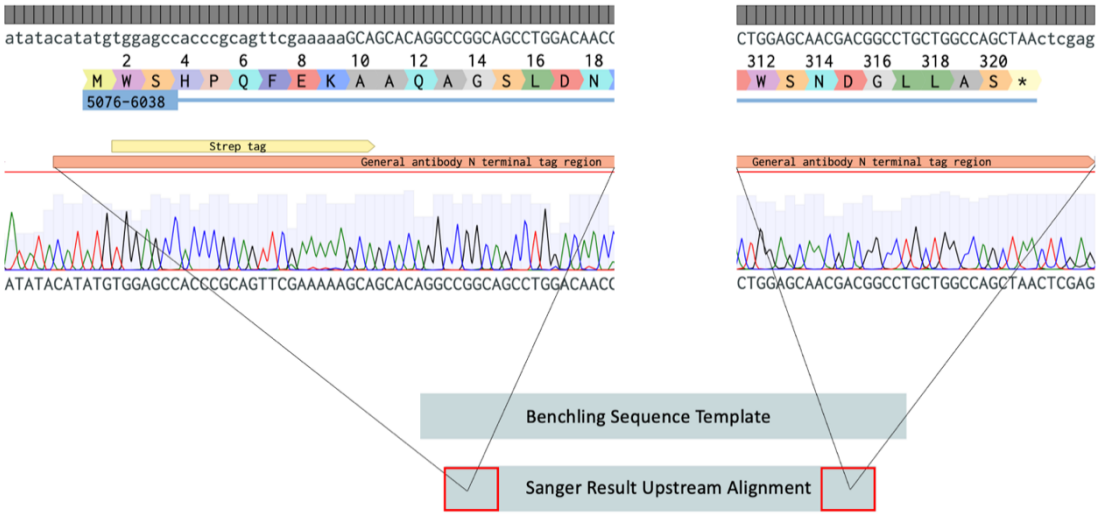


Figure 5.11: Sequencing alignment confirming successful construction of pET29a-System Type 2. Grey coloured bars represent exact sequence of System Type 2 conserved DNA fragment. Second line shows sequencing chromatograms that confirm the presence of the sequence. Absence of red colouring of the grey bars indicates no mutations accumulated within the fragment during insertion.

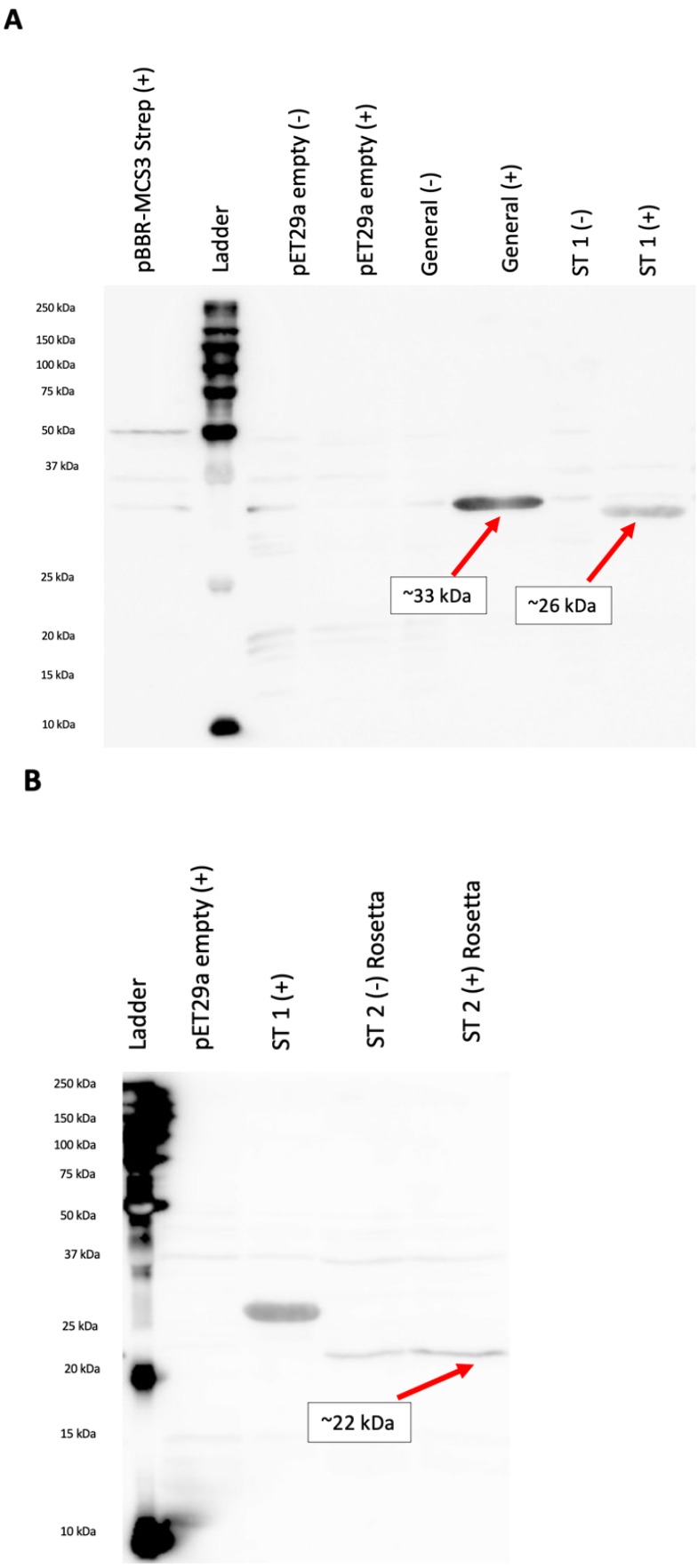


Figure 5.12: Western blot analysis confirms expression of all three CdiA^{Strep} proteins via StrepII tag detection and visualisation using Immobilon HRP substrate peroxidase. (A) General and System Type (ST) 1 induced recombinant protein expression band (33 and 26 kDa respectively), (B) System Type (ST) 2 induced recombinant protein expression band (22 kDa). Western blot analysis of whole cell lysate of uninduced (-) or IPTG induced (+) strains encoding the Strep-tagged conserved CdiA regions show expression of recombinant proteins, pBBR_AbATPbetaSII and empty pET29a were used as controls. This confirms expression of all three recombinant proteins. Successful expression is indicated by red arrows.

5.3.2 Recombinant protein expression enables purification for antibody production

Expression and purification of recombinant proteins is a common method employed to produce polyclonal antibodies against a specific epitope from a large native protein (Wah Liew *et al.*, 2021). Previously, antibodies have been generated to identify the presence and activity of the T6SS in *P. aeruginosa* (Allsopp *et al.*, 2017) and T5SSs in *E. coli* (Allsopp *et al.*, 2010, 2012), indicating this may be a method of detection for extracellular CdiA-NT in *P. aeruginosa* (Ruhe *et al.*, 2018). Although the conserved regions identified in Chapter 3 were cloned and expressed, purification and ability to produce the quantity required for immunogenic doses for the polyclonal antibody production was determined here.

After confirmation of successful construction of these inducible vectors, the next step was to validate the capture of recombinant proteins via Strep-Tactin® Sepharose® resin. Expression induction was conducted as previously outlined in 5.3.1. Cells were then sonicated before applying to a resin column. Ability to bind and purify recombinant proteins was evaluated via western blot analysis. Strep purification was only successful for ST2 recombinant protein (Figure 5.13), as General and ST1 remained within the solid fraction. I performed PCR mutagenesis to replace the StrepII tag with a His tag to increase purification likelihood through higher concentration buffers which are not compatible with the StrepII tag i.e. urea buffers (Figure 5.14). Direct mutagenesis was confirmed via sequencing (Figure 5.15). Purification of General and ST1 used TALON® His resin and was evaluated via western blot analysis, which was successful for both the General and ST1 (Figure 5.16). To ensure protein samples were of high purity, repeats were performed to optimise wash steps to collect the

samples of highest purity. Elutions were pooled and dialysed overnight before quantification. Each purified protein was then split into four doses at 0.5 mg/ml.

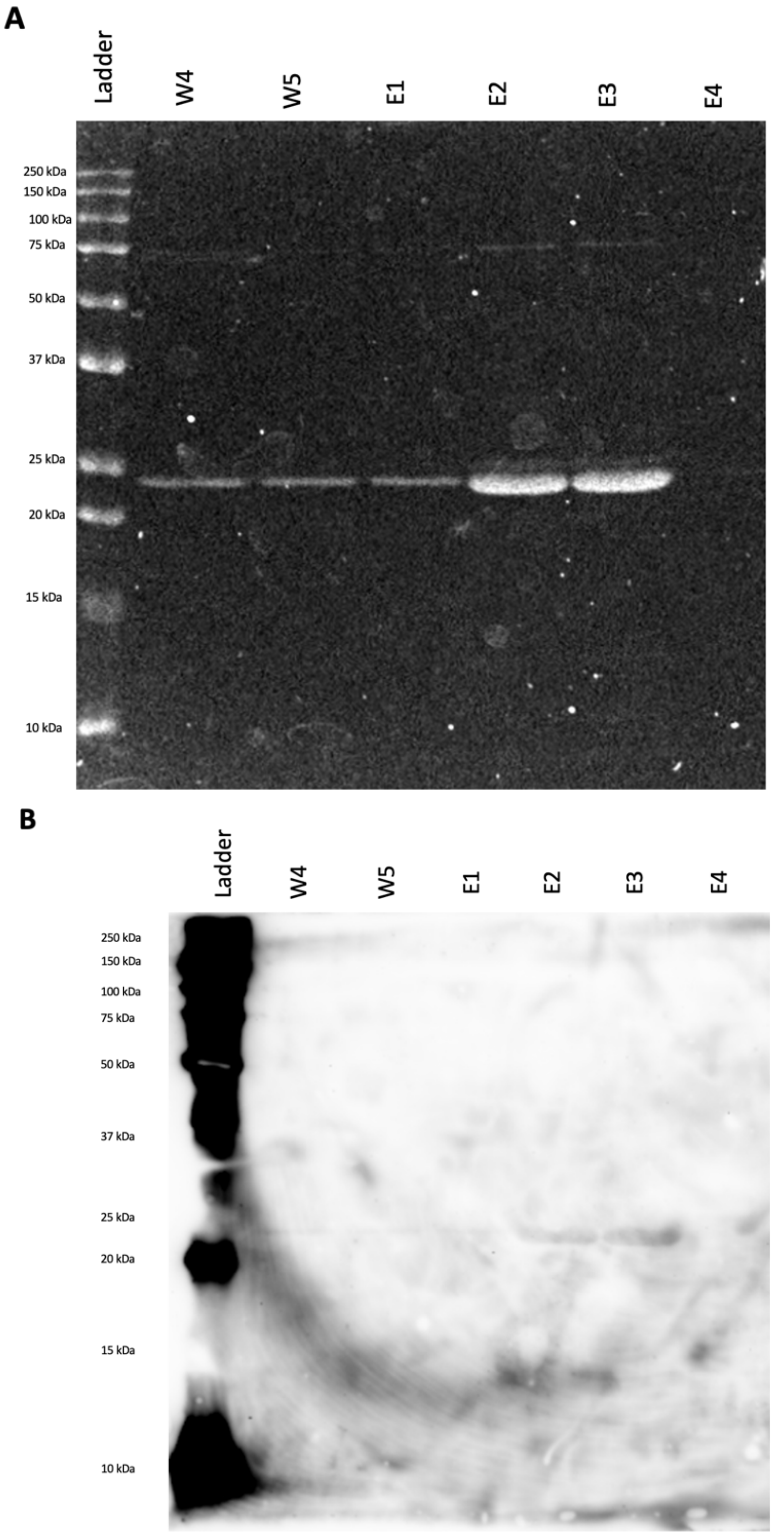


Figure 5.13: SDS-PAGE Coomassie stained gel and western blot analysis confirms Strep-Tactin mediated purification of System Type 2 recombinant protein. SDS-PAGE and western blot analysis of washes and elutions from Strep-Tactin protein purification of whole cell lysate protocol shows successful purification and elution of the System Type (ST) 2 recombinant protein. (A) Coomassie stained gel of Strep-Tactin mediated washes and elutions of ST2 recombinant protein purification predicted size ~22 kDa. Gel indicates (B) Western blot analysis of Strep-Tactin mediated washes and elutions from recombinant protein purification confirms ST2 purification. Coomassie stain indicates whether extra bands are present. Band present at 75 kDa may indicate protein is forming a trimer. This indicates ST2 recombinant protein has been purified to high purity.

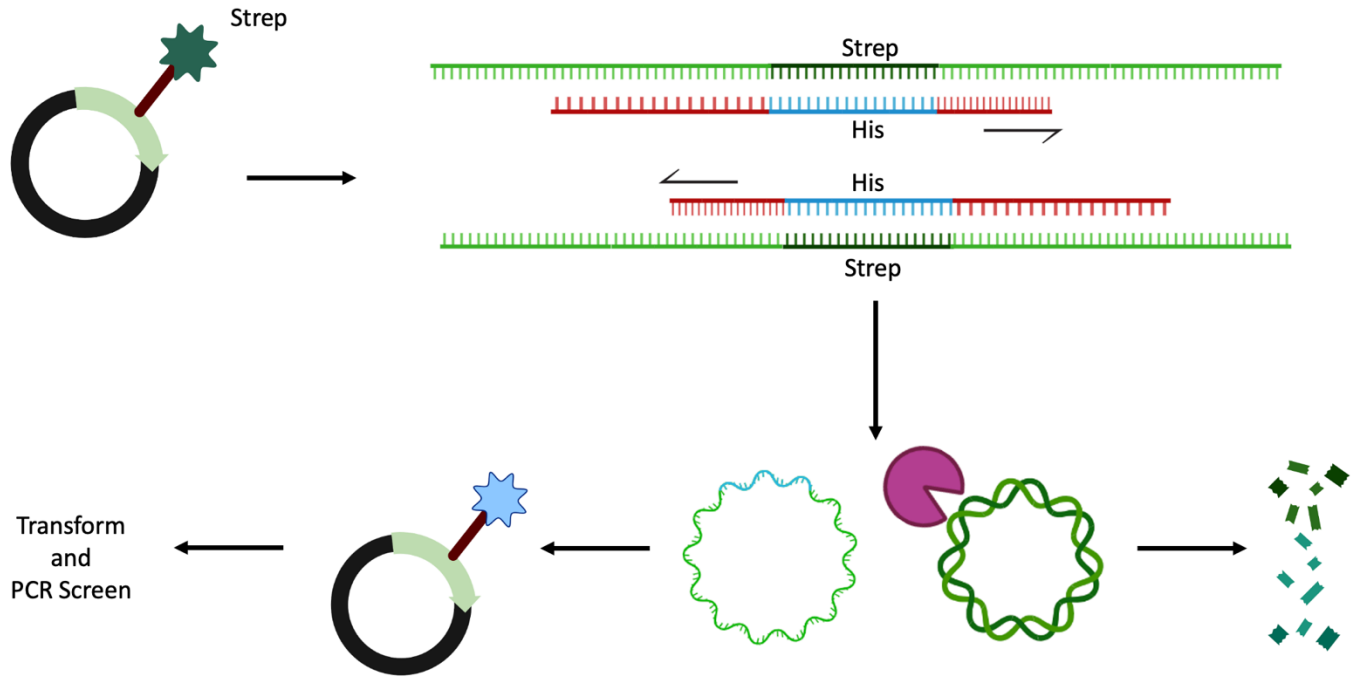


Figure 5.14: Direct mutagenesis of StrepII tag to His tag. PCR mutagenesis was used to replace the DNA encoding the StrepII tag for both the General and System Type 1 constructs due to difficulty in purification. His tags enable the use of higher concentration buffers for protein purification, which was required here to increase the likelihood of purification as these recombinant proteins were remaining in the solid pellet fraction of the cell lysate during the purification process. PCR using the designed primers enabled the replacement of the DNA encoding the tag. DpnI digestion was used to degrade the template DNA. Vectors were then transformed into *E. coli* BL21 competent cells.

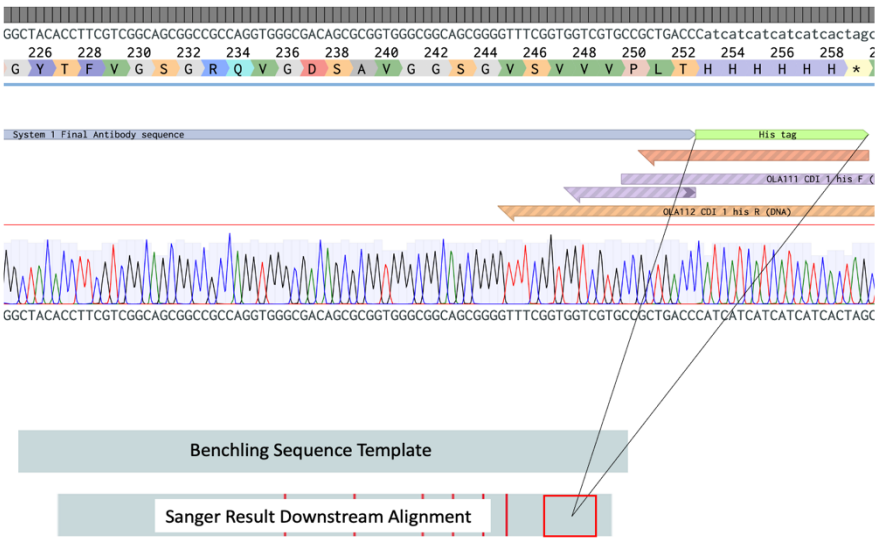


Figure 5.15: Sequencing alignment confirming successful mutagenesis and replacement of StrepII tag to His tag. Grey coloured bars represent exact sequence of System Type 1 conserved DNA fragment. Second and third lines show sequencing chromatograms that confirm the presence of the sequence. Red colouring of the grey bars indicates no mutations accumulated within the fragment during insertion, however these changes were determined to encode the same amino acids.

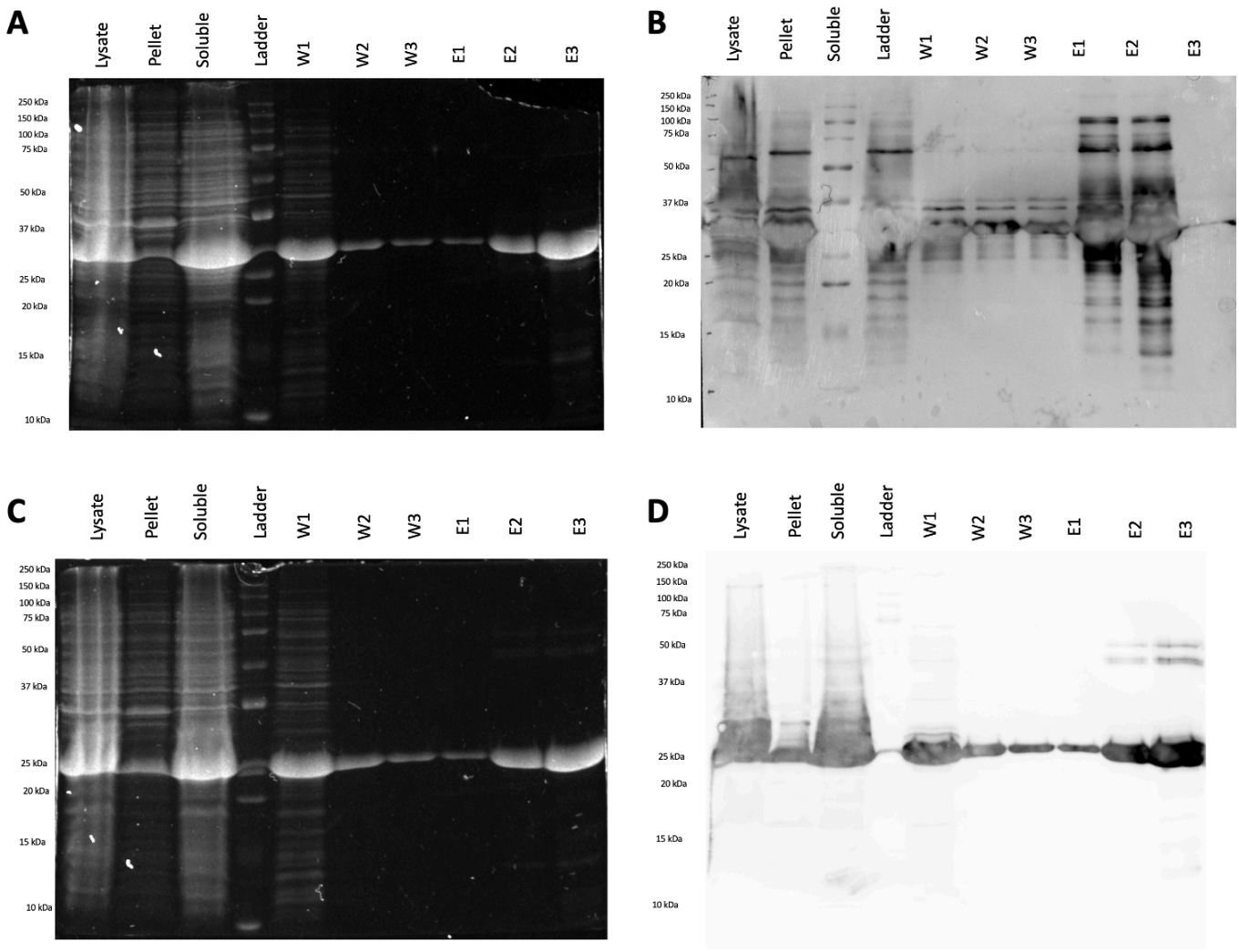


Figure 5.16: SDS-PAGE Coomassie stained gel and western blot analysis confirms TALON-resin purification of General and System Type 1 recombinant proteins. (A) Coomassie stained gel of TALON-mediated washes and elutions from General recombinant protein purification expected size ~33 kDa, (B) matched western blot analysis of TALON-mediated General recombinant protein purification using an anti-His antibody and chemiluminescent visualisation, (C) Coomassie stained gel of TALON-mediated washes and elutions from System Type 1 recombinant protein purification expected size ~26 kDa, (D) matched western blot analysis of System Type 1 recombinant protein purification. Figures show successful purification from whole cell lysates with clean elutions for the General and System Type (ST) 1 recombinant proteins. IPTG was used for inductions. Coomassie stain indicates greater than 99% purity for elutions.

5.3.3 Polyclonal antibodies successfully detect their corresponding recombinant proteins

To generate specific antisera for the three proteins General, ST1 and ST2 produced in 5.3.2, doses were sent to Eurogentec for injection into rabbits. Each protein had purified quantities sufficient to produce doses for immunization periods of two rabbits each, a total of six rabbits between the three proteins. Each rabbit was injected with doses for one protein, to raise a polyclonal immunogenic response against a single protein. Due to project time constraints and previous success with this program, the speedy 28 day custom polyclonal antibody service was used (Figure 5.17). Four injections were given per rabbit, where proteins were added to a non-Freund adjuvant to enhance immune response for faster production turn around, producing primarily IgG antibodies in the final bleed. Pre-immune, medium and final bleeds were taken and included in the received shipment alongside rabbit designation numbers and bleed acronyms (Table 5.1).

Upon receival, 1 ml aliquots of each sample were made and stored at -80 °C. Initially, cross-reaction of polyclonal antibodies against purified proteins used to challenge the rabbits was used to determine if an immune response was raised (Figure 5.18). From western blot analyses, this was confirmed as antibodies cross reacted against each recombinant protein as strong clear bands are observed for General (32 kDa), ST1 (26 kDa) and ST2 (29 kDa). The next step was to validate whether these antibodies could identify the presence of these systems in *P. aeruginosa* lab strains and my WSDM strain panel.

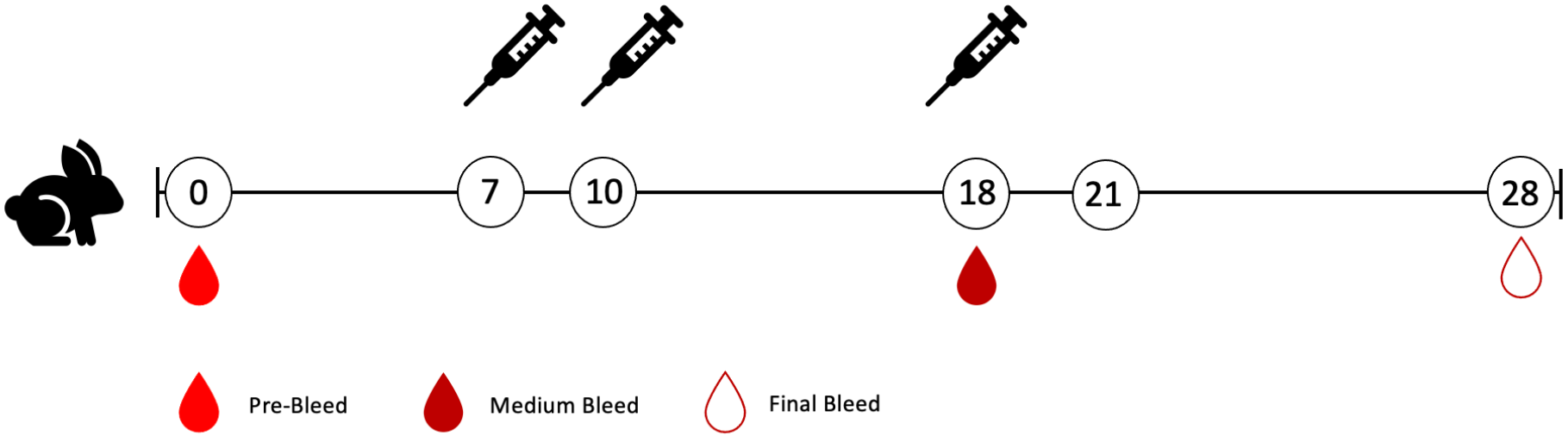


Figure 5.17: Eurogentec speedy 28-day custom polyclonal antibody service protocol. Antibody production was conducted by Eurogentec to produce custom polyclonal antibodies against the three recombinant proteins purified in 5.3.2. Non-Freund adjuvant was added to the doses as part of the speedy protocol in order to enhance the immune response for the shortened immunogen exposure period. Pre-bleed is taken to determine which fraction of antibodies is already present in the animal. A medium-bleed is taken once antibody levels have been detected to have increased to sufficient levels within the animal once the adaptive immune response has commenced. The final-bleed is then collected, the serum separated, and the animal is then sacrificed. Syringes denote days where immunogen exposure occurred.

Table 5.1: Rabbit identification numbers with immunogen used for sera production

Rabbit Number	Recombinant Protein
R1550	General
R1551	General
R1552	ST1
R1553	ST1
R1548	ST2
R1549	ST2

*Each rabbit bleed protocol produced three samples per rabbit. PPI- pre-bleed, GP- medium bleed, SAB- final bleed.

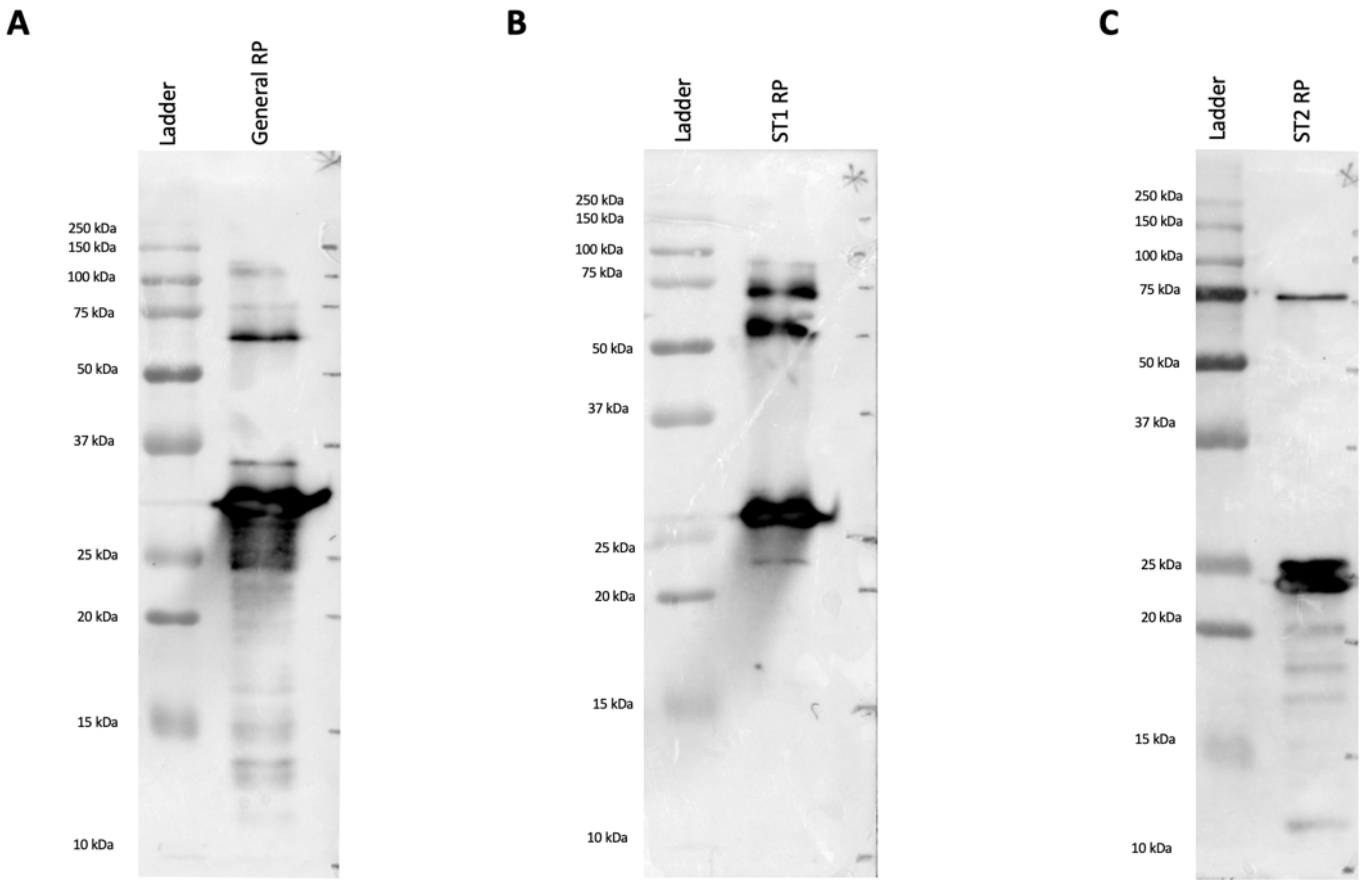


Figure 5.18: Western blot analysis shows cross-reaction between CdiA regions from final bleed sera. Western blot analysis of whole cell lysate was used to determine whether raised antibodies cross-reacted with purified recombinant proteins produced in 5.3.2 for one rabbit of each protein. HRP substrate peroxidase enabled detection and visualisation of expressed CdiA proteins. (A) General RP induced antibody R1550 showed detection of RP. (B) ST1 RP induced antibody R1552 showed detection of RP. (C) ST2 RP induced antibody R1549 showed detection of RP. This confirms rabbits produced a robust immune response during the immunisation protocol conducted during the Eurogentec speedy 28 day custom polyclonal antibody service.

5.3.4 Polyclonal antibodies do not detect CdiA in P. aeruginosa laboratory strains or whole system deletion mutants

After confirmation of a successful immune response, the next step was to validate the efficacy of these antibodies in detecting CDI systems in laboratory strains and my WSDM strain panel. Initially pre-bleed sera were tested via western blot analysis to determine whether cross reaction would occur with other components of the *P. aeruginosa* strains (Figure 5.19). Cross reaction was observed with the pre-bleeds due to the presence of multiple bands, indicating the rabbits may have been exposed to other gram-negative bacteria or have potentially seen *P. aeruginosa* before. However, as a strong HRP substrate peroxidase and long exposure time of 2 mins on the blot was used, the post-immunisation sera were considered to potentially produce a stronger reaction than those observed by the pre-bleeds.

The next step was to assess whether the expression of the CdiA^{00510} and CdiA^{32790} could be detected by the final bleed sera. Initially, WSDMs in the *rsmA* strain background were used as *rsmA* is a negative regulator of the CDI systems (Mercy *et al.*, 2016) and therefore these strains should have elevated levels of expression, increasing the likelihood of detection. These strains included *rsmA* ΔCDI^{00510}, *rsmA* ΔCDI^{32790}, *rsmA* CDI^{00510}CDI^{32790} (Chapter 4 Figure 4.4), and were utilised to determine the specificity of the antibodies as any bands observed should be absent for these mutants (Table 5.2). From the final-bleed antibodies, none appeared to identify the presence of CDI systems (Figure 5.20). Due to the high background signal observed in the pre- and final-bleeds, I attempted to lower background signal by adsorbing the antibodies individually against *rsmA* CDI^{00510}CDI^{32790} cell lysates. Conceptually, this would remove antibodies that cross react with the other proteins from the pre-bleeds, leaving

antibodies that would cross-react with CdiA^{00510} and CdiA^{32790} or both systems in the soluble faction. However, this also did not appear to yield a change in detection (Figure 5.21).

The next potential reason for the inability to detect the presence of these systems was due to the large size of the native CdiA^{00510} and CdiA^{32790} proteins, 353 kDa and 532 kDa respectively. Therefore Invitrogen Tris-Acetate 3-8% gradient NuPAGE gels were utilised and changing from a semi-dry to wet transfer protocol based on the literature available for visualising proteins of this size (Mishra, Tiwari & Gomes, 2017). Using the adsorbed antibodies and these protocol changes, the western blot analyses were repeated (Figure 5.22). Here other controls such as *rsmF, rsmArsmF* and *rsmArpoN* were used to enhance the expression of these systems by removing any potential negative regulation to increase the likelihood of detection further. Again, detection was unclear and although some bands at high kDa were observed, they were not absent in the deletion mutants indicating CdiA were not being detected here. Therefore, due to the lack of clear binding using these antibodies this part of the project was stopped due to time constraints and the clinical strains from the PAPA repository where not screened.

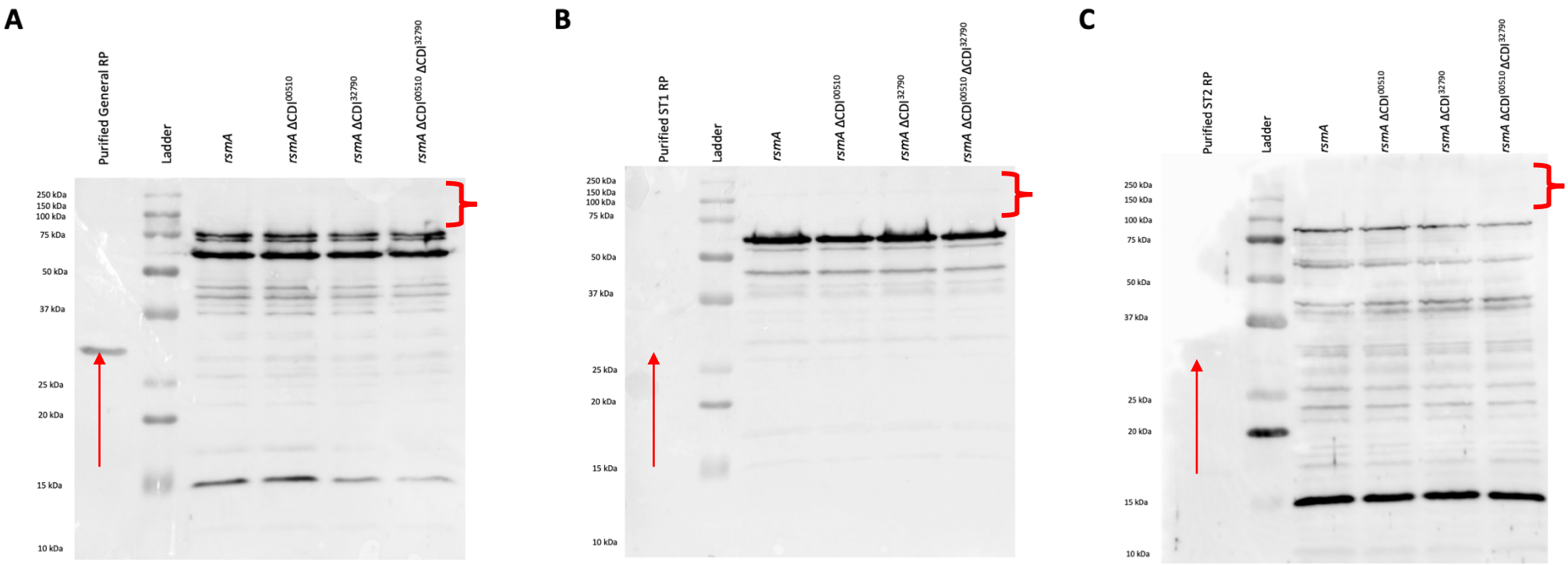


Figure 5.19: Western blot analysis shows cross-reaction occurs between CdiA regions from pre-bleed sera using rabbit antibody detection and visualisation via Immobilon HRP substrate peroxidase. Western blot analysis of whole cell lysate was used to determine whether raised antibodies cross-reacted with CdiA from ΔCDI mutant strains, purified proteins were used as controls and exposure time of 2 mins was utilised. HRP substrate peroxidase was unable to detect and visualise expression of CdiA proteins. (A) General RP induced antibody R1550 showed no detection of CdiA^{00510} or CdiA^{32790} (32 kDa). Some cross-reaction was observed with purified protein indicating this may not be naïve to the rabbit. (B) ST1 RP induced antibody R1552 showed no detection of CdiA^{00510} (26 kDa). (C) ST2 RP induced antibody R1549 showed no detection of CdiA^{32790} (29 kDa). This confirms rabbits were naïve to this protein. Red arrows indicate where recombinant protein bands are expected. Red brackets indicate where CdiA bands are expected.

Table 5.2: Detection of CDI expected to be observed by final-bleed antibodies

Recombinant Protein Antibody	*rsmA*	*rsmA* ΔCDI^{00510}	*rsmA* ΔCDI^{32790}	*rsmA* ΔCDI^{00510} ΔCDI^{32790}
General	☑	☑	☑	
ST1	☑		☑	
ST2	☑	☑		

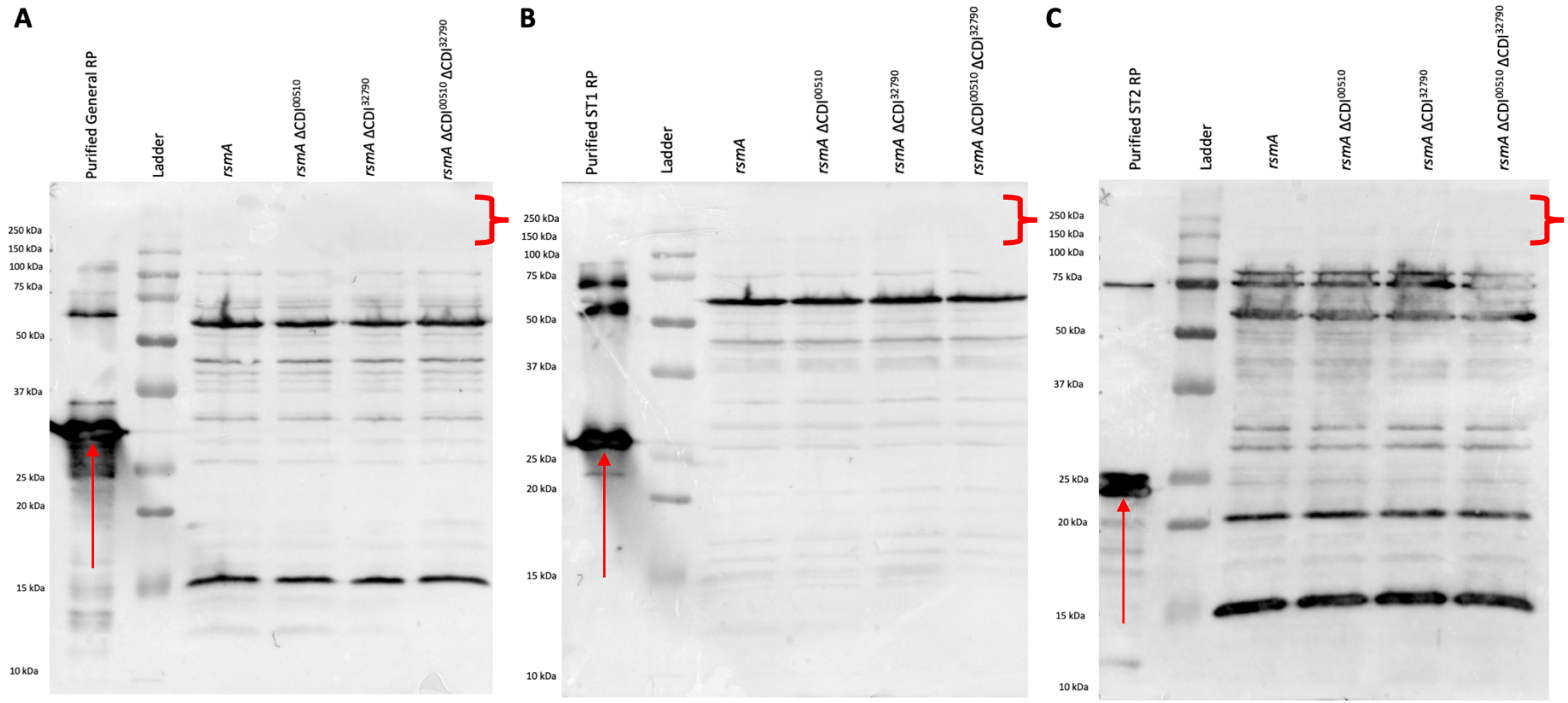


Figure 5.20: Western blot analysis using final-bleed polyclonal antibodies shows no cross-reaction occurs with native CdiA from *P. aeruginosa* strain PA14 that should be absent in the corresponding deletion mutant strains. Western blot analysis of whole cell lysate was used to determine whether antibodies would cross-react with CdiA from *rsmA* ΔCDI mutant strains. HRP substrate peroxidase was unable to detect and visualise expression of CdiA proteins. All recombinant proteins were detected by final-bleed polyclonal antibodies. (A) General adsorbed antibody R1550 showed no detection of $CdiA^{00510}$ detection. (B) ST1 RP adsorbed antibody R1552 no detection of $CdiA^{00510}$. (C) ST2 adsorbed antibody R1549 showed no detection of $CdiA^{00510}$. Red arrows indicate recombinant protein bands. Red brackets indicate where CdiA bands are expected.

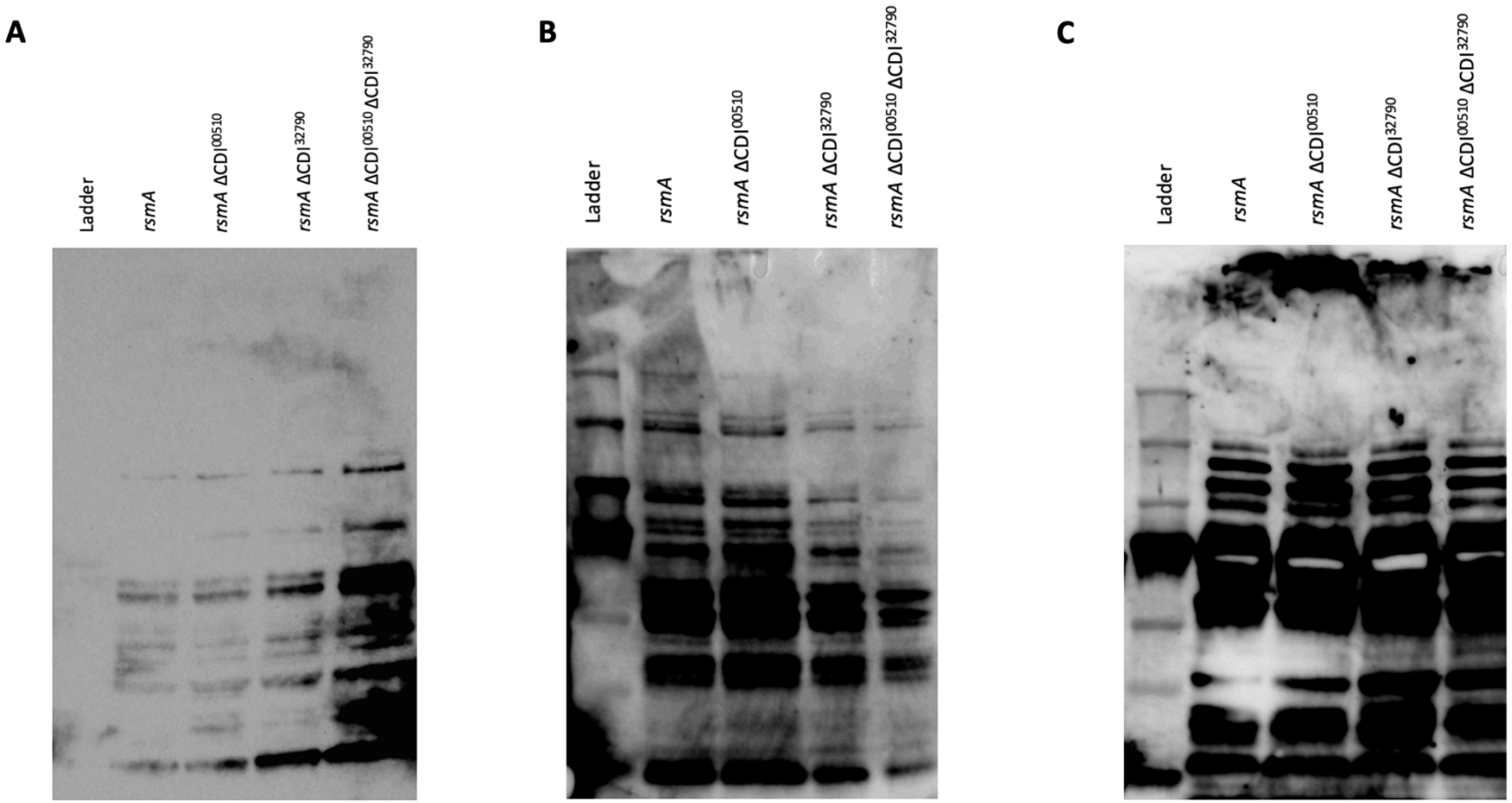


Figure 5.21: Western blot analysis using adsorbed polyclonal antibodies shows no cross-reaction occurs with native CdiA from *P. aeruginosa* strain PA14 that should be absent in the corresponding deletion mutant strains. Western blot analysis of whole cell lysate was used to determine whether antibodies would cross-react with CdiA from *rsmA* ΔCDI mutant strains after rabbit sera containing polyclonal antibodies underwent adsorption. HRP substrate peroxidase was unable to detect and visualise expression of CdiA proteins. (A) General adsorbed antibody R1550 showed no detection of $CdiA^{00510}$ detection. (B) ST1 RP adsorbed antibody R1552 no detection of $CdiA^{00510}$. (C) ST2 adsorbed antibody R1549 showed no detection of $CdiA^{00510}$.

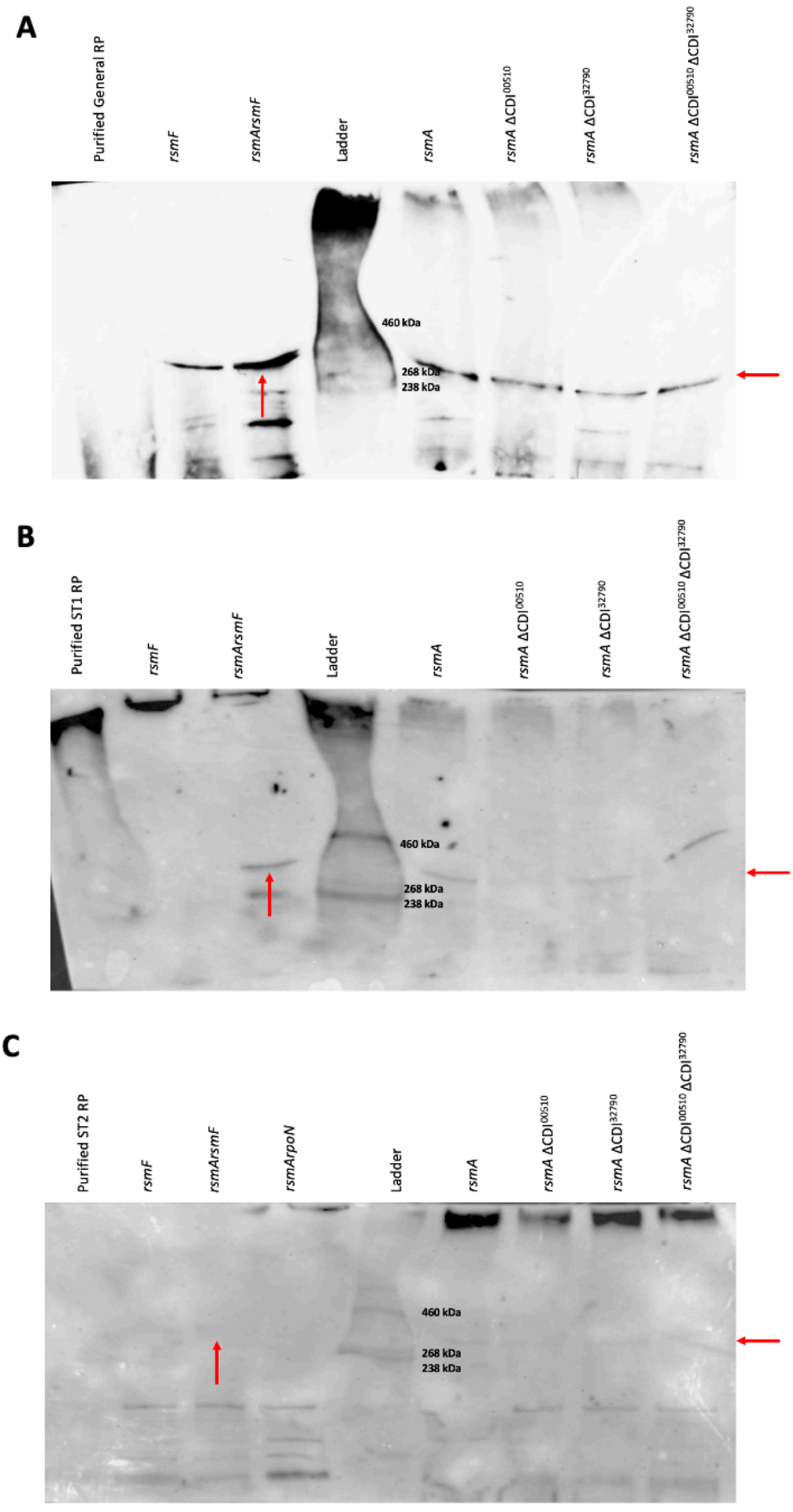


Figure 5.22: Tris-Acetate NuPAGE, wet transfer and western blot analysis using adsorbed polyclonal antibodies shows no cross-reaction occurs with native CdiA from *P. aeruginosa* strain PA14 that should be absent in the corresponding deletion mutant strains. Western blot analysis of whole cell lysate was used to determine whether antibodies would cross-react with CdiA from *rsmA* ΔCDI mutant strains after rabbit sera containing polyclonal antibodies underwent adsorption. (A) General adsorbed antibody R1550 showed no detection of $CdiA^{00510}$ detection. (B) ST1 RP adsorbed antibody R1552 no detection of $CdiA^{00510}$. (C) ST2 adsorbed antibody R1549 showed no detection of $CdiA^{00510}$. Red arrows indicate potential CdiA identification bands.

5.4 Discussion

The use of antibodies to study the activity of contact-dependent systems in *P. aeruginosa* has previously been described (Allsopp *et al.*, 2010, 2012, 2017; Nolan *et al.*, 2021). However, to date no attempt has been made to utilise them in studying CDI systems in *P. aeruginosa*. The results presented in Chapter 5 of this thesis outline the production of three proteins: General, ST1 and ST2, their expression, extraction, and purification for polyclonal antibody production. I show that these antibodies successfully cross react with the purified proteins. However, I show the antibodies were unable to indicate CDI activity in my CDI mutant strain panel. The inability to detect CDI via all three antibodies was unexpected having used three antigens and two rabbits per antigen to increase the likelihood that specific anti-CDI antibodies would be generated. This was a disappointing result, and an alternative approach will need to be taken to assess expression that is beyond the scope of this PhD.

Elucidating the presence and activity of these systems in clinical strains would provide insight into differences between strains, their importance in *P. aeruginosa* ability to compete for a niche, in addition to the reason these systems are conserved in strains associated with long-term chronic infections in immunocompromised individuals. Detecting the presence and activation status of these systems in clinical *P. aeruginosa* strains would demonstrate the ability to detect these systems *in vitro*. Further inter- and intra-bacterial competition experiments could determine if differential expression of these systems occurs based on the competitors *P. aeruginosa* faces, particularly against other pathogens associated with the polymicrobial community found within the CF lung.

5.4.1 Can conserved CdiA-NT regions be cloned to generate inducible recombinant protein vectors?

One of the major methods employed by molecular biologists to easily detect the presence and activity of various proteins of interest is through western blot analysis which uses antibodies specific to a protein or a protein tag (Begum, Murugesan & Tangutur, 2022). However, when studying a mechanism or system in clinical strains, protein tags are redundant. Therefore, establishing a way to identify the native protein *in vitro* is required to study any system of interest. Large proteins provide a multitude of potential antigenic epitope peptides where their DNA sequences can be cloned into vectors to assemble recombinant proteins for the production of polyclonal antibodies for detection of the native protein (Figure 5.1) (Trier, Hansen & Houen, 2012; Wah Liew *et al.*, 2021). Therefore, to raise antibodies against the two CDI systems in *P. aeruginosa* strain PA14, I constructed strains that possessed DNA encoding conserved regions that would enable the expression and purification of recombinant proteins to raise polyclonal antibodies against them (Figure 5.2).

Using the three conserved regions identified in Chapter 3, primers were successfully designed to enable cloning (Figure 5.3). These regions were successfully cloned into the expression vector pET29a (Figure 5.4-5.8). Cloning regions within secretion systems can be difficult due to their highly repeatable regions, which are genetically and structurally similar to many other OM proteins (Kajava *et al.*, 2001; Allen & Hauser, 2019). Indeed, I encountered multiple difficulties during the cloning step due to the highly repeatable units within these conserved regions. Optimisation steps were required which included changing annealing temperatures and polymerases but still had limited success. To overcome this difficulty in part, these regions

were initially cloned into high efficacy vector pCR Blunt-II TOPO before restriction digestion and ligation into the final expression vector pET29a could occur. This method was only successful for producing the ST1 strain specific to CDI^{00510} homologous systems.

After many attempts at General and ST2 vector production and due to time constraints ThermoFisher GeneArt service was used to design codon optimised versions of the conserved regions to accelerate vector engineering (Figure 5.9). From these vectors, restriction digestion, ligation into pET29a and transformation into *E. coli* was performed and confirmed via sequencing (Figure 5.10-5.11). These methods produced three strains; General, ST1 and ST2, respective to the three regions identified. Polyclonal antibodies were made against the CDI systems (general), those genetically homologous to CDI^{00510} (ST1), and those genetically homologous to CDI^{32790} (ST2) (Figure 5.2). These strains were shown to express the recombinant proteins under IPTG induction at 2 hrs (Figure 5.12).

5.4.2 Can recombinant proteins be expressed and purified to enable antibody production?

The utilisation of recombinant proteins in molecular biology has not only revolutionised research but the pharmaceutical industry as well. *E. coli* is the leading bacteria used for expression of recombinant proteins due to its ability to produce high levels of proteins whilst remaining stable, making it an ideal candidate for protein purification (Deo *et al.*, 2022). However the affinity of various tags differs, as well as the concentration of the buffers you can use in order to purify recombinant proteins (Labrou, 2014). Therefore, picking an optimal tag for purification is crucial to obtain purified products suitable to send for antibody production. Purifying regions of a larger native protein provides a specific antigen and

multiple epitopes to ideally raise a good immunogenic response in animals such as mice or rabbits to produce polyclonal antibodies specific to the native protein, whilst getting around issues with isolating large proteins. Having high purity protein samples for antibody generation is crucial for antibody specificity to ensure no off-target cross-reaction occurs. Additionally, the amount of protein required for raising an immune response is quite high, therefore generating enough protein for the doses requires optimisation of the expression and purification protocols. Here I produced high purity samples and sufficient quantities of protein (Figure 5.13 and 5.16). However for 1 of the antigens (ST2) I only used the minimum amount of protein required to raise the antibodies. Retrospectively, repeating this procedure I would ensure the maximum amount for all three proteins would be used.

5.4.3 Are polyclonal antibodies raised in rabbits effective at detecting both recombinant proteins and the presence of CDI systems in P. aeruginosa CDI deletion mutants?

Antibodies are used in many areas of molecular research as a tool to study the presence and expression levels of various proteins. The exploitation of antibodies has not only enhanced research but changed diagnostics and treatment, where antibodies are used from standard assays such as immunohistochemistry to treatments against viral infections (Bordeaux *et al.*, 2010; Pantaleo *et al.*, 2022). As the field of protein science has exploded in recent years, the use of antibodies provides a major advantage in enabling researchers to not only identify native proteins but specific epitopes too (Trier, Hansen & Houen, 2012) and provides the ability to study proteins in *in vitro* and *in vivo* assays (Lim *et al.*, 2022; Vacca, Sala & Rappuoli, 2022). Antibodies are also now used to identify pathogens or the presence of pathogenic toxins during infections based off recombinant protein technology. However, antibodies to

identify the presence and activity of CDI systems has not previously been developed for *P. aeruginosa*. Most commonly polyclonal antibodies are raised against native proteins, or recombinant proteins, based on the size of the native protein/specificity of the antibodies. This increases the likelihood of detection *in vitro* as polyclonal antibodies are raised against multiple epitopes of those proteins.

Many animals are used for antibody production. Most commonly small animals such as mice and rabbits, although large animals such as goats, sheep and horses are used depending on the desired antibody and immune response (Leenaars & Hendriksen, 2005; Thompson *et al.*, 2016). Rabbits provide a particular advantage as small animal conduits due to their: ability to respond to a wider variety of antigens, size, spleen size, and large antibody yield produced based on a larger sera volume (Stills, 2012). Therefore rabbits were selected here to produce anti-CDI antibodies for *P. aeruginosa*. Clear cross-reaction was observed for all three recombinant proteins (Figure 5.18) indicating successful generation of an immune response.

Laboratory PA14 mutant strains were utilised to attempt to detect the CDI. I used the *rsmA* mutant strains, including *rsmA* CDI^{00510}, *rsmA* CDI^{32790} and *rsmA* $CDI^{00510}CDI^{32790}$ of my mutant strain panel. Additional mutant strains *rsmF, rsmArsmF* and *rsmArpoN* were screened. Evidence has shown that RpoN is a regulator of the T6SSs (Bernard *et al.*, 2011; Sana *et al.*, 2013; Shao *et al.*, 2018). As the major alternative sigma factor, it may also control regulation of CDI due to its interplay with the Gac/Rsm pathway which includes RsmA and RsmF as well as its broad range of regulating multiple systems involved in virulence (Sana *et al.*, 2013; Allsopp *et al.*, 2017, 2022; Corley, Intile & Yahr, 2022). The high cross-reaction background observed in the pre-bleed blots (Figure 5.19) indicates the rabbits had been previously

exposed to gram-negative bacteria. As they are living animals which have their own microbiota this is highly likely. An alternative explanation is the rabbits were previously exposed to *P. aeruginosa*. This is likely as *P. aeruginosa* is ubiquitous and can even be found in drinking water (Crone *et al.*, 2020), and is a likely candidate for the high background levels observed in the pre-bleed sera. However, CdiA could not be detected by the final-bleeds (Figure 5.20) or adsorbed final-bleed sera (Figure 5.21). This was unexpected, however upon further rumination the large size of native CdiA (350-530 kDa) was a potential reason for lack of detection. Therefore tris-acetate NuPAGE was performed alongside wet-transfer to increase the likelihood of detection (Figure 5.22). Although this was able to outline some protein bands above the 250 kDa maximum size visualised via SDS-PAGE, detection of potential CdiA bands was unclear due to their unexpected presence in deletion mutant samples and outlined in Table 5.2.

Due to project time constraints and the lack of clear binding observed, this portion of the project was terminated at this stage. Therefore validating the efficacy of these antibodies and the presence and activity of these systems in both laboratory and clinical strains from the PAPA strain repository was not attempted. This was disappointing due to the trouble shooting involved which was moving in the right direction for validating these antibodies. Given more time to trouble shoot, I believe these may be a useful tool in detecting CDI systems. However, whether the conformation of these recombinant proteins mimic that of these CdiA regions *in situ* is unknown and could be a potential reason for detection difficulties as the recombinant protein antigenic epitopes may not be exposed to enable generated antibodies to bind native protein. The purification of the full length CdiA protein could be a good positive control in testing this theory. However, this would present its own challenges such as difficulties in

cloning. Alternatively internal epitope tags may be used; however this would be redundant in testing clinical strains. In future work, these antibodies may be improved through purification of more protein to conduct an antibody affinity purification. Additionally, due to the size of the full length CdiA proteins, they may be too large to run through standard gels. Optimising this was attempted with the Invitrogen tris-acetate 3-8% gradient gels but this did not improve detection. Alternatively, protein electrophoresis using agarose gels could be tested which have previously been shown to be effective in separating proteins larger than 600 kDa (Greaser & Warren, 2012). Another potential method is indirect immunofluorescence, where $CdiA^{00510}$, $CdiA^{32790}$ or $CdiA^{00510}CdiA^{32790}$ bacterial strains could be bound to the microplate before addition of the polyclonal sera. Presence could then be detected through the utilisation of a secondary antibody which would be attached to a fluorophore that could be detected via a plate reader (Chen *et al.*, 2021). An alternative to using antibodies if unsuccessful could be through RT-qPCR to detect CDI mRNA levels using designed primers to quantify CDI mRNA during competition but not assess protein levels.

5.5 Conclusions

The main conclusions associated with the cloning and purification of recombinant proteins, and the subsequent production and validation of their associated antibodies are as follows:

1. StrepII tag purification of ST1 recombinant protein was successful
2. StrepII tag purification of General and ST2 recombinant protein was unsuccessful however the alternative His tag re-engineering strategy enabled purification

3. Recombinant proteins designed from CdiA-NT give rise to polyclonal antibodies in rabbits
4. Polyclonal antibodies produced cross-react with purified recombinant proteins
5. No evidence for detection of CDI systems in *P. aeruginosa* CDI system deletion mutant strains via polyclonal antibodies was observed

Therefore, the results presented in Chapter 5 meant the antibodies generated were unable to be utilised for the characterisation of the presence and activation status of each CDI system in clinical *P. aeruginosa* strains. However, given more time to optimise detection methods, these antibodies may be successful in detection in the future outside the scope of this project.

So, the final step was to consider whether these results supported or refuted the hypotheses proposed at the beginning of this chapter.

Hypothesis 1: The conserved regions identified in Chapter 3 of this thesis can be cloned into recombinant proteins. **This was accepted.**

Hypothesis 2: These recombinant proteins can be expressed using the StrepII tag. **This was accepted.**

Hypothesis 3: These recombinant proteins can be purified using the StrepII tag. **This was refuted. Only System Type 1 recombinant protein could be purified using the StrepII tag, the General and System Type 2 recombinant proteins had to undergo direct mutagenesis to replace the StrepII tag with a His tag before being purified.**

Hypothesis 4: The purified recombinant proteins give rise to polyclonal antibodies from rabbits. **This was accepted.**

Hypothesis 5: Polyclonal antibodies can detect CDI systems in my CDI mutant strain panel. **This was refuted.**

Hypothesis 6: Polyclonal antibodies can be used to screen the presence of CDI systems in laboratory strains PA14 and respective CDI mutants. **This was not tested due to time constraints and poor diagnostic value of the CdiA antibodies.**

The ability to produce a tool to enable identification of CDI systems from clinical *P. aeruginosa* isolates would have aided our understanding of their presence and activity in strains associated with infection and poor clinical outcomes in patients with CF. This is a prerequisite for conducting phenotypic assays and profiling whether CDI systems are active in laboratory and clinical strains, and if disparate systems are expressed under different conditions and/or in the presence of specific competitors. Although due to the time frame these antibodies were not able to be validated as a tool to identify the CDI systems, there is still scope for providing a useful tool in future CDI studies. The inherent difficulty in trying to visualise large proteins such as the CdiA-NT, as well as conformation of the cloned recombinant region *in situ* means these antibodies require more troubleshooting than other smaller expressed proteins associated with large multi-protein complexes such as Hcp by T6SS (Allsopp *et al.*, 2017). The development of these antibody tools will be useful in informing our understanding of the utilisation of these systems in *P. aeruginosa* dominance during infection in polymicrobial settings. Such a specific antibody could also bind to the CdiA and potentially block/partially inhibit CdiA mediated delivery of the effector domain.

6. Determining the role of CDI and T6SSs in interbacterial competition between *P. aeruginosa* laboratory strains

6.1 Introduction

It is established in the literature that CDI and T6SS systems are encoded in *P. aeruginosa* and have been identified in clinical strain genomes from patients with cystic fibrosis (Mercy *et al.*, 2016; Allen *et al.*, 2020; Allsopp *et al.*, 2022; Robinson *et al.*, 2023). These systems are found in other virulent pathogens associated with CF such as *Burkholderia* species *dolosa* and *thailandensis*, as well as *Acinetobacter* spp. (Perault & Cotter, 2018; Lin *et al.*, 2022), where studies have shown their correlation with increased pathogenesis. The system diversity between strains observed upon genomic analyses of the same species from similar niches suggests a role for these systems in strain ecology (Allen & Hauser, 2019). This observation is reflected in studies from other physiological locations such as the gut via contact dependent competition systems in other bacterial species such as *Bacteroides* (Ross *et al.*, 2019b), with their role in ecology and consequently evolution believed to be mediated through the competitive mechanisms these systems employ. This is suggested to be mediated through the maintenance of 'immunity' genes that encode specific antidote proteins to prevent intoxication (Aoki *et al.*, 2010; Hood *et al.*, 2010) to control strain presence and consequently the composition of the polymicrobial community itself upon toxin deployment. If utilised by *P. aeruginosa*, it would allow control of the CF lung and indicate a major role in the dominance and strain succession observed in chronic infection (Flight *et al.*, 2015). However, the role of CDI in clinical strains of *P. aeruginosa* from CF patients remains to be elucidated.

P. aeruginosa is a highly competitive bacteria which has been shown to interact with other bacteria within its environment (Basler, Ho & Mekalanos, 2013). Most commonly associated with the T6SSs for interbacterial competition (Mougous *et al.*, 2006; Chen *et al.*, 2015; Allsopp *et al.*, 2020), its use of other competitive systems such as the CDI has been shown (Mercy *et al.*, 2016; Melvin *et al.*, 2017). The Mercy *et al.* 2016 study identified a role for CDI in PAO1 biofilm production and interbacterial competition. This supported the literature that a subset of the T5bSS is involved in contact-dependent inhibition (Guérin *et al.*, 2017) and indicated these systems may play a role in *Pseudomonas* spp. pathogenesis. Melvin *et al.* in 2017 showed an additional role for PAO1 CDI in swarming motility. These roles in biofilm production and motility indicate potentiation of bacterial cooperative capabilities or CDS (Ocasio & Cotter, 2019) which may impact *P. aeruginosa* behaviour. Although CDI presence is outlined within genomes of *Pseudomonas* species and other bacterial genera (Allen & Hauser, 2019; Cuthbert, Hayes & Goulding, 2022), most are yet to be validated experimentally. Increasing evidence associates the competitive systems with enhanced pathogenesis against the microbiota and host, driving research to determine their roles in infection- particularly in polymicrobial contexts (Allsopp *et al.*, 2020). Therefore confirming CDI roles in interbacterial competition in other *P. aeruginosa* strains is important in enhancing our understanding of their role in infection and dominance of the pulmonary environment in cystic fibrosis. Research into CDI competition has largely focussed on interbacterial competition (Aoki *et al.*, 2010). Therefore, determining any roles in intrabacterial competition would be pertinent in understanding dominance in CF and is yet to be shown experimentally.

6.2 Aims of this study

From the current literature and based on the results confirming the functionality of the *P. aeruginosa* strain PA14 CDI systems toxin-immunity modules outlined in Chapter 4 of this thesis, I have one major hypothesis to address in this chapter:

CDI systems of *P. aeruginosa* influence motility, biofilm production and competition

This chapter summarises research conducted to enable the validation of the role of the two CDI systems in *P. aeruginosa* strain PA14 in inter- and intrabacterial competition through addressing the following aims:

1. Conducting swimming motility assays using constructed WSDM strains
2. Conducting swarming motility assays using constructed WSDM strains
3. Conducting crystal violet biofilm production assays using constructed WSDM strains
4. Conducting interbacterial competition assays via *lacZ*, fluorescence and antibiotic resistance reporter systems
5. Conducting intrabacterial competition assays with other common CF pathogens

6.3 Results

6.3.1 CDI systems in P. aeruginosa strain PA14 do not play a role in motility

Bacteria can move via the use of various appendages. The flagella is one such appendage which enables two types of movement; swimming due to flagellar movement and swarming

due to a QS group-mediated movement response (previously outlined in 1.3). Motility is a mechanism often used to indicate altered gene expression as it is controlled through the Gac/Rsm and c-di-GMP regulons (Goodman *et al.*, 2004; Merritt *et al.*, 2007; Martínez-Granero *et al.*, 2012), which control multiple virulence mechanisms bacteria employ during infection. Research to date has shown PAO1 CDI systems play a role in bacterial swarming motility (Melvin *et al.*, 2017). Melvin *et al.* showed enhanced motility in ΔCDI^{PA0041} strains, a system in PAO1 homologous to CDI^{00510} in PA14 studied here, indicating CDI systems are associated with negative post-transcriptional regulation of motility as deletion of the system increased motility in a 24 hr time-dependent assay. However, the role of CDI systems in influencing motile capabilities other *Pseudomonas* genera or *P. aeruginosa* strains is yet to be determined. Therefore I set out to determine the role of CDI systems from PA14 in motility here. Based on WSDMs constructed in Chapter 4, swimming and swarming assays were conducted to validate their role in PA14 CDI systems. Confirming a role for these systems in motility will support a species-related role in controlling bacterial motility.

First swimming assays were conducted to assess whether CDI systems affect flagella-based motility. Using low percentage agar to enable flagellar-based movement through the agar, strains were inoculated and left to incubate for 24 hrs at 37 °C (Figure 6.1). From this, photographs were taken and swimming motility area after 24 hrs was calculated using ImageJ processing software (Schneider, Rasband & Eliceiri, 2012). Control strains *flgK, flgKpilA* and *pilA* used validated the experimental conditions. No significant difference in swimming motility in the CDI WSDM single or double mutants was observed compared with their respective parent strain backgrounds in all cases (Figure 6.2). A significant difference was observed between PA14/H123 and *rsmA*/ *rsmA*H123 strain backgrounds, which was expected

as *rsmA* deletion has been shown to negatively regulate flagellar formation and biofilm formation (Irie *et al.*, 2020). Although no differences were observed in flagellar-based swimming motility assays for the CDI WSDMs, the next step was to determine whether these systems played a role in group-mediated swarming motility.

Swarming assay was repeated as per the swimming assay, instead using low percentage and nutrient agar to enable group-mediated movement over the agar (Figure 6.3). No significant difference in swarming motility was observed in the CDI WSDM single or double mutants compared with their respective parent strain backgrounds in all cases (Figure 6.4). Again, a significant difference was observed between PA14 and *rsmA*/ *rsmA*H123 strain backgrounds, which was expected as *rsmA* deletion has been shown to reduce swarming motility (Miller *et al.*, 2016). Having determined PA14 CDI systems do not play a role in motility, their role in biofilm formation was then assessed.

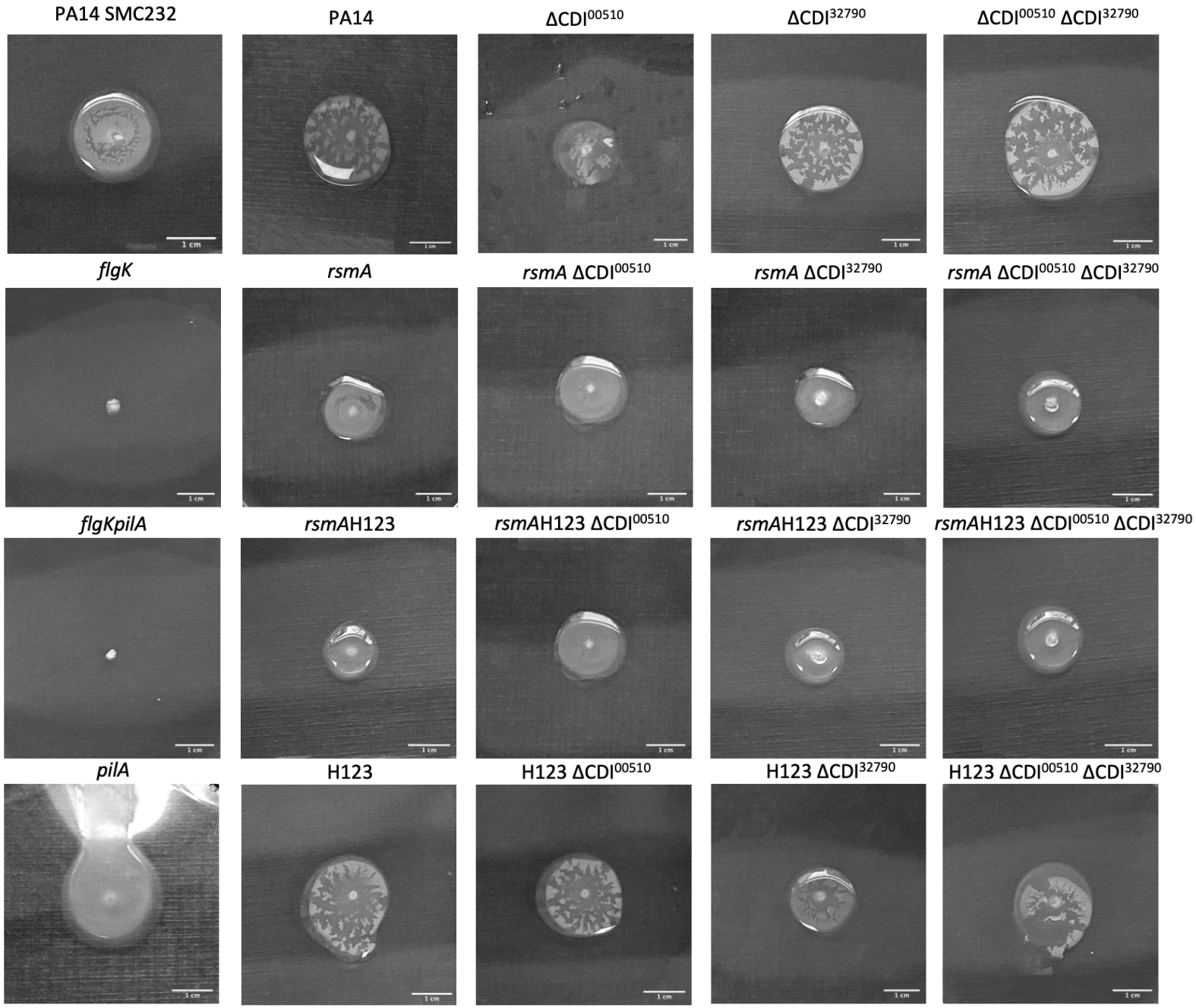


Figure 6.1: Swimming motility of *cdiBAI*^{00510} and *cdiBAI*^{32790} whole system deletion mutants in the background strains. Image for each strain indicates swimming motility area covered after 24 hrs. Flagellar and pili mutants (*flgK, pilA, flgKpilA*) were included in the strain panel as controls for altered motility. It is published that under these conditions the flgK mutants should be most impaired. Note: PA14 SMC232, *flgK*, *flgKpilA* and *pilA* are George O'Toole lab strains for baseline (O'Toole & Kolter, 1998), high and low motility controls. White scale bar is 1 cm.

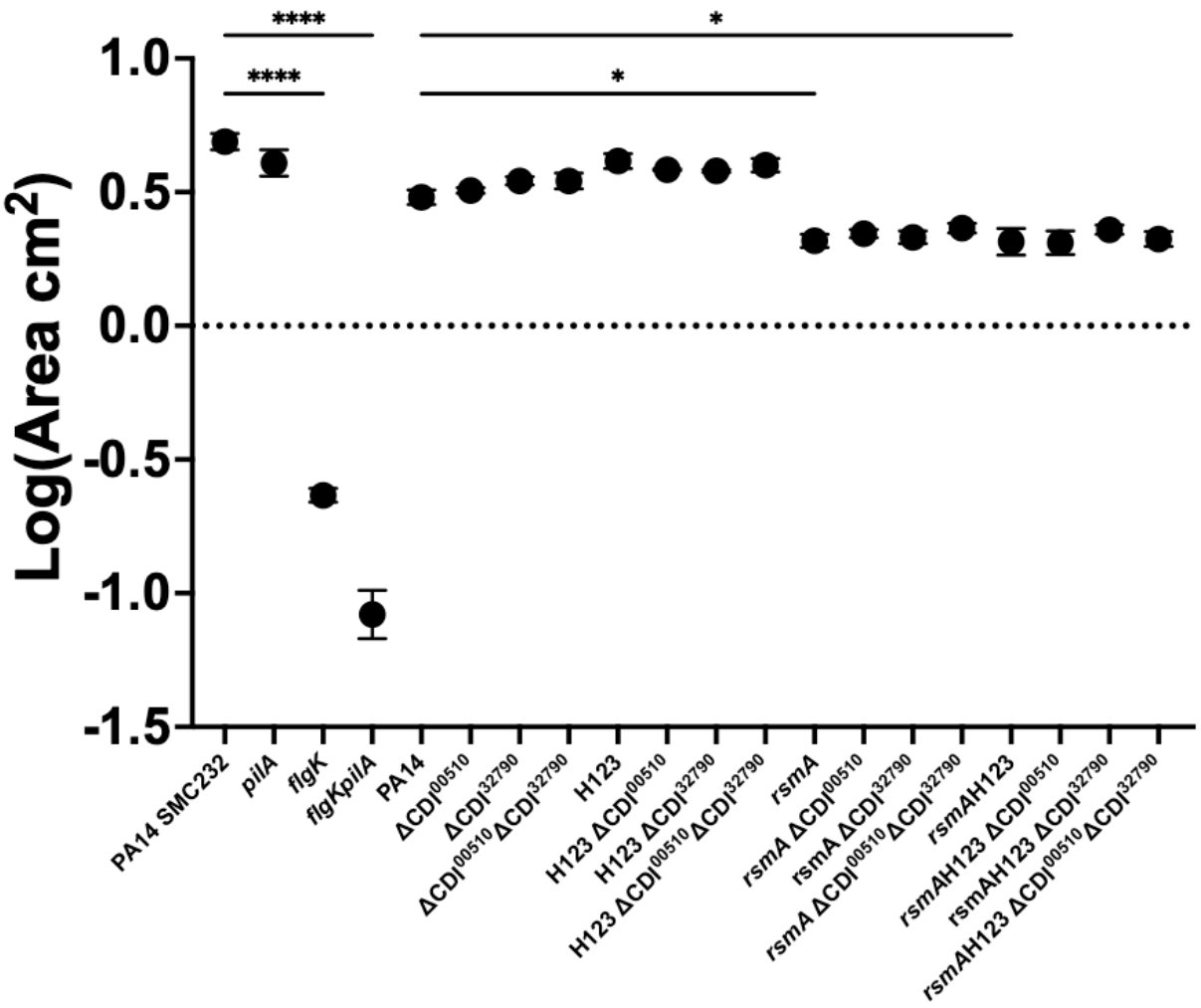


Figure 6.2: Deletion of *cdiBAI*^{00510} and *cdiBAI*^{32790} has no effect on swimming motility. Graph showing motility area after 24hr incubation. Average motility area of three assay replicates and standard error are indicated above. A One-Way ANOVA was performed on the log transformed average areas for each strain, statistically significant for 24 hrs motility to ****P<0.0001. Post-hoc statistical significance of CDI mutant motility compared with those of WT strain were determined using Šídák's test (n=3, six technical replicates). Note: PA14 SMC232, *flgK*, *flgKpilA* and *pilA* are George O'Toole lab strains for baseline (O'Toole & Kolter, 1998), high and low motility controls separate to the Allsopp lab and whole system deletion mutant strains. No significant difference was observed in swimming motility for CDI deletion mutant strains.

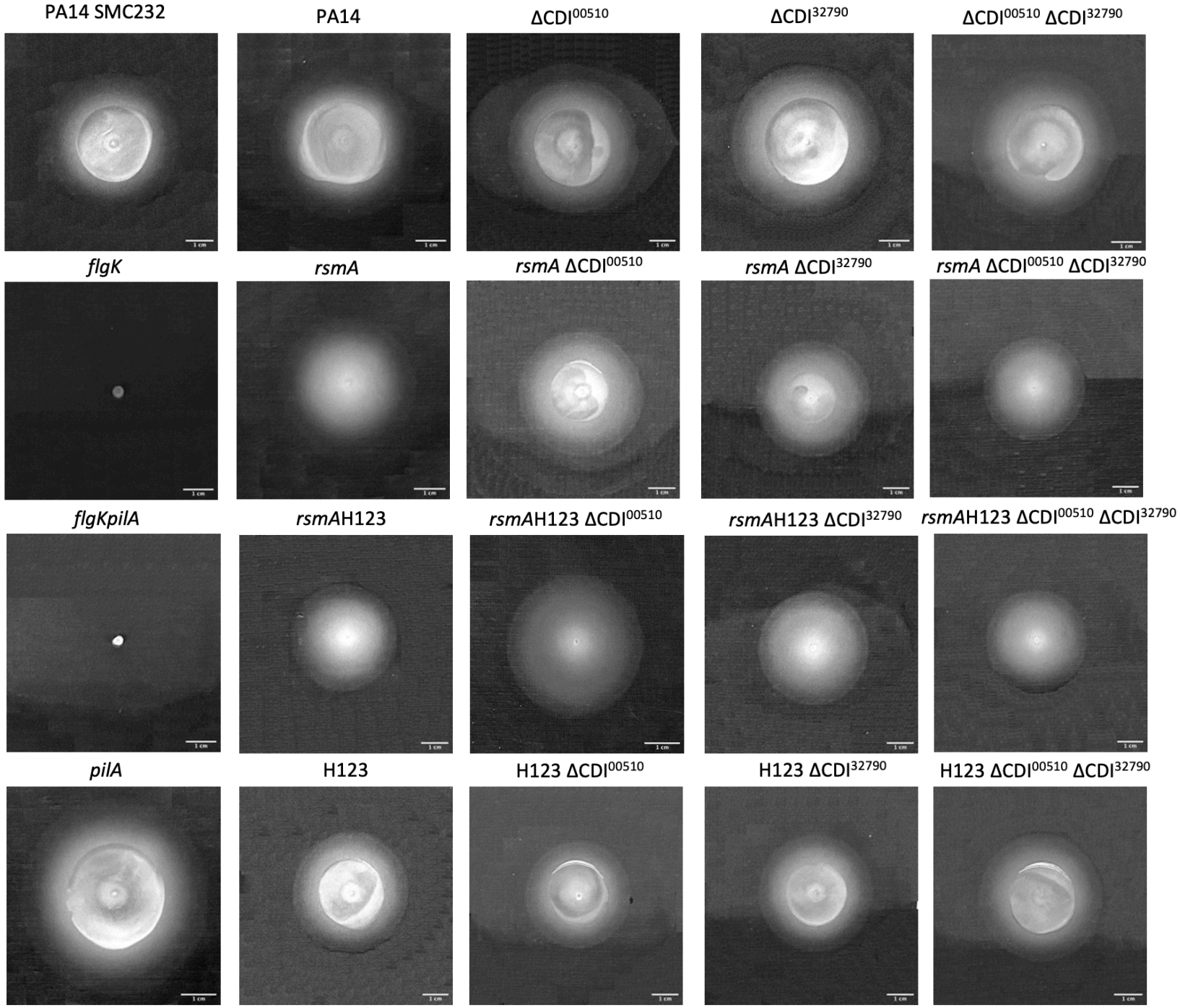


Figure 6.3: Swarming motility of *cdiBAI*^{00510} and *cdiBAI*^{32790} whole system deletion mutants in their respective background strains. Image for each strain indicates swarming motility area covered after 24 hrs. Flagellar and pili mutants (*flgK, pilA, flgKpilA*) were included in the strain panel as controls with altered motility. Note: PA14 SMC232, *flgK*, *flgKpilA* and *pilA* are George O'Toole lab strains for baseline (O'Toole & Kolter, 1998), high and low motility controls separate to the Allsopp lab and whole system deletion mutant strains.

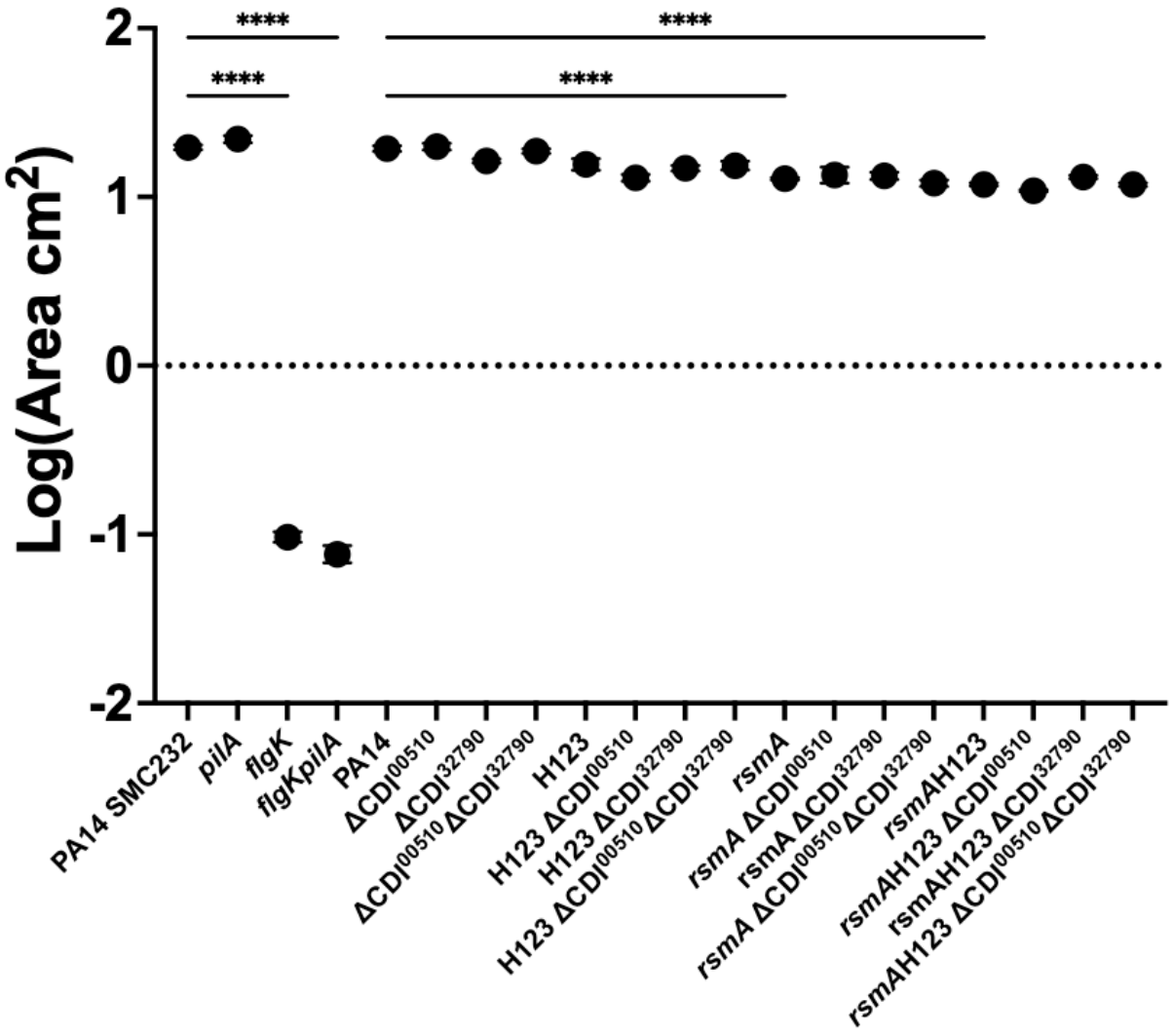


Figure 6.4: Deletion of *cdiBAI*^{00510} and *cdiBAI*^{32790} has no effect on swarming motility. Graph showing motility area after 24hr incubation. Average area of three assay replicates and standard error are indicated above. One-Way ANOVA was performed on the log transformed average areas for each strain, statistically significant for 24 hrs motility to ****P<0.0001. Post-hoc statistical significance of CDI mutant motility compared with those of WT strain were determined using Šídák's test (n=3, six technical replicates). Note: PA14 SMC232, *flgK*, *pilA* and *flgKpilA* are George O'Toole lab strains for motility controls (O'Toole & Kolter, 1998). No significant difference was observed in swarming motility for CDI deletion mutant strains.

6.3.2 CDI systems in P. aeruginosa strain PA14 do not play a role in biofilm formation

Biofilms are groups of bacterial cells within a protective polysaccharide-based matrix for protection and prevention of cell death via desiccation and antibiotic therapy (Sharma, Misba & Khan, 2019). Biofilm production is a mechanism linked to motility via an inverse regulatory relationship (Guo *et al.*, 2014) as well as being under various other regulators such as c-di-GMP and sRNAs (Fazli *et al.*, 2014). Therefore it is another commonly used indicator of coregulation with other virulence mechanisms by its association with infection establishment (Singh *et al.*, 2000; Liao *et al.*, 2022). Previous research showed reduced biofilm formation in ΔCDI^{0041} and ΔCDI^{2462} strains indicating both PAO1 CDI play a role in biofilm formation (Mercy *et al.*, 2016). This same effect is observed in other CDI-encoding bacterial pathogens (Garcia *et al.*, 2013; Ruhe *et al.*, 2015; Roussin *et al.*, 2019) suggesting a conserved mechanism. However, the role of CDI systems in biofilm formation in other *P. aeruginosa* strains remains to be evaluated. Here I assessed the role of the two CDI systems from PA14.

A 24 hr 96 well crystal violet assay was conducted at 37 °C (Pardee, 1959; O'Toole & Kolter, 1998). Biofilms were stained with Crystal violet and washed before elution with ethanol and OD readings were taken and averaged to determine mean biofilm production per strain (Figure 6.5). No significant difference in biofilm production was observed with most CDI WSDMs compared with the WT. A significant difference was observed between *rsmA* compared with WT. This was expected as RsmA negatively regulates biofilm production (Irie *et al.*, 2020). For this reason a significant difference was also expected in the *rsmA*H123 strain background but was not observed here. Therefore, the experiment was redesigned using a randomised well format to compensate for confounding factors such as oxygen gradients and

variations in volatile compound production from other strains within the plate (Chapter 2 method 2.14). Figure 6.6 showed no significant difference in biofilm production with most CDI WSDMs compared with the WT. A significant difference was observed between *rsmA* and *rsmAH123* strain backgrounds compared with WT/H123, aligning with the expected result based on the literature (Irie *et al.*, 2020). The only other significant difference observed was between *rsmA* and *rsmA* ΔCDI^{32790} which indicates the second CDI system may play a role in biofilm production via *rsmA*-mediated negative regulation. However, as this result was not observed in the double ΔCDI^{00510}ΔCDI^{32790} strain or in other strain backgrounds it may not be a biologically significant result.

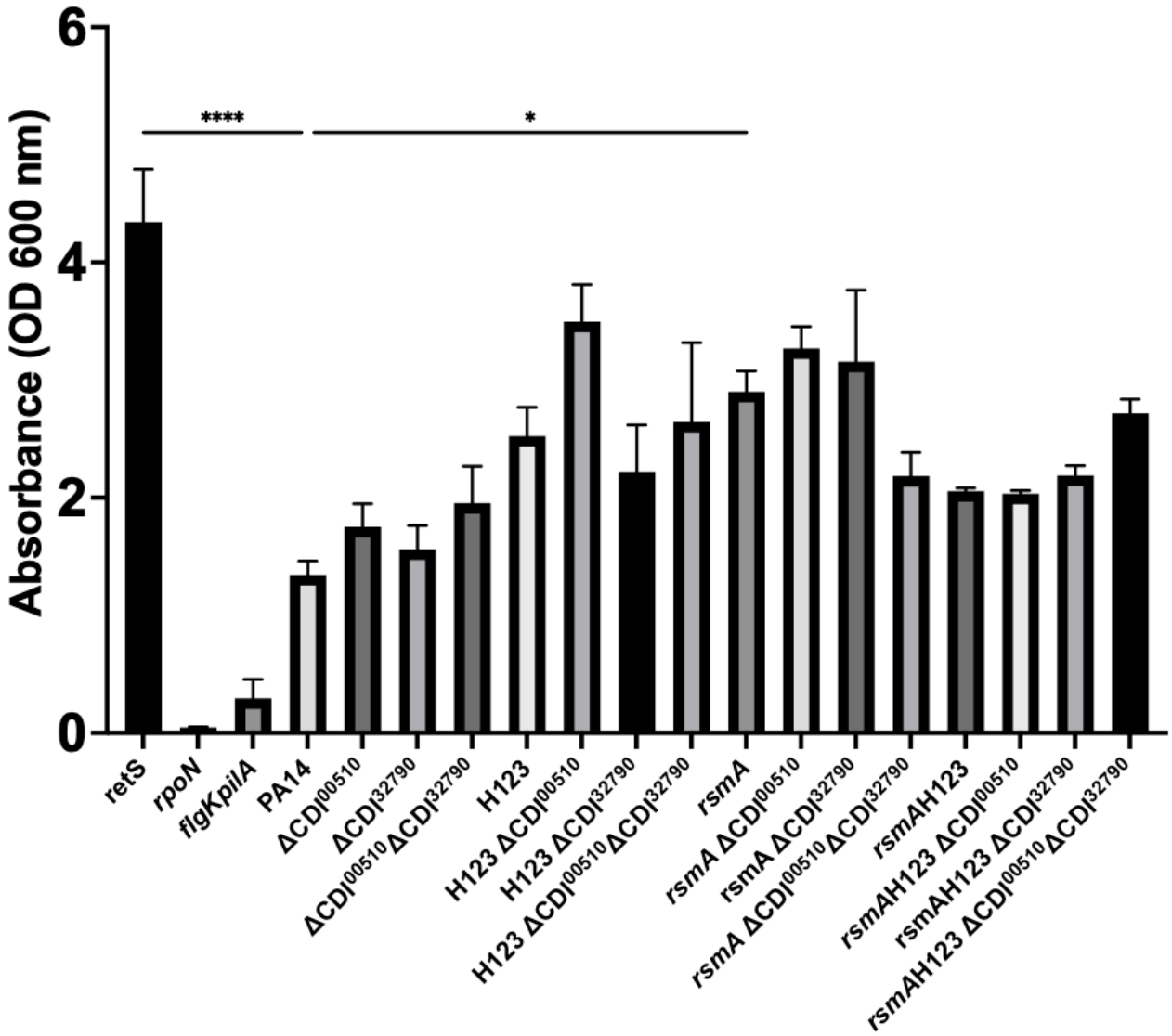


Figure 6.5: Deletion of *cdiBAI*^{00510} and *cdiBAI*^{32790} has no effect on biofilm biomass production. Graph showing biofilm biomass produced after 24hr incubation. Average area of three assay replicates and standard error are indicated above. A One-Way ANOVA was performed on the average absorbance for each strain, statistically significant for 24 hrs biofilm production to ****P<0.0001. Post-hoc statistical significance of CDI mutants compared with those of WT strain were determined using Šídák's test (n=6, seven technical replicates). A flagellar and pili (*flgKpilA*) and sigma factor (*rpoN*) mutant were included in the strain panel as low biofilm producing controls. A histidine kinase (*retS*) mutant was included in the strain panel as a high biofilm producing control.

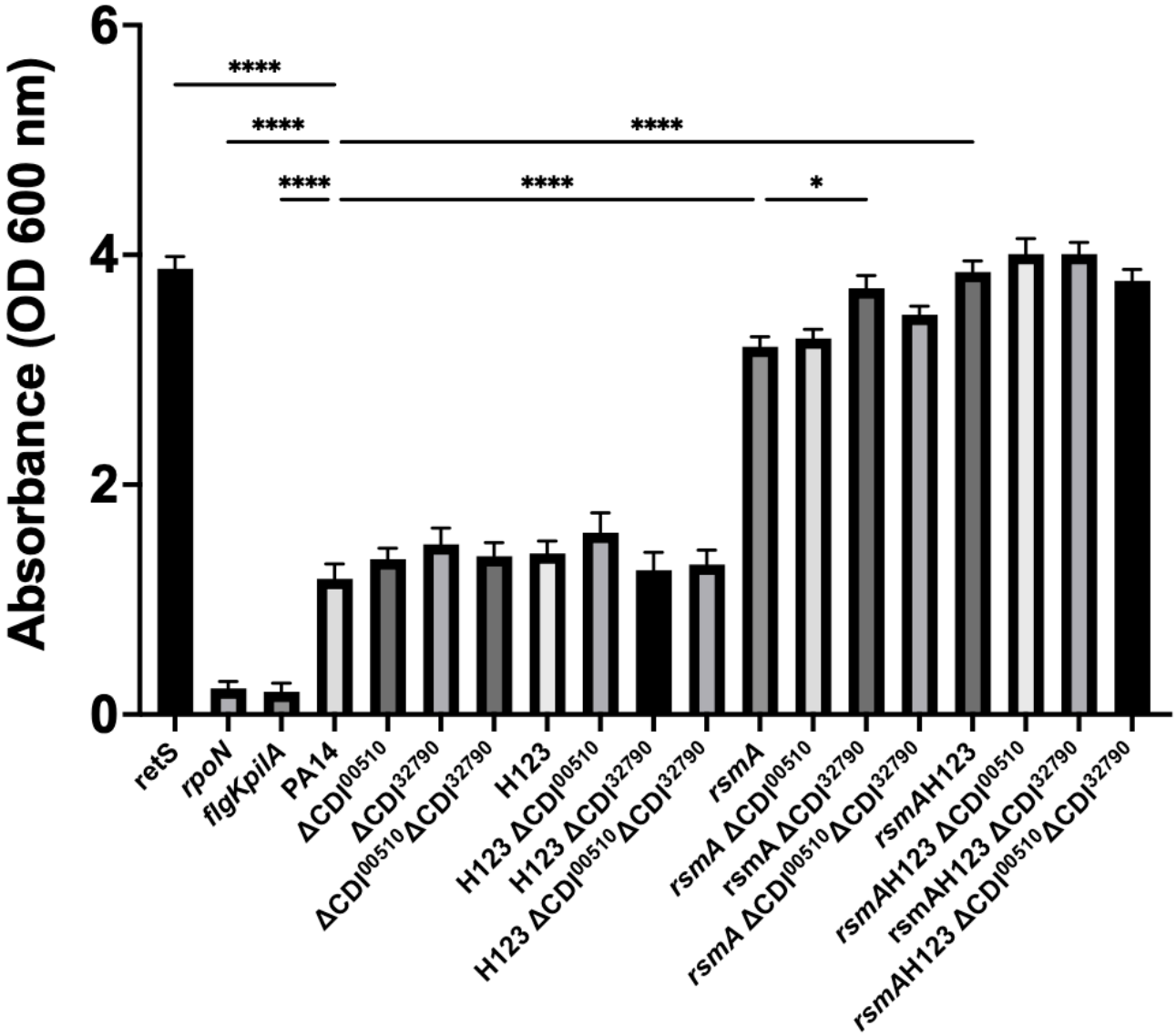


Figure 6.6: Randomised well format confirms deletion of *cdiBAI*^{00510} and *cdiBAI*^{32790} has no effect on biofilm biomass production. Graph showing biofilm biomass produced after 24hr incubation. Average area of six assay replicates and standard error are indicated above. A One-Way ANOVA was performed on the average absorbance for each strain, statistically significant for 24 hrs biofilm production to ****P<0.0001. Post-hoc statistical significance of CDI mutants compared with those of WT strain were determined using Šídák's test (n=6, seven technical replicates). A flagellar and pili (*flgKpilA*) and sigma factor (*rpoN*) mutant were included in the strain panel as low biofilm producing controls. A histidine kinase (*retS*) mutant was included in the strain panel as a high biofilm producing control.

6.3.3 Both CDI systems in P. aeruginosa strain PA14 play a role in interbacterial competition

CDI systems are a subset of the T5SS associated with interbacterial competition (Aoki *et al.*, 2005, 2010). Therefore the presence and activity of these systems may be an indicator of a conserved mechanism contributing to niche dominance and influencing niche dynamics during infection. Mercy *et al.* was able to show a competitive role for both systems CDI^{0041} and CDI^{2462}, which was enhanced in a *rsmA* strain background- identifying RsmA as a negative regulator. Therefore, the role of the two PA14 CDI systems in interbacterial competition was determined here. Characterising a role for these systems in competition will support the Mercy *et al.* study from 2016 that *P. aeruginosa* uses CDI as a mechanism for interbacterial competition which may shed light onto whether these conserved systems are actively utilised in infection establishment and niche dominance. Furthermore the use of the T6SS system mutants may also reveal an interplay between the systems as a H123 $\Delta CDI^{00510}\Delta CDI^{32790}$ strains should have all known contact dependent killing systems deleted or inactivated (note not all T6SS toxin-immunity pairs were removed, rather the three structural T6SS operons, H1-, H2- and H3-T6SS, have been truncated rendering them inactive).

Using the WSDM strain panel constructed in 4.3.2 of this thesis, competition was initially assessed by competing PA14::*lacZ* WT attacker against the entire panel (Figure 4.4) as prey strains. Bacteria were mixed in a 1:1 ratio and left to compete on an agar plate for 24 hrs at 37 °C. Counting blue vs white colonies on X-gal plates enabled calculation of a competitive index from the output vs input attacker:prey ratio and averaged over three repeats (Figure 6.7). In this assay a competitive index of 1 means no competition whilst >1 means attacker is outcompeting the prey. Broadly these results show the competitive effect is higher against

the *rsmA* strain background, supporting the Mercy *et al.* 2016 study. This was negated in the *rsmA*H123 background, indicating the competitive effect observed may be mediated by the T6SSs which are still active and upregulated in the *rsmA* background (Mercy *et al.*, 2016; Allsopp *et al.*, 2017). For the PA14 and H123 mutant strain backgrounds, a significantly enhanced competitive index was observed for the ΔCDI^{00510} and ΔCDI^{00510}ΔCDI^{32790} strain backgrounds, indicating CDI^{00510} plays a role in interbacterial competition. As this effect was observed for both PA14 and H123 strain backgrounds, this indicates the effect observed was not due to the T6SSs. No significant differences were observed for the *rsmA* strain background. Although, for the *rsmA*H123 strain background a significant increase was observed for *rsmA*H123 ΔCDI^{00510}ΔCDI^{32790}. This effect can be attributed to the complete lack of competitive system expression within the prey.

Upon incubation of the X-gal plates (Figure 6.8), a difference in blue colouration was observed at higher dilutions indicating potential attacker repression which did not reflect the competitive effects represented in Figure 6.7. As CDI is contact dependent with the toxins pertaining to intercellular targets that could be bacteriostatic (Aoki *et al.*, 2010; Poole *et al.*, 2011), this assay may have missed the true competitive effect by enabling recovery in the lower cell densities. Figure 6.8a shows increased blue (attacker) for ΔCDI^{00510} indicating it is outcompeted. This was observed in ΔCDI^{00510}ΔCDI^{32790} whilst ΔCDI^{32790} had no observable difference and indicates that CDI^{00510} plays a role in interbacterial competition. For *rsmA* prey strains, increased blue colouration is observed for all CDI deletions indicating they are outcompeted and both systems play a role in interbacterial competition. Figure 6.8b shows increased blue (attacker) for all *rsmA*H123 CDI deletion strains indicating they are all outcompeted. Blue colouration is particularly enhanced in the *rsmA*H123 ΔCDI^{32790} and

*rsmA*H123 ΔCDI^{00510}ΔCDI^{32790} indicating that both systems play a role in interbacterial competition but CDI^{32790} outlines an enhanced role. For H123 prey strain, increased blue colouration is observed for all CDI deletions indicating both systems play a role in interbacterial competition. As previous studies have shown a role for CDI in *P. aeruginosa* in interbacterial competition (Mercy *et al.*, 2016), and the results for the *rsmA*H123 background did not follow the expected result (Figure 6.7), the experiment was then redesigned to incorporate GFP-tagged WSDMs to investigate prey survival further.

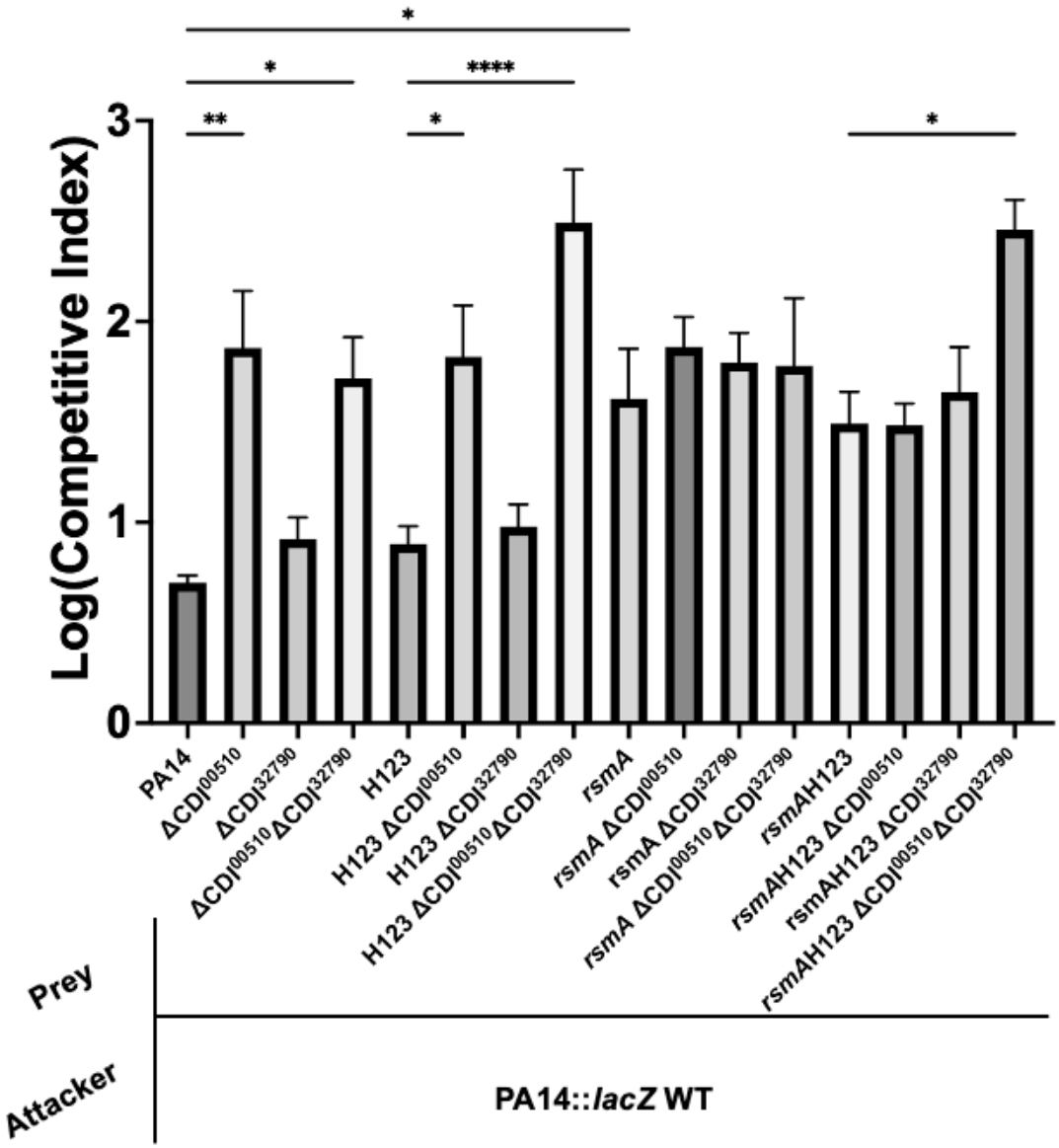


Figure 6.7: Deletion of *cdiBAI*^{00510} in the PA14 backgrounds but not in the *rsmA* backgrounds render prey susceptible to killing by PA14::*lacZ* WT attacker. Graph showing competitive index after 24hr competition. A

value of 1 indicates no competitive difference. Average colony count of three replicates for each competition and standard error are indicated above. For PA14 and H123 strain backgrounds, statistically significant competitive indices are observed for ΔCDI^{00510} and ΔCDI^{00510} ΔCDI^{32790} strains indicating a role for CDI^{00510} in competition. No statistically significant competitive indices were observed for the *rsmA* strain background. For the *rsmA*H123 strain background, statistically significant competitive index is observed for the *rsmA*H123 ΔCDI^{00510} ΔCDI^{32790} strains, indicating a competitive effect is observed when prey have all competitive systems removed. A One-Way ANOVA was performed on these counts for each competition, statistically significant for 24 hrs competition to ****P<0.0001. Post-hoc statistical significance of CDI mutant competitions compared with those with WT strain were determined using Šídák's test (n=3, three technical replicates).

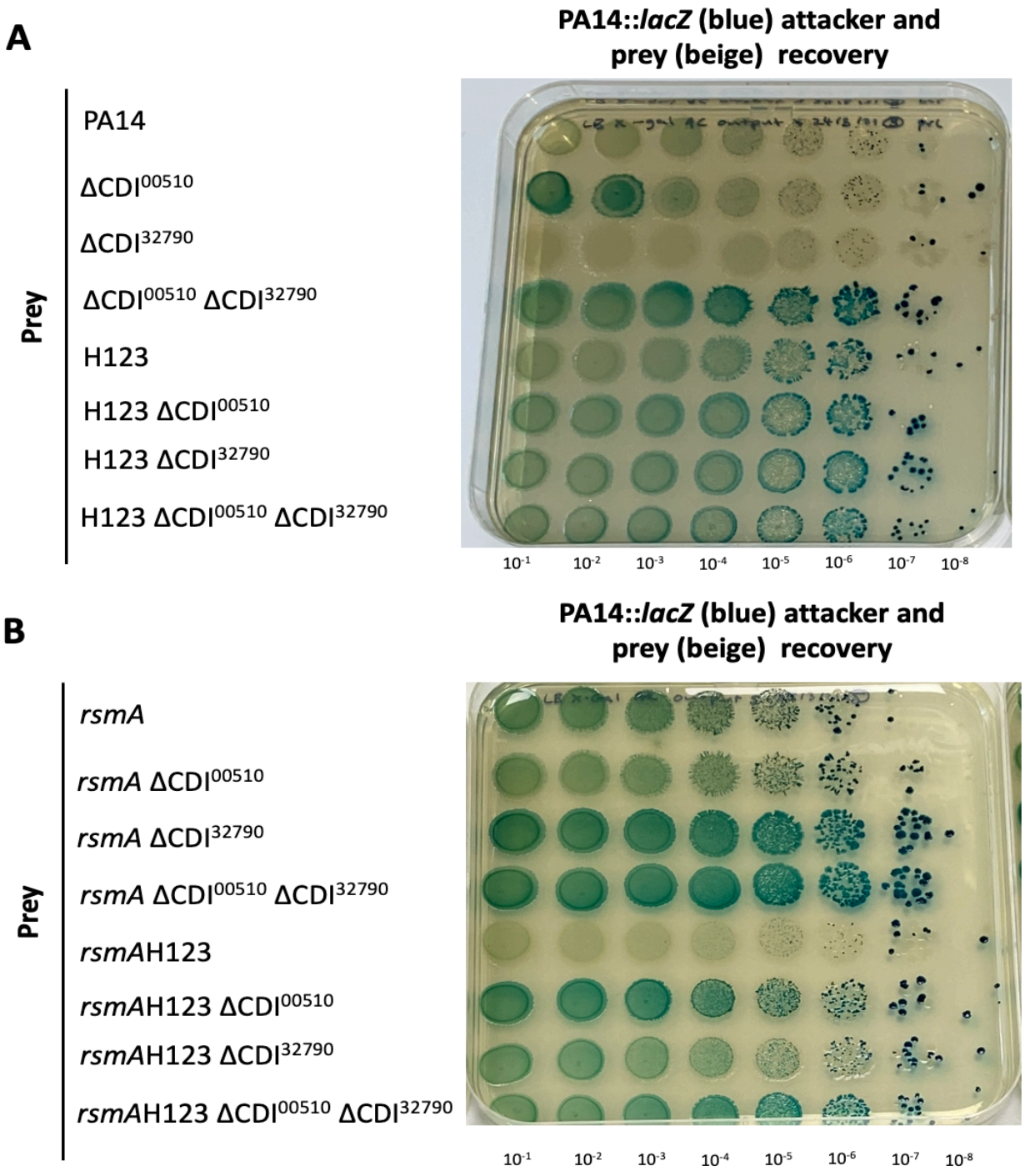


Figure 6.8: X-gal based competition assays show a role for both CDI systems dependent on the strain background used. Images showing output plates from competition of CDI mutant prey strain against a PA14::*lacZ* attacker strain. The more vivid blue the colony, the higher the better the attacker is doing. Red boxes for each panel highlights competition dilutions of 10^{-2} discussed here in relation to attacker vs prey strain survival. Different blue intensities between different prey strain competitions are observed at this higher dilution. This experimental approach delivers different results from those outlined in Figure 6.6. (A) PA14::*lacZ* (blue) vs PA14 (beige) WT strains show a more intense blue when attacker competes with Δ00510 prey. This

indicates more attacker is present suggesting the attacker is killing more prey that is dependent upon the presence and absence of the CDI^{00510} system. This is not seen with ΔCDI^{32790} but is for the ΔCDI^{00510} ΔCDI^{32790} prey. PA14::*lacZ* (blue) vs *rsmA* (beige) strains show a more intense blue against all *rsmA*ΔCDI mutant prey strains compared with *rsmA* prey strain. This indicates more attacker is present suggesting the attacker is killing more prey with either or both CDI systems removed. This shows a role for both systems in competition. (B) PA14::*lacZ* (blue) vs *rsmA*H123 (beige) strains show a more intense blue when attacker competes with ΔCDI^{32790} prey. This indicates more attacker is present suggesting the attacker is killing more prey. This is not seen with ΔCDI^{00510} but is for the ΔCDI^{00510} ΔCDI^{32790} prey. This shows a clear result for the CDI^{32790} system but not for CDI^{00510} which is unexpected. PA14::*lacZ* (blue) vs H123 (beige) strains show a more intense blue when attacker competes with all prey. This indicates more attacker is present suggesting the attacker is killing more prey. Therefore in the WT and H123 settings CDI^{00510} appears to be expressed and playing a role in competition in this setting suggesting the immunity CdiI^{00510} is required. For the *rsmA*H123 setting CDI^{32790} appears to be expressed and playing a role in competition in this setting suggesting the immunity CdiI^{32790} is required. However for the *rsmA* setting both CDI^{00510} and CDI^{32790} appear to be expressed and playing a role in competition suggesting both immunities are required. This indicates both systems in conjunction with *rsmA* are important in interbacterial competition in this setting and shows differential expression/dependence upon these systems depending on the attacker.

Three partner conjugation was used to fluorescently tag the WSDM prey strains via the mini-Tn7:GFP vector. The killing assay was repeated as per the *lacZ* assay, however after 24 hr incubation of output dilution series spot plates the 10^{-2} dilution was recovered and resuspended in LB before inputting samples into a black 96-well plate and measuring the fluorescence of the prey. This method was adapted from similar assays outlined in three studies; Hachani *et al.* 2014 and Pissaridou and Allsopp *et al.* 2018. This was used to evaluate CDI mutant prey strain survival at higher bacterial cell densities where competition is sustained for the following 24hrs in the diluted output spot. From the fluorescence measured, average fluorescence was determined over three repeats (Figure 6.9). Figure 6.9a shows

reduced fluorescence for ΔCDI^{00510} and ΔCDI^{00510}ΔCDI^{32790} indicating they are outcompeted and that CDI^{00510} plays a role in interbacterial competition, supporting the results from Figure 6.7. Figure 6.9b shows reduced fluorescence for H123 ΔCDI^{00510}, H123 ΔCDI^{32790} and H123 ΔCDI^{00510} ΔCDI^{32790}. This supports the results from Figure 6.7 and indicates CDI^{00510} plays a role in interbacterial competition. Unlike the previous results, an additional role is observed for H123 ΔCDI^{32790} at higher cell densities, indicating both systems play a role in interbacterial competition. This difference between PA14 and H123 for ΔCDI^{32790} was unexpected and will be commented upon in the discussion. For the *rsmA* and *rsmA*H123 strain backgrounds (Figure 6.9c-d), no significant differences in fluorescence levels were observed. As the PA14 strain appears to exhibit increased survival compared with *rsmA*, this indicates survival is not dependent on CDI systems. However, comparing *rsmA* with *rsmA*H123 prey, an increased level of fluorescence indicates removal of H123 enables PA14 to have a marginally increased survival. The significant difference in competition observed in Figure 6.7 with *rsmA*H123 ΔCDI^{00510}ΔCDI^{32790} was no longer observed. However, as the attacker strain still contained all competitive systems, this may be a confounding factor masking the true effect of each CDI. The assay was redesigned again using the WSDMs as attacker strains and double CDI mutants as the prey.

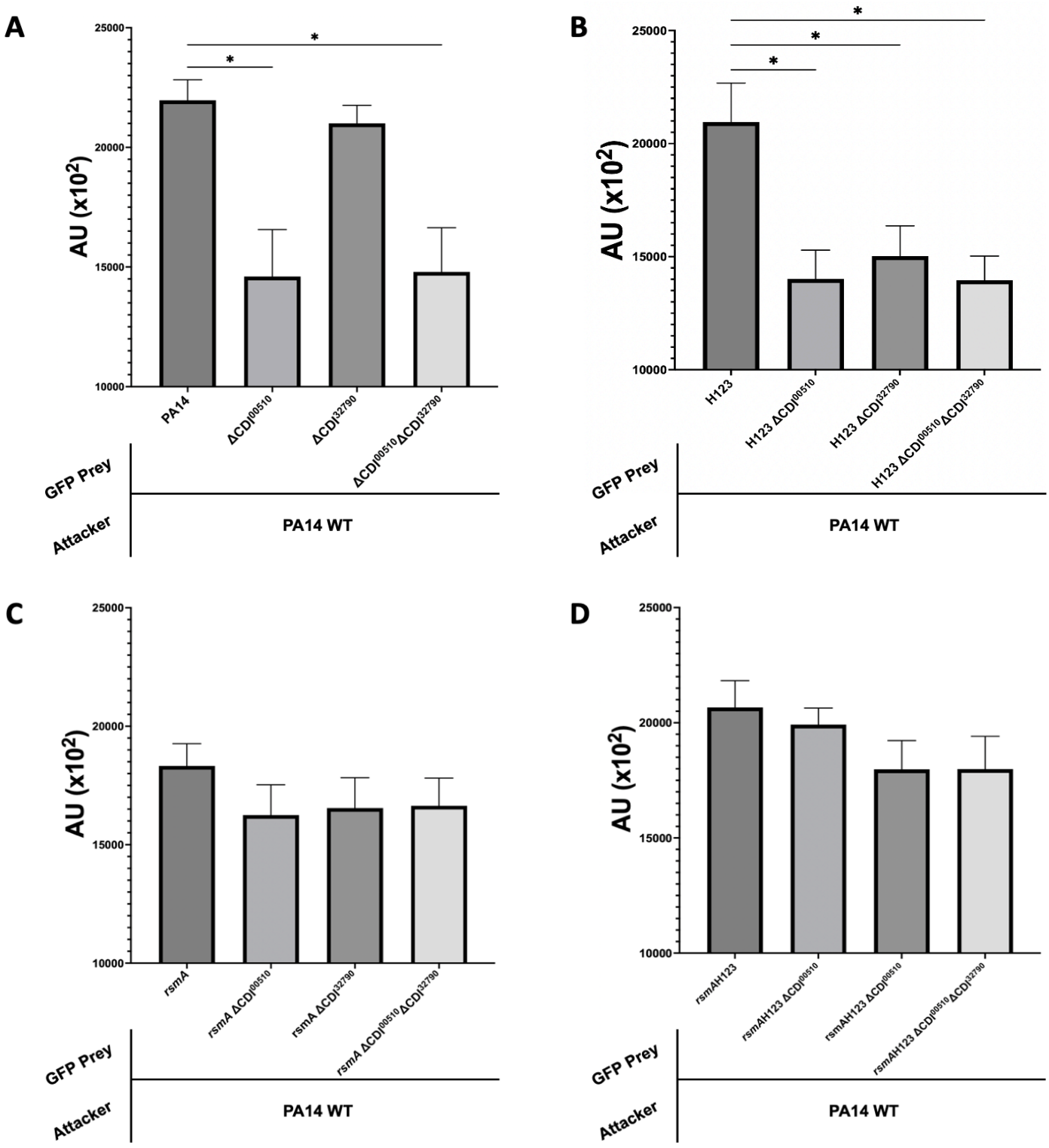


Figure 6.9: Deletion of *cdiBAI*^{00510} in the PA14 background and deletion of *cdiBAI*^{000510} and *cdiBAI*^{32790} in the H123 background but not in the *rsmA* and *rsmA*H123 backgrounds render prey susceptible to killing by PA14 WT attacker. Graph showing fluorescence levels (AU = 1300) of attacker strains after 24hr competition. Average fluorescence of four replicates for each competition and standard error are indicated above. (A) PA14 strain

background shows statistically significant reduction in fluorescence for ΔCDI^{00510} and ΔCDI^{00510} ΔCDI^{32790} strains indicating a role for CDI^{00510} in competition. (B) H123 strain background shows statistically significant reduction in fluorescence for H123 ΔCDI^{00510}, H123 ΔCDI^{32790} and H123 ΔCDI^{00510} ΔCDI^{32790} strains indicating a role for CDI^{00510} and CDI^{32790} in competition. (C-D) No statistically significant differences in fluorescence were observed for *rsmA* and *rsmA*H123 strain backgrounds. A One-Way ANOVA was performed on these counts for each competition, statistically significant for 24 hrs competition to ****P<0.0001. Post-hoc statistical significance of CDI mutant competitions compared with those with WT strain were determined using Šídák's test (n=4, three technical replicates).

Three partner conjugation was used to transfer pBBR-MCS5 gentamycin resistant plasmid into PA14 ΔCDI^{00510}ΔCDI^{32790} prey strain to selectively isolate prey to determine survival directly. The killing assay was repeated the same as the previous, with several notable differences. Based on the protocol outlined by the Mercy *et al.* study from 2016, strains were initially subcultured to OD 0.1 and grown to OD 0.3 at 32 °C – a physiologically relevant temperature for the lungs (McFadden *et al.*, 1985; Khosravi *et al.*, 2021). Post competition, prey were recovered on gentamycin 50 µg/ml plates, where colonies were counted over three repeats conducted three times (Figure 6.10). A significant reduction in prey survival was observed between *rsmA* and *rsmA*H123 strain backgrounds compared with WT which was expected as per reasons previously stated (Mercy *et al.*, 2016; Allsopp *et al.*, 2017). Therefore deletion of *rsmA* in these strains upregulates the competitive systems increasing killing. For the PA14 strain background, prey survival was enhanced for ΔCDI^{00510} and ΔCDI^{00510}ΔCDI^{32790} supporting the previous results observed in Figure 6.7, 6.8 and 6.9, indicating CDI^{00510} plays a clear role in interbacterial competition. For the H123 strain background, prey survival was enhanced for H123 ΔCDI^{00510}, H123 ΔCDI^{00510} and H123 ΔCDI^{00510}ΔCDI^{32790} in an additive manner. This indicates both systems play a role in interbacterial competition, supporting the

results observed in 6.8D and 6.9B. This indicates a compensatory effect is observed in the PA14 ΔCDI^{32790} prey strain which may be actively using the T6SSs masking the true effect observed in H123 and *rsmA*H123 strain backgrounds. Strikingly, we could clearly see competitive differences absent in Figures 6.7 and 6.9 but observed in Figure 6.8. For example when using the *rsmA* strain background as the attackers, prey survival was enhanced against *rsmA* ΔCDI^{00510}, *rsmA* ΔCDI^{32790} and *rsmA* ΔCDI^{00510}ΔCDI^{32790} indicating both systems play a role in interbacterial competition. However, the results here show prey survival against *rsmA* ΔCDI^{00510} and *rsmA* ΔCDI^{00510}ΔCDI^{32790} was recovered to a similar level compared with *rsmA* ΔCDI^{32790} and not to the level of ΔCDI^{00510}ΔCDI^{32790} strains from the other backgrounds. A potential explanation could be due to the T6SSs in this strain background being upregulated resulting in a compensatory competitive effect but could not be fully elucidated within this assay. However, it is an unexpected result I cannot fully explain. Finally, for the *rsmA*H123 strain background, prey survival was enhanced for *rsmA*H123 ΔCDI^{32790} and *rsmA*H123 ΔCDI^{00510}ΔCDI^{32790}. However survival was not enhanced for the *rsmA*H123 ΔCDI^{00510}. This indicates CDI^{32790}, but not CDI^{00510}, plays a role in interbacterial competition. Therefore both CDI systems appear to play a role in interbacterial competition in PA14, with a potential interplay between post-transcriptional regulation via RsmA and the T6SSs. This assay was repeated using a H123 ΔCDI^{00510} ΔCDI^{32790} pBBR-MCS5 prey strain to determine whether some of the competitive effect observed was partly influenced by the presence of the active T6SSs in this prey background (Figure 6.11).

In Figure 6.11 a significant difference was observed between *rsmA* and *rsmA*H123 strain backgrounds compared with WT which was expected as per reasons previously stated (Mercy *et al.*, 2016; Allsopp *et al.*, 2017). The results here mimic those observed in Figure 6.10

indicate the results observed were due to the CDI alone and were not influenced by the T6SSs in this context. In summary, both CDI systems appear to play a role in interbacterial competition in PA14 dependent upon the genetic mutants used. A potential interplay was observed between post-transcriptional regulation via RsmA and the T6SSs. Having determined the role of CDI systems in interbacterial competition, the next step was to determine their role in intrabacterial competition with other pathogens commonly associated with CF infection. However, due to project time constraints, the intrabacterial competition experiments were terminated before the assay could undergo trouble shooting and therefore this aim was not addressed within this thesis (data not shown).

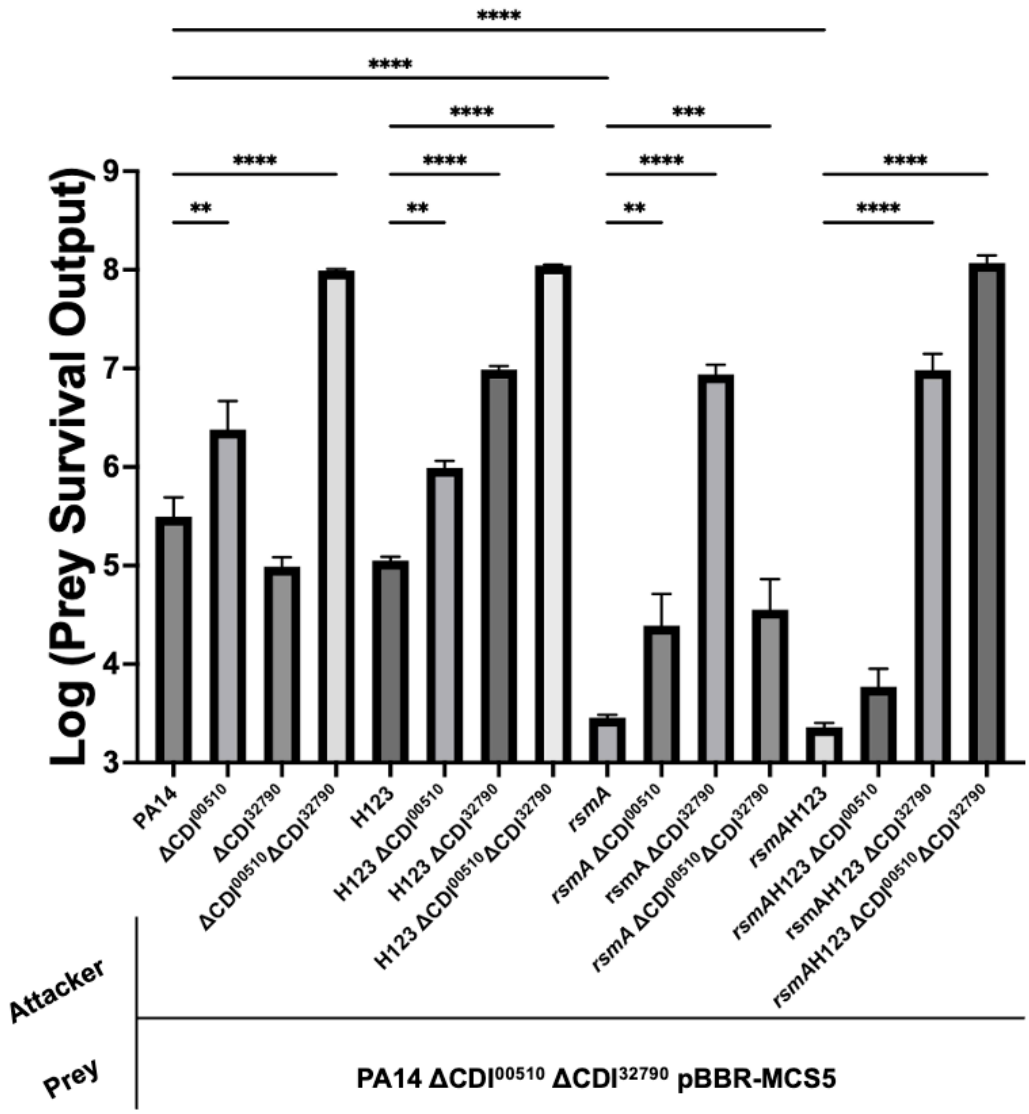


Figure 6.10: Deletion of CDI^{00510} in the PA14 and *rsmA* backgrounds and deletion of CDI^{32790} in the H123, *rsmA* and *rsmA*H123 backgrounds enhances PA14 ΔCDI^{00510} ΔCDI^{32790} prey survival. In this graph PA14 ΔCDI^{00510} ΔCDI^{32790} was used as the prey. The attacking strains have deletions of the genes encoding the CDI systems which should lower their ability to kill and result in increased prey survival if they are active in the attacking strains. Graph showing competitive index after 24hr competition. Average colony count of three replicates for each competition and standard error are indicated above. For PA14 and H123 strain backgrounds, statistically significant increased prey survival is observed against ΔCDI^{00510} strains indicating a role for CDI^{00510} in attacker strain dominance during competition. For the H123, *rsmA* and *rsmA*H123 strain backgrounds, statistically significant prey survival is observed against the ΔCDI^{32790} strains, indicating a role for CDI^{32790} in attacker dominance during competition. For all strain backgrounds statistically significant prey survival is observed for the ΔCDI^{00510} ΔCDI^{32790} strains compared with the parent strain indicating reduced competition occurs between strains when both CDI systems are removed. An additive effect was observed for the CDIs observed for the *rsmA*H123 and H123 backgrounds. Unexpectedly, no increase in prey survival was observed for *rsmA* ΔCDI^{00510} ΔCDI^{32790} compared with *rsmA* ΔCDI^{32790} as seen in the other strain backgrounds. This disparity may indicate

some interplay occurring between the CDI and T6SSs, which is an interesting concept. A One-Way ANOVA was performed on these counts for each competition, statistically significant for 24 hrs competition to ****P<0.0001. Post-hoc statistical significance of CDI mutant competitions compared with those with strain WT were determined using Šídák's test (n=3, three technical replicates).

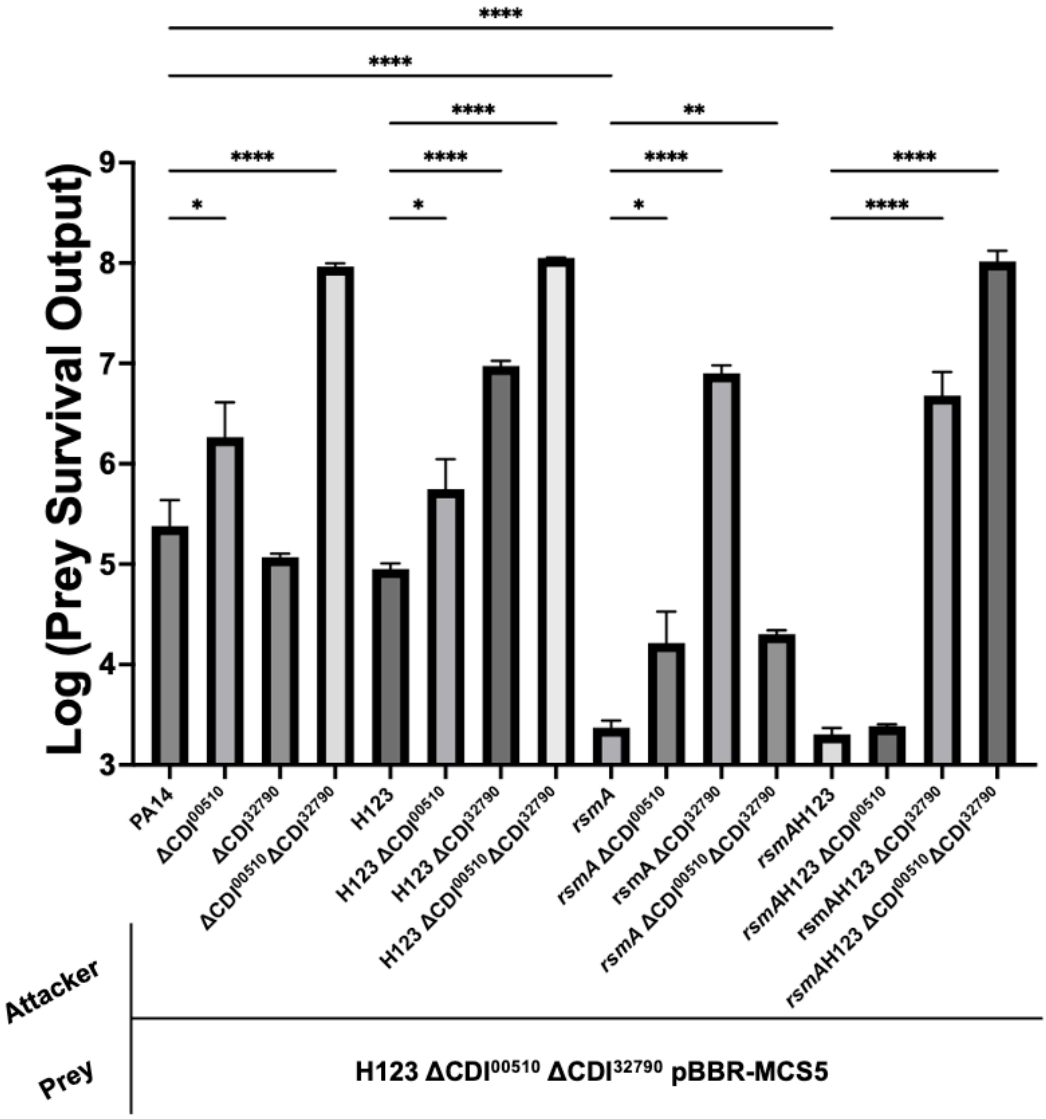


Figure 6.11: Deletion of CDI^{00510} in the PA14 and *rsmA* backgrounds and deletion of CDI^{32790} in the H123, *rsmA* and *rsmA*H123 backgrounds enhances H123 ΔCDI^{00510} ΔCDI^{32790} prey survival. In this graph PA14 ΔCDI^{00510} ΔCDI^{32790} was used as the prey. The attacking strains have deletions of the genes encoding the CDI systems which should lower their ability to kill and result in increased prey survival if they are active in the attacking strains. Graph showing competitive index after 24hr competition. Average colony count of three replicates for each competition and standard error are indicated above. For PA14 and H123 strain backgrounds, statistically significant increased prey survival is observed against ΔCDI^{00510} strains indicating a role for CDI^{00510} in attacker strain dominance during competition. For the H123, *rsmA* and *rsmA*H123 strain backgrounds, statistically significant prey survival is observed against the ΔCDI^{32790} strains, indicating a role for CDI^{32790} in attacker dominance during competition. For all strain backgrounds statistically significant prey survival is observed for

the ΔCDI^{00510} ΔCDI^{32790} strains compared with the parent strain indicating reduced competition occurs between strains when both CDI systems are removed. An additive effect was observed for the CDIs observed for the *rsmA*H123 and H123 backgrounds. Unexpectedly, no increase in prey survival was observed for *rsmA* ΔCDI^{00510} ΔCDI^{32790} compared with *rsmA* ΔCDI^{32790} as seen in the other strain backgrounds. This disparity may indicate some interplay occurring between the CDI and T6SSs, which is an interesting concept. A One-Way ANOVA was performed on these counts for each competition, statistically significant for 24 hrs competition to ****P<0.0001. Post-hoc statistical significance of CDI mutant competitions compared with those with strain WT were determined using Šídák's test (n=3, three technical replicates).

6.4 Discussion

P. aeruginosa has been associated with utility of the CDI systems, engaging in interbacterial competition, enhanced biofilm production and enhanced motility (Mercy *et al.*, 2016; Melvin *et al.*, 2017). The results presented in Chapter 6 of this thesis outline the role of *P. aeruginosa* PA14 CDI systems in motility, biofilm formation and interbacterial competition. Here I delineate the role of CDI systems using the PA14, *rsmA*, *rsmA*H123 and H123 strain backgrounds in phenotypic mechanisms associated with increased pathogenesis and infection. I outline that the CDI systems in PA14 do not play a role in swimming and swarming motility or biofilm production. My results differ from those outlined in the Mercy *et al.* and Melvin *et al.* papers from 2016 and 2017 respectively. Finally, I outline the role these systems play in interbacterial competition, confirming both systems previously identified via *in silico* analysis in Chapter 3 are active and utilised in competition. These results thereby support those observed in the Mercy *et al.* study that CDI are used by *P. aeruginosa* when in competition with other *P. aeruginosa* strains.

6.4.1 Do the CDI systems in P. aeruginosa strain PA14 play a role in bacterial motility?

P. aeruginosa is a bacterium with a large genome which makes it highly adaptable to both the environment and the hostility found during host colonisation (Stover *et al.*, 2000; Moradali, Ghods & Rehm, 2017). As such it utilises many mechanisms to enable its survival and colonisation of multiple niches. One such mechanism is the utilisation of flagella to move in response to multiple stimuli or to a new environment (Berg & Anderson, 1973; Webre, Wolanin & Stock, 2003). Motility is regulated via an interplay between the Gac/Rsm pathway and c-di-GMP levels (Goodman *et al.*, 2004; Merritt *et al.*, 2007; Martínez-Granero *et al.*, 2012) which are linked to the regulation control of many other virulence factors including secretion system expression (Mercy *et al.*, 2016; Allsopp *et al.*, 2017). Therefore it is logical to assume the deletion of these surface expressed secretion systems many influence the ability to move or coordinate group mediated movement in response to stimuli. Additionally, a role has previously been observed for the CDI systems in *P. aeruginosa* strain PAO1 in biofilm production which is often inversely regulated with bacterial movement (Miller *et al.*, 2016; Melvin *et al.*, 2017). To evaluate if the PA14 CDI influence motility, CDI mutant strains in the PA14, *rsmA*, *rsmA*H123 and H123 strain backgrounds were assessed in both swimming and swarming assays. This was used to determine whether these systems play a mechanistic role by directly influencing flagellar based motility, also known as swimming, or a regulatory role by influencing group-mediated motility, also known as swarming.

No significant difference in swimming motility was observed in the CDI mutant strains (Figure 6.3). A One-Way ANOVA was conducted and determined the changes in swimming motility between all control and CDI WSDM strains was statistically significant to ****P<0.0001,

validating the experimental setup. Šídák's post-hoc test showed a statistically significant difference in swimming between PA14 WT and *rsmA* or *rsmA*H123 strains (*P<0.05) which was anticipated as RsmA positively regulates motility (Irie *et al.*, 2020). Therefore these strains were expected to have reduced swimming motility. As no previous studies have linked the PA14 CDI systems to swimming motility, the lack of statistical significance observed here adds to the currently available literature.

No significant difference in swarming motility was observed in the CDI mutant strains (Figure 6.4). A One-Way ANOVA was conducted and determined the changes in swarming motility between all control and CDI WSDM strains was statistically significant to ****P<0.0001, validating the experimental setup. Šídák's post-hoc test showed a statistically significant difference in swarming between PA14 WT and *rsmA* or *rsmA*H123 strains (****P<0.0001) which was anticipated as *rsmA* deletion reduces swarming motility (Miller *et al.*, 2016). Therefore these strains were expected to have reduced swarming motility. A previous study by Melvin *et al.* in 2017 linked swarming motility to deletion of PAO1 CDI. The lack of statistical significance in swarming motility observed here conflicts with the published literature. This may be because of the difference observed in PAO1 CDI as whilst they share high structural homology, they have distinct C-terminal effector domains. Alternatively, this could be due to nuances in regulation between strains. My results indicate PA14 CDI systems are not involved in motility.

Understanding whether CDI play a role in other mechanisms associated with pathogenesis is important in fully elucidating their role and understanding potential regulatory or mechanistic interplay between various virulence phenotypes. Previous research in *B. thailandensis* has

shown that CDI can be involved in interbacterial cooperation, where the formation of the toxin-immunity module acts as a signalling molecule which can influence gene expression and the exhibition of other phenotypes through CDS (Garcia *et al.*, 2016b). If the presence of CDI systems influences other mechanisms controlling bacterial phenotypes this can support a wider role in modulating bacterial behaviour and pathogenesis. This could enable us to further understand their utility and the reason they are so highly conserved in gram-negative bacteria (Henderson *et al.*, 2004; Aoki *et al.*, 2010). Additionally, this would shed light on the capacity of *P. aeruginosa* to dominate other bacteria co-inhabiting its niche by spreading to different locations (Flight *et al.*, 2015; Jean-Pierre *et al.*, 2021). Although there appears to be no interplay found between the CDI systems and motility in PA14, the roles found previously in the Melvin *et al.* study in 2017 may indicate that differences in sequence, target and regulation are maintained between different strains of the same species. Such regulators could be influenced by other factors such as environmental niche occupied and other bacteria frequently interacted with. The CF polymicrobial community is variable between patients (Rogers *et al.*, 2004; Zhao *et al.*, 2012) where patients can have substrain pathoadaptation to the lung's microenvironments (Clark *et al.*, 2015; Schick & Kassen, 2018). It is well documented that *P. aeruginosa* clinical strains vary in motile behaviours, where those associated with chronic infection exhibit reduced motility (Clark *et al.*, 2015; Lozano *et al.*, 2018). However, confirming CDI role in other mechanisms associated with virulence and cooperation such as biofilm formation is required.

6.4.2 Do the CDI systems in P. aeruginosa strain PA14 play a role in biofilm production?

P. aeruginosa adaptability is driven by its utilisation of protective mechanisms to ensure its survival in hostile and adverse environments (Moradali, Ghods & Rehm, 2017). One of these mechanisms is the production of biofilm, which makes the bacterium difficult to eradicate due to its desiccation resistance and inability for antibiotics to effectively diffuse through the matrix (Baker *et al.*, 2016). Biofilm production, like motility, is regulated via the Gac/Rsm pathway (Frangipani *et al.*, 2014) as well as other regulators such as accumulation of intracellular c-di-GMP and sRNAs (Fazli *et al.*, 2014). It is known to be coregulated with other virulence mechanisms such as the secretion systems (Mercy *et al.*, 2016; Gallique *et al.*, 2017; Thi, Wibowo & Rehm, 2020). Many surface proteins and especially T5SSs, both those mediating CDI and those that do not, have been linked to altered aggregation and biofilm formation (Klausen *et al.*, 2003b; Garcia *et al.*, 2013; Ruhe *et al.*, 2013; Melvin *et al.*, 2017). Therefore it is logical to assume CDI deletion may influence biofilm production during infection establishment. Additionally, a role in biofilm formation has previously been observed for the CDI systems in *P. aeruginosa* strain PAO1 (Mercy *et al.*, 2016).

No significant difference in biofilm production was observed in CDI mutant strains (Figure 6.5). A One-Way ANOVA was conducted and determined changes in biofilm production between all control and CDI WSDM strains was statistically significant to ****P<0.0001, validating the experimental setup. Šídák's post-hoc test showed a statistically significant difference in biofilm production between PA14 WT and *rsmA* strains (*P<0.05) which was anticipated as RsmA negatively regulates biofilm production (Irie *et al.*, 2020). Therefore this strain was expected to have an enhanced biofilm production phenotype. This effect was also

expected for the *rsmA*H123 strain background and was not observed here indicating the experimental setup might not reflect the true effect. The experiment was redesigned and repeated using a randomised well format to compensate for variations in oxygen gradients within the plate, as well as production of various volatile compounds produced during incubation. Again no significant difference in biofilm production was observed. Although a statistically significant increase in biofilm production was observed for *rsmA* ΔCDI^{32790}, it was not observed in the other strain background indicating that this is not a biologically relevant effect especially as it was only significant to *P<0.05. The T6SSs in the *rsmA* background are upregulated here and as T6SSs has been shown to positively regulate biofilm production this may be a compensatory effect observed (Chen *et al.*, 2020). A previous study conducted by Mercy *et al.* in 2016 showed a role for the CDI systems in positive regulation of biofilm formation, however my results indicate PA14 CDI systems in are not involved in biofilm production or cooperative behaviours.

An explanation for the differences observed in CDI role in biofilm production compared with the Mercy *et al.* 2016 study which outlined enhanced biofilm production in CDI^{0041} and CDI^{2462} mutants may be due to the documented differences in biofilm matrix composition between PAO1 and PA14 (Colvin *et al.*, 2012). PA14 biofilms utilises the Pel polysaccharide, whilst PAO1 additionally utilises Psl (Friedman & Kolter, 2004a, 2004b). This difference in polysaccharide composition will change biofilm structures and therefore the PA14 CDI may not be involved in biofilm production itself. It may instead be involved in biofilm formation and maturation which has previously been documented in *P. aeruginosa* from a homolog of the T5bSS system. In the Reichhardt *et al.* study from 2018, CdrA-NT was shown to contribute to structural maturation and stabilisation of biofilms in *P. aeruginosa*. CdrA has been linked to interactions with Psl,

which PA14 does not exhibit and could explain the discrepancy observed between strains here (Borlee *et al.*, 2010). Therefore, a role for these systems in biofilm formation may still be observed in the maturation of biofilm structures, however based on the literature it seems unlikely. Biofilm maturation and structure was not evaluated here and therefore this lies outside the scope of the project.

Although these results do not support those previously observed in the Mercy *et al.* study from 2016, there may be logical explanations for why this observed difference occurs between strains and therefore why these systems may have different roles between strains of the same species based on disparity in sequences e.g. C-terminal toxic function, regulation and physiology. Therefore the CDI systems under study here are not involved in interbacterial cooperation or CDS based on motility and biofilm production assay performed here. However, the main role associated with these systems is interbacterial competition. Therefore confirming their role in interbacterial competition was required to understand whether CDI systems in PA14 are active under lab conditions and play a role in interbacterial killing.

6.4.3 Do the CDI systems in P. aeruginosa strain PA14 play a role in interbacterial competition?

P. aeruginosa is a pathogen that has been extensively studied for its capacity to outcompete bacteria and dominate its environment (Giamarellos-Bourboulis *et al.*, 2015). The most well documented competitive system utilised is the T6SS. To date, less research has been conducted on CDI systems and therefore our understanding of their role in virulence is not as clear. Research has identified their conservation in many gram-negative bacteria (Henderson *et al.*, 2004; Allen *et al.*, 2020). However, the activity of these systems in other bacteria and

understanding their role in infection is an area currently being developed. The previous study conducted by Mercy *et al.* in 2016 identified a role for these systems in interbacterial competition in *P. aeruginosa* strain PAO1. To evaluate the PA14 CDI systems, WSDMs constructed in Chapter 4 were used in a *lacZ* competition assay to determine whether these systems actively contribute to interbacterial killing.

A significant difference was observed for some of the CDI mutant strains when competed against a PA14::*lacZ* attacker strain (Figure 6.7). A One-Way ANOVA was conducted and determined the competition between CDI WSDM strains was statistically significant to *P<0.05. Šídák's post-hoc test showed a statistically significant difference between PA14 WT competition and *rsmA* strain (*P<0.05). This was anticipated as RsmA negatively regulates the competitive systems (Mercy *et al.*, 2016; Allsopp *et al.*, 2017) and biofilm production, and positively regulates motility (Miller *et al.*, 2016; Irie *et al.*, 2020), therefore the increased competitive index was expected due to decreased motility and biofilm production. However, this effect was expected to be further enhanced in the other *rsmA* strains and was not observed here. A significant difference was only observed in *rsmA*H123 ΔCDI^{00510}ΔCDI^{32790}. This sole significant interaction may be due to the lack of all competitive systems in the prey which combined with reduced motility and biofilm phenotypes increases susceptibility to killing by the attacker strain. Focusing on the PA14 and H123 backgrounds, significantly higher competitive indices were observed for the ΔCDI^{00510}, ΔCDI^{00510}ΔCDI^{32790} H123 ΔCDI^{00510} and H123 ΔCDI^{32790} and strains. This indicates CDI^{00510} plays a role in interbacterial competition due to enhanced killing of these prey strains. However, in these assays, in the lower dilution spots (Figure 6.8), a clear difference in blue colouration indicating attacker repression was occurring. Contrastingly, this attacker repression pattern was not reflective of the results

obtained from the spot counts. Here, ΔCDI^{00510} and ΔCDI^{00510}ΔCDI^{32790} appears outcompeted by the attacker due to enhanced blue coloration. However, in *rsmA,* *rsmA*H123 and H123 backgrounds, deletion of either CDI system appears to enhance blue colouration, as well as *rsmA* itself. However this blue colouration was not observed in *rsmA*H123. As CDI systems need direct contact to induce the mechanism to facilitate the release of the toxin (Aoki *et al.*, 2005), the space between bacteria in the higher dilutions may enable recovery, particularly if toxins induce bacteriostatic effects on the prey, and therefore are not reflective of the true competitive effect. This assay was also performed using the *rsmA*::*lacZ* attacker strain (data not shown), however the noise in the data between repeats made data interpretation unfeasible. Therefore, the assay was redesigned and repeated using GFP tagged prey strains to quantify prey survival from these lower dilution spots.

A significant difference was observed for the GFP tagged CDI deletion mutant strains when competed against PA14 WT attacker (Figure 6.9). A One-Way ANOVA was conducted and determined the competition between CDI WSDM strains was statistically significant to ****P<0.0001. Šídák's post-hoc test showed a statistically significant difference between PA14 WT competition compared with ΔCDI^{00510} and ΔCDI^{00510}ΔCDI^{32790} strains (*P<0.05). This was also observed in H123 ΔCDI^{00510}, ΔCDI^{32790} and ΔCDI^{00510}ΔCDI^{32790} strains (*P<0.05). This indicates both systems play a role in interbacterial competition due to the enhanced killing of these prey strains during competition against the H123 strain panel. As the additional role for the CDI^{32790} was observed in the H123 ΔCDI^{32790} strain which was not observed in the PA14 prey strain background, this indicates some interplay may be occurring between the CDI^{32790} and T6SSs in the PA14 strain background. No significant difference was observed between the *rsmA* and *rsmA*H123 strains which again was unexpected due to the previous reasons

outlined. These data combined indicate this assay did not represent the effects of CDI deletion on interbacterial competition. Therefore the assay was redesigned to utilise PA14 and H123 ΔCDI^{00510}ΔCDI^{32790} pBBR-MCS5 gentamycin resistant prey strains against the WSDM deletion strain panel. The PA14 and H123 ΔCDI^{00510}ΔCDI^{32790} pBBR-MCS5 gentamycin resistant prey strains were utilised as successive removal of the CDI systems in the attacker should alter the survival of the prey. Strains for this assay were treated differently before input into the assay by subculturing and were grown to an OD 0.3 at 32 °C before mixing in a 1:10 ratio. Mercy *et al.* in 2016 outlined subculturing at 30 °C and growing statically from OD 0.1 to 0.3 as static culture enhances the production of extracellular components associated with the OM. This was attempted here, however was not utilised as incubation time to OD 0.3 was 9 hrs and not a feasible time frame to use. During trouble shooting, this subculture was conducted at both 30 and 37 °C to determine the temperature that CDI competition is observed (data not shown). No competitive effect was observed at 37 °C, whilst a small competitive effect was observed at 30 °C. Upon reviewing the literature, respiratory mucosa maintains a temperature of roughly 32 °C which was selected for this experiment as preliminary tests showed enhanced killing of prey at this temperature.

A significant difference was observed for PA14 and H123 ΔCDI^{00510}ΔCDI^{32790} pBBR-MCS5 gentamycin resistant prey against the WSDM attacker strain panel (Figure 6.10 and 6.11). A One-Way ANOVA was conducted and determined the competition between CDI WSDM strains was statistically significant to ****P<0.0001. Šídák's post-hoc test showed significant survival in PA14 ΔCDI^{00510}ΔCDI^{32790} pBBR-MCS5 prey strain when in competition with ΔCDI^{00510} and ΔCDI^{00510}ΔCDI^{32790} strains. This supported previous results from Figures 6.7 and 6.9 indicating CDI^{00510} plays a role in interbacterial competition but to a higher degree of

significance. Significant survival in PA14 ΔCDI^{00510}ΔCDI^{32790} pBBR-MCS5 prey strain was observed when in competition with all H123 strains. This differs from previous experiments and indicates both CDI play a role in interbacterial competition, in an additive manner. This was unexpected as it indicates a potential regulatory role between T6SSs and CDI^{32790} through a compensatory mechanism which is previously unseen in the literature and is outside the scope of this project to determine. Significant survival in PA14 ΔCDI^{00510}ΔCDI^{32790} pBBR-MCS5 prey strain was also observed when in competition with all *rsmA* strains. However, there is a decrease in survival by three logs in the *rsmA* ΔCDI^{00510}ΔCDI^{32790} strain compared with other double CDI mutant strains. This was an unexpected result, and outside the scope of this project to determine the reasons for this result. A potential reason for this observation may be due to the upregulation of the T6SSs in this strain which would increase interbacterial competition, however this could not be determined here. Finally, significant survival in PA14 ΔCDI^{00510}ΔCDI^{32790} pBBR-MCS5 prey strain was also observed when in competition with *rsmA*H123 ΔCDI^{32790} and *rsmA*H123 ΔCDI^{00510}ΔCDI^{32790} strains. This indicates CDI^{32790} plays a role in interbacterial competition and supports the results observed in the H123 strains here. This indicates that both systems play a role in interbacterial competition due to the enhanced killing of this prey strain during competition with WSDM attacker strains. The same results were observed for the H123 ΔCDI^{00510}ΔCDI^{32790} pBBR-MCS5 prey strain (Figure 6.11), indicating the competitive effects observed here are due to the CDI systems alone.

In this I confirm that both PA14 CDI are involved in interbacterial competition. This is the first study to indicate that these systems are optimally expressed at 32 °C, which is more physiologically relevant to the respiratory mucosal temperatures experienced *in vivo* (McFadden *et al.*, 1985; Khosravi *et al.*, 2021). These results support the Mercy *et al.* study

from 2016 and indicate that this is a conserved feature in *P. aeruginosa* infection biology which may contribute to pathogenesis and its ability to colonise and dominate a diverse range of niches. Therefore the systems here appear to be solely involved in competition and are not involved in cooperation between bacteria. This could therefore be a contributing factor of enhanced virulence in certain strains which are genetically related to the PA14 substrains associated with CF and increased clinical manifestations of respiratory disease including reduced lung function. Here I show these strains have a role in intra-strain competition within *P. aeruginosa*. It is likely they also play a role in inter-strain competition but the presence of the T6SS in other strains make this difficult to assess. CDI systems are commonly used to kill closely related organisms as they so far have been shown to require specific surface receptors to date (Ruhe *et al.*, 2017). However, as these systems have been associated with interbacterial competition, and previous studies on secretion systems have shown that polymicrobial communities can be controlled based on the possession of the immunity genes throughout other members (Ross *et al.*, 2019b), confirming their role in intrabacterial competition against other common pathogens associated with CF pulmonary infection is required to understand whether these systems play a role in *P. aeruginosa* dominance and control of the polymicrobial community composition.

Due to time constraints of the project, I was unable to show the role of these systems in intrabacterial competition. Trouble shooting was required for selective medias which needed more time than granted for this project. Repeats of interbacterial competition between *E. coli* prey and my WSDM strain panel in a similar assay to that outlined in Figures 6.10 and 6.11 were conducted, however high variability was observed between biological repeats and

therefore decreased certainty from preliminary experiments that these systems are involved in intrabacterial competition (data not shown).

6.5 Conclusions

The main conclusions associated with the cooperative and competitive roles of CDI systems are as follows:

1. CDI systems do not contribute to or influence swimming motility in PA14
2. CDI systems do not contribute to or influence swarming motility in PA14
3. CDI systems do not contribute to or influence biofilm production in PA14
4. Both CDI^{00510} and CDI^{32790} play a role in interbacterial competition depending on the genetic background used
5. CDI systems contribute to *P. aeruginosa* infection, niche colonisation and dominance

Therefore, these results presented in Chapter 6 support the current literature indicating that CDI systems play an important role in interbacterial competition in laboratory settings. These systems thus might play a role during niche colonisation and dominance, but unlike CDI systems from other *P. aeruginosa* strains and bacterial genera they do not influence other mechanisms such as biofilm production and motility in PA14. This chapter and its results support the *in silico* identification of these systems from Chapter 3 of this thesis. It also validates the utility of CDI systems via toxin-immunity modules elucidated in Chapter 4 of this thesis. The differences in utilisation of the two systems between different mutant strain

backgrounds show their potential differential use when engaging in interbacterial competition and support the intrastrain variation observed.

So, the final step was to consider whether these results supported or refuted the hypotheses proposed at the beginning of this chapter.

Hypothesis 1: The CDI systems do influence swimming motility. **This was refuted. No differences were observed in swimming motility. This is not in line with previous claims, suggesting this may not be a shared mechanism between all strains of a species, or indeed bacteria encoding CDI systems.**

Hypothesis 2: The CDI systems do influence swarming motility. **This was refuted. No differences were observed in swarming motility. This additionally refutes previous claims that CDI influence swarming motility further supporting the notion this is not a shared mechanism between strains of the same species.**

Hypothesis 3: The CDI systems do influence biofilm production. **This was refuted. No differences were observed in biofilm production in CDI deletion mutant strains. This refutes previous claims that CDI influence biofilm production and suggests this may not be a shared mechanism between all strains of a species, or indeed bacteria encoding CDI systems.**

Hypothesis 4: Both CDI systems are involved in interbacterial competition. **This was accepted.**

Hypothesis 5: CDI systems are involved in intrabacterial competition with other pathogens commonly associated with cystic fibrosis pulmonary infection. **This was not tested due to time constraints.**

Although this study did not identify a role for the CDI systems in cooperative bacterial behaviour which has been observed in other *P. aeruginosa* strains and pathogens, this may be a strain specific behaviour whilst the role in interbacterial competition appears the conserved feature, mandating further exploration which is outside the scope of this project. Validating their role in inter- and intrabacterial competition is a prerequisite warranting further exploration into these systems in clinical strains to elucidate the conservation of interbacterial competition via CDI which would enhance our understanding of strain dominance and clinical outcomes from *P. aeruginosa* infection in CF.

7. Regulation of contact dependent killing systems in *P. aeruginosa* strain PA14

The data shown in this chapter represents my independent work except where otherwise stated. Part of the research and methods pertaining to this chapter has been previously published in the following manuscript. Any contributions from the authors are acknowledged. The prior analysis and figures are necessary to integrate current knowledge with the work I contributed to and for context. This data is available for reuse here under the terms of the Creative Commons CC BY licence which permits unrestricted use, distribution, and reproduction in any medium, provided the original work is properly cited.

Allsopp LP, Collins ACZ, Hawkins E, Wood TE, Filloux A. RpoN/Sfa2-dependent activation of the *Pseudomonas aeruginosa* H2-T6SS and its cognate arsenal of antibacterial toxins. *Nucleic Acids Research*. 2022; 50(1): 1–16.

7.1 Introduction

Genomic sequencing has broadened our understanding of bacterial genomes by enabling identification of multiple distinct copies of a system within the genome which may not have been identified via *in vitro* experimentation alone (Fridman *et al.*, 2020). Previous research has shown that the genome of *P. aeruginosa* strains encodes three T6SSs known as the H1-, H2- and H3- (Filloux, Hachani & Bleves, 2008). Other studies, including the research conducted here, has outlined that *P. aeruginosa* also encodes two CDI systems (Mercy *et al.*, 2016; Allen *et al.*, 2020). The prevalence of both T5SS and T6SS systems across various gram-negative bacteria that suggest that these systems have distinct functions which may be beneficial

under certain conditions (Lin *et al.*, 2019; Allen *et al.*, 2020). H1-T6SSs has been shown to be triggered in a programmed response upon sensing kin cell lysis which increases deployment of antagonistic factors by de-repression of the Gac/Rsm cascade (LeRoux *et al.*, 2014). Additionally, the H1-T6SS utilises an effective tit-for-tat mechanism to respond to attack from competitor bacteria (Basler, Ho & Mekalanos, 2013). As there is an interplay between regulators, many studies of a similar nature delete the regulators of interest from the genome to determine their influence on expression levels of various mechanistic genes of interest (Belliveau *et al.*, 2018). Outlining the regulatory mechanisms for these systems is important in understanding their function, expression, roles in infection and the effectors deployed by each system in line with the current literature. This may shed light on their differential expression under various conditions, how this influences *P. aeruginosa* ability to dominate their environment and how this translates to the CF pulmonary polymicrobial community. Additionally, this is a useful tool to develop when studying systems which are repressed or not well expressed under laboratory conditions as construction of regulator deletions can upregulate them.

The three T6SSs, as well as the two CDI systems, in *P. aeruginosa* have been shown to be repressed by RsmA from the Gac/Rsm regulation pathway (Chapter 1.8.1 Figure 1.23) (Mercy *et al.*, 2016; Allsopp *et al.*, 2017). RsmA negatively regulates translation by binding conserved motifs most often with a GGA motifs frequently found near mRNA ribosomal binding sites (Brencic *et al.*, 2009). Their regulation via the Gac/Rsm indicates that these systems may be co-regulated with other phenotypic mechanisms associated with infection, biofilm formation and metabolism (Martínez-Granero *et al.*, 2012; Frangipani *et al.*, 2014). Whilst our

understanding of CDI and T6SS mechanistic and competitive capabilities is increasing, less is known about their regulation at the transcriptional level- especially for the CDI systems.

Previous research has outlined T6SSs are likely not co-expressed simultaneously but are transcriptionally regulated by multiple regulators including the global transcriptional regulator RpoN (Sana *et al.*, 2013). RpoN regulation is associated with genes involved in nitrogen and carbon metabolism, bacterial persistence and infection including biofilm formation and motility (Schulz *et al.*, 2015) allowing *P. aeruginosa* to sense and respond to its environment for survival in diverse environments. RpoN binds specific DNA binding sequences most often within the promoter regions of genes. It acts as a sigma factor through association with polymerase, but for open complex formation it requires additional enhancer binding proteins (EBPs) for transcription initiation which utilise ATP hydrolysis for RpoN-RNA polymerase remodelling (Bush & Dixon, 2012). RpoN has been linked to H2- and H3-T6SSs expression (Bernard *et al.*, 2011; Sana *et al.*, 2013; Shao *et al.*, 2018), whilst enhancer binding proteins have been suggested to be involved in T6SSs repression such as H2-T6SS via EBP sigma factor activator (Sfa) Sfa2 (Sana *et al.*, 2013). This raises the question- how are these systems differentially regulated? And are these systems coregulated with other mechanisms such as motility and biofilm formation?

To determine the regulatory mechanisms which activate specific systems, a study conducted by Sana *et al.* in 2013 focused on two EBP SFA genes encoded within the core clusters of the H2- and H3-T6SS. These SFA proteins were shown to repress both H2- and H3-T6SS and designated Sfa2 and Sfa3 based on their association with the H2- and H3-T6SSs respectively. This differed from our study and is outlined below. The study along with previous research

indicated some interplay may be occurring with RpoN and Sfa proteins to control regulation and expression of the three T6SSs (Filloux, Hachani & Bleves, 2008; Sana *et al.*, 2013).

As research into CDI systems is in a much earlier phase less is understood about their regulation. To date, in *P. aeruginosa* only RsmA has been shown to negatively regulate CDI post-transcriptionally and their transcriptional regulators are yet to be ascertained (Mercy *et al.*, 2016; Garcia *et al.*, 2016a). Therefore, identifying whether CDI systems are also transcriptionally regulated by RpoN will broaden our understanding of their regulation and whether this occurs in conjunction with T6SSs. If this is the case, other fine-tuning regulators may be used by these systems to control the expression of specific systems. This may then be linked to the potential interplay observed in Chapter 6 between CDI and T6SS in interbacterial competition and biofilm formation with CDI^{32790}, as well as outlining the involvement of various systems under different conditions. This would expand our understanding of the competitive systems in *P. aeruginosa* and may shed light on their evolutionary importance based on their ability to control the expression of different competitive systems or identify any potential cross-regulation.

7.2 Aims of this study

From the current literature and to broaden our understanding of the regulators involved in transcriptional regulation of the CDI and T6SSs, I have found two major hypotheses to address in this chapter:

1. Both CDI and T6SSs are controlled by the transcriptional regulator RpoN

2. H2- and H3-T6SS expression is controlled by SFA proteins Sfa2 and Sfa3 respectively

This chapter summarises research conducted to validate the role of RpoN, RsmA and Sfa2 in the expression of CDI and T6SSs in *P. aeruginosa* PA14 through addressing the following aims:

1. Conducting transcriptomic analysis based on RNA-seq data previously obtained by the Allsopp lab focusing on the T6SSs
2. Conducting β-galactosidase assays using previously constructed *lacZ* TssA2 and TssB3 transcriptional fusion strains
3. Conducting swimming motility assays using previously constructed regulator mutants
4. Conducting swarming motility assays using previously constructed regulator mutants
5. Conducting crystal violet biofilm production assays using previously constructed regulator mutants
6. Conducting transcriptomic analysis based on RNA-seq data previously obtained by the Allsopp lab focusing on the T5SSs

7.3 Summary of findings

In this chapter the role of RpoN and Sfa2 in T6SS regulation and expression is discussed. RNA-seq analysis of *rsmA*, *rsmAsfa2, rsmAsfa3* and *rsmArpoN* PA14 strain backgrounds revealed altered regulation of flagellar, H1-, H2-T6SS and H3-T6SS VgrG/Hcp genes. Upon *rsmA* deletion, almost all T6SS genes were derepressed. Positive regulation of H2-T6SS VgrG/Hcp genes via RpoN and Sfa2 was determined. An inverse regulation between the H1-/H3- and H2-T6SS shown. RpoN deletion abrogates H2-T6SS associated orphan VgrG production, and

this was fully restored upon complementation, indicating a role in core and tip complex expression coordination. Through β-galactosidase assays using TssA2 and TssB3 *lacZ* transcriptional fusions, I confirmed a role for RpoN and RsmA- validating RNA-seq results where *rpoN* deletion enhances H3-T6SS expression but reduces H2-T6SS expression. Subsequently, Sfa2 was shown to positively regulate H2-T6SS in conjunction with RpoN. Trans-complementation with Sfa3 could not restore H2-T6SS function upon Sfa2 deletion showing SFA protein specificity. I confirmed via *in vitro* experimentation that motility and biofilm production were not altered in these strains, supporting the RNA-seq analysis. Finally, I show that RpoN and RsmA impacts CDI mRNA levels.

7.4 Results

7.4.1 Analysis of RNA-seq data identifies differential transcriptional regulators of the CDI, TPS and T6SSs

To determine the global role of regulators on expression of genes or systems of interest transcriptomics tools such as RNA-seq are used to measure levels of RNA expression in strain backgrounds with various regulators deleted (Belliveau *et al.*, 2018; Muhammad *et al.*, 2020). *P. aeruginosa* encodes three T6SSs and two CDI systems within its genome (Filloux, Hachani & Bleves, 2008; Van Ulsen *et al.*, 2014) which are proposed to be highly energy expensive (Basler, 2015). They may be differentially regulated, potentially providing different advantageous functions as they may only be useful in certain environments whilst aggression may not be the most effective strategy. The post-transcriptional regulator RsmA was previously identified to play a role in CDI and T6SSs repression (Mercy *et al.*, 2016; Allsopp *et*

al., 2017). Additionally, RpoN and EBPs have been shown to play a role in T6SS activation (Bernard *et al.*, 2011; Sana *et al.*, 2013; Shao *et al.*, 2018). Therefore, assessing these regulators in concert is important as they likely have overlapping targets between CDI and T6SSs. To study the role of RpoN, RsmA and Sfa2/3 in regulation of CDI, TPS and T6SSs, regulator deletion mutants were used to conduct the transcriptional analysis.

7.4.1.1 RNA-seq data identifies RpoN and Sfa2 as transcriptional regulators of the T6SSs

P. aeruginosa PA14 mutants were used as a panel for transcriptomics analysis consisting of *rsmA*, *rsmAsfa2, rsmAsfa3* and *rsmArpoN* that was performed by Luke Allsopp. The *rsmA* background would upregulate the competitive systems to ensure any effects of *rpoN* deletion were observed (Allsopp *et al.*, 2017). RNA collection and subsequent transcriptomics data analysis was performed by Luke Allsopp and included in the Allsopp *et al.* 2022 publication. Genes differentially regulated to a threshold of 1.5 2log-fold change were deemed significant. From this analysis, dysregulation was observed in multiple flagellar genes (Figure 7.1) and one *gcbA* diguanylate cyclase (Table 7.1) indicating a link with motility and c-di-GMP that might influence biofilm formation. This was expected as RpoN and RsmA have previously shown a role in motility and biofilm formation (Irie *et al.*, 2020; Liu *et al.*, 2021). Significant alteration to T6SS genes were observed in *rsmArpoN* (Figure 7.2), where 55.4% of 112 genes exhibited ≥ 1.5- 2log-fold altered expression. Upon *rpoN* deletion, genes associated with H1- and H3-T6SS were moderately and significantly upregulated respectively, whilst many H2-T6SS genes were repressed. This outlines differential regulation for these T6SSs controlled by RpoN.

Further analysis conducted by Luke Allsopp outlined any potential role of EBPs Sfa2 and Sfa3 deletion and if this impacted any genes with a specific focus on components of H2- and H3-T6SSs. The Sfa2 regulon was observed to be much smaller than RpoN, with only 49 genes associated differentially expressed as opposed to 1554. 34 genes were associated with H2-T6SS, either reduced or modulated upon *sfa2* deletion, including the entire core cluster and multiple orphan islands (Figure 7.3). Additionally, *sfa2* deletion showed no dysregulation of flagellar of biofilm biosynthesis genes, unlike RpoN deletion (Figure 7.4, compared with 7.1), indicating Sfa2 is specific to H2-T6SS genes. For Sfa3, no dysregulation of flagellar or biofilm biosynthesis genes was observed (Figure 7.5). Analysis of *rsmAsfa3* results showed altered expression levels for 10 genes. As this was so few, they may be false positives (Figure 7.6). In addition, only 1 was a T6SS gene from the H2-T6SS and not the H3-T6SS. To strengthen and validate these results *in vitro* I conducted follow on experiments which I will outline in sections 7.4.2 and 7.4.3.

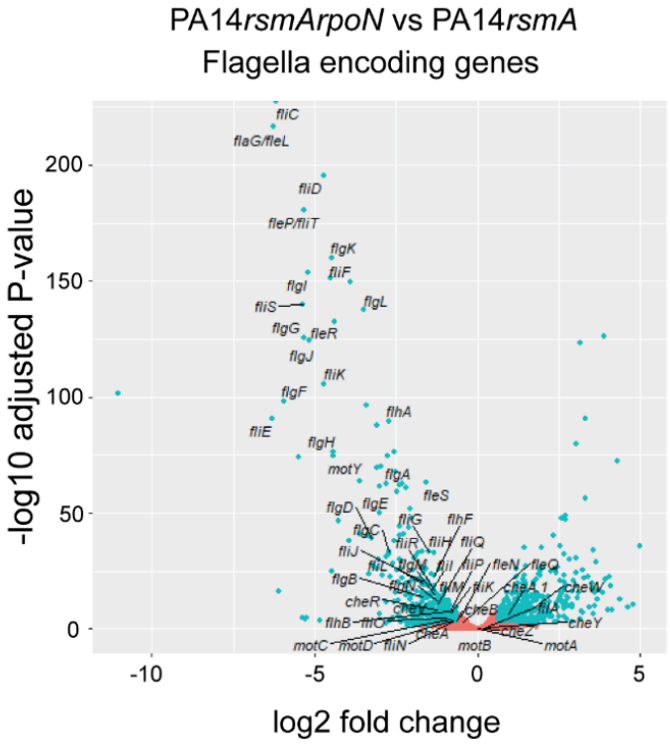


Figure 7.1: RpoN positively regulates the flagellar operon in *P. aeruginosa* strain PA14. Figure 2A Allsopp *et al.* 2022. 'Volcano plots of differentially expressed genes with colours indicating each gene's absolute log2 (fold change): orange ≤0.58; and blue >0.58 (1.5 fold) with a *P*adjusted <0.05 (*n* = 3). Significance was determined by a Wald test and adjusted for multiple comparisons using the Benjamini–Hochberg false-discovery rate correction using DESeq2.' Significant downregulation is observed in flagellar genes upon deletion of *rpoN*.

Table 7.1: Diguanylate cyclase gene is downregulated upon deletion of RpoN

rowname	baseMean	log2FoldChange	lfcSE	stat	pvalue	padj	old_locus_tag	symbol	flagella_motility	vgrG_hcp	T6SS	Protein_function	P.S. value and >0	P.S. value and <0	P.S. value and >0.58	P.S. value and <-0.58
PA14_RS26180	2742.64	-4.51707	0.170411	-26.507	8.06E-155	6.83E-152	PA14_64050	NA	NA	NA	NA	"2-oxo-hepta-3-ene-1,7-dioic acid hydratase"	FALSE	TRUE	FALSE	TRUE

From Allsopp *et al.* 2022 supplementary material, Table S5

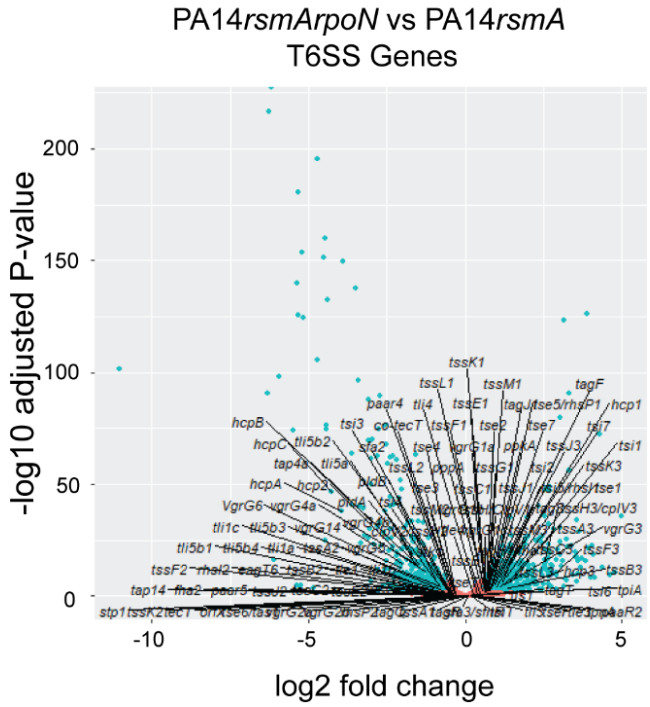


Figure 7.2: Deletion of *rpoN* significantly alters expression of T6SS associated genes. Figure S2B Allsopp *et al.* 2022. 'Volcano plots of differentially expressed genes with colours indicating each gene's absolute log2 (fold change): orange ≤0.58; and blue >0.58 (1.5 fold) with a *P*adjusted <0.05 (n = 3). Significance was determined by a Wald test and adjusted for multiple comparisons using the Benjamini–Hochberg false-discovery rate correction using DESeq2.' Significant downregulation of H2-T6SS genes, but significant upregulation of H1- and H3-T6SS genes is observed upon deletion of *rpoN*.

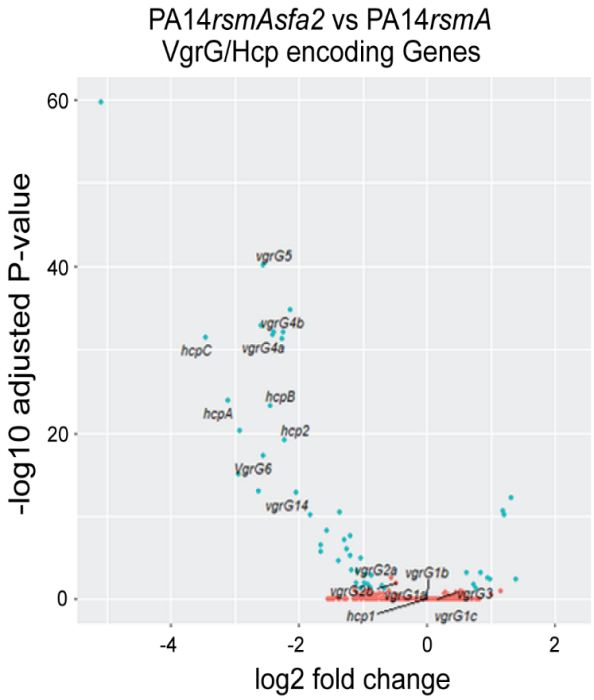


Figure 7.3: Sfa2 is essential for expression of H2-T6SS associated genes. Figure 4B Allsopp *et al.* 2022. 'Volcano plots of differentially expressed genes with colours indicating each gene's absolute log2 (fold change): orange ≤0.58; and blue >0.58 (1.5 fold) with a *P*adjusted < 0.05 (*n* = 3). Significance was determined by a Wald test with Benjamini–Hochberg correction.' Significant downregulation of H2-T6SS genes was observed upon deletion of *sfa2*.

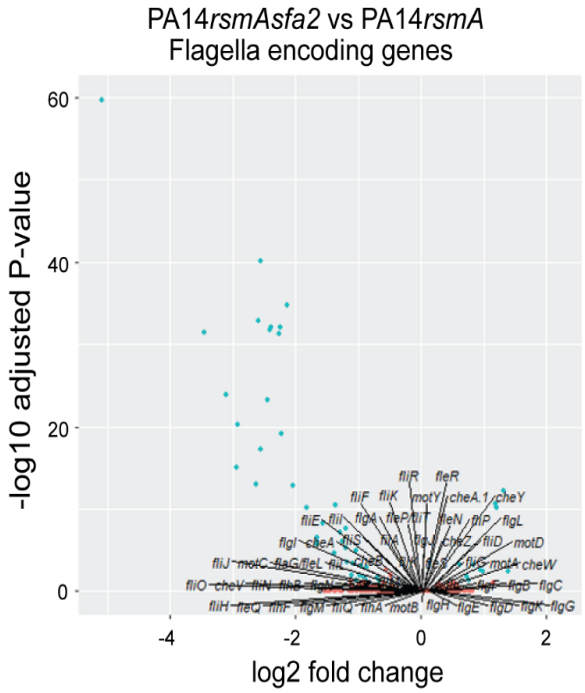


Figure 7.4: Flagella gene expression is unaffected by Sfa2. Figure 4C Allsopp *et al.* 2022. 'Volcano plots of differentially expressed genes with colours indicating each gene's absolute log2 (fold change): orange ≤0.58; and blue >0.58 (1.5 fold) with a *P*adjusted < 0.05 (*n* = 3). Significance was determined by a Wald test with Benjamini–Hochberg correction.' No significant difference is observed for flagella associated genes.

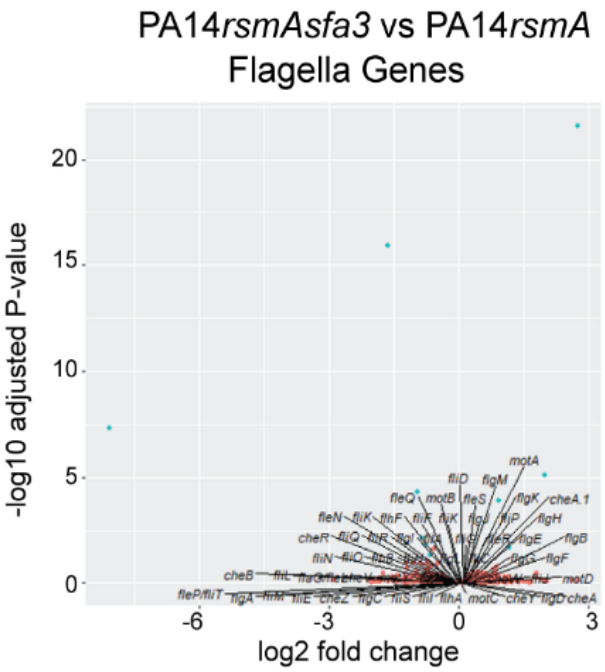


Figure 7.5: Flagella gene expression is unaffected by Sfa3. Figure S11B Allsopp *et al.* 2022. 'Volcano plots of differentially expressed genes with colours indicating each gene's absolute log2 (fold change): orange ≤0.58; and blue >0.58 (1.5 fold) with a *P*adjusted < 0.05 (*n* = 3). Significance was determined by a Wald test with Benjamini–Hochberg correction.' No significant difference is observed for flagella associated genes.

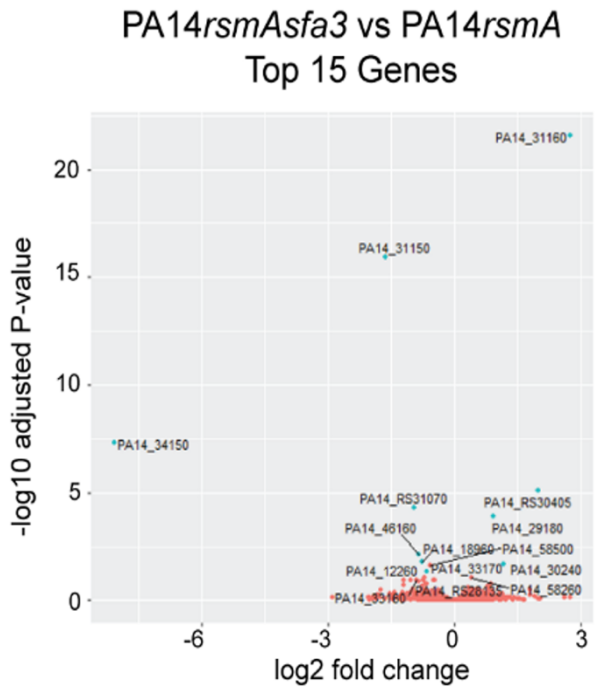


Figure 7.6: Altered gene expression is observed in 10 genes upon deletion of *sfa3*. Figure S11D Allsopp *et al.* 2022. 'Volcano plots of differentially expressed genes with colours indicating each gene's absolute log2 (fold change): orange ≤0.58; and blue >0.58 (1.5 fold) with a *P*adjusted < 0.05 (*n* = 3). Significance was determined by a Wald test with Benjamini–Hochberg correction.' Significant difference is observed for only one T6SS gene *tli5a* thought to be a H2-T6SS associated immunity encoding gene.

7.4.1.2 RNA-seq data identifies RsmA and RpoN as regulators of TPS and CDI systems

I conducted further analysis for this thesis after submission of the Allsopp *et al.* 2022 manuscript using this dataset to determine the regulation of TPS genes including CDI (Table 7.2). Immunity gene expression was not evaluated here due to the lack of gene designations for these small ORFs which were consequently not part of the dataset as a result. My analysis showed additional significant alteration of expression levels of 6/12 (50%) TPS/CDI (encoding 1 TPS and 2 CDI systems) genes, exhibited ≥ 1.5- 2log-fold altered expression in both *rsmA* and *rsmArpoN* backgrounds. Upon *rsmA* deletion (Figure 7.7) CDI gene expression is upregulated. CDI^{00510} genes PA14_00490 (*cdiB*) and PA14_00510 (*cdiA*) were upregulated 1.4 and 2.3 2log-fold respectively. CDI^{32790} genes PA14_32780 (*cdiB*) and PA14_32790 (*cdiA*) were upregulated 1.2 and 2 2log-fold respectively. This supports the Mercy *et al.* study from 2016 indicating RsmA negatively regulates CDI in *P. aeruginosa*. The differences in upregulation between the *cdiB* and *cdiA* were unexpected as the operons are thought to be under a single promoter so equal/similar 2log-fold increases in the levels would have been expected (Aoki *et al.*, 2005; Poole *et al.*, 2011). Additionally, one hypothetical CdrA/CdrB system showed significant upregulation upon *rsmA* deletion. PA14_61190 (*cdrB*) and PA14_61200 (*cdrA*) were upregulated 1.3 and 1.6 2log-fold respectively. This indicates CDI and some TPS are negatively regulated or repressed by RsmA.

Next, I explored the RNA-seq data upon *rpoN* deletion in the *rsmA* background (Figure 7.8). Genes encoding both CDI systems were significantly downregulated upon *rpoN* deletion. CDI^{00510} genes PA14_00490 (*cdiB*) and PA14_00510 (*cdiA*) were downregulated 1.6 and 0.7 2log-fold respectively. Whilst CDI^{32790} genes PA14_32780 (*cdiB*) and PA14_32790 (*cdiA*) were

downregulated 2.3 and 2.4 2log-fold respectively. This outlines a previously unseen role of RpoN as an activator of CDI. Additionally, the TPS CdrA/CdrB system homologue showed significant upregulation. PA14_61190 (*cdrB*) and PA14_61200 (*cdrA*) were upregulated 1 and 0.7 2log-fold respectively. Interestingly, this indicates that other TPS are negatively regulated by RpoN and inversely regulated with both CDI systems.

Table 7.2: TPS/CDI systems encoded in *P. aeruginosa* PA14

System	TpsB/CdiB	TpsA/CdiA
CDI	**PA14_00490**	**PA14_00510**
CDI	**PA14_32780**	**PA14_32790**
Hypothetical TPS	**PA14_61190**	**PA14_61200**
Hypothetical TPS	**PA14_55380**	**PA14_55400**
CupB5	**PA14_11110**	**PA14_11100**
Hypothetical TPS	**PA14_58890**	**PA14_58900**

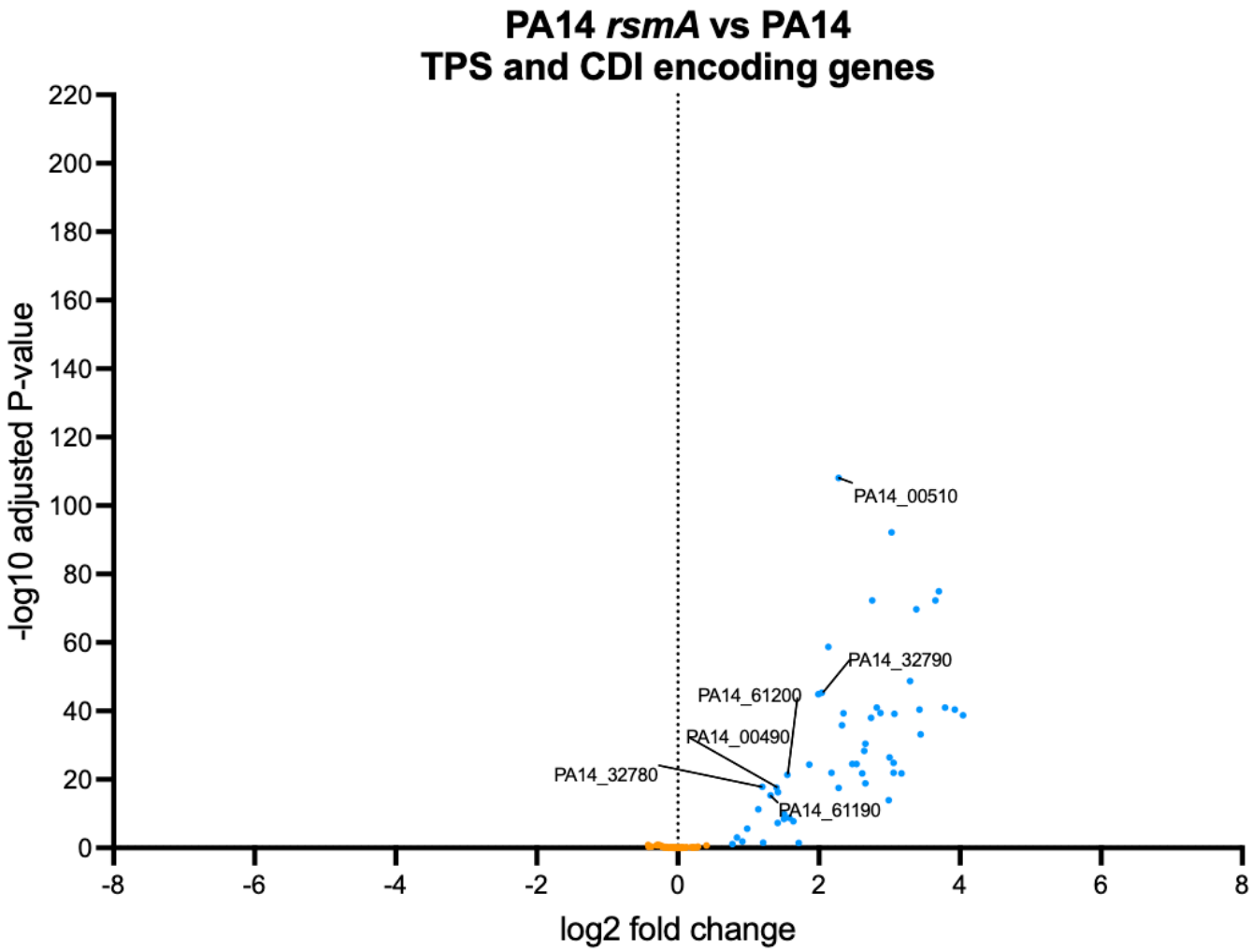


Figure 7.7: Deletion of *rsmA* enhances expression of CDI^{00510}, CDI^{32790} and TPS^{61200}. Volcano plot performed by me showing differentially gene expression with colours indicating each gene's absolute log2 (fold change): orange ≤0.58; and blue >0.58 (1.5 fold) with a -log10 *P*adjusted < 0.05 (*n* = 3). Significance was determined by a Wald test with Benjamini–Hochberg correction. Significant upregulation of CDI^{00510} and CDI^{32790} as well as one likely TPS PA14_61190/PA14_61120 with CdrB/CdrA homology is observed upon *rsmA* deletion. The three other TPS systems outlined in Table 7.2 are not significantly altered upon *rsmA* deletion.

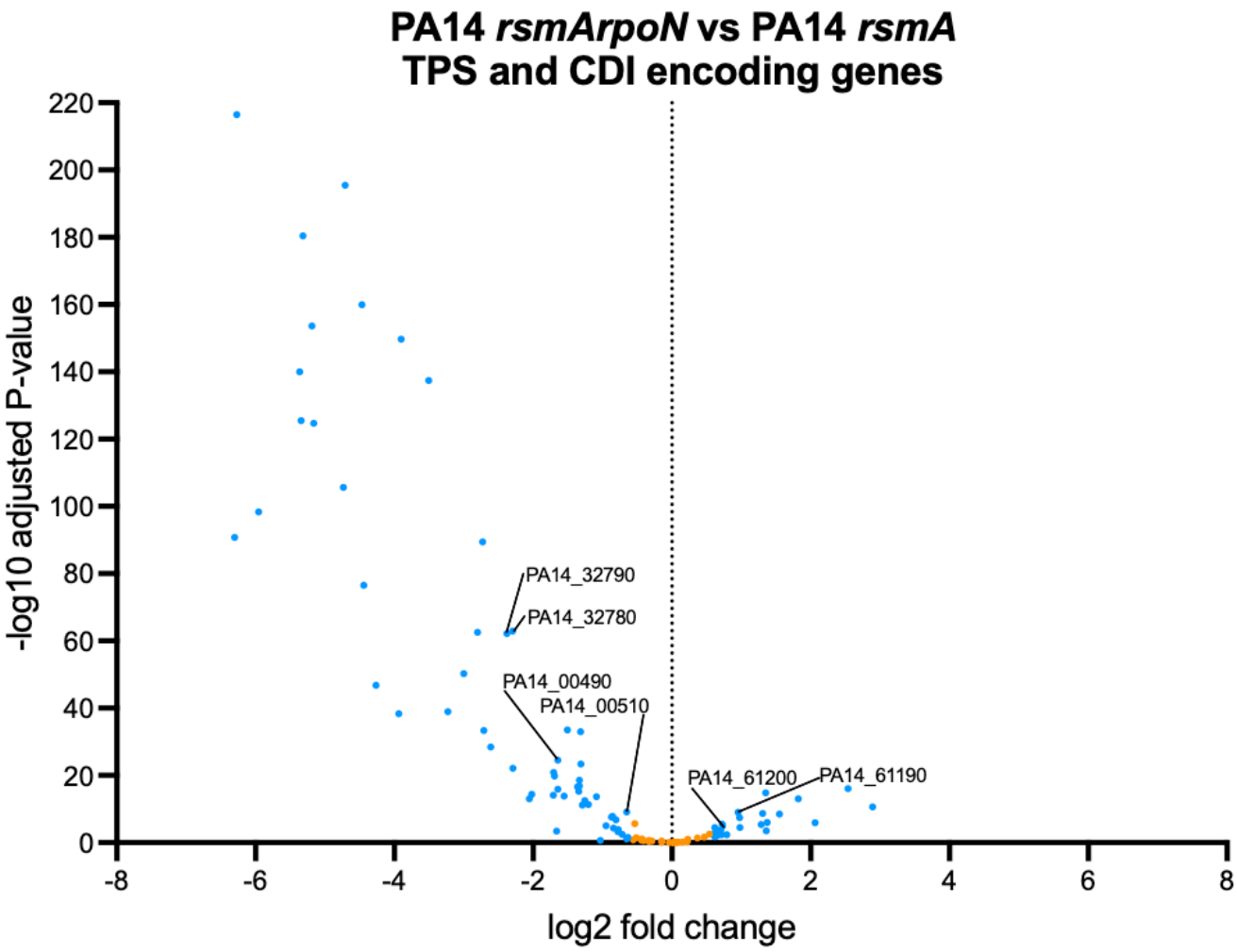


Figure 7.8: Deletion of *rpoN* reduces expression of CDI^{00510} and CDI^{32790} but increases expression of TPS^{61200}. Volcano plot showing differentially gene expression with colours indicating each gene's absolute log2 (fold change): orange ≤0.58; and blue >0.58 (1.5 fold) with a -log10 *P*adjusted < 0.05 (*n* = 3). Significance was determined by a Wald test with Benjamini–Hochberg correction. Significant downregulation of CDI^{00510} and CDI^{32790} is observed upon subsequent deletion of *rpoN* in and *rsmA* background. However, significant upregulation was observed for one previously identified hypothetical TPS PA14_61190/PA14_61120 with CdrB/CdrA homology is observed upon *rpoN* deletion. TPS systems outlined in Table 7.2 are not significantly altered upon *rpoN* deletion.

7.4.2 Transcriptional fusions enable investigation of the role of RpoN in the regulatory control of H2-T6SS in PA14

Previous research on *P. aeruginosa* T6SSs has utilised *lacZ* transcriptional fusions to determined gene expression levels from both WT and mutant strains (Podkovyrov & Larson, 1995; Allsopp *et al.*, 2017). To corroborate the role of RpoN in transcriptional control of the H2- and H3-T6SS *in vitro*, *lacZ* fusions were used to validate the RNA-seq analysis. Transcriptional fusions previously constructed by the Allsopp lab were used to determine whether expression of H2- and H3-T6SS changes upon subsequent deletion of *rpoN* in a *rsmA* strain background which would upregulate the competitive systems so to ensure any effects on *rpoN* deletion are observed.

P. aeruginosa PA14 transcriptional (tc) fusion of the *lacZ* gene to the first gene in the H2-T6SS (*tssA2*) and H3-T6SS (*tssB3*) operons were called A2tc and B3tc, respectively. These were constructed in WT, *rsmA* and *rsmArpoN* strain backgrounds by Luke Allsopp. I performed several β-galactosidase assays as part of this thesis, which was included in the Allsopp *et al.* 2022 publication. Initially, H2-T6SS regulation was determined using *tssA2*::*lacZ* fusions (Figure 7.9a). H2-T6SS is upregulated in A2tc *rsmA*, supporting results previously observed in Allsopp *et al.* 2017. Upon subsequent deletion of *rpoN*, expression is reduced, indicating RpoN positively regulates H2-T6SS supporting the transcriptional analysis conducted by Luke Allsopp in 7.4.1 (Figure 7.2). Next, H3-T6SS regulation was determined using *tssB3*::*lacZ* fusions (Figure 7.9b). H3-T6SS expression is upregulated in B3tc *rsmA*, supporting results previously observed in the Allsopp *et al.* 2017. Upon deletion of *rpoN*, expression is further enhanced, indicating RpoN negatively regulates H3-T6SS supporting the transcriptional

analysis conducted by Luke Allsopp in 7.4.1 (Figure 7.2). This validates an inverse relationship between the H2- and H3-T6SSs with RpoN indicating they are differentially expressed during interbacterial competition. Having determined the role of RpoN in the regulation of H2- and H3-T6SS, control of H2-T6SS via Sfa2 was confirmed *in vitro*.

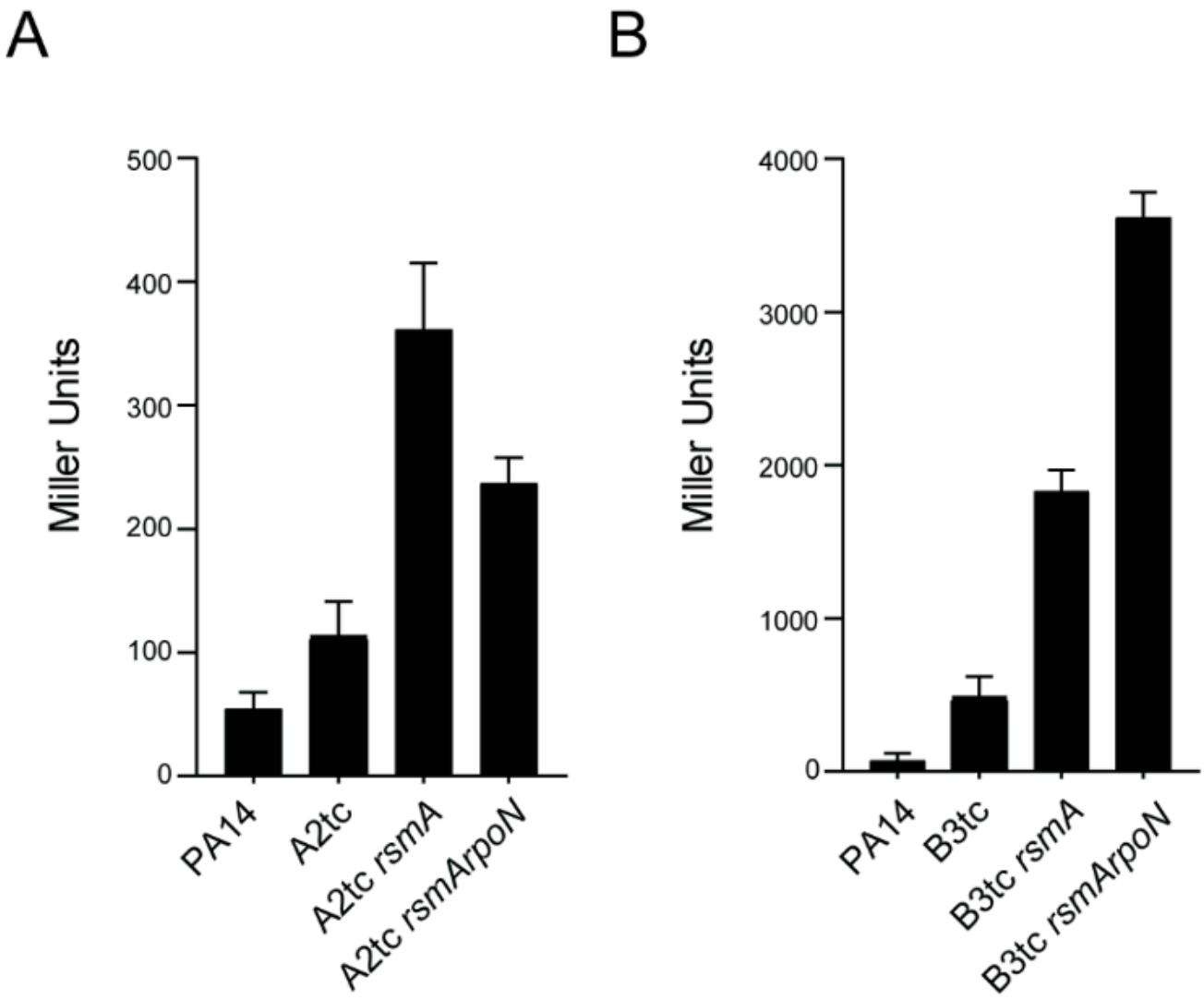


Figure 7.9: Deletion of *rpoN* reduces expression of H2-T6SS but increases expression of H3-T6SS. Figure 3AB Allsopp *et al.* 2022 that I performed. Graphs represents mean +SD (*n* = 3, ANOVA, Tukey's Multiple Comparison Test, *P* <0.01). Deletion of *rsmA* upregulated both the H2- and H3-T6SS fusions. Differential regulation was observed upon deletion of *rpoN*. (A) β-galactosidase assay using H2-T6SS *lacZ* transcriptional fusions A2tc, (B) β-galactosidase assay using H3-T6SS *lacZ* transcriptional fusions B3tc. This indicates that RpoN positively regulates H2-T6SS and negatively regulates the H3-T6SS.

7.4.3 In P. aeruginosa PA14, the regulator RpoN plays a clear role in motility, whilst enhancer binding protein Sfa2 may play a role, but Sfa3 does not

RpoN controls the expression of flagella (Dasgupta *et al.*, 2003). Figure 7.1 shows *rpoN* deletion has a large impact on flagella genes as expected, validating the results. However, Sfa2 transcriptomics analysis identified changes in expression for a subset of H2-T6SS genes alone (Figure 7.3). Additionally, Sfa3 appeared to play no role in H3-T6SS regulation, with few genes exhibiting altered expression (Figure 7.6). I performed swimming and swarming assays using deletion mutants previously constructed by the Allsopp lab to determine whether motility changes upon subsequent deletion of *rpoN, sfa2* or *sfa3* in a *rsmA* background. Again, the *rsmA* background would upregulate the competitive systems to ensure effects on *rpoN/sfa2/sfa3* deletion are observed. As the transcriptomics analysis outlined in 7.4.2 indicated Sfa2 is specific to H2-T6SS expression and Sfa3 had no discernible role, assessing these regulators in other phenotypes will validate the RNA-seq results.

Swimming motility assays were performed on a mutant panel of; PA14 WT, *rsmA*, *sfa2, sfa3, rsmAsfa2, rsmAsfa3, rpoN* and *rsmArpoN,* to encompass all regulation variants under study. Additionally, a panel of strains from the O'Toole strain repository were also used as controls (Limoli *et al.*, 2019), consisting of PA14 SMC232, *flgK, pilA* and *flgKpilA* as flagellar and pili mutant controls (Figure 7.10). Swimming assays were performed to determine any impact for Sfa2/Sfa3 on flagellar-mediated motility (Figure 7.11). A significant decrease was observed with the flagellar controls, *flgK* and *flgKpilA* compared with PA14 WT. This was expected as flagella are involved in bacterial swimming motility (O'Toole & Kolter, 1998; Conrad *et al.*, 2011). A significant decrease was observed for *rsmA*, *rpoN* and *rsmArpoN* strains compared

with PA14 WT. Additionally a significant decrease was observed with *rsmArpoN* compared with *rsmA*. Reduced swimming motility for *rsmA* and *rpoN* was expected as RsmA and RpoN are positive regulators of flagellar formation and therefore motility (Irie *et al.*, 2020; Liu *et al.*, 2021). Unexpectedly, a modest but significant reduction in swimming motility was observed for *sfa2* compared with PA14 WT. This difference was negated comparing *rsmA* and *rsmAsfa2* which may indicate the influence of another regulator in the *sfa2* background was overridden in the *rsmA* mutant. Alternatively, there may be an unknown link to flagellar genes not observed here. No significant difference in swimming motility was observed for any of the *sfa3* deletion mutant strains.

Using the same strain panel swarming motility assay was conducted (Figure 7.12). Swarming assays were performed to determine any impact for Sfa2/Sfa3 on group-mediated motility (Figure 7.13). A significant decrease was observed with flagellar controls, *flgK* and *flgKpilA*. This was expected as flagella are involved in bacterial motility (Henrichsen, 1972). A significant decrease was observed with *rsmA* and *rpoN* strains compared with the PA14 WT. Additionally a significant decrease was observed with *rsmArpoN* compared with *rsmA*. The reduction in swarming motility observed for *rsmA* and *rpoN* was expected as RsmA and RpoN have previously been shown to be positive regulators of group-coordinated movement (Liaw *et al.*, 2003; Damron *et al.*, 2012; Miller *et al.*, 2016). No significant difference in swarming motility was observed for any of the *sfa2* or *sfa3* deletion mutant strains. This indicates RpoN plays a role in swimming and swarming motility, whilst Sfa2 may play a role, but Sfa3 does not. This supports transcriptomics results outlined in 7.4.1. Having determined the role of Sfa2/3 in motility, their role in biofilm production was confirmed *in vitro*.

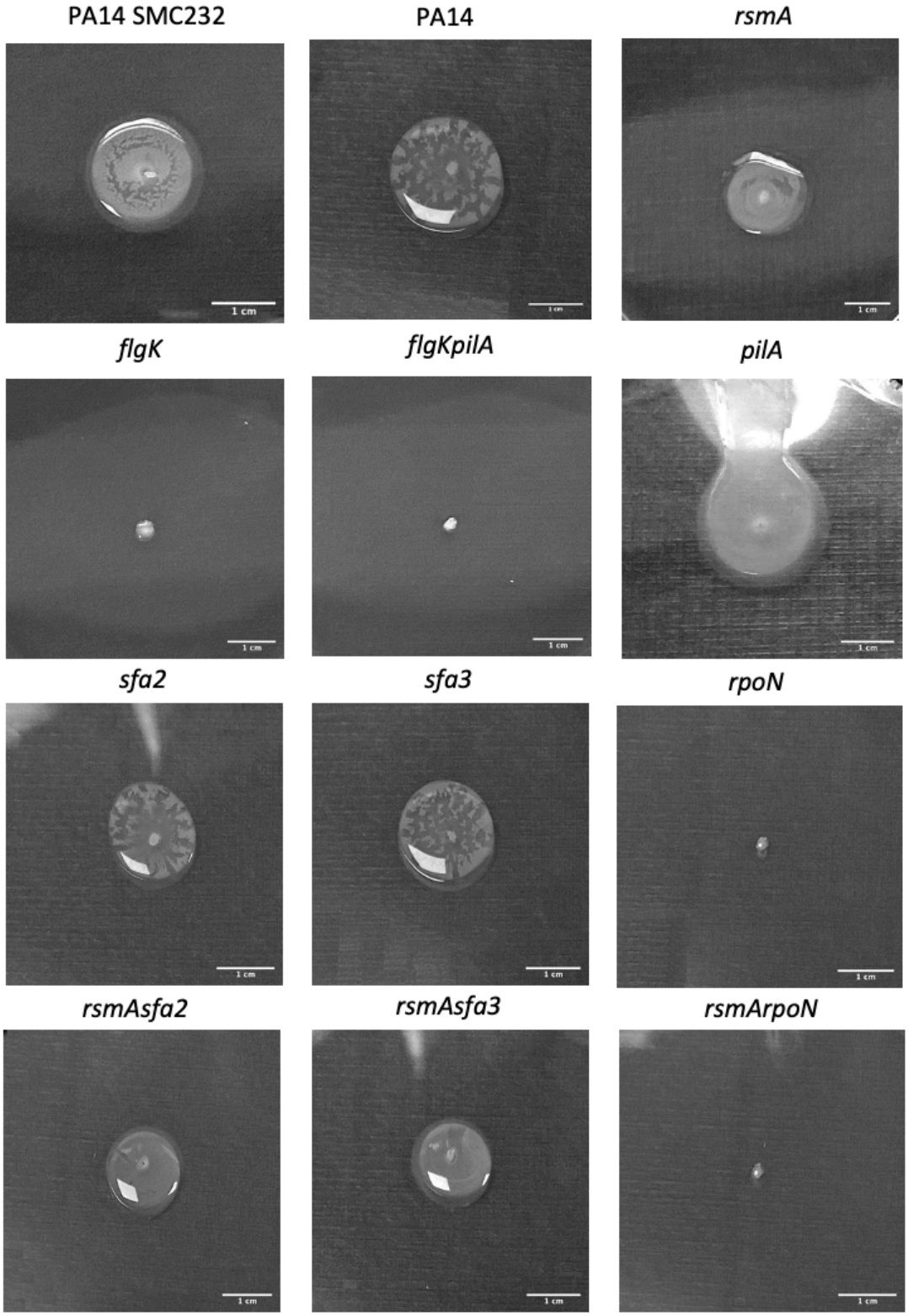


Figure 7.10: Swimming motility of *sfa2* and *sfa3* deletion mutants. Image for each strain indicates swimming motility area covered after 24 hrs. Flagellar and pili mutants (*flgK, pilA, flgKpilA*) were included in the strain panel as controls with altered motility. Note: PA14 SMC232, *flgK*, *flgKpilA* and *pilA* are George O'Toole lab strains for baseline, high (*pilA*) and low (*flgK, flgKpilA*) motility controls separate to the Allsopp lab and regulator deletion mutant strains. Some of this data is included in Allsopp *et al.* 2022 Figure S3.

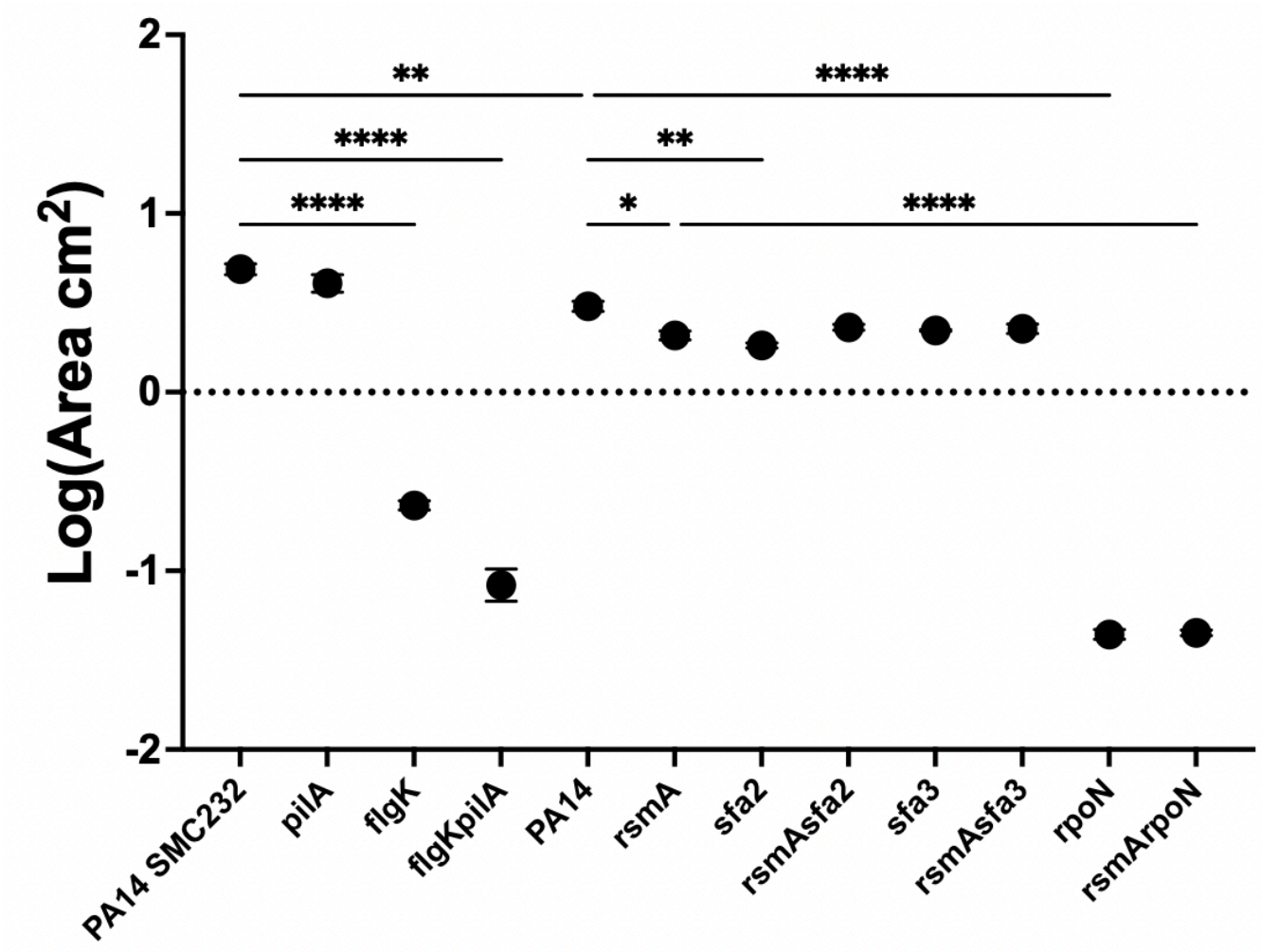


Figure 7.11: Deletion of *rpoN and rsmA* reduces swimming motility, but no effect is observed upon deletion of *sfa2* or *sfa3*. Graph showing motility area after 24hr incubation. Average motility area of three assay replicates and standard error are indicated. A One-Way ANOVA was performed on the log transformed average areas for each strain, statistically significant for 24 hrs motility to ****P<0.0001. Post-hoc statistical significance of regulator mutant motility compared with those of strain WT were determined using Šídák's test (n=3, six technical replicates). Note: PA14 SMC232, *flgK*, *flgKpilA* and *pilA* are George O'Toole lab strains for baseline, high (*pilA*) and low (*flgK, flgKpilA*) motility controls separate to the Allsopp lab strain panel. Significant reduction in *rpoN, rsmA* and *rsmArpoN* is observed indicating they influence swimming motility. No significant difference was observed upon deletion of *sfa3* indicating it plays no role in swimming motility. Unexpectedly a modest but significant reduction was observed in *sfa2* but not *rsmAsfa2* and indicates potential interplay of Sfa2 with other regulators which influences swimming motility. Some of this data is included in Allsopp *et al.* 2022 Figure S3.

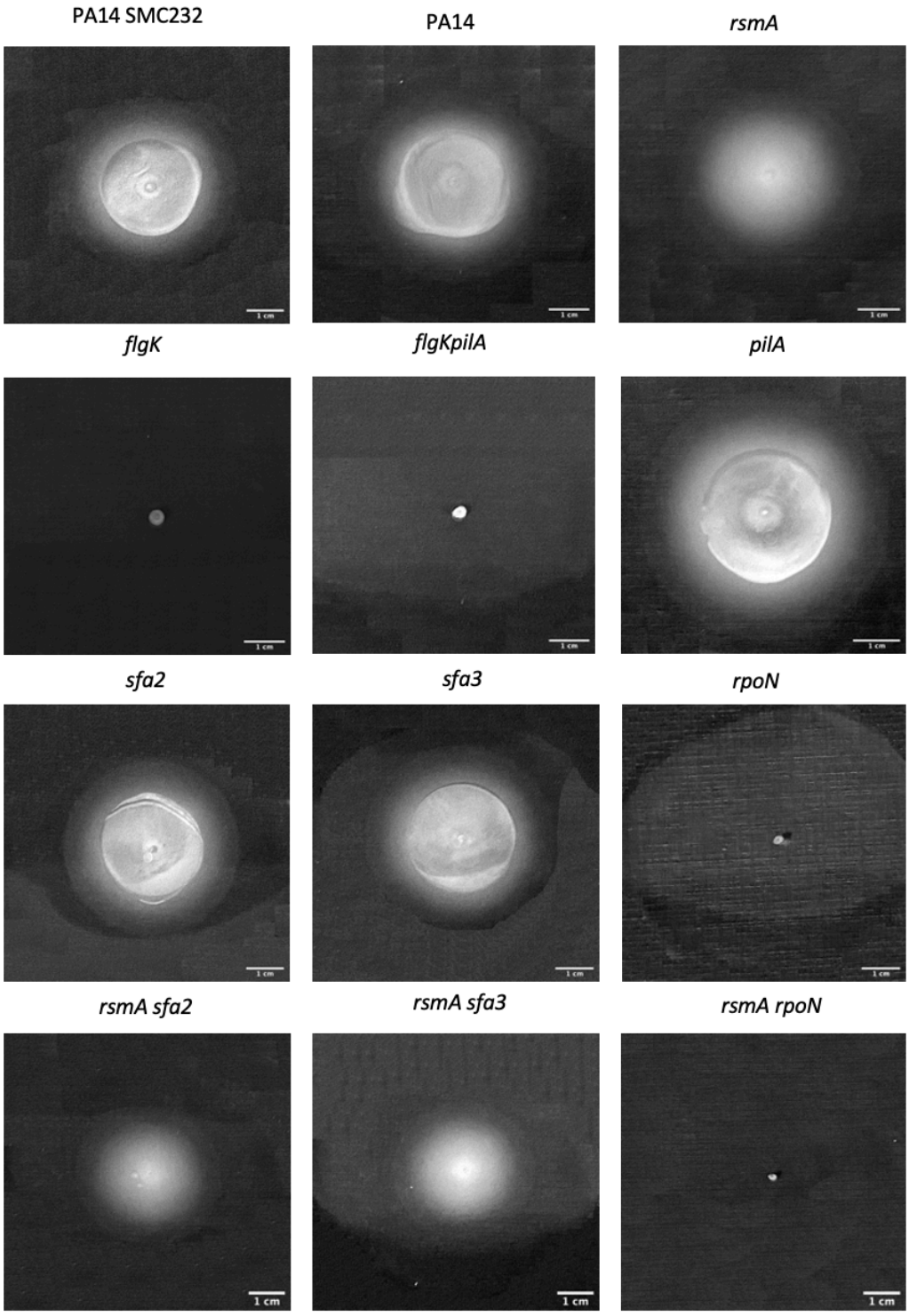


Figure 7.12: Swarming motility of *sfa2* and *sfa3* deletion mutants. Image for each strain indicates swarming motility area covered after 24 hrs. Flagellar and pili mutants (*flgK, pilA, flgKpilA*) were included in the strain panel as controls with altered motility. Note: PA14 SMC232, *flgK*, *flgKpilA* and *pilA* are George O'Toole lab strains for baseline, high (*pilA*) and low (*flgK, flgKpilA*) motility controls separate to the Allsopp lab and regulator deletion mutant strains. Some of this data is included in Allsopp *et al.* 2022 Figure S3.

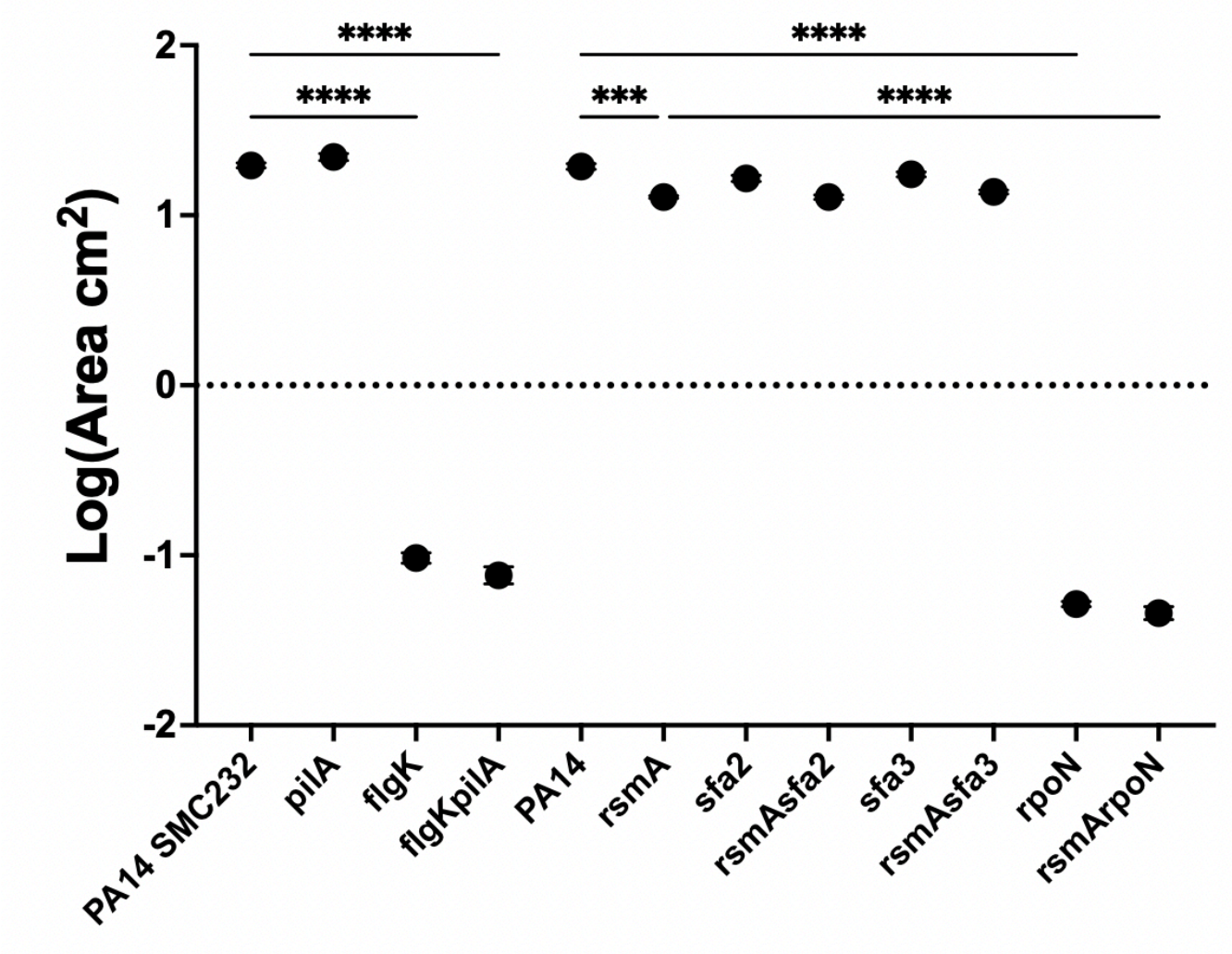


Figure 7.13: Deletion of *rpoN and rsmA* reduces swimming motility, but no effect is observed upon deletion of *sfa2* or *sfa3*. Graph showing motility area after 24hr incubation. Average motility area of three assay replicates and standard error are indicated. A One-Way ANOVA was performed on the log transformed average areas for each strain, statistically significant for 24 hrs motility to ****P<0.0001. Post-hoc statistical significance of regulator mutant motility compared with those of strain WT were determined using Šídák's test (n=3, six technical replicates). Note: PA14 SMC232, *flgK*, *flgKpilA* and *pilA* are George O'Toole lab strains for baseline, high (*pilA*) and low (*flgK, flgKpilA*) motility controls separate to the Allsopp lab strain panel. Significant reduction in *rpoN, rsmA* and *rsmArpoN* is observed indicating they influence swarming motility. No significant difference was observed upon deletion of *sfa2* or *sfa3* indicating they play no role in swarming motility.

7.4.4 Regulators RpoN and Sfa2 do not play a role in biofilm production in P. aeruginosa strain PA14

Previous research has shown the link between biofilm production and motility as an inverse relationship via the Gac/Rsm pathway, as well as to the expression of the T6SS (Merritt *et al.*, 2007; Martínez-Granero *et al.*, 2012; Guo *et al.*, 2014; Moscoso *et al.*, 2014; Chen *et al.*, 2020). Other regulators such as c-di-GMP levels and sRNAs are also involved (Fazli *et al.*, 2014). Thus *sfa2* deletion could alter biofilm production. Confirming whether Sfa2/Sfa3 do or do not play a role in biofilm formation is important in confirming Sfa2 specificity and if Sfa3 plays a role in biofilm production unseen from the RNA-seq results outlined in 7.4.2. To do this, a crystal violet biofilm production assay was conducted using the panel used in 7.4.4 exchanging *pilA* with the *retS* strain which is a hyper biofilm forming control.

No significant difference in biofilm production was observed in the *sfa2/sfa3* deletion mutants compared with the WT (Figure 7.14). A significant reduction was observed with the flagellar controls, *flgK* and *flgKpilA*. This was expected as flagella are inversely regulated with biofilm production (Winstanley, O'Brien & Brockhurst, 2016; Li *et al.*, 2017). A significant increase was observed for *retS* control which was also expected as RetS is a negative regulator of biofilm production (Kaler, Nix & Schubot, 2021). A significant increase was observed with *rsmA* and decrease with *rpoN* compared with the PA14 WT. Additionally a significant increase was observed with *rsmArpoN* compared with *rsmA*. The reduction in biofilm production observed for *rpoN*, and increase for *rsmA*, were expected as RpoN and RsmA positively and negatively regulate biofilm production, respectively (Irie *et al.*, 2020; Liu *et al.*, 2021). No significant difference was observed for the *sfa2* or *sfa3* deletion mutants. This indicates RpoN

plays a role in biofilm production, but Sfa2 and Sfa3 do not. This supports the transcriptomics results outlined in 7.4.1 outlining Sfa2 specificity to the regulation of the H2-T6SS.

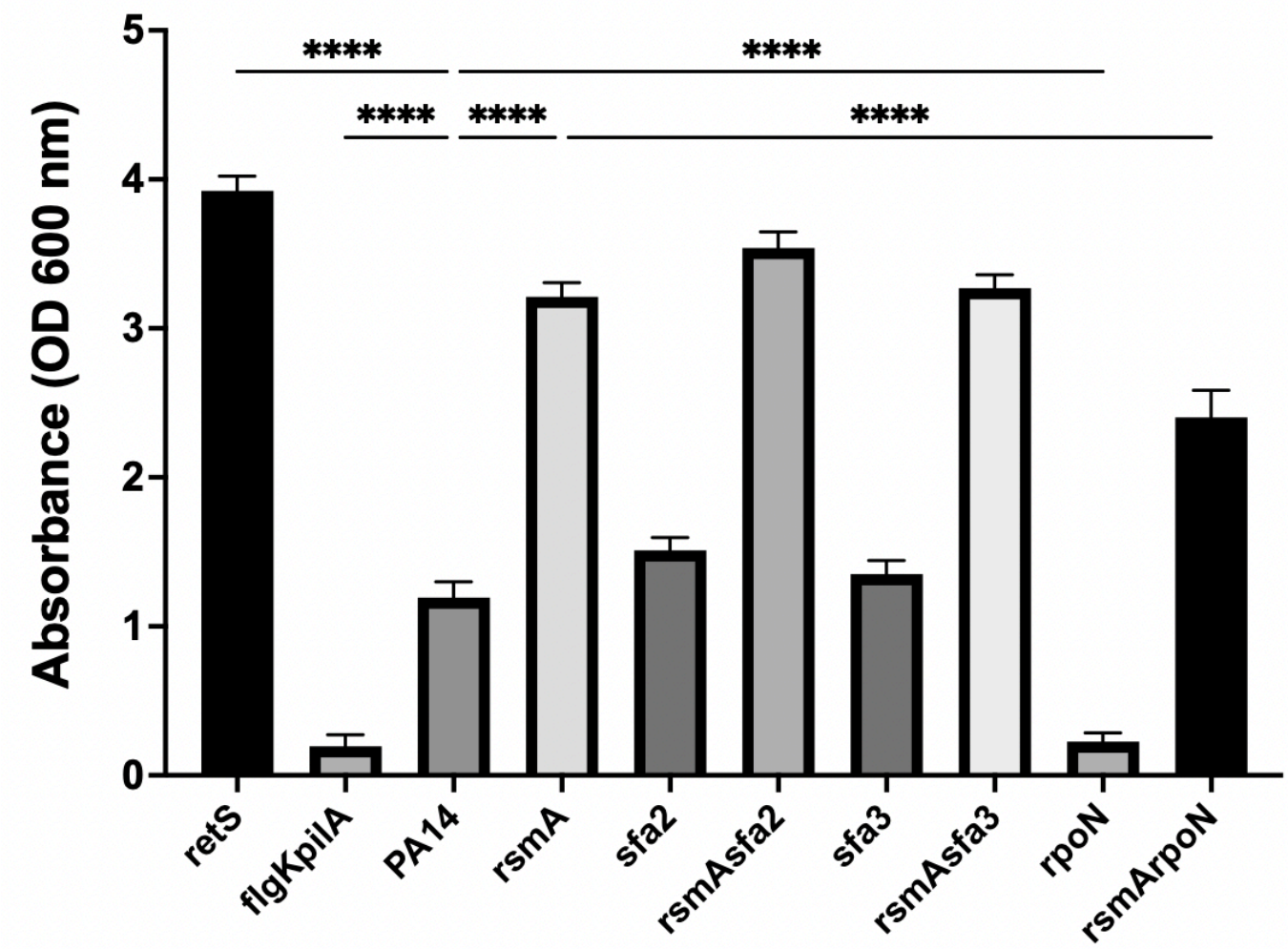


Figure 7.14: Deletion of *rpoN* and rsmA significantly alters biofilm formation, but no effect is observed upon deletion of *sfa2* or *sfa3*. Graph showing biofilm biomass produced after 24hr incubation. Average absorbance of three assay replicates and standard error are indicated above. A One-Way ANOVA was performed on the average absorbance for each strain, statistically significant for 24 hrs biofilm production to ****P<0.0001. Post-hoc statistical significance of regulator mutants compared with those of strain WT were determined using Šídák's test (n=6, seven technical replicates). A flagellar and pili (*flgKpilA*) and sigma factor (*rpoN*) mutant were included in the strain panel as low biofilm producing controls. A histidine kinase (*retS*) mutant was included in the strain panel as a high biofilm producing control. Significant increase in biofilm biomass was observed with *rsmA* and decrease with *rpoN* was observed compared to PA14 WT. Additionally a significant reduction in biomass was observed with *rsmArpoN* compared to *rsmA.* This indicates RsmA and RpoN play a role in biofilm production. Some of this data is included in Allsopp *et al.* 2022 Figure S4.

7.5 Discussion

The work outlined in this chapter shows a clear and broad impact of RsmA upon almost all T6SS and CDI genes. In addition, RpoN is necessary for CDI and H2-T6SS expression, where EBP Sfa2 works in conjunction to promote expression of the H2-T6SS core operon and orphan clusters. However, Sfa3 has limited impact upon gene expression with no clear role in expression of the H3-T6SS under the conditions tested here. This work has therefore enhanced our understanding of regulators of the CDI and T6SSs.

EBPs have previously been associated with the T6SS core operons in *P. aeruginosa*, indicating a potential role in the regulation of expression during interbacterial competition (Sana *et al.*, 2013; Allsopp *et al.*, 2017). My work has formed part of a larger project by our group which has shown that RpoN is a transcriptional regulator of all three T6SSs, where the H1- and H3-T6SSs are positively regulated whilst H2-T6SS is negatively regulated and requires EBP Sfa2 in the transcription polymerase complex to enable transcription initiation (data present here and in (Allsopp *et al.*, 2022)). We show a truly global impact of RsmA as a negative regulator of the T6SSs. We also show that, RpoN negatively regulates the H2-T6SS, whilst positively regulating the H1- and H3-T6SSs. I show Sfa2 plays a specific role in H2-T6SS expression which is not involved in regulation of other mechanisms such as swarming motility and biofilm production but appeared to play a very modest role in swimming motility. Finally, we outline no observable role for Sfa3 in H3-T6SS expression, motility, or biofilm formation. This expands on the Allsopp *et al*. study from 2017 indicating the T6SSs are controlled by RsmA and that EBPs such as Sfa2 are involved in fine-tuned control of the system in conjunction with RpoN.

Additionally, I show that RsmA negatively regulates CDI systems. These results thereby support those observed in the Mercy *et al.* study from 2016 inferring CDI are regulated by RsmA. Finally, I highlight a new role for RpoN as a positive regulator of CDI expression. This shows that multiple regulators work in tandem at the transcriptional and post-transcriptional level to control the expression of these systems. This coregulation and tight control by the various regulators explored in this chapter indicate these systems might be used as a mechanism for *P. aeruginosa* colonisation and dominance during CF pulmonary infection.

7.5.1 Can transcriptomics analysis identify regulators of CDI and T6SS?

Competitive systems are structurally and functionally complex and require tight regulation at the transcriptional, post-transcriptional and post-translational levels (Wang, Brodmann & Basler, 2019; Allsopp *et al.*, 2022; Nolan & Allsopp, 2022). To fully understand how they are regulated; transcriptomics analysis from data generated from techniques such as RNA-seq can address this (Belliveau *et al.*, 2018). RNA-seq can accurately assess RNA levels to pinpoint genes with significantly altered levels in a deletion mutant background compared with a WT strain. This is useful in identifying the role regulators play in operons of interest. The Gac/Rsm pathway is a regulator of CDI and T6SSs (Mercy *et al.*, 2016; Allsopp *et al.*, 2017), which acts at a post-transcriptional level to directly repress or alter the stability of mRNA transcripts but also regulates other regulators. Identifying transcriptional regulators is important in understanding when and how these systems are expressed.

Many operons are regulated transcriptionally by sigma factor activators which act as global regulators for transcription initiation of sets of genes (Browning & Busby, 2004). Regulons linked to virulence, stress and metabolism are often co-regulated by one sigma factor (Schulz

et al., 2015). RpoN is a sigma factor which is associated with the Gac/Rsm pathway by negatively regulating GacA expression, a component of the pathway (Heurlier *et al.*, 2003; Shang *et al.*, 2021). RpoN also mediates transcriptional control of motility and biofilm formation genes showing a degree of interconnectedness with RsmA (Damron *et al.*, 2012; Liu *et al.*, 2021). RpoN requires EBPs or SFAs for transcription initiation which often act to enable tight control of specific systems (Gao *et al.*, 2020). The presence of putative EBPs was observed in the core operons associated with H2- and H3-T6SS in a study by Filloux *et al.* in 2008 suggesting T6SSs could be additionally controlled using SFAs. To further characterise the role of RpoN and Sfa2/Sfa3 on T6SS gene expression, transcriptomics analysis was performed.

7.5.1.1 T6SS secretion systems

From the analysis performed by Luke Allsopp, deletion of RsmA upregulated all T6SSs (Allsopp *et al.*, 2022). Deletion of RpoN showed downregulation of flagellar genes (Figure 7.1) and a diguanylate cyclase gene (Table 7.1), whilst showing significant changes in expression of T6SS associated genes (Figure 7.2). Downregulation of flagella genes in *rsmArpoN* was expected as RpoN positively regulates the flagella operon (Liu *et al.*, 2021). Diguanylate cyclases are enzymes which catalyse c-di-GMP production- a regulator of biofilm production (Park & Sauer, 2022). As motility is linked to biofilm formation through an inverse regulatory relationship (Guo *et al.*, 2014), the differential regulation of this gene is an expected outcome. Therefore, these results support the current literature. RpoN deletion showed differential regulation of the T6SSs, where H1- and H3-T6SSs were upregulated whilst H2-T6SS was downregulated. This was later supported by my β-galactosidase assay in Figure 7.9. This expands the current literature showing RsmA represses all T6SSs and identifies RpoN as a regulator of all three T6SSs. As T6SSs are regulated under the Gac/Rsm pathway (Allsopp *et*

al., 2017), this indicates an interplay between RpoN and RsmA in the expression of T6SSs and outlines two levels of expression control at the transcriptional and post-transcriptional levels.

Deletion of Sfa2 showed no significant changes in flagellar expression (Figure 7.4), but a significant downregulation of H2-T6SS core cluster and orphan operons alone (Figure 7.3). This indicates Sfa2 is specific to H2-T6SS expression supporting the literature on the EBP specificity. Deletion of Sfa3, like Sfa2, showed no significant alteration in flagellar expression (Figure 7.5). However, unlike Sfa2, only 10 genes were shown to be significantly altered upon deletion of *sfa3* and did not include genes from H3-T6SS associated operons, but one gene associated with H2-T6SS *tli5a* (Figure 7.6). The lack of dysregulation observed indicates Sfa3 does not play a role in H3-T6SS regulation or interact with RsmA/RpoN.

This begs the question why is EBP regulation not observed in the H1- and H3-T6SS? The presence of Sfa3 in H3-T6SS core operon may indicate a divergence in the evolutionary role of the different *P. aeruginosa* T6SSs. As *sfa3* deletion outlined dysregulation of only 10 genes, this may indicate that Sfa3 no longer has a functional role which could be due to the variation in sequence homology observed in Allsopp *et al*. 2022. This could mean the role of Sfa3 in H3-T6SS fine-tuned expression was no longer required due to the evolving function of the system and its associated effectors, which may be why it is negatively regulated alongside H1-T6SS. If this is the case, the regulation of H2-T6SS by Sfa2 may mean it is still required due to the H2-T6SS role in bacterial competition or pathogenesis, or consequently it is a more potent and energy expensive mechanism only utilised under certain stressors or competitors. Alternatively, Sfa3 may interact with another regulator for expressional control of H3-T6SS.

7.5.1.2 CDI secretion systems

Using the transcriptomics data generated for the Allsopp *et al.* 2022 publication, I identified a role for RsmA and RpoN in the regulation of the expression of CDI systems in PA14. Here *rsmA* deletion (Figure 7.7) showed significant change in expression of CDI associated genes in addition to a CdrB/CdrA system homologue TPS^{61200} supporting results observed in the Mercy *et al.* study for CDI as well as the Colley *et al.* study for CdrB/CdrA (Colley *et al.*, 2016). Subsequent deletion of *rpoN* showed significant repression of CDI genes (Figure 7.8), indicating RpoN acts as a positive regulator of CDI- a previously undocumented result in the current literature. Here, TPS^{61200} was upregulated upon *rpoN* deletion indicating it is under a different transcriptional regulator. CdrB/CdrA system expression, supported by Figure 7.7, is controlled via RsmA which occurs through the expression of *rsmZ* in a SiaA/D dependent manner (Colley *et al.*, 2016). SiaD diguanylate cyclase is stimulated to produce c-di-GMP in a positive feedback loop upon expression of biofilm component *psl* (Irie *et al.*, 2012). As Psl is under RpoS regulation (Irie *et al.*, 2010), this indicates TPS^{61200} may instead be under RpoS control. This is interesting as CdrB/CdrA systems are linked to biofilm structure (Reichhardt *et al.*, 2018). The disparity in regulation may indicate that CDI systems in PA14 are not utilised upon expression of biofilm components, where they are downregulated and CdrA/CdrB TPS are upregulated. This could support the results previously observed in 6.3.2 (Figure 6.6), which indicated that deletion of CDI did not affect biofilm production despite a previously observed effect in PAO1 (Mercy *et al.*, 2016) and that the biofilm genes might be different between PA14/PAO1. This gives credence to the argument that CDI can be differentially regulated between strains.

This analysis shows that like the T6SS, RsmA and RpoN play an important role in the regulation of the expression of these competitive systems. It appears both CDI systems and the H2-T6SS are positively regulated by RpoN, whilst H1- and H3-T6SSs are negatively regulated. This co-regulation of CDI systems and H2-T6SS indicates these systems are likely co-expressed and therefore may have complementary roles such as enhancing killing through complementary toxin delivery, targeting a board array of bacteria, or kin selection. The CDI systems may allow the bacterium to sense an interaction with a neighbouring cell and then utilising the H2-T6SS in a retaliatory response a protection mechanism from incoming attackers. However, this tit-for-tat mechanism has only been observed for H1-T6SS to date (Basler, Ho & Mekalanos, 2013). A more likely explanation is that *P. aeruginosa* cells sense kin cell death which activates the *Pseudomonas aeruginosa* response to antagonism (PARA) response leading to H1-T6SS upregulation, in addition to the other T6SSs and CDI systems (LeRoux *et al.*, 2014; Mercy *et al.*, 2016; Allsopp *et al.*, 2017, 2022). This could be evaluated by RT-qPCR through interbacterial competition assays (Kim *et al.*, 2020). Alternatively fluorescently tagging each system and viewing firing events through time-lapse fluorescence microscopy such as conducted in LeRoux *et al.* 2014. Additionally, the antibodies developed in Chapter 5, if validated, alongside previously generated T6SS antibodies by the Allsopp lab could be utilised in identifying the expression each system under different conditions.

7.5.2 Is motility influenced by RpoN and SFA proteins?

Bacterial motility is a well-documented mechanism controlled by the sigma factor RpoN (Liu *et al.*, 2021). Here I show that deletion of *rpoN* renders PA14 non-motile to the same extent as a *flgK* flagella mutant, in line with the current literature (O'Toole & Kolter, 1998; Damron *et al.*, 2012; Liu *et al.*, 2021). The impact of Sfa2 and Sfa3 upon motility was unknown at the

start of this work. As EBP FleQ is associated with RpoN-mediated control of motility (Dasgupta *et al.*, 2003), here I investigated EBPs Sfa2 and Sfa3 for their potential roles in motility to validate the transcriptomics results outlined in 7.3.1 *in vitro* (Figure 7.10 and 7.12).

A significant reduction in swimming between PA14 WT and flagellar mutants; *flgK* and *flgKpilA*, was observed in line with the literature (O'Toole & Kolter, 1998). A significant reduction in swimming was also observed between PA14 WT compared with *rsmA* and *rpoN*, in addition to a reduction observed between *rsmA* compared with *rsmArpoN*. This indicates both *rpoN* and *rsmA* play a role in positive regulation of swimming motility, supporting current literature (Li *et al.*, 2017; Liu *et al.*, 2021). Unexpectedly, a significant reduction was observed upon *sfa2* deletion which may suggest some interplay with flagellar motility (Figure 7.11). However, as this result is not seen in the *rsmAsfa2* strain, this indicates the effect observed is not due to Sfa2 and may be due to another regulator which was negated in *rsmA*. Alternatively, there may be an unknown link to flagellar gene expression which was not observed in the results outlined here. To confirm a true significant difference, repeating the experiment with *sfa2* complemented strains would confirm whether another regulator was at play or if Sfa2 truly does influence swimming. No significant difference in swimming motility was observed for any of the *sfa3* deletion mutant strains indicating it does not play a role in swimming motility.

No significant difference in swarming motility was observed in the SFA mutant strains (Figure 7.13). There was significant reduction in swarming between PA14 WT and flagellar mutants; *flgK* and *flgKpilA*, in line with the literature (O'Toole & Kolter, 1998). A significant reduction in swarming was also observed between PA14 WT compared with *rsmA* and *rpoN*, in addition to a reduction observed between *rsmA* compared with *rsmArpoN*. This indicates both *rpoN*

and *rsmA* play a role in positive regulation of swarming motility, supporting current literature (Kohler *et al.*, 2000; Yeung *et al.*, 2009). No difference was observed in swarming motility for *sfa2* or *sfa3* strains indicating they play no role in group-mediated movement.

This analysis validates the specific role of Sfa2 in the control of H2-T6SS expression and not upon motility or biofilm. Understanding the role of regulators at the transcriptional and post-transcriptional levels expands our understanding of these mechanisms in bacterial survival and pathogenesis. This further supports the idea that the T6SSs have an important evolutionary role as the fine-tuned H2-T6SS expression appears to not be coregulated with other mechanisms associated with enhanced bacterial survival and persistence such as motility. This may be due to the energy expensive nature of motility and T6SSs (Basler, 2015; Schavemaker & Lynch, 2022). As motility and biofilm production are linked by an inverse regulatory relationship (Guo *et al.*, 2014) I next investigated biofilm formation.

7.5.3 Is biofilm production influenced by RsmA, RpoN and SFA proteins?

Biofilm production is another well-documented mechanism controlled by the sigma factor RpoN (Liu *et al.*, 2021). The RpoN regulon is vast and controls many mechanisms associated with bacterial survival and persistence and has been highlighted in many important mechanisms associated with *P. aeruginosa* infection (Schulz *et al.*, 2015). The RNA-seq analysis outlined in 7.4.1 showed that RpoN altered the expression of 1554 genes. To validate the scope of RpoN and the other regulators under study here in modulating biofilms, biofilm assays where performed. Here I show deletion of *rpoN* renders PA14 unable to produce biofilm to the same extent as a *flgKpilA* flagella and type IV pili double mutant, in line with the current literature (Damron *et al.*, 2012; Ha, Kuchma & O'Toole, 2014). The impact of Sfa2

and Sfa3 upon biofilm production was unknown at the start of this work. As EBP FleQ is associated with RpoN-mediated to control of biofilm (Baraquet *et al.*, 2012) here I investigated EBPs Sfa2 and Sfa3 for their potential roles in motility to validate the transcriptomics results outlined in 7.3.1 *in vitro* (Figure 7.14).

A significant reduction in biofilm production between PA14 WT and flagellar mutants; *flgKpilA*, was seen in line with the literature as positive regulators of biofilm production (Damron *et al.*, 2012; Ha, Kuchma & O'Toole, 2014). A significant increase in production was observed between PA14 WT and *retS* mutant, in line with the literature as RetS negatively regulates biofilm production (Kaler, Nix & Schubot, 2021). An additional significant reduction in biofilm production was also observed between PA14 WT compared with *rpoN,* whilst a significant increase was observed when compared with *rsmA*. This indicates *rpoN* and *rsmA* play an inverse role in regulating biofilm production, supporting current literature (Li *et al.*, 2017; Liu *et al.*, 2021). No difference was observed in swarming motility for *sfa2* or *sfa3* strains indicating they play no role in group-mediated movement.

As motility and biofilm formation have an inverse regulatory relationship (Guo *et al.*, 2014), the lack of role observed for these EBPs for both motility and biofilm production mechanisms was expected. This further supports the specificity of Sfa2 in H2-T6SS regulation. Although both biofilm production and T6SSs are associated with the same phase of infection and the T6SS in *P. aeruginosa* have been shown to play a role in biofilm formation (Chen *et al.*, 2020), Sfa2 appears to play a specific role in the modulation of the H2-T6SS. As we outlined RpoN's impact on all T6SSs, this indicates Sfa2 only activates RpoN at the site of specific genes in the genome. This gives further credence to the role of specific T6SSs upon sensing specific stimuli. Therefore the T6SSs may play different roles in infection, which warrants further research to

shed light on pathogenesis mechanisms of *P. aeruginosa* that may influence colonisation and formation of chronic infections in conditions such as CF.

7.6 Conclusions

The main conclusions associated with the transcriptomic RNA-seq analysis, and subsequent phenotypic validation studies *in vitro* are as follows:

1. RpoN and RsmA play a role in the expression of the CDI and T6SSs
2. RsmA negatively regulates all CDI and T6SSs
3. RpoN positively regulates the H1- and H3-T6SSs
4. RpoN negatively regulates the CDI and H2-T6SSs
5. RpoN does not play a role in swimming motility, but Sfa2 may
6. RpoN and Sfa2 do not play a role in swarming motility
7. RpoN and Sfa2 do not play a role in biofilm production

Therefore, these results presented in Chapter 7 build on the current literature indicating competitive systems are regulated by both RpoN and RsmA transcriptional and post-transcriptional regulators and show a clear example of EBP fine-tuning to control H2-T6SS core and orphan operon expression (Sana *et al.*, 2013; Mercy *et al.*, 2016; Allsopp *et al.*, 2017, 2022). This indicates the importance of specific regulators and the idea these systems are generally repressed by RsmA. However, the T6SS are differentially expressed by different regulators and may play separate roles in competition, survival, and subsequent dominance of a niche. Sfa2 specificity in H2-T6SS expression is indicative of specific control not observed

with the H3-T6SS associated EBP Sfa3, showing an unprecedented level of control. The differences in expression between the T6SSs support the idea for their differential expression and utilisation under different scenarios faced by the bacterium. As RsmA represses all three T6SS and both CDI systems and there is further overlap of regulators with RpoN between the CDI systems and the H2-T6SS, this suggests these systems may be expressed in the same environment or in response to the same environmental stimuli.

So, the final step was to consider whether these results supported or refuted the hypotheses proposed at the beginning of this chapter.

Hypothesis 1: Both CDI and T6SSs are controlled by the transcriptional regulator RpoN. **This was accepted.**

Hypothesis 2: T6SS expression is controlled by SFA proteins Sfa2 and Sfa3. **This was partially accepted and partially refuted. Whilst a clear and specific role was observed for Sfa2 in the expression of H2-T6SS, no role was observed for Sfa3 in control of the expression of T6SSs.**

Hypothesis 3: RpoN and Sfa2/3 play a role in motility in *P. aeruginosa* PA14. **This was refuted. The transcriptional RNA-seq analysis showed a clear impact of deletion of *rpoN* on multiple flagella genes. No observed change was indicated in the expression levels of flagellar genes in the *sfa2* and *sfa3* mutants. This was supported here as no role was observed on swarming for *sfa2* and *sfa3,* but a large effect was for *rpoN*. However, a modest role was observed in swimming motility for the *sfa2* mutant, but as this effect was negated in *rsmAsfa2* mutant this indicates this may be due to interplay with other regulators.**

Hypothesis 4: RpoN and Sfa2/3 play a role in biofilm formation in *P. aeruginosa* PA14. **This was refuted. No role was observed in biofilm formation in the *sfa2* and *sfa3* mutants, but a large effect was observed for *rpoN*.**

Confirming the transcriptional regulators for the CDI and T6SSs supports previous research conducted and the idea that these systems are differentially regulated in *P. aeruginosa*. The conserved regulation via RsmA and RpoN of the CDI and T6SSs indicates that certain systems have a degree of coregulation. This concept could support results outlined in the interbacterial competition observed in Chapter 6 where differences in CDI killing was observed in the presence or absence of the T6SS. This regulation interplay mandates further exploration into these systems. It would be interesting to define if these regulatory networks are employed by clinical strains. Outlining this regulation and any deviations/mutations which could be observed in clinical strains may give insight into their clinical importance and why some *P. aeruginosa* strains can outcompete other previously established and dominant *P. aeruginosa* strains. This knowledge could have clinical importance in understanding outcomes from *P. aeruginosa* infection in CF and potentially identify novel targets to switch off these systems for the development of novel treatments.

8. Final Discussion

The CDI systems are important tools in the bacterial arsenal to enable them to compete with other cells within their environment. CDI systems eliminate or suppress the growth of competing cells through the direct delivery of antibacterial toxins. Furthermore these systems enable kin recognition through shared toxin-immunity pairs. CDI systems are used by gram-negative bacteria in addition to another contact-dependent competitive system- the T6SS. Increasing evidence has shown that CDI and T6SSs play a role in pathogenesis to enable colonisation and dominance of a new niche. In this thesis, I have investigated the presence and domain structure of two '*E. coli*-type' CDI systems encoded in *P. aeruginosa* PA14, their functionality and roles in interbacterial competition and cooperation. I have also investigated T6SS and CDI regulation at the transcriptional and post-transcriptional level. In this chapter, I will discuss the overall implications of the results outlined in this thesis in the context of the wider field and assess their potential impact on our understanding of the systems themselves as well as their roles in *P. aeruginosa* infection in CF.

8.1 CDI secretion systems in *P. aeruginosa*

The ability for bacteria to survive can require the acquisition and utilisation of mechanisms to compete for space and resources that can result in an arms race. This is particularly the case between closely related organisms which likely share the same niche and use the same resources, increasing the odds of competition (Hibbing *et al.*, 2010). Possessing multiple competitive mechanisms may provide a fitness advantage that enables colonisation and establishment within a niche. CDI secretion systems are one such mechanism that has been

shown to play a role in bacterial survival in polymicrobial environments and are found in an array of different bacterial genera such as *Escherichia, Acinetobacter* and *Pseudomonas* (Aoki *et al.*, 2010; Mercy *et al.*, 2016; Harding *et al.*, 2017). *P. aeruginosa* encodes two CDI systems, which have previously been shown to play a role in interbacterial competition (Mercy *et al.*, 2016; Melvin *et al.*, 2017; Allen *et al.*, 2020). Although these systems were identified over a decade ago in an *E. coli* strain linked to pathogenesis and niche dominance (Aoki *et al.*, 2010), relatively little is elucidated about their presence and utilisation throughout gram-negative bacteria in comparison to other systems such as the T6SS. Therefore much remains to be determined about their roles in bacterial growth and infection. Since the first study in *P. aeruginosa* by Mercy *et al.* in 2016, these systems have been investigated for their role in interstrain competition and potential to contribute to *P. aeruginosa* dominance in both acute and chronic infection (Melvin *et al.*, 2017; Allen *et al.*, 2020). However, much of this research has utilised laboratory strain PAO1, the gold standard strain in *P. aeruginosa* research (Chandler *et al.*, 2019). Yet, the lab strain PA14 is considered more relevant when evaluating mechanisms in human infection due to its enhanced virulence arsenal and additional 800 genes which are yet to be characterised (Grace *et al.*, 2022).

Using PA14, I further bioinformatically investigate the two CDI encoded by *P. aeruginosa* PAO1 and PA14, highlighting differences in domain architecture via in depth analysis in addition to outlining disparities in previous distinctions of the entire genomic regions encoding PAO1 CDI operons. Presented in Chapter 3, these results show that domain architecture between systems is conserved, whilst function is highly specific, particularly at the 3' end. This is evident at the 3' end due to the high rates of homologous recombination which occur at these sites previously highlighted in the literature (Hayes *et al.*, 2014; Arenas

et al., 2013; Koskiniemi *et al.*, 2014). To date most studies have concluded the specificity of these systems even between strains from the same species (Allen & Hauser, 2019). However, the results presented here showed high sequence and structural similarities with toxins encoded between the PA14 and PAO1 systems in addition to instances of clear structural homology to genes from bacteria of different genera. This homology would help to facilitate HGT and HR of the genes encoding these polymorphic toxins beyond *Pseudomonas* spp. in line with previous studies (Zhang *et al.*, 2012).

As CDI toxin targets are intracellular (Cuthbert, Hayes & Goulding, 2022), and from this analysis effector encoding genes show high percentage identity to genes from other genera, CDI toxic functions may be more conserved than we think. Many of these targets are highly conserved within cells, particularly those targeting molecules of the central dogma, however many functions are yet to be identified. The presence of trans-kingdom effectors such as the CdiA-CT^{00510} tRNase, previously validated *in vitro* by Allen *et al.* in 2020, gives credence to the idea of conserved targets. Due to its conserved target in both prokaryotes and eukaryotes, and outlined role in *in vivo* mouse models of acute infection, CdiA-CT^{00510} tRNase may also be used against other eukarya such as fungi. This could expand the target range of these systems which to date has not been observed. However, the major limitation of CDI deployment is the requirement for specific receptors for C-terminal toxin domain uptake. There are many regions of the CdiA which have no defined function which could play a role in entry. Although a mechanism of eukaryotic entry is yet to be defined from the *in vivo* virulence studies conducted to date (Allen *et al.*, 2020), this supports the idea that these toxins have a much broader function.

Toxin sharing between different bacteria and divergent evolution into unique sequences would explain why these toxins have previously appeared novel as certain toxin-immunity modules were previously unidentified in the literature or had not been linked to other systems in various bacterial genera/species (Allen & Hauser, 2019). Wang *et al*. in 2022 was able to outline toxins which did not share sequence identity but had a matched topology and tRNase function. Therefore some of these toxins may have similar structures having evolved convergently to mediate a similar function and this builds the argument for targeting conserved internal functions within competing cells. Although much development in recent years has contributed to protein structural databases, they require more development and structural information before structural homologies between uncharacterised toxins can be ascertained this way more frequently.

Phylogenetic analyses of CDI systems have outlined diversity in CdiA toxin-passenger domains in *P. aeruginosa* strains (Allen *et al.*, 2020), but have not attempted to determine the genetic relatedness of these systems between other species within the *Pseudomonas* genera. The results outlined here identify the phylogenetic relationship between homologous systems, which clade together, in addition to their relationship to *cdiA* encoded in other *Pseudomonas* species. It was interesting that *cdiA*^{2462} was established as the most distantly related of the PA14 and PAO1 systems (which was found outside the clade encapsulating the other systems) and was instead found to be more closely related to *P. denitrificans* than the other three systems. CDI systems have been shown to be carried on plasmids therefore a conjugation event within the environment is plausible however this is yet to be shown in *P. aeruginosa* strains (Wäneskog *et al.*, 2021). Alternatively, these systems could have a common ancestral CDI operon which diversified at the 3’ end through HR events. Further studies on CDI

phylogeny throughout the genomes of multiple members of the polymicrobial community could shed light on why particular communities form, potentially based on toxin-immunity dissemination, which is driven by the acquisition or inherent presence of these systems in those members. This is a previously observed phenomenon in the gut by *Bacteroides* T6SSs (Ross *et al.*, 2019b), and may therefore be observed in the CF lung. As *P. aeruginosa* is not an inherently aggressive bacteria, the presence of shared immunities may be why certain members of the CF polymicrobial community survive during the reduction in diversity observed upon lung function decline or by not initiating competition with the pathogen.

As high sequence identity was observed between toxins and other proteins found in bacteria associated with CF infection, this could further support the idea that these toxins are used by *P. aeruginosa* and the other organisms to control the composition of the polymicrobial community. Despite these systems showing toxin homologies with other bacteria, the possession of multiple specific systems which have differences in toxic functions gives the strain a different combination of systems for competition, increasing the likelihood of dominance. In addition, different competition systems may enable the bacteria to respond specifically to a wider range of stimuli. Each system may be deployed based on different stimuli, which would provide an advantage over a single system. This would be beneficial to a bacterium such as *P. aeruginosa* which can survive in a wide range of environments including the human body to increase its likelihood of survival (Moradali, Ghods & Rehm, 2017). This ability to adapt to diverse environments may therefore involve specific CDI and/or T6SSs or be expressed together to enable survival and colonisation.

8.2 Function and specificity of CDI encoded toxin-immunity modules for interbacterial competition

Many CDI toxins have been reported in the literature that mediate interstrain competition due to their antibacterial activity (Aoki *et al.*, 2005, 2010; Mercy *et al.*, 2016; Salcedo *et al.*, 2019; Allen *et al.*, 2020; Wäneskog *et al.*, 2021). However, CDI toxins require interaction with receptors for import into the periplasm and others for import into the cytoplasm (Willett *et al.*, 2015a; Ruhe *et al.*, 2018; Bartelli *et al.*, 2019; Myers-Morales *et al.*, 2021). Through the use of specific receptor binding and YP domain classifications in recognising receptors on neighbouring cells (Aoki *et al.*, 2010; Allen *et al.*, 2020), CDI toxins can be transferred across membranes to gain access to their specific targets in the prey cell cytosol. The requirement of these receptors also likely limits the use of the CDI systems to closely related organisms. However, the extent of this specificity remains unknown as OM receptors for CDI deployment in *P. aeruginosa* are yet to be determined. To date, the DppBC IM receptor has been outlined for *P. aeruginosa* (Allen *et al.*, 2020) and this is a likely mechanism of toxin internalisation for the PA14 CDI systems.

P. aeruginosa CDI systems in PAO1, like many others, have been shown to encode specific toxin-immunity modules which enable toxin neutralisation and interact directly through cognate binding (Ruhe *et al.*, 2013; Willett *et al.*, 2015b). Although these toxins have been outlined in the literature, many of their putative functions throughout gram-negative bacteria are yet to be validated *in vitro*. Therefore much remains to be determined about CDI toxicity and potency and how this plays a role in invasion of pre-established niches. This is particularly

evident in *P. aeruginosa* as CDI toxin functions have only been outlined in two studies to date (Mercy *et al.*, 2016; Allen *et al.*, 2020).

Utilising the two CDI systems encoded in PA14, my results support the literature on the specificity, potency, and direct binding of toxin-immunity modules in *P. aeruginosa*. Presented in Chapter 4, these results show that these CDI are potent in antibacterial toxicity. The fact that only the matched immunity provided protection despite their similar putative tRNase toxin functions shows that the pairs are highly specific. As a low copy number vector was used for toxin cloning, this outlines these toxins as highly potent. However, many copies of the protein would be produced upon induction. It would therefore be interesting to determine if a single copy of the toxin can confer toxicity, but this is beyond the scope of this work. Although the toxin functions could not be validated *in vitro* in this timeframe, ongoing approaches through sequencing of isolates which survived toxin expression are in place to hopefully identify mutations which could alter the toxin targets potentially making the strains more permissive to growth in their presence.

The potency of these toxins is in line with tRNase function due to the rapid cessation and plateau in growth upon intoxication observed here and not a steep decline indicative of outright killing. The nuances observed in growth rate cessation between toxins, where CdiA-CT^{00510} induction resulted in immediate cessation and CdiA-CT^{32790} showed decreased growth and cessation 2 hours after induction, can be attributed to differences in function based on their homology to other tRNases. CdiA-CT^{00510} outlined immediate growth cessation, and through its 100% homology to a trans-kingdom tRNase (Allen *et al.*, 2020) indicates this toxin is a tRNase- supporting the potency observed. Alternatively, CdiA-CT^{32790} outlined delayed

growth cessation, and through its 62% sequence identity to *E. coli* O157:H7 tRNase shown to target specific tRNAs (Wang *et al.*, 2022) suggests that CdiA-CT^{32790} also encodes a tRNase which targets specific tRNAs. This supports the delayed growth cessation observed as the interaction of the *E. coli*-like tRNAse with specific intracellular tRNAs may therefore be concentration dependent, decreasing the rate in growth cessation. These differences in toxin targets support the idea that these systems are deployed to provide different fitness advantages in response to various stimuli. Alternatively these toxins may act synergistically to increase toxicity enacted via individual toxins. Additionally, the differences between YP domain classifications observed indicates different entry mechanisms which could increase bacterial target range. This work expands our understanding of CDI systems encoded within an individual *P. aeruginosa* strain.

The CDI toxicity observed was supported by the results outlined in Chapter 6, from interbacterial competition assays conducted using strains deleting each entire CDI system. Through these deletion mutants, I was able to confirm the role of both PA14-encoded CDI systems in interbacterial competition, supporting the literature outlining their use in other *P. aeruginosa* strains (Mercy *et al.*, 2016; Allen *et al.*, 2020). Most interestingly, these results highlighted potential regulation interplay between the CDI and T6SSs (Figure 6.10 and 6.11) previously unseen in the literature as CDI^{32790} only showed a role in interbacterial competition in the H123 strain background but not the PA14 background. This result gives credence to the idea these systems are co-expressed upon sensing various stimuli; however this interplay and purpose in differential expression are yet to be elucidated. Interestingly, deletion of *rsmA* in PA14 resulted in attacker strains that could kill PA14/H123 ΔCDI^{00510}ΔCDI^{32790} mutants showing that phenotypically RsmA does repress CDI^{32790}. However, an additive effect for

PA14/H123 ΔCDI^{00510}ΔCDI^{32790} mutant survival is not observed when attacked by *rsmA* ΔCDI^{00510}ΔCDI^{32790} compared to *rsmA* ΔCDI^{32790} or *rsmA* ΔCDI^{00510} and is still an incongruency in the results that cannot be explained but may be due to CDI and T6SS interplay.

Whilst deletion of these systems in PAO1 has previously shown a role in other phenotypes associated with virulence such as biofilm production and motility (Mercy *et al.*, 2016; Melvin *et al.*, 2017), I could not observe this for the PA14 CDI. This could be due to differences between strains in utility through variations in regulation/toxins, or alternatively indicates that these systems play different/broader roles in strain pathogenesis and lifestyle. In addition, genetic differences in strains even between labs may be accountable for the results observed here (Klockgether *et al.*, 2010) and repeating these assays in parallel using their strains could identify nuances between strains or scientists. Although CDI systems were not observed to play a role in other bacterial mechanisms such as biofilm and motility, these systems may be involved in other areas of infection in PA14 such as host interactions and colonisation. A study by Melvin *et al.* in 2017 was able to show PAO1 utilises CDI to compete on CF broncho-epithelial cells and contribute to acute infection in a non-competitive manner, although it was unclear whether this was direct or via another mechanism. Therefore these systems in PA14 could instead be used in host colonisation, which was not explored here but warrants further investigation- particularly as other studies in *E. coli* have shown an interplay between T6SSs and fimbral adhesins used for epithelial interactions (de Pace *et al.*, 2011). This however was not performed here as PA14 is a highly cytotoxic strain for eukaryotes and mutations in *pscC* would need to be engineered to disable the T3SS to remove this confounding factor (Mikkelsen, Mcmullan & Filloux, 2011).

Although this variation between systems between strains in biofilm production and motility was shown, their exact role in clinical strains remains unknown. This calls for the development of a tool to determine the presence and utility of these systems in different environments and in the presence of different competitors- including those in other genera. Whilst I performed attempts to assess CDI's role in intrabacterial competition, the reproducibility of which did not enable me to validate their role in controlling polymicrobial communities (data not shown), the results outlined can at least support the strain succession observed during CF chronic infection (Khanolkar *et al.*, 2020). Although antibodies were developed in Chapter 5 for use as a tool to check CDI expression in clinical strains, the time frame of this project would not allow for their validation and utilisation in assays to understand this relationship. These antibodies cross reacted well with the purified recombinant proteins constructed here but I could not detect clear expression in any strains tested. As the competition results from Chapter 6 showed these systems are expressed, these antibodies should have detected the presence of the target proteins, however this was not the case. Alternative assays to validate these antibodies in the future are outlined in 5.4.3. Such antibodies will be a useful tool in future experiments upon validation. Understanding when these systems are deployed, if specific CDI and T6SSs are used upon sensing specific stimuli or in the presence of specific competitors, and whether they are used in concert would elucidate their role in pathogenesis. This is particularly important in *P. aeruginosa* infection in CF as colonisation, dominance and decline in polymicrobial diversity are key features of its pathogenesis. If they are driven by these systems, their high conservation means these systems would provide excellent novel therapy targets for more successful infection control.

8.3 Regulation of T6SS and CDI in *P. aeruginosa*

The understanding of the regulation of CDI and T6SS systems could give us significant insight into their expression levels, deployment times and conditions. To date, more T6SS regulators in *P. aeruginosa* are known and some key regulators relevant to this report include the post-transcriptional negative regulator RsmA, c-di-GMP and transcriptional regulators AmrZ and RpoN (Bernard *et al.*, 2011; Sana *et al.*, 2013; Allsopp *et al.*, 2017; Shao *et al.*, 2018; Li *et al.*, 2020). Utilising transcriptional *lacZ* fusions, I confirmed the role of RpoN in the differential expression of the H2- and H3-T6SSs. Additionally I highlighted the specificity of enhancer binding protein Sfa2 in H2-T6SS expression through deletion mutants which showed no role in motility and biofilm production. Presented in Chapter 7, these results in conjunction with others published in our Allsopp *et al.* 2022 manuscript supported the paper's findings. These outlined an unprecedented level of T6SS control by identifying a role for RpoN in differential transcriptional regulation of the H2- and H3-T6SSs in addition to Sfa2 in the expression of H2-T6SS. This expands our understanding of the transcriptional regulation of these systems and clearly defines differences in expression of two of the T6SSs in *P. aeruginosa* previously unseen in the literature. The differences in expression profiles between the *P. aeruginosa*-encoded T6SSs gives credence to the idea that these systems are differentially expressed to provide select advantages to the encoding cell. This indicates that these systems may play different roles and be deployed at different points in colonisation by *P. aeruginosa*.

Far less is understood about the regulation of CDI, which was phenotypically linked to negative regulation by RsmA in one study (Mercy *et al.*, 2016). From the transcriptomics dataset generated for the Allsopp *et al.* 2022 paper, I was able to confirm the role of RsmA in

the negative regulation of the CDI whilst identifying a role for RpoN in the positive regulation of these systems previously unseen in the literature. As RsmA is a global regulator of many virulence genes (Shang *et al.*, 2021), confirming the role of RsmA in negative regulation of the CDI genes through transcriptomics analysis builds upon the Mercy *et al.* 2016 study. This indicates that all CDI and T6SS competitive systems are repressed in *P. aeruginosa* by RsmA and are thus likely de-repressed together from signals sensed via the Gac/Rsm pathway (Lapouge *et al.*, 2008; Mercy *et al.*, 2016; Allsopp *et al.*, 2020). This may be an important feature of the PARA mechanism as a method of rapidly deploying antibacterial factors upon cellular stress and derepression of the RsmA pathway (LeRoux *et al.*, 2014). As RpoN regulates multiple T6SSs in other bacterial genera, and I was able to show regulation of CDI via RpoN in *P. aeruginosa*, this begs the question- is this conserved for CDI in other bacteria? As both RsmA and RpoN are global regulators this may be a direct or indirect effect as they regulate other regulators within the bacterial cell as well as overlapping regulation between their regulons. Further experiments are required to elucidate the nature of the interactions with these promotors to determine if this happens in a direct or indirect manner such as reporter assays and ChIP-seq analysis. Although ChIP-seq was conducted for the Allsopp *et al.* 2022 manuscript, RpoN binding was not observed for CDI. However this may be due to the cell preparation at 37 °C. As CDI-mediated competition was observed at 32 °C, and RpoN binding sites were deemed present upstream of the CDI operons (data not shown), ChIP-seq may need to be repeated at this temperature to observe RpoN binding sites.

CDI systems have been proposed to additionally play a role in contact dependent signalling in kin cells in *B. thailandensis* through the formation of the toxin-immunity complex which influences cellular expression (Garcia *et al.*, 2016a). Understanding whether CDI in *P.*

aeruginosa control expression in kin cells via this mechanism will further outline their role in dominance of the CF polymicrobial community. Experiments such as RNA-seq and *lacZ* reporter assays to outline this would require additional mutants but is a potential reason for the discrepancy in killing between the PA14 and *rsmA* attacker strains upon PA14/H123 ΔCDI^{00510}ΔCDI^{32790} prey observed (Figure 6.11 and 6.12). This would validate the RNA-seq result to show that *rsmA* represses the CDI^{32790}. The antibodies generated in Chapter 5 if validated would have been used to confirm the increased expression observed in the *rsmA* mutant and *rpoN* backgrounds. Alternatively reporter fusions and introduction of point mutations in binding motifs could be used to validate *rpoN* binding and regulation of CDI.

From these results RpoN controls transcriptional expression, where CDI and H2-T6SS are positively regulated and H1- and H3-T6SSs are negatively regulated. This supports the notion that different systems can be expressed under different conditions. However, it also supports the idea these systems are co-regulated to respond to the same environmental stimuli via deployment of system pairs. Switching multiple systems on would result in different arrays of toxic effectors which could increases the cell's prey range and effectiveness at competition. Although the exact interplay between systems is yet to be elucidated, co-regulation could infer a specific role for these systems at different stages of colonisation and establishment of chronic infections by *P. aeruginosa* upon changes in the CF lung as function declines. This could provide insight into the steps between acute and chronic infection and their influence on *P. aeruginosa* dominance and control of the pulmonary polymicrobial community. This would be supported through further *in vivo* examinations upon defining their regulation. The conservation of these systems between gram-negative bacteria could provide novel targets

for therapies to prevent *P. aeruginosa* dominance in the lungs and block strain succession. This could be a game changer in CF treatments, improving prognosis and quality of life.

8.4 Conclusion

This thesis characterises the role of CDI systems in *P. aeruginosa*. I show that *P. aeruginosa* PA14 encodes two active CDI systems which can be studied via whole system deletions *in vitro*. I determine their specificity and role in interbacterial competition and have initiated the development of a molecular tool with the potential for use in CDI clinical strain studies *in vitro*. These results suggest differences in roles between strains, where PA14 CDI play roles in competition and kin recognition alone. Finally, I analysed the role of transcriptional and post-transcriptional regulators on expression of both the CDI and T6SS, outlining an unseen level of expression control for the H2- and H3-T6SS (Allsopp *et al.*, 2022) in addition to a previously unobserved link between CDI and known T6SS regulators. From these data, I propose co-regulation of these systems occurs during infection allowing *P. aeruginosa* to compete with other bacteria within its environment. As RpoN and RsmA are required for full expression of both CDI systems and the H2-T6SS, these systems may be switched on under low nutrient conditions where CDI/T6SS may help strains to kill other organisms for monopoly over food sources or alternatively enable the acquisition of enriched molecules from the competing cells upon their death. This could help *P. aeruginosa* to colonise and dominate a range of environments including in the CF pulmonary polymicrobial community. Therefore, the research presented in this thesis progresses the current understanding of these competition systems and reveals links between their regulation which expands the arsenal of systems that can be deployed together in *P. aeruginosa* that enable its hostile takeover of environments.

9. References

Abby, S.S., Cury, J., Guglielmini, J., Néron, B., et al. (2016) Identification of protein secretion systems in bacterial genomes. *Scientific Reports*. [Online] 6 (23080), 1–14. Available from: doi:10.1038/srep23080.

Aizenman, E., Engelberg-Kulkat, H. & Glaser, G. (1996) An Escherichia coli chromosomal 'addiction module' regulated by 3',5'-bispyrophosphate: A model for programmed bacterial cell death (stringent response/protein degradation/nutritional stress/programmed cell death). *Genetics*. 93, 6059–6063.

Ali-Ahmad, A., Fadel, F., Sebban-Kreuzer, C., Ba, M., et al. (2017) Structural and functional insights into the periplasmic detector domain of the GacS histidine kinase controlling biofilm formation in Pseudomonas aeruginosa OPEN. *Scientific Reports* . [Online] 7 (11262), 1–13. Available from: doi:10.1038/s41598-017-11361-3 [Accessed: 30 May 2023].

Ali, J., Cheang, U.K., Martindale, J.D., Jabbarzadeh, M., et al. (2017) Bacteria-inspired nanorobots with flagellar polymorphic transformations and bundling. *Scientific Reports*. [Online] 7 (1), 1–10. Available from: doi:10.1038/s41598-017-14457-y [Accessed: 21 May 2023].

Allen, J.P. & Hauser, A.R. (2019) Diversity of Contact-Dependent Growth Inhibition Systems of Pseudomonas aeruginosa. In: *Journal of Bacteriology*. [Online]. 2019 American Society for Microbiology. pp. 1–12. Available from: doi:10.1128/JB.00776-18.

Allen, J.P., Ozer, E.A., Minasov, G., Shuvalova, L., et al. (2020) A comparative genomics approach identifies contact-dependent growth inhibition as a virulence determinant. *Proceedings of the National Academy of Sciences of the United States of America*. [Online] 117 (12), 6811–6821. Available from: doi:10.1073/pnas.1919198117 [Accessed: 7 October 2021].

Allsopp, L.P., Beloin, C., Ulett, G.C., Valle, J., et al. (2012) Molecular characterization of upab and upac, two new autotransporter proteins of uropathogenic escherichia coli CFT073. *Infection and Immunity*. [Online] 80 (1), 321–332. Available from: doi:10.1128/IAI.05322-11.

Allsopp, L.P., Bernal, P., Nolan, L.M. & Filloux, A. (2020) Causalities of war: The connection between type VI secretion system and microbiota. *Cellular Microbiology*. [Online] 22 (3), 1–9. Available from: doi:10.1111/cmi.13153 [Accessed: 21 April 2020].

Allsopp, L.P., Collins, A.C.Z., Hawkins, E., Wood, T.E., et al. (2022) RpoN/Sfa2-dependent activation of the Pseudomonas aeruginosa H2-T6SS and its cognate arsenal of antibacterial toxins. *Nucleic Acids Research*. [Online] 50 (1), 1–16. Available from: doi:10.1093/nar/gkab1254 [Accessed: 5 January 2022].

Allsopp, L.P., Totsika, M., Tree, J.J., Ulett, G.C., et al. (2010) UpaH is a newly identified autotransporter protein that contributes to biofilm formation and bladder colonization by uropathogenic Escherichia coli CFT073. *Infection and Immunity*. [Online] 78 (4), 1659–1669. Available from: doi:10.1128/IAI.01010-09.

Allsopp, L.P., Wood, T.E., Howard, S.A., Maggiorelli, F., et al. (2017) RsmA and AmrZ orchestrate the assembly of all three type VI secretion systems in Pseudomonas aeruginosa. *Proceedings of the National Academy of Sciences of the United States of America*. [Online] 114 (29), 7707–7712. Available from: doi:10.1073/pnas.1700286114.

Almagro Armenteros, J.J., Tsirigos, K.D., Sønderby, C.K., Petersen, T.N., et al. (2019) SignalP

5.0 improves signal peptide predictions using deep neural networks. *Nature Biotechnology*. [Online] 37 (4), 420–423. Available from: doi:10.1038/s41587-019-0036-z.

Alsohim, A.S., Taylor, T.B., Barrett, G.A., Gallie, J., et al. (2014) The biosurfactant viscosin produced by Pseudomonas fluorescensSBW25 aids spreading motility and plant growth promotion. *Environmental Microbiology*. [Online] 16 (7), 2267–2281. Available from: doi:10.1111/1462-2920.12469 [Accessed: 13 January 2021].

Alvarez-Martinez, C.E. & Christie, P.J. (2009) Biological Diversity of Prokaryotic Type IV Secretion Systems. *Microbiology and Molecular Biology Reviews*. [Online] 73 (4), 775–808. Available from: doi:10.1128/MMBR.00023-09/ASSET/B3141931-49F4-49B2-9F39-107412990EA5/ASSETS/GRAPHIC/ZMR0040922300008.JPEG [Accessed: 19 May 2023].

Alvarez-Ortega, C. & Harwood, C.S. (2007) Responses of Pseudomonas aeruginosa to low oxygen indicate that growth in the cystic fibrosis lung is by aerobic respiration. *Molecular Microbiology*. [Online] 65 (1), 153–165. Available from: doi:10.1111/J.1365-2958.2007.05772.X.

Alwazzeh, M.J., Alkuwaiti, F.A., Alqasim, M., Alwarthan, S., et al. (2020) Infective Endocarditis Caused by Pseudomonas stutzeri: A Case Report and Literature Review. *Infectious Disease Reports 2020, Vol. 12, Pages 105-109*. [Online] 12 (3), 105–109. Available from: doi:10.3390/IDR12030020 [Accessed: 24 June 2023].

Ambreetha, S., Marimuthu, P., Mathee, K. & Balachandar, D. (2022) Plant-associated Pseudomonas aeruginosa strains harbour multiple virulence traits critical for human infection. *Journal of Medical Microbiology*. [Online] 71 (001493), 1–16. Available from: doi:10.1099/jmm.0.001493 [Accessed: 29 April 2023].

Amiel, E., Lovewell, R.R., O'Toole, G.A., Hogan, D.A., et al. (2010) Pseudomonas aeruginosa Evasion of Phagocytosis Is Mediated by Loss of Swimming Motility and Is Independent of Flagellum Expression. *Infection and Immunity*. [Online] 78 (7), 2945. Available from: doi:10.1128/IAI.00144-10 [Accessed: 21 May 2023].

Andersen, D.H. (1938) Cystic Fibrosis of the Pancreas and its Relation to Celiac Disease: a Clinical and Pathological Study. *American Journal of Diseases of Children*. [Online] 56 (2), 344–399. Available from: doi:10.1001/ARCHPEDI.1938.01980140114013 [Accessed: 10 May 2023].

Anderson, M.S., Garcia, E.C. & Cotter, P.A. (2012) The Burkholderia bcpAIOB Genes Define Unique Classes of Two-Partner Secretion and Contact Dependent Growth Inhibition Systems. *PLoS Genetics*. [Online] 8 (8), 1002877. Available from: doi:10.1371/JOURNAL.PGEN.1002877 [Accessed: 13 May 2022].

Andrews, S.C., Robinson, A.K. & Rodríguez-Quiñones, F. (2003) Bacterial iron homeostasis. *FEMS Microbiology Reviews*. [Online] 27 (2–3), 215–237. Available from: doi:10.1016/S0168-6445(03)00055-X [Accessed: 10 March 2022].

Anzai, Y., Kim, H., Park, J.-Y., Wakabayashi, H., et al. (2000) Phylogenetic affiliation of the pseudomonads based on 16S rRNA sequence. *International Journal of Systematic and Evolutionary Microbiology*. [Online] 50, 1563–1589. Available from: www.dsmz.de [Accessed: 26 April 2023].

Aoki, S.K., Diner, E.J., De Roodenbeke, C.T.K., Burgess, B.R., et al. (2010) A widespread family of polymorphic contact-dependent toxin delivery systems in bacteria. *Nature*. [Online] 468 (7322), 439–442. Available from: doi:10.1038/nature09490.

Aoki, S.K., Malinverni, J.C., Jacoby, K., Thomas, B., et al. (2008) Contact-dependent growth inhibition requires the essential outer membrane protein BamA (YaeT) as the receptor

and the inner membrane transport protein AcrB. *Molecular microbiology*. [Online] 70 (2), 323–340. Available from: doi:10.1111/J.1365-2958.2008.06404.X [Accessed: 8 February 2022].

Aoki, S.K., Pamma, R., Hernday, A.D., Bickham, J.E., et al. (2005) Microbiology: Contact-dependent inhibition of growth in Escherichia coli. *Science*. [Online] 309 (5738), 1245–1248. Available from: doi:10.1126/SCIENCE.1115109/SUPPL_FILE/AOKI-SOM.PDF [Accessed: 4 February 2022].

Aoki, S.K., Webb, J.S., Braaten, B.A. & Low, D.A. (2009) Contact-Dependent Growth Inhibition Causes Reversible Metabolic Downregulation in Escherichia coli. *Journal of Bacteriology*. [Online] 191 (6), 1777–1786. Available from: doi:10.1128/JB.01437-08 [Accessed: 14 January 2022].

Arenas, J., Schipper, K., van Ulsen, P., van der Ende, A., et al. (2013) Domain exchange at the 3' end of the gene encoding the fratricide meningococcal two-partner secretion protein A. *BMC genomics*. [Online] 14 (1), 1–14. Available from: doi:10.1186/1471-2164-14-622 [Accessed: 26 May 2023].

Armbruster, C.R., Coenye, T., Touqui, L. & Bomberger, J.M. (2020) Interplay between host-microbe and microbe-microbe interactions in cystic fibrosis. *Journal of Cystic Fibrosis*. [Online] 19, S47–S53. Available from: doi:10.1016/j.jcf.2019.10.015.

Assani, K., Shrestha, C.L., Robledo-Avila, F., Rajaram, M. V., et al. (2017) Human Cystic Fibrosis Macrophages Have Defective Calcium-Dependent Protein Kinase C Activation of the NADPH Oxidase, an Effect Augmented by Burkholderia cenocepacia. *Journal of Immunology* . [Online] 198 (5), 1985–1994. Available from: doi:10.4049/JIMMUNOL.1502609 [Accessed: 10 May 2023].

Azimi, A. (2015) 'Cystic fibrotics could survive cholera, choleraics could survive cystic fibrosis'; hypothesis that explores new horizons in treatment of cystic fibrosis. *Medical Hypotheses*. [Online] 85 (6), 715–717. Available from: doi:10.1016/j.mehy.2015.10.023.

Bains, M., Fernández, L. & Hancock, R.E.W. (2012) Phosphate Starvation Promotes Swarming Motility and Cytotoxicity of Pseudomonas aeruginosa. *Applied and Environmental Microbiology*. [Online] 78 (18), 6762–6768. Available from: doi:10.1128/AEM.01015-12.

Baker, A.E. & O'Toole, G.A. (2017) Bacteria, rev your engines: Stator dynamics regulate flagellar motility. *Journal of Bacteriology*. [Online] 199 (12), 1–8. Available from: doi:10.1128/JB.00088-17.

Baker, P., Hill, P.J., Snarr, B.D., Alnabelseya, N., et al. (2016) Exopolysaccharide biosynthetic glycoside hydrolases can be utilized to disrupt and prevent Pseudomonas aeruginosa biofilms. *BMC Research Notes*. [Online] 2 (e1501632), 1–9. Available from: doi:10.1126/sciadv.1501632.

Baraquet, C., Murakami, K., Parsek, M.R. & Harwood, C.S. (2012) The FleQ protein from Pseudomonas aeruginosa functions as both a repressor and an activator to control gene expression from the Pel operon promoter in response to c-di-GMP. *Nucleic Acids Research*. [Online] 40 (15), 7207–7218. Available from: doi:10.1093/nar/gks384.

Bardoel, B.W., Hartsink, D., Vughs, M.M., de Haas, C.J.C., et al. (2012) Identification of an immunomodulating metalloprotease of Pseudomonas aeruginosa (IMPa). *Cellular Microbiology*. [Online] 14 (6), 902–913. Available from: doi:10.1111/J.1462-5822.2012.01765.X [Accessed: 16 May 2023].

Bartelli, N.L., Sun, S., Gucinski, G.C., Zhou, H., et al. (2019) The cytoplasm-entry domain of antibacterial CdiA is a dynamic α-helical bundle with disulfide-dependent structural

features. *Journal of Molecular Biology*. [Online] 431 (17), 3203–3216. Available from: doi:10.1016/j.jmb.2019.05.049.
Bartholomew, J.W. & Mittwer, T. (1952) The Gram Stain. *Bacteriological Reviews*. [Online] 16 (1), 1. Available from: doi:10.1128/BR.16.1.1-29.1952 [Accessed: 30 April 2023].
Basler, M. (2015) Type VI secretion system: secretion by a contractile nanomachine. *Philosophical Transactions of the Royal Society B: Biological Sciences*. [Online] 370 (1679), 1–11. Available from: doi:10.1098/RSTB.2015.0021 [Accessed: 20 May 2023].
Basler, M., Ho, B.T. & Mekalanos, J.J. (2013) Tit-for-tat: Type VI secretion system counterattack during bacterial cell-cell interactions. *Cell*. [Online] 152 (4), 884–894. Available from: doi:10.1016/j.cell.2013.01.042.
Basler, M., Pilhofer, M., Henderson, G.P., Jensen, G.J., et al. (2012) Type VI secretion requires a dynamic contractile phage tail-like structure. *Nature*. [Online] 483 (7388), 182–186. Available from: doi:10.1038/nature10846.
Baud, C., Guérin, J., Petit, E., Lesne, E., et al. (2014) Translocation path of a substrate protein through its Omp85 transporter. *Nature Communications*. [Online] 5 (1), 1–9. Available from: doi:10.1038/ncomms6271 [Accessed: 11 July 2022].
Beck, C.M., Morse, R.P., Cunningham, D.A., Iniguez, A., et al. (2014) CdiA from Enterobacter cloacae delivers a toxic ribosomal RNase into target bacteria. *Structure*. [Online] 22, 707–718. Available from: doi:10.1016/J.STR.2014.02.012 [Accessed: 14 January 2022].
Beck, C.M., Willett, J.L.E., Cunningham, D.A., Kim, J.J., et al. (2016) CdiA Effectors from Uropathogenic Escherichia coli Use Heterotrimeric Osmoporins as Receptors to Recognize Target Bacteria. *PLOS Pathogens*. [Online] 12 (10), 1–26. Available from: doi:10.1371/journal.ppat.1005925 [Accessed: 22 April 2020].
Begum, H., Murugesan, P. & Tangutur, A.D. (2022) Western blotting: A powerful staple in scientific and biomedical research. *BioTechniques*. [Online] 73 (1), 59–69. Available from: doi:10.2144/BTN-2022-0003/ASSET/IMAGES/LARGE/FIGURE2.JPEG [Accessed: 24 November 2022].
van Beilen, J.B., Wubbolts, M.G. & Witholt, B. (1994) Genetics of alkane oxidation by Pseudomonas oleovorans. *Biodegradation*. 5, 161–174.
Belliveau, N.M., Barnes, S.L., Ireland, W.T., Jones, D.L., et al. (2018) Systematic approach for dissecting the molecular mechanisms of transcriptional regulation in bacteria. *Proceedings of the National Academy of Sciences of the USA*. [Online] 115 (21), E4796–E4805. Available from: doi:10.1073/PNAS.1722055115/SUPPL_FILE/PNAS.1722055115.SAPP.PDF [Accessed: 11 April 2023].
Benarroch, J.M. & Asally, M. (2020) The Microbiologist's Guide to Membrane Potential Dynamics. *Trends in Microbiology*. [Online] 28 (4), 304–314. Available from: doi:10.1016/J.TIM.2019.12.008.
Bennett, J.C.Q. & Hughes, C. (2000) From flagellum assembly to virulence: The extended family of type III export chaperones. *Trends in Microbiology*. [Online] 8 (5), 202–204. Available from: doi:10.1016/S0966-842X(00)01751-0.
Benz, I. & Schmidt, M.A. (2001) Glycosylation with heptose residues mediated by the aah gene product is essential for adherence of the AIDA-I adhesin. *Molecular Microbiology*. [Online] 40 (6), 1403–1413. Available from: doi:10.1046/J.1365-2958.2001.02487.X [Accessed: 26 June 2023].
Benz, J., Sendlmeier, C., Barends, T.R.M. & Meinhart, A. (2012) Structural insights into the effector - immunity system Tse1/Tsi1 from Pseudomonas aeruginosa. *PLoS ONE*.

[Online] 7 (7), 1–10. Available from: doi:10.1371/journal.pone.0040453.
Berg, H.C. & Anderson, R.A. (1973) Bacteria Swim by Rotating their Flagellar Filaments. *Nature*. [Online] 245 (5425), 380–382. Available from: doi:10.1038/245380a0 [Accessed: 7 April 2023].
Bernal, P., Christopher, R., Fecht, S., Leung, R.C.Y., et al. (2021) A novel stabilization mechanism for the type VI secretion system sheath. *Proceedings of the National Academy of Sciences of the United States of America*. [Online] 118 (7), 1–9. Available from: doi:10.1073/PNAS.2008500118/VIDEO-1 [Accessed: 23 March 2022].
Bernard, C.S., Brunet, Y.R., Gavioli, M., Lloubès, R., et al. (2011) Regulation of type VI secretion gene clusters by sigma54 and cognate enhancer binding proteins. *Journal of Bacteriology*. [Online] 193 (9), 2158–2167. Available from: doi:10.1128/JB.00029-11 [Accessed: 1 June 2023].
Berni, B., Soscia, C., Djermoun, S., Ize, B., et al. (2019) A type VI secretion system trans-kingdom effector is required for the delivery of a novel antibacterial toxin in Pseudomonas aeruginosa. *Frontiers in Microbiology*. [Online] 10 (June), 1–14. Available from: doi:10.3389/fmicb.2019.01218.
Bernstein, H.D. (2000) The biogenesis and assembly of bacterial membrane proteins. *Current Opinion in Microbiology*. [Online] 3 (2), 203–209. Available from: doi:10.1016/S1369-5274(00)00076-X.
Bhagirath, A.Y., Li, Y., Somayajula, D., Dadashi, M., et al. (2016) Cystic fibrosis lung environment and Pseudomonas aeruginosa infection. *BMC Pulmonary Medicine*. [Online] 16 (174), 1–22. Available from: doi:10.1186/s12890-016-0339-5.
Bingle, L.E., Bailey, C.M. & Pallen, M.J. (2008) Type VI secretion: a beginner's guide. *Current Opinion in Microbiology*. [Online] 11 (1), 3–8. Available from: doi:10.1016/J.MIB.2008.01.006.
Bisht, K., Baishya, J. & Wakeman, C.A. (2020) Pseudomonas aeruginosa polymicrobial interactions during lung infection. *Current Opinions in Microbiology*. [Online] 53, 1–8. Available from: doi:10.1016/j.mib.2020.01.014.
Bleves, S. (2016) Game of Trans-Kingdom Effectors. *Trends in Microbiology*. [Online] 24 (10), 773–774. Available from: doi:10.1016/j.tim.2016.08.002 [Accessed: 20 May 2023].
Bleves, S., Galán, J.E. & Llosa, | Matxalen (2019) Bacterial injection machines: Evolutionary diverse but functionally convergent. *Cellular Microbiology*. [Online] 22, 1–10. Available from: doi:10.1111/cmi.13157 [Accessed: 19 May 2023].
Böck, D., Medeiros, J.M., Tsao, H.F., Penz, T., et al. (2017) In situ architecture, function, and evolution of a contractile injection system. *Science* . [Online] 357 (6352), 717. Available from: doi:10.1126/SCIENCE.AAN7904 [Accessed: 20 May 2023].
De Boeck, K. (2020) Cystic fibrosis in the year 2020: A disease with a new face. *Acta Paediatrica, International Journal of Paediatrics*. [Online] 109 (5), 893–899. Available from: doi:10.1111/apa.15155.
Bondage, D.D., Lin, J.S., Ma, L.S., Kuo, C.H., et al. (2016) VgrG C terminus confers the type VI effector transport specificity and is required for binding with PAAR and adaptor-effector complex. *Proceedings of the National Academy of Sciences of the United States of America*. [Online] 113 (27), E3931–E3940. Available from: doi:10.1073/PNAS.1600428113/-/DCSUPPLEMENTAL [Accessed: 20 May 2023].
Bönemann, G., Pietrosiuk, A., Diemand, A., Zentgraf, H., et al. (2009) Remodelling of VipA/VipB tubules by ClpV-mediated threading is crucial for type VI protein secretion. *The EMBO journal*. [Online] 28 (4), 315–325. Available from:

doi:10.1038/EMBOJ.2008.269 [Accessed: 20 May 2023].
Bordeaux, J., Welsh, A.W., Agarwal, S., Killiam, E., et al. (2010) Antibody validation. *BioTechniques*. [Online] 48 (3), 197–209. Available from: doi:10.2144/000113382/ASSET/IMAGES/LARGE/FIGURE6.JPEG [Accessed: 29 November 2022].
Borlee, B.R., Goldman, A.D., Murakami, K., Samudrala, R., et al. (2010) Pseudomonas aeruginosa uses a cyclic-di-GMP-regulated adhesin to reinforce the biofilm extracellular matrixm mi_6991 827..842. *Molecular Microbiology*. [Online] 75 (4), 827–842. Available from: doi:10.1111/j.1365-2958.2009.06991.x [Accessed: 7 April 2023].
Boudaher, E. & Shaffer, C.L. (2019) MedChemComm Inhibiting bacterial secretion systems in the fight against antibiotic resistance. *Medicinal Chemistry Communications*. [Online] 10 (682), 1–11. Available from: doi:10.1039/c9md00076c.
Boyd, A. & Chakrabarty, A.M. (1995) Pseudomonas aeruginosa biofilms: role of the alginate exopolysaccharide. *Journal of Industrial Microbiology*. [Online] 15 (3), 162–168. Available from: doi:10.1007/BF01569821 [Accessed: 29 May 2023].
Brencic, A., Mcfarland, K.A., Mcmanus, H.R., Castang, S., et al. (2009) The GacS/GacA signal transduction system of Pseudomonas aeruginosa acts exclusively through its control over the transcription of the RsmY and RsmZ regulatory small RNAs. *Molecular Microbiology*. [Online] 73 (3), 434–445. Available from: doi:10.1111/j.1365-2958.2009.06782.x.
Broder, U.N., Jaeger, T. & Jenal, U. (2016) LadS is a calcium-responsive kinase that induces acute-to-chronic virulence switch in Pseudomonas aeruginosa. *Nature Microbiology*. [Online] 2 (October), 1–11. Available from: doi:10.1038/nmicrobiol.2016.184.
Brown, D.A. & Berg, H.C. (1974) Temporal Stimulation of Chemotaxis in Escherichia coli (bacterial taxis/temporal gradients/alanine aminotransferase/three-dimensional tracking). *Proceedings of the National Academy of Sciences USA*. [Online] 71 (4), 1388–1392. Available from: https://www.pnas.org [Accessed: 21 May 2023].
Browning, D.F. & Busby, S.J.W. (2004) The regulation of bacterial transcription initiation. *Nature Reviews Microbiology 2004 2:1*. [Online] 2 (1), 57–65. Available from: doi:10.1038/nrmicro787 [Accessed: 15 April 2023].
Bruel, N. & Genevaux, P. (2014) Biochimica et Biophysica Acta Chaperone networking facilitates protein targeting to the bacterial cytoplasmic membrane ☆☆. *BBA - Molecular Cell Research*. [Online] 1843 (8), 1442–1456. Available from: doi:10.1016/j.bbamcr.2013.11.007.
De Bruin, O.M., Ludu, J.S. & Nano, F.E. (2007) The Francisella pathogenicity island protein IglA localizes to the bacterial cytoplasm and is needed for intracellular growth. *BMC Microbiology*. [Online] 7 (1), 1–10. Available from: doi:10.1186/1471-2180-7-1/TABLES/1 [Accessed: 20 May 2023].
Bruner, S.D., Norman, D.P.G. & Verdine, G.L. (2000) Structural basis for recognition and repair of the endogenous mutagen 8-oxoguanine in DNA. *Nature*. [Online] 403 (6772), 859–866. Available from: doi:10.1038/35002510 [Accessed: 11 July 2022].
Buchanan, S.K., Botos, I. & Noinaj, N. (2017) Insertion of proteins and lipopolysaccharide into the bacterial outer membrane. *Philosophical Transactions of the Royal Society B: Biological Sciences*. [Online] 372 (1726), 1–9. Available from: doi:10.1098/rstb.2016.0224.
Bucior, I., Pielage, J.F. & Engel, J.N. (2012) Pseudomonas aeruginosa Pili and Flagella Mediate Distinct Binding and Signaling Events at the Apical and Basolateral Surface of

Airway Epithelium. *PLoS Pathogens*. [Online] 8 (4), 1–18. Available from: doi:10.1371/JOURNAL.PPAT.1002616 [Accessed: 29 May 2023].
Buck, M., Gallegos, M.T., Studholme, D.J., Guo, Y., et al. (2000) The bacterial enhancer-dependent sigma(54) (sigma(N)) transcription factor. *J Bacteriol*. [Online] 182 (15), 4129–4136. Available from: http://www.ncbi.nlm.nih.gov/entrez/query.fcgi?cmd=Retrieve&db=PubMed&dopt=Citation&list_uids=10894718.
Bush, M. & Dixon, R. (2012) The Role of Bacterial Enhancer Binding Proteins as Specialized Activators of σ 54 -Dependent Transcription . *Microbiology and Molecular Biology Reviews*. [Online] 76 (3), 497–529. Available from: doi:10.1128/mmbr.00006-12.
Byrd, M.S., Pang, B., Mishra, M., Edward Swords, W., et al. (2010) The Pseudomonas aeruginosa exopolysaccharide Psl facilitates surface adherence and NF-kappaB activation in A549 cells. *mBio*. [Online] 1 (3), 1–4. Available from: doi:10.1128/MBIO.00140-10 [Accessed: 29 May 2023].
Cai, Y.-M., Hutchin, A., Craddock, J., Walsh, M.A., et al. (2020) Differential impact on motility and biofilm dispersal of closely related phosphodiesterases in Pseudomonas aeruginosa. *Scientific Reports*. [Online] 10 (6232), 1–12. Available from: doi:10.1038/s41598-020-63008-5 [Accessed: 29 May 2023].
Caiazza, N.C. & O'Toole, G.A. (2004) SadB Is Required for the Transition from Reversible to Irreversible Attachment during Biofilm Formation by Pseudomonas aeruginosa PA14. *Journal of Bacteriology*. [Online] 186 (14), 4485. Available from: doi:10.1128/JB.186.14.4476-4485.2004 [Accessed: 29 May 2023].
Cantin, A.M., Hartl, D., Konstan, M.W. & Chmiel, J.F. (2015) Inflammation in cystic fibrosis lung disease: Pathogenesis and therapy. *Journal of cystic fibrosis : official journal of the European Cystic Fibrosis Society*. [Online] 14 (4), 419–430. Available from: doi:10.1016/J.JCF.2015.03.003 [Accessed: 11 May 2023].
Carson, M.R., Travis, S.M. & Welsh, M.J. (1995) The two nucleotide-binding domains of cystic fibrosis transmembrane conductance regulator (CFTR) have distinct functions in controlling channel activity. *The Journal of biological chemistry*. [Online] 270 (4), 1711–1717. Available from: doi:10.1074/JBC.270.4.1711 [Accessed: 10 May 2023].
Casabona, M.G., Silverman, J.M., Sall, K.M., Boyer, F., et al. (2013) An ABC transporter and an outer membrane lipoprotein participate in posttranslational activation of type VI secretion in Pseudomonas aeruginosa. *Environmental Microbiology*. [Online] 15 (2), 471–486. Available from: doi:10.1111/j.1462-2920.2012.02816.x.
Cascales, E., Buchanan, S.K., Duché, D., Kleanthous, C., et al. (2007) Colicin Biology. *Microbiology and Molecular Biology Reviews*. [Online] 71 (1), 158–229. Available from: doi:10.1128/MMBR.00036-06/ASSET/6521DD60-FD25-4B1D-B9CE-60362A473A6F/ASSETS/GRAPHIC/ZMR0010721490025.JPEG [Accessed: 26 May 2023].
Castang, S., Mcmanus, H.R., Turner, K.H. & Dove, S.L. (2008) H-NS family members function coordinately in an opportunistic pathogen. *Proceeding of the National Academy of Sciences USA*. 105 (48).
Castellani, C., Cuppens, H., Macek, M., Cassiman, J.J., et al. (2008) Consensus on the use and interpretation of cystic fibrosis mutation analysis in clinical practice. *Journal of Cystic Fibrosis*. [Online] 7 (3), 179–196. Available from: doi:10.1016/J.JCF.2008.03.009.
Chambonnier, G., Redelberger, D., Fadel, F. & Filloux, A. (2016) *The Hybrid Histidine Kinase LadS Forms a Multicomponent Signal Transduction System with the GacS / GacA Two-Component System in Pseudomonas aeruginosa*. [Online] 1–30. Available from:

doi:10.1371/journal.pgen.1006032.
Chandler, C.E., Horspool, A.M., Hill, P.J., Wozniak, D.J., et al. (2019) Genomic and phenotypic diversity among ten laboratory isolates of Pseudomonas aeruginosa PAO1. *Journal of Bacteriology*. [Online] 201 (5), 595–613. Available from: doi:10.1128/JB.00595-18/FORMAT/EPUB [Accessed: 29 April 2023].
Chen, J., Boyaci, H. & Campbell, E.A. (2021) Diverse and unified mechanisms of transcription initiation in bacteria. *Nature Reviews Microbiology*. [Online] 19, 1–15. Available from: doi:10.1038/s41579-020-00450-2 [Accessed: 26 June 2023].
Chen, J.S., Witzmann, K.A., Spilker, T., Fink, R.J., et al. (2001) Endemicity and inter-city spread of Burkholderia cepacia genomovar III in cystic fibrosis. *Journal of Pediatrics*. [Online] 139 (5), 643–649. Available from: doi:10.1067/mpd.2001.118430.
Chen, L., Zou, Y., Asmaa, |, Kronfl, A., et al. (2020) Type VI secretion system of Pseudomonas aeruginosa is associated with biofilm formation but not environmental adaptation. *Microbiology Open*. [Online] 9 (e991), 1–10. Available from: doi:10.1002/mbo3.991 [Accessed: 13 April 2023].
Chen, L., Zou, Y., She, P. & Wu, Y. (2015) Composition, function, and regulation of T6SS in Pseudomonas aeruginosa. *Microbiological Research*. [Online] 172, 19–25. Available from: doi:10.1016/j.micres.2015.01.004.
Chen, R., Shang, H., Niu, X., Huang, J., et al. (2021) Establishment and evaluation of an indirect ELISA for detection of antibodies to goat Klebsiella pneumonia. *BMC Veterinary Research*. [Online] 17 (1), 1–10. Available from: doi:10.1186/s12917-021-02820-1.
Cheng, X. (1995) Struction and function of DNA methyltransferases Xiaodong Cheng. *Annual Reviews of Biophysics and Biomolecular Structure*. [Online] 24, 293–318. Available from: www.annualreviews.org [Accessed: 22 March 2022].
Cherrak, Y., Flaugnatti, N., Durand, E., Journet, L., et al. (2019) Structure and Activity of the Type VI Secretion System. *Microbiology Spectrum*. [Online] 7 (4), 1–12. Available from: doi:10.1128/MICROBIOLSPEC.PSIB-0031-2019 [Accessed: 24 June 2023].
Chevalier, N., Moser, M., Koch, H.G., Schimz, K.L., et al. (2005) Membrane Targeting of a Bacterial Virulence Factor Harbouring an Extended Signal Peptide. *Journal of Molecular Microbiology and Biotechnology*. [Online] 8 (1), 7–18. Available from: doi:10.1159/000082076 [Accessed: 26 May 2023].
Chioccioli, M., Feriani, L., Kotar, J., Bratcher, P.E., et al. (2019) Phenotyping ciliary dynamics and coordination in response to CFTR-modulators in Cystic Fibrosis respiratory epithelial cells. *Nature Communications*. [Online] 10 (1), 1–11. Available from: doi:10.1038/S41467-019-09798-3 [Accessed: 10 May 2023].
Choi, P.S. & Bernstein, H.D. (2010) Sequential translocation of an Escherchia coli two-partner secretion pathway exoprotein across the inner and outer membranes. *Molecular Microbiology*. [Online] 75 (2), 440–451. Available from: doi:10.1111/J.1365-2958.2009.06993.X.
Chow, S., Gu, K., Jiang, L. & Nassour, A. (2011) Salicylic Acid Affects Swimming, Twitching and Swarming Motility in Pseudomonas aeruginosa, resulting in Decreased Biofilm Formation. *Journal of Experimental Microbiology and Immunology*.15.
Cianciotto, N.P. (2005) Type II secretion: A protein secretion system for all seasons. *Trends in Microbiology*. [Online] 13 (12), 581–588. Available from: doi:10.1016/j.tim.2005.09.005.
Ciofu, O., Moser, C., Østrup Jensen, P. & Høiby, N. (2022) Tolerance and resistance of microbial biofilms. *Nature Reviews Microbiology*. [Online] 20, 621–635. Available from:

doi:10.1038/s41579-022-00682-4 [Accessed: 28 May 2023].
Clark, S.T., Caballero, J.D., Cheang, M., Coburn, B., et al. (2015) Phenotypic diversity within a Pseudomonas aeruginosa population infecting an adult with cystic fibrosis. *Scientific Reports*. [Online] 5 (1), 1–10. Available from: doi:10.1038/srep10932 [Accessed: 7 April 2023].
Clausen, M., Koomey, M. & Maier, B. (2009) Dynamics of type IV Pili Is controlled by switching between multiple states. *Biophysical Journal*. [Online] 96 (3), 1169–1177. Available from: doi:10.1016/j.bpj.2008.10.017.
Coburn, B., Wang, P.W., Diaz Caballero, J., Clark, S.T., et al. (2015) Lung microbiota across age and disease stage in cystic fibrosis. *Scientific Reports* . [Online] 5 (1), 1–12. Available from: doi:10.1038/srep10241 [Accessed: 25 May 2023].
Coenye, T., Vandamme, P., Govan, J.R.W. & Lipuma, J.J. (2001) Taxonomy and Identification of the Burkholderia cepacia Complex. *Journal of Clinical Microbiology*. [Online] 39 (10), 3427–3436. Available from: doi:10.1128/JCM.39.10.3427-3436.2001.
Cohen-Cymberknoh, M., Kerem, E., Ferkol, T. & Elizur, A. (2013) Airway inflammation in cystic fibrosis: Molecular mechanisms and clinical implications. *Thorax*. [Online] 68 (12), 1157–1162. Available from: doi:10.1136/thoraxjnl-2013-203204.
Cole, S.J., Records, A.R., Orr, M.W., Linden, S.B., et al. (2014) Catheter-associated urinary tract infection by Pseudomonas aeruginosa is mediated by exopolysaccharide-independent biofilms. *Infection and Immunity*. [Online] 82 (5), 2048–2058. Available from: doi:10.1128/IAI.01652-14.
Colley, B., Dederer, V., Carnell, M., Kjelleberg, S., et al. (2016) SiaA/D interconnects c-di-GMP and RsmA signaling to coordinate cellular aggregation of Pseudomonas aeruginosa in response to environmental conditions. *Frontiers in Microbiology*. [Online] 7, 1–13. Available from: doi:10.3389/fmicb.2016.00179.
Colvin, K.M., Irie, Y., Tart, C.S., Urbano, R., et al. (2012) The Pel and Psl polysaccharides provide Pseudomonas aeruginosa structural redundancy within the biofilm matrix. *Environmental Microbiology*. [Online] 14 (8), 1–26. Available from: doi:10.1111/j.1462-2920.2011.02657.x.
Condren, M.E. & Bradshaw, M.D. (2013) Ivacaftor: A Novel Gene-Based Therapeutic Approach for Cystic Fibrosis. *The Journal of Pediatric Pharmacology and Therapeutics*. [Online] 18 (1), 13. Available from: doi:10.5863/1551-6776-18.1.8 [Accessed: 10 May 2023].
Conrad, J.C., Gibiansky, M.L., Jin, F., Gordon, V.D., et al. (2011) Flagella and pili-mediated near-surface single-cell motility mechanisms in P. aeruginosa. *Biophysical Journal*. [Online] 100 (7), 1608–1616. Available from: doi:10.1016/j.bpj.2011.02.020.
Conway, S. (2008) Segregation is good for patients with cystic fibrosis. *Journal of the Royal Society of Medicine*. [Online] 101 (Suppl 1), 35. Available from: doi:10.1258/JRSM.2008.S18007 [Accessed: 11 May 2023].
Coppens, F., Castaldo, G., Debraekeleer, A., Subedi, S., et al. (2018) Hop-family Helicobacter outer membrane adhesins form a novel class of Type 5-like secretion proteins with an interrupted β-barrel domain. *Molecular Microbiology*. [Online] 110 (1), 33–46. Available from: doi:10.1111/MMI.14075 [Accessed: 26 May 2023].
Corley, J.M., Intile, P. & Yahr, T.L. (2022) Direct Inhibition of RetS Synthesis by RsmA Contributes to System. *Journal of Bacteriology*. 204 (3), 1–14.
Costa, S., Almeida, A., Castro, A., Domingues, L., et al. (2014) Fusion tags for protein solubility, purification, and immunogenicity in Escherichia coli: the novel Fh8 system.

Frontiers in Microbiology. [Online] 5 (63), 1–20. Available from: doi:10.3389/fmicb.2014.00063 [Accessed: 25 November 2022].
Costa, T.R.D., Felisberto-Rodrigues, C., Meir, A., Prevost, M.S., et al. (2015) Secretion systems in Gram-negative bacteria: Structural and mechanistic insights. *Nature Reviews Microbiology*. [Online]. 13 (6) pp.343–359. Available from: doi:10.1038/nrmicro3456.
Costa, T.R.D., Harb, L., Khara, P., Zeng, L., et al. (2021) Type IV secretion systems: Advances in structure, function, and activation. *Mol Microbiol*. [Online] 115 (3), 436–452. Available from: doi:10.1111/mmi.14670.
Cover, T.L., Borden Lacy, D. & Ohi, M.D. (2020) The Helicobacter pylori Cag Type IV Secretion System. *Trends in Microbiolgy*. [Online] 28 (8), 682–695. Available from: doi:10.1016/j.tim.2020.02.004.
Cowley, E.S., Kopf, S.H., Lariviere, A., Ziebis, W., et al. (2015) Pediatric Cystic Fibrosis Sputum Can Be Chemically Dynamic, Anoxic, and Extremely Reduced Due to Hydrogen Sulfide Formation. *mBio*. [Online] 6 (4), 1–15. Available from: doi:10.1128/mBio.00767-15.
Craig, L., Volkmann, N., Arvai, A.S., Pique, M.E., et al. (2006) Type IV pilus structure by cryo-electron microscopy and crystallography: implications for pilus assembly and functions. *Molecular cell*. [Online] 23 (5), 651–662. Available from: doi:10.1016/J.MOLCEL.2006.07.004 [Accessed: 21 May 2023].
Cramer, N., Klockgether, J., Wrasman, K., Schmidt, M., et al. (2011) Microevolution of the major common Pseudomonas aeruginosa clones C and PA14 in cystic fibrosis lungs. *Environmental Microbiology*. [Online] 13 (7), 1690–1704. Available from: doi:10.1111/J.1462-2920.2011.02483.X.
Crone, S., Vives-Flórez, M., Kvich, L., Saunders, A.M., et al. (2020) The environmental occurrence of Pseudomonas aeruginosa. *Journal of Pathology, Microbiology and Immunology*. [Online] 128 (3), 220–231. Available from: doi:10.1111/apm.13010.
Cuthbert, B.J., Hayes, C.S. & Goulding, C.W. (2022) Functional and Structural Diversity of Bacterial Contact-Dependent Growth Inhibition Effectors. *Frontiers in Molecular Biosciences*. [Online] 9 (866854), 1–20. Available from: doi:10.3389/fmolb.2022.866854.
Cuthbertson, L., Walker, A.W., Oliver, A.E., Rogers, G.B., et al. (2020) Lung function and microbiota diversity in cystic fibrosis. *Microbiome*. [Online] 8 (45), 1–13. Available from: doi:10.1186/S40168-020-00810-3 [Accessed: 25 May 2023].
Daccò, V., Alicandro, G., Consales, A., Rosazza, C., et al. (2023) Cepacia syndrome in cystic fibrosis: A systematic review of the literature and possible new perspectives in treatment. *Pediatric Pulmonology*. [Online] 58 (5), 1337–1343. Available from: doi:10.1002/PPUL.26359 [Accessed: 11 May 2023].
Dalsing, B.L., Truchon, A.N., Gonzalez-Orta, E.T., Milling, A.S., et al. (2015) Ralstonia solanacearum Uses Inorganic Nitrogen Metabolism for Virulence, ATP Production, and Detoxification in the Oxygen-Limited Host Xylem Environment. *mBio*. [Online] 6 (2). Available from: doi:10.1128/MBIO.02471-14 [Accessed: 29 April 2023].
Damron, F.H., Owings, J.P., Okkotsu, Y., Varga, J.J., et al. (2012) Analysis of the Pseudomonas aeruginosa Regulon Controlled by the Sensor Kinase KinB and Sigma Factor RpoN. *Journal of Bacteriology* . [Online] 194 (6), 1317–1330. Available from: doi:10.1128/JB.06105-11 [Accessed: 13 April 2023].
Dasgupta, N., Wolfgang, M.C., Goodman, A.L., Arora, S.K., et al. (2003) A four-tiered transcriptional regulatory circuit controls flagellar biogenesis in Pseudomonas aeruginosa. *Molecular Microbiology*. [Online] 50 (3), 809–824. Available from:

doi:10.1046/J.1365-2958.2003.03740.X [Accessed: 21 January 2022].
Dautin, N. (2021) Folding Control in the Path of Type 5 Secretion. *Toxins*. [Online] 13 (5). Available from: doi:10.3390/TOXINS13050341 [Accessed: 20 May 2022].
Davies, J.C., Alton, E.W.F.W. & Bush, A. (2007) Cystic fibrosis. *The BMJ*. [Online] 335, 1255–1259. Available from: doi:10.1136/bmj.39391.713229.AD.
Davis, P.B. & Di Sant'Agnese, P.A. (1984) Diagnosis and Treatment of Cystic Fibrosis: An Update. *Chest*. [Online] 85 (6), 802–809. Available from: doi:10.1016/S0012-3692(16)62421-2.
Delforge, D., Depiereux, E., De Bolle, X., Feytmans, E., et al. (1993) Similarities between Alanine Dehydrogenase and the N-Terminal Part of Pyridine Nucleotide Transhydrogenase and Their Possible Implication in the Virulence Mechanism of Mycobacterium tuberculosis. *Biochemical and Biophysical Research Communications*. [Online] 190 (3), 1073–1079. Available from: doi:10.1006/BBRC.1993.1158.
Dell'Anno, A. & Danovaro, R. (2005) Extracellular DNA plays a key role in deep-sea ecosystem functioning. *Science* . [Online] 309 (5744), 2179. Available from: doi:10.1126/SCIENCE.1117475 [Accessed: 28 May 2023].
Deng, W., Marshall, N.C., Rowland, J.L., McCoy, J.M., et al. (2017) Assembly, structure, function and regulation of type III secretion systems. *Nature Reviews Microbiology*. [Online] 15 (6), 323–337. Available from: doi:10.1038/nrmicro.2017.20.
Denise, R., Abby, S.S. & Rocha, E.P.C. (2019) *Diversification of the type IV filament superfamily into machines for adhesion, protein secretion, DNA uptake, and motility*. [Online]. Available from: doi:10.1371/journal.pbio.3000390.
Deo, S., Turton, K.L., Kainth, T., Kumar, A., et al. (2022) Strategies for improving antimicrobial peptide production. *Biotechnology Advances*. [Online] 59 (107968), 1–17. Available from: doi:10.1016/J.BIOTECHADV.2022.107968.
Desvaux, M., Scott-Tucker, A., Turner, S.M., Cooper, L.M., et al. (2007) A conserved extended signal peptide region directs posttranslational protein translocation via a novel mechanism. *Microbiology*. [Online] 153, 59–70. Available from: doi:10.1099/MIC.0.29091-0 [Accessed: 21 February 2022].
Devanga Ragupathi, N.K., Veeraraghavan, B., Karunakaran, E. & Monk, P.N. (2022) Editorial: Biofilm-mediated nosocomial infections and its association with antimicrobial resistance: Detection, prevention, and management. *Frontiers in Medicine*. [Online] 9, 2322. Available from: doi:10.3389/FMED.2022.987011/BIBTEX.
Di, A., Brown, M.E., Deriy, L. V, Li, C., et al. (2006) CFTR regulates phagosome acidification in macrophages and alters bactericidal activity. *Nature Cell Biology*. [Online] 8 (9). Available from: doi:10.1038/ncb1456.
Diggle, S.P. & Whiteley, M. (2020) Microbe Profile: Pseudomonas aeruginosa: opportunistic pathogen and lab rat. *Microbiology*. [Online] 166, 30–33. Available from: doi:10.1099/mic.0.000860.
Doggett, R.G. (1969) Incidence of mucoid Pseudomonas aeruginosa from clinical sources. *Applied Microbiology*. [Online] 18 (5), 936–937. Available from: doi:10.1128/AM.18.5.936-937.1969 [Accessed: 28 May 2023].
Dolores, J.S., Agarwal, S., Egerer, M. & Satchell, K.J.F. (2015) Vibrio cholerae MARTX toxin heterologous translocation of beta-lactamase and roles of individual effector domains on cytoskeleton dynamics. *Molecular microbiology*. [Online] 95 (4), 590. Available from: doi:10.1111/MMI.12879 [Accessed: 16 May 2023].
Dorman, C.J. (2004) H-NS : A Universal Rregulator for a Dynamic Genome. *Nature Reviews*

Microbiology. [Online] 2 (May), 1–10. Available from: doi:10.1038/nrmicro883.
Douzi, B., Spinelli, S., Blangy, S., Roussel, A., et al. (2014) Crystal Structure and Self-Interaction of the Type VI Secretion Tail-Tube Protein from Enteroaggregative Escherichia coli. *PLoS ONE*. [Online] 9 (2), 1–9. Available from: doi:10.1371/JOURNAL.PONE.0086918 [Accessed: 20 May 2023].
Drenkard, E. (2003) Antimicrobial resistance of Pseudomonas aeruginosa biofilms. *Microbes and Infection*. [Online] 5 (13), 1213–1219. Available from: doi:10.1016/j.micinf.2003.08.009 [Accessed: 29 May 2023].
Drobnak, I., Braselmann, E., Chaney, J.L., Leyton, D.L., et al. (2015) Of linkers and autochaperones: an unambiguous nomenclature to identify common and uncommon themes for autotransporter secretion. *Molecular Microbiology*. [Online] 95 (1), 1–16. Available from: doi:10.1111/MMI.12838 [Accessed: 24 May 2023].
Dufour, P., Jarraud, S., Vandenesch, F., Greenland, T., et al. (2002) High Genetic Variability of the agr Locus in Staphylococcus Species. *Journal of Bacteriology*. [Online] 184 (4), 1180–1186. Available from: doi:10.1128/JB.184.4.1180-1186.2002 [Accessed: 11 March 2022].
Duong, F., Bonnet, E., Géli, V., Lazdunski, A., et al. (2001) The AprX protein of Pseudomonas aeruginosa: a new substrate for the Apr type I secretion system. *Gene*. [Online] 262 (1–2), 147–153. Available from: doi:10.1016/S0378-1119(00)00541-2.
Durand, E., Nguyen, V.S., Zoued, A., Logger, L., et al. (2015) Biogenesis and structure of a type VI secretion membrane core complex. *Nature*. [Online] 523 (7562), 555–560. Available from: doi:10.1038/nature14667.
Durda-Masny, M., Goździk-Spychalska, J., John, A., Czaiński, W., et al. (2021) The determinants of survival among adults with cystic fibrosis—a cohort study. *Journal of Physiological Anthropology*. [Online] 40 (1), 1–9. Available from: doi:10.1186/S40101-021-00269-7/FIGURES/5 [Accessed: 10 May 2023].
Edelheit, O., Hanukoglu, A. & Hanukoglu, I. (2009) Simple and efficient site-directed mutagenesis using two single-primer reactions in parallel to generate mutants for protein structure-function studies. *BMC Biotechnology*. [Online] 9 (1), 1–8. Available from: doi:10.1186/1472-6750-9-61/FIGURES/3 [Accessed: 14 June 2023].
Elhosseiny, N.M. & Attia, A.S. (2018) Acinetobacter: An emerging pathogen with a versatile secretome review-article. *Emerging Microbes and Infections*. [Online] 7 (1), 1–15. Available from: doi:10.1038/s41426-018-0030-4.
Elkins, M.R. & Bye, P.T.P. (2011) Mechanisms and applications of hypertonic saline. *Journal of the Royal Society of Medicine*. [Online] 104, S5. Available from: doi:10.1258/JRSM.2011.S11101 [Accessed: 10 May 2023].
Emsley, P., Charles, I.G., Fairweather, N.F. & Isaacs, N.W. (1996) Structure of Bordetella pertussis virulence factor P.69 pertactin. *Nature*. [Online] 381 (6577), 90–92. Available from: doi:10.1038/381090a0.
Erickson, H.P. (2021) How Teichoic Acids Could Support a Periplasm in Gram-Positive Bacteria, and Let Cell Division Cheat Turgor Pressure. *Frontiers in Microbiology*. [Online] 12 (May), 1–11. Available from: doi:10.3389/fmicb.2021.664704.
Evans, L.R. & Linker, A. (1973) Production and characterization of the slime polysaccharide of Pseudomonas aeruginosa. *Journal of bacteriology*. [Online] 116 (2), 915–924. Available from: doi:10.1128/JB.116.2.915-924.1973 [Accessed: 28 May 2023].
Fan, K., Cao, Q. & Lan, L. (2021) Genome-Wide Mapping Reveals Complex Regulatory Activities of BfmR in Pseudomonas aeruginosa. *Microorganisms*. 9 (3), 1–22.

Farber, S., Shwachman, H. & Maddock, C.L. (1943) Pancreatic Function and Disease in Early Life. I. Pancreatic Enzyme Activity and the Celiac Syndrome. *Journal of Clinical Investigation*. [Online] 22 (6), 827. Available from: doi:10.1172/JCI101456 [Accessed: 10 May 2023].

Farrell, P., Férec, C., Macek, M., Frischer, T., et al. (2018) Estimating the age of p.(Phe508del) with family studies of geographically distinct European populations and the early spread of cystic fibrosis. *European Journal of Human Genetics*. [Online] 26 (12), 1832–1839. Available from: doi:10.1038/s41431-018-0234-z.

Farrell, P.M., White, T.B., Ren, C.L., Hempstead, S.E., et al. (2017) Diagnosis of Cystic Fibrosis: Consensus Guidelines from the Cystic Fibrosis Foundation. *Journal of Pediatrics*. [Online] 181, S15. Available from: doi:10.1016/j.jpeds.2016.09.064 [Accessed: 24 June 2023].

Faure, L.M., Garvis, S., de Bentzmann, S. & Bigot, S. (2014) Characterization of a novel two-partner secretion system implicated in the virulence of Pseudomonas aeruginosa. *Microbiology (United Kingdom)*. [Online] 160, 1940–1952. Available from: doi:10.1099/mic.0.079616-0.

Faure, L.M., Llamas, M.A., Bastiaansen, K.C., De, S., et al. (2013) Phosphate starvation relayed by PhoB activates the expression of the Pseudomonas aeruginosa σ vreI ECF factor and its target genes To cite this version : HAL Id : hal-03012634 Phosphate starvation relayed by PhoB activates the expression of the Pseudomona. *Microbiolofy*. [Online] 159, 1315–1327. Available from: doi:10.1099/mic.0.067645-0.

Fazli, M., Almblad, H., Rybtke, M.L., Givskov, M., et al. (2014) Regulation of biofilm formation in Pseudomonas and Burkholderia species. *Environmental Microbiology*. [Online] 16 (7), 1961–1981. Available from: doi:10.1111/1462-2920.12448.

Feldman, M., Bryan, R., Rajan, S., Scheffler, L., et al. (1998) Role of Flagella in Pathogenesis of Pseudomonas aeruginosa Pulmonary Infection. *Infection and Immunity*. 66 (1), 43–51.

Felisberto-Rodrigues, C., Durand, E., Aschtgen, M.S., Blangy, S., et al. (2011) Towards a Structural Comprehension of Bacterial Type VI Secretion Systems: Characterization of the TssJ-TssM Complex of an Escherichia coli Pathovar. *PLoS Pathogens*. [Online] 7 (11), 1–11. Available from: doi:10.1371/JOURNAL.PPAT.1002386 [Accessed: 20 May 2023].

Festa, R.A. & Thiele, D.J. (2011) Copper: an Essential Metal in Biology. *Current biology*. [Online] 21 (21), R883. Available from: doi:10.1016/J.CUB.2011.09.040 [Accessed: 20 May 2023].

Figurski, D.H. & Helinski, D.R. (1979) Replication of an origin-containing derivative of plasmid RK2 dependent on a plasmid function provided in trans. *Proceedings of the National Academy of Sciences of the United States of America*. [Online] 76 (4), 1652. Available from: doi:10.1073/PNAS.76.4.1648 [Accessed: 27 June 2023].

Filloux, A. (2022) Bacterial protein secretion systems: Game of types. *REVIEW Filloux, Microbiology*. [Online] 168 (5), 1–16. Available from: doi:10.1099/mic.0.001193.

Filloux, A. (2011) Protein secretion systems in Pseudomonas aeruginosa: An essay on diversity, evolution, and function. *Frontiers in Microbiology*. [Online] 2 (155), 1–21. Available from: doi:10.3389/fmicb.2011.00155.

Filloux, A., Hachani, A. & Bleves, S. (2008) The bacterial type VI secretion machine: yet another player for protein transport across membranes. *Microbiology*. [Online] 154, 1570–1583. Available from: doi:10.1099/mic.0.2008/016840-0 [Accessed: 10 April 2023].

Fischer, S., Klockgether, J., Sorribes, M.G., Dorda, M., et al. (2021) Sequence diversity of the Pseudomonas aeruginosa population in loci that undergo microevolution in cystic fibrosis airways. *Access Microbiology*. [Online] 3 (12), 1–15. Available from: doi:10.1099/ACMI.0.000286 [Accessed: 29 April 2023].

Flemming, H.-C., Wingender, J., Szewzyk, U., Steinberg, P., et al. (2016) Biofilms: an emergent form of bacterial life. *Nature Publishing Group*. [Online] 14, 563–575. Available from: doi:10.1038/nrmicro.2016.94 [Accessed: 28 May 2023].

Flight, W.G., Smith, A., Paisey, C., Marchesi, J.R., et al. (2015) Rapid detection of emerging pathogens and loss of microbial diversity associated with severe lung disease in cystic fibrosis. *Journal of Clinical Microbiology*. [Online] 53 (7), 2022–2031. Available from: doi:10.1128/JCM.00432-15.

Förster, A., Planamente, S., Manoli, E., Lossi, N.S., et al. (2014) Coevolution of the ATPase ClpV, the sheath proteins TssB and TssC, and the accessory protein TagJ/HsiE1 distinguishes type VI secretion classes. *The Journal of Biological Chemistry*. [Online] 289 (47), 33032–33043. Available from: doi:10.1074/JBC.M114.600510 [Accessed: 20 May 2023].

Francis, V.I., Stevenson, E.C., Porter, S.L., Biosciences, †, et al. (2017) Two-component systems required for virulence in Pseudomonas aeruginosa. *FEMS Microbiology Letters*. [Online] 364 (11), 1–22. Available from: doi:10.1093/femsle/fnx104 [Accessed: 30 May 2023].

Francke, C., Groot Kormelink, T., Hagemeijer, Y., Overmars, L., et al. (2011) Comparative analyses imply that the enigmatic sigma factor 54 is a central controller of the bacterial exterior. *BMC Genomics*. [Online] 12 (385), 1–21. Available from: doi:10.1186/1471-2164-12-385 [Accessed: 21 January 2022].

Frangipani, E., Visaggio, D., Heeb, S., Kaever, V., et al. (2014) The Gac/Rsm and cyclic-di-GMP signalling networks coordinately regulate iron uptake in Pseudomonas aeruginosa. *Environmental Microbiology*. [Online] 16 (3), 676–688. Available from: doi:10.1111/1462-2920.12164.

Freeman, L. (1916) Chronic General Infection with the Bacillus pyocyaneus. *Annals of Surgery*. [Online] 64 (2), 202. Available from: doi:10.1097/00000658-191608000-00005 [Accessed: 29 April 2023].

Freschi, L., Bertelli, C., Jeukens, J., Moore, M.P., et al. (2018) Genomic characterisation of an international Pseudomonas aeruginosa reference panel indicates that the two major groups draw upon distinct mobile gene pools. *FEMS Microbiology Letters*. [Online] 365 (14), 1–11. Available from: doi:10.1093/femsle/fny120.

Freschi, L., Vincent, A.T., Jeukens, J., Emond-Rheault, J.G., et al. (2019) The Pseudomonas aeruginosa Pan-Genome Provides New Insights on Its Population Structure, Horizontal Gene Transfer, and Pathogenicity. *Genome Biology and Evolution*. [Online] 11 (1), 109–120. Available from: doi:10.1093/GBE/EVY259 [Accessed: 29 April 2023].

Fridman, C.M., Keppel, K., Gerlic, M., Bosis, E., et al. (2020) A comparative genomics methodology reveals a widespread family of membrane-disrupting T6SS effectors. *Nature Communications*. [Online] 11 (1). Available from: doi:10.1038/S41467-020-14951-4 [Accessed: 10 April 2023].

Friedman, L. & Kolter, R. (2004a) Genes involved in matrix formation in Pseudomonas aeruginosa PA14 biofilms. *Molecular Microbiology*. [Online] 51 (3), 675–690. Available from: doi:10.1046/J.1365-2958.2003.03877.X [Accessed: 7 April 2023].

Friedman, L. & Kolter, R. (2004b) Two genetic loci produce distinct carbohydrate-rich

structural components of the Pseudomonas aeruginosa biofilm matrix. *Journal of Bacteriology*. [Online] 186 (14), 4457–4465. Available from: doi:10.1128/JB.186.14.4457-4465.2004/FORMAT/EPUB [Accessed: 7 April 2023].

Gallique, M., Decoin, V., Barbey, C., Rosay, T., et al. (2017) Contribution of the Pseudomonas fluorescens MFE01 Type VI Secretion System to Biofilm Formation Eric Cascales (ed.). *PLOS ONE*. [Online] 12 (1), 1–19. Available from: doi:10.1371/journal.pone.0170770 [Accessed: 30 May 2020].

Gambello, M.J. & Iglewski, B.H. (1991) Cloning and Characterization of the Pseudomonas aeruginosa lasR Gene a Transcriptional Activator of Elastase Expression. *Journal of Bacteriology*. 173 (9), 3000–3009.

Gao, F., Danson, A.E., Ye, F., Jovanovic, M., et al. (2020) Bacterial Enhancer Binding Proteins-AAA + Proteins in Transcription Activation. *Biomolecules*. [Online] 10 (351), 1–12. Available from: doi:10.3390/biom10030351 [Accessed: 15 April 2023].

Gao, R., Mack, T.R. & Stock, A.M. (2007) Bacterial response regulators: versatile regulatory strategies from common domains. *Trends in Biochemical Sciences*. [Online] 32 (5), 225–234. Available from: doi:10.1016/J.TIBS.2007.03.002.

Gao, R. & Stock, A.M. (2009) Biological Insights from Structures of Two-Component Proteins. *Annual Reviews Microbiology*. [Online] 63, 133–154. Available from: doi:10.1146/annurev.micro.091208.073214 [Accessed: 30 May 2023].

Garcia, E.C., Anderson, M.S., Hagar, J.A. & Cotter, P.A. (2013) Burkholderia BcpA mediates biofilm formation independently of interbacterial contact dependent growth inhibition. *Molecular Microbiology*. [Online] 89 (6), 1213. Available from: doi:10.1111/MMI.12339 [Accessed: 4 April 2023].

Garcia, E.C., Perault, A.I., Marlatt, S.A. & Cotter, P.A. (2016a) Interbacterial signaling via Burkholderia contact-dependent growth inhibition system proteins. *Proceedings of the National Academy of Sciences of the United States of America*. [Online] 113 (29), 8296–8301. Available from: doi:10.1073/pnas.1606323113 [Accessed: 9 October 2020].

Garcia, E.C., Perault, A.I., Marlatt, S.A. & Cotter, P.A. (2016b) Interbacterial signaling via Burkholderia contact dependent growth inhibition system proteins. *Proceedings of the National Academy of Sciences of the United States of America*. [Online] 113 (29), 8296–8301. Available from: doi:10.1073/pnas.1606323113.

Garde, S., Chodisetti, P.K. & Reddy, M. (2021) Peptidoglycan: Structure, Synthesis, and Regulation. *EcoSal Plus*. [Online] 9 (2), 1–35. Available from: doi:10.1128/ECOSALPLUS.ESP-0010-2020/FORMAT/EPUB.

Gaussian, C.F. (1809) *Theoria Motus Corporum Coelestium in Sectionibus Conicis Solem Ambientium*. Lowfield Heath.

Gentle, I., Gabriel, K., Beech, P., Waller, R., et al. (2004) The Omp85 family of proteins is essential for outer membrane biogenesis in mitochondria and bacteria. *The Journal of Cell Biology*. [Online] 164 (1), 19–24. Available from: doi:10.1083/JCB.200310092 [Accessed: 26 May 2023].

Gentle, I.E., Burri, L. & Lithgow, T. (2005) Molecular architecture and function of the Omp85 family of proteins. *Molecular Microbiology*. [Online] 58 (5), 1216–1225. Available from: doi:10.1111/J.1365-2958.2005.04906.X [Accessed: 26 January 2023].

Gerlai, R. (2005) *Genetic Background*. [Online]. Springer, Berlin, Heidelberg. Available from: doi:10.1007/3-540-29623-9_2370 [Accessed: 23 September 2022].

Gessmann, D., Chung, Y.H., Danoff, E.J., Plummer, A.M., et al. (2014) Outer membrane β-barrel protein folding is physically controlled by periplasmic lipid head groups and

BamA. *Proceedings of the National Academy of Sciences USA*. [Online] 111 (16), 5878–5883. Available from: doi:10.1073/pnas.1322473111.
Ghigo, A., Prono, G., Riccardi, E. & De Rose, V. (2021) Dysfunctional inflammation in cystic fibrosis airways: From mechanisms to novel therapeutic approaches. *International Journal of Molecular Sciences*. [Online] 22 (4), 1–23. Available from: doi:10.3390/ijms22041952.
Giamarellos-Bourboulis, E., Xu, L., Christaki, E., Van Delden, C., et al. (2015) Metabolic pathways of Pseudomonas aeruginosa involved in competition with respiratory bacterial pathogens. *Frontiers in Microbiology*. [Online] 6 (321), 1–12. Available from: doi:10.3389/fmicb.2015.00321 [Accessed: 7 April 2023].
Gibiansky, M.L., Conrad, J.C., Jin, F., Gordon, V.D., et al. (2010) Bacteria use type IV pili to walk upright and detach from surfaces. *Science*. [Online] 330 (6001), 8–10. Available from: doi:10.1126/science.1194238.
Gibson, L.E. & Cooke, R.E. (1959) A test for concentration of electrolytes in sweat in cystic fibrosis of the pancreas utilizing pilocarpine by iontophoresis. *Pediatrics*. 23 (3), 545–549.
Gibson, R.L., Burns, J.L. & Ramsey, B.W. (2003) Pathophysiology and management of pulmonary infections in cystic fibrosis. *American journal of respiratory and critical care medicine*. [Online] 168 (8), 918–951. Available from: doi:10.1164/RCCM.200304-505SO [Accessed: 24 June 2023].
Gloag, E.S., Turnbull, L., Huang, A., Vallotton, P., et al. (2013) Self-organization of bacterial biofilms is facilitated by extracellular DNA. *Proceedings of the National Academy of Sciences of the United States of America*. [Online] 110 (28), 11541–11546. Available from: doi:10.1073/PNAS.1218898110 [Accessed: 28 May 2023].
Goeders, N. & Van Melderen, L. (2014) Toxin-Antitoxin Systems as Multilevel Interaction Systems. *Toxins*. [Online] 6 (1), 304. Available from: doi:10.3390/TOXINS6010304 [Accessed: 5 April 2023].
Gomila, M., Peña, A., Mulet, M., Lalucat, J., et al. (2015) Phylogenomics and systematics in Pseudomonas. *Frontiers in Microbiology*. [Online] 6 (MAR), 214. Available from: doi:10.3389/FMICB.2015.00214/ABSTRACT.
González-Magaña, A., Altuna, J., Queralt-Martín, M., Largo, E., et al. (2022) The P. aeruginosa effector Tse5 forms membrane pores disrupting the membrane potential of intoxicated bacteria. *Communications Biology*. [Online] 5 (1), 1–15. Available from: doi:10.1038/s42003-022-04140-y.
Goodman, A.L., Kulasekara, B., Rietsch, A., Boyd, D., et al. (2004) A Signaling Network Reciprocally Regulates Genes Associated with Acute Infection and Chronic Persistence in Pseudomonas aeruginosa. *Developmental Cell*. [Online] 7 (5), 745–754. Available from: doi:10.1016/J.DEVCEL.2004.08.020.
Goodman, A.L., Merighi, M., Hyodo, M., Ventre, I., et al. (2009) Direct interaction between sensor kinase proteins mediates acute and chronic disease phenotypes in a bacterial pathogen. *Genes & Development*. [Online] 23 (2), 249–259. Available from: doi:10.1101/GAD.1739009 [Accessed: 20 May 2023].
Gorasia, D.G., Veith, P.D. & Reynolds, E.C. (2020) The Type IX Secretion System: Advances in Structure, Function and Organisation. *Microorganisms*. [Online] 8 (8), 1–9. Available from: doi:10.3390/MICROORGANISMS8081173 [Accessed: 19 May 2023].
Goss, C.H. & Burns, J.L. (2007) Exacerbations in cystic fibrosis. 1: Epidemiology and pathogenesis. *Thorax*. [Online] 62 (4), 360–367. Available from:

doi:10.1136/THX.2006.060889 [Accessed: 24 June 2023].
Grace, A., Sahu, R., Owen, D.R. & Dennis, V.A. (2022) Pseudomonas aeruginosa reference strains PAO1 and PA14: A genomic, phenotypic, and therapeutic review. *Frontiers in Microbiology*. [Online] 13 (October), 1–15. Available from: doi:10.3389/fmicb.2022.1023523.
Granato, E.T., Meiller-Legrand, T.A. & Foster, K.R. (2019) The Evolution and Ecology of Bacterial Warfare. *Current Biology*. [Online] 29 (11), R521–R537. Available from: doi:10.1016/J.CUB.2019.04.024.
Greaser, M.L. & Warren, C.M. (2012) *Protein electrophoresis in agarose gels for separating high molecular weight proteins*. [Online]. Humana Press, Totowa, NJ. Available from: doi:10.1007/978-1-61779-821-4_10/FIGURES/1 [Accessed: 17 June 2023].
Green, E.R. & Mecsas, J. (2016) Bacterial Secretion Systems: An Overview. *Microbiology Spectrum*. [Online] 4 (1), 1–19. Available from: doi:10.1128/MICROBIOLSPEC.VMBF-0012-2015 [Accessed: 11 May 2023].
Greene, N.P., Kaplan, E., Crow, A. & Koronakis, V. (2018) Antibiotic resistance mediated by the MacB ABC transporter family: A structural and functional perspective. *Frontiers in Microbiology*. [Online] 9 (950), 1–17. Available from: doi:10.3389/fmicb.2018.00950.
Grijpstra, J., Arenas, J., Rutten, L. & Tommassen, J. (2013) Autotransporter secretion: varying on a theme. *Research in Microbiology*. [Online] 164 (6), 562–582. Available from: doi:10.1016/J.RESMIC.2013.03.010.
Grohmann, E., Christie, P.J., Waksman, G. & Backert, S. (2018) Type IV secretion in Gram-negative and Gram-positive bacteria. *Mol Microbiol*. [Online] 107 (4), 455–471. Available from: doi:10.1111/mmi.13896.
Guérin, J., Bigot, S., Schneider, R., Buchanan, S.K., et al. (2017) Two-partner secretion: Combining efficiency and simplicity in the secretion of large proteins for bacteria-host and bacteria-bacteria interactions. *Frontiers in Cellular and Infection Microbiology*. [Online] 7 (148), 1–23. Available from: doi:10.3389/FCIMB.2017.00148/BIBTEX.
Guerin, J., Botos, I., Zhang, Z., Lundquist, K., et al. (2020) Structural insight into toxin secretion by contact-dependent growth inhibition transporters. *eLife*. [Online] 9 (e58100), 1–22. Available from: doi:10.7554/eLife.58100 [Accessed: 7 October 2021].
Guillaume, O., Butnarasu, C., Visentin, S. & Reimhult, E. (2022) Interplay between biofilm microenvironment and pathogenicity of Pseudomonas aeruginosa in cystic fibrosis lung chronic infection. *Biofilm* . [Online] 4, 1–14. Available from: doi:10.1016/j.bioflm.2022.100089 [Accessed: 29 May 2023].
Guo, Q., Kong, W., Jin, S., Chen, L., et al. (2014) PqsR-dependent and PqsR-independent regulation of motility and biofilm formation by PQS in Pseudomonas aeruginosa PAO1. *Journal of Basic Microbiology*. [Online] 54 (7), 633–643. Available from: doi:10.1002/JOBM.201300091 [Accessed: 4 April 2023].
Gupta, K., Marques, C.N.H., Petrova, O.E. & Sauer, K. (2013) Antimicrobial tolerance of Pseudomonas aeruginosa biofilms is activated during an early developmental stage and requires the two-component hybrid SagS. *Journal of bacteriology*. [Online] 195 (21), 4975–4987. Available from: doi:10.1128/JB.00732-13 [Accessed: 29 May 2023].
Guzman, L.M., Belin, D., Carson, M.J. & Beckwith, J. (1995) Tight regulation, modulation, and high-level expression by vectors containing the arabinose PBAD promoter. *Journal of Bacteriology*. [Online] 177 (14), 4121–4130. Available from: doi:10.1128/JB.177.14.4121-4130.1995 [Accessed: 5 April 2023].
Ha, D.G., Kuchma, S.L. & O'Toole, G.A. (2014) Plate-based assay for swarming motility in

Pseudomonas aeruginosa. *Methods in Molecular Biology*. [Online] 1149, 67–72. Available from: doi:10.1007/978-1-4939-0473-0_8 [Accessed: 20 November 2020].
Hachani, A., Allsopp, L.P., Oduko, Y. & Filloux, A. (2014) The VgrG proteins are 'à la carte' delivery systems for bacterial type VI effectors. *Journal of Biological Chemistry*. [Online] 289 (25), 17872–17884. Available from: doi:10.1074/jbc.M114.563429.
Hachani, A., Lossi, N.S., Hamilton, A., Jones, C., et al. (2011) Type VI secretion system in Pseudomonas aeruginosa: Secretion and multimerization of VgrG proteins. *Journal of Biological Chemistry*. [Online] 286 (14), 12317–12327. Available from: doi:10.1074/jbc.M110.193045.
Hachani, A., Wood, T.E. & Filloux, A. (2016) Type VI secretion and anti-host effectors. *Current opinion in microbiology*. [Online] 29, 81–93. Available from: doi:10.1016/J.MIB.2015.11.006 [Accessed: 14 January 2022].
Hagan, C.L., Silhavy, T.J. & Kahne, D. (2011) β-Barrel Membrane Protein Assembly by the Bam Complex. *Annu. Rev. Biochem*. [Online] 80, 189–210. Available from: doi:10.1146/annurev-biochem-061408-144611 [Accessed: 2 May 2023].
Halte, M. & Erhardt, M. (2021) Protein export via the type iii secretion system of the bacterial flagellum. *Biomolecules*. [Online] 11 (2), 1–19. Available from: doi:10.3390/biom11020186.
Halter, R., Pohlner, J. & Meyer, T.F. (1984) IgA protease of Neisseria gonorrhoeae: isolation and characterization of the gene and its extracellular product. *The EMBO Journal*. [Online] 3 (7), 1595–1601. Available from: doi:10.1002/J.1460-2075.1984.TB02016.X [Accessed: 24 May 2023].
Han, Y., Wang, T., Chen, G., Pu, Q., et al. (2019) A Pseudomonas aeruginosa type VI secretion system regulated by CueR facilitates copper acquisition. *PLoS Pathogens*. [Online] 15 (12), 1–25. Available from: doi:10.1371/JOURNAL.PPAT.1008198 [Accessed: 20 May 2023].
Hanson, T.E., Zulie Ma, L., Ivan Nikel, P., Hindré, T., et al. (2017) SuhB Regulates the Motile-Sessile Switch in Pseudomonas aeruginosa through the Gac/Rsm Pathway and c-di-GMP Signaling. *Frontiers in Microbiology*. [Online] 8 (1045), 1–11. Available from: doi:10.3389/fmicb.2017.01045 [Accessed: 29 May 2023].
Hansson, G.C. (2019) Mucus and mucins in diseases of the intestinal and respiratory tracts. *Journal of internal medicine*. [Online] 285 (5), 479–490. Available from: doi:10.1111/JOIM.12910 [Accessed: 29 May 2023].
Harding, C.M., Pulido, M.R., Di Venanzio, G., Kinsella, R.L., et al. (2017) Pathogenic Acinetobacter species have a functional type i secretion system and contact-dependent inhibition systems. *Journal of Biological Chemistry*. [Online] 292 (22), 9075–9087. Available from: doi:10.1074/jbc.M117.781575.
Harvey, C., Weldon, S., Elborn, S., Downey, D.G., et al. (2022) The Effect of CFTR Modulators on Airway Infection in Cystic Fibrosis. *International Journal of Molecular Sciences*. [Online] 23 (7). Available from: doi:10.3390/ijms23073513.
Hatziagorou, E., Orenti, A., Drevinek, P., Kashirskaya, N., et al. (2020) Changing epidemiology of the respiratory bacteriology of patients with cystic fibrosis–data from the European cystic fibrosis society patient registry. *Journal of Cystic Fibrosis*. [Online] 19 (3), 376–383. Available from: doi:10.1016/J.JCF.2019.08.006.
Hauser, A.R. (2009) The type III secretion system of Pseudomonas aeruginosa: Infection by injection. *Nature Reviews Microbiology*. [Online] 7 (9), 654–665. Available from: doi:10.1038/nrmicro2199.

Hayes, C.S., Koskiniemi, S., Ruhe, Z.C., Poole, S.J., et al. (2014) Mechanisms and Biological Roles of Contact-Dependent Growth Inhibition Systems. *Cold Spring Harbor Perspectives in Medicine*. [Online] 4 (4), 1–12. Available from: doi:10.1101/cshperspect.a010025 [Accessed: 26 January 2023].

He, C., Li, Y., Huang, C., Chen, F., et al. (2018) Genome Sequence and Metabolic Analysis of a Fluoranthene-Degrading Strain Pseudomonas aeruginosa DN1. *Frontiers in Microbiology*. [Online] 9, 1–10. Available from: doi:10.3389/FMICB.2018.02595/FULL [Accessed: 29 April 2023].

Heinz, E. & Lithgow, T. (2014) A comprehensive analysis of the Omp85/TpsB protein superfamily structural diversity, taxonomic occurrence, and evolution. *Frontiers in microbiology*. [Online] 5 (370), 1–13. Available from: doi:10.3389/FMICB.2014.00370 [Accessed: 26 May 2023].

Henderson, I.R. & Nataro, J.P. (2001) Virulence Functions of Autotransporter Proteins. *Infection and Immunity*. [Online] 69 (3), 1231–1243. Available from: doi:10.1128/IAI.69.3.1231-1243.2001.

Henderson, I.R., Navarro-Garcia, F., Desvaux, M., Fernandez, R.C., et al. (2004) Type V Protein Secretion Pathway: the Autotransporter Story. *Microbiology and Molecular Biology Reviews*. [Online] 68 (4), 692–744. Available from: doi:10.1128/MMBR.68.4.692-744.2004 [Accessed: 21 April 2020].

Hendrickson, E.L., Plotnikova, J., Mahajan-Miklos, S., Rahme, L.G., et al. (2001) Differential roles of the Pseudomonas aeruginosa PA14 rpoN gene in pathogenicity in plants, nematodes, insects, and mice. *Journal of Bacteriology*. [Online] 183 (24), 7126–7134. Available from: doi:10.1128/JB.183.24.7126-7134.2001 [Accessed: 1 June 2023].

Henrichsen, J. (1972) Bacterial surface translocation: a survey and a classification. *Bacteriological reviews*. [Online] 36 (4), 478–503. Available from: doi:10.1128/BR.36.4.478-503.1972 [Accessed: 21 May 2023].

Hentzer, M., Teitzel, G.M., Balzer, G.J., Heydorn, A., et al. (2001) Alginate overproduction affects pseudomonas aeruginosa biofilm structure and function. *Journal of Bacteriology*. [Online] 183 (18), 5395–5401. Available from: doi:10.1128/JB.183.18.5395-5401.2001/ASSET/494F0096-71FA-4497-84E9-3818EF3C9C39/ASSETS/GRAPHIC/JB1810188005.JPEG [Accessed: 28 May 2023].

Heriot, M., Nottelet, B., Garric, X., D'Este, M., et al. (2019) Interaction of gentamicin sulfate with alginate and consequences on the physico-chemical properties of alginate-containing biofilms. *International journal of biological macromolecules*. [Online] 121, 390–397. Available from: doi:10.1016/J.IJBIOMAC.2018.10.025 [Accessed: 28 May 2023].

Hernandez, R.E., Gallegos-Monterrosa, R. & Coulthurst, S.J. (2020) Type VI secretion system effector proteins: Effective weapons for bacterial competitiveness. *Cellular Microbiology*. [Online] 22 (9), 1–9. Available from: doi:10.1111/CMI.13241 [Accessed: 20 May 2023].

Heurlier, K., Denervaud, V., Pessi, G., Reimmann, C., et al. (2003) The Integrated OR: New Horizons in Improving the Surgical Workflow. *Journal Of Bacteriology*. [Online] 185 (7), 2227–2235. Available from: doi:10.1128/JB.185.7.2227.

Hibbing, M.E., Fuqua, C., Parsek, M.R. & Peterson, S.B. (2010) Bacterial competition: surviving and thriving in the microbial jungle. *Nature Reviews Microbiology*. [Online] 8 (1), 15–25. Available from: doi:10.1353/sew.2015.0002.

Higashi, T. (1960) Physiological study on the oxygen- and nitrate respiration of

pseudomonas aeruginosa. *Journal of Biochemistry*. [Online] 47 (3), 326–334. Available from: doi:10.1093/OXFORDJOURNALS.JBCHEM.A127070/2/47-3-326.PDF.GIF [Accessed: 24 June 2023].

Hinsa, S.M., Espinosa-Urgel, M., Ramos, J.L. & O'Toole, G.A. (2003) Transition from reversible to irreversible attachment during biofilm formation by Pseudomonas fluorescens WCS365 requires an ABC transporter and a large secreted protein. *Molecular Microbiology*. [Online] 49 (4), 905–918. Available from: doi:10.1046/J.1365-2958.2003.03615.X [Accessed: 29 May 2023].

Ho, B.T., Dong, T.G. & Mekalanos, J.J. (2014) A view to a kill: the bacterial type 6 secretion system. *Cell host & microbe*. [Online] 15 (1), 9–21. Available from: doi:10.1016/J.CHOM.2013.11.008 [Accessed: 4 May 2022].

Hoffman, L.R., Kulasekara, H.D., Emerson, J., Houston, L.S., et al. (2009) Pseudomonas aeruginosa lasR mutants are associated with cystic fibrosis lung disease progression . *Journal of Cystic Fibrosis*. [Online] 8 (1), 66–70. Available from: doi:10.1016/j.jcf.2008.09.006.

Hoffmann, A., Bukau, B. & Kramer, G. (2010) Biochimica et Biophysica Acta Structure and function of the molecular chaperone Trigger Factor. *BBA - Molecular Cell Research*. [Online] 1803 (6), 650–661. Available from: doi:10.1016/j.bbamcr.2010.01.017.

Hoiczyk, E., Roggenkamp, A., Reichenbecher, M., Lupas, A., et al. (2000) Structure and sequence analysis of Yersinia YadA and Moraxella UspAs reveal a novel class of adhesins. *The EMBO Journal*. [Online] 19 (22), 5989–5999. Available from: doi:10.1093/EMBOJ/19.22.5989 [Accessed: 26 May 2023].

Holloway, B.W. (1955) Genetic recombination in Pseudomonas aeruginosa. *Journal of general microbiology*. [Online] 13 (3), 572–581. Available from: doi:10.1099/00221287-13-3-572/CITE/REFWORKS [Accessed: 24 June 2023].

Holm, S. (1979) A Simple Sequentially Rejective Multiple Test Procedure. *Scandinavian Journal of Statistics*. 6 (2), 65–70.

Homma, M., Oota, H., Kojima, S., Kawagishi, I., et al. (1996) Chemotactic responses to an attractant and a repellent by the polar and lateral flagellar systems of Vibrio alginolyticus. *Microbiology (Reading, England)*. [Online] 142 (Pt 10) (10), 2777–2783. Available from: doi:10.1099/13500872-142-10-2777 [Accessed: 21 May 2023].

Hood, R.D., Singh, P., Hsu, F.S., Güvener, T., et al. (2010) A type VI secretion system of Pseudomonas aeruginosa targets a toxin to bacteria. *Cell host & microbe*. [Online] 7 (1), 25–37. Available from: doi:10.1016/J.CHOM.2009.12.007 [Accessed: 14 January 2022].

Hosu, B.G., Nathan, V.S.J. & Berg, H.C. (2016) Internal and external components of the bacterial flagellar motor rotate as a unit. *Proceedings of the National Academy of Sciences of the United States of America*. [Online] 113 (17), 4783–4787. Available from: doi:10.1073/PNAS.1511691113/-/DCSUPPLEMENTAL [Accessed: 21 May 2023].

Hou, L., Debru, A., Chen, Q., Bao, Q., et al. (2019) AmrZ Regulates Swarming Motility Through Cyclic di-GMP-Dependent Motility Inhibition and Controlling Pel Polysaccharide Production in Pseudomonas aeruginosa PA14. *Frontiers in Microbiology*. [Online] 10, 1847. Available from: doi:10.3389/FMICB.2019.01847/BIBTEX.

Hsu, F., Schwarz, S. & Mougous, J.D. (2009) TagR Promotes PpkA-Catalyzed Type VI Secretion Activation in Pseudomonas aeruginosa. *Molecular Microbiology*. [Online] 72 (5), 1111–1125. Available from: doi:10.1111/j.1365-2958.2009.06701.x.TagR.

Huang, H., Shao, X., Xie, Y., Wang, T., et al. (2019) An integrated genomic regulatory network of virulence-related transcriptional factors in Pseudomonas aeruginosa.

Nature Communications . [Online] 10 (2931), 1–13. Available from: doi:10.1038/s41467-019-10778-w [Accessed: 31 May 2023].

Huang, Y.J. & LiPuma, J.J. (2016) The Microbiome in Cystic Fibrosis. *Clinics in Chest Medicine*. [Online]. 37 (1) pp.59–67. Available from: doi:10.1016/j.ccm.2015.10.003.

Humair, B., Wackwitz, B. & Haas, D. (2010) GacA-controlled activation of promoters for small RNA genes in pseudomonas fluorescens. *Applied and Environmental Microbiology*. [Online] 76 (5), 1497–1506. Available from: doi:10.1128/AEM.02014-09/SUPPL_FILE/TABLE_S1.DOC [Accessed: 30 May 2023].

Hutchings, M., Truman, A. & Wilkinson, B. (2019) Antibiotics: past, present and future. *Current Opinion in Microbiology*. [Online] 51, 72–80. Available from: doi:10.1016/J.MIB.2019.10.008.

Iadanza, M.G., Higgins, A.J., Schiffrin, B., Calabrese, A.N., et al. (2016) Lateral opening in the intact b-barrel assembly machinery captured by cryo-EM. *Nature Communications*. [Online] 7 (12865), 1–12. Available from: doi:10.1038/ncomms12865 [Accessed: 2 May 2023].

Ibáñez de Aldecoa, A.L., Zafra, O. & González-Pastor, J.E. (2017) Mechanisms and Regulation of Extracellular DNA Release and Its Biological Roles in Microbial Communities. *Frontiers in Microbiology*. [Online] 8 (1390), 1–19. Available from: doi:10.3389/FMICB.2017.01390 [Accessed: 28 May 2023].

Ikeda, M., Arai, M., Okuno, T. & Shimizu, T. (2003) TMPDB: a database of experimentally-characterized transmembrane topologies. *Nucleic Acids Research*. [Online] 31 (1), 406–409. Available from: doi:10.1093/nar/gkg018 [Accessed: 22 May 2020].

Irie, Y., Borlee, B.R., O'Connor, J.R., Hill, P.J., et al. (2012) Self-produced exopolysaccharide is a signal that stimulates biofilm formation in Pseudomonas aeruginosa. *Proceedings of the National Academy of Sciences of the United States of America*. [Online] 109 (50), 20632–20636. Available from: doi:10.1073/PNAS.1217993109/-/DCSUPPLEMENTAL [Accessed: 20 June 2023].

Irie, Y., La Mensa, A., Murina, V., Hauryliuk, V., et al. (2020) Hfq-Assisted RsmA Regulation Is Central to Pseudomonas aeruginosa Biofilm Polysaccharide PEL Expression. *Frontiers in Microbiology*. [Online] 11 (482585), 1–15. Available from: doi:10.3389/FMICB.2020.482585/FULL [Accessed: 3 April 2023].

Irie, Y., Starkey, M., Edwards, A.N., Wozniak, D.J., et al. (2010) Pseudomonas aeruginosa biofilm matrix polysaccharide Psl is regulated transcriptionally by RpoS and post-transcriptionally by RsmAm mi_7320 158..172. *Molecular Microbiology*. [Online] 78 (1), 158–172. Available from: doi:10.1111/j.1365-2958.2010.07320.x [Accessed: 20 June 2023].

Ismailov, I.L., Awayda, M.S., Jovov, B., Berdiev, B.K., et al. (1996) Regulation of epithelial sodium channels by the cystic fibrosis transmembrane conductance regulator. *The Journal of biological chemistry*. [Online] 271 (9), 4725–4732. Available from: doi:10.1074/JBC.271.9.4725 [Accessed: 10 May 2023].

Iyer, L.M., Zhang, D., Rogozin, I.B. & Aravind, L. (2011) Evolution of the deaminase fold and multiple origins of eukaryotic editing and mutagenic nucleic acid deaminases from bacterial toxin systems. *Nucleic Acids Research*. [Online] 39 (22), 9473–9497. Available from: doi:10.1093/nar/gkr691.

Jackson, K.D., Starkey, M., Kremer, S., Parsek, M.R., et al. (2004) Identification of psl, a locus encoding a potential exopolysaccharide that is essential for Pseudomonas aeruginosa PAO1 biofilm formation. *Journal of Bacteriology*. [Online] 186 (14), 4466–4475.

Available from: doi:10.1128/JB.186.14.4466-4475.2004 [Accessed: 28 May 2023].
Jander, G., Rahme, L.G. & Ausubel, F.M. (2000) Positive correlation between virulence of Pseudomonas aeruginosa mutants in mice and insects. *Journal of Bacteriology*. [Online] 182 (13), 3843–3845. Available from: doi:10.1128/JB.182.13.3843-3845.2000 [Accessed: 30 May 2023].
Janssen, K.H., Diaz, M.R., Golden, M., Graham, J.W., et al. (2018) Functional Analyses of the RsmY and RsmZ Small Noncoding Regulatory RNAs in Pseudomonas aeruginosa. *Journal of Bacteriology*. [Online] 200 (11), 1–15. Available from: doi:10.1128/JB [Accessed: 30 May 2023].
Jayathilake, P.G., Li, B., Zuliani, P., Curtis, T., et al. (2019) Modelling bacterial twitching in fluid flows: a CFD-DEM approach. *Scientific Reports*. [Online] 9 (1), 1–10. Available from: doi:10.1038/s41598-019-51101-3.
Jean-Pierre, F., Vyas, A., Hampton, T.H., Henson, M.A., et al. (2021) One versus many: Polymicrobial communities and the cystic fibrosis airway. *mBio*. [Online] 12 (2), 1–7. Available from: doi:10.1128/MBIO.00006-21/ASSET/EE5D1BC5-F184-4BFC-B1E2-FDAF5474A562/ASSETS/IMAGES/MEDIUM/MBIO.00006-21-F0002.GIF [Accessed: 7 April 2023].
Jenkinson, A.C., Mulligan, M., White, R., Power, N., et al. (2021) Acinetobacter baumannii Infection in a Child with Cystic Fibrosis. *Journal of Paediatrics and Child Health*. [Online] 57 (7), 1148–1149. Available from: doi:10.1111/JPC.15536.
Jennings, L.K., Dreifus, J.E., Reichhardt, C., Storek, K.M., et al. (2021) Pseudomonas aeruginosa aggregates in cystic fibrosis sputum produce exopolysaccharides that likely impede current therapies. *Cell Reports*. [Online] 34 (8), 1–9. Available from: doi:10.1016/j.celrep.2021.108782 [Accessed: 28 May 2023].
Jennings, L.K., Storek, K.M., Ledvina, H.E., Coulon, C., et al. (2015) Pel is a cationic exopolysaccharide that cross-links extracellular DNA in the Pseudomonas aeruginosa biofilm matrix. *Proceedings of the National Academy of Sciences of the United States of America*. [Online] 112 (36), 11353–11358. Available from: doi:10.1073/PNAS.1503058112/SUPPL_FILE/PNAS.1503058112.SM01.AVI [Accessed: 28 May 2023].
Jiang, F., Wang, X., Wang, B., Chen, L., et al. (2016) The Pseudomonas aeruginosa Type VI Secretion PGAP1-like Effector Induces Host Autophagy by Activating Endoplasmic Reticulum Stress. *Cell Reports*. [Online] 16 (6), 1502–1509. Available from: doi:10.1016/J.CELREP.2016.07.012 [Accessed: 20 May 2023].
Jiang, F., Waterfield, N.R., Yang, J., Yang, G., et al. (2014) A Pseudomonas aeruginosa type VI secretion phospholipase D effector targets both prokaryotic and eukaryotic cells. *Cell host & microbe*. [Online] 15 (5), 600–610. Available from: doi:10.1016/J.CHOM.2014.04.010 [Accessed: 14 January 2022].
Jimenez, L. (2007) Microbial Diversity in Pharmaceutical Product Recalls and Environments. *PDA Journal of Pharmaceutical Science and Technology*. 61 (5), 383–399.
Jin, C., Kang, S.M., Kim, D.H. & Lee, B.J. (2021) Structural and functional analysis of the Klebsiella pneumoniae MazEF toxin-antitoxin system. *IUCrJ*. [Online] 8 (Pt 3), 362–371. Available from: doi:10.1107/S2052252521000452 [Accessed: 16 May 2022].
Johnson, M., Zaretskaya, I., Raytselis, Y., Merezhuk, Y., et al. (2008) NCBI BLAST: a better web interface. *Nucleic Acids Research*. [Online] 36, 5–9. Available from: doi:10.1093/nar/gkn201 [Accessed: 22 May 2020].
Johnson, P.M., Beck, C.M., Morse, R.P., Garza-Sánchez, F., et al. (2016) Unraveling the

essential role of CysK in CDI toxin activation. *Proceedings of the National Academy of Sciences of the United States of America*. [Online] 113 (35), 9792–9797. Available from: doi:10.1073/PNAS.1607112113/SUPPL_FILE/PNAS.201607112SI.PDF [Accessed: 26 May 2023].

Jones, A.M., Garza-Sánchez, F., So, J., Hayes, C.S., et al. (2017) Activation of contact-dependent antibacterial tRNase toxins by translation elongation factors. *Proceedings of the National Academy of Sciences of the United States of America*. [Online] 114 (10), E1951–E1957. Available from: doi:10.1073/PNAS.1619273114/SUPPL_FILE/PNAS.201619273SI.PDF [Accessed: 26 May 2023].

Jones, C.J., Newsom, D., Kelly, B., Irie, Y., et al. (2014) ChIP-Seq and RNA-Seq Reveal an AmrZ-Mediated Mechanism for Cyclic di-GMP Synthesis and Biofilm Development by Pseudomonas aeruginosa. *PLoS Pathogens*. [Online] 10 (3), 1–18. Available from: doi:10.1371/JOURNAL.PPAT.1003984 [Accessed: 1 June 2023].

Jones, C.J., Ryder, C.R., Mann, E.E. & Wozniak, D.J. (2013) AmrZ modulates pseudomonas aeruginosa biofilm architecture by directly repressing transcription of the psl operon. *Journal of Bacteriology*. [Online] 195 (8), 1637–1644. Available from: doi:10.1128/JB.02190-12 [Accessed: 1 June 2023].

Jouault, A., Saliba, A.M. & Touqui, L. (2022) Modulation of the immune response by the Pseudomonas aeruginosa type-III secretion system. *Frontiers in Cellular and Infection Microbiology*. [Online] 12 (11), 1–8. Available from: doi:10.3389/fcimb.2022.1064010.

Juhas, M. (2015) Type IV secretion systems and genomic islands-mediated horizontal gene transfer in Pseudomonas and Haemophilus. *Microbiological Research*. [Online] 170, 10–17. Available from: doi:10.1016/J.MICRES.2014.06.007.

Jurado-Martín, I., Sainz-Mejías, M. & McClean, S. (2021) Pseudomonas aeruginosa: An Audacious Pathogen with an Adaptable Arsenal of Virulence Factors. *International Journal of Molecular Sciences*. [Online] 22 (6), 1–37. Available from: doi:10.3390/IJMS22063128 [Accessed: 11 May 2023].

Jyot, J., Balloy, V., Jouvion, G., Verma, A., et al. (2011) Type II secretion system of pseudomonas aeruginosa: In vivo evidence of a significant role in death due to lung infection. *Journal of Infectious Diseases*. [Online] 203 (10), 1369–1377. Available from: doi:10.1093/infdis/jir045.

Kajava, A. V., Cheng, N., Cleaver, R., Kessel, M., et al. (2001) Beta-helix model for the filamentous haemagglutinin adhesin of Bordetella pertussis and related bacterial secretory proteins. *Molecular Microbiology*. [Online] 42 (2), 279–292. Available from: doi:10.1046/J.1365-2958.2001.02598.X [Accessed: 5 April 2023].

Kaler, K.M.R., Nix, J.C. & Schubot, F.D. (2021) RetS inhibits Pseudomonas aeruginosa biofilm formation by disrupting the canonical histidine kinase dimerization interface of GacS. *Journal of Biological Chemistry*. [Online] 297 (4), 1–13. Available from: doi:10.1016/J.JBC.2021.101193.

Kang'ethe, W. & Bernstein, H.D. (2013) Charge-dependent secretion of an intrinsically disordered protein via the autotransporter pathway. *Proceedings of the National Academy of Sciences of the United States of America*. [Online] 110 (45), E4246–E4255. Available from: doi:10.1073/PNAS.1310345110/SUPPL_FILE/PNAS.201310345SI.PDF [Accessed: 24 May 2023].

Kanonenberg, K., Spitz, O., Erenburg, I.N., Beer, T., et al. (2018) Type I secretion system-it takes three and a substrate. *FEMS Microbiology Letters*. [Online] 365 (11), 1–10.

Available from: doi:10.1093/femsle/fny094 [Accessed: 16 May 2023].
Kaur, G., Iyer, L.M., Burroughs, A.M. & Aravind, L. (2021) Bacterial death and tradd-n domains help define novel apoptosis and immunity mechanisms shared by prokaryotes and metazoans. *eLife*. [Online] 10, 1–36. Available from: doi:10.7554/eLife.70394.
Kaushik, S., He, H. & Dalbey, R.E. (2022) Bacterial Signal Peptides- Navigating the Journey of Proteins. *Frontiers in Physiology*. [Online] 13 (July), 1–25. Available from: doi:10.3389/fphys.2022.933153.
Kay, E., Humair, B., Dénervaud, V., Riedel, K., et al. (2006) Two GacA-dependent small RNAs modulate the quorum-sensing response in Pseudomonas aeruginosa. *Journal of bacteriology*. [Online] 188 (16), 6026–6033. Available from: doi:10.1128/JB.00409-06 [Accessed: 14 January 2022].
Kazmierczak, B.I., Schniederberend, M. & Jain, R. (2015) Cross-regulation of Pseudomonas motility systems: the intimate relationship between flagella, pili and virulence. *Current opinion in microbiology*. [Online] 28, 78–82. Available from: doi:10.1016/J.MIB.2015.07.017 [Accessed: 19 January 2022].
Kelley, L.A., Mezulis, S., Yates, C.M., Wass, M.N., et al. (2015) The Phyre2 web portal for protein modeling, prediction and analysis. *Nature Protocols*. [Online] 10 (6), 845–858. Available from: doi:10.1038/nprot.2015.053.
Kerem, B.S., Rommens, J.M., Buchanan, J.A., Markiewicz, D., et al. (1989) Identification of the cystic fibrosis gene: Genetic analysis. *Science*. [Online] 245 (4922), 1073–1080. Available from: doi:10.1126/SCIENCE.2570460 [Accessed: 10 May 2023].
Khanolkar, R.A., Clark, S.T., Wang, P.W., Hwang, D.M., et al. (2020) Ecological Succession of Polymicrobial Communities in the Cystic Fibrosis Airways. *mSystems*. [Online] 5 (6), 1–16. Available from: https://doi.org/10 [Accessed: 23 June 2023].
Khosravi, M., Lin, R.L., Maskey, A.P., Pandey, S., et al. (2021) A Distinct Difference Between Air and Mucosal Temperatures in Human Respiratory Tract. *Frontiers in Medicine*. [Online] 8 (650637), 1–7. Available from: doi:10.3389/FMED.2021.650637/BIBTEX.
Kida, Y., Higashimoto, Y., Inoue, H., Shimizu, T., et al. (2008) A novel secreted protease from Pseudomonas aeruginosa activates NF-kB through protease-activated receptors. *Cellular Microbiology* . [Online] 10 (7), 1491–1504. Available from: doi:10.1111/j.1462-5822.2008.01142.x [Accessed: 24 May 2023].
Kierbel, A., Gassama-Diagne, A., Mostov, K. & Engel, J.N. (2005) The Phosphoinositol-3-Kinase–Protein Kinase B/Akt Pathway Is Critical for Pseudomonas aeruginosa Strain PAK Internalization. *Molecular Biology of the Cell*. [Online] 16 (5), 2585. Available from: doi:10.1091/MBC.E04-08-0717 [Accessed: 20 May 2023].
Kim, N., Kim, J.J., Kim, I., Mannaa, M., et al. (2020) Type VI secretion systems of plant-pathogenic Burkholderia glumae BGR1 play a functionally distinct role in interspecies interactions and virulence. *Molecular Plant Pathology*. [Online] 21 (8), 1055–1069. Available from: doi:10.1111/mpp.12966.
Kimkes, T.E.P. & Heinemann, M. (2019) How bacteria recognise and respond to surface contact. *FEMS Microbiology Reviews*. [Online] 44 (1), 106–122. Available from: doi:10.1093/femsre/fuz029.
King, J.D., Kocíncová, D., Westman, E.L. & Lam, J.S. (2009) Lipopolysaccharide biosynthesis in Pseudomonas aeruginosa. *Innate Immunity*. [Online] 15 (5), 261–312. Available from: doi:10.1177/1753425909106436.
Kingsley, R.A., Keestra, A.M., De Zoete, M.R. & Bäumier, A.J. (2004) The ShdA adhesin binds to the cationic cradle of the fibronectin 13FnIII repeat module: evidence for molecular

mimicry of heparin binding. *Molecular Microbiology*. [Online] 52 (2), 345–355. Available from: doi:10.1111/J.1365-2958.2004.03995.X [Accessed: 4 April 2022].
Klausen, M., Aaes-Jørgensen, A., Molin, S. & Tolker-Nielsen, T. (2003a) Involvement of bacterial migration in the development of complex multicellular structures in Pseudomonas aeruginosa biofilms. *Molecular microbiology*. [Online] 50 (1), 61–68. Available from: doi:10.1046/J.1365-2958.2003.03677.X [Accessed: 21 May 2023].
Klausen, M., Heydorn, A., Ragas, P., Lambertsen, L., et al. (2003b) Biofilm formation by Pseudomonas aeruginosa wild type, flagella and type IV pili mutants. *Molecular Microbiology*. [Online] 48 (6), 1511–1524. Available from: doi:10.1046/J.1365-2958.2003.03525.X [Accessed: 29 May 2023].
Klauser, T., Pohlner, J. & Meyer, T.F. (1993) The secretion pathway of IgA protease-type proteins in gram-negative bacteria. *BioEssays*. [Online] 15 (12), 799–805. Available from: doi:10.1002/BIES.950151205 [Accessed: 24 May 2023].
Klein, T.A., Ahmad, S. & Whitney, J.C. (2020) Contact-Dependent Interbacterial Antagonism Mediated by Protein Secretion Machines. *Trends in Microbiology*. [Online] 28 (5), 387–400. Available from: doi:10.1016/j.tim.2020.01.003.
Klockgether, J., Munder, A., Neugebauer, J., Davenport, C.F., et al. (2010) Genome Diversity of Pseudomonas aeruginosa PAO1 Laboratory Strains. *Journal of Bacteriology*. [Online] 192 (4), 1121. Available from: doi:10.1128/JB.01515-09 [Accessed: 29 June 2023].
Koch, M.D., Fei, C., Wingreen, N.S., Shaevitz, J.W., et al. (2021) Competitive binding of independent extension and retraction motors explains the quantitative dynamics of type IV pili. *Proceedings of the National Academy of Sciences of the United States of America*. [Online] 118 (8). Available from: doi:10.1073/PNAS.2014926118/-/DCSUPPLEMENTAL [Accessed: 21 May 2023].
Kohler, T., Curty, L.K., Barja, F., Van Delden, C., et al. (2000) Swarming of Pseudomonas aeruginosa is dependent on cell-to-cell signaling and requires flagella and pili. *Journal of Bacteriology*. [Online] 182 (21), 5990–5996. Available from: doi:10.1128/JB.182.21.5990-5996.2000 [Accessed: 21 May 2023].
Kohler, V., Probst, I., Aufschnaiter, A., Büttner, S., et al. (2017) Conjugative type IV secretion in Gram-positive pathogens: TraG, a lytic transglycosylase and endopeptidase, interacts with translocation channel protein TraM. *Plasmid*. [Online] 91, 9–18. Available from: doi:10.1016/J.PLASMID.2017.02.002.
Korotkov, K. V., Sandkvist, M. & Hol, W.G.J. (2012) The type II secretion system: biogenesis, molecular architecture and mechanism. *Nature Reviews Microbiology*. [Online] 10 (5), 359–375. Available from: doi:10.1038/nrmicro2762.The.
Koskiniemi, S., Garza-Sánchez, F., Sandegren, L., Webb, J.S., et al. (2014) Selection of Orphan Rhs Toxin Expression in Evolved Salmonella enterica Serovar Typhimurium. *PLoS Genet*. [Online] 10 (3), 1–10. Available from: doi:10.1371/journal.pgen.1004255 [Accessed: 26 May 2023].
Krasauskas, R., Skerniškytė, J., Armalytė, J. & Sužiedėlienė, E. (2019) The role of Acinetobacter baumannii response regulator BfmR in pellicle formation and competitiveness via contact-dependent inhibition system. *BMC Microbiology*. [Online] 19 (241), 1–12. Available from: doi:10.1186/S12866-019-1621-5 [Accessed: 31 May 2023].
Kuchma, S.L., Brothers, K.M., Merritt, J.H., Liberati, N.T., et al. (2007) BifA, a cyclic-Di-GMP phosphodiesterase, inversely regulates biofilm formation and swarming motility by Pseudomonas aeruginosa PA14. *Journal of bacteriology*. [Online] 189 (22), 8165–8178.

Available from: doi:10.1128/JB.00586-07 [Accessed: 21 May 2023].
Kuchma, S.L., Delalez, N.J., Filkins, L.M., Snavely, E.A., et al. (2015) Cyclic di-GMP-mediated repression of swarming motility by Pseudomonas aeruginosa PA14 Requires the MotAB stator. *Journal of Bacteriology*. [Online] 197 (3), 420–430. Available from: doi:10.1128/JB.02130-14 [Accessed: 20 November 2020].
Kuhlen, L., Abrusci, P., Johnson, S., Gault, J., et al. (2018) Structure of the core of the type iii secretion system export apparatus. *Nature Structural and Molecular Biology*. [Online] 25 (7), 583–590. Available from: doi:10.1038/s41594-018-0086-9.
Kumar, S., Stecher, G., Li, M., Knyaz, C., et al. (2018) MEGA X: Molecular Evolutionary Genetics Analysis across Computing Platforms. *Molecular Biology and Evolution*. [Online] 35 (6), 1547–1549. Available from: doi:10.1093/molbev/msy096 [Accessed: 23 March 2020].
Kuru, E., Hughes, H.V., Brown, P.J., Hall, E., et al. (2012) In situ probing of newly synthesized peptidoglycan in live bacteria with fluorescent D-amino acids. *Angewandte Chemie - International Edition*. [Online] 51 (50), 12519–12523. Available from: doi:10.1002/anie.201206749.
Labrou, N.E. (2014) Protein purifi cation: An overview. *Methods in Molecular Biology*. [Online] 1129, 3–10. Available from: doi:10.1007/978-1-62703-977-2_1/TABLES/1 [Accessed: 16 June 2023].
Lairson, L.L., Henrissat, B., Davies, G.J. & Withers, S.G. (2008) Glycosyltransferases: Structures, Functions, and Mechanisms. *Annual Reviews of Biochemistry*. [Online] 77, 521–555. Available from: doi:10.1146/ANNUREV.BIOCHEM.76.061005.092322 [Accessed: 20 May 2022].
Lanzer, M. & Bujard, H. (1988) Promoters largely determine the efficiency of repressor action (RNA polymerase/repressor competition/operator position/Ic operon). *Proceedings of the National Academy of Sciences USA*. 85, 8973–8977.
Lapouge, K., Schubert, M., Allain, F.H.T. & Haas, D. (2008) Gac/Rsm signal transduction pathway of γ-proteobacteria: From RNA recognition to regulation of social behaviour. *Molecular Microbiology*. [Online] 67 (2), 241–253. Available from: doi:10.1111/J.1365-2958.2007.06042.X.
Lara-Tejero, M., Kato, J., Wagner, S., Liu, X., et al. (2011) A sorting platform determines the order of protein secretion in bacterial type III systems. *Science*. [Online] 331 (6021), 1188–1191. Available from: doi:10.1126/science.1201476.
Latour, X. (2020) The evanescent GacS signal. *Microorganisms*. [Online] 8 (11), 1–25. Available from: doi:10.3390/microorganisms8111746.
Le, N.-H., Pinedo, V., Lopez, J., Cava, F., et al. (2021) Killing of Gram-negative and Gram-positive bacteria by a bifunctional cell wall-targeting T6SS effector. *Proceedings of the National Academy of Sciences*. [Online] 118 (40), 1–6. Available from: doi:10.1073/pnas.2106555118/-/DCSupplemental [Accessed: 11 October 2021].
Leard, L.E., Holm, A.M., Valapour, M., Glanville, A.R., et al. (2021) Consensus document for the selection of lung transplant candidates: An update from the International Society for Heart and Lung Transplantation. *Journal of Heart and Lung Transplantation*. [Online] 40 (11), 1349–1379. Available from: doi:10.1016/J.HEALUN.2021.07.005/ATTACHMENT/99ECCBCB-5318-4552-94E8-B6CFCE092466/MMC1.DOCX [Accessed: 11 May 2023].
Lederberg, J. & Tatum, E.L. (1946) Gene Recombination in Escherichia Coli. *Nature*. [Online] 158 (4016), 558–558. Available from: doi:10.1038/158558a0 [Accessed: 4 February

2022].
Leduc, M., Frehel, C., Siegel, E. & Van Heijenoort, J. (1989) Multilayered distribution of peptidoglycan in the periplasmic space of Escherichia coli. *Journal of general microbiology*. [Online] 135 (5), 1243–1254. Available from: doi:10.1099/00221287-135-5-1243 [Accessed: 2 May 2023].
Lee, I. & Schindelin, H. (2008) Structural Insights into E1-Catalyzed Ubiquitin Activation and Transfer to Conjugating Enzymes. *Cell*. [Online] 134 (2), 268–278. Available from: doi:10.1016/J.CELL.2008.05.046.
Lee, J. & Zhang, L. (2015) The hierarchy quorum sensing network in Pseudomonas aeruginosa. *Protein Cell*. [Online] 6 (1), 26–41. Available from: doi:10.1007/s13238-014-0100-x.
Lee, S. & Lee, D.K. (2018) What is the proper way to apply the multiple comparison test? *Korean Journal of Anesthesiology*. [Online] 71 (5), 353–360. Available from: doi:10.4097/kja.d.18.00242.
Leenaars, M. & Hendriksen, C.F.M. (2005) Critical Steps in the Production of Polyclonal and Monoclonal Antibodies: Evaluation and Recommendations. *ILAR Journal*. [Online] 46 (3), 269–279. Available from: doi:10.1093/ILAR.46.3.269 [Accessed: 27 January 2023].
van Leewenhoeck, A. (1677) Observations, communicated to the publisher by Mr. Antony van Leewenhoeck, in a dutch letter of the 9th Octob. 1676. here English'd: concerning little animals by him observed in rain-well-sea- and snow water; as also in water wherein pepper had lain infus. *Philosophical Transactions of the Royal Society of London*. [Online] 12 (133), 821–831. Available from: doi:10.1098/RSTL.1677.0003 [Accessed: 26 April 2023].
Leo, J.C., Oberhettinger, P., Schütz, M. & Linke, D. (2015) The inverse autotransporter family: Intimin, invasin and related proteins. *International Journal of Medical Microbiology*. [Online] 305 (2), 276–282. Available from: doi:10.1016/J.IJMM.2014.12.011.
LeRoux, M., Kirkpatrick, R.L., Montauti, E.I., Tran, B.Q., et al. (2014) Kin cell lysis is a danger signal that activates antibacterial pathways of Pseudomonas aeruginosa. *eLife*. [Online] 4, 15–2. Available from: doi:10.7554/eLife.05701.001.
Lesic, B., Lépine, F., Déziel, E., Zhang, J., et al. (2007) Inhibitors of pathogen intercellular signals as selective anti-infective compounds. *PLoS Pathogens*. [Online] 3 (9), 1229–1239. Available from: doi:10.1371/journal.ppat.0030126.
Lesic, B., Starkey, M., He, J., Hazan, R., et al. (2009) Quorum sensing differentially regulates Pseudomonas aeruginosa type VI secretion locus I and homologous loci II and III, which are required for pathogenesis. *Microbiology*. [Online] 155 (9), 2845–2855. Available from: doi:10.1099/mic.0.029082-0.
Lethem, M.I., James, S.L., Marriott, C. & Burke, J.F. (1990) The origin of DNA associated with mucus glycoproteins in cystic fibrosis sputum - PubMed. *European Respiratory Journal*. [Online] 3 (1), 19–23. Available from: https://pubmed.ncbi.nlm.nih.gov/2107097/ [Accessed: 28 May 2023].
Létoffé, S., Redeker, V. & Wandersman, C. (1998) Isolation and characterization of an extracellular haem-binding protein from Pseudomonas aeruginosa that shares function and sequence similarities with the Serratia marcescens HasA haemophore. *Molecular Microbiology*. [Online] 28 (6), 1223–1234. Available from: doi:10.1046/J.1365-2958.1998.00885.X [Accessed: 16 May 2023].
Létoffé, S., Wu, Y., Darch, S.E., Beloin, C., et al. (2022) Pseudomonas aeruginosa Production

of Hydrogen Cyanide Leads to Airborne Control of Staphylococcus aureus Growth in Biofilm and in Vivo Lung Environments. *mBio*. [Online] 13 (5). Available from: doi:10.1128/MBIO.02154-22/SUPPL_FILE/MBIO.02154-22-S0007.PDF [Accessed: 29 April 2023].

Letunic, I. & Bork, P. (2017) 20 years of the SMART protein domain annotation resource. *Nucleic Acids Research*. [Online] 46, 493–496. Available from: doi:10.1093/nar/gkx922 [Accessed: 22 May 2020].

Lewis, J.M., Deveson Lucas, D., Harper, M. & Boyce, J.D. (2019) Systematic identification and analysis of acinetobacter baumannii type vi secretion system effector and immunity components. *Frontiers in Microbiology*. [Online] 10 (OCT), 2440. Available from: doi:10.3389/FMICB.2019.02440/BIBTEX.

Leyton, D.L., Johnson, M.D., Thapa, R., Huysmans, G.H.M., et al. (2014) ARTICLE A mortise-tenon joint in the transmembrane domain modulates autotransporter assembly into bacterial outer membranes. *Nature Communications*. [Online] 5 (4239), 1–11. Available from: doi:10.1038/ncomms5239 [Accessed: 24 May 2023].

Li, H., Hao, C. & Xu, D. (2017) Development of a novel vector for cloning and expressing extremely toxic genes in Escherichia coli. *Electronic Journal of Biotechnology*. [Online] 30, 88–94. Available from: doi:10.1016/J.EJBT.2017.10.004.

Li, K., Yang, G., Debru, A.B., Li, P., et al. (2017) SuhB regulates the motile-sessile switch in Pseudomonas aeruginosa through the Gac/Rsm pathway and c-di-GMP signaling. *Frontiers in Microbiology*. [Online] 8 (1045), 1–11. Available from: doi:10.3389/FMICB.2017.01045/BIBTEX.

Li, M., Le Trong, I., Carl, M.A., Larson, E.T., et al. (2012) Structural basis for type VI secretion effector recognition by a cognate immunity protein. *PLoS Pathogens*. [Online] 8 (4), 1–13. Available from: doi:10.1371/journal.ppat.1002613.

Li, X., Gu, N., Huang, T.Y., Zhong, F., et al. (2022) Pseudomonas aeruginosa: A typical biofilm forming pathogen and an emerging but underestimated pathogen in food processing. *Frontiers in Microbiology*. [Online] 13, 1–8. Available from: doi:10.3389/FMICB.2022.1114199 [Accessed: 29 April 2023].

Li, Y., Chen, L., Zhang, P., Bhagirath, A.Y., et al. (2020) ClpV3 of the H3-Type VI Secretion System (H3-T6SS) Affects Multiple Virulence Factors in Pseudomonas aeruginosa. *Frontiers in Microbiology*. [Online] 11 (1096), 1–14. Available from: doi:10.3389/FMICB.2020.01096/BIBTEX.

Li, Y. & Ni, X. (2019) Molecular Evolution and Functional Analysis of Rubredoxin-Like Proteins in Plants. *BioMed Research International*. [Online] 2019, 1–14. Available from: doi:10.1155/2019/2932585 [Accessed: 10 March 2022].

Liao, C., Huang, X., Wang, Q., Yao, D., et al. (2022) Virulence Factors of Pseudomonas Aeruginosa and Antivirulence Strategies to Combat Its Drug Resistance. *Frontiers in Cellular and Infection Microbiology*. [Online] 12 (926758), 1–17. Available from: doi:10.3389/FCIMB.2022.926758 [Accessed: 4 April 2023].

Liaw, S.J., Lai, H.C., Ho, S.W., Luh, K.T., et al. (2003) Role of RsmA in the regulation of swarming motility and virulence factor expression in Proteus mirabilis. *Journal of Medical Microbiology*. [Online] 52 (1), 19–28. Available from: doi:10.1099/jmm.0.05024-0.

Lim, G.M., Kim, J.K., Kim, E.J., Lee, C.S., et al. (2022) Generation of a recombinant antibody for sensitive detection of Pseudomonas aeruginosa. *BMC Biotechnology*. [Online] 22 (1), 1–11. Available from: doi:10.1186/s12896-022-00751-9.

Limoli, D.H., Warren, E.A., Yarrington, K.D., Donegan, N.P., et al. (2019) Interspecies interactions induce exploratory motility in pseudomonas aeruginosa. *eLife*. [Online] 8, 1–24. Available from: doi:10.7554/eLife.47365.

Lin, J.-S., Wu, H.-H., Hsu, P.-H., Ma, L.-S., et al. (2014) Fha Interaction with Phosphothreonine of TssL Activates Type VI Secretion in Agrobacterium tumefaciens. *PLoS Pathogens*. [Online] 10 (3), 1–16. Available from: doi:10.1371/journal.ppat.1003991 [Accessed: 3 June 2023].

Lin, J., Yang, J., Cheng, J., Zhang, W., et al. (2023) Pseudomonas aeruginosa H3-T6SS Combats H2O2 Stress by Diminishing the Amount of Intracellular Unincorporated Iron in a Dps-Dependent Manner and Inhibiting the Synthesis of PQS. *International Journal of Molecular Sciences*. [Online] 24 (2), 1–20. Available from: doi:10.3390/ijms24021614.

Lin, J., Zhang, W., Cheng, J., Yang, X., et al. (2017) A Pseudomonas T6SS effector recruits PQS-containing outer membrane vesicles for iron acquisition. *Nature Communications*. [Online] 28 (8), 1–12. Available from: doi:10.1038/ncomms14888 [Accessed: 20 May 2023].

Lin, L., Capozzoli, R., Ferrand, A., Plum, M., et al. (2022) Subcellular localization of Type VI secretion system assembly in response to cell–cell contact. *The EMBO Journal*. [Online] 41 (13), e108595. Available from: doi:10.15252/EMBJ.2021108595 [Accessed: 3 April 2023].

Lin, L., Lezan, E., Schmidt, A. & Basler, M. (2019) Abundance of bacterial Type VI secretion system components measured by targeted proteomics. *Nature Communications*. [Online] 10 (1), 1–11. Available from: doi:10.1038/s41467-019-10466-9.

Link, A.J., Phillips, D. & Church, G.M. (1997) Methods for generating precise deletions and insertions in the genome of wild-type Escherichia coli: Application to open reading frame characterization. *Journal of Bacteriology*. [Online] 179 (20), 6228–6237. Available from: doi:10.1128/jb.179.20.6228-6237.1997.

Linker, A. & Jones, R.S. (1964) A Polysaccharide Resembling Alginic Acid from a Pseudomonas Micro-Organism. *Nature*. [Online] 204 (4954), 187–188. Available from: doi:10.1038/204187A0 [Accessed: 28 May 2023].

LiPuma, J.J. (2010) The changing microbial epidemiology in cystic fibrosis. *Clinical Microbiology Reviews*. [Online]. 23 (2) pp.299–323. Available from: doi:10.1128/CMR.00068-09.

Lister, P.D., Wolter, D.J. & Hanson, N.D. (2009) Antibacterial-Resistant Pseudomonas aeruginosa: Clinical Impact and Complex Regulation of Chromosomally Encoded Resistance Mechanisms. *Clinical Microbiology Reviews*. [Online] 22 (4), 582–610. Available from: doi:10.1128/CMR.00040-09.

Liu, X., Ye, Y., Zhu, Y., Wang, L., et al. (2021) Involvement of RpoN in Regulating Motility, Biofilm, Resistance, and Spoilage Potential of Pseudomonas fluorescens. *Frontiers in Microbiology*. [Online] 12 (641844), 1–14. Available from: doi:10.3389/FMICB.2021.641844/FULL [Accessed: 19 January 2022].

Liu, Y., Gloag, E.S., Hill, P.J., Parsek, M.R., et al. (2022) Interbacterial Antagonism Mediated by a Released Polysaccharide. *Journal of Bacteriology*. [Online] 204 (5), 1–14. Available from: doi:10.1128/JB.00076-22 [Accessed: 28 May 2023].

Loper, J.E., Hassan, K.A., Mavrodi, D. V., Davis, E.W., et al. (2012) Comparative Genomics of Plant-Associated Pseudomonas spp.: Insights into Diversity and Inheritance of Traits Involved in Multitrophic Interactions. *PLOS Genetics*. [Online] 8 (7), 1–27. Available

from: doi:10.1371/JOURNAL.PGEN.1002784.
De Lorenzo, V., Herrero, M., Jakubzik, U. & Timmis, K.N. (1990) Mini-Tn5 transposon derivatives for insertion mutagenesis, promoter probing, and chromosomal insertion of cloned DNA in gram-negative eubacteria. *Journal of Bacteriology*. [Online] 172 (11), 6572. Available from: doi:10.1128/JB.172.11.6568-6572.1990 [Accessed: 13 June 2023].
Losada, P.M., Chouvarine, P., Dorda, M., Hedtfeld, S., et al. (2016) The cystic fibrosis lower airways microbial metagenome. *ERJ Open Research*. [Online] 2 (2). Available from: doi:10.1183/23120541.00096-2015 [Accessed: 11 May 2023].
Lossi, N.S., Dajani, R., Freemont, P. & Filloux, A. (2011) Structure–function analysis of HsiF, a gp25-like component of the type VI secretion system, in Pseudomonas aeruginosa. *Microbiology*. [Online] 157 (Pt 12), 3305. Available from: doi:10.1099/MIC.0.051987-0 [Accessed: 20 May 2023].
Lozano, C., Manuel Azcona-Gutiérrez, J., Van Bambeke, F. & Sá Enz, Y. (2018) Great phenotypic and genetic variation among successive chronic Pseudomonas aeruginosa from a cystic fibrosis patient. *PLoS ONE*. [Online] 13 (9), 1–15. Available from: doi:10.1371/journal.pone.0204167 [Accessed: 7 April 2023].
Lu, D., Shang, G., Yu, Q., Zhang, H., et al. (2013) Expression, purification and preliminary crystallographic analysis of the T6SS effector protein Tse3 from Pseudomonas aeruginosa. *Acta Crystallographica Section F: Structural Biology and Crystallization Communications*. [Online] 69 (5), 524–527. Available from: doi:10.1107/S1744309113007148.
Lu, S., Wang, J., Chitsaz, F., Derbyshire, M.K., et al. (2020) CDD/SPARCLE: the conserved domain database in 2020. *Nucleic Acids Research*. [Online] 48 (1), 265–268. Available from: doi:10.1093/nar/gkz991.
Lung, T.W.F., Charytonowicz, D., Beaumont, K.G., Howden, B.P., et al. (2022) Klebsiella pneumoniae induces host metabolic stress that promotes tolerance to pulmonary infection. *Cell Metabolism*. [Online] 34, 761–774. Available from: doi:10.1016/j.cmet.2022.03.009 [Accessed: 20 May 2023].
Lynch, J.P., Sayah, D.M., Belperio, J.A. & Weigt, S.S. (2015) Lung transplantation for cystic fibrosis: Results, indications, complications, and controversies. *Seminars in Respiratory and Critical Care Medicine*. [Online]. pp.299–320. Available from: doi:10.1055/s-0035-1547347.
Mackman, N., Nicaud, J.M., Gray, L. & Holland, I.B. (1985) Identification of polypeptides required for the export of haemolysin 2001 from E. coli. *MGG Molecular & General Genetics*. [Online] 201 (3), 529–536. Available from: doi:10.1007/BF00331351/METRICS [Accessed: 16 May 2023].
Madeira, F., Mi Park, Y., Lee, J., Buso, N., et al. (2019) The EMBL-EBI search and sequence analysis tools APIs in 2019. *Nucleic Acids Research*. [Online] 47 (1), 636–641. Available from: doi:10.1093/nar/gkz268 [Accessed: 22 May 2020].
Mahenthiralingam, E., Campbell, M.E. & Speert, D.P. (1994) Nonmotility and phagocytic resistance of Pseudomonas aeruginosa isolates from chronically colonized patients with cystic fibrosis. *Infection and immunity*. [Online] 62 (2), 596–605. Available from: doi:10.1128/IAI.62.2.596-605.1994 [Accessed: 29 May 2023].
Majerczyk, C., Brittnacher, M., Jacobs, M., Armour, C.D., et al. (2014) Global analysis of the Burkholderia thailandensis quorum sensing-controlled regulon. *Journal of Bacteriology*. [Online] 196 (7), 1412–1424. Available from: doi:10.1128/JB.01405-13.

Malgieri, G., Palmieri, M., Russo, L., Fattorusso, R., et al. (2015) The prokaryotic zinc-finger: structure, function and comparison with the eukaryotic counterpart. *The FEBS Journal*. [Online] 282 (23), 4480–4496. Available from: doi:10.1111/FEBS.13503 [Accessed: 10 March 2022].

Mall, M., Hipper, A., Greger, R. & Kunzelmann, K. (1996) Wild type but not deltaF508 CFTR inhibits Na+ conductance when coexpressed in Xenopus oocytes. *FEBS letters*. [Online] 381 (1–2), 47–52. Available from: doi:10.1016/0014-5793(96)00079-8 [Accessed: 10 May 2023].

Mall, M.A., Danahay, H. & Boucher, R.C. (2018) Emerging concepts and therapies for mucoobstructive lung disease. *Annals of the American Thoracic Society*. [Online] 15 (Suppl 3), S216–S226. Available from: doi:10.1513/ANNALSATS.201806-368AW/SUPPL_FILE/DISCLOSURES.PDF [Accessed: 11 May 2023].

Marc, F., Weigel, P., Legrain, C., Almeras, Y., et al. (2000) Characterization and kinetic mechanism of mono- and bifunctional ornithine acetyltransferases from thermophilic microorganisms. *European Journal of Biochemistry*. [Online] 267 (16), 5217–5226. Available from: doi:10.1046/J.1432-1327.2000.01593.X [Accessed: 23 February 2022].

Marietou, A., Røy, H., Jørgensen, B.B. & Kjeldsen, K.U. (2018) Sulfate transporters in dissimilatory sulfate reducing microorganisms: A comparative genomics analysis. *Frontiers in Microbiology*. [Online] 9 (309), 1–21. Available from: doi:10.3389/FMICB.2018.00309/FULL [Accessed: 11 March 2022].

Marra, R., Sgalla, G., Richeldi, L., Conte, E.G., et al. (2020) Role of Stenotrophomonas maltophilia isolation in patients with non-CF bronchiectasis. *QJM: An International Journal of Medicine*. [Online] 113 (10), 726–730. Available from: doi:10.1093/QJMED/HCAA120 [Accessed: 12 July 2022].

Marsac, C., Berdah, L., Thouvenin, G., Sermet-Gaudelus, I., et al. (2021) Achromobacter xylosoxidans airway infection is associated with lung disease severity in children with cystic fibrosis. *ERJ Open Research*. [Online] 7 (2), 00076–02021. Available from: doi:10.1183/23120541.00076-2021 [Accessed: 12 July 2022].

Martínez-Gil, M., Ramos-González, M.I. & Espinosa-Urgel, M. (2014) Roles of cyclic Di-GMP and the Gac system in transcriptional control of the genes coding for the Pseudomonas putida adhesins LapA and LapF. *Journal of Bacteriology*. [Online] 196 (8), 1484–1495. Available from: doi:10.1128/JB.01287-13 [Accessed: 31 May 2023].

Martínez-Granero, F., Navazo, A., Barahona, E., Redondo-Nieto, M., et al. (2012) The Gac-Rsm and SadB Signal Transduction Pathways Converge on AlgU to Downregulate Motility in Pseudomonas fluorescens. *PLoS ONE*. [Online] 7 (2), 31765. Available from: doi:10.1371/journal.pone.0031765 [Accessed: 4 April 2023].

Marvig, R.L., Sommer, L.M., Molin, S. & Johansen, H.K. (2014) Convergent evolution and adaptation of Pseudomonas aeruginosa within patients with cystic fibrosis. *Nature Genetics* . [Online] 47 (1), 57–64. Available from: doi:10.1038/ng.3148 [Accessed: 30 May 2023].

Massung, R.F., Esposito, J.J., Liu, L.I., Qi, J., et al. (1993) Potential virulence determinants in terminal regions of variola smallpox virus genome. *Nature*. [Online] 366 (6457), 748–751. Available from: doi:10.1038/366748a0 [Accessed: 11 March 2022].

Da Mata Madeira, P.V., Zouhir, S., Basso, P., Neves, D., et al. (2016) Structural Basis of Lipid Targeting and Destruction by the Type v Secretion System of Pseudomonas aeruginosa. *Journal of Molecular Biology*. [Online] 428 (9), 1790–1803. Available from: doi:10.1016/j.jmb.2016.03.012 [Accessed: 21 April 2020].

Mathee, K. (2018) Forensic investigation into the origin of pseudomonas aeruginosa PA14 — Old but not lost. *Journal of Medical Microbiology*. [Online] 67 (8), 1019–1021. Available from: doi:10.1099/JMM.0.000778/CITE/REFWORKS [Accessed: 29 April 2023].

Le Mauff, F., Razvi, E., Reichhardt, C., Sivarajah, P., et al. (2022) The Pel polysaccharide is predominantly composed of a dimeric repeat of α-1,4 linked galactosamine and N-acetylgalactosamine. *Communications Biology 2022 5:1*. [Online] 5 (1), 1–7. Available from: doi:10.1038/s42003-022-03453-2 [Accessed: 28 May 2023].

May, T.B., Shinabarger, D., Maharaj, R., Kato, J., et al. (1991) Alginate synthesis by Pseudomonas aeruginosa: a key pathogenic factor in chronic pulmonary infections of cystic fibrosis patients. *Clinical Microbiology Reviews*. [Online] 4 (2), 191–206. Available from: doi:10.1128/CMR.4.2.191 [Accessed: 28 May 2023].

McBride, M.J. (2019) Bacteroidetes Gliding Motility and the Type IX Secretion System. *Microbiology spectrum*. [Online] 7 (1), 1–9. Available from: doi:10.1128/MICROBIOLSPEC.PSIB-0002-2018 [Accessed: 19 May 2023].

McCormick, J., Green, M.W., Mehta, G., Culross, F., et al. (2002) Demographics of the UK cystic fibrosis population: Implications for neonatal screening. *European Journal of Human Genetics*. [Online] 10, 583–590. Available from: doi:10.1038/sj.ejhg.5200850.

McDougal, L.K., Steward, C.D., Killgore, G.E., Chaitram, J.M., et al. (2003) Pulsed-Field Gel Electrophoresis Typing of Oxacillin-Resistant Staphylococcus aureus Isolates from the United States: Establishing a National Database. *Journal of Clinical Microbiology*. [Online] 41 (11), 5113–5120. Available from: doi:10.1128/JCM.41.11.5113-5120.2003.

McFadden, E.R., Pichurko, B.M., Bowman, H.F., Ingenito, E., et al. (1985) Thermal mapping of the airways in humans. *Journal of Applied Physiology*. [Online] 58 (2), 564–570. Available from: doi:10.1152/JAPPL.1985.58.2.564.

Melvin, J.A., Gaston, J.R., Phillips, S.N., Springer, M.J., et al. (2017) Pseudomonas aeruginosa Contact-Dependent Growth Inhibition Plays Dual Role in Host-Pathogen Interactions. *mSphere*. [Online] 2 (6), 1–13. Available from: doi:10.1128/msphere.00336-17.

Meng, G., Surana, N.K., St Geme, J.W. & Waksman, G. (2006) Structure of the outer membrane translocator domain of the Haemophilus influenzae Hia trimeric autotransporter. *The EMBO journal*. [Online] 25 (11), 2297–2304. Available from: doi:10.1038/SJ.EMBOJ.7601132 [Accessed: 26 May 2023].

Mercy, C., Ize, B., Salcedo, S.P., de Bentzmann, S., et al. (2016) Functional Characterization of Pseudomonas Contact Dependent Growth Inhibition (CDI) Systems Min Wu (ed.). *PLOS ONE*. [Online] 11 (1), 1–21. Available from: doi:10.1371/journal.pone.0147435 [Accessed: 13 November 2019].

Merritt, J.H., Brothers, K.M., Kuchma, S.L. & O'Toole, G.A. (2007) SadC Reciprocally Influences Biofilm Formation and Swarming Motility via Modulation of Exopolysaccharide Production and Flagellar Function. *Journal of Bacteriology*. [Online] 189 (22), 8154. Available from: doi:10.1128/JB.00585-07 [Accessed: 4 April 2023].

Merz, A.J., So, M. & Sheetz, M.P. (2000) Pilus retraction powers bacterial twitching motility. *Nature*. [Online] 407 (6800), 98–102. Available from: doi:10.1038/35024105.

Meuskens, I., Saragliadis, A., Leo, J.C. & Linke, D. (2019) Type V secretion systems: An overview of passenger domain functions. *Frontiers in Microbiology*. [Online]. 10 (1163) pp.1–19. Available from: doi:10.3389/fmicb.2019.01163.

Michalska, K., Quan Nhan, D., Willett, J.L.E., Stols, L.M., et al. (2018) Functional plasticity of antibacterial EndoU toxins. *Molecular Microbiology*. [Online] 109 (4), 509–527. Available from: doi:10.1111/mmi.14007.

Mikkelsen, H., Mcmullan, R. & Filloux, A. (2011) The Pseudomonas aeruginosa Reference Strain PA14 Displays Increased Virulence Due to a Mutation in ladS. *PLoS Pathogens*. [Online] 6 (12), 1–7. Available from: doi:10.1371/journal.pone.0029113 [Accessed: 30 May 2023].

Miller, C.L., Romero, M., Rajasekhar Karna, S.L., Chen, T., et al. (2016) RsmW, Pseudomonas aeruginosa small non-coding RsmA-binding RNA upregulated in biofilm versus planktonic growth conditions. *BMC Microbiology*. [Online] 16 (155), 1–16. Available from: doi:10.1186/s12866-016-0771-y.

Miller, S.I. & Salama, N.R. (2018) The gram-negative bacterial periplasm: Size matters. *PLoS Biology*. [Online] 16 (1), 1–7. Available from: doi:10.1371/JOURNAL.PBIO.2004935 [Accessed: 30 April 2023].

Mishra, M., Byrd, M.S., Sergeant, S., Azad, A.K., et al. (2012) Pseudomonas aeruginosa Psl polysaccharide reduces neutrophil phagocytosis and the oxidative response by limiting complement-mediated opsonization. *Cellular Microbiology*. [Online] 14 (1), 95–106. Available from: doi:10.1111/J.1462-5822.2011.01704.X [Accessed: 29 May 2023].

Mishra, M., Tiwari, S. & Gomes, A. V. (2017) Protein purification and analysis: next generation Western blotting techniques. *Expert review of proteomics*. [Online] 14 (11), 1053. Available from: doi:10.1080/14789450.2017.1388167 [Accessed: 17 June 2023].

Mitri, C., Xu, Z., Bardin, P., Corvol, H., et al. (2020) Novel Anti-Inflammatory Approaches for Cystic Fibrosis Lung Disease: Identification of Molecular Targets and Design of Innovative Therapies. *Frontiers in pharmacology*. [Online] 11 (1096), 1–25. Available from: doi:10.3389/FPHAR.2020.01096 [Accessed: 29 May 2023].

Miyata, M., Robinson, R.C., Uyeda, T.Q.P., Fukumori, Y., et al. (2020) Tree of motility – A proposed history of motility systems in the tree of life. *Genes to Cells*. [Online] 25 (1), 6–21. Available from: doi:10.1111/GTC.12737 [Accessed: 21 May 2023].

Moore, N.M. & Flaws, M.L. (2011) Introduction: Pseudomonas aeruginosa. *American Society for Clinical Laboratory Science*. [Online] 24 (1), 41–42. Available from: doi:10.29074/ASCLS.24.1.41 [Accessed: 26 April 2023].

Moradali, M.F., Ghods, S. & Rehm, B.H.A. (2017) Pseudomonas aeruginosa Lifestyle: A Paradigm for Adaptation, Survival, and Persistence. *Frontiers in Cellular and Infection Microbiology*. [Online] 7 (39), 1–29. Available from: doi:10.3389/fcimb.2017.00039.

Morse, R.P., Nikolakakis, K.C., Willett, J.L.E., Gerrick, E., et al. (2012) Structural basis of toxicity and immunity in contact-dependent growth inhibition (CDI) systems. *Proceedings of the National Academy of Sciences of the United States of America*. [Online] 109 (52), 21480–21485. Available from: doi:10.1073/PNAS.1216238110/-/DCSUPPLEMENTAL [Accessed: 8 July 2022].

Morse, R.P., Willett, J.L.E., Johnson, P.M., Zheng, J., et al. (2015) Diversification of β-augmentation interactions between CDI toxin/immunity proteins. *Journal of Molecular Biology*. [Online] 427 (23), 3766–3784. Available from: doi:10.1016/J.JMB.2015.09.020.

Moscoso, J.A., Jaeger, T., Valentini, M., Hui, K., et al. (2014) The diguanylate cyclase SadC is a central player in Gac/Rsm-mediated biofilm formation in Pseudomonas aeruginosa. *Journal of Bacteriology*. [Online] 196 (23), 4081–4088. Available from: doi:10.1128/JB.01850-14.

Moser, C., Jensen, P.Ø., Thomsen, K., Kolpen, M., et al. (2021) Immune Responses to Pseudomonas aeruginosa Bio film Infections. *Frontiers in Immunology*. [Online] 12 (625597), 1–15. Available from: doi:10.3389/fimmu.2021.625597.

Mougous, J.D., Cuff, M.E., Raunser, S., Shen, A., et al. (2006) A virulence locus of

Pseudomonas aeruginosa encodes a protein secretion apparatus. *Science*. [Online] 312 (5779), 1526–1530. Available from: doi:10.1126/science.1128393.
Mougous, J.D., Gifford, C.A., Ramsdell, T.L. & Mekalanos, J.J. (2007) Threonine phosphorylation post-translationally regulates protein secretion in Pseudomonas aeruginosa. *Nature Cell Biology*. [Online] 9 (7), 797–803. Available from: doi:10.1038/ncb1605.
Muhammad, I.I., Kong, S.L., Nor, S., Abdullah, A., et al. (2020) Molecular Sciences RNA-seq and ChIP-seq as Complementary Approaches for Comprehension of Plant Transcriptional Regulatory Mechanism. *International Journal of Molecular Sciences*. [Online] 21 (167), 1–30. Available from: doi:10.3390/ijms21010167 [Accessed: 11 April 2023].
Mukhopadhyay, S., Kapatral, V., Xu, W. & Chakrabarty, A.M. (1999) Characterization of a Hank's type serine/threonine kinase and serine/threonine phosphoprotein phosphatase in Pseudomonas aeruginosa. *Journal of Bacteriology*. [Online] 181 (21), 6615–6622. Available from: doi:10.1128/jb.181.21.6615-6622.1999.
Mulcahy, H., Charron-Mazenod, L. & Lewenza, S. (2008) Extracellular DNA chelates cations and induces antibiotic resistance in Pseudomonas aeruginosa biofilms. *PLoS pathogens*. [Online] 4 (11), 1–12. Available from: doi:10.1371/JOURNAL.PPAT.1000213 [Accessed: 28 May 2023].
Mulcahy, H., Charron-Mazenod, L. & Lewenza, S. (2010) Pseudomonas aeruginosa produces an extracellular deoxyribonuclease that is required for utilization of DNA as a nutrient source. *Environmental Microbiology*. [Online] 12 (6), 1621–1629. Available from: doi:10.1111/J.1462-2920.2010.02208.X [Accessed: 28 May 2023].
Mulet, M., Gomila, M., Scotta, C., Sánchez, D., et al. (2012) Concordance between whole-cell matrix-assisted laser-desorption/ionization time-of-flight mass spectrometry and multilocus sequence analysis approaches in species discrimination within the genus Pseudomonas. *Systematic and Applied Microbiology*. [Online] 35 (7), 455–464. Available from: doi:10.1016/J.SYAPM.2012.08.007.
Murray, T.S. & Kazmierczak, B.I. (2008) Pseudomonas aeruginosa Exhibits Sliding Motility in the Absence of Type IV Pili and Flagella. *Journal of Bacteriology*. [Online] 190 (8), 2708. Available from: doi:10.1128/JB.01620-07 [Accessed: 21 May 2023].
Murzin, A.G., Brenner, S.E., Hubbard, T. & Chothia, C. (1995) SCOP: A structural classification of proteins database for the investigation of sequences and structures. *Journal of Molecular Biology*. [Online] 247 (4), 536–540. Available from: doi:10.1016/S0022-2836(05)80134-2 [Accessed: 23 March 2022].
Myers-Morales, T., Sim, M.M.S., DuCote, T.J. & Garcia, E.C. (2021) Burkholderia multivorans requires species-specific GltJK for entry of a contact-dependent growth inhibition system protein. *Molecular Microbiology*. [Online] 116 (3), 957–973. Available from: doi:10.1111/MMI.14783.
Naskar, S., Hohl, M., Tassinari, M. & Low, H.H. (2021) The structure and mechanism of the bacterial type II secretion system. *Molecular Microbiology*. [Online] 115 (3), 412–424. Available from: doi:10.1111/mmi.14664.
Newmark, P. (1985) Testing for cystic fibrosis. *Nature* . [Online] 318 (6044), 309–309. Available from: doi:10.1038/318309a0 [Accessed: 10 May 2023].
Nguyen, V.S., Logger, L., Spinelli, S., Legrand, P., et al. (2017) Type VI secretion TssK baseplate protein exhibits structural similarity with phage receptor-binding proteins and evolved to bind the membrane complex. *Nature Microbiology* . [Online] 2 (9), 1–9.

Available from: doi:10.1038/nmicrobiol.2017.103 [Accessed: 20 May 2023].
Nikaido, H. & Vaara, M. (1985) Molecular basis of bacterial outer membrane permeability. *Microbiological Reviews*. [Online] 49 (1), 1–32. Available from: doi:10.1128/mmbr.49.1.1-32.1985.
Nikolaidis, M., Mossialos, D., Oliver, S.G. & Amoutzias, G.D. (2020) Comparative Analysis of the Core Proteomes among the Pseudomonas Major Evolutionary Groups Reveals Species-Specific Adaptations for Pseudomonas aeruginosa and Pseudomonas chlororaphis. *Diversity*. [Online] 12 (289), 1–21. Available from: doi:10.3390/d12080289 [Accessed: 26 April 2023].
Noegel, A., Rdest, U., Springer, W. & Goebel, W. (1979) Plasmid cistrons controlling synthesis and excretion of the exotoxin α-haemolysin of Escherichia coli. *Molecular & General Genetics*. [Online] 175 (3), 343–350. Available from: doi:10.1007/BF00397234.
Nolan, L.M. & Allsopp, L.P. (2022) *Antimicrobial Weapons of Pseudomonas aeruginosa*. [Online]. Available from: doi:10.1007/978-3-031-08491-1_8.
Nolan, L.M., Cain, A.K., Clamens, T., Furniss, R.C.D., et al. (2021) Identification of Tse8 as a Type VI secretion system toxin from Pseudomonas aeruginosa that targets the bacterial transamidosome to inhibit protein synthesis in prey cells. *Nature Microbiology*. [Online] 6 (9), 1199–1210. Available from: doi:10.1038/s41564-021-00950-8 [Accessed: 5 April 2023].
Novotny, L.A., Amer, A.O., Brockson, M.E., Goodman, S.D., et al. (2013) Structural Stability of Burkholderia cenocepacia Biofilms Is Reliant on eDNA Structure and Presence of a Bacterial Nucleic Acid Binding Protein. *PLoS ONE*. [Online] 8 (6), 1–15. Available from: doi:10.1371/JOURNAL.PONE.0067629 [Accessed: 10 May 2023].
Nummelin, H., Merckel, M.C., Leo, J.C., Lankinen, H., et al. (2004) The Yersinia adhesin YadA collagen-binding domain structure is a novel left-handed parallel beta-roll. *The EMBO journal*. [Online] 23 (4), 701–711. Available from: doi:10.1038/SJ.EMBOJ.7600100 [Accessed: 26 May 2023].
O'May, C. & Tufenkji, N. (2011) The swarming motility of Pseudomonas aeruginosa is blocked by cranberry proanthocyanidins and other tannin-containing materials. *Applied and Environmental Microbiology*. [Online] 77 (9), 3061–3067. Available from: doi:10.1128/AEM.02677-10.
O'Toole, G.A. (2016) Classic Spotlight: How the Gram Stain Works. *Journal of Bacteriology*. [Online] 198 (23), 3128–3128. Available from: doi:10.1128/JB.00726-16 [Accessed: 30 April 2023].
O'Toole, G.A. & Kolter, R. (1998) Flagellar and twitching motility are necessary for Pseudomonas aeruginosa biofilm development. *Molecular Microbiology*. [Online] 30 (2), 295–304. Available from: doi:10.1046/j.1365-2958.1998.01062.x [Accessed: 15 August 2019].
Oakley, A.J., Loscha, K. V., Schaeffer, P.M., Liepinsh, E., et al. (2005) Crystal and Solution Structures of the Helicase-binding Domain of Escherichia coli Primase: o. *Journal of Biological Chemistry*. [Online] 280 (12), 11495–11504. Available from: doi:10.1074/JBC.M412645200.
Oberhettinger, P., Schütz, M., Leo, J.C., Heinz, N., et al. (2012) Intimin and Invasin Export Their C-Terminus to the Bacterial Cell Surface Using an Inverse Mechanism Compared to Classical Autotransport. *PLOS ONE*. [Online] 7 (10), 1–15. Available from: doi:10.1371/JOURNAL.PONE.0047069 [Accessed: 26 May 2023].
Ocasio, A.B. & Cotter, P.A. (2019) CDI/CDS system-encoding genes of Burkholderia

thailandensis are located in a mobile genetic element that defines a new class of transposon. *PLOS Genetics*. [Online] 15 (1), 1–24. Available from: doi:10.1371/journal.pgen.1007883 [Accessed: 9 October 2020].
Ochsner, U.A. & Reiser, J. (1995) Autoinducer-mediated regulation of rhamnolipid biosurfactant synthesis in Pseudomonas aeruginosa. *Proceeding of the National Academy of Sciences USA*. 92 (July), 6424–6428.
Ogier, J.C., Duvic, B., Lanois, A., Givaudan, A., et al. (2016) A new member of the growing family of contact-dependent growth inhibition systems in Xenorhabdus doucetiae. *PLoS ONE*. [Online] 11 (12), 1–19. Available from: doi:10.1371/journal.pone.0167443.
Opal, S.M. (2009) A Brief History of Microbiology and Immunology. *Vaccines: A Biography*. [Online] 10, 56. Available from: doi:10.1007/978-1-4419-1108-7_3 [Accessed: 26 April 2023].
Oppegaard, O., Mylvaganam, H., Skrede, S., Lindemann, P.C., et al. (2017) Emergence of a Streptococcus dysgalactiae subspecies equisimilis stG62647-lineage associated with severe clinical manifestations. *Scientific Reports*. [Online] 7 (1), 1–10. Available from: doi:10.1038/s41598-017-08162-z [Accessed: 12 July 2022].
Orenti, A., Zolin, A., Jung, A., van Rens, J., et al. (2021) *ECFS Patient Registry*. [Online]. Available from: www.ecfs.eu/ecfspr [Accessed: 16 May 2022].
Ostrowski, A., Cianfanelli, F.R., Porter, M., Mariano, G., et al. (2018) Killing with proficiency: Integrated post-translational regulation of an offensive Type VI secretion system Melanie Blokesch (ed.). *PLOS Pathogens*. [Online] 14 (7), 1–25. Available from: doi:10.1371/journal.ppat.1007230 [Accessed: 16 January 2020].
de Pace, F., de Paiva, J.B., Nakazato, G., Lancellotti, M., et al. (2011) Characterization of icmF of the type VI secretion system in an avian pathogenic Escherichia coli (APEC) strain. *Microbiology*. [Online] 157 (10), 2954–2962. Available from: doi:10.1099/MIC.0.050005-0/CITE/REFWORKS [Accessed: 19 January 2022].
Pang, Z., Raudonis, R., Glick, B.R., Lin, T.J., et al. (2019) Antibiotic resistance in Pseudomonas aeruginosa: mechanisms and alternative therapeutic strategies. *Biotechnology Advances*. [Online] 37 (1), 177–192. Available from: doi:10.1016/J.BIOTECHADV.2018.11.013.
Pantaleo, G., Correia, B., Fenwick, C., Joo, V.S., et al. (2022) Antibodies to combat viral infections: development strategies and progress. *Nature Reviews Drug Discovery*. [Online] 21, 676–696. Available from: doi:10.1038/s41573-022-00495-3 [Accessed: 29 November 2022].
Papanikou, E., Karamanou, S. & Economou, A. (2007) Bacterial protein secretion through the translocase nanomachine. *Nature Reviews Microbiology*. [Online] 5 (11), 839–851. Available from: doi:10.1038/nrmicro1771 [Accessed: 21 February 2022].
Pardee, A.B. (1959) The genetic control and cytoplasmic expression of “Inducibility” in the synthesis of β-galactosidase by E. coli. *Journal of Molecular Biology*. [Online] 1 (2), 165–178. Available from: doi:10.1016/S0022-2836(59)80045-0.
Park, S. & Sauer, K. (2022) Controlling biofilm development through cyclic di-GMP signaling. *Advances in Experimental Medicine and Biology*. [Online] 1386, 69–94. Available from: doi:10.1007/978-3-031-08491-1_3.
Park, Y.J., Lacourse, K.D., Cambillau, C., DiMaio, F., et al. (2018) Structure of the type VI secretion system TssK–TssF–TssG baseplate subcomplex revealed by cryo-electron microscopy. *Nature Communications* . [Online] 9 (1), 1–11. Available from: doi:10.1038/s41467-018-07796-5 [Accessed: 20 May 2023].

Parkins, M.D. & Floto, R.A. (2015) Emerging bacterial pathogens and changing concepts of bacterial pathogenesis in cystic fibrosis. *Journal of cystic fibrosis : official journal of the European Cystic Fibrosis Society*. [Online] 14 (3), 293–304. Available from: doi:10.1016/J.JCF.2015.03.012 [Accessed: 11 May 2023].

Parmely, M., Gale, A., Clabaugh, M., Horvat, R., et al. (1990) Proteolytic inactivation of cytokines by Pseudomonas aeruginosa. *Infection and Immunity*. [Online] 58 (9), 3009–3014. Available from: doi:10.1128/IAI.58.9.3009-3014.1990 [Accessed: 16 May 2023].

Parte, A.C. (2014) LPSN—list of prokaryotic names with standing in nomenclature. *Nucleic Acids Research*. [Online] 42, D613–D616. Available from: doi:10.1093/NAR/GKT1111 [Accessed: 26 April 2023].

Partridge, J.D. & Harshey, R.M. (2013) Swarming: flexible roaming plans. *Journal of bacteriology*. [Online] 195 (5), 909–918. Available from: doi:10.1128/JB.02063-12 [Accessed: 21 May 2023].

Paz De Oliveira, E., Flá Via Da, A., Rovida, S., Martins, J.G., et al. (2021) Tolerance of Pseudomonas strain to the 2,4-D herbicide through a peroxidase system. *PLoS ONE*. [Online] 16 (12), 1–18. Available from: doi:10.1371/journal.pone.0257263 [Accessed: 29 April 2023].

Pena, R.T., Blasco, L., Ambroa, A., González-Pedrajo, B., et al. (2019) Relationship between quorum sensing and secretion systems. *Frontiers in Microbiology*. [Online]. 10 (1100) pp.1–14. Available from: doi:10.3389/fmicb.2019.01100.

Penesyan, A., Paulsen, I.T., Kjelleberg, S. & Gillings, M.R. (2021) Three faces of biofilms: a microbial lifestyle, a nascent multicellular organism, and an incubator for diversity. *NPJ Biofilms and Microbiomes*. [Online] 7 (80), 1–9. Available from: doi:10.1038/s41522-021-00251-2 [Accessed: 28 May 2023].

Perault, A.I., Chandler, C.E., Rasko, D.A., Ernst, R.K., et al. (2020) Host Adaptation Predisposes Pseudomonas aeruginosa to Type VI Secretion System-Mediated Predation by the Burkholderia cepacia Complex. *Cell Host & Microbe*. [Online] 28 (4), 547. Available from: doi:10.1016/J.CHOM.2020.06.019.

Perault, A.I. & Cotter, P.A. (2018) Three distinct contact-dependent growth inhibition systems mediate interbacterial competition by the cystic fibrosis pathogen burkholderia dolosa. *Journal of Bacteriology*. [Online] 200 (22), 1–17. Available from: doi:10.1128/JB.00428-18 [Accessed: 22 April 2020].

Perez Mora, B., Giordano, R., Permingeat, V., Calderone, M., et al. (2023) BfmRS encodes a regulatory system involved in light signal transduction modulating motility and desiccation tolerance in the human pathogen Acinetobacter baumannii. *Scientific Reports* . [Online] 13 (1), 1–13. Available from: doi:10.1038/s41598-022-26314-8 [Accessed: 31 May 2023].

Perikleous, E.P., Gkentzi, D., Bertzouanis, A., Paraskakis, E., et al. (2023) Antibiotic Resistance in Patients with Cystic Fibrosis: Past, Present, and Future. *Antibiotics*. [Online] 12 (217), 1–13. Available from: doi:10.3390/antibiotics12020217 [Accessed: 3 May 2023].

Petrou, G. & Crouzier, T. (2018) Mucins as multifunctional building blocks of biomaterials. *Biomaterials Science*. [Online] 6 (9), 2282–2297. Available from: doi:10.1039/C8BM00471D [Accessed: 29 May 2023].

Picot, R., Das, I. & Reid, L. (1978) Pus, deoxyribonucleic acid, and sputum viscosity. *Thorax*. [Online] 33 (2), 242. Available from: doi:10.1136/THX.33.2.235 [Accessed: 28 May 2023].

Pietrosiuk, A., Lenherr, E.D., Falk, S., Bönemann, G., et al. (2011) Molecular basis for the unique role of the AAA+ chaperone ClpV in type VI protein secretion. *The Journal of biological chemistry*. [Online] 286 (34), 30010–30021. Available from: doi:10.1074/JBC.M111.253377 [Accessed: 20 May 2023].

Pissaridou, P., Allsopp, L.P., Wettstadt, S., Howard, S.A., et al. (2018) The Pseudomonas aeruginosa T6SS-VgrG1b spike is topped by a PAAR protein eliciting DNA damage to bacterial competitors. *Proceedings of the National Academy of Sciences of the United States of America*. [Online] 115 (49), 12519–12524. Available from: doi:10.1073/pnas.1814181115.

Podkovyrov, S.M. & Larson, T.J. (1995) A new vector-host system for construction of lacZ transcriptional fusions where only low-level gene expression is desirable. *Gene*. [Online] 156 (1), 151–152. Available from: doi:10.1016/0378-1119(95)00053-9.

Poole, S.J., Diner, E.J., Aoki, S.K., Braaten, B.A., et al. (2011) Identification of Functional Toxin/Immunity Genes Linked to Contact-Dependent Growth Inhibition (CDI) and Rearrangement Hotspot (Rhs) Systems. *PLOS Genetics*. [Online] 7 (8), 1–14. Available from: doi:10.1371/journal.pgen.1002217 [Accessed: 23 March 2022].

del Porto, P., Cifani, N., Guarnieri, S., Di Domenico, E.G., et al. (2011) Dysfunctional CFTR Alters the Bactericidal Activity of Human Macrophages against Pseudomonas aeruginosa. *PLoS ONE*. [Online] 6 (5), 19970. Available from: doi:10.1371/JOURNAL.PONE.0019970 [Accessed: 10 May 2023].

Potvin, E., Sanschagrin, F. & Levesque, R.C. (2008) Sigma factors in Pseudomonas aeruginosa. *FEMS Microbiology Reviews*. [Online] 32 (1), 38–55. Available from: doi:10.1111/j.1574-6976.2007.00092.x.

Pukatzki, S., Ma, A.T., Revel, A.T., Sturtevant, D., et al. (2007) Type VI secretion system translocates a phage tail spike-like protein into target cells where it cross-links actin. *Proceedings of the National Academy of Sciences of the United States of America*. [Online] 104 (39), 15508–15513. Available from: doi:10.1073/PNAS.0706532104 [Accessed: 20 May 2023].

Pukatzki, S., Ma, A.T., Sturtevant, D., Krastins, B., et al. (2006) Identification of a conserved bacterial protein secretion system in Vibrio cholerae using the Dictyostelium host model system. *Proceedings of the National Academy of Sciences of the United States of America*. [Online] 103 (5), 1533. Available from: doi:10.1073/PNAS.0510322103 [Accessed: 20 May 2023].

Purevdorj-Gage, B., Costerton, W.J. & Stoodley, P. (2005) Phenotypic differentiation and seeding dispersal in non-mucoid and mucoid Pseudomonas aeruginosa biofilms. *Microbiology* . [Online] 151 (Pt 5), 1569–1576. Available from: doi:10.1099/MIC.0.27536-0 [Accessed: 29 May 2023].

Purtschert-Montenegro, G., Cárcamo-Oyarce, G., Pinto-Carbó, M., Agnoli, K., et al. (2022) Pseudomonas putida mediates bacterial killing, biofilm invasion and biocontrol with a type IVB secretion system. *Nature Microbiology* . [Online] 7 (10), 1547–1557. Available from: doi:10.1038/s41564-022-01209-6 [Accessed: 19 May 2023].

Qin, X., Emerson, J., Stapp, J., Stapp, L., et al. (2003) Use of Real-Time PCR with Multiple Targets To Identify Pseudomonas aeruginosa and Other Nonfermenting Gram-Negative Bacilli from Patients with Cystic Fibrosis. *Journal of Clinical Microbiology*. [Online] 41 (9), 4312–4317. Available from: doi:10.1128/JCM.41.9.4312-4317.2003.

Quinton, P.M. (1983) Chloride impermeability in cystic fibrosis. *Nature*. 271, 9–173.

Radics, J., Königsmaier, L. & Marlovits, T.C. (2014) Structure of a pathogenic type 3 secretion

system in action. *Nature Structural and Molecular Biology*. [Online] 21 (1), 82–87. Available from: doi:10.1038/nsmb.2722.
Rahme, L.G., Stevens, E.J., Wolfort, S.F., Shao, J., et al. (1995) Common virulence factors for bacterial pathogenicity in plants and animals. *Science*. [Online] 268 (5219), 1899–1902. Available from: doi:10.1126/science.7604262.
Ramirez-Peralta, A., Stewart, K.A. V., Thomas, S.K., Setlow, B., et al. (2012) Effects of the SpoVT regulatory protein on the germination and germination protein levels of spores of Bacillus subtilis. *Journal of Bacteriology*. [Online] 194 (13), 3417–3425. Available from: doi:10.1128/JB.00504-12/FORMAT/EPUB [Accessed: 25 May 2022].
Randall, L.L. & Hardy, S.J.S. (2002) SecB, one small chaperone in the complex milieu of the cell. *Cellular and Molecular Life Sciences* . 59, 1617–1623.
Reichhardt, C., Wong, C., da Silva, D.P., Wozniak, D.J., et al. (2018) CdrA interactions within the pseudomonas aeruginosa biofilm matrix safeguard it from proteolysis and promote cellular packing. *Journal of Molecular Biology and Physiology*. [Online] 9 (5), 1–12. Available from: doi:10.1128/mBio.01376-18.
Reimmann, C., Ginet, N., Michel, L., Keel, C., et al. (2002) Genetically programmed autoinducer destruction reduces virulence gene expression and swarming motility in Pseudomonas aeruginosa PAO1. *Microbiology*. [Online] 148 (4), 923–932. Available from: doi:10.1099/00221287-148-4-923/CITE/REFWORKS [Accessed: 21 May 2023].
Ribeiro Da Cunha, B., Fonseca, L.P. & Calado, C.R.C. (2019) Antibiotic Discovery: Where Have We Come from, Where Do We Go? *Antibiotics*. [Online] 8 (45), 1–21. Available from: doi:10.3390/antibiotics8020045 [Accessed: 3 May 2023].
Rich, J.J., Kinscherf, T.G., Kitten, T. & Willis, D.K. (1994) Genetic evidence that the gacA gene encodes the cognate response regulator for the lemA sensor in Pseudomonas syringae. *Journal of Bacteriology*. [Online] 176 (24), 7468–7475. Available from: doi:10.1128/JB.176.24.7468-7475.1994 [Accessed: 30 May 2023].
Riordan, J.R., Rommens, J.M., Kerem, B.S., Alon, N.O.A., et al. (1989) Identification of the Cystic Fibrosis Gene: Cloning and Characterization of Complementary DNA. *Science*. [Online] 245 (4922), 1066–1073. Available from: doi:10.1126/SCIENCE.2475911 [Accessed: 10 May 2023].
Riordan, J.T. & Mitra, A. (2017) Regulation of Escherichia coli Pathogenesis by Alternative Sigma Factor N. *EcoSal Plus*. [Online] 7 (2), 1–15. Available from: doi:10.1128/ECOSALPLUS.ESP-0016-2016/ASSET/141CC2DE-E83B-4F70-9A5C-B2D556446F12/ASSETS/GRAPHIC/ESP-0016-2016_FIG_004.GIF [Accessed: 26 June 2023].
Robb, C.S., Assmus, M., Nano, F.E. & Boraston, A.B. (2013) Structure of the T6SS lipoprotein TssJ1 from Pseudomonas aeruginosa. *Acta Crystallographica Section F: Structural Biology and Crystallization Communications*. [Online] 69 (Pt 6), 607–610. Available from: doi:10.1107/S1744309113012220 [Accessed: 20 May 2023].
Robb, C.S., Robb, M., Nano, F.E. & Boraston, A.B. (2016) The Structure of the Toxin and Type Six Secretion System Substrate Tse2 in Complex with Its Immunity Protein. *Structure*. [Online] 24 (2), 277–284. Available from: doi:10.1016/j.str.2015.11.012.
Robertson, J.B., Gochtt, M., Marahielt, M.A. & Zuber, P. (1989) AbrB, a regulator of gene expression in Bacillus, interacts with the transcription initiation regions of a sporulation gene and an antibiotic biosynthesis gene. *Proceedings of the National Academy of Sciences of the United States of America*. 86, 8457–8461.
Robinson, C. & Bolhuis, A. (2004) Tat-dependent protein targeting in prokaryotes and

chloroplasts. *Biochimica et Biophysica Acta (BBA) - Molecular Cell Research*. [Online] 1694 (1–3), 135–147. Available from: doi:10.1016/J.BBAMCR.2004.03.010.
Robinson, J.A. (2019) Folded synthetic peptides and other molecules targeting outer membrane protein complexes in Gram-negative bacteria. *Frontiers in Chemistry*. [Online] 7, 1–11. Available from: doi:10.3389/fchem.2019.00045.
Robinson, L., Liaw, J., Omole, Z., Xia, D., et al. (2021) Bioinformatic Analysis of the Campylobacter jejuni Type VI Secretion System and Effector Prediction. *Frontiers in Microbiology*. [Online] 12 (June), 1–20. Available from: doi:10.3389/fmicb.2021.694824.
Robinson, L.A., Collins, A.C.Z., Murphy, R.A., Davies, J.C., et al. (2023) Diversity and prevalence of type VI secretion system effectors in clinical Pseudomonas aeruginosa isolates. *Frontiers in Microbiology*. [Online] 13, 4966. Available from: doi:10.3389/FMICB.2022.1042505/BIBTEX.
Rocha, G.A., Lima, D.F., Rodrigues, E.R., Leão, R.S., et al. (2018) Species distribution, sequence types and antimicrobial resistance of Acinetobacter spp. from cystic fibrosis patients. *Epidemiology and infection*. [Online] 146 (4), 524–530. Available from: doi:10.1017/S0950268817002849 [Accessed: 16 May 2022].
Rogers, G.B., Carroll, M.P., Serisier, D.J., Hockey, P.M., et al. (2004) Characterization of Bacterial Community Diversity in Cystic Fibrosis Lung Infections by Use of 16S Ribosomal DNA Terminal Restriction Fragment Length Polymorphism Profiling. *Journal of Clinical Microbiology*. [Online] 42 (11), 5176–5183. Available from: doi:10.1128/JCM.42.11.5176-5183.2004 [Accessed: 7 April 2023].
Ross, B.D., Verster, A.J., Radey, M.C., Schmidtke, D.T., et al. (2019a) Human gut bacteria contain acquired interbacterial defence systems. *Nature*. [Online] 575 (7781), 224–228. Available from: doi:10.1038/s41586-019-1708-z.
Ross, B.D., Verster, A.J., Radey, M.C., Schmidtke, D.T., et al. (2019b) Human gut bacteria harbor acquired interbacterial defense systems. *Nature*. [Online] 575 (7781), 228. Available from: doi:10.1038/S41586-019-1708-Z [Accessed: 7 July 2022].
Roussel-Jazédé, V., Jongerius, I., Bos, M.P., Tommassen, J., et al. (2010) NalP-mediated proteolytic release of lactoferrin-binding protein B from the meningococcal cell surface. *Infection and Immunity*. [Online] 78 (7), 3083–3089. Available from: doi:10.1128/IAI.01193-09/FORMAT/EPUB [Accessed: 26 June 2023].
Roussin, M., Rabarioelina, S., Cluzeau, L., Cayron, J., et al. (2019) Identification of a Contact-Dependent Growth Inhibition (CDI) System That Reduces Biofilm Formation and Host Cell Adhesion of Acinetobacter baumannii DSM30011 Strain. *Frontiers in Microbiology*. [Online] 10 (2450), 1–14. Available from: doi:10.3389/fmicb.2019.02450 [Accessed: 21 April 2020].
Roy, A.B., Petrova, O.E. & Sauer, K. (2012) The Phosphodiesterase DipA (PA5017) Is Essential for Pseudomonas aeruginosa Biofilm Dispersion. *Journal of Bacteriology*. [Online] 194 (11), 2904–2915. Available from: doi:10.1128/JB.05346-11 [Accessed: 29 May 2023].
Ruhe, Z.C., Low, D.A. & Hayes, C.S. (2020) Annual Review of Microbiology Polymorphic Toxins and Their Immunity Proteins: Diversity, Evolution, and Mechanisms of Delivery. *Annual Reviews*. [Online] 74, 497–520. Available from: doi:10.1146/annurev-micro-020518 [Accessed: 9 October 2020].
Ruhe, Z.C., Nguyen, J.Y., Chen, A.J., Leung, N.Y., et al. (2016) CDI Systems Are Stably Maintained by a Cell-Contact Mediated Surveillance Mechanism. *PLOS Genetics*. [Online] 12 (6), 1–21. Available from: doi:10.1371/journal.pgen.1006145.

Ruhe, Z.C., Nguyen, J.Y., Xiong, J., Koskiniemi, S., et al. (2017) CdiA effectors use modular receptor-binding domains to recognize target bacteria. *mBio*. [Online] 8 (2), 1–16. Available from: doi:10.1128/mBio.00290-17.

Ruhe, Z.C., Subramanian, P., Song, K., Nguyen, J.Y., et al. (2018) Programmed Secretion Arrest and Receptor-Triggered Toxin Export during Antibacterial Contact-Dependent Growth Inhibition. *Cell*. [Online] 175 (4), 921–933. Available from: doi:10.1016/j.cell.2018.10.033.

Ruhe, Z.C., Townsley, L., Wallace, A.B., King, A., et al. (2015) CdiA promotes receptor-independent intercellular adhesion. *Molecular Microbiology*. [Online] 98 (1), 175–192. Available from: doi:10.1111/mmi.13114 [Accessed: 22 April 2020].

Ruhe, Z.C., Wallace, A.B., Low, D.A. & Hayes, C.S. (2013) Receptor polymorphism restricts contact-dependent growth inhibition to members of the same species. *mBio*. [Online] 4 (4), 1–9. Available from: doi:10.1128/MBIO.00480-13/SUPPL_FILE/MBO004131574ST3.DOCX [Accessed: 8 February 2022].

Ruiz-Perez, F., Henderson, I.R., Leyton, D.L., Rossiter, A.E., et al. (2009) Roles of Periplasmic Chaperone Proteins in the Biogenesis of Serine Protease Autotransporters of Enterobacteriaceae. *Journal of Bacteriology*. [Online] 191 (21), 6571–6583. Available from: doi:10.1128/JB.00754-09 [Accessed: 24 May 2023].

Rumbaugh, K.P. & Sauer, K. (2020) Biofilm dispersion. *Nature Reviews Microbiology*. [Online] 18 (10), 571–586. Available from: doi:10.1038/S41579-020-0385-0 [Accessed: 29 May 2023].

Russell, A.B., Hood, R.D., Khai Bui, N., Leroux, M., et al. (2012) Type VI secretion delivers bacteriolytic effectors to target cells HHS Public Access. *Nature*. [Online] 475 (7356), 343–347. Available from: doi:10.1038/nature10244 [Accessed: 20 May 2023].

Russell, A.B., Leroux, M., Hathazi, K., Agnello, D.M., et al. (2013) Diverse type VI secretion phospholipases are functionally plastic antibacterial effectors HHS Public Access. *Nature*. [Online] 496 (7446), 508–512. Available from: doi:10.1038/nature12074 [Accessed: 20 May 2023].

Russell, A.B., Peterson, S.B. & Mougous, J.D. (2014) Type VI secretion system effectors: Poisons with a purpose. *Nature Reviews Microbiology*. [Online] 12 (2), 137–148. Available from: doi:10.1038/nrmicro3185.

Russell, A.B., Wexler, A.G., Harding, B.N., Whitney, J.C., et al. (2014a) A type VI secretion-related pathway in Bacteroidetes mediates interbacterial antagonism. *Cell Host and Microbe*. [Online] 16 (2), 236. Available from: doi:10.1016/J.CHOM.2014.07.007 [Accessed: 20 May 2023].

Russell, A.B., Wexler, A.G., Harding, B.N., Whitney, J.C., et al. (2014b) A type VI secretion-related pathway in Bacteroidetes mediates interbacterial antagonism. *Host Cell Microbe*. [Online] 16 (2), 227–236. Available from: doi:10.1016/j.chom.2014.07.007.

Rybtke, M., Jensen, P.Ø., Nielsen, C.H. & Tolker-Nielsen, T. (2020) The Extracellular Polysaccharide Matrix of Pseudomonas aeruginosa Biofilms is a Determinant of Polymorphonuclear Leukocyte Responses. *Infection and Immunity*. 89 (1), 1–15.

Rytkönen, A. & Holden, D.W. (2007) Bacterial Interference of Ubiquitination and Deubiquitination. *Cell Host & Microbe*. [Online] 1 (22), 13. Available from: doi:10.1016/J.CHOM.2007.02.003 [Accessed: 21 February 2022].

Sah, S., Krishnani, S. & Singh, R. (2021) Pseudomonas mediated nutritional and growth promotional activities for sustainable food security. *Current Research in Microbial Sciences*. [Online] 2, 1–12. Available from: doi:10.1016/j.crmicr.2021.100084

[Accessed: 29 April 2023].
Salacha, R., Kovačić, F., Brochier-Armanet, C., Wilhelm, S., et al. (2010) The *Pseudomonas aeruginosa* patatin-like protein PlpD is the archetype of a novel Type V secretion system. *Environmental Microbiology*. [Online] 12 (6), 1498–1512. Available from: doi:10.1111/j.1462-2920.2010.02174.x [Accessed: 21 April 2020].
Salcedo, S.P., Roussin, M., Rabarioelina, S., Cluzeau, L., et al. (2019) Identification of a Contact-Dependent Growth Inhibition (CDI) System That Reduces Biofilm Formation and Host Cell Adhesion of Acinetobacter baumannii DSM30011 Strain. *Frontiers in Microbiology*. [Online] 10 (2450), 1–14. Available from: doi:10.3389/fmicb.2019.02450 [Accessed: 9 October 2020].
Salih, O., He, S., Planamente, S., Stach, L., et al. (2018) Atomic Structure of Type VI Contractile Sheath from Pseudomonas aeruginosa. *Structure*. [Online] 26 (2), 336. Available from: doi:10.1016/J.STR.2017.12.005 [Accessed: 20 May 2023].
Salsgiver, E.L., Fink, A.K., Knapp, E.A., LiPuma, J.J., et al. (2016) Changing Epidemiology of the Respiratory Bacteriology of Patients With Cystic Fibrosis. *Chest*. [Online] 149 (2), 390–400. Available from: doi:10.1378/CHEST.15-0676 [Accessed: 11 May 2023].
Sana, T.G., Bleves, S. & Berni, B. (2016) The T6SSs of Pseudomonas aeruginosa Strain PAO1 and Their Effectors: Beyond Bacterial-Cell Targeting. *Frontiers in Cellular and Infection Microbiology | www.frontiersin.org*. [Online] 6 (61), 1–8. Available from: doi:10.3389/fcimb.2016.00061 [Accessed: 26 June 2023].
Sana, T.G., Hachani, A., Bucior, I., Soscia, C., et al. (2012) The Second Type VI Secretion System of Pseudomonas aeruginosa Strain PAO1 Is Regulated by Quorum Sensing and Fur and Modulates Internalization in Epithelial Cells . *The Journal of Biological Chemistry*. [Online] 287 (32), 27095–27105. Available from: doi:10.1074/jbc.M112.376368.
Sana, T.G., Soscia, C., Tonglet, C.M., Garvis, S., et al. (2013) Divergent Control of Two Type VI Secretion Systems by RpoN in Pseudomonas aeruginosa. *PLOS ONE*. [Online] 8 (10), 1–10. Available from: doi:10.1371/journal.pone.0076030.
Sanders, D.B., Bittner, R.C.L., Rosenfeld, M., Hoffman, L.R., et al. (2010) Failure to Recover to Baseline Pulmonary Function after Cystic Fibrosis Pulmonary Exacerbation. *American Journal of Respiratory and Critical Care Medicine*. [Online] 182 (5), 632. Available from: doi:10.1164/RCCM.200909-1421OC [Accessed: 11 May 2023].
Sanguinetti, M., Ardito, F., Fiscarelli, E., Sorda, M. LA, et al. (2001) Fatal pulmonary infection due to multidrug-resistant Mycobacterium abscessus in a patient with cystic fibrosis. *Journal of Clinical Microbiology*. [Online] 39 (2), 816–819. Available from: doi:10.1128/JCM.39.2.816-819.2001 [Accessed: 11 May 2023].
di Sant'agnese, P., Darling, R.C., Perara, G.A. & Shea, E. (1953) Abnormal Electrolyte Composition of Sweat in Cystic Fibrosis of the Pancreas: Clinical Significance and Relationship to the Disease. *Pediatrics*. [Online] 12 (5), 549–563. Available from: doi:10.1542/PEDS.12.5.549 [Accessed: 10 May 2023].
di Sant'agnese, P.A. (1956) Fibrocystic Disease of the Pancreas, a Generalised Disease of Exocrine Glands. *Journal of the American Medical Association*. [Online] 160 (10), 846–853. Available from: doi:10.1001/JAMA.1956.02960450028007 [Accessed: 10 May 2023].
Santin, Y.G., Doan, T., Lebrun, R., Espinosa, L., et al. (2018) In vivo TssA proximity labelling during type VI secretion biogenesis reveals TagA as a protein that stops and holds the sheath. *Nature Microbiology* . [Online] 3 (11), 1304–1313. Available from:

doi:10.1038/s41564-018-0234-3 [Accessed: 24 June 2023].
Sato, K., Naito, M., Yukitake, H., Hirakawa, H., et al. (2010) A protein secretion system linked to bacteroidete gliding motility and pathogenesis. *Proceedings of the National Academy of Sciences of the United States of America*. [Online] 107 (1), 276–281. Available from: doi:10.1073/PNAS.0912010107 [Accessed: 19 May 2023].
Sauer, K., Stoodley, P., Goeres, D.M., Hall-Stoodley, L., et al. (2022) The biofilm life cycle: expanding the conceptual model of biofilm formation. *Nature Reviews Microbiology*. [Online] 20, 608–620. Available from: doi:10.1038/s41579-022-00767-0 [Accessed: 29 May 2023].
Sauvonnet, N., Vignon, G., Pugsley, A.P. & Gounon, P. (2000) Pilus formation and protein scretion by the same machinery in Escherichia coli. *The EMBO Journal*. 19 (10), 2221–2228.
Sawa, T., Shimizu, M., Moriyama, K. & Wiener-Kronish, J.P. (2014) Association between Pseudomonas aeruginosa type III secretion, antibiotic resistance, and clinical outcome: A review. *Critical Care*. [Online] 18 (1), 1–12. Available from: doi:10.1186/S13054-014-0668-9/TABLES/2 [Accessed: 24 June 2023].
Schaffer, K. (2015) Epidemiology of infection and current guidelines for infection prevention in cystic fibrosis patients. *Journal of Hospital Infection*. [Online] 89 (4), 309–313. Available from: doi:10.1016/j.jhin.2015.02.005.
Schavemaker, P.E. & Lynch, M. (2022) Flagellar energy costs across the tree of life. *eLife*. [Online] 11, 1–22. Available from: doi:10.7554/ELIFE.77266.
Schick, A. & Kassen, R. (2018) Rapid diversification of Pseudomonas aeruginosa in cystic fibrosis lung-like conditions. *Proceedings of the National Academy of Sciences of the USA*. [Online] 115 (42), 10714–10719. Available from: doi:10.1073/PNAS.1721270115/SUPPL_FILE/PNAS.1721270115.SAPP.PDF [Accessed: 7 April 2023].
Schleifer, K.H. & Kandler, O. (1972) Peptidoglycan types of bacterial cell walls and their taxonomic implications. *Bacteriological reviews*. [Online] 36 (4), 407–477. Available from: doi:10.1128/mmbr.36.4.407-477.1972.
Schloer, S., Pajonczyk, D. & Rescher, U. (2018) Annexins in Translational Research: Hidden Treasures to Be Found. *International Journal of Molecular Sciences*. [Online] 19 (6), 1–17. Available from: doi:10.3390/IJMS19061781 [Accessed: 23 March 2022].
Schlüter, D.K., Southern, K.W., Dryden, C., Diggle, P., et al. (2019) Impact of newborn screening on outcomes and social inequalities in cystic fibrosis: A UK CF registry-based study. *Thorax*. [Online] 75, 123–131. Available from: doi:10.1136/thoraxjnl-2019-213179.
Schneider, C.A., Rasband, W.S. & Eliceiri, K.W. (2012) NIH Image to ImageJ: 25 years of image analysis. *Nature Methods*. [Online]. 9 (7) pp.671–675. Available from: doi:10.1038/nmeth.2089.
Schniederberend, M., Williams, J.F., Shine, E., Shen, C., et al. (2019) Modulation of flagellar rotation in surface-attached bacteria: A pathway for rapid surface-sensing after flagellar attachment. *PLOS Pathogens*. [Online] 15 (11), 1–30. Available from: doi:10.1371/JOURNAL.PPAT.1008149 [Accessed: 28 May 2023].
Schraidt, O. & Marlovits, T.C. (2011) Three-Dimensional Model of Salmonella's Needle Complex at Subnanometer Resolution. *Science*. 331 (March), 1192–1196.
Schroeder, G.N. (2017) The Toolbox for Uncovering the Functions of Legionella Dot/Icm Type IVb Secretion System Effectors: Current State and Future Directions. *Frontiers in*

Cellular and Infection Microbiology. [Online] 7 (582), 1–10. Available from: doi:10.3389/FCIMB.2017.00528 [Accessed: 20 May 2023].
Schulz, S., Eckweiler, D., Bielecka, A., Nicolai, T., et al. (2015) Elucidation of Sigma Factor-Associated Networks in Pseudomonas aeruginosa Reveals a Modular Architecture with Limited and Function-Specific Crosstalk. *PLOS Pathogens*. [Online] 11 (2), 1–21. Available from: doi:10.1371/journal.ppat.1004744.
Schwab, U., Abdullah, L.H., Perlmutt, O.S., Albert, D., et al. (2014) Localization of Burkholderia cepacia Complex Bacteria in Cystic Fibrosis Lungs and Interactions with Pseudomonas aeruginosa in Hypoxic Mucus. *Infection and Immunity*. [Online] 8 (11), 4729–4745. Available from: doi:10.1128/IAI.01876-14 [Accessed: 29 April 2023].
Scotet, V., Duguépéroux, I., Saliou, P., Rault, G., et al. (2012) *Evidence for decline in the incidence of cystic fibrosis: a 35-year observational study in Brittany, France*. [Online]. Available from: doi:10.1186/1750-1172-7-14.
Seeger, M.A., Schiefner, A., Eicher, T., Verrey, F., et al. (2006) Structural asymmetry of AcrB trimer suggests a peristaltic pump mechanism. *Science*. [Online] 313 (5791), 1295–1298. Available from: doi:10.1126/science.1131542.
Serapio-Palacios, A., Woodward, S.E., Vogt, S.L., Deng, W., et al. (2022) Type VI secretion systems of pathogenic and commensal bacteria mediate niche occupancy in the gut. *Cell Reports*. [Online] 39 (4), 1–16. Available from: doi:10.1016/J.CELREP.2022.110731.
Serra, D.O. & Hengge, R. (2014) Stress responses go three dimensional – the spatial order of physiological differentiation in bacterial macrocolony biofilms. *Environmental Microbiology*. [Online] 16 (6), 1455–1471. Available from: doi:10.1111/1462-2920.12483 [Accessed: 29 May 2023].
Seveau, S.M., Pizarro-Cerda, J., Warawa, J.M., Stevens, J.M., et al. (2019) Burkholderia pseudomallei BimC Is Required for Actin-Based Motility, Intracellular Survival, and Virulence. *Frontiers in Cellular and Infection Microbiology | www.frontiersin.org*. [Online] 9 (63), 1–9. Available from: doi:10.3389/fcimb.2019.00063 [Accessed: 29 April 2023].
Shang, L., Yan, Y., Zhan, Y., Ke, X., et al. (2021) A regulatory network involving Rpo, Gac and Rsm for nitrogen-fixing biofilm formation by Pseudomonas stutzeri. *NPJ Biofilms and Microbiomes*. [Online] 7 (1), 1–15. Available from: doi:10.1038/s41522-021-00230-7 [Accessed: 15 April 2023].
Shao, X., Zhang, X., Zhang, Y., Zhu, M., et al. (2018) RpoN-Dependent Direct Regulation of Quorum Sensing and the Type VI Secretion System in Pseudomonas aeruginosa PAO1. *Journal of Bacteriology*. [Online] 200 (16), 1–17. Available from: doi:10.1128/JB.00205-18 [Accessed: 2 December 2021].
Sharma, A., Leach, R.N., Gell, C., Zhang, N., et al. (2014) Domain movements of the enhancer-dependent sigma factor drive DNA delivery into the RNA polymerase active site: Insights from single molecule studies. *Nucleic Acids Research*. [Online] 42 (8), 5177–5190. Available from: doi:10.1093/nar/gku146.
Sharma, D., Misba, L. & Khan, A. (2019) Antibiotics versus biofilm: an emerging battleground in microbial communities. *Antimicrobial Resistance and Infection Control*. 8, 76.
Shi, J., Jin, Y., Bian, T., Li, K., et al. (2015) SuhB is a novel ribosome associated protein that regulates expression of MexXY by modulating ribosome stalling in Pseudomonas aeruginosa. *Molecular Microbiology*. [Online] 98 (2), 370–383. Available from: doi:10.1111/MMI.13126.
Shneider, M.M., Buth, S.A., Ho, B.T., Basler, M., et al. (2013) PAAR-repeat proteins sharpen

and diversify the type VI secretion system spike. *Nature*. [Online] 500 (7462), 350–353. Available from: doi:10.1038/NATURE12453 [Accessed: 20 May 2023].
Silby, M.W., Winstanley, C., Godfrey, S.A.C., Levy, S.B., et al. (2011) Pseudomonas genomes: diverse and adaptable. *FEMS Microbiology Reviews*. [Online] 35 (4), 652–680. Available from: doi:10.1111/J.1574-6976.2011.00269.X [Accessed: 24 June 2023].
Silhavy, T.J., Kahne, D. & Walker, S. (2010) The Bacterial Cell Envelope1 T. J. Silhavy, D. Kahne and S. Walker, . *Cold Spring Harb Perspect Biol*. [Online] 2, 1–16. Available from: https://www.ncbi.nlm.nih.gov/pmc/articles/PMC2857177/pdf/cshperspect-PRK-a000414.pdf.
Silverman, J.M., Austin, L.S., Hsu, F., Hicks, K.G., et al. (2011) Separate inputs modulate phosphorylation-dependent and - independent type VI secretion activation. *Molecular Microbiology*. [Online] 82 (5), 1277–1290. Available from: doi:10.1111/j.1365-2958.2011.07889.x.Separate.
Simm, R., Morr, M., Kader, A., Nimtz, M., et al. (2004) GGDEF and EAL domains inversely regulate cyclic di-GMP levels and transition from sessibility to motility. *Molecular Microbiology*. [Online] 53 (4), 1123–1134. Available from: doi:10.1111/j.1365-2958.2004.04206.x.
Simonin-Le Jeune, K., Le Jeune, A., Jouneau, S., Belleguic, C., et al. (2013) Impaired Functions of Macrophage from Cystic Fibrosis Patients: CD11b, TLR-5 Decrease and sCD14, Inflammatory Cytokines Increase. *PloS ONE*. [Online] 8 (9), 1–14. Available from: doi:10.1371/journal.pone.0075667 [Accessed: 10 May 2023].
Singh, P., Montano, A. & Bostick, A. (2021) Rapid severe sepsis from Pseudomonas fluorescens/putida bacteremia due to skin and soft tissue infection – A case report. *Annals of Medicine and Surgery*. [Online] 70. Available from: doi:10.1016/J.AMSU.2021.102845.
Singh, P.K., Schaefer, A.L., Parsek, M.R., Moninger, T.O., et al. (2000) Quorum-sensing signals indicate that cystic fibrosis lungs are infected with bacterial biofilms. *Nature 2000 407:6805*. [Online] 407 (6805), 762–764. Available from: doi:10.1038/35037627 [Accessed: 4 April 2023].
Skerker, J.M. & Berg, H.C. (2001) Direct observation of extension and retraction of type IV pili. *Proceedings of the National Academy of Sciences of the United States of America*. [Online] 98 (12), 6901–6904. Available from: doi:10.1073/pnas.121171698.
Sønderholm, M., Kragh, K.N., Koren, K., Jakobsen, T.H., et al. (2017) Pseudomonas aeruginosa Aggregate Formation in an Alginate Bead Model System Exhibits In Vivo-Like Characteristics. *Applied and Environmental Microbiology*. [Online] 83 (9), e00113–e00117. Available from: doi:10.1128/AEM.00113-17 [Accessed: 28 May 2023].
Song, H., Li, Y. & Wang, Y. (2023) Two-component system GacS/GacA, a global response regulator of bacterial physiological behaviors. *Engineering Microbiology*. [Online] 3 (1), 100051. Available from: doi:10.1016/j.engmic.2022.100051.
Song, K.S., Lee, W.J., chung, K.C., Koo, J.S., et al. (2003) Interleukin-1 beta and tumor necrosis factor-alpha induce MUC5AC overexpression through a mechanism involving ERK/p38 mitogen-activated protein kinases-MSK1-CREB activation in human airway epithelial cells. *The Journal of Biological Chemistry*. [Online] 278 (26), 23243–23250. Available from: doi:10.1074/JBC.M300096200 [Accessed: 29 May 2023].
Sorg, J.A., Blaylock, B. & Schneewind, O. (2006) Secretion signal recognition by YscN, the Yersinia type III secretion ATPase. *Proceedings of the National Academy of Sciences of the United States of America*. [Online] 103 (44), 16490–16495. Available from:

doi:10.1073/pnas.0605974103.
Soria-Bustos, J., Ares, M.A., Gómez-Aldapa, C.A., González-y-Merchand, J.A., et al. (2020) Two Type VI Secretion Systems of Enterobacter cloacae Are Required for Bacterial Competition, Cell Adherence, and Intestinal Colonization. *Frontiers in Microbiology*. [Online] 11, 2137. Available from: doi:10.3389/FMICB.2020.560488/BIBTEX.
Southern, K.W., Munck, A., Pollitt, R., Travert, G., et al. (2007) A survey of newborn screening for cystic fibrosis in Europe. *Journal of cystic fibrosis : official journal of the European Cystic Fibrosis Society*. [Online] 6 (1), 57–65. Available from: doi:10.1016/J.JCF.2006.05.008 [Accessed: 10 May 2023].
De Soyza, A., Hall, A.J., Mahenthiralingam, E., Drevinek, P., et al. (2013) Developing an international Pseudomonas aeruginosa reference panel. *Microbiology Open*. [Online] 2 (6), 1023. Available from: doi:10.1002/MBO3.141 [Accessed: 29 April 2023].
Stanford, G.E., Dave, K. & Simmonds, N.J. (2021) Pulmonary Exacerbations in Adults With Cystic Fibrosis: A Grown-up Issue in a Changing Cystic Fibrosis Landscape. *Chest*. [Online] 159 (1), 102. Available from: doi:10.1016/J.CHEST.2020.09.084 [Accessed: 11 May 2023].
Stanier, R.Y., Palleroni, N.J. & Doudoroff, M. (1966) The Aerobic Pseudomonads: a Taxonomic Study. *Journal of General Microbiology*. 43, 159–271.
Stanley, S.A., Raghavan, S., Hwang, W.W. & Cox, J.S. (2003) Acute infection and macrophage subversion by Mycobacterium tuberculosis require a specialized secretion system. *Proceedings of the National Academy of Sciences of the United States of America*. [Online] 100 (22), 13001–13006. Available from: doi:10.1073/PNAS.2235593100 [Accessed: 19 May 2023].
Stebbins, C.E. & Galán, J.E. (2001) Maintenance of an unfolded polypeptide by a cognate chaperone in bacterial type III secretion. *Nature*. [Online] 414 (6859), 77–81. Available from: doi:10.1038/35102073.
Stewart, P.S. & Franklin, M.J. (2008) Physiological heterogeneity in biofilms. *Nature reviews. Microbiology*. [Online] 6 (3), 199–210. Available from: doi:10.1038/NRMICRO1838 [Accessed: 29 May 2023].
Stills, H.F. (2012) *Polyclonal Antibody Production*. [Online]. Academic Press. Available from: doi:10.1016/B978-0-12-380920-9.00011-0.
Stingl, K., Müller, S., Scheidgen-Kleyboldt, G., Clausen, M., et al. (2010) Composite system mediates two-step DNA uptake into Helicobacter pylori. *Proceedings of the National Academy of Sciences of the United States of America*. [Online] 107 (3), 1189. Available from: doi:10.1073/PNAS.0909955107 [Accessed: 19 May 2023].
Stock, A.M., Robinson, V.L. & Goudreau, P.N. (2000) Two-Component Signal Transduction. *Annual Reviews Biochemistry*. [Online] 69, 183–215. Available from: www.annualreviews.org [Accessed: 30 May 2023].
Stolle, A.-S., Meader, B.T., Toska, J. & Mekalanos, J.J. (2021) Endogenous membrane stress induces T6SS activity in Pseudomonas aeruginosa. *Proceedings of the National Academy of Sciences*. [Online] 118 (1), 1–12. Available from: doi:10.1073/PNAS.2018365118 [Accessed: 22 October 2021].
Stover, C.K., Pham, X.Q., Erwin, A.L., Mizoguchi, S.D., et al. (2000) Complete genome sequence of Pseudomonas aeruginosa PAO1, an opportunistic pathogen. *Nature*. [Online] 406 (6799), 959–964. Available from: doi:10.1038/35023079 [Accessed: 7 April 2023].
Suarez, G., Sierra, J.C., Kirtley, M.L. & Chopra, A.K. (2010) Role of Hcp, a type 6 secretion

system effector, of Aeromonas hydrophila in modulating activation of host immune cells. *Microbiology*. [Online] 156 (12), 3678–3688. Available from: doi:10.1099/mic.0.041277-0.

Suria, A.M., Smith, S., Speare, L., Chen, Y., et al. (2022) Prevalence and diversity of type VI secretion systems in a model beneficial symbiosis. *Frontiers in Microbiology*. [Online] 13 (September), 1–13. Available from: doi:10.3389/fmicb.2022.988044.

Suvorova, I.A., Korostelev, Y.D. & Gelfand, M.S. (2015) GntR Family of Bacterial Transcription Factors and Their DNA Binding Motifs: Structure, Positioning and Co-Evolution. *PLOS ONE*. [Online] 10 (7), 1–21. Available from: doi:10.1371/journal.pone.0132618 [Accessed: 21 February 2022].

Symmons, M.F., Bokma, E., Koronakis, E., Hughes, C., et al. (2009) The assembled structure of a complete tripartite bacterial multidrug efflux pump. *Proceedings of the National Academy of Sciences of the United States of America*. [Online] 106 (17), 7173–7178. Available from: doi:10.1073/pnas.0900693106.

Talà, L., Fineberg, A., Kukura, P. & Persat, A. (2019) Pseudomonas aeruginosa orchestrates twitching motility by sequential control of type IV pili movements. *Nature Microbiology*. [Online] 4 (5), 774–780. Available from: doi:10.1038/s41564-019-0378-9.

Tan, J., Zhang, X., Wang, X., Xu, C., et al. (2021) Structural basis of assembly and torque transmission of the bacterial flagellar motor. *Cell*. [Online] 184 (10), 2665-2679.e19. Available from: doi:10.1016/J.CELL.2021.03.057 [Accessed: 21 May 2023].

Tayeb, S., Chama, Z., Tifrit, A., Zohra, F., et al. (2015) Antagonistic activity of Pseudomonas aeruginosa ATCC 27853 against pathogenic bacteria. *Journal of Chemical and Pharmaceutical Research*. [Online] 7 (7), 362–369. Available from: www.jocpr.com.

Taylor, N.M.I., Prokhorov, N.S., Guerrero-Ferreira, R.C., Shneider, M.M., et al. (2016) Structure of the T4 baseplate and its function in triggering sheath contraction. *Nature* . [Online] 533 (7603), 346–352. Available from: doi:10.1038/nature17971 [Accessed: 20 May 2023].

Teschler, J.K., Jiménez-Siebert, E., Jeckel, H., Singh, P.K., et al. (2022) VxrB Influences Antagonism within Biofilms by Controlling Competition through Extracellular Matrix Production and Type 6 Secretion. *mBio*. [Online] 13 (4). Available from: doi:10.1128/mbio.01885-22.

Thi, M.T.T., Wibowo, D. & Rehm, B.H.A. (2020) Pseudomonas aeruginosa Biofilms. *International Journal of Molecular Sciences*. [Online] 21 (22), 1–25. Available from: doi:10.3390/IJMS21228671 [Accessed: 6 April 2023].

Thomas, B.S., Okamoto, K., Bankowski, M.J., Seto, T.B., et al. (2013) A Lethal Case of Pseudomonas putida Bacteremia Due to Soft Tissue Infection. *Infect Dis Clin Pract*. [Online] 21 (3), 147–213. Available from: doi:10.1097/IPC.0b013e318276956b.

Thomas, D., Morgan, D.G. & DeRosier, D.J. (2001) Structures of bacterial flagellar motors from two FliF-FliG gene fusion mutants. *Journal of Bacteriology*. [Online] 183 (21), 6404–6412. Available from: doi:10.1128/JB.183.21.6404-6412.2001.

Thompson, M.K., Fridy, P.C., Keegan, S., Chait, B.T., et al. (2016) Optimizing selection of large animals for antibody production by screening immune response to standard vaccines. *Journal of Immunological Methods*. [Online] 430, 56–60. Available from: doi:10.1016/J.JIM.2016.01.006.

Thornton, C.S., Acosta, N., Surette, M.G. & Parkins, M.D. (2022) Exploring the Cystic Fibrosis Lung Microbiome: Making the Most of a Sticky Situation. *Journal of the Pediatric Infectious Diseases Society*. [Online] 11 (Suppl 2), S13–S22. Available from:

doi:10.1093/JPIDS/PIAC036 [Accessed: 11 May 2023].
Tomás, A., Lery, L., Regueiro, V., Pérez-Gutiérrez, C., et al. (2015) Functional genomic screen identifies klebsiella pneumoniae factors implicated in blocking nuclear factor κB (NF-κB) signaling. *Journal of Biological Chemistry*. [Online] 290 (27), 16678–16697. Available from: doi:10.1074/jbc.M114.621292.
Toska, J., Ho, B.T. & Mekalanos, J.J. (2018) Exopolysaccharide protects Vibrio cholerae from exogenous attacks by the type 6 secretion system. *Proceedings of the National Academy of Sciences of the United States of America*. [Online] 115 (31), 7997–8002. Available from: doi:10.1073/pnas.1808469115.
Toutain, C.M., Zegans, M.E. & O'Toole, G.A. (2005) Evidence for Two Flagellar Stators and Their Role in the Motility of Pseudomonas aeruginosa. *Journal of Bacteriology*. [Online] 187 (2), 777. Available from: doi:10.1128/JB.187.2.771-777.2005 [Accessed: 21 May 2023].
Trier, N.H., Hansen, P.R. & Houen, G. (2012) Production and characterization of peptide antibodies. *Methods*. [Online] 56 (2), 136–144. Available from: doi:10.1016/J.YMETH.2011.12.001.
Trunk, K., Peltier, J., Liu, Y.C., Dill, B.D., et al. (2018) The type VI secretion system deploys antifungal effectors against microbial competitors. *Nature Microbiology*. [Online] 3 (8), 920–931. Available from: doi:10.1038/s41564-018-0191-x.
Tsay, T. Bin, Jiang, Y.Z., Hsu, C.M. & Chen, L.W. (2016) Pseudomonas aeruginosa colonization enhances ventilator-associated pneumonia-induced lung injury. *Respiratory Research*. [Online] 17 (1), 1–9. Available from: doi:10.1186/s12931-016-0417-5.
Tsui, L.-C. & Dorfman, R. (2013) The Cystic Fibrosis Gene: A Molecular Genetic Perspective. *Cold Spring Harbor Perspectives in Medicine*. [Online] 3, 1–14. Available from: doi:10.1101/cshperspect.a009480.
Tu, Z., He, G., Li, K.X., Chen, M.J., et al. (2005) An improved system for competent cell preparation and high efficiency plasmid transformation using different Escherichia coli strains. *Electronic Journal of Biotechnology*. [Online] 8 (1), 717–3458. Available from: http://www.ejbiotechnology.info/content/vol8/issue1/full/8/ [Accessed: 28 February 2020].
Tulchinsky, T.H. (2018) John Snow, Cholera, the Broad Street Pump; Waterborne Diseases Then and Now. *Case Studies in Public Health*. [Online] 9 (6), 77. Available from: doi:10.1016/B978-0-12-804571-8.00017-2 [Accessed: 26 April 2023].
Typas, A., Banzhaf, M., Gross, C.A. & Vollmer, W. (2012) From the regulation of peptidoglycan synthesis to bacterial growth and morphology. *Nature Reviews*. [Online] 10, 123–136. Available from: doi:10.1038/nrmicro2677 [Accessed: 2 May 2023].
Ulhuq, F.R., Gomes, M.C., Duggan, G.M., Guo, M., et al. (2020) A membrane-depolarizing toxin substrate of the Staphylococcus aureus type VII secretion system mediates intraspecies competition. *Proceedings of the National Academy of Sciences of the United States of America*. [Online] 117 (34), 20836–20847. Available from: doi:10.1073/PNAS.2006110117/-/DCSUPPLEMENTAL [Accessed: 19 May 2023].
Van Ulsen, P., Rahman, S. ur, Jong, W.S.P., Daleke-Schermerhorn, M.H., et al. (2014) Type V secretion: From biogenesis to biotechnology. *Biochimica et Biophysica Acta - Molecular Cell Research*. [Online]. 1843 (8) pp.1592–1611. Available from: doi:10.1016/j.bbamcr.2013.11.006.
Vacca, F., Sala, C. & Rappuoli, R. (2022) Monoclonal Antibodies for Bacterial Pathogens: Mechanisms of Action and Engineering Approaches for Enhanced Effector Functions.

Biomedicines. [Online] 10 (9), 1–12. Available from: doi:10.3390/BIOMEDICINES10092126 [Accessed: 29 November 2022].
Vakulskas, C.A., Potts, A.H., Babitzke, P., Ahmer, B.M.M., et al. (2015) Regulation of Bacterial Virulence by Csr (Rsm) Systems. *Microbiology and Molecular Biology Reviews*. [Online] 79 (2), 193–224. Available from: doi:10.1128/MMBR.00052-14/FORMAT/EPUB.
Valentini, M., Gonzalez, D., Mavridou, D.A. & Filloux, A. (2017) Lifestyle transitions and adaptive pathogenesis of Pseudomonas aeruginosa. *Current Opinions in Microbiology*. [Online] 41, 15–20. Available from: doi:10.1016/j.mib.2017.11.006 [Accessed: 30 May 2023].
Vandamme, P., Moore, E.R.B., Cnockaert, M., De Brandt, E., et al. (2013) Achromobacter animicus sp. nov., Achromobacter mucicolens sp. nov., Achromobacter pulmonis sp. nov. and Achromobacter spiritinus sp. nov., from human clinical samples. *Systematic and Applied Microbiology*. [Online] 36 (1), 1–10. Available from: doi:10.1016/J.SYAPM.2012.10.003.
Vasseur, P., Vallet-Gely, I., Soscia, C., Phane Genin, S., et al. (2005) The pel genes of the Pseudomonas aeruginosa PAK strain are involved at early and late stages of biofilm formation. *Microbiology*. [Online] 151, 985–997. Available from: doi:10.1099/mic.0.27410-0 [Accessed: 28 February 2020].
Veit, G., Avramescu, R.G., Chiang, A.N., Houck, S.A., et al. (2016) From CFTR biology toward combinatorial pharmacotherapy: expanded classification of cystic fibrosis mutations. *Molecular Biology of the Cell*. [Online] 27 (3), 433. Available from: doi:10.1091/MBC.E14-04-0935 [Accessed: 10 May 2023].
Ventre, I., Goodman, A.L., Vallet-Gely, I., Vasseur, P., et al. (2006) Multiple sensors control reciprocal expression of Pseudomonas aeruginosa regulatory RNA and virulence genes. *Proceeding of the National Academy of Sciences USA*. [Online] 103 (1), 171–176. Available from: www.pnas.orgcgidoi10.1073pnas.0507407103 [Accessed: 30 May 2023].
Vettiger, A., Winter, J., Lin, L. & Basler, M. (2017) The type VI secretion system sheath assembles at the end distal from the membrane anchor. *Nature Communications*. [Online] 8 (16088), 1–9. Available from: doi:10.1038/NCOMMS16088 [Accessed: 20 May 2023].
Wadhwa, N. & Berg, H.C. (2022) Bacterial motility: machinery and mechanisms. *Nature Reviews Microbiology*. [Online] 20 (March), 161–173. Available from: doi:10.1038/s41579-021-00626-4.
Wagner, J.K., Heindl, J.E., Gray, A.N., Jain, S., et al. (2009) Contribution of the Periplasmic Chaperone Skp to Efficient Presentation of the Autotransporter IcsA on the Surface of Shigella flexneri. *Journal of Bacteriology*. [Online] 191 (3), 815–821. Available from: doi:10.1128/JB.00989-08 [Accessed: 24 May 2023].
Wah Liew, O., M Ling, S.S., Lilyanna, S., Zhou, Y., et al. (2021) Epitope-directed monoclonal antibody production using a mixed antigen cocktail facilitates antibody characterization and validation. *Nature Communications Biology*. [Online] 4 (441), 1–17. Available from: doi:10.1038/s42003-021-01965-x.
Wäneskog, M., Halvorsen, T., Filek, K., Xu, F., et al. (2021) Escherichia coli EC93 deploys two plasmid-encoded class I contact-dependent growth inhibition systems for antagonistic bacterial interactions DATA SUMMARY. *Microbial Genomics*. [Online] 7 (534), 1–14. Available from: doi:10.1099/mgen.0.000534.
Wang, J., Brodmann, M. & Basler, M. (2019) Assembly and Subcellular Localization of

Bacterial Type VI Secretion Systems. *Annual Review of Microbiology*. [Online] 73 (1), 621–638. Available from: doi:10.1146/annurev-micro-020518-115420 [Accessed: 21 April 2020].

Wang, J., Yashiro, Y., Sakaguchi, Y., Suzuki, T., et al. (2022) Mechanistic insights into tRNA cleavage by a contact-dependent growth inhibitor protein and translation factors. *Nucleic Acids Research*. [Online] 50 (8), 4712–4731. Available from: doi:10.1093/NAR/GKAC228 [Accessed: 15 June 2022].

Wang, S., Liu, X., Liu, H., Zhang, L., et al. (2015) The exopolysaccharide Psl-eDNA interaction enables the formation of a biofilm skeleton in Pseudomonas aeruginosa. *Environmental Microbiology Reports*. [Online] 7 (2), 330–340. Available from: doi:10.1111/1758-2229.12252 [Accessed: 28 May 2023].

Wang, T., Du, X., Ji, L., Han, Y., et al. (2021) Pseudomonas aeruginosa T6SS-mediated molybdate transport contributes to bacterial competition during anaerobiosis. *Cell Reports*. [Online] 35 (2). Available from: doi:10.1016/j.celrep.2021.108957 [Accessed: 26 June 2023].

Wang, Y., Bian, Z. & Wang, Y. (2022) Biofilm formation and inhibition mediated by bacterial quorum sensing. *Applied Microbiology and Biotechnology* . [Online] 106 (19), 6365–6381. Available from: doi:10.1007/S00253-022-12150-3 [Accessed: 28 May 2023].

Wang, Y., Stieglitz, K.A., Bubunenko, M., Court, D.L., et al. (2007) The structure of the R184A mutant of the inositol monophosphatase encoded by suhB and implications for its functional interactions in Escherichia coli. *The Journal of biological chemistry*. [Online] 282 (37), 26989–26996. Available from: doi:10.1074/JBC.M701210200 [Accessed: 29 May 2023].

Webre, D.J., Wolanin, P.M. & Stock, J.B. (2003) Bacterial chemotaxis Run Tumble Run Attractant Repellent B A Current Biology. *Current Biology*. 13 (2), R47–R49.

Weil, D.N. & Wilde, J. (2014) How Relevant Is Malthus for Economic Development Today? HHS Public Access. *American Economic Review*. 100 (2), 1–10.

Weiser, R., Oakley, J., Ronchetti, K., Tame, J.D., et al. (2022) The lung microbiota in children with cystic fibrosis captured by induced sputum sampling. *Journal of Cystic Fibrosis*. [Online] 21 (6), 1006–1012. Available from: doi:10.1016/J.JCF.2022.01.006.

Wettstadt, S., Wood, T.E., Fecht, S. & Filloux, A. (2019) Delivery of the Pseudomonas aeruginosa Phospholipase Effectors PldA and PldB in a VgrG- and H2-T6SS-Dependent Manner. *Frontiers in Microbiology*. [Online] 10 (1718), 1–18. Available from: doi:10.3389/fmicb.2019.01718 [Accessed: 26 June 2023].

Wheeler, D.L., Church, D.M., Federhen, S., Lash, A.E., et al. (2003) Database resources of the National Center for Biotechnology. *Nucleic Acids Research*. [Online] 31 (1), 28–33. Available from: doi:10.1093/nar/gkg033 [Accessed: 2 April 2020].

Whitchurch, C.B., Tolker-Nielsen, T., Ragas, P.C. & Mattick, J.S. (2002) Extracellular DNA required for bacterial biofilm formation. *Science*. [Online] 295 (5559), 1487. Available from: doi:10.1126/SCIENCE.295.5559.1487 [Accessed: 28 May 2023].

White, J., Gilbert, J., Hill, G., Hill, E., et al. (2011) Culture-Independent Analysis of Bacterial Fuel Contamination Provides Insight into the Level of Concordance with the Standard Industry Practice of Aerobic Cultivation. *Applied and Environmental Microbiology*. [Online] 77 (13), 4538. Available from: doi:10.1128/AEM.02317-10 [Accessed: 29 April 2023].

Whitney, J.C., Quentin, D., Sawai, S., Goodlett, D.R., et al. (2015) An Interbacterial NAD(P) + Glycohydrolase Toxin Requires Elongation Factor Tu for Delivery to Target Cells

Accession Numbers 4ZV0 4ZUY 4ZV4 Whitney et al Article An Interbacterial NAD(P) + Glycohydrolase Toxin Requires Elongation Factor Tu for Delivery to Target Cells. *Cell*. [Online] 163, 607–619. Available from: doi:10.1016/j.cell.2015.09.027 [Accessed: 16 May 2022].

WHO (2017) *WHO publishes list of bacteria for which new antibiotics are urgently needed*. [Online]. 27 February 2017. Available from: https://www.who.int/news/item/27-02-2017-who-publishes-list-of-bacteria-for-which-new-antibiotics-are-urgently-needed [Accessed: 3 May 2023].

Wilhelm, S., Gdynia, A., Tielen, P., Rosenau, F., et al. (2007) The autotransporter esterase EstA of Pseudomonas aeruginosa is required for rhamnolipid production, cell motility, and biofilm formation. *Journal of Bacteriology*. [Online] 189 (18), 6695–6703. Available from: doi:10.1128/JB.00023-07.

Willett, J.L.E., Gucinski, G.C., Fatherree, J.P., Low, D.A., et al. (2015a) Contact-dependent growth inhibition toxins exploit multiple independent cell-entry pathways. *Proceedings of the National Academy of Sciences of the United States of America*. [Online] 112 (36), 11341–11346. Available from: doi:10.1073/pnas.1512124112.

Willett, J.L.E., Ruhe, Z.C., Goulding, C.W., Low, D.A., et al. (2015b) Contact-Dependent Growth Inhibition (CDI) and CdiB/CdiA Two-Partner Secretion Proteins. *Journal of Molecular Biology*. [Online]. 427 (23) pp.3754–3765. Available from: doi:10.1016/j.jmb.2015.09.010.

Williams, F.D. & Schwarzhoff, R.H. (1978) Nature of the swarming phenomenon in Proteus. *Annual review of microbiology*. [Online] 32, 101–122. Available from: doi:10.1146/ANNUREV.MI.32.100178.000533 [Accessed: 21 May 2023].

Winstanley, C., O'Brien, S. & Brockhurst, M.A. (2016) Pseudomonas aeruginosa Evolutionary Adaptation and Diversification in Cystic Fibrosis Chronic Lung Infections. *Trends in Microbiology*. [Online] 24 (5), 327–337. Available from: doi:10.1016/j.tim.2016.01.008 [Accessed: 21 May 2023].

Wood, T.E., Howard, S.A., Vollmer, W., Freemont, P.S., et al. (2019) The Pseudomonas aeruginosa T6SS Delivers a Periplasmic Toxin that Disrupts Bacterial Cell Morphology. *Cell Reports*. [Online] 29, 187–201. Available from: doi:10.1016/j.celrep.2019.08.094 [Accessed: 10 March 2020].

Wuichet, K., Cantwell, B.J. & Zhulin, I.B. (2010) Evolution and phyletic distribution of two-component signal transduction systems. *Current Opinion in Microbiology*. [Online] 13 (2), 219–225. Available from: doi:10.1016/J.MIB.2009.12.011.

Wurtzel, O., Y1. Wurtzel O, Yoder-Himes DR, Han K, Dandekar AA, Edelheit S, Greenberg EP, et al. The Single-Nucleotide Resolution Transcriptome of Pseudomonas aeruginosa Grown in Body Temperature. PLOS Pathog [Internet]. 2012 Sep [cited 2023 Jun 1];8(9). Available fro, D.R., Han, K., Dandekar, A.A., et al. (2012) The Single-Nucleotide Resolution Transcriptome of Pseudomonas aeruginosa Grown in Body Temperature. *PLOS Pathogens*. [Online] 8 (9), 1–17. Available from: doi:10.1371/JOURNAL.PPAT.1002945 [Accessed: 1 June 2023].

Xie, Z.D., Hershberger, C.D., Shankar, S., Ye, R.W., et al. (1996) Sigma factor-anti-sigma factor interaction in alginate synthesis: inhibition of AlgT by MucA. *Journal of Bacteriology*. [Online] 178 (16), 4996. Available from: doi:10.1128/JB.178.16.4990-4996.1996 [Accessed: 28 May 2023].

Yan, Q., Lopes, L.D., Shaffer, B.T., Kidarsa, T.A., et al. (2018) Secondary metabolism and interspecific competition affect accumulation of spontaneous mutants in the GacS-

GacA regulatory system in Pseudomonas protegens. *mBio*. [Online] 9 (1). Available from: doi:10.1128/MBIO.01845-17/SUPPL_FILE/MBO001183653SF5.TIF [Accessed: 30 May 2023].

Yang, X., Liu, H., Zhang, Y. & Shen, X. (2021) Roles of Type VI Secretion System in Transport of Metal Ions. *Frontiers in Microbiology*. [Online] 12, 1–7. Available from: doi:10.3389/FMICB.2021.756136/BIBTEX.

Yeung, A.T.Y., Torfs, E.C.W., Jamshidi, F., Bains, M., et al. (2009) Swarming of Pseudomonas aeruginosa is controlled by a broad spectrum of transcriptional regulators, including MetR. *Journal of Bacteriology*. [Online] 191 (18), 5592–5602. Available from: doi:10.1128/JB.00157-09.

Yuan, X., Johnson, M.D., Zhang, J., Lo, A.W., et al. (2018) Molecular basis for the folding of β-helical autotransporter passenger domains. *Nature Communications*. [Online] 9 (1), 1–12. Available from: doi:10.1038/s41467-018-03593-2 [Accessed: 24 June 2023].

Zhang, D., de Souza, R.F., Anantharaman, V., Iyer, L.M., et al. (2012) Polymorphic toxin systems: Comprehensive characterization of trafficking modes, processing, mechanisms of action, immunity and ecology using comparative genomics. *Biology direct*. [Online] 7 (18), 1–76. Available from: doi:10.1186/1745-6150-7-18 [Accessed: 16 May 2022].

Zhang, H.P., Be'er, A., Florin, E.L. & Swinney, H.L. (2010) Collective motion and density fluctuations in bacterial colonies. *Proceedings of the National Academy of Sciences of the United States of America*. [Online] 107 (31), 13626–13630. Available from: doi:10.1073/PNAS.1001651107/-/DCSUPPLEMENTAL/PNAS.1001651107_SI.PDF [Accessed: 21 May 2023].

Zhang, N., Joly, N., Burrows, P.C., Jovanovic, M., et al. (2009) The role of the conserved phenylalanine in the σ54 -interacting GAFTGA motif of bacterial enhancer binding proteins. *Nucleic Acids Research*. [Online] 37 (18), 5981–5992. Available from: doi:10.1093/nar/gkp658.

Zhang, Z.X., Nong, F.T., Wang, Y.Z., Yan, C.X., et al. (2022) Strategies for efficient production of recombinant proteins in Escherichia coli: alleviating the host burden and enhancing protein activity. *Microbial Cell Factories*. [Online] 21 (1), 1–18. Available from: doi:10.1186/s12934-022-01917-y.

Zhao, J., Schloss, P.D., Kalikin, L.M., Carmody, L.A., et al. (2012) Decade-long bacterial community dynamics in cystic fibrosis airways. *Proceedings of the National Academy of Sciences USA*. [Online] 109 (15), 5809–5814. Available from: doi:10.1073/pnas.1120577109.

Zheng, M., Cooper, D.R., Grossoehme, N.E., Yu, M., et al. (2009) Structure of Thermotoga maritima TM0439: implications for the mechanism of bacterial GntR transcription regulators with Zn2+-binding FCD domains. *Acta crystallographica*. [Online] 65, 356–365. Available from: doi:10.1107/S0907444909004727 [Accessed: 21 February 2022].

Zhou, T., Huang, J., Liu, Z., Lin, Q., et al. (2022) The Two-Component System FleS/FleR Represses H1-T6SS via Cyclic di-GMP Signaling in Pseudomonas aeruginosa. *Applied and Environmental Microbiology*. [Online] 88 (2). Available from: doi:10.1128/AEM.01655-21/FORMAT/EPUB [Accessed: 1 June 2023].

Zhou, Y., Tao, J., Yu, H., Ni, J., et al. (2012) Hcp family proteins secreted via the type VI secretion system coordinately regulate Escherichia coli K1 interaction with human brain microvascular endothelial cells. *Infection and Immunity*. [Online] 80 (3), 1243–1251. Available from: doi:10.1128/IAI.05994-11.

Zimmer, J., Nam, Y. & Rapoport, T.A. (2008) Structure of a complex of the ATPase SecA and the protein-translocation channel. *Nature*. [Online] 455, 939--943. Available from: doi:10.1038/nature07335.

Zoued, A., Brunet, Y.R., Durand, E., Aschtgen, M.S., et al. (2014) Architecture and assembly of the Type VI secretion system. *Biochimica et Biophysica Acta (BBA) - Molecular Cell Research*. [Online] 1843 (8), 1664–1673. Available from: doi:10.1016/J.BBAMCR.2014.03.018.

Zoued, A., Durand, E., Brunet, Y.R., Spinelli, S., et al. (2016) Priming and polymerization of a bacterial contractile tail structure. *Nature*. [Online] 531 (7592), 59–63. Available from: doi:10.1038/nature17182.

10. Appendix

Supplementary 1 (S1): Bioinformatic analysis of annotated CDI system genes in PAO1 and PA14

System	ORF	Blast	SMART Domains	Cdd Domain	Phobius	Signal P	TMpred
A	0040	PORTA domain ShlB type family / TpsB2	**27**- ShlB/FhaC/HecB hemolysin secretion/activation **53**- PORTA ShlB-type / TpsB1 / TpsB2 **Pfam:ShlB, SCOP, PDB, UBA_e1_C, DEATH, Tim44, TIR, x2Pfam:PORTA, x2Pfam:PORTA_2, x2 Pfam:PORTA_3, BTAD, Autotransporter, EF1G, CTNS**	FhaC	T	Sec/SPI	x3 I-to-O x2 O-to-I O-I, I-O = N out
	0041	TpsA2 / hemagglutinin / CdiA	**1699**- filamentous hemagglutinin N-terminal / TpaA1 / putative large exoprotein / heme utilization/adhesion (FhaB) large exoprotein / tRNA nuclease CdiA-2 / IbpA **1854**- filamentous hemagglutinin N-terminal / TpaA1 / putative large exoprotein / heme utilization/adhesion (FhaB) large exoprotein / 16S rRNA endonuclease CdiA / / tRNA nuclease CdiA-2 **2270**- hemagglutinin / filamentous hemagglutinin N-terminal / TpsA2 / hemolysin precursor / 16S rRNA endonuclease CdiA **2307**- hemagglutinin **3394**- hemagglutinin / filamentous hemagglutinin N-terminal / **SCOP(d1hv9a1)**- filamentous hemagglutinin / S-layer protein **SCOP(d1jmva)**- S-layer protein / p120 / hemagglutinin **SCOP(d1k28a2)**- filamentous hemagglutinin / ParB N-terminal domain **SCOP(d1jaya)**- DUF 627 domain / filamentous hemagglutinin / TpsA2 **x3 Haemagg_act, x47 Pfam:Fil_haemagg,, x4 Pfam:DUF637, PDB, transmembrane region, CPSase_sm_chain, x2 internal repeat 1, x2 internal repeat 2, internal repeat 3, AdoHcyase_NAD, ZnF_RBZ, NIDO, HBM, Why, ALAD, CHASE, PGRP, OMPdecase, BTAD, Spc7_N, S4, tRNA_SAD, PUA, Int_alpha, H-kinase_dim, RPOLD, PHB, MA, LRR_RI, DeoRC, Germane, Amb_all, TSPc, B_lectin, CASH, LINK, BID_1, ADSL_C, Prim-Pol, H2A, SH3b, Flavin_Reduct, CA, PepX_C, Arg_tRNA_synt_N, CHRD, TFIIA, PP2Cc, CO_deh_flav_C, Tubulin_C, LamGL, CDC48_N, ZipA_C, Glyco_25, Biotin_carb_C, LANC_like, Milton, RICIN, PKS_DH,**	DUF637 / Haemagg_act / CDI_toxin_Bp1026b_like / x2 FhaB / x2 PRK15319 / Fil_haemagg_2	T	Sec/SPI	x25 I-to-O x21 O-to-I O-I, I-O = N out

			UreE_N, Resolvase, APC2, FCH, DUF3160, PAP-1, FIST, PBPb, PLDc, BPI1, t_SNARE, KIND, A1pp, ELFV_dehydrog, Ycel, Calx_beta, Kelch, CBD_IV, G8, A2M, SCPU, PYNP_C, GTase_5, PAX, DAGKc, Ribosomal_L2_C, PGA_cap, RuBisCO_small, Amelin, FTCD_N, DSPc, PKS_TE, CTD, CBD_II, Fop_duplication, Adenylsucc_synt, DUF1767, AIP3, CHAD, PKS_PP, DUF1944, GARS_C, RES, RobI_LC7, HAS, EB_DH, alkPPc, POLAc, D-ser_dehydrat, Aamy, HMG17, MoCF_biosynth, DM14, BAG, efhand_Ca_insen, PKS_AT, Transket_pyr, Alpha_l_AF_C, PKS_ER, VKc, OmpH, Enolase_C, Dak2, AICARFT_IMPCHas, Gln-synt_C, SecA_DEAD, Frataxin_Cyay, BTP, EAL, 6PGB, Cutinase, GGDEF, DSRM, MHC_II_alpha, ProQ, FCD, Malic_M, DDE_Tnp_IS1595, HTH_ASR, WNT1, SPEC, ParB, Aerolysin, Protease, IB, CVNH, Ala_racemase_C, Galanin				
	0042	CdiA/I	Pfam CAP	-	N/T	Lipo-Sec/SPII	x1 I-to-O x1 O-to-I O-I, I-O = N out
	0043	-	**1**- glycine zipper 2TM / Jouberin **94**- patatin-like phospholipase **117**- AMP-binding / spore germination / endospore germination permease / TPA chromate efflux transporter / subtilase / S8 serine peptidase / DUF1161 **171**- Rho / NtaA/DmoA FMN-dependent monooxygenase / aldehyde dehydrogenase / class I SAM-dependent RNA methyltransferase / ImuB / ubiquitin thioesterase / DEAD/DEAH helicase / AraC DNA binding protein / HTH transcriptional regulator **288**- tetratricopeptide repeat / pentraxin PTX3 / GAF domain **306**- zinc finger Xfin / zinc fingers and homeoboxes protein 3 / ClpA / RpoD / MAST domain / DGCR14 / 3-hydroxyisobutyryl-CoA hydrolase-like / α-ketoacid dehydrogenase kinase / HliD / DUF4010 . cytochrome c **338**- resolvase / E3 ubiquitin ligase WAV3 / AAA ATPase / disulphide oxidoreductase **354**- TIGR02680 / integrase **394**- LOB domain / Ig-like / cobalt-zinc-cadmium efflux system **SCOP(d1jj2c)**- S12 methyltransferase accessory factor **SCOP(d1kkea2)**- ROK / carbohydrate binding **CDC48_N, BTAD, Pro-rich, x2 Pfam:DUF4778, TFIIA, RES, IRF**	PRK12678	-	-	x1 I-to-O x2 O-to-I
B	00490		**27**- TpsB2 / ShlB/FhaC/HecB hemolysin secretion/activation **54**- PORTA ShlB-type / TpsB1 / TpsB2	FhaC	T	Sec/SPI	x3 I-to-O x2 O-to-I

		TpsB2 / ShlB/FhaC/HecB hemolysin secretion/activation	**Pfam:ShlB, SCOP, PDB, UBA_e1_C, DEATH, Tim44, TIR, x2Pfam:PORTA, x2Pfam:PORTA_2, x2 Pfam:PORTA_3, BTAD, Autotransporter, EF1G, CTNS**				O-I, I-O = N out
	00510	Putative hemagglutinin / TpsA2 / CdiA / hemolysin precursor	**1699**- filamentous hemagglutinin / TpsA1/ 16S rRNA endonuclease CdiA / FhaB / IbpA precursor 2200- filamentous hemagglutinin N-terminal **2270**- filamentous hemagglutinin N-terminal / TpsA2 / hemolysin precursor / 16S rRNA endonuclease CdiA **2306**- filamentous hemagglutinin N-terminal / TpsA2 / 16S rRNA endonuclease CdiA **2930**- TpsA2 / putative ShlA/HecA/FhaA exoprotein / hemolysin precursor / 16S rRNA endonuclease CdiA / adhesin HecA **3320**- TpsA2 / hemolysin / CdiA / adhesin HecA **SCOP(d1hv9a1)**- hemagglutinin / S-layer protein / **SCOP(d1a59)**- TpsA2 / hemagglutinin **x3 Haemagg_act, x46 Pfam:Fil_hemagg, x5 Pfam:DUF637, PDB, transmembrane region, CPSase_sm_chain, x2 internal repeat 2, AdoHcyase_NAD, ZnF_RBZ, NIDO, Why, ALAD, PGRP, FtsA, OMPdecase, BTAD, Spc7_N, HBM, S4, HAMP, FCD, x2 internal repeat 1, PUA, Int_alpha, H-kinase_dim, RPOLD, CoA_trans, MA, LRR_RI, DeoRC, Germane, Amb_all, Dak2, CASH, LINK, BID_1, ADSL_C, SH3b, GGDEF, PepC_C, Arg_tRNA_synt_N, MGS, CHRD, PP2Cc, Tubulin_C, LamGL, eIF6, CDC48_N, ZipA_C, Glyco_25, Biotin_carb_C, UreE_N, Resolvase, APC2, FCH, DUF3160, D-ser_dehydrat, PAPA-1, FIST, Glyco_32, PLDc, B_lectin, CO_deh_flav_C, BPI1, PKS_DH, t_SNARE, Glyco_18, ELFV_dehydrog, Ycel, Kelch, Alpha-L-AF_C, LamG, Frataxin_Cyay, CBD_IV, G8, A2M, SCPU, PYNP_C, GATase_5, PAX, DAGKc, Ribosomal_L2_C, PGA_cap, RuBisCO_small, Amelin, FTCD_N, PKS_TE, CTD, FoP_duplication, Adenylsucc_synt, AIP3, PKS_PP, TFIIA, DUF1944, GARS_C, RES, CHAD, HAS, EB_dh, alkPPc, POLAc, Aamy, PLAc, M60-like, Candida_ALS_N, HMG17, MoCF_biosynth, LeuA_dimer, AdoHcyase, TR_FER, PP2C_SIG, DM14, DUF1237, Iso_dh, POU, CHB_HEX, Dak1_2, ETF, PKS_ER, H2A, CHASE, G3P_acyltransf, VKc, DeoC, PBPb, B561, RFX5_DNA_bdg, Romo1, Flavin_Reduct, Cache_2, RTC4, AFOR_N, SAR, Enolase_N, DDRGK, CLa, ILWEQ, AICARFT_IMPCHas, MgtE_N, YaeQ, BTP, PSA, ALBUMIN, LSM14, DUF1899, AD**	Haemagg_act / x2 FhaB / DUF637 / Fil_haemagg_2 / x2 PRK15319	T	Sec/SPI	x25 I-to-O x21 O-to-I O-I, I-O = N out

	00520	Transposase / CdiA/I	**27**- WD repeat-containing protein slp1 / metalloprotease / fibulin-2-like / cytospin B **SCOP**- CPBP intermembrane metalloprotease	-	C	-	-
	00530	CdiA/I	Pfam CAP	-	N/T	Lipo-Sec/SPII	x1 I-to-O x1 O-to-I O-I, I-O = N out
	00550	MgtC/SapB protein	**11 and 193**-MgtC/SapB **448**- DUF4010 / MgtC/SapB **x2 SCOP, x3 Pfam:MgtC, x3 Pfam:DUF4010, G3P_acyltransf, Pfam:Methyltranf_RNA, B561, TOG, HTTM, VKc, acidPPc, Bac_rhodopsin, CHAD, TLC, FCD, Solute_trans_a, PKS_TE, Cg6151-P, HTH_DTXR, Mab-21, Cornichon, UME, KbaA, PSN, DUF106, BC10, Haemolytic, Pfam:Spore_YhaL, Asparaginase, flavin_reduct, Transket_pyr, PKS_AT, DM14, rADc,, PKS_DH, GIT**	COG3174	T	-	x12 I-to-O x11 O-to-I O-I, I-O = N out
C	2456	-	**SCOP(d15xa)**- WD repeat-comtaining / collagen α-1 chain-like / TonB dependent siderophore receptor **SCOP(d1cm5a)**- ketoacyl-ACP synthase III / LysR transcription regulator **DysFC**	-	N/T	Sec/SPI	x2 I-to-O x1 O-to-I I-O, O-I = N in
	2457	RHS repreat	**x7 Pfam:RHS_repeat** **SCOP**- aminomethyl-transferring glycine dehydrogenase **FN3, LamB, RICIN, PKD, CBD_II, CTD, Prim_Zn_Ribbon**	RhsA	N	-	x1 I-to-O
	2458	RHS repeat / sugar binding	x7 RHS, x2 SCOP, Strep_pep, CADG, Aamy, WD40, HBM, ArrestinC, Aerolysin, ZnF_DBF, DKCLD	RhsA	T	-	x1 I-to-O x1 O-to-I I-O, O-I = N in
	2459	PA2459	SCOP / Cyt-b5 / Ala_racemase_C / DUF862 / ZnF_CHCC / END	-	-	-	x1 I-to-O x1 O-to-I
	2460	VENN motif pre-toxin / EndoU	**SCOP**- VENN motif / filamentous haemagglutinin **PT-VENN, EGF_CA**	PT-VENN	N	Sec/SPI	x1 I-to-O x1 O-to-I
	2461	Pentapeptide repeat-containing protein	**x5 Pfam, PDB, SCOP**- pentapeptide repeats **Semialdhyde_dh**	YjbI	N	-	x1 I-to-O x1 O-to-I O-I, I-O = N out
	2462	TpsA1 / p120 / hemagglutinin / FhaB / 16S rRNA endonuclease CdiA	**333**- TpsA1 / filamentous hemagglutinin N-terminal domain / putative large exoprotein / 16S rRNA endonuclease CdiA / heme utilization FhaB / tRNA nuclease CdiA-2	Haemagg_act / DUF637 / x2 FhaB / EndoU_bacteria / Fil_haemagg_2 / x3 PRK15319	T	Sec/SPI	x30 I-to-O x31 O-to-I O-I, I-O = N out

			670 and 1085- TpsA1 / filamentous hemagglutinin N-terminal domain / putative large exoprotein / 16S rRNA endonuclease CdiA / tRNA nuclease CdiA-2 / IbpA / p120 **3577**- filamentous hemagglutinin N-terminal domain / TpsA1 / NCGM2_3464 / putative large exoprotein / 16S rRNA endonuclease CdiA / tRNA nuclease CdiA-2 / IbpA **5042**- DUF637 / p120 / adhesin / CdiA / IbpA / hemagglutinin / DNase CdiA **5365**- filamentous hemagglutinin N-terminal domain / TpsA1 / Y89_2739 / putative large exoprotein / 16S rRNA endonuclease CdiA / tRNA nuclease CdiA-2 IbpA / p120 **5495**- TpsA1 / filamentous hemagglutinin N-terminal domain / 16S rRNA endonuclease CdiA / p120 / EndoU domain putative large exoprotein **SCOP(d1exba) and SCOP(d1k28a2)**- filamentous hemagglutinin N-terminal domain / TpsA1 / putative large exoprotein / 16S rRNA endonuclease CdiA / **x4 Haemagg_act, x82 Pfam:Fil_haemagg, Pfam:EndoU_bacteria, PDB, transmembrane region, CPSase_sm_chain, x2 internal repeat 2, TOP2c, AdoHcyase_NAD, ZnF_RBZ, NIDO, HBM, Why, ALAD, PGRP, FtsA, OMPdecase, BTAD, S4, UTRA, FCD, Bgal_small_N, x2 internal repeat 1, Int_alpha, PUA, ASCH, t_SNARE, HAMP, H15, ZipA_C, TECPR, Glyco_25, rADc, FIST_C, VWD, HELICc, DeoC, Milton, HTH_MARR, LINK, DHDPS, STI, GatB_Yqey, Spc7_N, PKS_AT, AHS2, PKS_MT, COG6, Aamy_C, STN, LNS2, CpcD, LytTR, MA, POL3Bc, BPI1, CVNH, DSX_dimer, PhnA_Zn_Ribbon, UreE_N, B_lectin, BID_1, D-ser_dehydrat, CASH, PBPb, PP2C_SIG, G8, CHRD, PKS_PP, AIP3, RobI_LC7, LysM, Frataxin_Cyay, CTNS, BID_2, DUF1907, BBC, Galanin, x4 ANTAR, Germane, GA, PHB, Arg_tRNA_synt_N, MGS, SAF, TSPc, DUF1900, ParB, Amb_all, CHAD, ADSL_C, Prim-Pol, H2A, SH3b, PepX_C, Cation_ATPase_N, PP2Cc, Tubilin_C, LamGL, CDC48_N, Biotin_carb_C, DUF3160, PAPA-1, Glyco_32, ILWEQ, PLDc, CO_de_flav_C, Glyco_18, ELFV_dehydrog, Ycel, Kelch, Alpha-L-AF_C, LamG, A2M, Enolase_C, PAX, CBM_10, CPSase_L_D3, EFG_IV, Tet_JBP, GARS_C, Carb_anhydrase, RICIN, P68HR, PKS_TE, CobW_C, CBD_II, PKS_DH, TFIIA, PLAc, NPP, UBA_e1_C, eIF5C, FeoA, H2TH, HDc, Ad_cyc_g-alpha, CBD_IV, alkPPc, LYZ2, Semialdhyde_dh, NPCBM, Cpl-7, Ald_Xan_dh_C, FDX-ACB, C345C, FMN_bind, Aamy, Candida_ALS_N, ING, MoCF_biosynth, PTX,**			

			Enolase_N, Ribosomal_L15E, efhand_Ca_insen, EB_dh, Dak2, AIRC, G3P_acyltransf, Bac_rhodopsin, Transket_pyr, PLEC, GATase_5, ClB_D2-small, DZF, AlaDh_PNT_N, PROF, PKS_KR, Tubulin, ENDO3c, ITAM, DM14, HisKA, PQQ, DysFC				
	2463	TspB1	**30**- ShlB/FhaC/HecB hemolysin secretion/activation **57**- OM BamA / ShlB/FhaC/HecB hemolysin secretion/activation / PORTA domain ShlB-type / TpsB1/2 **x3 SCOP, PDB, DNAG_DnaB_bind, FCD, Tim44, TIR, x2 Pfam:PORTA, x2 Pfam:PORTA2, Pfam:PORTA3, Pfam:ShlB, BTAD, Autotransporter, EF1G, CTNS**	FhaC	T	Sec/SPI	x3 I-to-O x2 O-to-I O-I, I-O = N out
D	32780	TpsB1	**30**- ShlB/FhaC/HecB hemolysin secretion/activation **57**- OM BamA / ShlB/FhaC/HecB hemolysin secretion/activation / PORTA domain ShlB-type / TpsB1/2 **x3 SCOP, PDB, DNAG_DnaB_bind, FCD, Tim44, TIR, x2 Pfam:PORTA, x2 Pfam:PORTA2, Pfam:PORTA3, Pfam:ShlB, BTAD, Autotransporter, EF1G, CTNS**	FhaC	T	Sec/SPI	x3 I-to-O x2 O-to-I O-I, I-O = N out
	32790	filamentous hemagglutinin N-terminal domain / TpsA1 / 16S rRNA endonuclease CdiA / tRNA nuclease CdiA-2 / IbpA	**670 and 4945**- TpsA1 / filamentous hemagglutinin N-terminal / 16S rRNA endonuclease CdiA / FhaB / IbpA / p120 **1993**- filamentous hemagglutinin N-terminal / TpsA1 / NCGM2_3464 / putative large exoprotein / FhaB / tRNA nuclease CdiA-2 / IbpA **4622**- DUF367 / p120 / CdiA / adhesin / IbpA / DNase CdiA / hemagglutinin **5075**- filamentous hemagglutinin N-terminal / TpsA1 / IbpA / p120 **SCOP(d1k5ca)**- adhesin/hemagglutinin / filamentous hemagglutinin N-terminal **SCOP(d1cby)**- tRNA nuclease CdiA-2 /16S rRNA endonuclease CdiA / TpsA1 / filamentous hemagglutinin, intein -containing / CdiA / S-layer protein / IbpA **SCOP(d1k28a2)**- hemagglutinin / adhesin HecA / p120 / IbpA / S-layer protein / DNase CdiA / ParB n-terminal **SCOP, x4 Haemagg_act, x75 Pfam:Fil_haemagg, PDB, transmembrane domain, CPSase_sm_chain, x2 internal repeat 3, X2 internal repeat 2, TOP2c, AdoHcyase_NAD, ZnF_RBZ, NIDO, ALAD, PGRP, FtsA, OMPdecase, BTAD, HBM, S4, UTRA, Bgal_small_N, x2 internal repeat 1, Int_alpha, H-kinase_dim, PUA, ASCH, t_SNARE, PKS_MT, HAMP, H15, TECPR, Glyco_25, WHy, GARS_C, GatB_Yqey, FIST_C, AAMY_C, STN, LNS2, CpcD, CADG, LytTR, MA, POL3Bc, Prim-Pol, HA2, BPI1, CVNH, DSX_dimer, PhnA_Zn_Ribbon, CASH, BID_1, PBPb, AIP3,**	Haemagg_act / DUF637 / x2 FhaB / Fil_haemagg_2 / x3 PRK15319	T	Sec/SPI	x30 I-to-O x31 O-to-I O-I, I-O = N out

			PP2C_SIG, G8, CHRD, PKS_PP, Ribosomal_S19e, CTNS, BID_2, Galanin, Fapy_DNA_glyco, x4 ANTAR, Germane, MCM, LINK, GA, MeTrc, Arg_tRNA_synt_N, PHB, MGS, PKS_ER, Jag_N, CAT_RBD, SAF, TSPc, DUF1900, ParB, Amb_all, ADSL_C, H2A, SH3b, GGDEF, PepX_C, PP2Cc, Tubulin_C, LamGL, EIF6, CDC48_N, ZipA_C, Biotin_carc_C, UreE_N, Resolvase, APC2, FCH, DUF3160, PAPA-1, DeoC, FIST, Glyco_32, PLDc, B_lectin, CO_deh_flav_C, Glyco_18, ELFV_dehydrog, Ycel, Kelch, LamG, YaeQ, Frataxin_Cyay, CBD_IV, JHBP, A2M, PYNP_C, A1pp, Spc7_N, EF1G, SPRY, CobW_C, PKS_TE, Pro-rich, CBD_II, Cpl-7, PDZ, TFIIA, PLAc, UBA_e1_C, Cation_ATPase_N, eIF5C, FeoA, H2TH, HDc, STI, Ad_cyc_g-alpha, AHS2, RFX5_DNA_bdg, alkPPc, LYZ2, Semialdhyd_dh, NPCBM, COLFI, D-ser_dehydrat, Ald_Xan_dh_C, FDX-ACB, C345C, FMN_bind, Aamy, Candida_ALS_N, MoCF_biosynth, PTX, efhand_CA_insen, EB_dh, Dak2, AIRC, ETF, G3P_acyltransf, Transket_pyr, PLEC, GATase_5, SRP54_N, ClpB_D2-small, DZF, PROF, AP2Ec, PKS_KR, Tubulin, ENDO3c, ITAM, AICARFT_IMPCHas, AlaDh_PNT_N, DM14, HisKA, N-glycanase_N, CBM_2, SWIB				
	32810	putative haemagglutinin	**68**- filamentous hemagglutinin N-terminal domain / TpsA1 exoprotein / putative large exoprotein (involved in heme utilization or adhesion) / hemagglutinin / adenosine monophosphate-protein transferase and cysteine protease IbpA precursor / p120 **SCOP**- filamentous hemagglutinin **CO_deh_flav_C, HisKA**	-	-	-	x1 O-to-I
	32820	filamentous hemagglutinin / 16S rRNA endonuclease CdiA / CdiA / adhesin/hemagglutinin, HecA	**68**- 16S rRNA endonuclease CdiA / filamentous hemagglutinin /CdiA / p120 / hemolysin precursor / adhesin/hemagglutinin, HecA / EndoU domain / mafB19-like deaminase family **SCOP(d1l8aa3)**- CdiA / 16S rRNA endonuclease CdiA / filamentous hemagglutinin **SCOP(d1qh4a2)**- CdiA / 16S rRNA endonuclease CdiA **SCOP(d1qkra), PKS_TE, Pro_CA, SMC_hinge, HhH1, NADH_4Fe-4S**	-	-	-	x1 O-to-I
	32830	-	**79-** mechanosensitive ion channel / T2SS F protein / phosphatase PAP2 / SLC13 permease **170-** non-ribosomal peptide synthetase / linear gramicidin synthase subunit D / WYL domain / fimbrial assembly protein / glutamate dehydrogenase / multi-sensor hybrid histidine kinase / response regulator / carbamoyl transferase / tetratricopeptide repeat / σ54 dependent Fis transcriptional regulator / PAS domain	-	T	Sec/SPI	x16 I-to-O x16 O-to-I I-O, O-I = N in

			/ AMP-binding / NADH-quinone oxidoreductase / leucyl aminopeptidase / aminotransferase class III-fold pyridoxal phosphate-dependent **211-** DUF2339 / universal stress proteins / maleylpyruvate isomerase mycothiol-dependent enzyme **260-** FliN / ATP-binding cassette / SppA / PilB / DUF952 / p65 /ATP binding **307-** OM lipoprotein / membrane protein / glycine zipper 2TM domain **409-** L-ribulose-5-phosphate 4-epimerase AraD **504-** TPA cytochrome oxidase assembly protein / cation transporter / MFS transporter / GGDEF domain / acyltransferase **578-** site specific recombinase, phage integrase / FtsA **620-** TPA / ABC transporter ATP binding protein **703-** methyltransferase domain / β-glucosidase **WAP, GDNF, Cyclin_C, RING, Flavin_Reduct, CheW, CHAD, FIST, A2M, Asparaginase, Bac_rhodopsin, D-er_dehydrat, SATase_N, rADc, B12-binding_2, ARM, AlkA_N, G3P_acyltransf, HBM, Cutinase, Int_α, DUF167, VRR_NUC, FTP, BTAD, FIST_C, ETF NL, HWE_HK, PLEC, HELICc2, DALR_1, CHASE MA, GatB_Yqey, S1, SpoU_sub_bind, UreE_N, YqgFc, H2HT, CoA_binding, V4R, ANTAR**				
	32840	-	**1**- HD domain / RibD **60**- membrane protein / calcium binding / sodium:calcium antiporter **80**- phosphoribosylamine--glycine ligase **171**- transglutaminase domain / major facilitator superfamily / MFS transporter / ABC transporter permease / C4-dicarboxyl ABC transporter / mannosyltransferase /DUF2029 / spermidine/putrescine transport system permease protein / EamA transporter / EAL domain / glycine/betaine ABC transporter permease / CysT / protein kinase **SCOP(d1jpya)**- oxygen-regulated protein 1 / amino acid adenylation domain **x2 SCOP, HA2, AFOR_N, IG_GLMN, Gln-synt_C, FIST, PYNP_C, Bac_rhodopsin, KbaA, MAPKK1_Int, Transket_pyr, Ald_Xan_dh_C, ETF, CAT_RBD, Cu_FIST, Copper-fist, Excalibur, ZnF_C2**	-	T	-	x7 I-to-O x7 O-to-I O-I, I-O = N out
	32850	-	**39**- E3 ubiquitin-protein ligase RNF182 / ribosomal protein S6 kinase-like / β-propeller fold lactonase	-	T	-	x7 I-to-O x8 O-to-I

			178- oxidoreductase / NADH dehydrogenase / CHAT domain / tetratricopeptide-repeat / pH adaptation potassium efflux system protein A / chloride channel protein / two-partner sensor histidine kinase / AI-2E transporter / NADH-quinone oxidoreductase subunit 5 / M48 metalloprotease / ABC transporter permease / FtsX-like permease / MFS transporter **215**- PAS domain S-box / RNA methyltransferase / ribokinase **262**- sphingosine kinase / TPA:DNRLRE domain / hexose kinase / two-component histidine kinase / sensory histidine kinase UhpB **313**- 4-aminobutyrate—2-oxoglutarate transaminase **SCOP(d1gqea)**- DUF116 domain / amidohydrolase / sodium/hydrogen exchanger **SCOP(d1ekea)**- aspartate aminotransferase, 4-aminobutyrate—2-oxoglutarate transaminase / 3-carboxy-cis,cis-muconate cycloisomerase / glycosyltranferase **SCOP, AFO_N, DAGKc, PKS_KS, MGS, DHDPS, CoA_binding, Lactamase_B, FCD, PKS_AT, CHAD, BTAD, PTX, Pro-kuma_activ, CheW**				O-I, I-O = N out
	32860	-	**3**- talin-2 / DUF3504 / glycoside hydrolase / ABC transporter ATP binding / methyl-accepting chemotaxis protein / sterol desaturase / cytochrome P450 / RNA 3' terminal phosphate cyclase / DMT transporter / polysaccharide biosynthesis / cyclin dependent serine-threonine kinase / ITN1-like protein **29**- Rne/Rng ribonuclease / ribonuclease E/G **ENDO3c, ProQ, PBP5_C, HABP4_PAI-RBP1, PKS_DH, HTH_XRE, DUF1716, C8**	-	N	-	-
	32880	-	**19**- M23 metallopeptidase / IclR transcriptional regulator **80**- transglutimase domain / formimidoylglutamate deiminase / acetyl-CoA carboxylase biotin carboxyl carrier protein subunit / PAS domain **196**- DJ-1/Pfpl/YhbO deglycase/protease / molybdenum-dependent oxidoreductase / FAD-binding oxidoreductase / monodehydroascorbate reductase **225**- YbaB/EbfC nucleoid-associated / PAS domain S-box **SCOP**- Cysteinyl-tRNA synthetase / response regulator / FAD-dependent oxidoreductase / PAS domain S-box / golgin subfamily B member 1-like / replication-associated recombination protein A / TPA: hydantoinase/oxoprolinase **CP12, DSS1_SEM1**	-	N		x2 I-to-O x2 O-to-I
	32950	Esterase / DUF3327	**105**- enterochelin esterase / esterase	Fes	N	Sec/SPI	x2 I-to-O

			Pfam DUF3327 **PDB:3C8HID**- esterase **SCOP**- esterase **Fn3_like, cNMP, AlkA_N, PKS_DH, CHAD, SpoVT_AbrB, RFX5_DNA_bdg, FATC, PepX_C, Pfam:Abhydrolase_1, Pfam:Peptidase_S9**				x2 O-to-I I-O, O-I = N in

Note: ORF column, blue = OM β-barrel, red = toxin, green = orphan toxin-immunity region downstream toxin. SMART domains column, if more information or multiple similarities for a domain the domains are highlighted in bold. Domains are in order from upstream to downstream of the gene sequence. Phobius column; N = non-cytoplasmic, C = cytoplasmic, T= transmembrane. TMpred column; O = out, I = in, I-O = in to out, O-I = out to in, N in = N-terminal preferred inside model, N out = N-terminal preferred outside model.

Supplementary 2 (S2): Small ORF bioinformatics analysis

System	ORF	Blast	SMART Domains	Cdd	Phobius	Signal P	TMpred
PA0041	6	CdiA/I	Rubredoxin/Zn ribbon	-	C	-	-
	20	N/A	N/A	-	C	-	-
	69	TssM / asparaginase	N/A	-	C/T	-	-
	7	Transposase/ RayT	POLAc / ING / CPSase / CO dehydrogenase / transglutimase / S4 / A-T hook / BHD_2 / Y1_Tnp	-	N	-	-
	55	Zn finger (*Penicillium* / *Aspergillus*)	C1	-	C	-	-
	45	Transposase	BHD_2 / Y1_Tnp		N		x1 I-to-O
	23	PA0042/ CdiA/I	IG / CAPN	-	N/T	Lipo-Sec/SPII	x1 O-to-I
	11		**2**- metallopeptidase / transcriptional regulator **30**- AAA ATPase / DNA binding / σ^{54} binding **70**- sortase **SCOP**- helicase / ATPase/ P3K **FOP**	-	N	TAT- Sec/SPI	-
PA14_00510	54	CdiA/I	**32, 78, SCOP**- Chain B immune protein **AgrD** **Pox_P35**	-	N/T	-	x1 I-to-O
	9	CdiA/I	**SCOP**- Zn metalloprotease / ammonium transporter / diguanylate cyclase	-	T	-	x1 O-to-I
	67	FtsK	**-**	-	C	-	-

	10	Aminoacyl-tRNA hydrolase / GPI de-N-acetylase / peptidase/ cation transporting ATPase	-	-	N	-	-
	55	CdiI / CdiA/I	**SCOP(d1npsa)**- Hlip **SCOP(d1gg3a2)**- CdiI **XTALbg**- β/γ crystallins **CUE**	-	N	-	-
	82	-	**SCOP**- TVP38/TMEM64 / signal recognition particle / alcohol dehydrogenase / BatD	-	C/T	-	x1 I-to-O x1 O-to-I I-O, O-I= N in
	66	-	**SCOP**- ATP binding cassette / RNA binding transcription accessory protein / glycoside hydrolase	-	N	-	-
	39	Transposase / CdiA/I	**27**- Slp1 / metalloprotease / fibulin-like 2 / cytospin B **SCOP**- CPBP intramembrane metalloprotease	-	C	-	-
	56	CdiA/I	**17, SCOP**- hypothetical **CAPN**		T	Lipo-Sec/SPII	x1 O-to-I
	41	-	**2**- metallopeptidase / transcription regulation **30**- AAA ATPase / DNA binding / σ^{54} binding **70**- sortase **SCOP**- helicase / ATPase / P3K **FOP**	-	N	TAT- Sec/SPI	-
PA2462	65	Acetyltransferase	-	-	C/T	-	x1 I-to-O x1 O-to-I I-O, O-I = N in
	40	Cell adhesion / ABC transporter permease	-	-	N	-	-
	41	-	**SCOP**- ATP/GTP binding protein / peptidase / metallophosphatase	-	C	-	-
	68	-	-	-	C	-	-
	44	tRNA nucleotidyl transferase / methylcitrate synthase	-	-	N	TAT- Sec/SPI	-
	69	-	**SCOP**- ATPase / non-ribosomal peptide synthetase / Bcrnrps 6	-	N	-	-
	142	FAD binding oxidoreductase	-	-	N	-	x1 O-to-I

	70	-	**SCOP**- Slyx / T1SS C-terminal / cell wall associated protease **FIMAC**	-	N	-	-
	132	-	**7**- sulfate permease **SCOP**- N-6 DNA methylase	-	T	-	x1 I-to-O x1 O-to-I O-I, I-O = N out
PA14_32790	VectorNTI	-	**SCOP** **AXN**- annexin repeats binding phospholipids in a calcium-dependent manner	-	-	-	x1 I-to-O
	163	MAM / S8 family peptidase	-	-	T	Lipo-Sec/SPII	x1 I-to-O x1 O-to-I O-I, I-O = N out
	87	ig-h3	-	-	T	Lipo-Sec/SPII	x1 I-to-O x1 O-to-I O-I, I-O = N out
	57	ABC transporter	**33**- glycosyltransferase **SCOP**- ABC transporter	-	T	-	x1 I-to-O x1 O-to-I O-I, I-O = N out
	201	-	-	-	C	-	-
	29	Class II aldolase/adducin family / ribulose-5-phosphate 4 epimerase/fuculose-1-phosphate aldolase / ATPase / histidine kinase / DNA gyrase / HSP90 ATPase / A1-2E family transporter	-	-	N	-	-
	200	-	-	-	N	-	-
	60	-	**SCOP**- Lrp/AsnC transcription regulator	-	N/T	-	x1 I-to-O x1 O-to-I O-I, I-O = N out
	92	CdiI	**66**- CdiI / GNAT N-acetyltransferase / DUF 87 / ATPase **SCOP(d1f1za1)**- CdiI / SfsA **SCOP(d1f2da)**- NAD-dependent epimerase / TPA **RAP**	-	N	-	-

	95	Wall association protein / insulinase / RhsB / metallophosphoesterase	-	-	N	Sec/SPI	x1 I-to-O x1 O-to-I I-O, O-I= N in
	111	-	**6**- molybdenum cofactor systhesis domain **55**- FliN / ABC domain / signal peptide peptidase / PilB **102**- OM lipoprotein / membrane protein / glycine zipper 2TM domain **125**- exo-α-sialidase / SppA / efflux RND transporter periplasmic adaptor / ion transporter / protein-tyrosine kinase / CwsA **SCOP(d1fyc)**- putative elongation factor TS **D-ser_dehydrat, SATase_N, BTAD, ARM, Tail_VII**	-	N	-	x3 I-to-O x3 O-to-I O-I, I-O= N out
	98	Aminotransferase class I and II / histidinol-phosphate aminotransferase / dihydropyrimidine dehydrogenase NADP+ / monovalent cation H+ antiporter subunit A	-	-	N	-	-
	195	-	**SCOP**- KICSTOR complex C12orf66 homologue isoform X1/X2 / A-T hook DNA binding motif / ankyrin repeat and death domain **TMEM71**	-	N	-	-
	62	-	37- TonB / chloroplast OM family protein / AAA ATPase SCOP- AMP binding protein / pentatricopeptide repeat / PCI-domain	-	N	-	x1 I-to-O
	100	JAB domain containing	**51**- 50S / KS-AT-KR-ACP domain **75**- ATP binding / PRM10 phermone-regulated / carbohydrate responsive element binding **142**- spectrin α chain erythrocytic 1 / dedicator of cytokinesis protein / TetR/AcrR / chaperonin / Fe ABC transporter permease / pwi / enoyl-CoA hydratase **214**- HTH transcription regulation / AMP binding / PAS domain / histidine kinase / AAA ATPase **SCOP**- JAB **SOCS-box, FA-GDNF, GRAN, FOLN**	-	N	-	x2 I-to-O x1 O-to-I O-I, I-O= N out

	106	-	**3**- talin-2 / glycoside hydrolase / TPA ABC transporter ATP binding protein / methyl-accepting chemotaxis protein / sterol desaturase / T2SS F protein / RNA 3' terminal phosphate cyclase / DMT transporter / polysaccharide biosynthesis / cyclin dependent serine/threonine kinase / ankyrin repeat **93**- Rne/Rng ribonuclease **ENDO3c, ProQ, PBP5_C, HABP4_PAI, PKS_DH, HTH_XRE, DUF1716, C8**	-	N	-	-
	70	Class I SAM-dependent methyltransferase	FBA, TPMT, TehB, Ubie_methyltran, CHAD, PYNP_C, LON, LysM, HX	AdoMet_MTases	N/T	-	x2 I-to-O x2 O-to-I O-I, I-O= N out
	190	Phosphatidylinositol 4-phosphate 3 kinase C2 domain	SCOP- TraN / glycerol transporter / HTH transcriptional regulator	-	N	-	-
	39	YgdI/R lipoprotein	-	DUF903	T	Lipo-Sec/SPII	x1 I-to-O x1 O-to-I I-O, O-I= N in
	73	Esterase	**105**- enterochelin esterase **Pfam DUF3327**- enterochelin esterase **PDB:3C8ID**- esterase **SCOP**- esterase **Fn3_like, cNMP, AlkA_N, PKS_DH, CHAD, SpoVT_AbrB, RFX5_DNA_bdg, FATC, PepX_C, Pfam Abhydrolase_1, Pfam peptidase**	Fes	N	Sec/SPI	x2 I-to-O x2 O-to-I O-I, I-O= N in

Note: SMART domains column, if more information or multiple similarities for a domain the domains are highlighted in bold. Phobius column; N = non-cytoplasmic, C = cytoplasmic, T= transmembrane. TMpred column; O = out, I = in, I-O = in to out, O-I = out to in, N in = N-terminal preferred inside model, N out = N-terminal preferred outside model.